Technical/Regulatory Guidance

Implementing Advanced Site Characterization Tools

IMPORTANT: This guidance document was developed for use on the web. Please review the following disclaimers before using the PDF version of the web-based document:

- Hyperlinks will send users to the web-based document.
- Glossary terms and references are not hyperlinked.

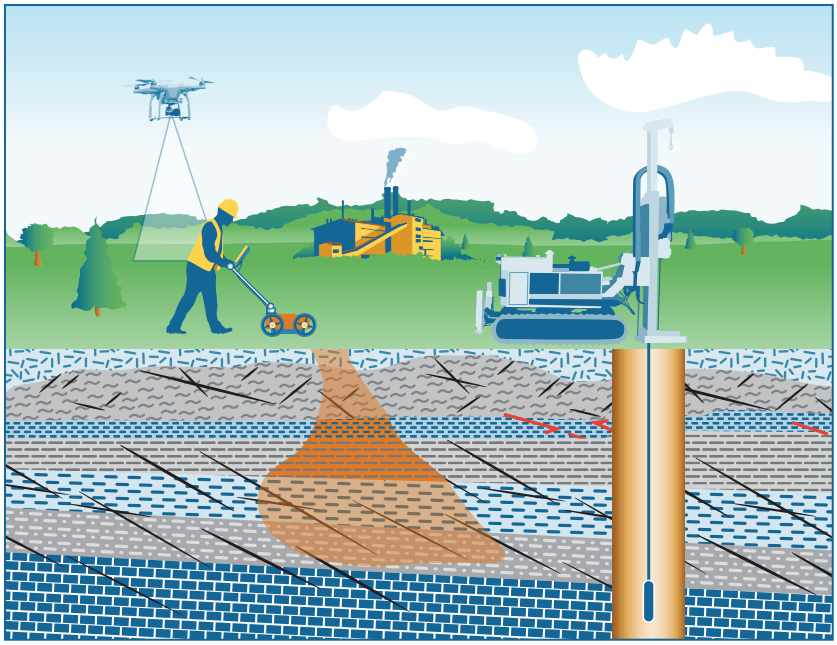

December 2019

Prepared by
The Interstate Technology & Regulatory Council
Implementing Advanced Site Characterization Tools Team

Table of Contents

About ITRC

The Interstate Technology and Regulatory Council (ITRC) is a state-led coalition working to reduce barriers to the use of innovative environmental technologies and approaches so that compliance costs are reduced and cleanup efficacy is maximized. ITRC produces documents and training that broaden and deepen technical knowledge and expedite quality regulatory decision making while protecting human health and the environment. With private and public sector members from all 50 states and the District of Columbia, ITRC truly provides a national perspective. More information on ITRC is available at www.itrcweb.org. ITRC is a program of the Environmental Research Institute of the States (ERIS), a 501(c)(3) organization incorporated in the District of Columbia and managed by the Environmental Council of the States (ECOS). ECOS is the national, nonprofit, nonpartisan association representing the state and territorial environmental commissioners. Its mission is to serve as a champion for states; to provide a clearinghouse of information for state environmental commissioners; to promote coordination in environmental management; and to articulate state positions on environmental issues to Congress, federal agencies, and the public.

Disclaimer

Advanced Site Characterization Tools (ASCT) in this document are organized into four sections: Section 3 – Direct Sensing, Section 4 – Borehole Geophysical, Section 5 – Surface Geophysical, and Section 6 – Remote Sensing. For each tool within these sections, the document provides a discussion of:

- the information the tool provides,
- how it works,
- advantages and limitations of the tool,
- quality assurance/quality control considerations,
- data collection design,
- data interpretation and presentation, and
- cost considerations

An ASCT Selection Tool, along with Summary Tables, Case Studies, and Checklists are included with this document to support the selection and use of these tools.

The ASCT Selection Tool provides an interactive dataset to identify appropriate tools for collecting geologic, hydrologic, and chemical data. It can be accessed using the Selection Tool icon on the icon bar that is available at the top of each page. By selecting four general criteria about a site, the ASCT Selection Tool provides a list of ASCT that may be appropriate to collect the needed data. Prospective tools can be further evaluated using the discussions of the tool provided in the tool section of the document and the:

- Summary Tables that provide additional information to evaluate the applicability of each tool,
- Case Studies that provide examples of the use of the tools at a site, and
- Checklists that provide information to be considered when planning to use a tool, describe typical content of a report, and identify appropriate quality control checks.

These can be accessed using the icons on the icon bar or from links within the ASCT Selection Tool. Training Videos are also available to provide an overview of the ASCT document and example application of select tools. These can be accessed using the icon on the icon bar.

Publication Date: December 2019

1 Introduction

An effective site characterization begins with developing or updating a conceptual site model (CSM) based on a thorough review of existing information. A CSM describes the locations and timing of potential past releases to the environment; soil properties and geology; hydrogeologic conditions; contaminant nature and extent; information regarding utilities; and other preferential pathways, potential receptors, and additional relevant data. After a thorough review of the CSM, data gaps are identified, acceptable levels of uncertainty are assessed, and the goals of the next stage of investigation is determined. Additional information regarding the development of a CSM and data quality objectives are provided in the following documents:

- Characterization and Remediation in Fractured Rock. FracRx-1 (ITRC 2017).
- Integrated DNAPL Site Characterization and Tools Selection. ISC-1 (ITRC 2015).
- USEPA Guidance on Systematic Planning Using the Data Quality Objectives Process (USEPA 2006)
- Expedited Site Assessment Tools for Underground Storage Tank Sites: A Guide for Regulators (USEPA 2016c)
- Best Practices for Data Management Technical Guide (USEPA 2018a)

Advanced site characterization tools (ASCTs) are capable of rapid implementation and data generation and can be used to provide data for a more precise and accurate CSM. ASCTs deliver semi-quantitative or qualitative data that provides a means to identify locations and depths where quantitative data should be collected to improve or complete a CSM or allow decisions to be made. Specifically, ASCTs offer images of site conditions in three dimensions, providing spatial context of variations in geology and contaminant distribution. These capabilities help target investigations and remedial actions in the most beneficial areas, potentially reducing characterization and monitoring costs while improving results. Similarly, tools designed to provide contaminant-related data are often combined with tools designed to generate geologic data that allows a better understanding of the subsurface. This understanding enhances the CSM and allows for the development of more effective remedial strategies.

ASCTs have greatly expanded the ability to understand contaminant concentration and mass, as well as the stratigraphy of the contaminated media. Although these tools have been available for several years, they often are not used because users perceive them to be expensive and unavailable or do not understand how ASCTs work and how to interpret the acquired data. Yet advances in computing and supporting technologies have vastly improved data analysis, presentation, and user experience with these tools. The amount of data collected versus time invested exceeds that provided by more traditional approaches, and the number of companies offering these services and their geographic range have increased. Despite this progress and evolution, ASCTs continue to be underutilized.

ASCTs are valuable resources and cost effective when available, understood, and used appropriately. We hope that the value of advanced site characterization tools will be reflected in future regulatory expectations and requirements.

ASCTs expand and enhance CSMs by providing a better understanding of contaminant concentration, mass, and distribution in the subsurface and the stratigraphy, geology, and hydrogeology of a site.

1.1 Purpose and Scope

The purpose of this document is to improve stakeholders' fundamental understanding of environmental projects and foster responsible decision making as follows:

- Assist in appropriately selecting and applying ASCTs and performing basic data interpretation.
- Use the results from ASCTs to update CSMs, evaluate cleanup options, and meet the technical needs of projects.

This guidance does not include all available tools but includes those most widely used and readily available. While this document contains extensive information on various ASCTs, it is not a guide to designing CSMs or a user's manual for any specific tool.

1.2 Technologies

The ASCTs in this document are divided into four general categories: direct sensing tools, borehole geophysical tools, surface geophysical tools, and remote sensing tools. These tools may be deployed together to collect multiple streams of

data and provide multiple lines of evidence. Specific information for the applications and technical limitations of each tool are described in the section addressing each tool. Each section also provides the information needed to ensure the tools are used only where appropriate. Some tools are expected to be modified and improved in the future while others are expected to be developed for widespread use.

1.2.1 Direct Sensing

Direct sensing tools included here are technologies that measure the parameter of interest through direct contact or precise, discrete sampling. Several of these tools are advanced into the subsurface to obtain logs of lithology or the permeability of soils or unconsolidated formations. Some tools provide logs about the presence and level of volatile organic compounds (VOCs) while others are used to provide information about the presence of nonaqueous phase liquids (NAPLs). Tools can also be combined to provide sensors for both contaminant detection and lithologic identification in one device to provide insight into lithologic control on contaminant migration.

1.2.2 Borehole and Surface Geophysics

Geophysics is the measurement of contrasts in the physical properties of different materials (through active or passive detection methods) that are used to indirectly infer or estimate parameters of interest. For example, contrasts observed in gamma radiation can be used to infer changes in lithology while changes in temperature in a borehole can be used to infer groundwater flow direction and velocity. Geophysical methods have been used in resource exploration, civil engineering, and the environmental industry to characterize subsurface conditions.

This guidance divides geophysical methods into borehole geophysics and surface geophysics. Borehole geophysics is used in open or cased wells or boreholes to collect data that can be correlated to other nearby boreholes or wells or related site information. Surface geophysical methods are non-intrusive and used to evaluate the subsurface over large areas.

1.2.3 Remote Sensing

Remote Sensing generally refers to use of satellite or aircraft-based sensors to detect and classify objects on the ground surface, in the atmosphere, and in surface water based on propagated signals [typically electromagnetic (EM) radiation]. The rising availability of remotely piloted aircraft systems (RPAS) has opened new opportunities for remote sensing and spurred the development of new technologies and applications that are being applied at the typical spatial extent of site characterization activities. Remote sensing may be split into active remote sensing (when a signal is emitted by a satellite or aircraft and its reflection by the object is detected by the sensor) and passive remote sensing (when a signal from the surface of interest, such as heat via infrared, is detected by the sensor).

This guidance provides a broad overview of remote sensing technologies, discusses in more detail how RPAS can be used to provide site information, and describes how to overcome the barriers associated with using RPAS.

1.3 How to Use this Document

The ASCT in this document are divided into four general categories: direct sensing tools, borehole geophysical tools, surface geophysical tools, and remote sensing tools. Using the table of contents or the figure on the main page, you can go to one of the four sections that describe the tools under a general category or go directly to an individual tool. Tool summary tables, case studies, and checklists are also included. The summary tables provide additional information to evaluate the applicability of each tool. Case studies are examples of the use of these tools at a site. Checklists provide information to be considered when planning to use a tool, describe typical content of a report, and identify appropriate quality control checks.

If you are interested in identifying and reviewing tools that might address a data need for a site, you can use the ASCT Selection Tool. The ASCT Selection Tool is a Microsoft Excel spreadsheet that can be downloaded from the ITRC ASCT page. To select tools to evaluate you will need to provide the following information using the pulldown boxes on the spreadsheet:

- **The type of data needed** – chemistry (chemical identification, NAPL presence, contaminant concentration, pH, conductivity, organic content, total organic solids), geology (lithology, stratigraphy, fractures, structural, physical properties), or hydrology (porosity, permeability, flux, groundwater flow, hydraulic conductivity, hydraulic gradient)
- **The type of subsurface** – consolidated/bedrock (cannot penetrate with direct-push platforms) or unconsolidated
- **Data quality needed** – quantitative (for chemistry – concentrations based on standards, for geo or hydro –

parameter measurements that are generally repeatable), semi-quantitative (measurements that fall within a range), or qualitative (an indirect measurement)

- **Data collection characteristics** – invasive (requires a boring or subsurface access), non-invasive (, access restrictions (surface cover, topology or other characteristics that may restrict or make access difficult).

Based on your input, the selection tool will provide a list of tools that meet these four criteria. Once a shortlist of tools has been identified, you can follow links to the category section, individual tool subsections, summary tables, case studies, and checklists.

2 ASCT Implementation

The implementation of ASCTs involves selecting the appropriate tool, applying the tool in an appropriate location, and performing basic data interpretation. Considerations for use of an ASCT may include but are not limited to:

- Does it fill data gaps and meet data quality needs?
- Is it technically feasible? (for example, are there constraints on use of the ASCT such as limitations due to area and depth of coverage or availability of the tool)
- Will it be approved by the regulator? (for example, use may vary by purpose such as screening versus investigation)
- Are trained and qualified contractors available within the geographic area?
- Is it sensitive to the contaminant of concern?
- Does it provide additional value or potential value to the investigation?
- Does it support existing data for multiple lines of evidence?
- What is the data collection objective? (for example, screening, delineation, pilot testing, monitoring, remediation)
- What is the form of data output? (for example, real-time data, electronic usability)
- Is it a dynamic or static tool? (for example, is it supplemental to an existing investigation?)
- What is the urgency? (for example, is it a public or ecological risk? Is the affected public demanding action?)
- How much time will it take to complete?
- Will it help evaluate site concerns and achieve end goals?

2.1 Tool Selection

Selection and proper use of any investigative tool is fundamental to a successful project and is the responsibility of the project team. The use of an ASCT should be considered at the onset of an investigation. Final selection of appropriate investigation tools and techniques occurs once a CSM is developed, data gaps are identified, and data collection planning is complete.

2.1.1 Data Needs

Often, several different tools can be used to meet a specific data collection objective. In addition, many ASCTs provide qualitative rather than quantitative data which is important to consider. Selecting the optimum tool or combination of tools relies on several factors, including:

- ability of the tool to effectively provide data given site conditions
- availability and cost of the tool
- reliability of the tool
- familiarity with the tool
- expertise required to use the tool
- expertise required to interpret data from the tool
- acceptability of data generated to stakeholders

2.1.2 Cost and Value Considerations

ASCTs are generally perceived as expensive to use; however, the amount, precision, and accuracy of data generated using ASCTs are often greater than traditional sampling techniques (for example, soil borings, monitoring wells) and can result in cost savings over the life of the project. The value of an approach is not always monetary, but may also be measured based on time, convenience, social impact, or other qualitative impacts. During the tool selection process, it is important to consider the monetary costs, the value added by the investigation, and whether the technology is appropriate for the site.

2.1.3 Cost Benefit Comparison of Traditional Tools vs. ASCTs

A cost-benefit analysis using the following approach allows the merits of advanced and traditional tools at a particular site to be evaluated:

- Outline all potential costs that will be incurred using a particular tool or approach.
- Compare to the total expected benefit to determine whether the proposed action is advisable. (Note: The overall benefit associated with a proposed action should outweigh the incurred costs.)
- Compare to alternatives for which all potential costs are also outlined.
- Record all anticipated benefits associated with the potential action.
- Weigh all identified costs relative to the expected benefits to determine whether the positive benefits outweigh the negative costs.

2.2 Tool Application

Advanced site characterization tools (ASCTs) can be used to identify locations and depths where quantitative data should be collected, to support the characterization of subsurface geology and hydrogeology, and to improve or complete a CSM. Applying ASCTs is particularly effective:

- at sites where conventional tools are incapable of providing data of sufficient density or quality
- in complex hydrogeological conditions (for example, fractured bedrock, karst, intricate alluvial channel systems)
- at sites where existing remedial strategies have not been effective or where remedial strategy effectiveness is sensitive to the precise distribution of a contaminant in the subsurface
- during emergency response situations when timely decision making is required

3 Direct Sensing

Most direct sensing tools are screening tools used to rapidly and efficiently detect the presence of contamination and characterize subsurface conditions. These tools provide high-resolution subsurface lithologic and groundwater data to aid in site assessment and improve the CSM, which allows a site or project to progress more rapidly toward cleanup or closure. Aside from profiling tools, where physical samples are collected (such as groundwater grab samples), many direct sensing tools are qualitative or semi-quantitative. Data generated with these tools can be used to select confirmatory soil boring and monitoring well locations to verify and enhance the direct sensing results.

Direct sensing tools are typically deployed using direct-push technology or are deployed in open boreholes. Given the potential for a high resolution of data, direct sensing investigations can be developed on a variety of scales based on the CSM and data objectives. Direct sensing tools can significantly improve a site CSM as well as help in the development of a more robust remedial design that addresses mass distribution, heterogeneity, and hydraulics by aiding in the understanding of the following:

- exposure pathways
- processes affecting fate and transport of contaminants
- contaminant mass distribution and flux by phase and media
- how remedial measures will affect the contaminant

The general adoption of direct sensing tools requires overcoming multiple barriers, such as misperceptions that the tools are not readily available or too expensive and beliefs that the resulting data are perplexing or subjective. The latter may result from a lack of knowledge of the basic principles underlying the function of direct sensing tools. Finally, the lack of guidance for the application of direct sensing tools and integrating them into a project to meet characterization and remedy objectives results in a hesitancy to use these tools.

3.1 How to Select and Apply Direct Sensing Tools Using this Document

Direct sensing tools evaluated in this section are based on subsurface advancement using direct-push technologies for the following data:

- downhole analytical [laser-induced fluorescence (LIF), optical image profiler (OIP), and membrane interface probe (MIP)]
- downhole physical [cone penetrometer testing (CPT) and electrical conductivity (EC)]
- hydraulic profiling [hydraulic profiling tool (HPT), Waterloo® advanced profiling system (APS) and HPT-groundwater profiler (HPT-GWP)]
- flexible liners [flexible underground technology (FLUTe™)]

In this guidance, each tool section includes a discussion of what the tool tells you, how it works, variations, benefits, appropriate use, limitations (both technical and nontechnical), data collection design, quality controls, data interpretation and presentation (including data extrapolations and misuse), which tools can be used together, costs, and references. The Direct Sensing Tool Summary Table allows you to select direct sensing tools to satisfy characterization requirements for a specific topic of interest. This table can help you identify the attributes and limitations of a selected tool. Direct Sensing Checklists (.xlsx version) are provided to support use of a selected tool and project management.

3.1.1 Tool Availability

The direct sensing tools described in this section are generally available in North America and many countries around the world. The systems associated with the tools are often portable and, with a trained operator, can be relatively easily transported if a local platform (for example, direct push rig) to “drive” the sensors is available.

3.1.2 Regulatory Considerations

Most direct sensing tools described in this section have proven histories of use and have been approved by regulators for use at particular sites across North America. Some regulators may not be familiar with the tools; however, this guidance provides information to assist those regulators in understanding the use and limitations of these tools. Nevertheless,

practitioners should be prepared to provide regulators with information, case studies, and explanations of the tool's use in the field.

3.1.3 Public Acceptance

While the public may be unaware of direct sensing tools, acceptance and common use by practitioners and regulators who support and promote the technology generally leads to greater public acceptance. Direct sensing tools can significantly reduce the degree of uncertainty in the CSM by providing detailed three-dimensional data. The level of detail and the way the information is presented can increase the public's understanding of the CSM and potential receptor impact posed by the site. In turn, a clearer understanding of the site for all stakeholders can facilitate agreement of the best path toward closure.

3.1.4 Access

Most direct sensing tools use direct-push platforms to drive sensors and, therefore, need appropriate site clearance for this equipment. Probes can be advanced with smaller track-mounted direct-push-type drill rigs (versus large truck-mounted drilling rigs) that allow access to areas with low overhead clearance limitations (for example, inside buildings) and soft or unstable ground. Most direct sensing tools can be operated remotely from the platform, providing significant versatility.

When a direct-push platform is used, the application of direct sensing tools is limited to use in unconsolidated sediments or lightly consolidated or cemented rocks because cobbles and boulders can prevent the sensors from being driven into the subsurface. To investigate bedrock and other consolidated strata, boreholes can be drilled using other methods (for example, sonic, air-rotary casing hammer), but these investigations must be custom designed and are not routine.

3.1.5 Data Collection Design

To ensure that the data collected during the investigation using direct sensing tools is useful and cost-effective it is particularly important to define the purpose of the investigation (for example, identifying locations for soil borings/monitoring wells, assisting in the design of a remedial system, geotechnical investigation). Some pre-implementation data that may be useful for enhancing the CSM prior to beginning any direct sensing investigation include:

- point(s) of release or source area(s) information
- historic use of the property
- location of underground utilities or structures
- available soil and groundwater sampling data
- depth to groundwater and bedrock

These data should be used to develop proposed boring locations, and measurements of depth to groundwater and depth to bedrock can assist in estimating the total depth of the proposed borings.

Direct sensing tools can be used in conjunction with either static or dynamic sampling approaches. If using a fixed sampling approach or as the initial step in a dynamic sampling approach, boring locations are placed on a grid pattern so that resulting data aids in the understanding of the total subsurface. This approach is more useful in areas where little is known regarding contaminant distribution and hydrological conditions at a site. If the project budget is limited, sampling transects across key areas helps develop a site-wide understanding of the subsurface geology. Dynamic work strategies can use the flexibility provided by these tools to adapt the sampling plan (for example, modify or add sampling locations) in real-time to resolve uncertainties. The number of sampling locations needed for investigations using direct sensing tools varies from site to site and may be determined by defining the number of data points required to assess the geology, hydrogeology, and preferential migration pathways.

Similar to traditional drilling tools, direct sensing tools carry the risk of cross contamination depending on the depth of penetration. Cross contamination occurs when two or more transmissive zones that are separated by a lower permeability barrier are connected. If one of the transmissive zones contains NAPL or high contaminant concentrations, it is preferable to stop the penetration at the top of the lower permeability barrier so that the potential to open a pathway for contamination to migrate into a deeper, less contaminated or cleaner zone is limited.

While it is expected that direct sensing tools act as a seal when in direct contact with the subsurface, this is not the case during tool retrieval. If a monitoring device will not be installed, grouting the hole is the general best practice to prevent vertical migration of contaminants. Most states have rules or guidelines for sealing such boreholes under their water well drilling program.

3.1.6 Cost Considerations

A site characterization cost estimate should compare direct sensing technologies to traditional approaches to assess the most cost-effective method of filling the identified data need. Most direct sensing tools described herein provide real-time data evaluation, and, therefore, reduce the need for multiple mobilizations by allowing the investigation scope to be adjusted in the field as data are collected. The cost saved by avoiding multiple mobilizations should be considered, particularly when mobilizing equipment to remote areas or areas without established equipment and personnel.

As with all site investigation technologies, the primary considerations affecting cost are the number and depth of borings. Other common cost considerations of direct-push, direct sensing technologies are as follows:

- Mobilization – lump sum cost to mobilize the tool to the site, which varies depending on site location and proximity to tool suppliers and contractors
- Tool rental – day rate to operate the tool, including costs for drilling (daily rental rate)
- Logging/data generation– data management or data generation fee that is charged on a per day or per foot (ft) basis, including time to log the linear feet of drilling
- Duplicate borings for QA/QC
- Confirmation sampling (coring) and analysis for QA/QC
- Grout – per ft basis cost for use of material, if needed
- Oversight – labor cost for consultant to direct contractor on-site
- Weekend-in-place and/or per diem– an amount of money provided to a contractor to spend each day while working on lengthy investigations or investigations in remote locations
- Lost tooling or equipment –fee for tools or equipment lost down the borehole; the bid should clearly identify who is responsible for lost tools and the timing for replacement).
- Data post-processing and analysis – Additional costs may also be associated with post-processing and analysis of data, depending on project needs.

3.1.7 Supporting Tools

A variety of supporting tools may be used to strengthen and verify the results from the various technologies described in this section. Supporting tools are considered primary screening tools in some situations; therefore, the project scope should include the overall goals of the investigation and identify technical lines of evidence that need to be developed when methods and technologies are being selected. These supporting tools can be used to determine sample types, locations, and depths and analytical parameters so that specific compounds are identified, and actual mass concentrations are measured. Using these data in conjunction with other tools guides additional sampling efforts and monitoring well placement and screening. Like when using any tool, the user should be aware of tools' limitations in all applications.

3.1.7.1 Sampling

Advanced sampling tools provide physical samples of the media being investigated for field or laboratory analysis. These tools use methods that allow sample collection (groundwater, soil, or soil gas) over discrete depths (from a few ft to a few inches) and generally are employed at multiple depth intervals in a boring to provide a high-resolution vertical profile of analyte concentrations or physical properties across a formation. Samples are analyzed using appropriate field analytical or laboratory methods.

Advanced sampling tools include direct-push temporary well point systems and multi-level groundwater monitoring systems.

Direct-push temporary well point systems include Geoprobe Systems® Screen Point (SP) samplers (SP16, SP22, or SP60) and Sonic Screen Points. Multi-level groundwater monitoring systems include the Solinst Continuous Multichannel Tubing (CMT) system, Solinst Waterloo Multilevel Groundwater Monitoring System, Westbay® System, and Flexible Liner Underground Technologies (FLUTe™) system. Use of small diameter pre-packed well screens can also improve sample integrity compared to conventional well completions. Piezometric testing or monitoring can also be conducted with some of these systems. The Direct Sensing Tool Summary Table provides additional information on some of these tools.

Environmental soil sampling has traditionally included methods originally designed for geotechnical sampling, such as hollow-stem auger and sampling with drop hammer split-spoon samplers, which result in large data gaps and excessive waste soil. Better alternatives to these traditional methods include advanced site characterization technologies such as direct-push continuous dual-tube systems (for example, Geoprobe DT22 and DT325); hollow-stem auger continuous core systems; and, in more difficult drilling lithologies, sonic dual-tube continuous coring systems.

3.1.7.2 Analysis

Advanced analysis tools, rather than providing physical samples for subsequent analysis, are used to derive information from these samples or to directly assess flow characteristics or interconnectedness in bedrock. Logging bedrock cores and measuring fracture flow in open boreholes are examples of advanced analysis tools. The discrete-fracture network (DFN) method is an example of a complete system approach, developed by Dr. Beth Parker and her research team at the University of Guelph and summarized in (Parker 2007), to improve contamination characterization in fractured rock.

3.1.7.3 Field Analyses

Where direct sensing tools need actual soil, soil gas, or groundwater confirmation, direct sampling methods can be conducted, and samples can be analyzed in a conventional laboratory or by using mobile laboratories, various field instrumentals, or test kits. Where direct sensing tools cannot be used due to site geology, contaminant type, or other constraints and high-resolution soil, soil gas, or groundwater samples are collected instead, analysis using these methods can still allow real-time evaluations applying adaptive management strategies to the site characterization, similar to using direct sensing tools. A partial list of examples of supporting field analysis tools and methods is as follows:

- mobile laboratories (many analytical methods available)
- portable gas chromatograph (GC)
- portable gas chromatography /mass spectrometry (GC/MS)
- handheld organic vapor detectors such as photoionization detector (PID) and flame ionization detector (FID)
- air and landfill gas meters (for example, O_2, CO_2, CH_4)
- radiation meters
- vapor-sensing colorimetric tubes
- handheld metal detectors such as X-ray fluorescence (XRF)
- water quality meters (for example, pH, eH, conductivity, turbidity, temperature)
- water titration or colorimetric test kits
- soil and water test kits
- immunoassay and enzymatic assays

3.2 Membrane Interface Probe

A MIP is an ASCT that is deployed using a direct-push or CPT platform. The tool consists of a probe fitted with a small gas permeable membrane connected to flowing stream of inert carrier gas that is directed uphole to one or more detectors (for example, a PID). The probe also contains a block heater and a small EC array. The MIP can detect VOCs and some semi-volatile organic compounds (SVOCs) in the subsurface and generates real-time logs of detector response (Christy 1996); (ASTM 2017). MIP is typically used to assess relative concentrations of hydrocarbons or solvents in the subsurface and the depth of their occurrence. The MIP can assist the user in overcoming the challenges associated with fully understanding contaminant distribution in heterogeneous unconsolidated or semiconsolidated materials. The MIP is rarely used as a standalone tool and instead is combined with other direct sensing tools (for example, HPT and EC) that allow for a more thorough understanding of subsurface contaminant distribution and potential migration pathways. In the interest of simplicity, this section primarily focuses on the MIP tool. Additional tools commonly used in tandem with the MIP are discussed in subsequent sections.

The primary uses of the MIP are as follows:

- a timely and cost-effective method for detecting VOCs (combined sorbed, vapor phase, and dissolved) in saturated and unsaturated zones by recording qualitative to semiquantitative levels of total VOCs in situ with depth
- real-time data collection for dynamic work plan implementation

The primary benefits of the MIP are as follows:

- optimizes site assessment and remedial efforts by providing a rapid, high-resolution depiction of contaminant distribution in the subsurface to identify discrete targets (for example, hot spots) for more effective sampling, monitoring well screen placement, and remediation
- with some limitations, infers the presence of light nonaqueous phase liquid (LNAPL) and dense nonaqueous phase liquid (DNAPL)
- obtains information about local geologic conditions when combined, as is typically the case, with other direct-push sensors (EC, HPT, CPT)
- supports collaborative data visualization and analysis and decision making via logs that can be transmitted with secure, cloud-based, real-time data management systems and presented with two-dimensional (2-D) and three-dimensional (3-D) mapping tools
- distinguishes between different classes of VOCs (for example, halogenated versus nonhalogenated compounds) when used with multiple detectors
- presents significantly less potential for worker exposure to impacted media versus conventional sampling methods

The MIP can significantly reduce the amount of data gaps in the CSM because it provides a detailed set of data along the depth of the borehole (typically at 1-ft intervals), rather than at the coarser intervals typically associated with conventional soil sampling methods. MIP data can be used to create one-dimensional (1-D) profiles, 2-D transects, and 3-D interpolated visualizations and interactive maps. Each method of presentation can help refine the CSM and develop a remedial approach, leading to a clearer understanding of the site also that all stakeholders can support a common path forward.

3.2.1 Tool Description

The MIP was developed by Geoprobe Systems® as a logging tool to detect the presence of VOCs in situ (Christy 1996).

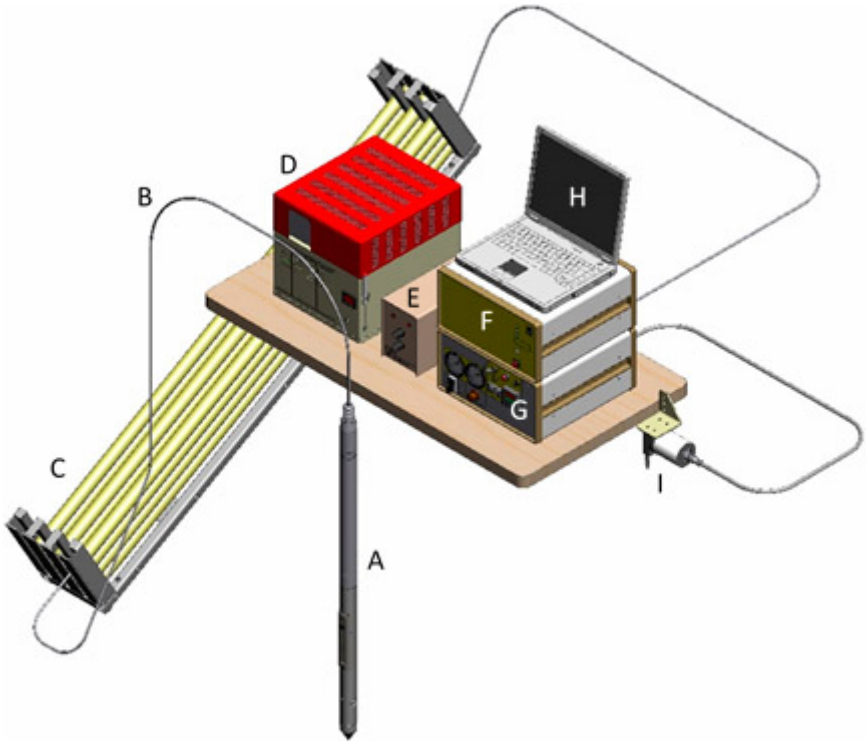

Figure 3-1. Components of a typical MIP system.

Source: Geoprobe Systems®, Used with permission

The MIP system consists of A) the MIP probe, B) prestrung trunk line within the probe, C) probe rods organized in rack, D) GC with gas-phase detectors, E) detector controller, F) field instrument that converts analog signal to digital data, G) MIP control, H) laptop computer, and I) string potentiometer that measures depth of probe advancement (see Figure 3-1).

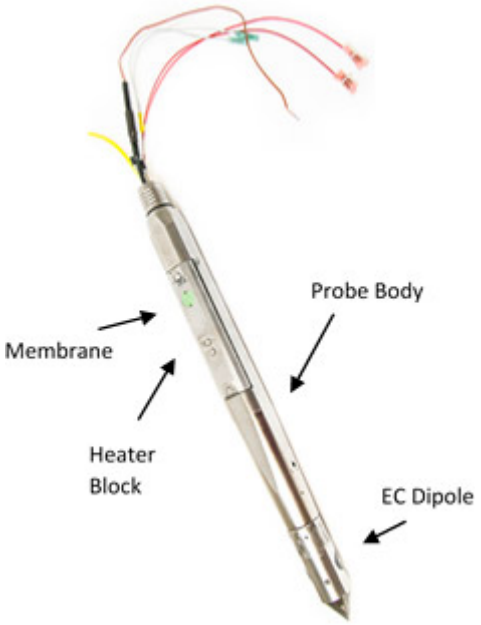

Figure 3-2. The MIP probe.

Source: Geoprobe Systems®, Used with permission

The MIP is a 24-inch (60-centimeter (cm))-long steel probe with a maximum diameter of approximately 2 inches (50 millimeters (mm)) (see Figure 3-2). A semipermeable membrane about ½ inch (12 mm) in diameter is located on the side of the probe. The membrane is reinforced with stainless-steel mesh, allowing advancement into soil and unconsolidated (and some poorly consolidated) formations with direct-push methods. A polymer clad trunk line is prestrung through the drive rods and connects the downhole probe and sensors to the uphole instrumentation (see Figure 3-1).

MIP operation is straightforward. VOCs in the formation cross the semipermeable membrane and enter the carrier gas flow to be swept up the trunk line to gas-phase detectors at the surface (see Figure 3-3) (Christy 1996). Volatilization of subsurface contaminants is enhanced by heating the soil, groundwater, and vapor in the soil pore space adjacent to the membrane with a heater block. The MIP log viewing software allows the detector response to be logged versus depth in real-time.

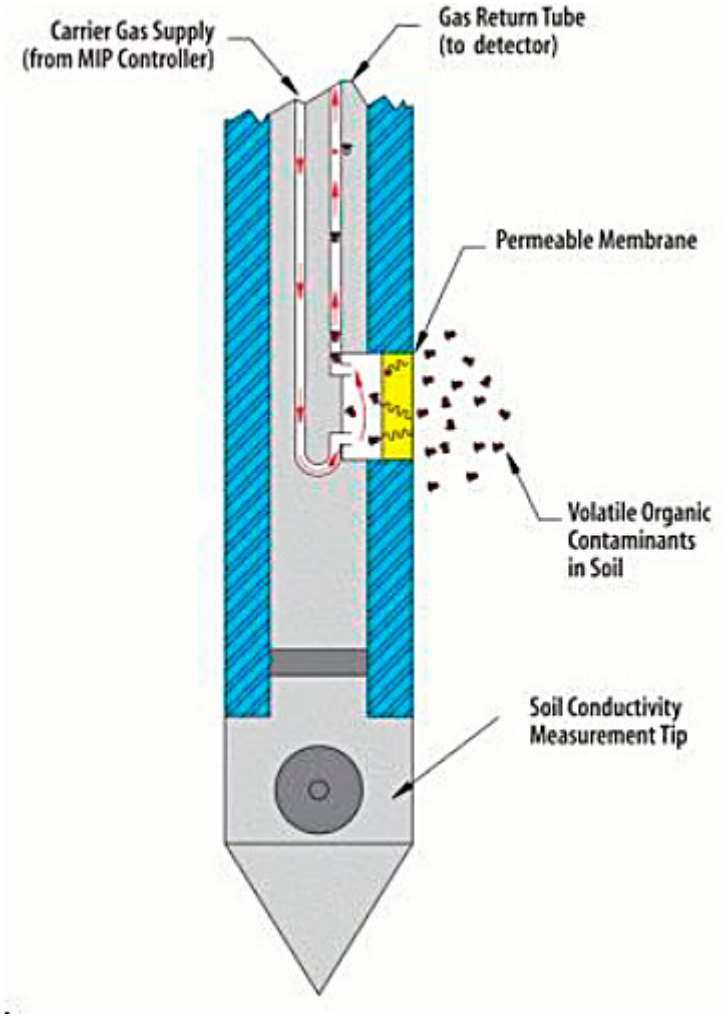

Figure 3-3. MIP principles of operation.

Source: Geoprobe Systems®, Used with permission

The MIP is nominally advanced in 1-ft increments, stopping at each increment to heat the soil, water, and vapor for a consistent period to ensure the surrounding VOCs in the subsurface are volatilized and, therefore, screened consistently. VOC data are collected every 0.05 ft, but the most representative VOC measurements are collected at the 1-ft increments in which the MIP stops. Tandem EC and HPT sensors provide lithologic data every 0.05 ft (about 15 mm) as the probe is advanced. Site lithologic characteristics dictate how fast the probe can be advanced and the refusal penetration depth. The type of contaminant and its associated boiling point and vapor pressure dictate the length of the heating cycle at each depth, typically 45 to 60 seconds (sec). These parameters should be established in the field by conducting performance testing and determining the time required for contaminant(s) of conern to travel across the MIP membrane prior to deployment (Geoprobe 2015b); (ASTM 2017).

Total VOCs are detected using a PID, FID, and a halogen-specific detector (XSD). An EC probe located on the probe also measures the EC of the soil adjacent to the probe. Graphic logs of VOC detector responses are recorded as the MIP is advanced with depth. The PID responds to VOC molecules with an ionization potential below 10.6 electron volt (eV), which includes aromatic hydrocarbons and molecules with carbon double bonds [tetrachloroethene (PCE); trichloroethylene (TCE); and benzene, toluene, ethylbenzene, and xylenes (BTEX)]. The FID generally responds to VOC molecules with a carbon-hydrogen bond, which includes most VOCs that combust in the H_2-air flame. The XSD responds only to halogenated (fluorine, chlorine, bromine) VOCs and has largely replaced the older electron capture detector (ECD) for detecting these compounds.

Figure 3-4 shows a MIP log of gasoline contamination in an alluvial aquifer setting. The left panel is the log of bulk formation EC. Higher EC readings in the upper 30 ft of the log indicate clay-dominated materials; below 30 ft, decreased EC indicates the presence of sandy materials with some silt-clay lenses. Panels 2 and 3 are the PID and FID detector responses, respectively. Baseline readings down to about 23 ft indicate no response above background. Elevated PID and FID detector responses between 23 ft and 35 ft indicate that significant hydrocarbons are present. The baseline reading on the XSD indicates that no detectable chlorinated solvents are present at this location.

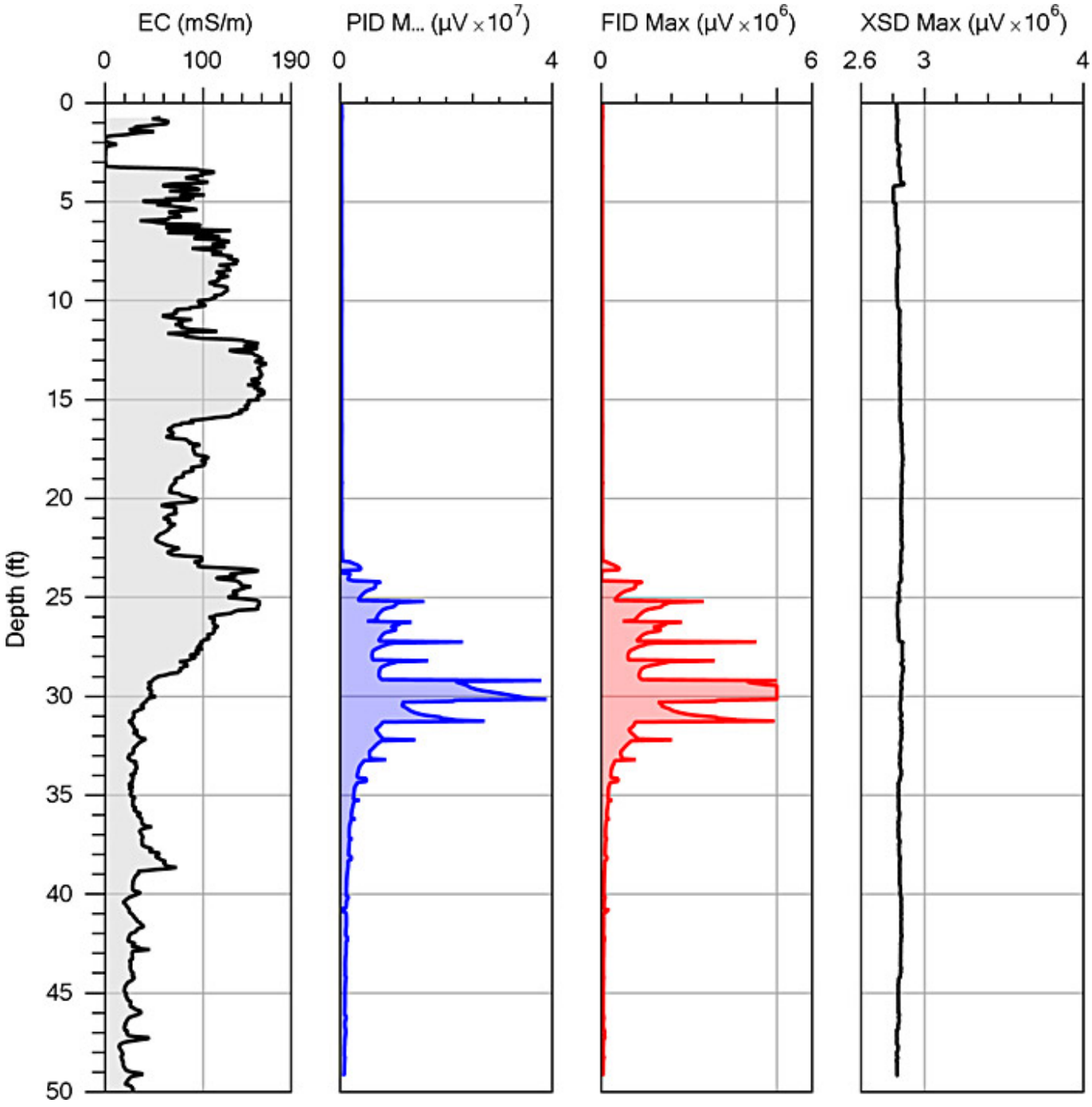

Figure 3-4. A MIP log of gasoline contamination in an alluvial aquifer setting.

Source: Geoprobe Systems®, Used with permission

3.2.2 Technical Limitations

The MIP system provides qualitative to semiquantitative results for total VOC levels (combination of sorbed, vapor, and dissolved VOCs) in the bulk formation. Because a chromatography column is not used to separate analytes in the sample gas stream before their introduction to the gas-phase detectors, specific analyte identification is not possible. Using multiple detectors that are sensitive to different groups of contaminants (for example, aromatic hydrocarbons, chlorinated VOCs) helps to identify the type of contaminant(s) present. In some modified systems, the MIP gas stream can be sampled for

further analysis with additional assay methods (for example, GC/MS) (Costanza and Davis 2000); (Van de Putte et al. 2012); (Considine and Robbat 2008). The MIP should not replace traditional soil sampling and monitoring wells but is a means to optimize a reduced number of boreholes and monitoring wells to achieve site characterization and long-term monitoring objectives.

In recent years, there has been significant interest in defining the presence and extent of NAPL in the subsurface. The MIP can be used to infer the presence of subsurface concentrations consistent with the presence of fuel NAPL (residual or saturated); however, the Ultraviolet Optical Screening Tool® (UVOST®) (see Section 3.4.1.1) or OIP-Ultraviolet (OIP-UV) (see Section 3.3) logging methods are more accurate and efficient for this task. When NAPL is encountered during MIP operation, the membrane, carrier gas tubing, and detector may become overloaded. This overload can produce artificially high background readings as the MIP is advanced past the NAPL zone. Once the lines and detectors are oversaturated, purging the lines and system can take some time and may require pulling the tool out of the ground.

3.2.2.1 Detection Limits

MIP detection limits depend on many factors, including, but not limited to, the analyte characteristics (boiling point, volatility, solubility), soil type, temperature at the membrane face, and detector used. Table 3-1 provides estimated lower limits of detection in bulk formation for several contaminant classes for common detectors.

Table 3-1. A guide to analyte detection levels in bulk formation using the MIP system and typical detectors

Source: Geoprobe Systems®, Used with permission

Detector	Analyte detection limits [parts per million (ppm)]								
	BTEX	**Gasoline**	**Diesel**	**TCE, PCE**	**CCl_4**	**DCE**	**VC**	**DCA, TCA**	**CH_4**
PID*	0.5 – 5	3 – 10+	10 – >25	0.5 – 3	N/A	5 – 10	>5	N/A	N/A
FID†	1 – 10	1 – 5	3 – 10	>500	>500	25 – 50+	>50	10 – 25	100 (ppm-v)
XSD‡	N/A	N/A	N/A	0.2 – 0.5	0.2 – 0.5	0.2 – 0.5	0.2 – 0.5	0.2 – 0.5	N/A
ECD§	N/A	N/A	N/A	0.2 – 0.5	0.1 – 0.5	25 – 50	>100	1 – 25	N/A
*PID – photoionization detector; †FID – flame ionization detector; ‡XSD – halogen-specific detector; §ECD – electron capture detector									
BTEX – benzene, toluene, ethylbenzene, and xylenes; CCl_4— carbon tetrachloride; DCE — dichloroethylene; VC — vinyl chloride; DCA — dichloroethane; TCA – trichloroethane, ppm: parts per million CH_4: methane, ppm-v: parts per million by volume in air NA: not applicable, this detector not sensitive to this analyte.									

The MIP and associated detectors are generally appropriate for investigating common VOCs, including chlorinated solvents, light oil and fuel mixtures, and those VOCs that are not fully miscible in water and have low-to-moderate boiling points (see Table 3-1). Multiple detectors are available for analyzing the effluent gas, including the PID, FID, XSD, and ECD. If a detector option is available, then the detector, or more likely, combination of detectors should be selected based on the properties of the compounds being investigated (Table 3-2). It is worth noting that the FID detects all hydrocarbon VOCs, including methane, which is common when anaerobic degradation is occurring. The other two detectors (PID, XSD) do not detect methane. If a response is present on the FID and not on the PID or XSD, then methane is likely present.

Table 3-2. Inferring analyte category based on response(s) of MIP multidetector system

Source: Modified from Geoprobe Systems®, Used with permission

MIP Detector	Chlorinated or fluorinated ethenes	Chlorinated alkanes	Gasoline, diesel, or similar petroleum fuel	BTEX, Naphthalene	Methane	Mixed petroleum fuel or BTEX and halogenated VOCs
	Relative detector response(s) to analyte categories					
PID	Moderate to High	None to Low	Moderate to High	High	NA	Moderate to High
FID	Low (See notes below)	Low	High	High	High	Moderate to High
ECD	Low to High	High	NA	NA	NA	Low to High
XSD	Moderate to High	High	NA	NA	NA	Moderate to High
Notes	FID often Responds in Chlorinated DNAPL	Detection of chlorinated alkenes on PID can differentiate chlorinated alkanes which don't respond on PID	Relative PID-FID response Will Vary with degree of weathering	Other non-chlorinated VOCs may give similar response pattern	Useful for tracking landfill gas plumes, releases of natural gas or for monitoring methane produced by anaerobic insitu bio projects	

Soil type, saturation level, and proximity of contaminants to the surface of the probe can significantly affect the ability of the MIP to detect subsurface contamination. Different soil types and variations in degree of saturation can influence the ability of the MIP probe to volatize compounds and may result in variability in detection levels that are unrelated to the mass concentrations present. The MIP volatilizes chemicals in media that are in direct contact with its heated membrane and not from media located further out into the surrounding formation. If contaminant distribution is highly heterogeneous, as is often the case, the MIP may fail to detect contaminants that are too distant from the probe.

Low-level MIP systems can be used when lower detection limits (for example, below the ppm level) are required such as when halogenated VOCs are the contaminant. A low-level MIP system includes an additional carrier gas flow modulating controller to start and stop the carrier gas flow at desired times and depths. Using the low-level system increases the detection level of the MIP system by approximately an order of magnitude for many contaminants.

3.2.2.2 Interferences

In zones with high concentrations, carryover or cross contamination of the membrane sampling port and return carrier gas line may occur as the MIP is advanced. Carryover or cross contamination results in slow bleed off of signal response for an extended depth below the interval where the high concentrations were encountered. At lower concentrations, complex mixtures (for example, gasoline) containing lower volatility and higher molecular weight compounds travel through the gas line at a slower rate, arriving at the detector(s) sometime after the more volatile contaminants, resulting in a delayed or shifted response. These effects can result in detector responses being plotted at greater depth than where the analytes were located in the formation. This carryover effect (Bumberger et al. 2011); (Adamson et al. 2014); (McCall et al. 2014) often has been mischaracterized as a physical drag down of contaminants. Actual physical drag down of contaminants while logging appears to be much less common than carryover effects.

As the MIP provides for total VOC detection without analyte separation and specificity, interference between analytes is common. Interference can be most pronounced on sites where both chlorinated VOCs like TCE and PCE are present as well as BTEX compounds. TCE, PCE, and BTEX compounds cause a response on the PID detector (see Table 3-2). Thus, it is necessary to look also at the XSD where only chlorinated compounds cause a response and the FID where only BTEX causes

a response. Using multiple detectors helps identify classes of contaminants and reduce interferences.

Additionally, some natural and manmade compounds are nonhazardous but cause a detector response. Natural pine oil or similar natural aromatic compounds from pine tree or juniper roots may yield a response if touched by the MIP membrane at depth. Some potential nonhazardous manmade interferents may include isopropyl alcohol (rubbing alcohol) or windshield washer fluid (with alcohol) recently spilled at a targeted boring log location. If the MIP system is operated with a Nafion™ dryer, then low concentrations of alcohol may be removed, but higher concentrations may be detected. The site should be investigated to assess the potential presence of nonhazardous VOCs and, if identified, these interferents should be included in the data interpretation, if they cannot be eliminated.

3.2.3 Data Collection Design

General information pertaining to data collection and design for direct sensing tools is provided in Section 3.1.5. Additional considerations to design effective MIP investigations are as follows:

- Select appropriate detectors and supporting technology.
- Determine verification requirements.

Selecting the appropriate complementary tools can help define contaminant migration pathways, geologic barriers, flux, and other parameters of interest. Appropriate detectors should be selected based on the contaminants at a site (see Table 3-1). Although it is not necessary to use multiple detectors simultaneously at all sites, it is typical. Since the FID destroys the vapor sample being analyzed it is usually the last detector to receive the MIP carrier gas stream. Similarly, MIP are routinely used in tandem with other logging tools such as an EC array, HPT [or membrane interface HPT (MiHPT)], or CPT sensor. It is important to note that the CPT sensor can be used only on CPT-type direct-push rigs, not percussion-driven, direct-push rigs. Complementary tools should be selected based on known and anticipated hydrogeological properties of the site.

Because data produced by the MIP is qualitative to semiquantitative and susceptible to interference (see Section 3.2.2.2), it is important to supplement MIP data with quantitative data from confirmation samples collected and analyzed on site or in a lab. In general, laboratory confirmation samples should be collected from areas of high, low, and medium response to verify the ability to detect the target contaminants in all desired concentration ranges. Verification sampling should also consider the number and location of geologic layers, as detector response may be affected by subsurface geology. In addition, regulatory agencies may have specific requirements for verification sampling.

3.2.4 Quality Assurance and Quality Control (QA/QC)

Proper operator training in using the MIP system is critical to obtaining logs that represent subsurface conditions. Training includes proper operation of MIP system electronics, GC, and operating software, as well as understanding MIP advancement methods and component maintenance. Improper operation and lack of maintenance can result in poor-quality and even inaccurate data.

Chemical response testing is an important QA measure used to validate each log by demonstrating the integrity of the GC detectors and MIP system. A response test must be performed before and after each log. The response test standard should be made from one or more VOCs found at the site under investigation. A MIP reference test must be performed by preparing a working standard in a 40-milliliter (mL) volatile organic analyte (VOA) vial, inverting it over the membrane, and leaving it in place for 45 sec to 60 sec. A clean vial with deionized water may be used to run a blank test in the same fashion (see Figure 3-5). For example, at a site where both gasoline and PCE were released, the stock standard may be made with benzene and PCE to verify performance of the MIP system and GC detectors for these analytes. Gas standards of much lighter VOCs (such as methane) can also be applied to the membrane.

Figure 3-5. Response test – method of introducing an aqueous standard to the membrane.

Source: Geoprobe Systems®, Used with permission

In a laboratory setting, precision is usually assessed by comparing the results of duplicate analyses; however, because MIP samples are obtained in situ, it is not possible to collect true duplicate samples. Instead, an estimate of the instrumental precision can be obtained for the entire system by evaluating the results from multiple measurements of response test samples, which are analyzed before and after each push.

QC is performed during and after each log is generated. Log QC addresses the following concerns to ensure that the log data are valid (Geoprobe 2015b):

- Proper functioning of the MIP system. Does the log look correct? Does anything in the MIP log and detector responses make you suspect that the MIP system wasn't working correctly (for example, sudden changes in pressure, flow or temperature that correspond with a shift in detector response)?
- Consistency between chemical response tests. As more logs are completed, do they show general consistency between chemical response tests?
- Significant changes seen in the response factor(s). As multiple logs are completed, a Response factor is defined as the amount of signal response divided by the signal response increase on a response test.Control charts of response test results over time can be used to gauge typical MIP system and detector response factor variations; however, response factors vary due to numerous variables, including the membrane condition and age, trunk-line type and length, and ambient temperatures.
- Log repeatability and system consistency. Review log overlays or a cross section of logs in the log viewing software to evaluate log repeatability and system consistency. Replicate logs may be run every 10 to 20 locations to verify repeatability. Run replicate logs with a 0.5-m to 1.5-m spacing (approximately 3-ft offset from original borehole) for optimum results. Small-scale variability is common; large-scale patterns are usually consistent.

- Comparison of sample results to log responses. Collect targeted soil cores or groundwater samples guided by MIP detector responses. Analyze the cores in an on-site mobile laboratory or send off site for rapid turnaround analysis. If possible, compare sample results to log responses as the field work proceeds so that adjustments or maintenance to the MIP system/GC detectors can be performed if needed.

3.2.5 Data Interpretation and Presentation

Since multiple sensors are typically used and readings are recorded at 0.05-ft intervals, investigations using MIP generates a significant quantity of data. If available, field notes recorded during an investigation using an MIP should include an interpretation of the sensor results for each log run. A more rigorous analysis should follow shortly after each day or mobilization and may include the generation of maps, cross sections, 3-D figures or animations, and other types of data displays. Data can be used to update the working CSM in the field to allow the CSM to evolve real-time in the field as additional data are generated. The final data presentation includes the interpreted MIP results as well as relevant CSM components (for example, source locations, geologic strata and properties, groundwater elevations and flow, mass flux). The following subsections provide summaries of the stages of data interpretation and presentation for an investigation using MIP.

3.2.5.1 Field Log Interpretation

As the investigation proceeds, the field team should view a graphical presentation of the sensor results on a computer monitor as the MIP is advanced. Depending on the sensors used, the field investigator may be able to determine, in real-time, the (1) relative level of impact at the boring location compared to other boring locations, (2) vertical distribution of impacts, (3) location of the groundwater table (see Section 3.2.6) and (4) vertical distribution of lithologic units. Step-out locations can be selected in the field based on this initial real-time data review.

It is possible to use the level of detector response or lack of response from the different detectors in the MIP system to tentatively identify the category of VOCs present. For example, when the XSD and PID give strong responses but the FID has a weak response, the analytes being detected are most likely chlorinated ethenes like PCE or TCE. More examples are provided in Table 3-2. To confirm an analyte category or to identify a specific analyte, colocated samples of environmental media need to be collected and submitted for laboratory analysis.

While all logs are visible on a laptop screen as work progresses, printed or electronic logs are typically made available by the operator at the end of the log run, end of day or by the following morning. Overlays of two or more logs can be created for comparison and simple cross sections may be created using the field logs to evaluate site hydrogeology and potential contaminant migration pathways or contaminant storage zones. Such information can be useful when implementing adaptive sampling plans. Logs can be used in the field to help answer the following questions:

- Have all relevant geologic layers been investigated (that is, have the MIP borings penetrated to the bedrock or a sufficient distance below the impacted zone to confirm vertical extent)?
- Are additional borings required to complete horizontal and vertical delineation?
- Where should confirmatory soil and groundwater samples be collected?

These questions and other data objectives are established in the planning phase prior to mobilization.

3.2.5.2 Data Presentation

Deliverables from the operator at the end of the project should include a field report, digital copies of the log files for use in the Direct Image Viewer software, and text files of the raw sensor data. The required deliverables should be specified in the contract before field work is initiated.

The field report may vary from company to company, but should describe the sensors used, include response test procedures and final logs for each boring, provide a table of borings drilled and provide basic boring information such as boring ID, total depth, date and time, and a location map or coordinates. An experienced service provider should be able to provide a summary report that includes a QC review of all logs and describes issues associated with individual log runs. The consultant or site owner should request a copy of the raw or final edited logs files for recordkeeping purposes. Data from these logs can be reviewed for QA later. Scaling of the log graphs is an important consideration when comparing results from multiple locations as several factors other than concentration can influence peak responsess and sensor responses can span several orders of magnitude. Many providers will provide two sets of logs prints, one set with common sensor scaling for all the boring logs, and another set where each boring log is scaled individually to show the most detail for each sensor in that individual boring.

3.2.6 Tool and Data Misuses

Lithology, saturation, the presence of multiple compounds, and other factors make direct correlation of MIP response to compound concentrations problematic. Detection levels measured in volts may not correlate directly to concentrations. In some cases when compared with physical sample analyses, MIP results have poor quantitative correlation, especially if limited samples were collected (Quinnan 2010); (Adamson et al. 2014). MIP values may vary by orders of magnitude from one location to another and are not absolute or unique to a specific compound or concentration.

A lack of MIP response does not necessarily indicate that the soil column investigated is free of VOCs or SVOCs because MIP detection limits (Table 3-1) are typically well above regulatory action levels. The MIP cannot, therefore, be used to directly determine whether health-based levels have been exceeded in a particular media.

3.2.7 Supporting and Enhancing Instruments and Technologies

Attempting to use the standard MIP configuration to characterize low-level or high-level contaminated sites can be challenging. In some cases, modified field procedures or slightly modified versions of the tool allow characterization at these sites. The low-level MIP system is used to detect lower VOC concentrations by pausing the return carrier gas to concentrate the VOC signal seen by the detectors by approximately an order of magnitude. Heated transfer line MIP (HTL-MIP) incorporates a heated trunk line to minimize trunk line analyte retention that occurs with high-level analyte concentrations or condensation in colder ambient conditions. Both methods require hardware modifications to the standard MIP.

The MIP is typically used in conjunction with other direct sensing tools to allow as much subsurface information to be gathered as possible during a single push. The MIP is equipped with a small dipole EC array (see Section 3.7 near the end of the probe to acquire a log of bulk formation EC as the probe is advanced. In many cases, the MIP is equipped with a HPT port (MiHPT) to conduct injection logging. Tandem HPT logging provides an injection flow and pressure log versus depth to help evaluate formation permeability (see Section 3.5). Used together, the EC and HPT logs can help better define stratigraphic and hydrostratigraphic characteristics of the subsurface. Plotting MIP detector logs with HPT and EC logs can help identify contaminant migration pathways or low permeability back-diffusion sources of VOCs. The MIP can also be advanced in tandem with a CPT cone (see Section 3.5) to obtain information on soil type and material strength. Targeted sampling of sedimentary layers is recommended to confirm MIP log data for VOC distribution and lithologic interpretation.

3.2.8 Case Studies

The following case studies describe specific implementation of MIP:

- MIP Boring Data Allow On-Site Decisions to Fill Data Gaps and Reduce Uncertainty during Triad Approach Evaluation at Five South Dakota Sites
- MIP Allows Real-Time Identification and Delineation of DNAPL Plume at a Former Naval Air Station in California

3.2.9 Additional Information

- Alaska Department of Environmental Conservation, Division of Spill Prevention and Response Contaminated Sites Program, Field Sampling Guide (ADEC 2017).
- Montana Light Non-Aqueous Phase Liquid (LNAPL) Recovery and Monitoring Guidance (MDEQ 2013).
- Senate Bill 96 (2015) Status of $7,000,000 Appropriation from the Orphan Share Account Environmental Quality Council – Final Report (MDEQ 2017).
- Final Proposed Plan, Former Kirksville Air Force Station Missouri, Fuds Project No. B07MO023204 (USACE 2008).
- Final Supplemental Groundwater Characterization Report, Bishop Tube Site, East Whiteland Township, Chester County, Pennsylvania (Baker 2004).
- A study of Managing Decision Uncertainties using the Triad Approach (SDPRCF 2015).
- Virginia DEQ's Northern Region Petroleum Program current understanding of the Robinson Terminal North – the former Washington Post paper depot (VDEQ 2017).
- High Resolution Site Characterization: A Sustainable Risk Management Approach (Fiacco 2010).
- The Triad Approach to Managing, Decision Uncertainty for Better Cleanup Projects (USEPA 2004).
- Membrane Interface Hydraulic Profiling Tool (MiHPT) (Cascade 2019).
- Membrane Interface Probe (MIP) Standard Operating Procedure (Geoprobe 2015b).
- USEPA CLU-IN, Membrane Interface Probe (MIP) (USEPA 2018c).

3.3 Optical Image Profiler

The OIP, manufactured and marketed by Geoprobe Systems®, is a field-screening tool used for characterizing the subsurface distribution of products (NAPL) containing polycyclic aromatic hydrocarbons (PAHs). The system provides qualitative to semiquantitative results for product and PAHs levels in the bulk formation. The OIP system employs a 275-nanometer (nm) UV light-emitting diode (LED) to induce fluorescence in PAHs, a visible (white) light (VIS) LED to examine the media, and an integrated camera to capture images of both. Each of these instruments are housed opposite a sapphire window within a 2-ft-long, 2-inch-diameter probe. Fluorescence is logged as a percent area of the camera's field of view or "percent% area of fluorescence." The system is deployed using either direct-push technology with hydraulic hammer or a CPT unit.

The OIP-UV takes advantage of the fact that PAHs fluoresce in the presence of UV light (Lakowicz 1999). The UV light causes electrons in the molecules to jump to a higher energy state and, after a short period of time, the electrons return to the normal, lower-energy state by releasing a photon of light (fluorescing). Light is released by these molecules at specific wavelengths depending on the compounds being excited. Smaller PAH molecules, such as naphthalene, emit shorter wavelengths while larger molecules emit longer wavelengths. In all cases, the light emitted by these molecules is of a longer wavelength than the exciting source (Aldstadt 2002). Naphthalene emissions are primarily in the UV range. For mixtures containing larger PAH molecules, fluorescence occurs at visible wavelengths (Berlman 1971); (Dixon 2005) (see Section 3.4 for a more in-depth description). The OIP camera cannot detect most UV emissions, but is sensitive to emissions in the visible portion of the EM spectrum. An OIP probe equipped with a green wavelength (520 nm) laser diode is available to detect coal tars and creosote. These heavier compounds do not fluoresce or fluoresce only weakly under UV light but do fluoresce well under the green light source.

The OIP-UV is primarily used to identify the presence and distribution of hydrocarbon LNAPL such as gasoline, diesel fuel, used motor oil, and similar compounds in contaminated subsurface soils and sediments. OIP-UV can also be used to estimate certain physical properties of overburden materials. The device also is equipped with a VIS LED to provide images of soil texture and color at selected depths, which allows grain-size distribution and permeability to be estimated. The system does not allow the user to discriminate between types or mixtures of LNAPL present (for example, gasoline versus diesel versus jet fuel); therefore, some prior knowledge of the type of release is required (McCall, Christy, Pipp, Jaster, Bean, et al. 2018).

3.3.1 Tool Description

The OIP system consists of a probe, the field instrument, optical interface, and laptop computer (see Figure 3-6 and Figure 3-7). The field instrument interfaces with, provides power to, and allows data transfer from an EC dipole mounted on the probe and a string potentiometer located at the surface. The string potentiometer is mounted to the direct-push unit and provides information on probe depth and push rate. The optical interface delivers power to the downhole camera and LED and transmits images to the laptop computer for analysis. A trunk line connects the probe directly to the optical interface (McCall, Christy, Pipp, Jaster, White, et al. 2018).

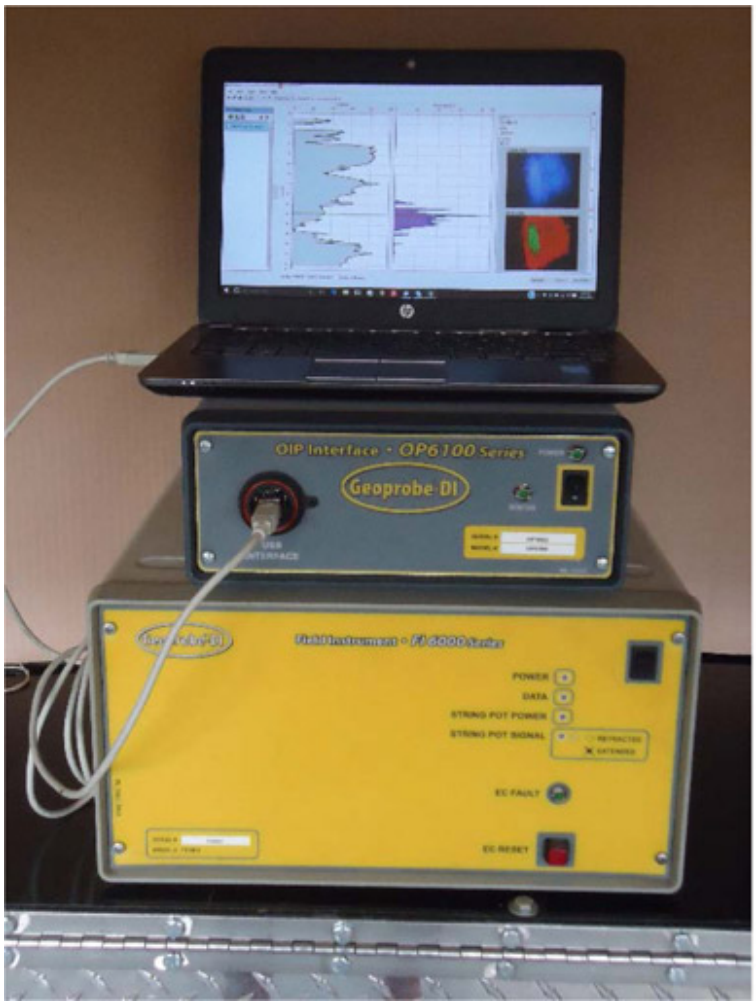

Figure 3-6. Aboveground OIP system components.

Source: Geoprobe Systems®, Used with permission

System operation is straight forward. The OIP probe is advanced using direct push percussion probing methods into soils and unconsolidated formations at a rate of approximately 2 cm/sec (4 ft/minute). The standard probe (see Figure 3-7) used during petroleum investigations, is equipped with both UV (275 nm) LED (UV LED) and a visible spectrum (VIS) LED stationed behind a sapphire window. Either of these LEDs may be used to illuminate the formation outside the sapphire window. To capture the illuminated image, a small complementary metal-oxide semiconductor camera is mounted behind the window, inside the probe. As the probe is advanced, the camera captures images of fluorescence at 30 frames/sec. One image is saved for every 0.05 ft (~15mm) of probe advancement. The system operator can halt probe advancement at any depth and capture a still fluorescence or VIS image. Still images provide better clarity and detail than images captured as the probe is advancing. VIS images may help to define formation texture, structure, and color. As the probe is advanced, an integrated EC array provides real-time readings of the EC of the formation.

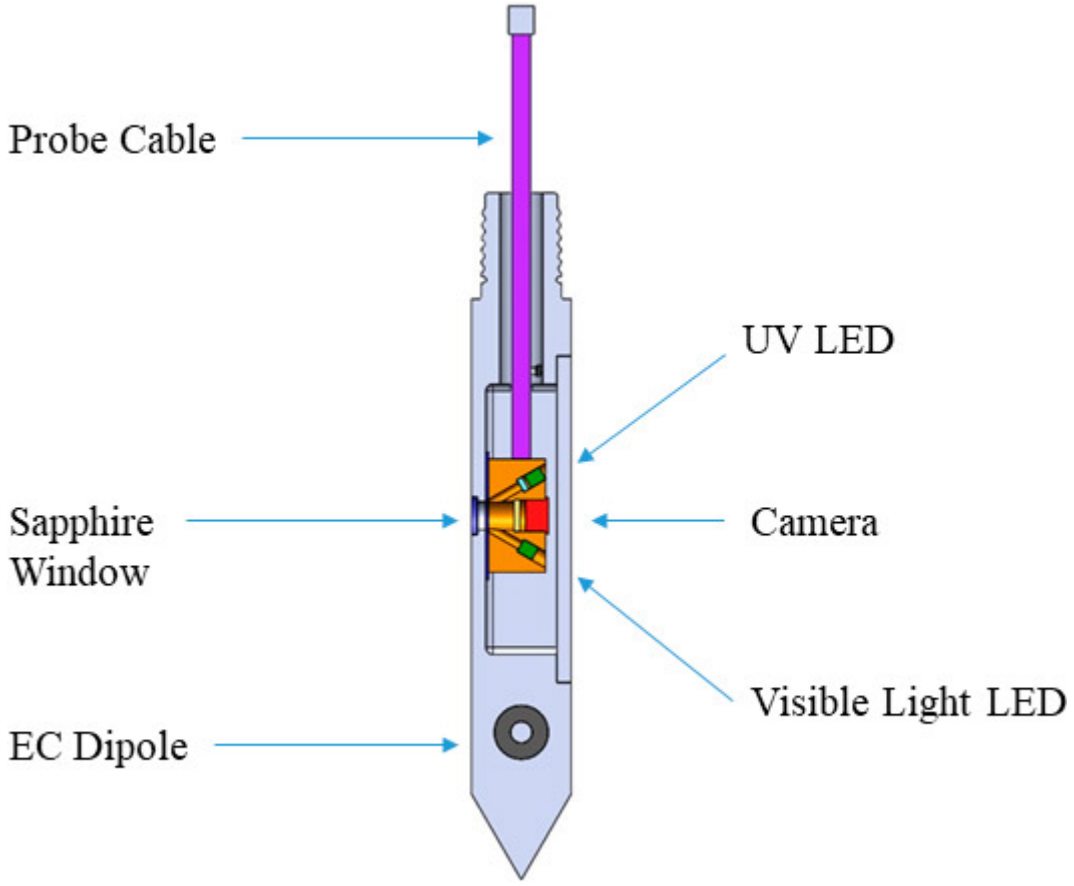

Figure 3-7. Standard OIP-UV probe with integrated EC array (The OIP-G probe is configured with a Green LED instead of the UV LED, and an Infra-Red LED instead of the Visible Light LED.).

Source: Geoprobe Systems®, Used with permission

The left side of Figure 3-8 shows the EC and percent area of fluorescence logs versus depth; the right side presents captured still images. The UV images, both still and dynamic, are analyzed by software and displayed on a laptop computer for interpretation in the field. As seen in Figure 3-8, the captured image represents the unfiltered image as detected by the complementary metal-oxide semiconductor sensor. The analyzed image is what remains of the unfiltered image following the application of digital filters. These filters eliminate pixels that are unrepresentative of fuel fluorescence. The average area illuminated per frame is calculated using multiple filtered frames obtained over a 0.05-ft interval to calculate the percent area of fluorescence which is then plotted on the log.

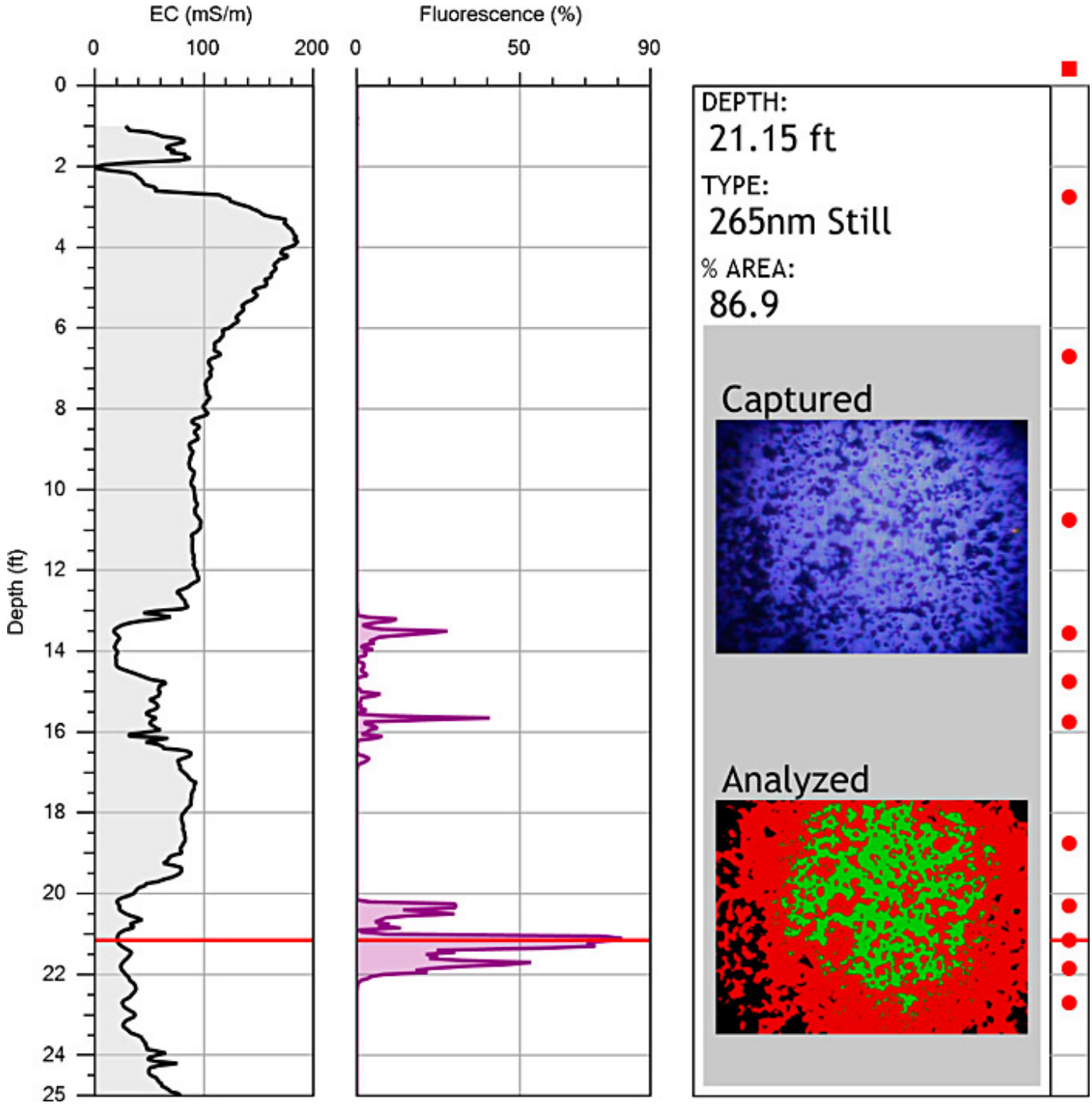

Figure 3-8. OIP software display.

Source: Geoprobe Systems®, Used with permission

OIP data are rarely viewed in isolation but combined with information obtained from complimentary sensors. All OIP probes are equipped with a small dipole EC array near the end of the tool to acquire logs of bulk formation EC as the probe is advanced (see Section 3.5). Most OIP probes can be fitted with a HPT port to conduct injection logging. Information from these sensors can be viewed together with the OIP percent area of fluorescence data and EC log information. In addition, OIP probes can be fitted with a CPT cone (see Section 3.5) to obtain information on soil type and material strength (see Figure 3-9).

Figure 3-9. OIP probe with attached CPT cone.

Source: Geoprobe Systems®, Used with permission

Tandem HPT logging is used to provide a pressure log versus depth to help evaluate formation permeability (see Section 3.6.1.1). Viewing these logs alongside the OIP fluorescence logs can help to better define contaminant migration pathways or low permeability back-diffusion sources. In Figure 3-10, the low EC (see Section 3.7) and low HPT pressure (see Section 3.6) from about 23.5 ft to 25 ft indicate the presence of a dry sand (not water wet). The image of fluorescence at 25.35 ft indicates the presence of LNAPL globules in the formation. The percent fluorescence log shows that NAPL is present in the sandy layer bounded above and below by silty clays. These data indicate that the sandy layer is behaving as a migration pathway for the LNAPL at this site.

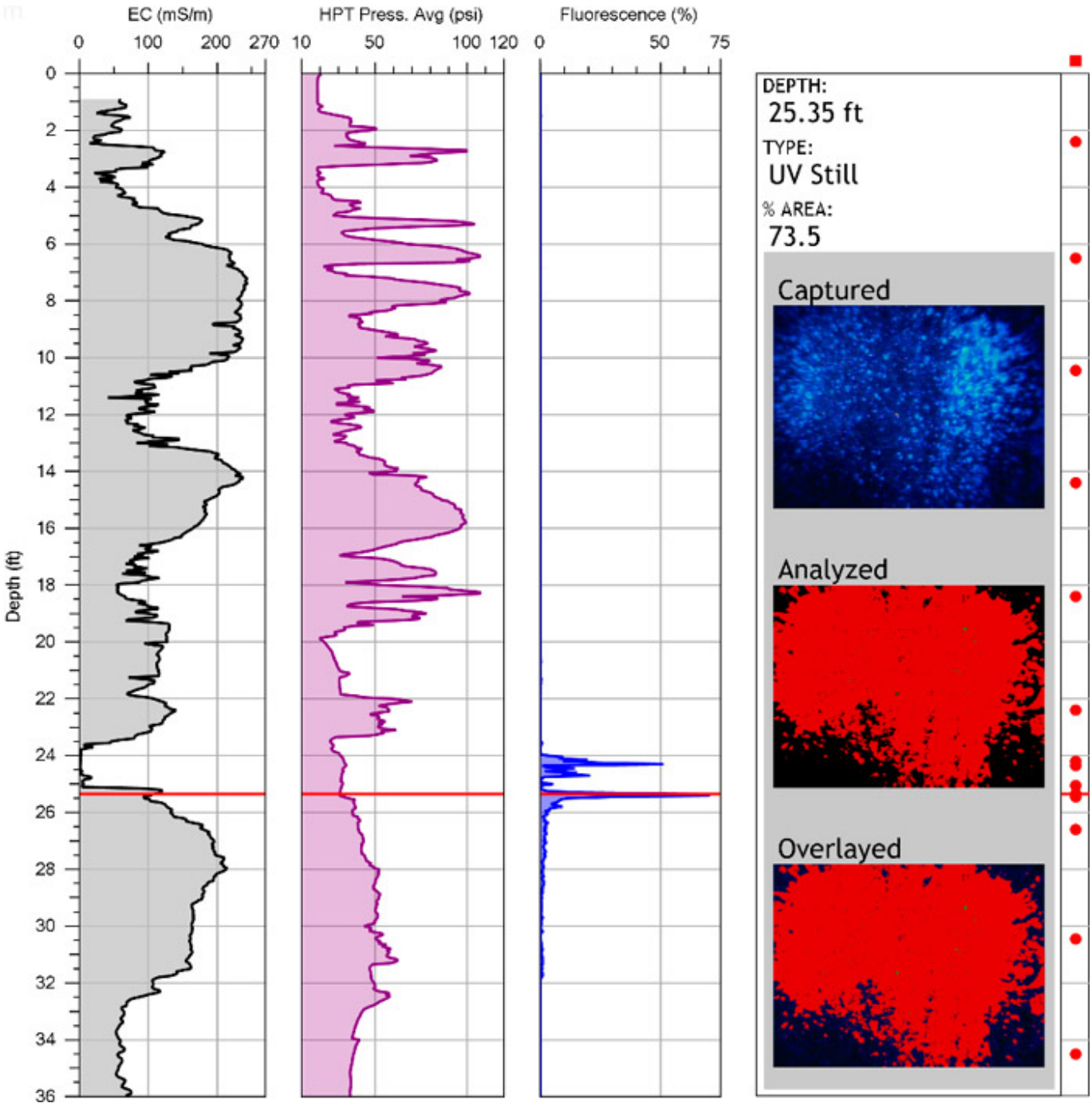

Figure 3-10. An OIP-HPT log with (EC on left, HPT injection pressure on middle, and percent area of fluorescence on right).

Source: Geoprobe Systems®, Used with permission

Coal tars, creosote, and some heavy fuels do not fluoresce consistently under UV illumination but do fluoresce under green wavelength light. An OIP probe, the OIP-Green (OIP-G), has been designed with a green (525nm) laser diode for investigation of these contaminants. Because of the low pass filter used over the camera to exclude the green source light, this probe is equipped with an infrared (IR) LED to view soil texture and structure at selected depths. The operational process for the OIP-G probe is the same as described above for the OIP-UV system.

3.3.2 Technical Limitations

The ability of the OIP to detect various contaminants depends on a variety of physical and chemical factors. Interferences, such as mineral fluorescence, can cause false positive results. Confirmatory sampling and analysis is needed when using the OIP data to assist with interpretation of these potential interferences, as well as to compare soil sample concentrations to the fluorescence response results. These technical limitations are discussed in the subsections below.

3.3.2.1 Detection Limits

OIP sensitivity depends on chemical characteristics, the soil type, and other factors. The OIP cannot detect disseminated or dissolved contamination; it only detects NAPL phase. NAPL that is PAH deficient may exhibit little to no fluorescence signature. The detection level for gasoline is higher than that for diesel, crude oil, or motor oil due to lower PAH concentrations (McCall, Christy, Pipp, Jaster, White, et al. 2018). Weathering and biodegradation of the product often result in lower levels of fluorescence and, therefore, higher detection limits. With the OIP-UV system products that are PAH rich with heavier molecular weight compounds may also exhibit reduced fluorescence due to quenching.

LIF response tends to be stronger in coarser-grained materials and weaker in fine-grained materials such as clay (Apitz et al. 1993) (see Section 3.4). The OIP, as a fluorescent-based detection tool, is likely to be similarly affected by grain size. OIP fluorescence data does not provide an indication of product type (for example, gasoline versus diesel versus jet fuel); sampling and analysis are required to specifically identify the product present in the subsurface.

Pure chlorinated contaminants are invisible to the OIP because chlorinated NAPL do not fluoresce under UV, unless they are mixed with PAHs (such as degreasing wastes). Chlorinated DNAPL can be detected with dye LIF (see Section 3.4.1.3), and chlorinated VOCs, including DNAPL, can be detected with the MIP (see Section 3.2).

3.3.2.2 Interferences

Natural and manmade materials fluoresce and potentially result in false positive results. Probably the most common natural interferant is calcite, a mineral in limestone, seashells, and caliche soils. Calcite fluorescence appears to be minimal under OIP-UV illumination. Soil sampling is required to verify if false positive fluorescence is observed with the OIP system. Many manmade materials (for example, paper and plastics) fluoresce, so investigations at landfills or similar facilities may be challenging. (see Section 3.3.3.2 for further discussion).

3.3.2.3 Confirmatory Sampling

Because the OIP is a screening tool, some form of confirmatory soil sampling and analysis is recommended. Using log data to target specific locations and depth intervals to collect confirmatory samples is recommended. Samples should be collected from high, moderate, and low fluorescence intervals as well as a few nondetect zones. Confirmation of OIP results using traditional, fixed-based sampling methods may be problematic because NAPL distribution tends to be in the form of diffuse ganglia or through preferential pathways in heterogeneous materials. In most case, the goal is to determine whether the OIP results indicate the presence of product in the same area as samples collected and analyzed in a laboratory. A specific OIP sample cannot be used to determine site contamination; a larger picture of contamination based on multiple samples is the goal. Therefore, confirmatory samples should be collected to confirm the presence of NAPL generally and, perhaps, not to directly compare paired, colocated samples. Quantitative correlation of OIP and other chemical log data to laboratory analysis of samples is often low due to several factors, including, but not limited to, the differences in analytical methods and qualitative nature of in situ tests compared to rigorous quantitative laboratory procedures. Furthermore, a core sample taken only 0.5 m from the log location may have a different NAPL distribution due to heterogeneity challenges discussed previously.

3.3.3 QA/QC

QA/QC standards must be established and followed to ensure reliable data. QC should be performed during and after each log is generated and care should be taken to ensure that the operator is performing the necessary QC tasks. In addition to comprehensive operator training (which may be verified prior to commencing work) and an operator track record of successful use, approved field procedures must be understood and followed before, during, and after OIP logging activities. The manufacturer's SOP must be reviewed prior to initiating field work (Geoprobe 2019).

3.3.3.1 QA Prior to Use

Site conditions, the type of subsurface contamination, and the project objectives should be evaluated to determine if OIP is the appropriate tool. One such evaluation can include collection of NAPL and soil samples prior to initiating field work to test and assess NAPL response and the potential for false positives and background interference. Another important pre-mobilization consideration is determination of how probe refusal will be defined for the site. Many investigations using direct-push technologies define refusal as an advancement rate (plotted on screen) below 0.5 ft/minute.

The equipment operator should complete all required QA tests prior to advancing the OIP in accordance with the manufacturer's SOP (Geoprobe 2019). These tests assure that the probe is undamaged prior to use, that interferences are

absent, and that the probe sensor is responding appropriately to reference standards. QA test data obtained prior to beginning work should be saved to a log file and should include all images and fluorescence responses to known products tested. The file may be reviewed any time after logging is completed. Typically, the same QA test sequence is performed after each log is completed (or at least after the last log of the day) to verify data quality for the final log. QA test data obtained after logging should also be saved to a log file.

3.3.3.2 QC During Use

When using the OIP, frequent communication between the probe machine operator and OIP operators is the primary key to success. The OIP and probe operators should agree on verbal commands and hand signals to alert the probe operator when to halt probe advancement so still images can be captured. Good still images in zones of high fluorescence (UV and VIS) or where lithology changes occur (VIS) are valuable when reviewing logs and ultimately developing the CSM.

Real-time images of fluorescence are displayed on screen as the OIP probe is advanced. These images may be used to confirm the indicated presence or absence of fluorescence plotted in the percent area of the fluorescence log. The fluorescence images on screen (and saved to file) are dark if fluorescence is absent. For fuel investigations, the OIP-UV-generated images show blue light typical of fuel fluorescence. Occasionally, fluorescent light of a wavelength outside of that defined for fuels under OIP-UV may be observed but the digital filters in the software do not recognize this fluorescent light as a contaminant of concern. Unfiltered images are captured at a rate 30 frames/sec and saved at a rate of one image/0.5 ft of probe advancement. Multiple (unsaved) images obtained over the 0.05 ft interval are processed (filtered and averaged) to obtain the percent area of fluorescence for that interval (McCall, Christy, Pipp, Jaster, White, et al. 2018).

In some cases, viewing the images of fluorescent light and visible (reflected) light or infrared images may help to identify materials causing false positive responses. The UV and tandem VIS (OIP-UV only) or infrared (OIP-G only) images may help identify objects with identifiable shapes or patterns in the subsurface, such as paper or seashells (see Figure 3-11). Caliche nodules in soils can develop and may have a characteristic shape and size that differs from fluid products. Targeted sampling at some locations may be needed to verify materials suspected of causing false positive responses.

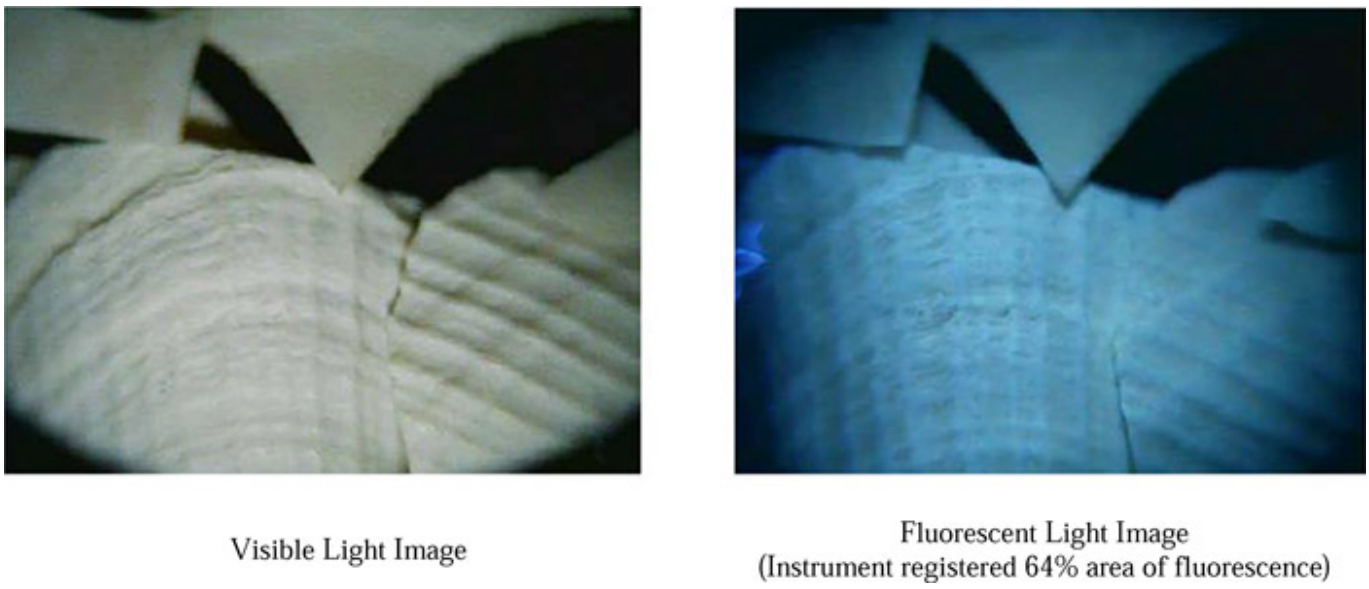

Figure 3-11. Bench-scale test images of seashell chips as seen under visible (left) and UV (right) light using OIP sensor.

Source: Geoprobe Systems®, Used with permission

3.3.3.3 QC After Use

A response check is run before and after each log run, including the last run of the day. QC tasks after using the OIP include inspecting the tool window for damage and contamination, checking to ensure that the camera frame rate is not consistently low, checking consistency between response tests, and verifying that no contamination is present on the optical window or inside the optical cavity by checking the focus and clarity of the visual image test, and verifying a non-detect response on the and black box test (Geoprobe 2019). In addition, occasionally performing replicate log runs to verify repeatability and collecting targeted confirmation soil samples for analysis is part of the post-log QC process.

3.3.4 Tool and Data Misuse

The OIP provides photographic images of NAPL fluorescence in situ. These images can provide photographic verification of PAH fluorescence in the subsurface and some indication of the relationship between the fluorescent NAPL and the formation matrix and the NAPL distribution in the formation (for example, suspended droplets, blebs, ganglia, massive saturation in the pore space). The OIP is unable to detect NAPL that are significantly PAH deficient (for example, chlorinated NAPL) and should not be used for this purpose.

Because various factors can affect OIP response, care should be taken to prevent overly simplistic interpretations when reviewing logs. The formation and any contained NAPL are disturbed and compressed when the probe is advanced into the formation. This disturbance and compression may lead to local increases in NAPL-saturated pore space at the sapphire window. Thus, the images (and resultant percent area of fluorescence log) may overestimate the amount of NAPL observed at any given depth. Conversely, soft clays may smear over the sapphire window and block the fluorescence of small amounts of NAPL. Confirmatory sampling can help to verify these misrepresentations if they occur.

3.3.5 Case Studies

The following case study describes the use of the OIP:

- OIP-Green Probe Delineates Extent of Coal Tar NAPL at a Former Gas Manufacturing Plant in KansasLaser-Induced Fluorescence

3.4 Laser-Induced Fluorescence

LIF is a field-portable system that detects NAPL in the subsurface, including most refined fuels through heavy crude petroleum. LIF employs laser light to excite fluorescent molecules in NAPL, including jet fuel/kerosene, petroleum fuels/oils, coal tars, and creosotes. In addition, LIF detects fluorescent compounds added to nonfluorescent NAPLs. The system is deployed using either direct-push technology with hydraulic hammer or a CPT unit and provides qualitative to semiquantitative, real-time results. LIF does not typically respond to dissolved- or vapor-phase PAHs that result from the presence of NAPL. Fluorescence is logged as %RE: the response relative to the response from a reference emitter (RE) calibration standard.

LIF works by using a laser to excite PAH electrons in the NAPL to a higher-energy state. The excited PAH electrons return to ground state, releasing photons with wavelengths longer than the excitation laser. The resulting fluorescence is recorded by a detector. PAHs are fundamental components of most fossil fuels and tar-like substances. They are multiple aromatic ring structures, with the simplest being naphthalene (two rings). Gasoline contains fewer PAH than diesel. Tar-like substances such as asphalt and creosote contain greater weight percentages of both smaller and larger PAH molecules. Light is emitted by PAHs at specific wavelengths that are indicative of their size and degree of substitution. Smaller PAH molecules such as naphthalene emit shorter UV wavelengths; larger PAHs emit increasingly longer wavelengths that extend out into the red and even infrared spectrum.

Under the right conditions, the intensity of the fluorescence is proportional to the quantity of the NAPL present. In addition, different PAHs continue to emit fluorescence after excitation more or less quickly (differing lifetimes). Some NAPLs fluoresce for a short time [1 nanosecond (ns) to 2 ns] following excitation (for example, coal tar), whereas other NAPLs (for example, diesel) fluoresce for longer (50 ns to 100 ns) following excitation (Aldstadt 2002).

3.4.1 Tool Description

LIF system consists of several components: a direct-push (either percussion or static) system with attached sapphire-windowed probe, a pulsed laser, wavelength selection module, a photomultiplier tube, an oscilloscope, and a computer to control the components and record the data (Aldstadt 2002). The probe containing the sapphire window is pushed or hammered into the ground at a rate of about 2 cm/sec (ASTM 2010), with a measurement obtained approximately every 0.05 foot. A fiber-optic cable transmits the pulsed laser light downhole to the window where the light exits the probe and illuminates the adjacent soils and sediments and NAPL, if present (see Figure 3-12). The laser excites aromatic compounds in the NAPL, which emit photons (fluorescence). A portion of the soil-scattered laser excitation along with a portion of detected fluorescence are returned to the surface through a second fiber-optic line, and results are displayed in real-time.

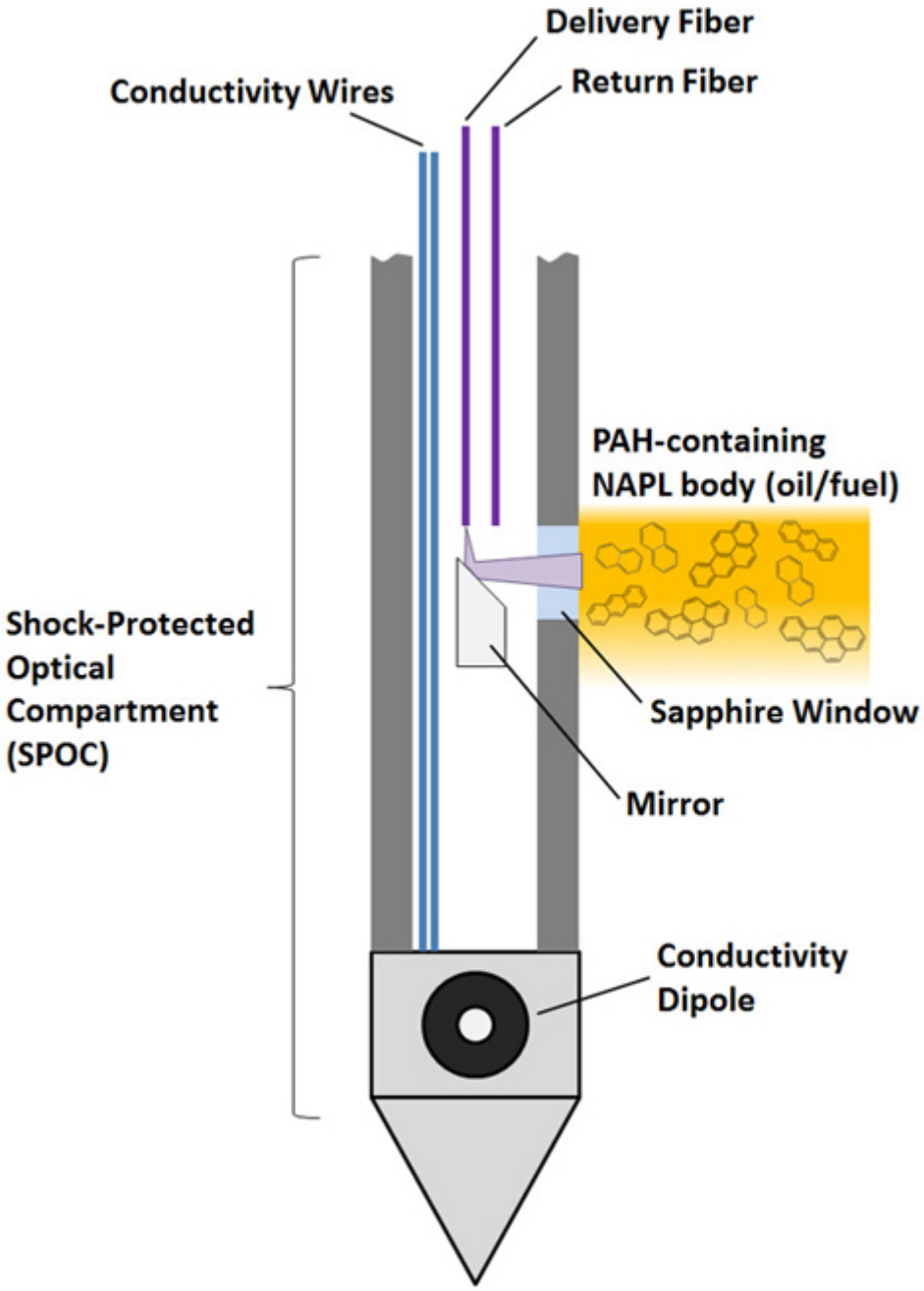

Figure 3-12. LIF tool and associated sensor (EC).
Dakota Technologies, Inc. Used with Permission.

LIF's versatility originates from its use of *pulsed* laser light as the excitation source. The laser light's narrow excitation range and high power produce very low detection limits, while the pulsed nature of the light provides LIF the ability to measure fluorescence decay times. This ability to simultaneously detect the intensity, color and lifetime of the fluorescence outside the probe provides LIF with the capability to identify target fluorophores (fluorescent chemical compounds of interest) while simultaneously identifying non-target fluorophores (for example, false positives such as peat or minerals). Careful selection of excitation lasers also optimizes its ability to respond to certain target chemistries while ignoring others.

Optimizing detection capabilities for the unique chemistry of one class of NAPL means other NAPLs cannot be properly detected with the same LIF system. LIF technology developers have crafted a family of LIF systems that strike a balance between optimized detection of some important classes of NAPL and the ability to detect other NAPL classes. Although a universally responsive tool is technically feasible, its high cost and complexity is currently beyond industry's ability to pay for its implementation. The three currently available LIF systems strike a balance between specialization and broad applicability. Figure 3-13 illustrates how these LIF systems relate to each other and the various NAPL types commonly encountered in the subsurface.

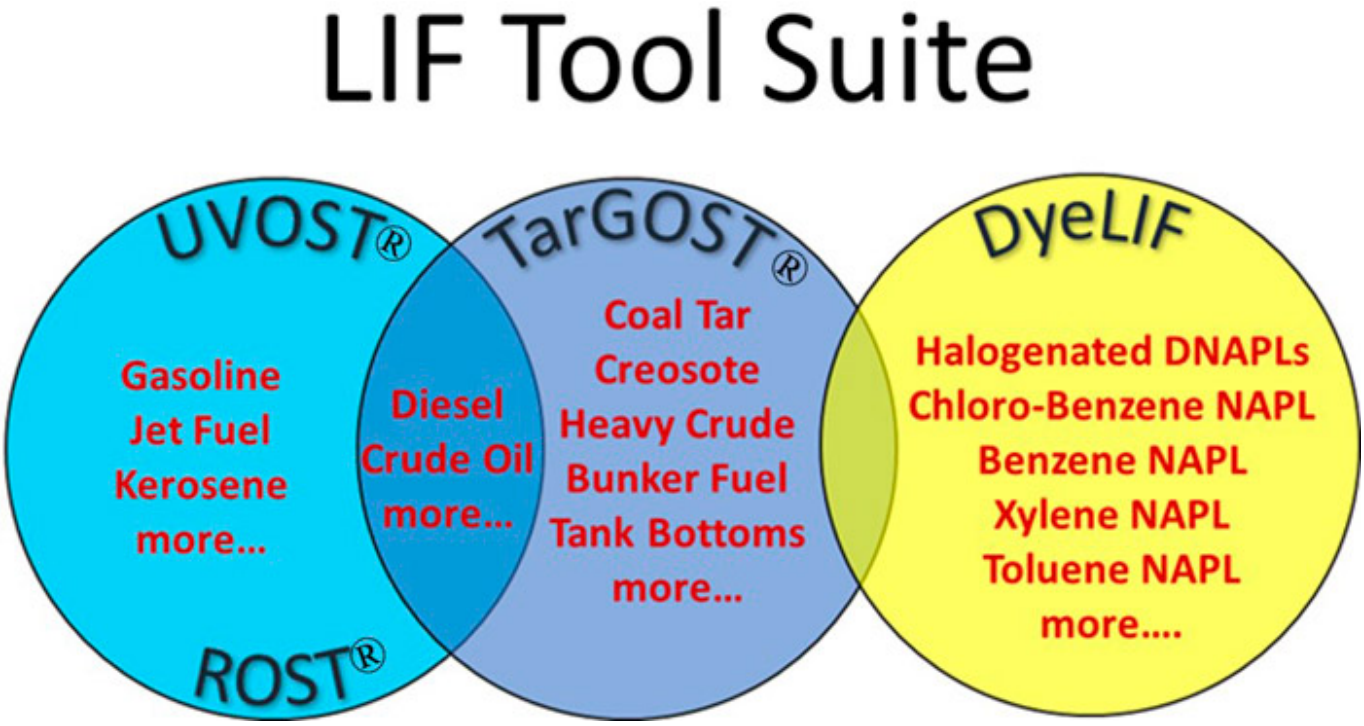

Figure 3-13. The three LIF systems and their associated NAPL types.
Dakota Technologies, Inc. Used with Permission.

This LIF tool description is divided into three parts according to three major NAPL classes and LIF systems that were designed to detect them. The section headings mirror the elements described in Figure 3-13.

- The UVOST® and Rapid Optical Screening Tool (ROST®) LIF systems are nearly identical UV-laser-based systems optimized to detect most petroleum products, oils, and lubricants. They detect LNAPL common to most releases at gas stations, refineries, pipelines, and bulk-handling facilities.
- TarGOST® is a visible-wavelength laser system that was designed to detect heavier hydrocarbons. These heavy NAPLs are commonly DNAPL due to their higher density, and include coal tars, creosote, tank bottoms, bunker (marine) fuel, and chlorinated solvents that were used for degreasing (used for cleaning items contaminated with hydrocarbons).
- The DyeLIF is a dye-enhanced laser-induced fluorescence system designed for chlorinated solvents and similar compounds that do not naturally fluoresce. DyeLIF is similar to TarGOST® but involves the injection of a fluorescent marker dye that renders the NAPL fluorescent prior to the arrival of the LIF probe.

UVOST® and ROST® were the first time-resolved LIF systems to be commercialized and are closely associated with the generic label "LIF." The description in Section 3.4.1 and Section 3.4.1.1 uses this class of LIF to discuss the general hardware and tool functions shared by all LIF systems. The subsequent sections describing TarGOST® and DyeLIF systems focus on the unique attributes of those systems, challenges typically encountered when characterizing their unique classes of target NAPL, and best practices for success for deployment.

LIF works by using a laser to excite PAH electrons in the NAPL to a higher-energy state. The excited PAH electrons return to ground state, releasing photons with longer wavelengths. The resulting fluorescence (%RE: the response relative to a reference emitter calibration standard) is recorded by a detector. PAHs are fundamental components of most fossil fuels and tar-like substances. They are multiple aromatic ring structures with the simplest being naphthalene (two rings). Gasoline contains fewer PAH than diesel. Tar-like substances such as asphalt and creosote contain greater weight percentages of smaller and larger PAH molecules. Light is released by molecules at specific wavelengths that are indicative of the compounds being excited. Smaller PAH molecules such as naphthalene emit shorter UV wavelengths; larger molecules emit increasingly longer wavelengths that extend out into the red and even infrared spectrum. Under the right conditions, the intensity of the fluorescence is proportional to the quantity of the compound present. In addition, different PAHs emit radiation after excitation more or less quickly (differing lifetimes). Some NAPLs fluoresce for a short time [1 nanosecond (Ns) to 2 Ns] following excitation (for example, coal tar), whereas other NAPLs (for example, diesel) fluoresce for longer (50 Ns to

100 Ns) following excitation (Aldstadt 2002).

When LNAPL and DNAPL are present in the subsurface environment, delineating their occurrence can be difficult with traditional methods, especially in heterogeneous geology. To gain a comprehensive understanding of the subsurface contaminant distribution, many soil samples need to be collected and analyzed at great cost. Modified forms of LIF have been successful at detecting chlorinated compounds (which are often DNAPL) as described above, and, in some cases, chlorinated DNAPL contains sufficient fluorophores to allow LIF detection without modification.

When used in conjunction with direct-push delivery, LIF can rapidly obtain high-density diagnostic data over a wide area and to sufficient subsurface depth to provide a cost-effective delineation of NAPL phase "body". The large amounts of gathered information can be displayed on a borehole-by-borehole basis or sitewide using 3-D visualization software (see Figure 3-14). Multiple LIF logs from NAPL release sites provide a basis for a detailed CSM (St. Germain 2011). In the case of some refined fuels, LIF can help the investigator discriminate between weathered and nonweathered LNAPL based on the fluorescence's spectral (color) and lifetime properties. Seek guidance from the vendor and consider results of any validation sampling or benchtop testing when determining a proper NAPL threshold for the site. When used in conjunction with other downhole tools (for example, CPT, EC, or HPT) the investigator can gain a better understanding of how site geology is controlling the contaminant distribution.

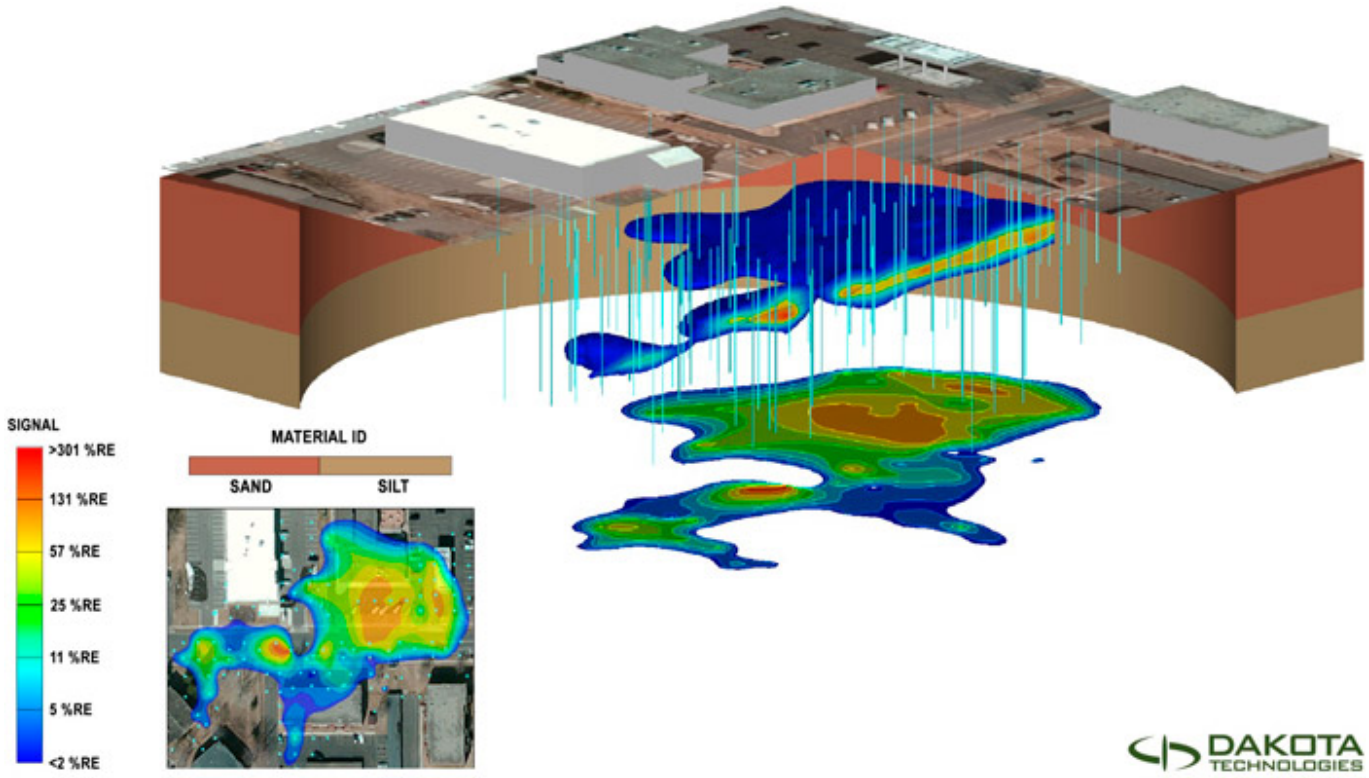

Figure 3-14. CSM with LIF logs plotted in 3-D (colors are relative %RE with red being highest)
Source: Dakota Technologies, Inc., Used with Permission

3.4.1.1 UVOST®

As discussed in the tool description (Section 3.4.1), a portion of the soil-scattered laser excitation along with a portion of detected fluorescence are returned to the surface through a second fiber-optic line, and results are displayed in real time.

The scattered laser light used for UVOST® is filtered out from the fluorescence return fiber, after which the light is split into four wavelength channels each of which responds to different size distributions of PAHs. Using different lengths of fiber optics, these four channels are delayed in time before being directed to the photomultiplier tube detector for conversion from light intensity to electric current. The current from the photomultiplier tube is sent to a digital oscilloscope that measures the intensity and the decay rate of the four wavelength channels to generate what is called a waveform. The waveforms, along with depth information, are analyzed and displayed graphically in real-time with signal strength;

waveforms are normalized to the %RE waveform (Aldstadt 2002). Figure 3-15 presents an example UVOST® log. The shape of the waveform is representative of both the color and lifetime of the fluorescence, which provides insight into the fuel type

(see Figure 3-16). Increasing NAPL in the soil pores results in increasing fluorescence, causing increases in the size of the waveform.

In general, the intensity of the total fluorescence response is expected to increase with increasing NAPL pore saturation. In benchtop tests (where the soil and NAPL are held constant), the behavior between NAPL content and %RE is typically linear across three to four orders of magnitude depending on the NAPL and %RE is typically linear (monotonic) across three to four orders of magnitude depending on the NAPL and soil types (Coleman 2006); (St. Germain and Martin 2008). Such monotonic performance through several orders of magnitude is typical across all LIF systems, until the NAPLs become too rich in PAHs and internal quenching mechanisms begin to dominate. At that point the response begins to weaken; plateaus across all concentrations; and, in many cases, decreases with increasing NAPL concentration. A monotonic relationship between fluorescence intensity and NAPL pore saturation is assumed but is not guaranteed due to a host of other factors that can enhance or quench this ideal behavior. It is, therefore, important to fully understand the numerous factors affecting the fluorescence response prior to interpreting LIF logs. Figure 3-17 illustrates the monotonic (linear) response of the same data shown on Figure 3-16.

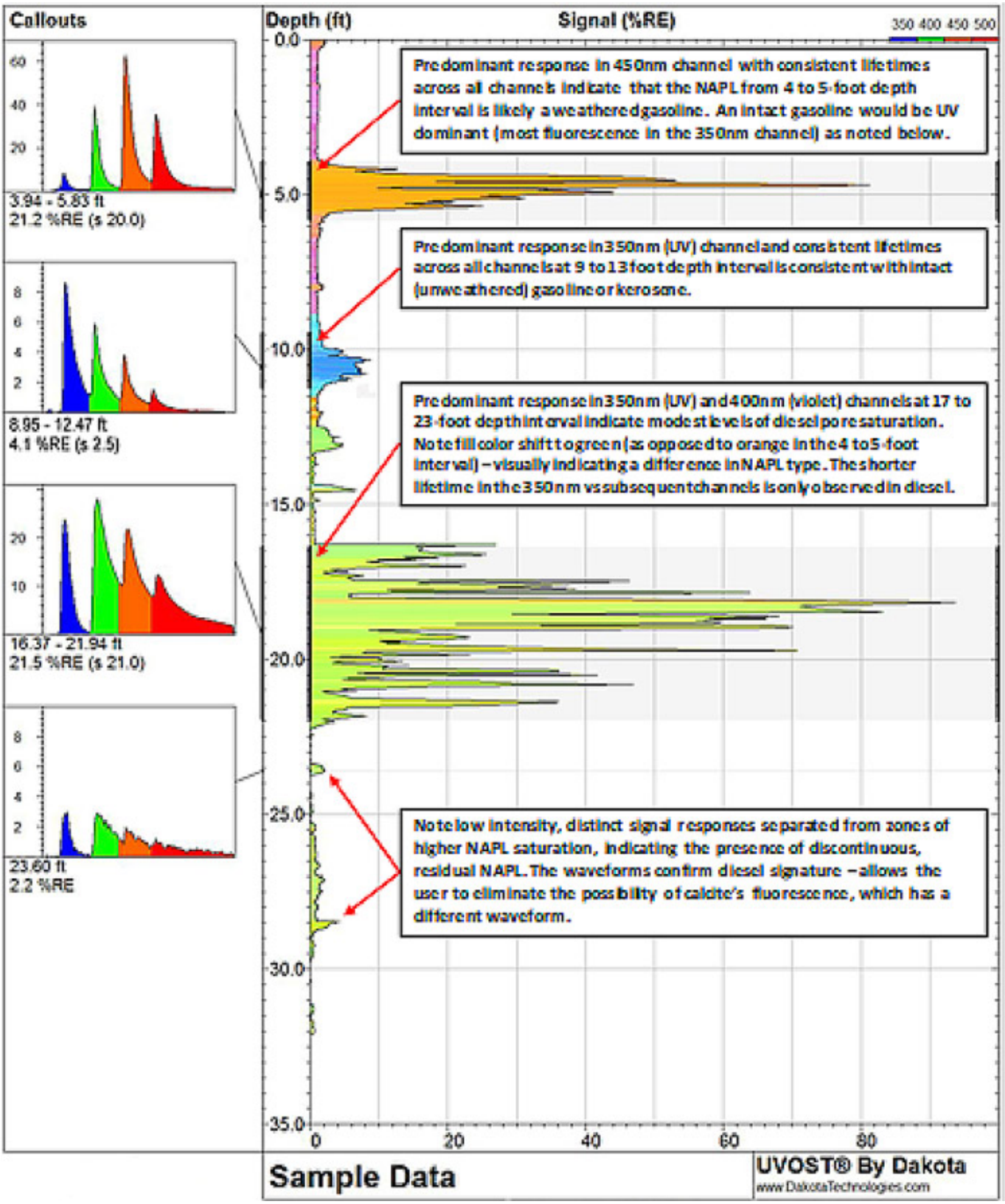

Figure 3-15. Example UVOST® log.

Source: Dakota Technologies, Inc., Used with Permission

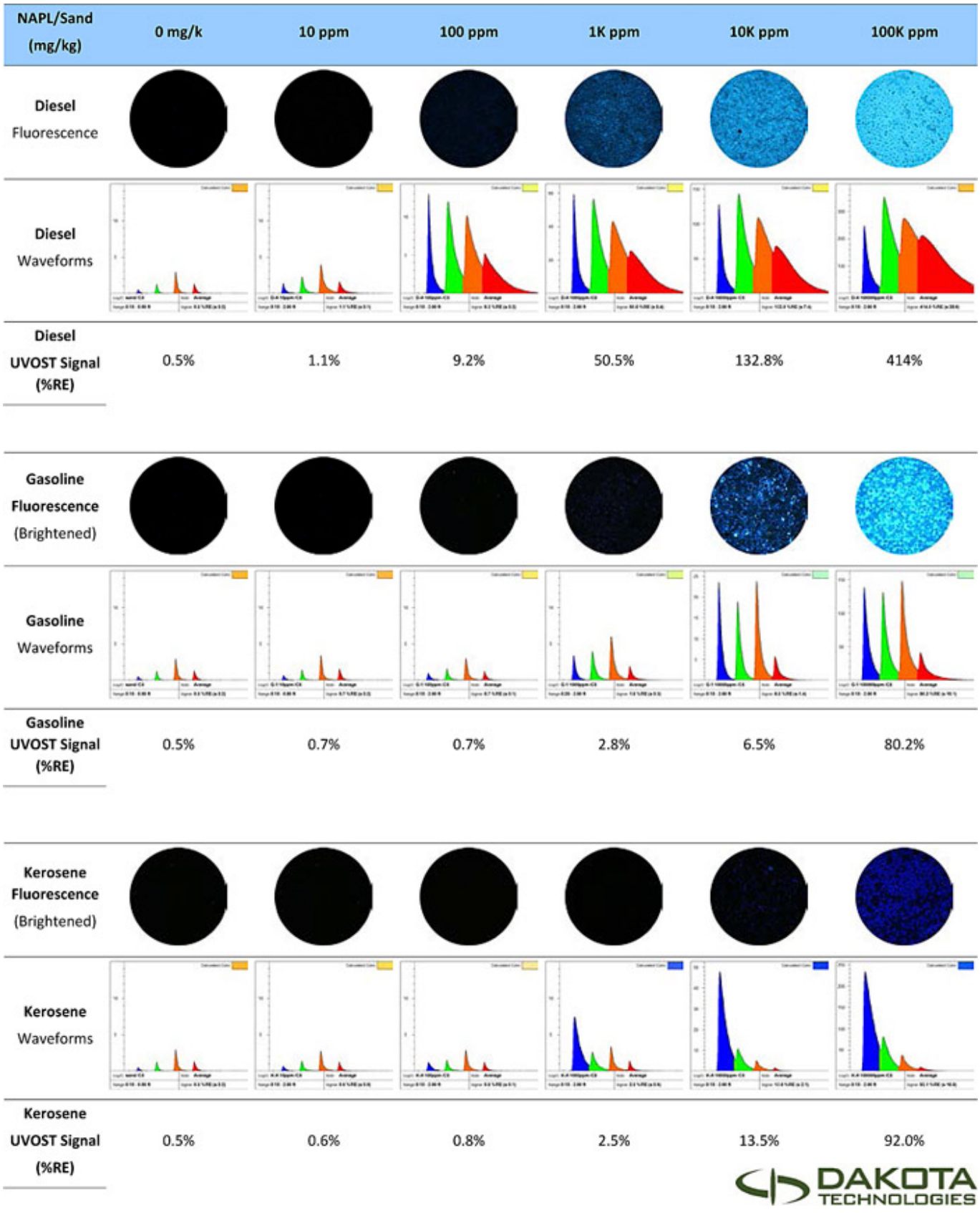

Figure 3-16. Fluorescence photos (308-nm laser) with UVOST® waveforms for common NAPLs in 20-40 mesh silica/quartz sand at 10% moisture.

Source: Dakota Technologies, Inc., Used with Permission

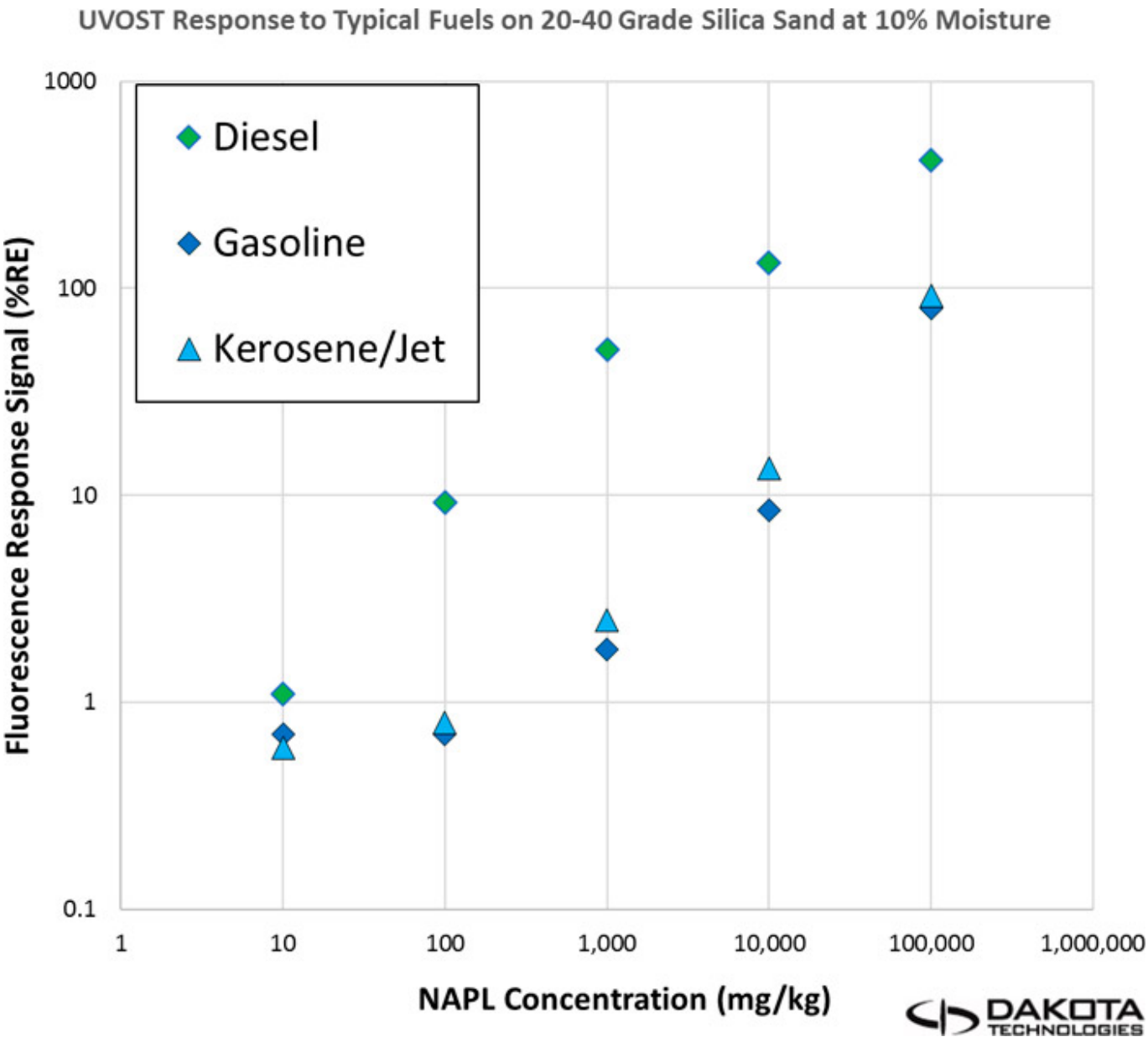

Figure 3-17. UVOST® response (%RE) of common fuels across a wide range of NAPL concentrations.
Source: Dakota Technologies, Inc., Used with Permission

3.4.1.2 TarGOST®

Field trials of existing ultra-violet excitation LIF tools were found to consistently generate erroneous data when applied to "heavy NAPL" such as coal tars, creosotes, and bunker fuels. Due to severe NAPL fluorescence quenching caused by large PAHs combined with unexpected bright fluorescence of small dissolved-phase PAHs, Dakota Technologies, Inc. developed the TarGOST® to overcome these confounding behaviors. The first successful field trials of TarGOST® delineating coal tar at manufactured gas plants are documented by (Coleman 2006).

Shifting the excitation laser to longer wavelength (weaker energy) light targets the larger PAH molecules directlysince 2- and 3-ring PAHs do not absorb this longer wavelength light. In addition, TarGOST® shifts to detecting the longer wavelength fluorescence emitted by very large PAH molecules, which eliminates some degree of the quenching. Even with this optimization, multiple-wavelength waveforms (and their associated lifetime decay) remain a crucial component in differentiating between target NAPL fluorescence and false positive fluorescence of peat, meadow mat, wood, calcites and the like. The TarGOST® system has been used at hundreds of coal tar, creosote, and heavy fuel projects to date. An example TarGOST® log is presented as Figure 3-18.

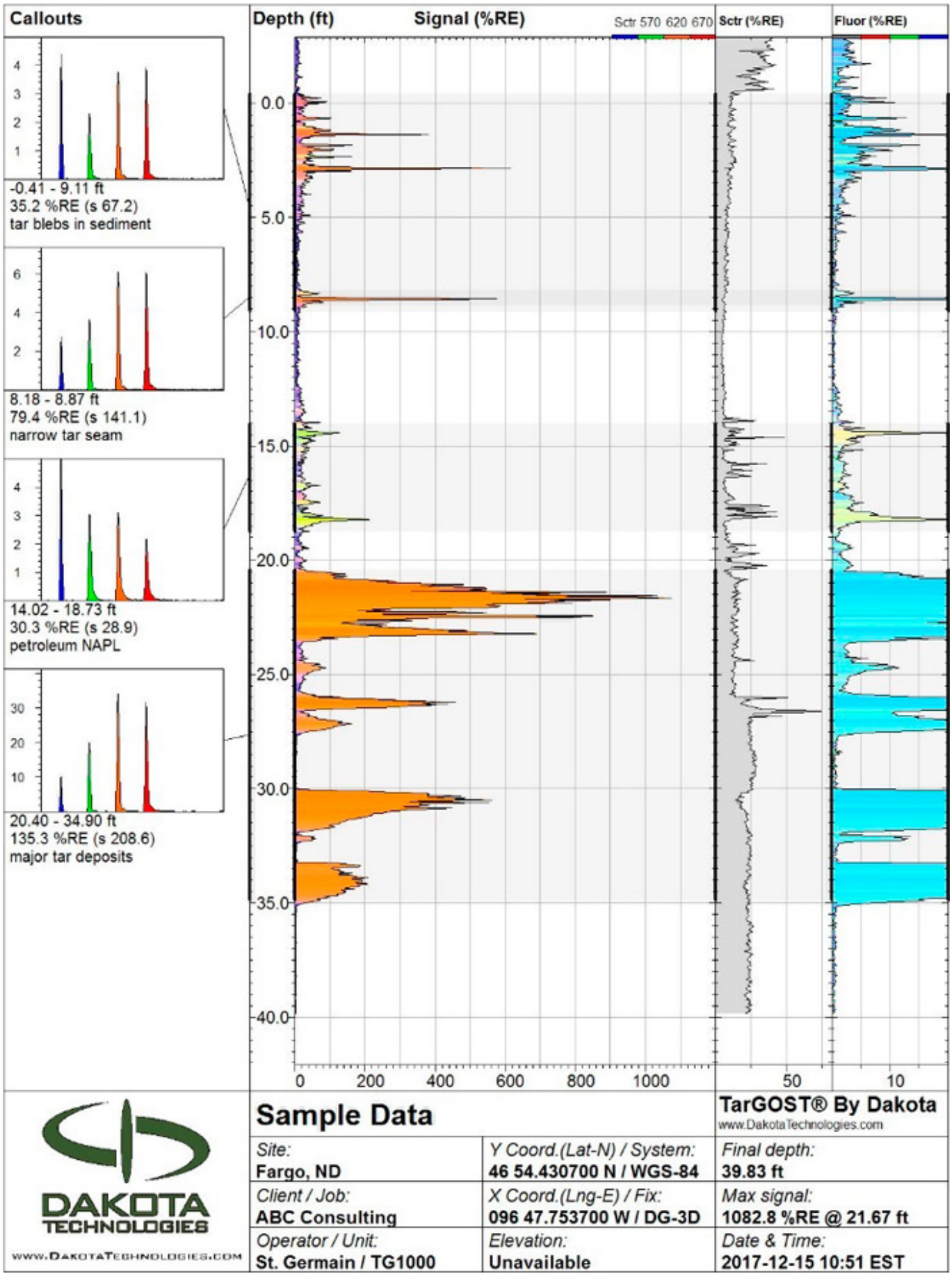

Figure 3-18. Example TarGOST® log.

Source: Dakota Technologies, Inc., Used with Permission

The advantages of the TarGOST® system over UVOST® LIF for heavy NAPL include the following:

- a robust response to most coal tars and creosotes
- excellent linearity of response for coal tars and creosotes (see Figure 3-19) across many orders of magnitude
- no possibility of response to dissolved-phase PAHs since the TarGOST® laser is incapable of exciting water-soluble PAHs

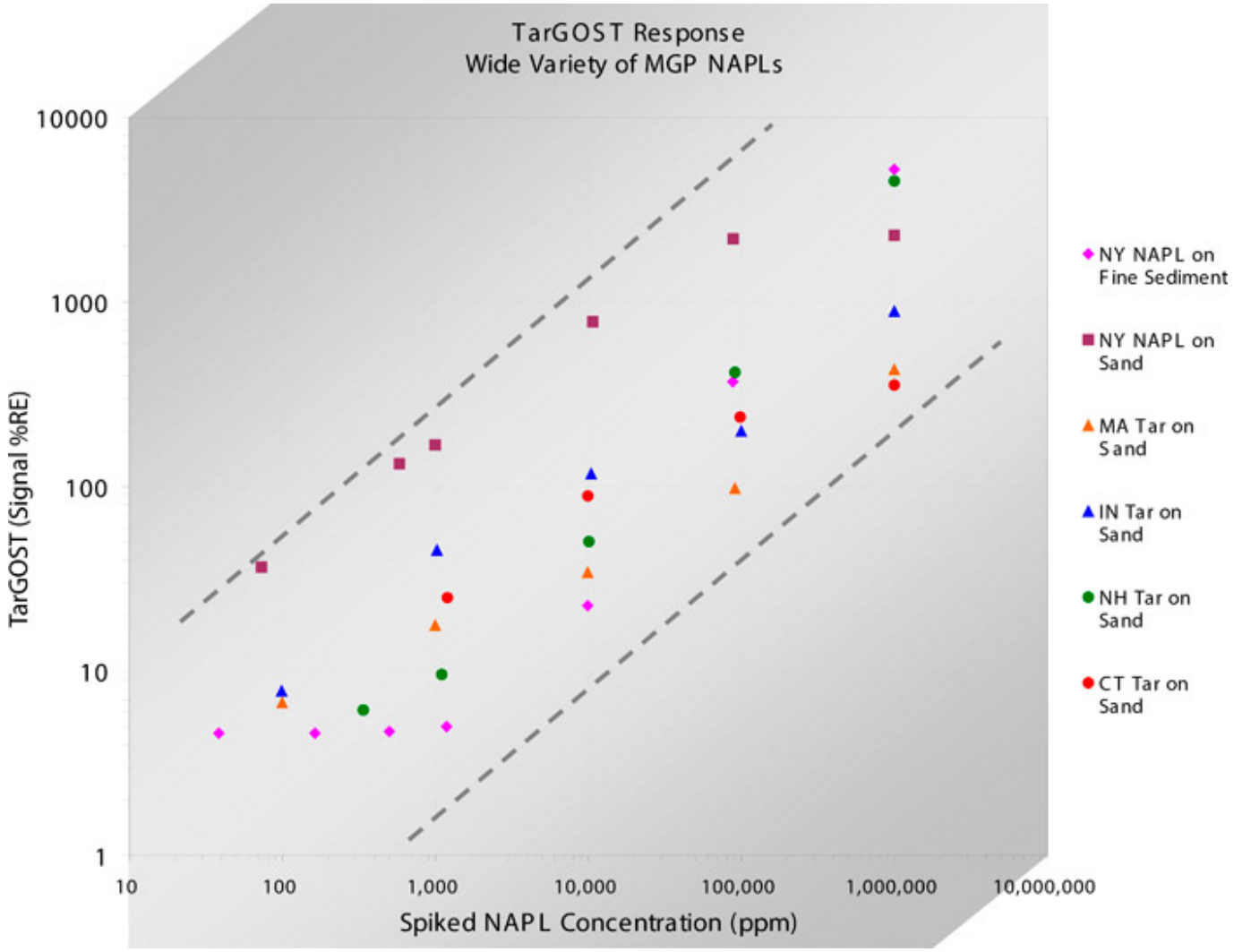

Figure 3-19. Example TarGOST® responses versus heavy NAPL content (mg/kg).
Source: Dakota Technologies, Inc., Used with Permission

The following facts are important to keep in mind when characterizing heavy NAPL with a system like TarGOST®:

- Coal tars, creosotes, bunkers, and other DNAPLs distribute themselves in highly heterogenous fashion.
- NAPL denser than water may be distributed deeper than LNAPL.
- Wood treatment sites and manufactured gas plants are typically located along waterways, so the likelihood of encountering false positive fluorophores such as wood, calcareous sands, shell hash, peat, meadow mat, and associated wetland debris is high.
- A typical detection limit range for most mixed-component DNAPL (for example, coal tars and creosotes) is 100 milligrams (mg) to 1,000 mg NAPL per kilogram (kg) soil. This limit of detection is close to human observation.

The following actions are recommended when implementing the TarGOST® system:

- Contact the TarGOST® vendor to arrange for bench-top testing of representative NAPLs from the site.
- Do not apply too high of a %RE threshold to the site. While the long-term average threshold indicative of tar and creosote has ranged from 7% RE to 50% RE, each site is unique and requires site-specific interpretation.

- Budget for limited targeted validation sampling in conjunction with the NAPL threshold determination.
- Average the %RE over a selected depth range rather than choosing narrow peak TarGOST® values spanning just one or two readings.

3.4.1.3 DyeLIF

The DyeLIF tool is a specialized form of LIF that was developed to improve the detectability and reliability of LIF for chlorinated NAPLs (St. Germain et al. 2014);

(Einarson et al. 2018). The DyeLIF tool injects a small amount (<1 g per 50-ft log) of proprietary fluorescent dye (noncarcinogenic and relatively nontoxic) into the formation several centimeters ahead of the LIF sensor. The dye mixes with and elicits a response from the nonfluorescing NAPL, as described in more detail below. In addition, dye injection pressure and flow are monitored to produce estimated hydraulic conductivity values, similar to the HPT (see Section 3.6.1.1).

As previously described, NAPL fluorescence depends on conditions such as PAH content, solvent-body conditions, and fluorescence excitation and emission energies. The molecular structures of chlorinated DNAPLs such as PCE and TCE lack aromaticity and therefore do not fluoresce. However, chlorinated NAPLs can contain remnant PAHs from manufacturing processes (for example, picked up while cleaning or degreasing), and naturally occurring fluorophores solvated after release can fluoresce sufficiently to allow for detection (Kram et al. 2004). Unfortunately, false negatives remain likely; therefore,

UVOST® and TarGOST® should not be used for chlorinated NAPL detection without first establishing that the site-specific NAPL fluoresces sufficiently by bench testing of site DNAPL if available.

Figure 3-20 illustrates the concept of injecting dye below the LIF sensor to render NAPL fluorescent for subsequent detection. Rather than changing from a black to red color like Oil Red O or Sudan IV dye shake tests (Cohen et al. 1992), theDyeLIF dye fluoresces orders of magnitude more intensely when it contacts NAPL. It also changes color and the fluorescence lifetimes increase – all of which are recorded in the DyeLIF waveforms. The dye currently used in the DyeLIF tool fluoresces more intensely and is more universally effective than the original dye, which was robustly responsive to TCE and PCE but lacked sufficient response to reliably detect some other classes of DNAPL. The current dye performs well with monoaromatics such as benzene and toluene as well as chlorobenzenes, dichloroethane, trichloroethane, TCE, PCE, and chloroform. DyeLIF is expected to respond to nearly all halogenated solvents but conducting site-specific NAPL bench testing is always advised. Nitrobenzenes are a notable exception, having been found to quench both versions of DyeLIF indicator dye fluorescence significantly.

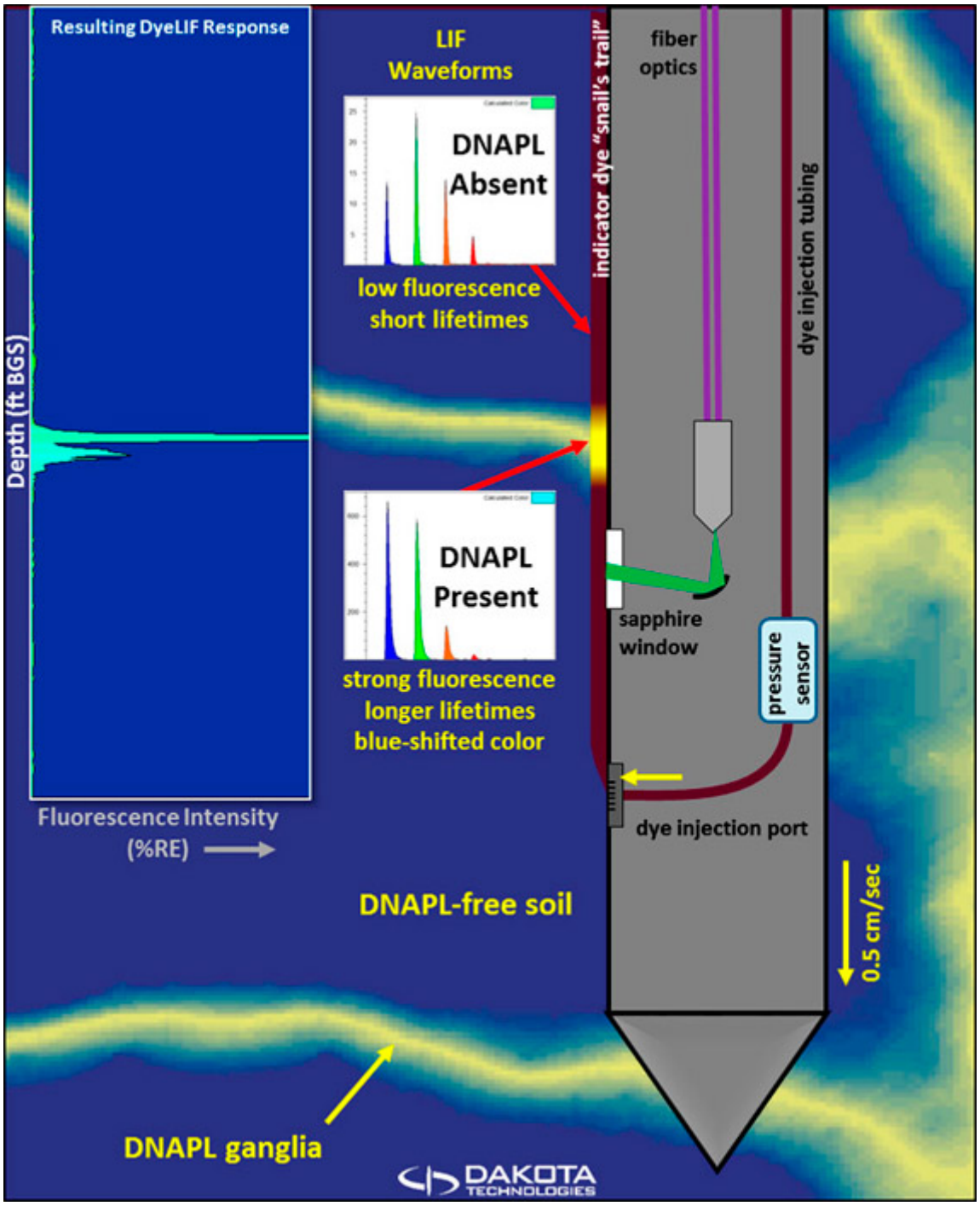

Figure 3-20. Conceptual diagram showing a DyeLIF probe passing through a DNAPL-impacted soil formation.
Source: Dakota Technologies, Inc., Used with Permission

Figure 3-21 shows a typical DyeLIF field log. The results of a nonnegative least squares (NNLS) analysis data are plotted (in red) to indicate zones of chlorinated NAPL-exclusive fluorescence (false positives are removed vis NNLS analysis).

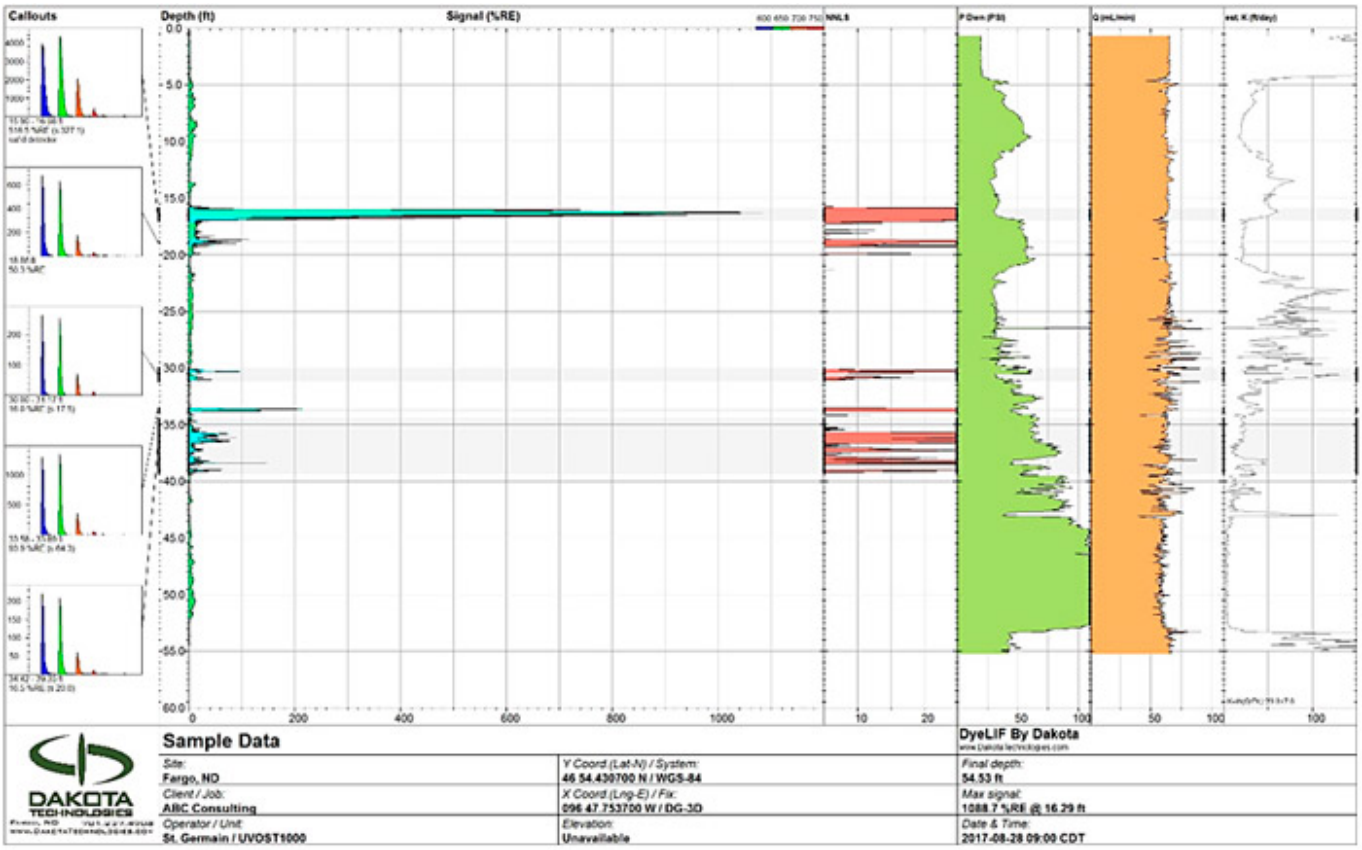

Figure 3-21. Example DyeLIF log.

Source: Dakota Technologies, Inc., Used with Permission

he following actions are recommended when implementing the DyeLIF system:

- Because investigating chlorinated NAPLs is always challenging, time should be invested in discussing the applicability of the DyeLIF tool to the site with the vendor prior to initiating work.
- It is important to note that DyeLIF is unresponsive to dissolved-, vapor-, or adsorbed-phase chlorinated solvent contamination, making it truly NAPL-specific.
- This tool, like TarGOST®, is relatively unresponsive to light fuels like kerosene and gasoline.
- DyeLIF responds well to diesel and heavier fuels, which can interfere greatly with using the tool for specifically detecting chlorinated solvents NAPLs.
- The DyeLIF responds monotonically to chlorinated NAPL saturation when the soil grain size is fixed. Finer soil particles dampen the response while coarser grained soils enhance the response.

3.4.1.4 Proper LIF Selection

Selecting the proper LIF tool to target specific NAPL is essential. Some LIF systems are blind to certain NAPLs, many of which carry higher risk than the target NAPL. For example, UVOST® is designed to characterize light-fuel LNAPL and is unresponsive to many coal tars, which are DNAPLs with potentially hundreds of times more toxicity and recalcitrance than diesel. The Tar-specific Green Optical Screening Tool (TarGOST®) system, on the other hand, is designed for coal tar delineation but fails to detect gasoline. Selecting the inappropriate LIF tool may result in overlooking contaminants and wasting money, effort, and remediation efficacy. Before selecting an LIF system for a project, contacting the developers of LIF systems is recommended. They can answer questions, provide guidance in selecting the appropriate system, and can possibly provide testing services for a target NAPL or even advise whether LIF is appropriate for a site.

3.4.2 Technical Limitations

The technical limitations of LIF systems are similar to other direct-push that are constrained by problematic geology, detection confirmation issues, NAPL detection, NAPL detection and interferences.

3.4.2.1 Geologic Setting

LIF is typically advanced through unconsolidated overburden where it has the same limitations as other direct-push tools. However, LIF has been successfully used in harder bedrock by advancing direct-push technology with LIF in a previously cored borehole filled with a sand and organoclay mixture (Hale 2011).

3.4.2.2 Confirmatory Sampling

Confirmatory soil sampling for comparison to LIF results can prove unsuccessful for the following reasons:

- Sampling in NAPL-friendly geology (such as sands, gravels) can result in poor correlation between sample results and the subsurface NAPL location, possibly due to mismatching depths between sampling methods (especially when NAPL occurs in thin horizons).
- Coarser materials, which often contain substantial NAPL, can be more difficult to sample or retain in a sampling device. Be prepared for sampling difficulty exactly where it's critical you get good recovery.
- Confirmation samples are often collected from different boreholes, and, although the boreholes may be close to the LIF being confirmed, natural lithologic heterogeneity can be significant over short distances. To control for this, laboratory confirmation sample splits can be reanalyzed with LIF (benchtop testing) to ensure the same sample is measured by both the LIF and confirming laboratory technique. This approach is recommended to assure the two methods are analyzing the same sample.
- The laboratory tests selected may not include the primary compounds present in the NAPL if the NAPL has not been separately characterized. If laboratory results do not indicate detection, then further laboratory analysis is required to identify fluorescing material.

3.4.2.3 Detection Limitations

LIF does not generally detect dissolved- or vapor-phase impacts related to NAPL. Unusual NAPLs that have not been classified as detectable or NAPL for which there is no information on the LIF response should always be sent to the vendor for testing. This is critical to success, because false negatives (NAPL in the subsurface that don't respond to LIF) result in an uncharacterized contaminant mass unless there is significant co-sampling – a potentially daunting and expensive task at NAPL release sites. Knowing the limitations of the ability of a technology to detect all NAPL types that might exist at a site is critical to success for any sensor, including LIF. Aviation gasolines are a notable example for all fluorescence systems, having failed to generate a satisfactory LIF response at a number of sites and in laboratory testing.

3.4.2.4 Interferences

False positives can be caused by organic matter, sea shells, peat, calcite (limestone), and calcareous sands. These false positives can often be recognized and removed from the CSM because they typically generate a signature (waveform) that varies from that of the NAPL, giving investigators some evidence for identifying false positives versus NAPL. Disposal sites such as landfills also contain anthropogenic materials that often fluoresce (for example, plastic and paper), which interferes with LIF. Other materials that can cause false positives include peat and meadow mat, asphalt, stiff and viscous tars, tree roots, sewer lines, coal, and quicklime (St. Germain 2008).

Fine-grained, organic-rich sediments are challenging. High surface area and small grain size soils (for example, clays) can hide NAPL so that it cannot be detected by LIF; under these conditions, the NAPL in the interstitial spaces of clay is not visible to the sensor unless there is clear line of sight. LIF sensitivity to petroleum hydrocarbons in soil has been shown to be inversely proportional to the available surface area of the soils. Sandy soils tend to have a much lower total available surface area than clay soils, so hydrocarbon compounds in sandy soils generally yield a higher fluorescence response than they do in clay-rich soils. These environments can result in high backgrounds readings and wandering baselines that can be deleterious to proper interpretation and can mask smaller signals, often requiring advanced data analysis.

Other factors related to soil type that can affect fluorescence response include mineralogy, degree of soil aggregation, and moisture content (Apitz et al. 1993). Increasing water content tends to impede LIF response in sand but enhances response in clay, while having negligible effect in sand-clay mixtures where their respective effects offset one another (Apitz et al. 1993).

3.4.3 Data Collection Design

General information about ASCT data collection and design is provided in Section 3.1.5. Additional considerations for LIF include NAPL type (for example, gasoline, diesel, kerosene, jet fuel, crude oil) and the age of the release.

3.4.4 Quality Control

QC standards must be established and followed to ensure reliable data. In addition to comprehensive operator training (which may be verified prior to commencing work) and an operator track record of successful use, approved field procedures must be understood and followed before, during, and after LIF activities.

3.4.4.1 Quality Control Prior to Use

During project planning stages, site conditions and the project objectives should be evaluated to determine if LIF is the appropriate tool. If desired, NAPL and soil samples can be collected and tested to assess NAPL response and the potential for false positives and background interference. It should be noted that benchtop NAPL analysis can also be performed after fieldwork, but this delay eliminates the possibility of factoring these responses into real-time interpretation of the logs.

Prior to beginning work, discuss with the operator how hard they should push when advancing becomes difficult so that the likelihood of breaking equipment or getting the equipment stuck is reduced. The equipment operator should complete the following prior to advancing LIF tools and systems:

- Test the equipment, and verify it is in good working order. This includes:
    - Ensure proper setup and alignment of the shock-protected optical compartment and evaluate and mitigate fogging, if necessary.
    - Recording and evaluating the %RE
    - Recording and evaluating the system background response (nothing on the sapphire window). Foreign materials inside the probe can fluoresce, masking the response occurring from outside the window in the formation. Background should never exceed 1% RE, with <0.5% preferred, if possible. This makes small responses outside the window easier to detect and interpret.
- Acquire baseline soil response (for example, from calcium-carbonate-rich soils.) to understand whether small contaminant responses may be masked. This is usually in an area of the site where no previous impacts have been reported. If such an area has not been identified, the background response usually can be determined during LIF advancement from intervals that do not appear impacted.
- If product sample(s) are available, apply to sapphire window to record site-specific response(s). Low-viscosity NAPLs such as gasoline need to be applied to a small volume of moist sand piled onto the probe window so as to prevent thin-sheeting and evaporation that may produce artificially low fluorescent responses.

3.4.4.2 Quality Control During Use

During fieldwork, the equipment operator must repeat the following quality control measures prior to every log:

- Verify the shock-protected optical compartment is in good working order and there is no fogging.
- Record the %RE to calibrate the tool for that log.
- Record the system background response (clean window). Again, background should never exceed 1% RE, with <0.5% preferred, if possible.

The waveforms and other concurrent outputs should be evaluated throughout the LIF advancement to identify potential non-NAPL materials, potential background interference, or evidence that a previously unidentified form of NAPL exists at the site.

The advancement (push) rate, typically about 2 cm/sec, must be monitored for deviations to account for associated response variations. The rate should not exceed that specified for the method. Although advancement rates slower than the standard rate produce higher data densities with minimal risk to data quality, these slower rates negatively impact daily production.

3.4.4.3 Quality Control After Use

Following each LIF push, the operator should inspect the sapphire window for fogging, chips, cracks, or other issues.

Soil samples may be collected (or existing samples used) to confirm potential non-NAPL or unidentified NAPL signatures and to understand lithology that may affect response (for example, porosity effects from clayey versus sandy material) and natural soil fluorescence interference as described in Section 3.4.2.4. These results are incorporated into the final report from the LIF operator.

Targeted follow-up soil sampling (when data suggest the need) may be useful. However, sample results may not always correlate well with LIF results. Multiple lines of evidence are necessary, including lithology, other soil and groundwater

samples, visual observations, and field testing. To achieve this goal, the LIF operator may place recovered materials onto the LIF system, either on-site or by sending samples to the vendor postinvestigation.

After completing the investigation, it is critical that an individual with LIF data interpretation experience (for example, technology developer) assists in reviewing the LIF data in a sitewide context. The LIF waveforms contain a wealth of information that can provide insights into fuel types, weathering, false positives, and unknown NAPL existence and can be the key to differentiating NAPL from mineral fluorescence. If no individual on the project team has the experience necessary, the LIF vendor should be contacted for assistance.

3.4.5 Tool and Data Misuse

Like results from similar investigation methods, LIF results should not be interpreted without understanding the CSM and, if available, other lines of evidence. Because of the potential for interferences and sequestered NAPL (in fine-grained materials), results must be maintained in the context of available information and investigation requirements. For example, monotonic behavior between fluorescence intensity and NAPL pore saturation may be assumed but is not guaranteed. In addition, applying an inappropriate fluorescence method may result in lack of NAPL detection.

Possible misinterpretations of LIF data may result during data transformation or interpolation. Statistical methods may incorrectly represent datasets if the data condition is not well understood or the wrong method is used. The following common mistakes are made during LIF implementation and data interpretation:

- failure to have the LIF vendor perform testing on NAPL samples (if available) to ascertain that the site NAPL has an appropriately bright fluorescence response and to select the most suitable LIF technology (most intense and unique waveform possible)
- failure to identify and remove false positives by comparing other lines of evidence to waveforms, clustering diagrams, and log fill color
- failure to recognize and consider that different NAPL have inherently different fluorescence intensities (for example, applying diesel intensity values to gasoline LIF causes an underestimation of gasoline NAPL impacts)
- applying too high of a %RE threshold to gasoline sites (using 5, 10, or 20% RE as indicative of NAPL) (Note: Even the smallest response indicates gasoline NAPL as long as the waveform (blue-shifted with long lifetimes) supports it.
- failure to recognize that gasoline weathers rapidly and its fluorescence covers a wide spectrum of signatures, eventually fading to an orange fill and waveform that is easily confused with limestone fill and calcites
- failure to understand that the limits of detection must be based on benchtop or in situ multiple lines of evidence
- failure to apply LIF well below the groundwater surface, which results in overlooking substantial trapped NAPL below the water table
- failure to budget for limited targeted validation sampling, leaving all stakeholders in doubt as to how to properly interpret data
- Choosing the single highest LIF value rather than averaging the RE over some minimum depth range
- failing to select a depth range (over which LIF data are averaged) that correctly represents subsurface conditions
- Failing to assess the applicability of the different LIF techniques for each site, even if the responses among them may be related
- failure to appreciate that extremely short-lived and red-shifted responses (UVOST®) can indicate the existence of unreported dramatically high PAH-content NAPL like creosote or coal tar
- waiting too long after the project to review and interpret data (before memories fade)
- Failure to understand that additional LIF logs and other data are required to understand how a LIF log represents the general surroundings.

3.4.6 Case Studies

The following case studies demonstrate potential applications of LIF systems:

- LIF Survey with UOVOST® Provides More Accurate Representation of LNAPL Plume at a Former Bulk Petroleum Storage Facility in New Hampshire
- UVOST Differentiates LNAPL Types to Allocate Financial Liabilities at a Retail Petroleum Facility in Tennessee
- TarGOST Determines DNAPL Extent and HPT Confirms Site Lithology at a Former Creosote Facility in Louisiana

3.5 Cone Penetrometer Testing

CPT is used to characterize geologic (lithology) and hydrologic properties of the subsurface. It is generally applied to sites with unconsolidated lithology but may also be effective in soft rock. CPT is useful for characterizing sites with discrete horizons or discontinuous lenses. The detailed lithology provided by CPT may be used to identify zones of high or low permeability, further defining groundwater migration pathways and potential groundwater storage zones.

3.5.1 Tool Description

CPT is used to evaluate the stratigraphy, soil types, water table, and engineering parameters of the subsurface. Data are logged directly to a field computer and can be assessed in real-time by the on-site geotechnical engineer or scientist.

CPT uses the weight of the CPT truck to advance a 55° to 60° cone through the subsurface at a constant rate, usually 2 cm/sec. CPT probes vary in size, typically 10 cm^2 to 15 cm^2 (cone surface area). This technology is generally applied to depths up to 150 ft but has been used as deep as 300 ft. Penetration depth may be improved by using an expanded coupling behind the cone, which reduces friction on the rods by enlarging the borehole. CPT probes are designed for push-only applications and cannot be driven with a hydraulic hammer or other percussion methods, which may limit penetration depth in some settings. Greater penetration depths may be achieved by predrilling through intervals where CPT data are not needed or where subsurface conditions limit cone advancement.

A traditional CPT platform is a hydraulic ram mounted on a CPT truck; a string of 1-meter long threaded rod segments is used to push probes into the subsurface. The system includes the following components:

- an electrical penetrometer
- a hydraulic pushing system with rods
- cable or transmission device
- depth recorder
- piezoelectric element to measure pore pressure
- strain gauges to measure the tip resistance and sleeve friction
- data acquisition unit

Figure 3-22 illustrates a typical CPT platform and system. Note the inclinometer on the probe to measure deviation from vertical, which should not exceed 2° (Robertson and Cabal 2008).

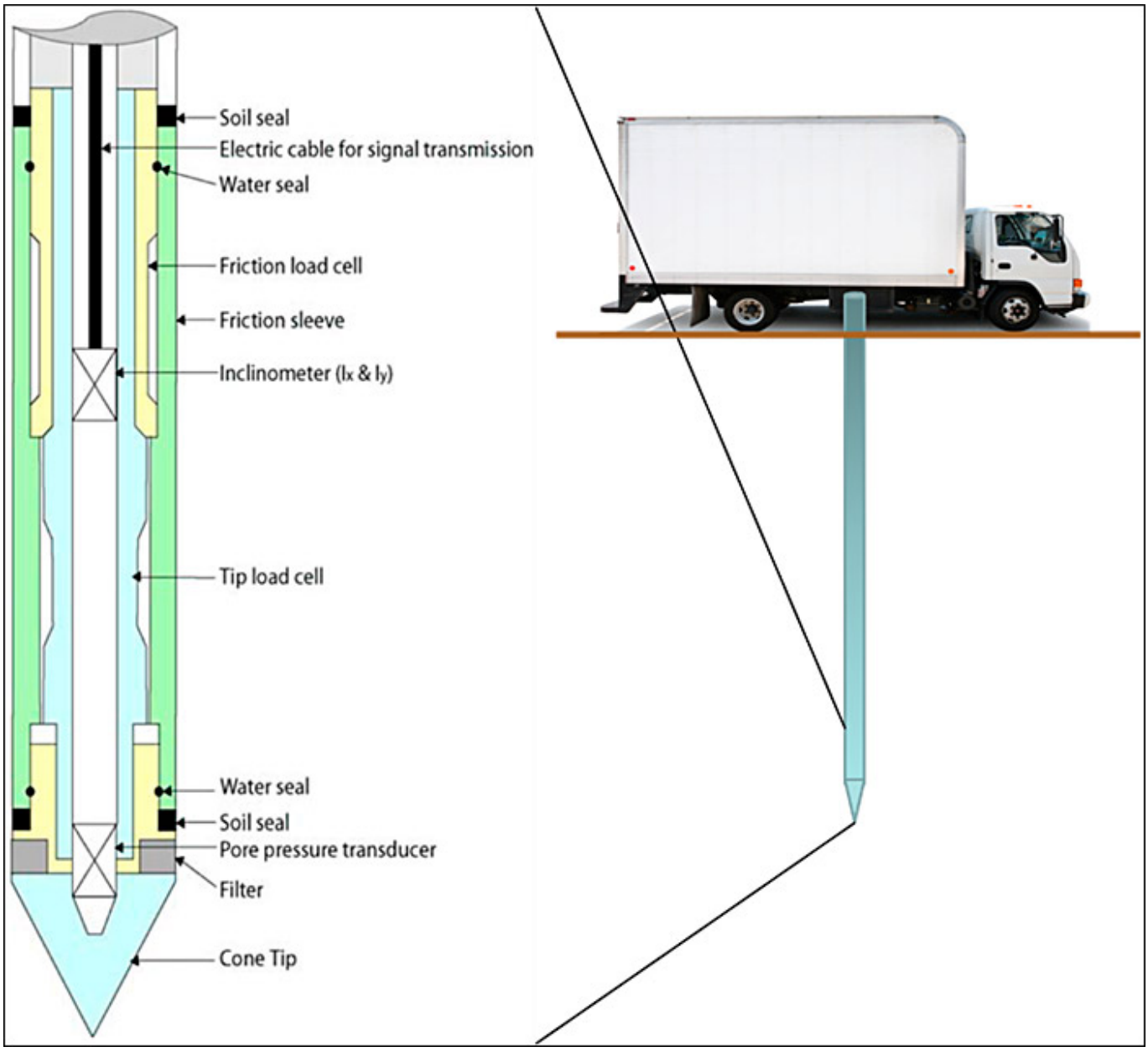

Figure 3-22. Typical CPT configuration.
Source: Gregg Drilling & Testing, Inc. Used with permission

CPT measures tip resistance (qc) and sleeve friction (fs), typically at 1- to 5-cm intervals. Tip resistance is theoretically related to the undrained shear strength of a saturated, cohesive material and measured with an embedded load cell. The sleeve friction is theoretically related to the friction of the horizon being penetrated and measured using tension load cells embedded in the sleeve (USDA 2009). Generally, clay soils have high sleeve friction and sandy soils have high tip resistance; however, values are dependent on individual soils (ScienceDirect 2016).

Tip resistance and sleeve friction are often plotted as the friction ratio (Rf) to aid in interpreting soil type (for example, sand, silt, clay; see Figure 3-23) based on various soil classification schemes (Robertson 1986); (Robertson 1990). CPT probes may also be equipped with a pore-pressure sensor[1] (Lunne, Robertson, and Powell 1997) to improve soil classification data. Dissipation tests conducted with a piezocone penetrometer (CPTμ) also assist in estimating approximate hydraulic head and soil permeability or hydraulic conductivity at the point of measurement (Robertson et al. 2011). A typical CPT log is shown on Figure 3-24.

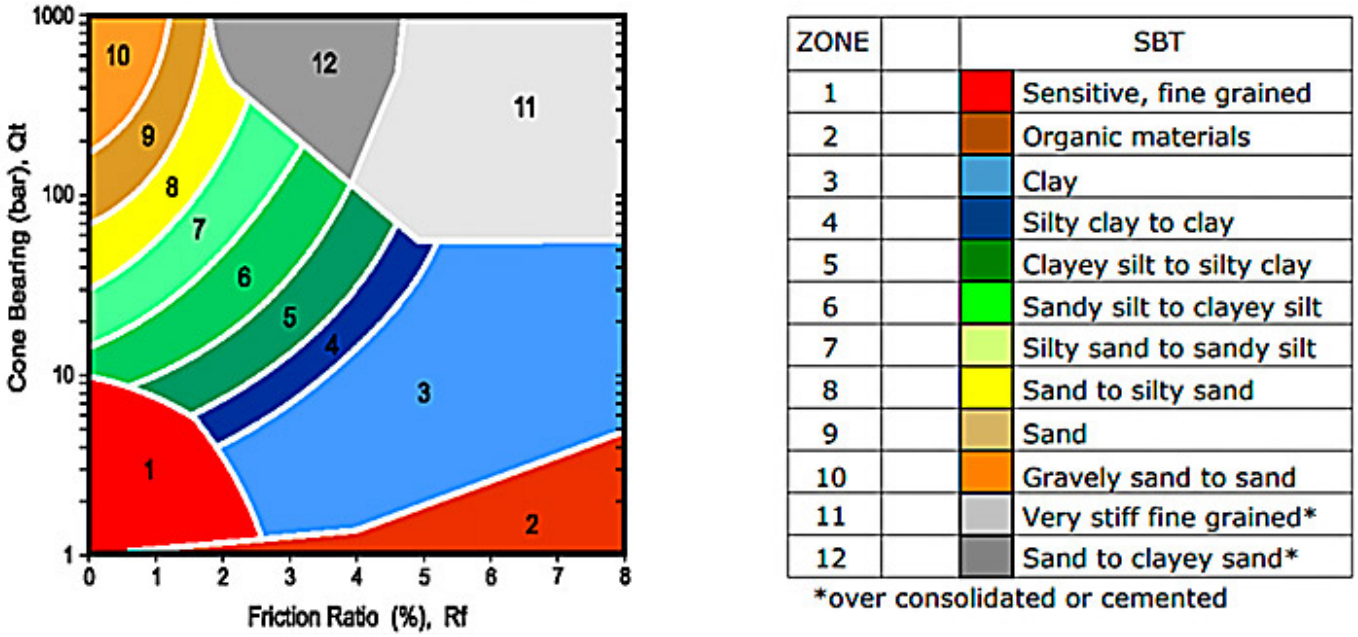

ZONE		SBT
1		Sensitive, fine grained
2		Organic materials
3		Clay
4		Silty clay to clay
5		Clayey silt to silty clay
6		Sandy silt to clayey silt
7		Silty sand to sandy silt
8		Sand to silty sand
9		Sand
10		Gravely sand to sand
11		Very stiff fine grained*
12		Sand to clayey sand*

*over consolidated or cemented

Figure 3-23. Soil behavior types.

Source: Gregg Drilling & Testing, Inc. Used with permission

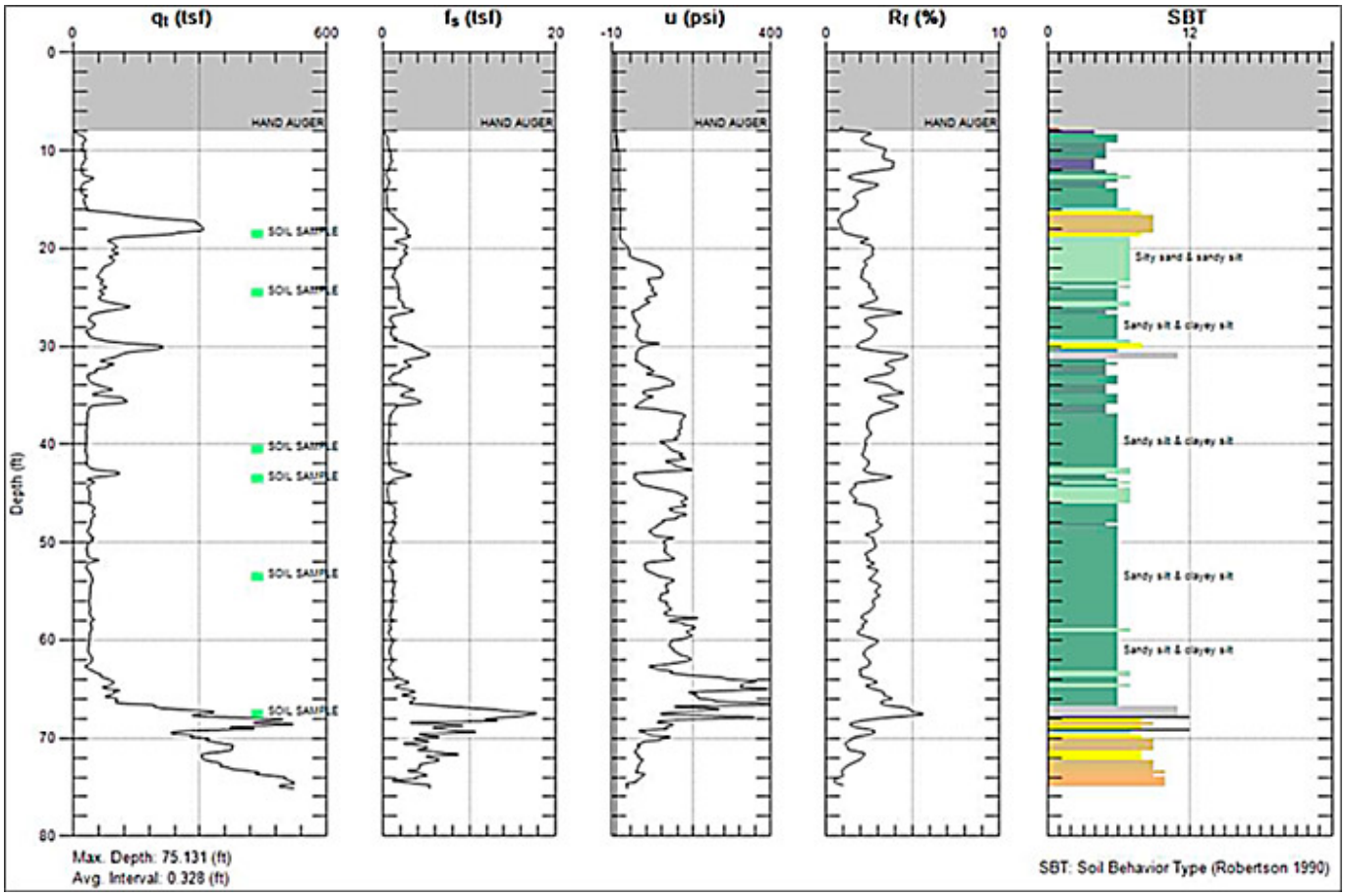

Total cone tip resistance (qt), sleeve friction (fs), friction ratio (Rf), pore pressure (u, pounds per square inch), Soil Behavior Type (SBT)

Figure 3-24. Typical CPT log

Source: Gregg Drilling & Testing, Inc., Used with permission

3.5.2 Technical Limitations

Similar to other direct-push technology methods, CPT use is limited to sites with unconsolidated lithology and possibly in soft rock. After the CPT drill rods are removed, an open borehole may remain. This borehole should be sealed as soon as practicable to reduce the likelihood of cross contamination. To avoid this situation and minimize borehole cross contamination, retraction grouting may be performed as drill rods are removed.

When using CPT, soil behavior types may present an ambiguous representation when soil properties are nonstandard (for example, very dense/stiff soil), and omit grain-size information. These soils may have both elevated tip resistance and sleeve friction values and are not always handled accurately by the algorithm that calculates the soil behavior type. Experience suggests that dense fine-grained sand, for example, may be identified this way.

3.5.3 Quality Assurance and Quality Control (QA/QC)

CPT soundings should be performed in accordance with (ASTM 2012a). CPT sensing devices should be properly calibrated using reference standards or by identifying readings considered reasonable by an experienced technician. Baseline readings should be measured before and after each sounding to assess measurement stability and consistency. Additional details are provided in the sections below.

3.5.3.1 Quality Assurance Prior to Use

Site conditions and objectives should be evaluated to determine the applicability of the CPT on site. Prior to use, the lithology to be penetrated, potential interferences, and potential refusal depth must be evaluated to the extent practicable.

3.5.3.2 Quality Control During Use

Progress should be carefully observed, and the screens should be viewed while advancing CPT tooling. The advancement (push) rate must be monitored for deviations to account for associated response variations; the rate should not exceed method specifications. Slower advancement rates produce higher data densities, with minimal risk to data quality, but reduce daily production.

3.5.3.3 Quality Control After Use

Targeted follow-up sampling (when data suggest the need) and comparison to existing logs, if available, may be used to validate CPT output. The results of dissipation tests and pore-pressure readings may require assistance from the CPT vendor for interpretation.

3.5.4 Tool and Data Misuse

CPT results should not be interpreted without understanding the CSM and, if available, other lines of evidence. CPT does not provide grain-size information, and soils that do not conform to the expected behavior types may be misinterpreted.

3.5.5 Supporting and Enhancing Instruments and Technologies

The following tools, also described in this section, may be paired with CPT to provide additional types of data:

- MIP (see Section 3.2 for a detailed description)
- OIP (see Section 3.3 for detailed description)
- LIF (see Section 3.4 for a detailed description)
- HPT (see Section 3.6.1.1 for a detailed description)
- EC arrays (see Section 7 for a detailed description)

Other sensors and tools that can be combined with CPT include the following (Cabal and Robertson, 2008):

- temperature – to identify frozen soil or contaminants that generate heat
- resistivity – to evaluate lithology and chemistry
- pH – to identify contaminants
- redox potential – to assess subsurface conditions undergoing bioremediation
- radioisotopes – to measure density and moisture content or to detect radioactive contaminants

3.5.6 Case Studies

The following case study demonstrates how CPT can be applied at sites:

- 9.7 CPT Borings and Hydropunch Sampler Optimize Site Characterization at an Aviation Industrial Complex in California

---

[1] A CPT cone equipped with a pore pressure sensor is refered to as a piezocone and CPT test using a piezocone is often abbreviated as CPTμ).

3.6 Hydraulic and Groundwater Profiling Tools

Hydraulic and groundwater profiling tools are a group of injection flow logging tools with the primary purpose to measure relative permeability or actual hydraulic conductivity. The advantage of hydraulic and groundwater profiling tools is that they are capable of collecting a high density of quantitative groundwater data. They can be used independently or in combination with other screening and sampling tools on a single tool string. Some versions of these tools also perform discrete interval groundwater sampling. These tools are used in conjunction with a direct-push platform and include the following:

- HPT – an injection-flow logging tool that measures pressure, flow, hydraulic conductivity, and soil and groundwater EC and can be used alone or integrated with MIP, OIP, and LIF
- Waterloo APS – an integrated injection-flow logging and discreet interval groundwater sampling tool that measures pressure, flow, and hydraulic conductivity
- HPT-GWS – an integrated injection-flow logging and discreet interval groundwater sampling tool that measures pressure, flow, hydraulic conductivity, EC, and groundwater-specific EC and operates similar to the Waterloo APS
- HPT-GWP – a smaller version of the HPT-GWS tool that measures injection pressure and flow and collects discrete groundwater samples but does not include the EC or downhole pressure sensor

These multipurpose tools generate real-time logs of formation permeability while advanced through the subsurface. The tools operate in unconsolidated formations, generally to depths of 100 ft below ground surface. The value of these tools is the dataset generated, which allows contaminant mass relative to formation permeability to be understood and groundwater storage zones and flow zones to be identified.

The primary benefits of hydraulic and groundwater profiling tools are that they:

- Optimize site assessment and remedial efforts by providing a high-resolution, real-time depiction of formation permeability, including potential contaminant flow pathways and potential confining layers, which can be used to optimize well and well screen placement.
- Identify the water table, infer lithology, identify confined or semiconfined aquifers, and estimate hydraulic conductivity in the saturated zone.
- Integrate with MIP, OIP, or LIF, understand the depth and distribution of contaminant mass relative to formation permeability, and infer relative mass flux.
- Collect discrete groundwater samples from a short-screen interval (2 inches to 6 inches), based on the evaluation of the formation permeability to generate quantitative groundwater analytical data.
- Rapidly characterize site contaminant impacts and hydrogeologic conditions without installing permanent monitoring wells.

3.6.1 How the Tools Work

Hydraulic and groundwater profiling tools are typically operated by trained professionals employed by a drilling company or other specialty vendor. No specific training is required for an environmental professional to use these tools, but it is recommended that a scientist familiar with site geology oversee tool operation to direct the contractor where to terminate borings and collect samples (if applicable) and assist the operator with the interpretation.

Injection-flow logging tools measure the pressure required by a water pump to inject a flow of clean water (generally dclean tap water) into the soil, through small screen port(s) on the side of the tool, as the probe is advanced into the subsurface. The tool produces a graphical log of injection pressure and flow with depth, which can be used to infer formation permeability and to calculate semi-qualitative values of hydraulic conductivity with depth. Injection flow logging is useful for understanding the heterogeneity of formation permeability, which often varies over short vertical, and to a lesser extent, horizontal distances.

The sampling version of these tools (HPT-GWS, HPT-GWP, and Waterloo APS) combine injection-flow logging with discreet interval groundwater sampling. Because the groundwater samples collected are analyzed using traditional laboratory techniques, these tools are not limited to detecting a certain type of contaminant. Deionized injection water may be required for certain applications, such as metals analysis, for purging the sampling lines prior to sampling. Once groundwater samples are evaluated by a laboratory, the collective dataset includes formation permeability and quantitative groundwater

analytical data.

Together, hydraulic and groundwater profiling tools are capable of generating a powerful dataset that can be used to understand contaminant mass in relation to formation permeability.

3.6.1.1 HPT

The HPT is an injection-flow logging tool manufactured by Geoprobe Systems® that measures the pressure required to inject a flow of water into the soil as a probe is advanced into the subsurface. The downhole components of the tool consist of the following (see Figure 3-25):

- probe equipped with an injection screen port and EC array
- injection and hydrostatic pressure sensor
- trunk line consisting of electrical wires and a water-injection line
- connection tube and drive head with the pressure sensor, electrical wires, and water-injection line
- probe rods (1.75- or 1.5-inch-diameter rods are typically used, successive rods are added as the probe is advanced with depth)

Figure 3-25. Downhole probe components of the HPT (The pressure sensor is shown outside of the connection rod but is actually located inside the rod during use).

Source: Geoprobe Systems®, Used with permission

The aboveground components of the tool look similar to the instruments shown in Figure 3-6 and consist of:

- data acquisition instrument – measures EC and acquires data from other instruments (such as MIP) if the HPT is being used in conjunction with another tool
- computer – receives data from acquisition instrument, displays logs and saves all data and operating parameters
- controller – regulates the flow of injected water and measures injection pressure to the HPT trunk line and probe

The injection-pressure log produced by the HPT is an indicator of relative formation permeability; higher injection pressures correspond to lower formation permeability (silts and clays) and lower injection pressures correspond to higher formation permeability (sands and gravels). The HPT operates by continuously injecting water as the tool advances, which creates a real-time log of average HPT pressure and flow at depth.

Following completion of the boring, HPT pressure data is corrected at each depth interval using a graph of absolute hydrostatic pressure, which is calculated from a dissipation test. The corrected HPT pressure graph can be used along with the HPT injection flow rate to calculate and plot estimated hydraulic conductivity (McCall 2010). Additional information about calculating estimated hydraulic conductivity is provided in (McCall 2010). The correction equation is:

Corrected HPT Pressure = Average HPT Pressure – Absolute Hydrostatic Pressure

To conduct a dissipation test, the operators identifies a depth below the water table to temporarily pause tool advancement and pause injection of water. At the selected depth, the operator turns off the water pump which allows the pressure of the

ambient formation to dissipate until it reaches the hydrostatic head at the depth of the tool. Typically, the pressure-dissipation tests should be completed in relatively high-permeability zones to allow full dissipation of ambient formation pressure over a relatively short duration of time.

Figure 3-26 provides an example HPT log showing:

1. average HPT pressure in pounds/ square inch (psi) (red line in second column in Figure 3-26)
2. corrected HPT pressure in psi (purple dashed line in first column in Figure 3-26)
3. average flow in mL/minute (green dashed line in fourth column in Figure 3-26)
4. estimated hydraulic conductivity in ft/day (blue line in fourth column in Figure 3-26)

As shown on Figure 3-26, injection-flow logging from the HPT can be combined with EC (black line in first column) as well as screening tools such as the MIP. The two tools are integrated and advanced into the subsurface together, creating an output log showing both formation permeability data from the HPT and screening data from the MIP (MiHPT log). Figure 3-26 also shows MIP data as the orange and blue lines in the third column.

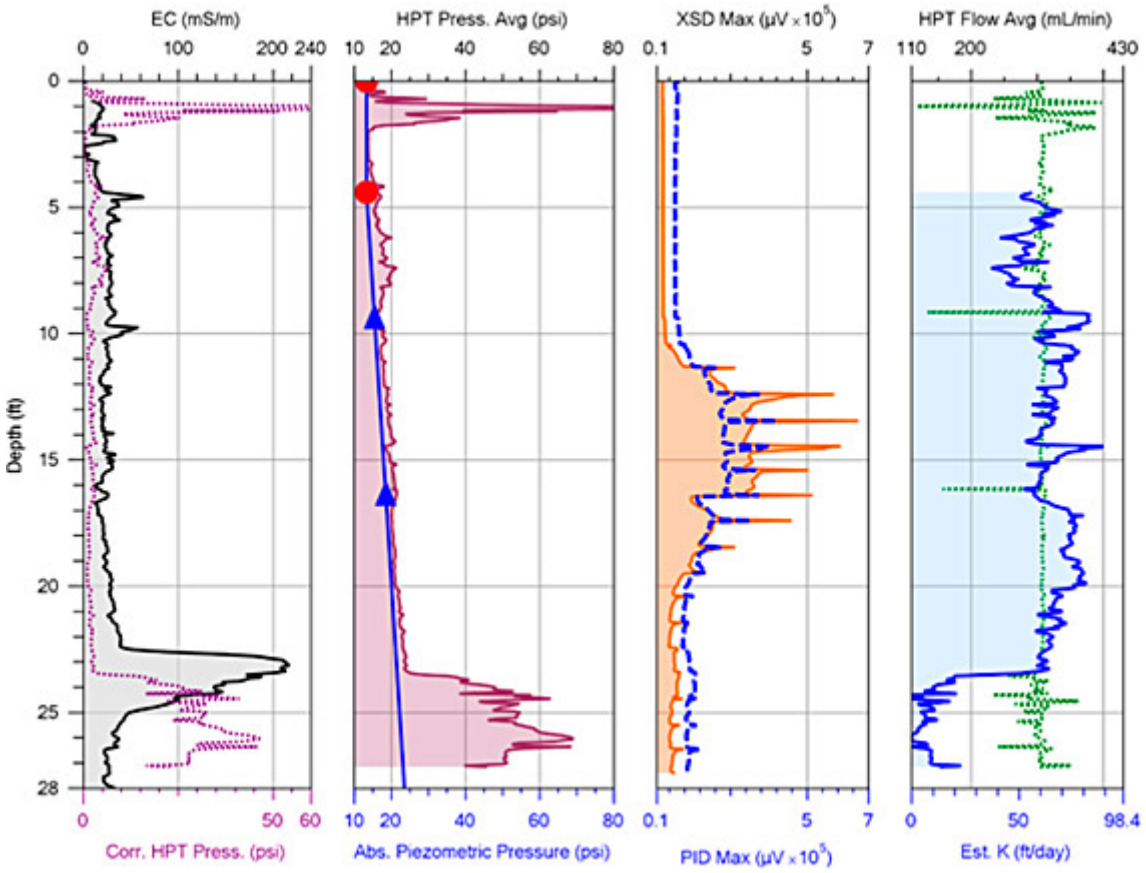

Figure 3-26. Example MiHPT log.

Source: Geoprobe Systems®, Used with permission

3.6.1.2 Waterloo Advanced Profiling System

The Waterloo APS is an integrated injection-flow logging and discreet interval groundwater sampling tool that is driven into unconsolidated soils using direct-push rods. It is a proprietary tool currently operated by Cascade Technical Services. The tool was developed and tested extensively at the University of Waterloo and was introduced to investigation and remediation professionals in 1994.

The downhole components of the Waterloo APS (see Figure 3-27) are:

- profiler tip consisting of a drive point with stainless-steel screened ports
- conventional direct-push rods
- up to three stainless-steel lines running through the drilling rods and connecting the profile head to the ground surface:

- KPRO line – injects water at a constant rate (typically 300 mL/min) into the subsurface
- sample line – conveys groundwater up through the drill rods to the surface via peristaltic or gas drive pump
- gas line – conveys nitrogen to operate the downhole pump

- nitrogen gas positive displacement pump for when the water table is below the suction limit of a peristaltic pump

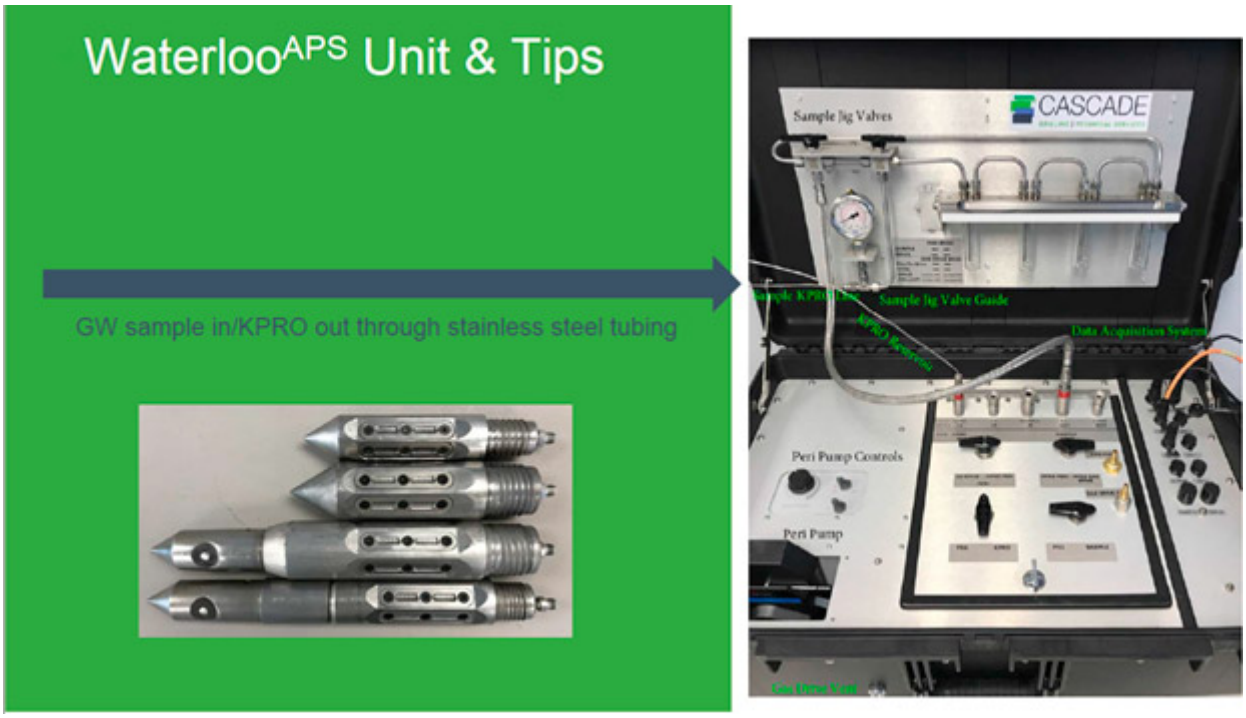

Figure 3-27. Waterloo APS tool tip options and instrument.
Source: Cascade Environmental, Used with permission

The aboveground components of the tool are:

- peristaltic pump
- multiparameter water-quality meter used to measure pH, temperature, oxidation-reduction potential (ORP), electrical conductivity, and turbidity of purged groundwater
- sensor and laptop computer equipped with software to measure and log the index of hydraulic conductivity, which is the pressure required to inject a flow of water into the subsurface

The injection-flow logging component of the tool operates similar to the HPT except that the tool logs relative formation permeability in real-time; dissipation tests are not completed, and the index of conductivity data is not corrected. Typically, the index of conductivity data is evaluated in real-time by the operator and are used to infer hydrogeologic conditions to determine sample depth. In relatively high-permeability formations such as sands and gravels, less pressure is required to inject into the subsurface; in relatively low-permeability formations such as silts and clays, more pressure is required to inject into the subsurface. The operator or consultant reviews the real-time log of relative formation permeability and directs the driller to stop advancing once the profile tip is at the target depth or within the target unit.

To collect a groundwater sample, drilling temporarily stops and groundwater is purged to the surface via a peristaltic or gas-drive pump and is monitored for geochemical parameters to determine stability (see Figure 3-28). Once stabilization is achieved, samples are collected for laboratory analysis and the profiler tip is advanced to the next targeted sample depth. The Waterloo APS is commonly fitted with a stainless-steel sample holder used to collect zero-headspace groundwater samples in 40 mL VOA vials, but the tool can be used to collect any type of groundwater sample.

Figure 3-28. Waterloo APS operator purging groundwater from the sample interval, recording water-quality parameters, and preparing for sample collection.
Source: Cascade Environmental, Used with permission

The Waterloo APS profiler tip is available in three sizes (2.25 inch, 1.75 inch, and 1.50 inch) and is attached directly to the direct-push rods used on the direct-push drilling platform. The larger diameter tip is used on a larger drill rig for maximal depth penetration and higher sampling rates; the smaller tip is used with smaller drill rigs to access tighter spaces where larger drill rigs cannot operate.

3.6.1.3 Hydraulic Profiling Tool – Groundwater Sampler (HPT-GWS)

The HPT-GWS combines the injection-flow logging of the HPT with discreet interval groundwater sampling and operates in a similar manner as the Waterloo APS. The HPT-GWS is designed for use on a 2.25-inch-diameter casing for advancement into the subsurface using direct-push methods (see Figure 3-29). The tool components are generally the same as the HPT described in Section 3.6.1.1, with the addition of a ¼-inch-outer-diameter sample line. The probe tip is equipped with 20 screened ports, each about ½-inch in diameter, installed in four rows around the probe circumference. The ports are distributed over a 4-inch vertical segment of the probe, providing for a discrete sample interval. Ten of the 20 screened ports are visible in Figure 3-29.

As with the HPT, a pressure transducer located just above the injection ports measures the pressure required to inject the water into the formation. This pressure is logged by uphole instrumentation. An EC array is positioned at the end of the probe to provide a log of bulk formation EC, and the EC and injection pressure are logged every 0.05 ft (about15 mm) of log depth. The log data guide selection of permeable zones for sampling; once the HPT-GWS has reached a desired sampling depth, advancement of the tool pauses temporarily, and the operator may conduct a dissipation test prior to sampling. To sample, groundwater is purged through the sample line using either a peristaltic or a bladder pump, depending on aquifer conditions. Following sample collection, the operator resumes HPT logging and the tool is advanced to the next sample depth.

Figure 3-29. The HPT-GWS probe.

Source: Geoprobe Systems®, Used with permission

The Waterloo APS and the HPT-GWS are both operated by a trained operator, who is typically a geologist that works for the drilling company. As such, no specific training is required for an environmental professional to use the tool, but it is recommended that a scientist familiar with the site geology oversee the tool operation to direct the operator where to sample.

3.6.1.4 Hydraulic Profiling Tool – Groundwater Profiler (HPT-GWP)

The HPT-GWP is a smaller diameter (1.75 inch) version of the HPT-GWS, which lacks the EC dipole and downhole pressure transducer. It measures injection flow and pressure (surface pump pressure) and has the 20-screen port arrangement for collecting groundwater samples at discrete intervals. Compared to the HPT-GWS, it is a simpler and more robust design because it only has two water lines. The HPT-GWP is used to collect multiple discrete groundwater samples from predetermined intervals.

3.6.2 Technical Limitations

The technical limitations associated with hydraulic and groundwater profiling tools are associated with applicability and accessibility such as formation permeability, tip clogging, and freezing conditions. These limitations are described in the subsections below.

3.6.2.1 Formation Permeability

The HPT system is able to resolve soil permeability within a hydraulic conductivity range of about 0.1 ft/day (3.5×10^{-5}

cm/sec) to 75 ft/day (2.7 x 10^{-2} cm/sec), approximately three orders of magnitude in range. The lower end of the range varies depending on flow rate, effective pressure, and the specific nature (density, grain size, moisture content) of the soil or sediment being penetrated. At the upper end of the range, formation permeability becomes sufficiently high to reduce the pressure required to inject fluid into the formation to relatively low. Under high hydraulic conductivity conditions, the injection pressure may be equal to or less than the pressure resulting from the internal friction due to fluid flow in the HPT probe. Under these conditions, the hydraulic conductivity of the formation is effectively above the upper limit of what the HPT can discern. Simply increasing flow rate to the probe does not alleviate this problem; it also increases the internal friction and pressure. In aquifer zones where the estimated hydraulic conductivity is near the upper limit, temporary piezometers (Geoprobe 2006); (Geoprobe 2010); (ASTM 2012b) can be installed across these intervals and slug tests (Geoprobe 2014); (ASTM 2013) can be performed to more precisely define higher hydraulic conductivity zones.

The HPT probe is currently designed with a 100 psi (about700 kilopascal) pressure transducer (equivalent to about 230 psi of water pressure). The effective upper operating limit is about 80 psi (550 kilopascal) or about 180 ft (about 55 m below the water table in an unconfined aquifer.

The Waterloo APS has a similar upper limit for differentiating relative formation permeability within high-permeability zones. Due to this upper limit, the index of conductivity log may not be able to differentiate between the most permeable zones, such as a coarse sand and gravel.

For all hydraulic and groundwater profiling tools, sample collection is limited by formation permeability because groundwater samples cannot be collected unless there is sufficient groundwater flow within the formation. Unlike a monitoring well, which can sometimes be sampled under low-recharge conditions (for example, purging the well dry and returning later to collect a sample), a groundwater sample cannot be collected unless there is sufficient flow. That said, if a particular depth interval does not produce sufficient flow for sample collection, it can be inferred that mass flux within that zone would be relatively low. Then, the tool can be advanced deeper to collect samples from subsequent depth intervals.

3.6.2.2 Tip Clogging

In silty geologic conditions, the HPT screen ports may clog, preventing sample collection. To unclog, the tool typically has to be removed from the hole to remove the clog from the tip. Additionally, the tip may clog when advancing through a viscous DNAPL.

3.6.2.3 Freezing Conditions

Groundwater profiling tools can be challenging to operate in subfreezing conditions because the injection-flow-logging component of the tool relies on a steady flow of water from the surface to the subsurface, and the profiling component of the tool requires groundwater to be pumped back up to the surface. In subfreezing conditions, tubing may freeze and prevent water flow in either direction. Heated tents can be used when profiling in subfreezing conditions, but additional health and safety precautions must be taken and productivity will likely be slower.

3.6.3 Quality Assurance/Quality Control

QA/QC standards must be established and followed to ensure reliable data. In addition to comprehensive operator training (which may be verified prior to commencing work) and an operator track record of successful use, approved field procedures must be understood and followed before, during, and after profiling activities. The manufacturer's SOP must be reviewed prior to initiating field work.

3.6.3.1 Quality Assurance Prior to Use

Prior to beginning investigation activities, the operator should calibrate and test hydraulic and groundwater profiling tools. Depending on the tool, testing may be conducted daily during a field program or at the beginning of each boring. The project team should ask the operator about the QC procedures specific to the tool and request that testing and calibration results be communicated to the field team and included within the final data report.

3.6.3.2 Quality Control During Use

Once data collection has begun, the operator must monitor the equipment throughout the data collection process. For most hydraulic and groundwater profiling tools, the operator monitors the rate of advancement, depth, EC, and injection pressure to ensure equipment responses are within normal ranges. Maintaining a constant rate of advancement (typically around 2 cm/sec) produces a representative log; a slower rate gives a more detailed log but affects the rate of production. A rate that

is too fast can miss smaller stratigraphic features. Daily productivity varies greatly depending on desired drilling depth and the number of times that drilling is stopped to either complete a dissipation test (if applicable) or collect a sample for laboratory analysis (if discreet interval samples are being collected). Generally, with the profiling tools, the factor that limits productivity is the number of samples collected per day for laboratory analysis.

Prior to beginning work, the depth of the local water table from a nearby well or temporary piezometer should be estimated as it is not always evident from the pressure injection log. Understanding the approximate depth of the water table helps the operator interpret the injection pressure log and generated contaminant screening data. If the tool is being used to collect discreet interval groundwater samples (Waterloo APS or HPT-GWS), the water table depth must be estimated to direct the depth at which sampling can begin.

For sampling tools, some trial and error may be necessary to determine the site-specific conditions under which groundwater samples can be efficiently collected. Sample flow may be directed through an in-line flow-through cell with a multiparameter water-quality meter and a sample interval is purged until stabilized criteria are met, which typically involves purging 400 mL to 1,000 mL. If deionized water is used for the injection fluid, a good contrast between the natural formation water and the deionized water is easily observed with the water-quality meter. If a water-quality meter is not being used, three system volumes should be purged before collecting samples for laboratory analysis.

After sample collection, sample-specific tubing is changed. Following completion of a boring, the drill rod, stainless-steel tubing, and profiling probe or tip is decontaminated between each profiling point with clean water or by following project-specific decontamination procedures.

3.6.3.3 Quality Controls After Use

Depending on investigation objectives, co-located groundwater and soil samples may be collected following completion of a hydraulic and groundwater profiling investigation to make defensible statements regarding the accuracy and precision of the data collected. For example, if HPT or index of conductivity (I_K) logs are being used to inform remedy design, it may be important to advance targeted soil borings within the low permeability zones where contaminant mass is retained to correlate injection pressure log data to a specific soil type. In another scenario, soil analytical samples may be collected to determine contaminant mass within the low permeability layers where groundwater samples have not been collected.

The investigation may also be supplemented with a select number of permanent monitoring wells if multiple rounds of groundwater data from a monitoring well are required for risk characterization or site closure. In this case, the hydraulic and groundwater profiling investigation can significantly reduce the scale and cost of the monitoring well network by informing the well network design so that screens are placed within specific hydrogeologic units identified by the hydraulic and groundwater profiling investigation.

3.6.4 Data Interpretation and Presentation

Logs provided by the contractor are often grouped together to form cross sections. The vertical variations in formation permeability are correlated horizontally and shaded to help the reader visualize the geologic strata. Laboratory analytical data are added to the cross section.

Boring log data provided by the contractor can be requested in spreadsheet format and input into visualization and modeling programs such as Earth Volumentric Studio (EVS), ArcGIS, or LeapFrog so that cross sections or 3-D visualization models can be created using other software programs as needed.

As site characterization progresses, additional types of data can be added to the cross sections, including monitoring wells and associated groundwater analytical data and soil borings and associated soil analytical data.

3.6.5 Data Misuses

Samples collected from groundwater profiling tools are different from traditional monitoring well screen samples because they are collected from a much smaller discreet interval. Samples from a 5- or 10-ft-long submerged well screen can originate from multiple lithological zones within the screened interval. These zones may exhibit different contaminant concentrations. Therefore, monitoring well data may represent a weighted-average concentration within the screened interval, which is often less reliable when developing a CSM. Weighted-average concentrations within a screened interval should not be compared directly to discreet intervals sampled by profiling tools without considering the potential dilution factors within the screened interval of the monitoring well.

3.6.6 Supporting and Enhancing Instruments and Technologies

An EC array is standard equipment on most profiling tools. EC is discussed in detail in Section 3.7.

3.6.7 Case Studies

The following case study demonstrates how hydraulic and groundwater profiling tools can be applied at sites:

- CPT Borings and Hydropunch Sampler Optimize Site Characterization at Naval Air Station North Island in California
- Waterloo APS, CPT, and LIF Data Update CSM and Help Optimize Selected Remedy at a Former Refinery in Oklahoma

3.7 Electrical Conductivity (EC) Probe

EC is the ability of a particular material (for example, soil, sediment) to conduct an electrical current measured in milli-Siemens per meter (mS/m) using an EC probe. The EC probe is typically deployed by direct-push methods (static or percussion) to measure the apparent EC of the bulk formation (solids and fluids) located adjacent to the advancing probe. The term “apparent conductivity” is used because the probe measures the bulk or average conductivity of materials near it.

As the probe is advanced, it produces a continuous log of apparent conductivity versus depth. Measurements of EC can be used to infer the presence of more highly conductive subsurface materials such as clays; but because EC can be influenced by several factors, EC probes are typically used in conjunction with other tools such as the HPT to better determine the true nature of the subsurface materials being investigated (USEPA 2016b).

Finer-grained soils, such as silts or clays, tend to produce higher EC signals than coarser-grained sands and gravels. While specific values cannot be assigned to each soil type, each soil type typically provides a different response. Figure 3-30 shows the typical EC measurements for sand, silt, and clay.

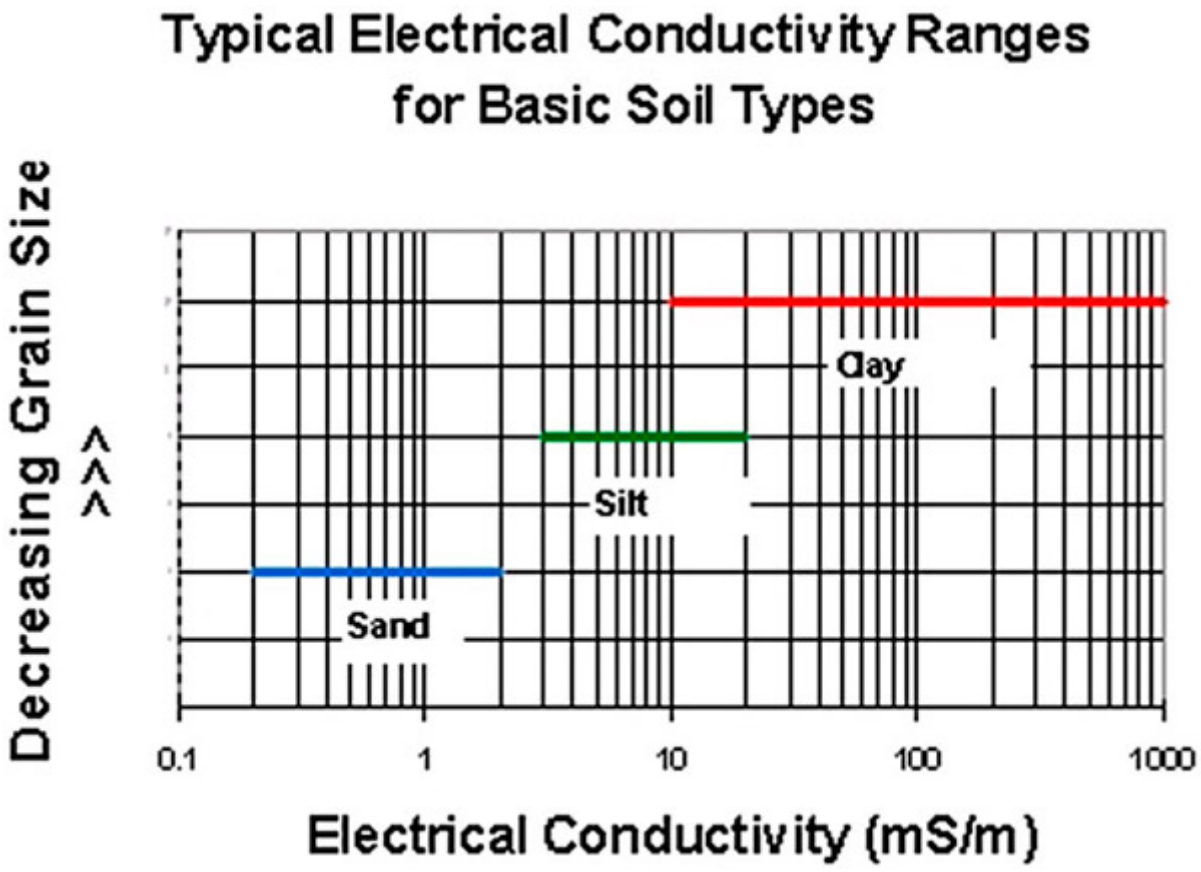

Figure 3-30. Typical EC measurements for sand, silt, and clay.
Source: Geoprobe 2015b, Used with permission

An EC probe is frequently used to map potential contaminant pathways. Zones of lower EC usually indicate coarser-grained, more permeable materials. These more permeable zones allow contaminants to migrate in the subsurface (path of least resistance). Finer-grained sediments (for example, clays) can trap and store contaminants. The EC gives the investigator real-time, on-screen logs for on-site decision making. Once multiple logs are generated, a cross-sectional view of a series of logs is helpful to visualize how these preferential pathways connect across a site (see Figure 3-31). Courser-grained sediments are located near 10 ft to 11 ft and 16 ft to 24 ft below ground surface and are also present near the bottom of the logs. More conductive finer-grained sediments are present elsewhere in the logs.

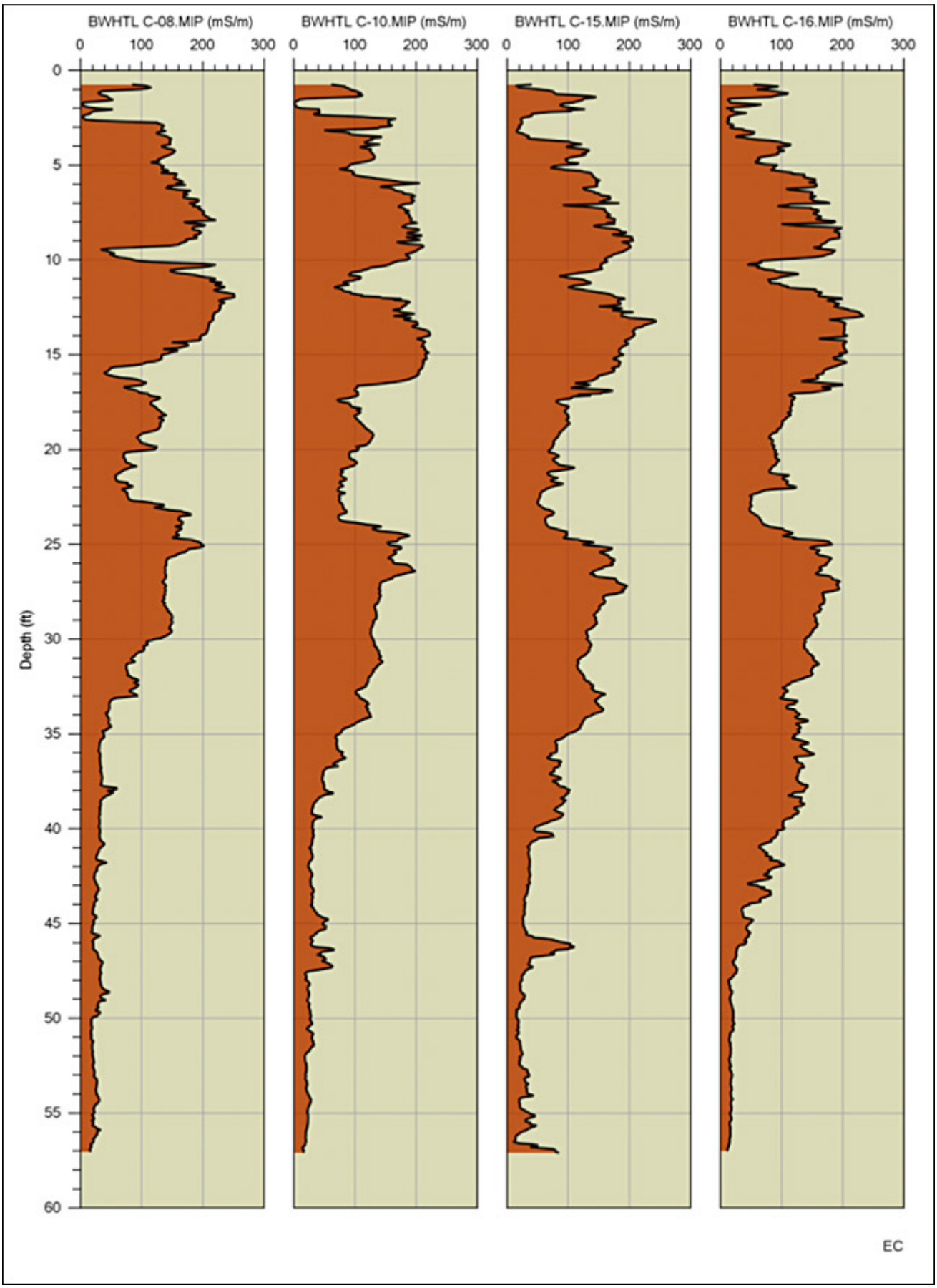

Figure 3-31. Example of EC logs along a cross section.

Source: Geoprobe Systems®, Used with permission

3.7.1 Tool Description

EC probes typically use either a four-pole Wenner array (see Figure 3-32) or a simple dipole array to measure apparent conductivity. Similar arrays are used during surface electrical resistivity surveys except that the probe electrodes in a downhole tool are fixed along the probe's surface. Consequently, the volume of material being measured is also fixed and does not extend far from the probe's surface. Of the two electrode configurations, the Wenner array measures a somewhat larger volume of the formation proportional to the length of the array. Using this configuration, more averaging is necessary to obtain the output signal in the log, so small-scale features, such as a 1-inch-thick clay lens in a sand body, may not be clearly distinguishable. Conversely, dipole arrays sample a smaller volume of the formation and therefore more easily distinguish the smaller-scale lithologic features. These probes measure bulk formation EC; thus, they provide a measure of the combined EC of the formation solids and any contained fluids and dissolved ions (Milsom and Eriksen 2011).

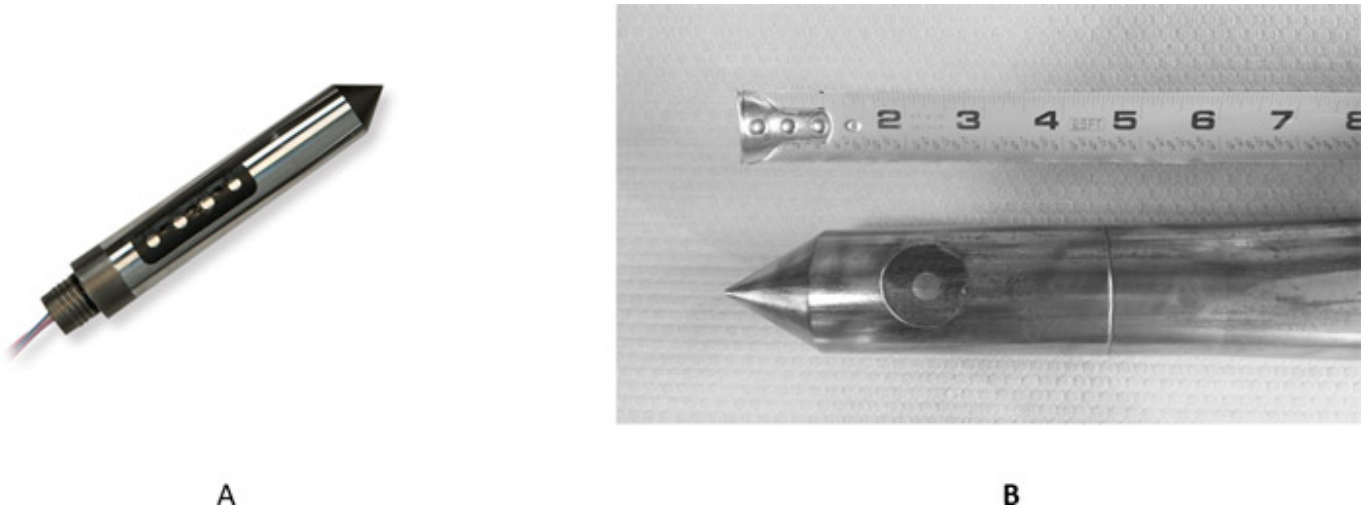

Figure 3-32. EC probe with four-pole Wenner array (left) and simple dipole EC array (right).

Source: Geoprobe Systems®, Used with permission

The EC tool consists of the probe, a trunk line to connect the probe to the field instrument (see Figure 3-33), a string pot to measure sensor depth, and a laptop to process and view the EC versus depth and probe advancement rate logs. The field instrument provides current to the probe and senses both downhole current and potential difference values. The probe is used in concert with a direct-push-type rig operated in either push or percussion mode.

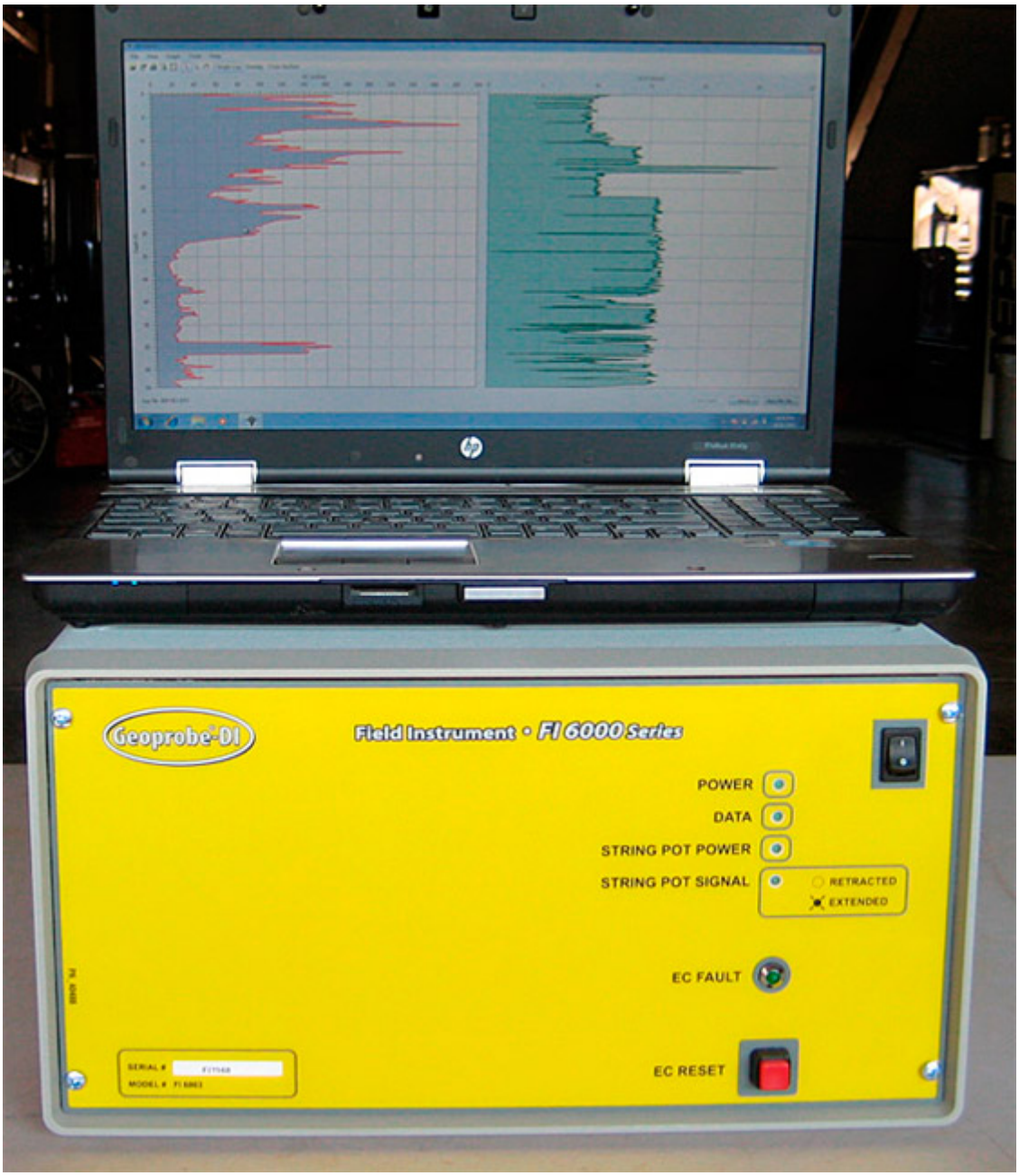

Figure 3-33. Geoprobe FI 6000 field instrument and laptop display.

Source: Geoprobe Systems®, Used with permission

EC probe operation is straight forward; using the Wenner configuration, the probe is positioned with two poles in the ground and the other half aboveground as the starting position for the log. Just prior to beginning the first subsurface push, a trigger is activated using the provided software, initiating logging for that particular boring. If needed, logging can be paused by using the software to switch the trigger off, which allows the user to disconnect the probe wires and add new rods as needed. As the probe is advanced into the ground, information from the field instrument is relayed to the field computer, which displays EC (in mS/m) and probe advancement rate (see Figure 3-33). Once downhole logging is complete, the trigger is set to "off" and the probe is extracted from the ground. A rubber sleeve at the ground surface removes soil residue from the probe as it is being extracted (Geoprobe 2015a). The log can then be used in concert with other information (for example, sediment logs, injection flow logging data) to map site hydrostratigraphy.

3.7.2 Technical Limitations

In fresh-water formations, elevated EC readings often indicate increased clay content, but not all clays exhibit high EC. The presence of elevated dissolved ions (such as sodium, calcium, chloride, or ionic remediation fluids like sodium persulfate) can further complicate EC log interpretation. High concentrations of dissolved ions can completely overwhelm and mask changes in EC due to lithologic variations. Because of these limitations, targeted soil and sometimes groundwater sampling

should be conducted to verify log interpretation (McCall, Christy, and Evald 2017). The EC probe can also be used in conjunction with HPT (see Section 3.6) as a means of addressing these limitations.

3.7.2.1 Detection Limits

EC logging resolution may depend upon several factors. The type of array configuration used (Wenner vs. dipole) may have some affect with respect to resolution, with the dipole configuration providing somewhat higher resolution (Geoprobe 1994); using the Wenner configuration, clay layers as thin as 2.5 cm have been identified. Clay type can also be a factor. Clays with high cation-exchange capacity such as smectite and montmorillonite are more conductive and therefore more easily resolvable than kaolinite clays. Probes measure conductivity every 1.5 cm as the probe is advanced (Schulmeister et al. 2003). The instrument measures the bulk conductivity of soils, sediments, pore fluids, or other materials located in the proximity of the probe, generally within 5 cm to 10 cm (Beck, Clark, and Puls 2000).

3.7.2.2 Interferences

The EC probe may be subject to certain interference that may hinder or prevent it from detecting stratigraphic changes. It is possible that highly mineralized or otherwise conductive pore waters may overwhelm the ability of the EC probe to detect discrete changes in lithology that may be of interest. For instance, a thin conductive clay layer surrounded by sands or gravels filled with saline pore water may not be resolvable. If work is being performed in a disturbed area, buried debris could affect readings if the debris were to come into direct contact with the probe array. Because the alternating current delivered to the probe's current electrodes is in the low hertz (Hz) range, the field instrument is designed to effectively filter out signal noise caused by underground electrical lines (60-Hz signals).

3.7.3 Data Collection Design

3.7.3.1 Identify Project Goals

Direct sensing survey design should always begin with a basic understanding of what is unknown and what the investigator hopes to learn by deploying a given technology. Once the goal of a survey is well understood, the investigator can begin to tailor use of the technology to the given need.

EC surveys are commonly used to help identify subsurface stratigraphic features that may be helping to control contaminant transport. If fine-grained deposits exist in the form of discontinuous lenses or as laterally continuous layers, then an EC survey combined with limited soil coring could be useful in helping to refine the CSM. The amount of heterogeneity present determines the density of survey boreholes required at a given site. In many cases, a gridded approach to survey design may be used, especially little is known about a particular site.

Alternatively, EC surveys can be used to better identify the location or width of a conductive groundwater plume. In this case, a courser-grained, relatively nonconductive sandy or gravelly sedimentary environment may be ideal because EC would be mainly a function of the ionic content of the pore water. Under such circumstances, laying out a series of borings in the form of a transect(s) downgradient plume source may be advantageous. Regardless of the survey goal, using other tools or methods as multiple lines of evidence is often advantageous to support survey conclusions.

3.7.3.2 Determine Verification Requirements

EC probe logs should not be taken at face value. Because EC can be affected by multiple factors, it is common to collect at least a single sediment core near an EC boring to confirm log interpretation and allow correlation with strata identified in the core. Ideally several core logs are available for a given site; other tools can be used in tandem with EC to assist with EC log interpretation.

3.7.4 Quality Control

Diagnostic tests should be run on the EC probe before and after each boring log. An EC load test confirms that the actual measured EC values are within 10% of the target values for three separate conductivity values. If the EC probe passes the load test, then the tool is ready for logging. If the EC probe fails the load test, then a separate set of tests must be run to troubleshoot the problem. If the EC probe is functioning as designed, then only pre- and post-load tests are required (Geoprobe 2015a).

3.7.5 Data Interpretation and Presentation

Interpretation and presentation of EC logging data is fairly straightforward. In many instances, elevated EC values indicate

the presence of finer-grained sedimentary layers (for example, silts or clays). Other tools can be used in conjunction with EC logging to identify situations where this relationship does not hold true. Figure 3-34 shows an EC log obtained from the Arkansas River alluvial aquifer. From the interpretation provided (verified by targeted sampling), increasing EC values in fresh water formations typically indicate increasing clay content. Yet this is not always true, as clay mineralogy and the presence of brines can affect EC log response. Here the water table is visible where clean sand goes from dry to saturated at about 9 ft below ground surface. In finer-grained materials, the water level is typically not discernable. When combined with the HPT, the HPT pressure correlates with the EC response unless ionic interferences are present (see Figure 3-34). Various data presentation options are available, with the most common being to display individual EC logs side by side.

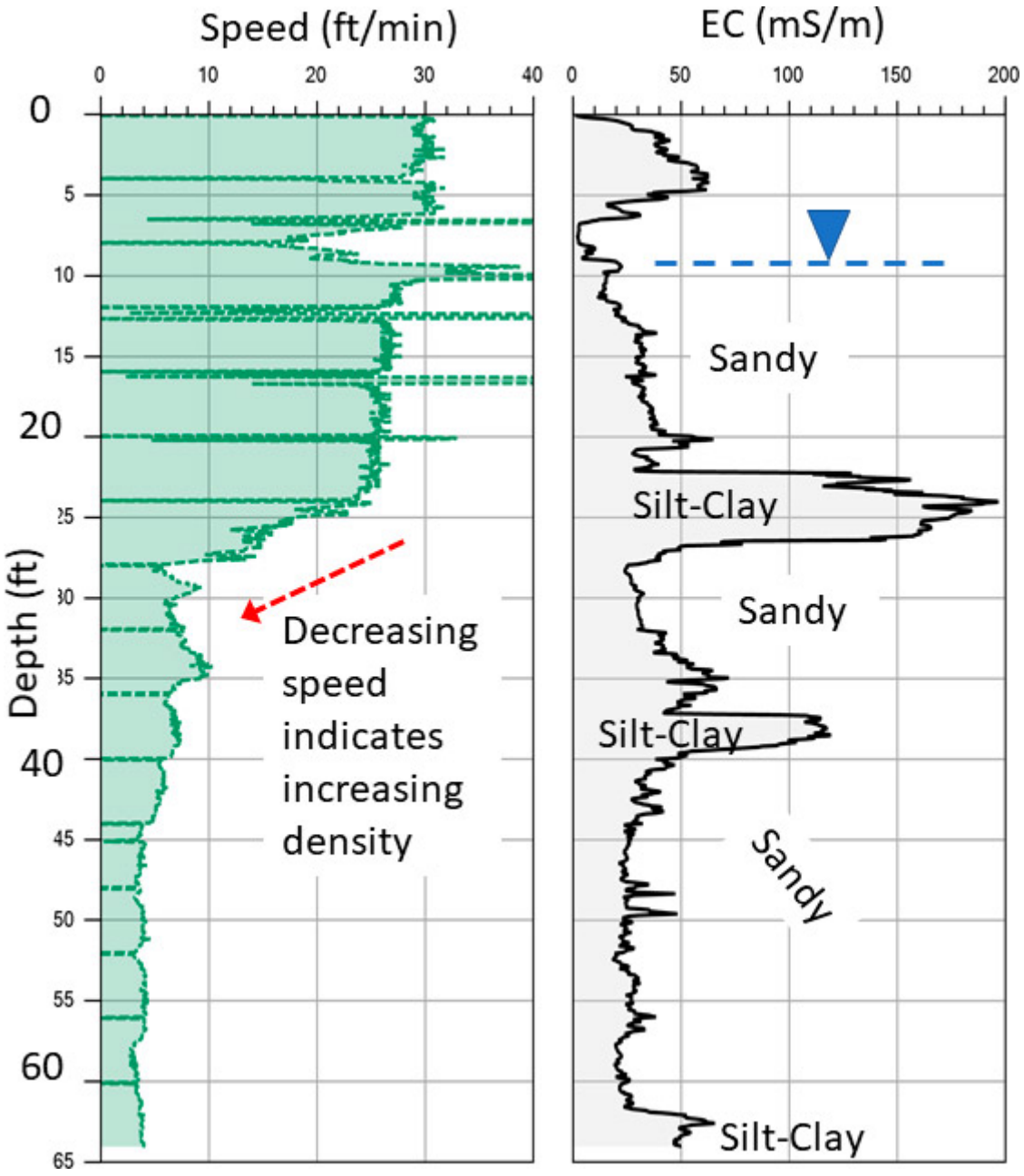

Figure 3-34. EC log (right) with associated probe advancement rate log (left).

Source: Geoprobe Systems®, Used with permission

EC field logs are initially displayed on a laptop computer as conductivity versus depth. A separate log indicating probe advancement rate is also displayed, primarily for field use and may or may not be included in a final report. The EC probe should be advanced at a rate of approximately 2 cm/sec through the logging process to ensure adequate contact between the probe and sediment and consistent results between adjacent boreholes. Because the probe is commonly used in tandem with other sensors that are more sensitive to advancement rate, advancement rates for each log should be confirmed to be close to the 2 cm/sec value.

If the ionic content of pore waters is believed to be fairly consistent at a given site, then EC should be primarily a function of grain size and clay content, with higher EC values being associated with smaller grain size and more conductive clays. Silts and clays are less permeable than coarser-grained sediments, which is why it is often advantageous to plot EC logs alongside hydraulic profiling logs obtained from the same borehole. When using this approach, a low-permeability clay should exhibit a similar signature on both the EC and hydraulic profiling logs. An inverse relationship (for example, high EC and low pressure) may indicate that higher EC values reflect coarser-grained materials containing conductive pore water. Figure 3-35 provides an example EC log that shows mostly sands and gravels present above approximately 23 ft and a clay till layer below this depth based on the abrupt rise on the HPT log below 23 ft. Note that the EC log peaks above the clay till layer. This effect is produced by the presence of sodium persulfate in the more permeable material located above the clay till.

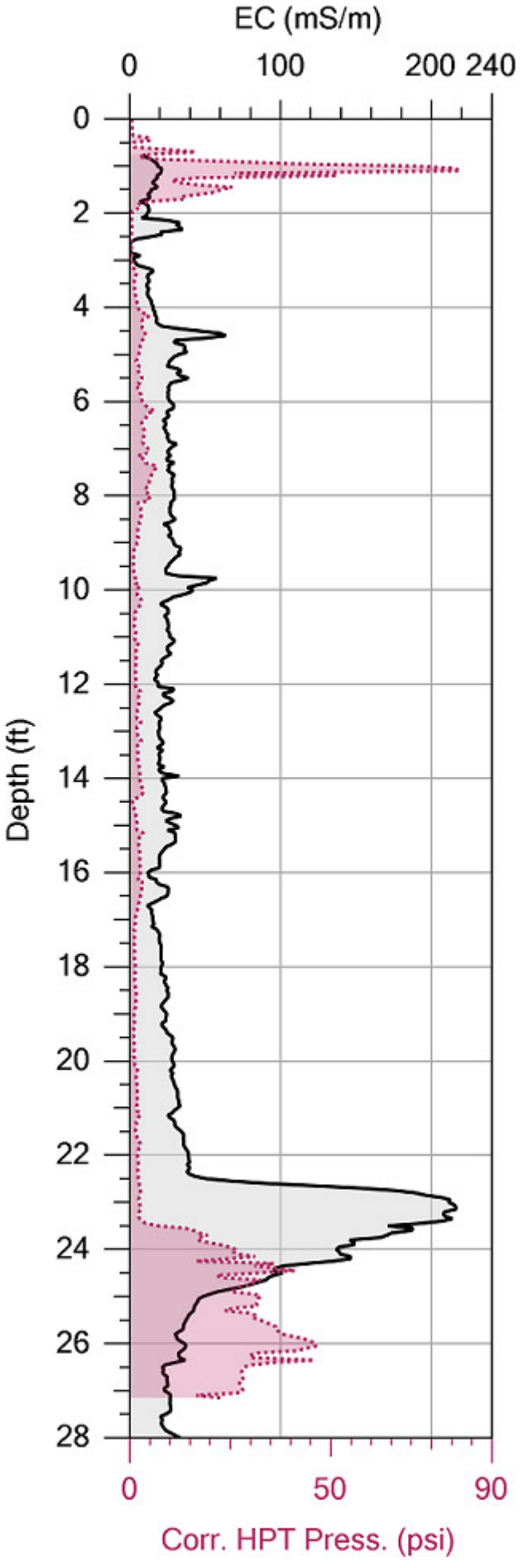
EC (mS/m)
0
100
200 240
0
2
4
6
8
10
12
14
16
18
20
22
24
26
28
Depth (ft)
0
50
90
Corr. HPT Press. (psi)

Figure 3-35. EC log (solid black line) and superimposed HPT pressure log (dashed purple line) corrected for hydrostatic pressure.

Source: Modified from McCall et al., 2014, Used with permission

There are several different options when it comes to displaying EC data. Typically, EC probe data are simply presented as a log of conductivity versus depth with multiple logs being displayed in a cross-section format (see Figure 3-31). If HPT is used in concert with the EC array, both sets of data (EC and corrected pressure curves) can be plotted on the same log or on adjacent logs to aid in data interpretation. While perhaps less common, plot plan view slice maps or even 3-D images of EC can be created using appropriate software. Whatever the presentation style, EC data should not be viewed in isolation but should be presented with some form of supporting information (for example, hydraulic profiling, natural gamma log).

3.7.6 Tool and Data Misuse

Using the EC probe in areas known to contain mainly coarser-grained, nonconductive soils (for example, coastal plain environments) may be of little benefit unless the survey goal is to map a zone of highly conductive pore water (for example, a salt-water intrusion zone). The EC probe is likely to be most useful in more heterogeneous unconsolidated environments where greater understanding of hydrostratagraphic relationships is required. It can also be useful for defining (in high resolution) acidic buried wastes, high-concentration total dissolved solid plumes in groundwater, and buried material that has an EC different from the deposits that contain the buried waste.

3.8 Flexible Liners

Flexible liners deployed in boreholes allow measurements of hydraulic conductivity, groundwater pressures, water quality, and NAPL distribution within a borehole and may also be used to conduct tracer tests and seal boreholes. Flexible liners have been developed to monitor landfills, augment horizontal drilling, provide groundwater pressure histories, and reline pipes and pull logging tools. Flexible liners are commercially available from Flexible Liner Underground Technologies, LLC (FLUTe™). A depiction of a flexible liner and its insertion into a borehole are shown on Figure 3-36.

Flexible liner measurement methods are simple and have been aided by the development of strong impermeable fabrics and the availability of data-recording pressure transducers. Because liners are deployed in open boreholes, they are typically used in bedrock.

Flexible liners can have multiple applications depending on the data needs of the investigation. When liners are used for multiple applications, a high-resolution dataset is generated at a borehole spatial resolution of several inches to several ft.

Some applications can be performed with minimal training; others require trained FLUTe™ personnel to perform the installations and data reduction. The following applications of flexible liners are described in more detail in this section:

1. sealing boreholes with liners
2. mapping transmissivity profiles (FLUTe™ T Profiler)
3. mapping NAPL distribution (NAPL FLUTe™)
4. mapping dissolved-phase contaminants [FLUTe™ Activated Carbon Technique (FACT)]

These applications often follow the numbered sequence above because they reuse the same flexible liner. The cost advantage of using FLUTe™ versus individual tools to achieve the same results is the multiple data streams that are derived from a single borehole and liner. In addition, FLUTe™ liners are readily removed unlike permanent subsurface installations.

3.8.1 Sealing Boreholes with Liners (FLUTe™)

FLUTe™ liners are used to seal a borehole. The advantages of this method are:

- ease of installation and removal
- continuous seal quality
- support from the liner to protect the borehole wall against slough
- tracer arrival detection because of transparent liner
- geophysics logs can “see” through the liner from the protected interior;
- installation of liner without heavy equipment
- same liner can be used for multiple methods (NAPL FLUTe™, FACT, FLUTe™ T profile, and the reverse-head profile).

Liners can be removed for repair or replacement if needed. Videos are available online from FLUTe™ to illustrate how to deploy liners, or a trained technician can be provided by FLUTe™.

The liner is used to seal the borehole to prevent cross connection between zones of different hydraulic head. The basic blank liner is installed using eversion, which advances a liner downhole by turning it right side-out. To facilitate the process, the liner is shipped inside out to the site on a reel. The installation/removal process is as follows:

1. Liner is pulled from the reel and secured to the borehole casing with a clamp.
2. Liner is pushed down inside the casing, forming an annular pocket in the liner.
3. Water is poured into the annular pocket; the weight of water in the liner causes the liner to evert down into the borehole, pulling the liner from the reel (see Figure 3-36*).* A minimum height of water is needed to drive the everting liner to the water table. Water may be pumped from the borehole using a pump below the liner.
4. Liner eversion stops at the water table, and more water is required to restore an excess head in the liner to continue eversion.

5. Liner eversion below the water table displaces water into the formation.
6. Liner descent by eversion continues until there is insufficient formation transmissivity beneath the everting liner to permit its further descent; at that time, the borehole is effectively sealed by the pressurized liner.
7. To invert (remove) the liner, the operator pulls upward on the tether and water is drawn into the borehole until the liner is fully removed.

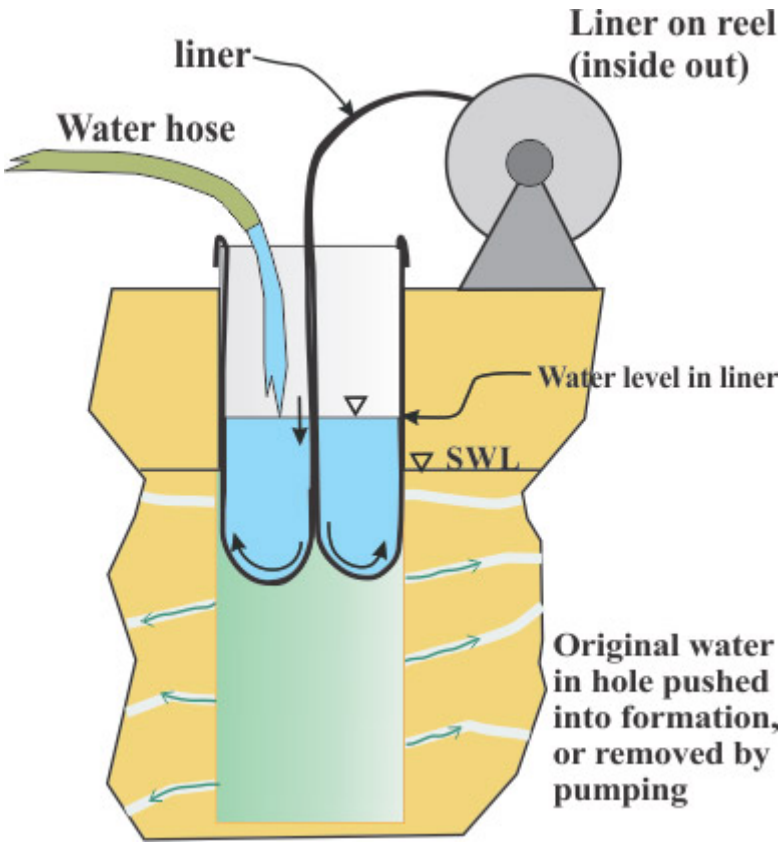

Figure 3-36. Simple eversion of flexible liner.
Source: Flexible Liner Underground Technologies, Used with permission

Water-filled liners effectively seal boreholes by tightly conforming to the borehole wall and sealing around cavities and fractures in the formation. The seal of the liner with its conforming capability is better than that of most inflatable well packers which are made from stiffer materials.

The excess water head against the everting end of the liner causes tension to develop on the liner and the tether attached to the inside end of the liner. This tension is used for various applications such as towing logging tools into angled and horizontal boreholes or carrying tubing and other devices into the borehole. Water is the common driving fluid for liner eversion, but other fluids (such as heavy mud or air) may be used. Liners have been everted through crooked pipes and upward in boreholes from inside mine tunnels. Gamma, neutrons, and sonic and electrical signals may be measured through everting liners, allowing geophysicaltools to be deployed in the protective interior of the liner, which prevents borehole collapse and contamination of the tools.

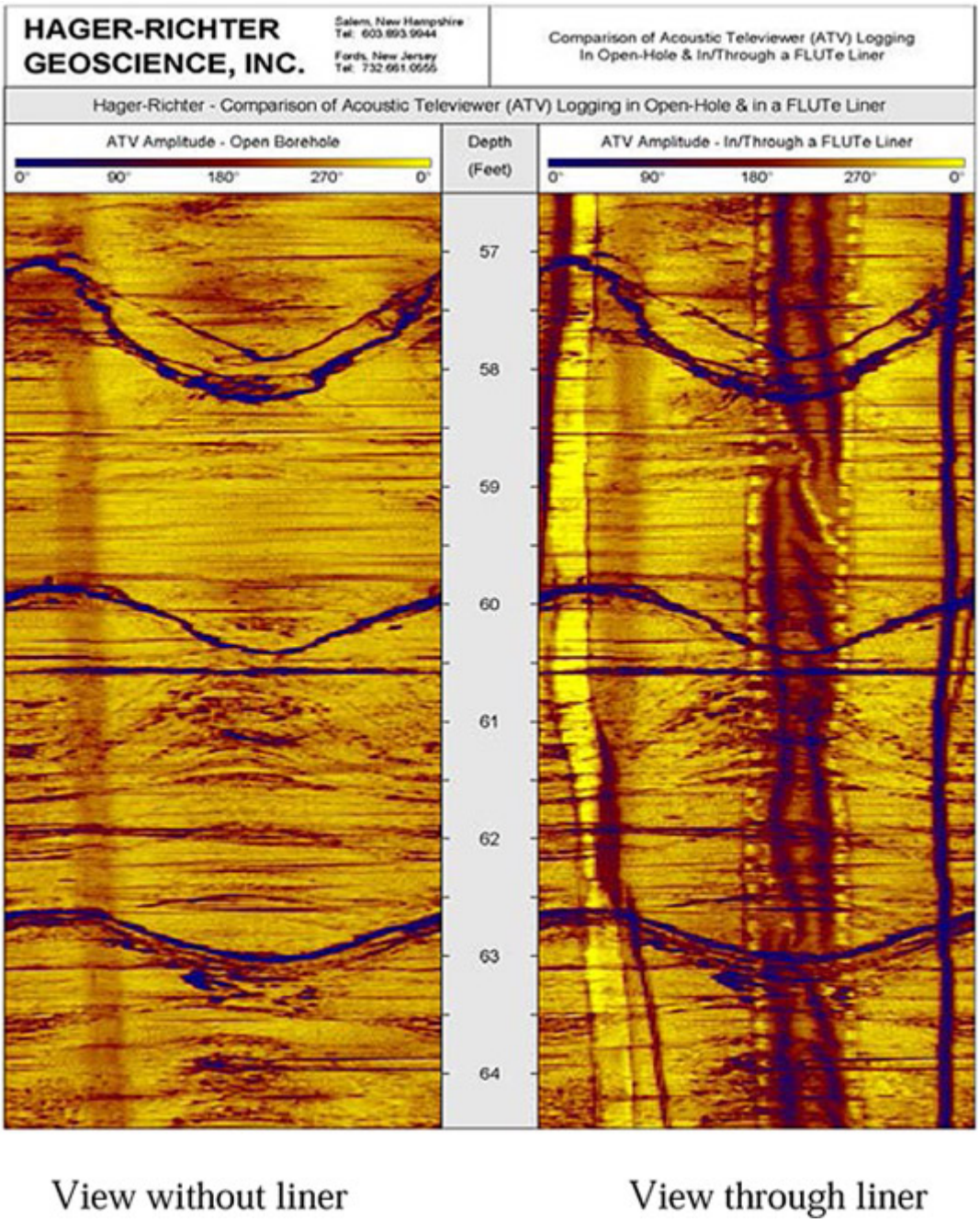

Figure 3-37. Acoustic televiewer logs recorded with and without a liner in the same borehole.
Source: Flexible Liner Underground Technologies, Used with permission

An image of a borehole can also be obtained through both opaque and clear liners. In the case of opaque liners, an acoustic televiewer can be used to obtain the image. Figure 3-37 shows views of an acoustic televiewer log (see Section 4.6) with (left) and without a liner (right). An interior sleeve (dark strip) and tether (right-most shadow) are visible in the view through the liner at right, but obscuration of the borehole wall by the liner is minimal; fracture locations are equally clear in both views. Transparent liners are also available, which may be useful to visually monitor the arrival of injected potassium permanganate within a borehole with a downhole camera.

3.8.2 Technical Limitations

Limitations when sealing boreholes with liners are as follows (for most sealing FLUTe™ and theFLUTe™ transmissivity profiler see Section 3.8):

- If the liner is exposed to extremely high concentrations of VOCs (NAPL), the VOCs diffuse into the liner interior water. Upon removal, the water must be treated as contaminated.
- Some compounds such as potassium permanganate degrade nylon liners; polyester liners are available for sites

with potassium permanganate in groundwater.
- The water level in the liner must be maintained to preserve the seal of the liner.
- For extreme downward gradients (>50 ft over the borehole depth), a stronger liner is required to prevent the liner from bursting.
- Although liners can be punctured by sharp rocks in the borehole wall, puncturing has only occurred in fewer than 1% of liner installations.

The limitations of the NAPL FLUTe™ liner include the following:

- An open stable hole or installation through drill casing is required.
- The dissolved phase is not detectable, and the liner must contact NAPL for a stain to develop.
- Solvents migrate in the cover material and, therefore, the size of the stain is not indicative of NAPL thickness.
- The NAPL type cannot be identified by the stain.
- Stains represent current NAPL locations; NAPL may be redistributed by the drilling process, resulting in scattered staining. (Scattered small stains usually occur in boreholes with large stains from the source of the scattered NAPL).

3.8.3 FLUTe™ Transmissivity Profiler

The liner descent rate in a water-filled borehole can be used to map the location and flow rates of water in the fractures intersecting the borehole. However, the procedure requires that the excess head driving the liner and the tension on the liner be maintained relatively constant. Under these conditions, the liner suffers a drop in its descent velocity each time a flowing fracture is sealed by the descending liner. The velocity change multiplied by the cross-sectional area of the borehole is the flow rate of the water in the fracture before it was sealed.

The transmissivity of the interval traversed by the liner in one recording time step is calculated using the Thiem equation:

$$\Delta T = \Delta Q/\Delta H_h \ln(r_a/r_h)/2\pi = (v_i - v_{i+1})\ A \ln(r_a/r_h)/(2\pi(H_h - H_a))$$

where ΔQ is the change in velocity (v_i) multiplied by the borehole cross section (A), ΔH_h is the difference between the borehole pressure (H_h) and the ambient pressure (H_a) in the formation at a distance (r_a) from the borehole center, and r_h is the borehole radius. Since r_a is often not well known, it is estimated.

Because it occurs in the long term, an error in the ratio is not a major error in the calculation. The spatial interval is dependent upon the recording time step (typically 0.5 sec) and the velocity of the liner. In other words, the faster the liner descents, the longer the interval traversed in one-time step. For example, when integrated over 1-ft intervals, the result is similar to that obtained from a series of 1-ft-long straddle packer tests.

3.8.4 The NAPL FLUTe™ Liner

The NAPL FLUTe™ liner maps the distribution of NAPL present at the borehole wall against the hydrophobic liner cover. Upon contact with NAPLs, dye in the liner is dissolved, producing a dark stain on the inside white surface of the hydrophobic cover. Stain colors vary from purple (a mixture of the dyes used) to dark brown or nearly black if the NAPL is mixed with oily residue as a spent solvent. The hydrophobic cover reacts only with pure NAPL, not dissolved-phase contamination, creating a visual log of free-phase product within the borehole, if present.

Advantages of the NAPL FLUTe™ liner are as follows:

- Stains observed are a reliable indication of the presence of NAPL at any depth within the borehole.
- Stains indicate the presence of NAPL not apparent through visual observation of a rock core.
- Stains are easy to observe and photograph and require minimal interpretation.
- Spatial resolution of NAPL is approximately 1 inch to 2 inches and presents a full 2-D map of the presence of NAPL.
- The NAPL FLUTe™ liner is a relatively inexpensive addition to a sealing liner used to prevent cross connection.

Many compounds have been tested for reactivity with the NAPL FLUTe™ liner; a list is available online from FLUTe™. To confirm reactivity, a confirmation staining test of the target NAPL with the FLUTe™ liner material should be conducted prior

to employing a FLUTe™ liner investigation program.

Figure 3-38. Everted dye-striped NAPL FLUTe™ liner cover.
Source: Flexible Liner Underground Technologies, Used with permission

When everting the NAPL FLUTe™ liner into a borehole, one borehole volume of water is pumped from beneath the liner during installation to reduce the injection of water into the fractures (the injection effect may displace NAPL from the borehole vicinity). Pumping should not be excessive so that significant mobilization of NAPL is avoided. It is important to note that water displaced into fractures during the eversion is likely extracted from the same fractures during the inversion of the liner from the borehole.

After a minimum of one hour, the liner is inverted from the borehole as shown on Figure 3-38. The dye-stripe liner cover is now inside of the inside-out liner. The liner cover is held as the liner is slipped off the liner cover, exposing the normally white inside surface of the liner. Visible stains on the white surface of the line indicate where NAPL has contacted the liner cover. A tape measure is placed next to the cover, and the stains are photographed to record the depth in the hole where NAPL contacted the liner cover.

Because the liner and liner cover are inverted from the borehole, the liner cover does not contact any other portion of the borehole than where it was everted against the borehole wall. The NAPL FLUTe™ cover is often installed on the blank liner for the initial emplacement to seal the borehole. Upon removal of the NAPL FLUTe™ cover, the liner is replaced to seal the borehole or perform other measurements described below.

As an example, Figure 3-39 shows stains from TCE, coal tar, xylene, and gasoline on the inside surface of a cover. The first three stains were obtained in open fractured rock boreholes, which are the conditions where this method is most commonly used. The LNAPL stain was the result of a thin gasoline film on water in a tube.

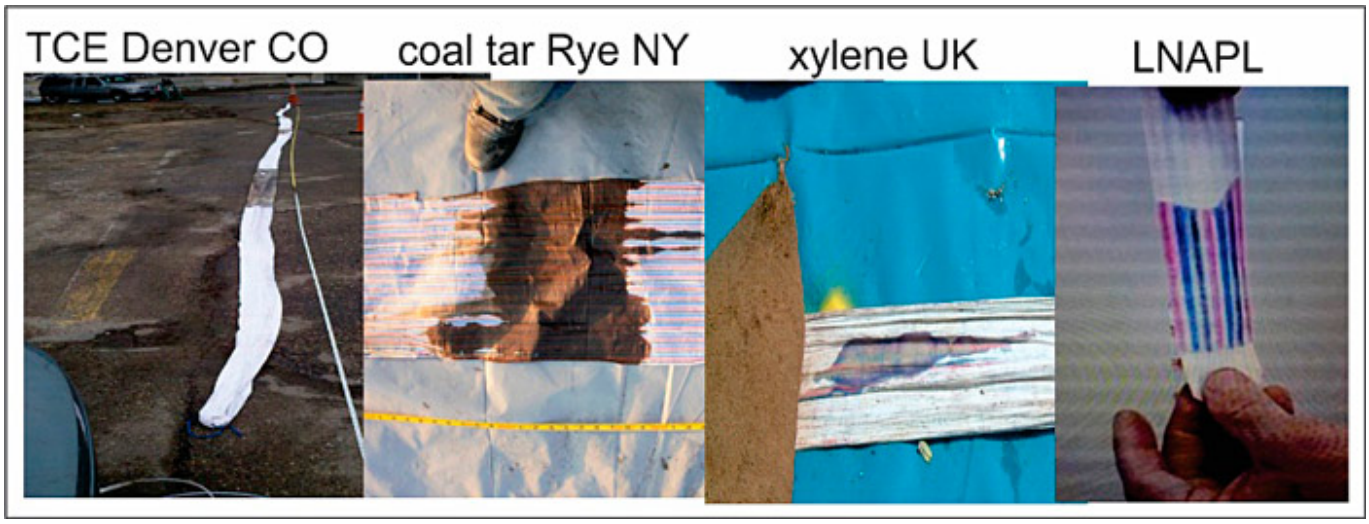

Figure 3-39. Examples of NAPL stains on the inside surface of a cover.
Source: Flexible Liner Underground Technologies, Used with permission

Rather than being deployed downhole, the NAPL FLUTe™ cover material may also be used as a bag to detect NAPL in extruded core material that is placed inside the bag. This technique is used if the borehole is not expected to remain open when casing is removed or if only a small section of core is to be tested. Similar to the liner, contact of NAPL in the core with the dye on the inside surface of the bag will produce a visible stain on the outside of the bag.

3.8.5 FLUTe™ Activated Carbon Technique

The NAPL FLUTe™ liner, described above, detects only NAPL in contact with the cover, but the FACT can detect contaminants in the pore space and in fractures of the formation at the borehole wall. The NAPL FLUTe™ liner and FACT may be deployed together, generating two datasets from the same borehole.

In the FACT, an activated carbon felt strip is pressed against the borehole wall when the sealing liner is everted into the borehole. The FACT strip is left in the borehole for up to two weeks during which the carbon adsorbs the dissolved phase of the contaminants.

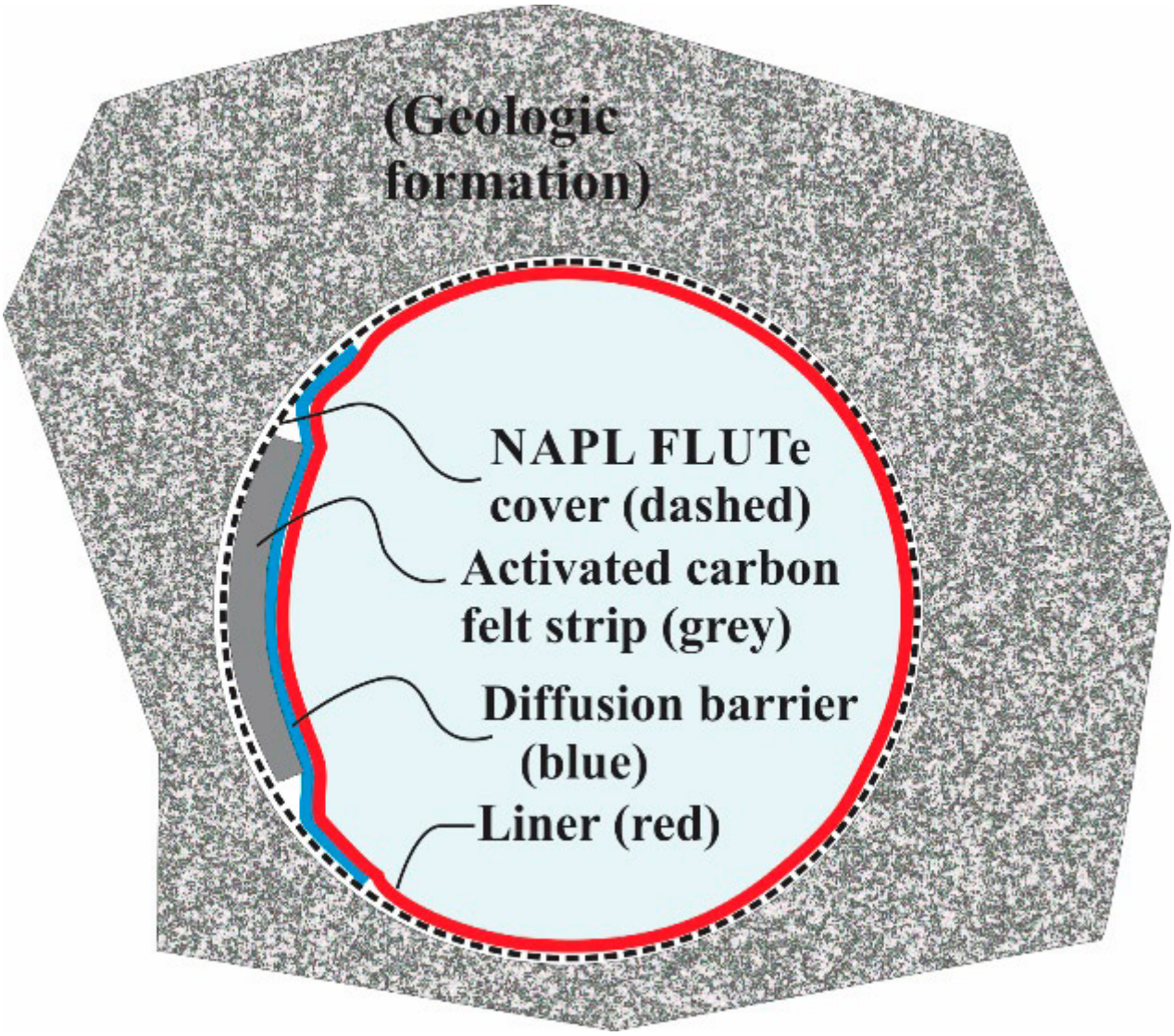

Figure 3-40. FACT components.
Source: Flexible Liner Underground Technologies, Used with permission

The construction of the FACT is shown in Figure 3-40. The FACT carbon strip (about 1.5-inches wide and 0.125-inches thick) is contained between the outer NAPL FLUTe™ cover material (dashed curve) and a diffusion barrier (blue) that is sewn into the inside surface of the thin (about 1 mil) cover material. The pressurized liner (red line) presses the diffusion barrier (blue line), the carbon felt (gray line), and the NAPL FLUTe™ cover (dashed line) against the borehole wall.

After two weeks in the borehole, the liner is inverted from the borehole with the NAPL FLUTe™ cover. As described in Section 3.8.4, the liner is slipped off the inverted cover, and NAPL stains, if present, are photographed. The diffusion barrier, which is now on the outside of the inverted cover, is slit and the carbon felt strip is removed, cut to desired lengths, and inserted into sample jars filled with deionized water. Carbon-felt samples are shipped to a laboratory for analysis according to USEPA Method 8265. Acceptable performance for the carbon-felt matrix should be demonstrated by matrix spikes or laboratory control samples with analytes spiked onto the carbon felt.

The spatial resolution of data is determined by the length of each carbon-felt strip, which is determined by the user. For a high-resolution dataset, the carbon strips may be cut into small (6 inch) pieces; for a lower resolution dataset, the carbon strips may be cut into larger (1 ft to 2 ft) pieces. Analyzing larger sections of FACT is less costly because fewer samples are generated, but a data set with lower resolution results. Regardless of sample length, the entire carbon strip must be analyzed because contaminants do not migrate in the carbon; failure to analyze the entire length of carbon can result an interval of elevated contamination being missed.

The right side of Figure 3-41 shows measurements of TCE (in ppm of carbon) in 6-inch carbon-felt segments from a 150-foot

borehole using the FACT. The graph also shows corresponding groundwater concentrations [in parts per billion (ppb)] obtained from 10 sample intervals 300 days (black bars in figure) and 700 days (blue triangles in figure) after the FACT carbon strip was removed. Water samples are plotted on the same scale regardless of unit, which shows the distribution similarity. The data comparison between the FACT and water sample results shows the accuracy of the measurements from the FACT and how the liner prevents borehole cross connections between different contaminated zones. The water samples are derived mainly from fracture flows, suggesting that the FACT is also sensitive to fracture flow concentrations. Because the FACT produces a diffusion-based measurement, contaminant concentration gradients are expected to be highest for water flowing past the FACT carbon strip as compared to water trapped in the pore space of the matrix. Thus, the mass of diffusion is directly dependent on the concentration gradient.

Measurements from the FACT generally agree with the contaminant concentration distribution in the core, but not necessarily with all locations in the borehole. The FACT draws from pore water and fracture water, whereas a core assessment measures the pore water of selected samples, not the entire core, or intervals of lost core. FLUTe™ is often a component of a DFN investigation (see Section 3.1.7.2), so a high-resolution comparison may be performed when both investigation methods are used.

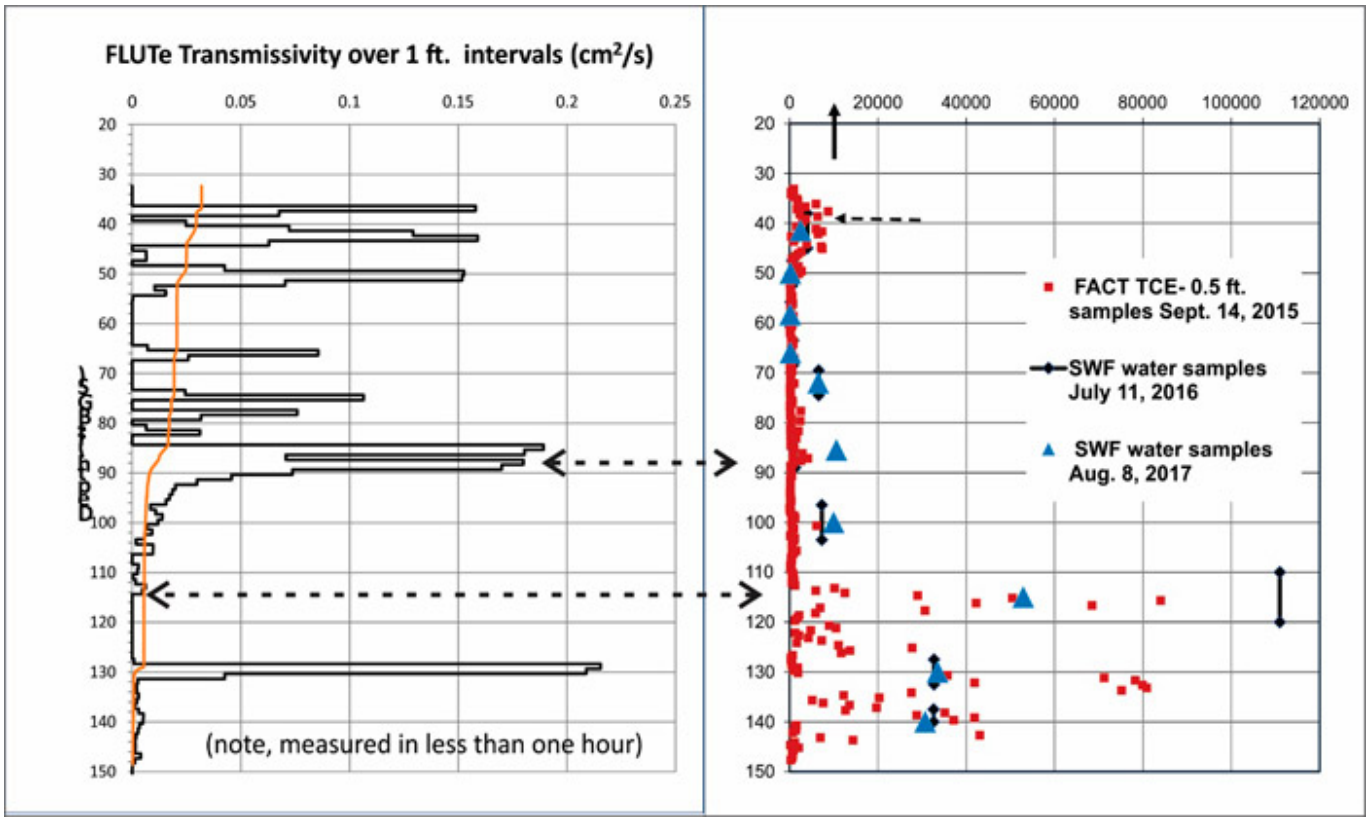

Figure 3-41. FACT results with transmissivity.

Source: Flexible Liner Underground Technologies, Used with permission

The left side of Figure 3-40 shows transmissivity over the intervals, providing a side-by-side comparison of the FACT results and the transmissive intervals measured. The arrows correlate two example high concentration intervals to corresponding transmissivity intervals. The highest concentrations are not always in the high flow zones. The highest concentration at 115 ft occurs within a low-transmissivity interval, and the relatively low concentration at 87 ft occurs within a high-transmissivity interval.

The FACT uses carbon-felt strips, which contain toluene that is known to be leached from the urethane-coated liner fabric. Leaching is unlikely to impact future water samples because the toluene dissipates relatively quickly from the liner, but not in the time frame of the FACT installation, and therefore will be seen in the analysis of the carbon strip.

Advantages of the FACT:

- Provides a continuous vertical map of the dissolved-phase contaminants (the entire length of the borehole is evaluated so no intervals are missed).

- Not dependent on prior judgement of where contaminants are residing.
- Results correlate to groundwater samples.
- Sensitive to both pore-space and fracture contamination.
- Can be added to the NAPL FLUTe™ cover at relatively small additional cost.
- Carrier liner can be reused to seal the borehole or to perform other high-resolution measurements.

4 Borehole Geophysics

Borehole geophysical tools provide high-resolution geologic, hydrogeologic, and geochemical data that aid in developing robust CSMs. Borehole geophysics is best applied where direct sensing methods cannot be used (typically too dense or too deep). Certain borehole geophysical tools [nuclear magnetic resonance (NMR), natural gamma, induction] can be used in existing wells as a cost-effective alternative to drilling new borings or using direct sensing methods. Borehole geophysical tools can also provide data on parameters that cannot be obtained with direct sensing tools, such as porosity.

A wide variety of geophysical tools are available to provide information on soil and bedrock lithology porosity; permeability and hydraulic conductivity; pore-fluid characteristics; fracture characterization; well construction; and other hydrologic parameters such as hydraulic head, residual saturation, and dynamic flow conditions. Data are commonly acquired using wireline methods in open boreholes, although some geophysical tools can be deployed in cased wells. Some tools can be deployed in dry, open holes, but most require fluid in the borehole (water or drilling mud) to transmit and collect data or are specifically designed to characterize fluid within the formation.

Borehole geophysical tools have been applied for decades to improve site characterization but are generally underused due to lack of understanding or awareness. The tools presented in this document can provide information concerning the physical (lithology), hydraulic (flow velocity), and chemical (dissolved solids) aspects of the subsurface. Borehole geophysics can provide relatively quick subsurface information without significant costs. Typically, a suite of tools is deployed either at once or in sequence, and the results of each are integrated to infer subsurface characteristics. Combinations of tools (See USGS Fractured Rock Geophysical Toolbox Method Selection Tool (USGS 2018b)) are appropriate for particular geologic environments and to describe the particular geologic properties that affect contaminant distribution and transport and fate and that inform decisions regarding remedial approaches.

4.1 How to Select and Apply Borehole Geophysical Tools Using this Document

Preparing a borehole geophysical tool logging program includes identifying the key project parameters and objectives, selecting the most appropriate geophysical tools, and communicating with the geophysicist. Before selecting a borehole geophysical tool, it is important to understand the parameters the tool can measure and the site-specific conditions the tool requires to acquire the data. Borehole geophysical tools described in this section are as follows: fluid temperature, fluid resistivity, mechanical caliper, optical and acoustic televiewers, natural gamma, borehole flow meters (heat-pulse flow meter and the flow impeller), and advanced borehole logging (electric resistivity, NMR, and borehole video).

The borehole geophysical program development and tool selection should consider the following:

- Project and data quality objectives
- Local and regional geology
- Site-specific logging logistics
- Drilling methods
- Anticipated borehole conditions
- Log analysis
- Cost

The tools presented in this section are summarized in Table 4-1. The project geophysicist may use various orders of deployment. Other factors such as cost, time, tool availability, or initial knowledge of rock type may mean certain tools are not necessary.

Table 4-1. Borehole logging tools discussed

Logging Tool	Primary Application
Fluid Temperature	Records borehole temperature
Fluid Resistivity (or Conductivity)	Measures electrical resistance of borehole fluids

Logging Tool	Primary Application
Mechanical Caliper	Measures borehole diameter
Optical Televiewer (OTV)	Optical image of borehole walls
Acoustic Televiewer (ATV)	Acoustical image of borehole wall
Natural Gamma	Measures gamma radiation emitted from formation

In this guidance, each tool section includes a discussion of what the tool tells you, how it works, variations, benefits, appropriate use, limitations (both technical and nontechnical), data collection design, quality controls, data interpretation and presentation (including data extrapolations and misuse), which tools can be used together, costs, and references. The ASCT Borehole Geophysical Tool Summary Table provides a screening process based on site and project parameters and objectives. More than one tool may provide the data required. By using different tools to collect similar data, supporting evidence is provided and data confidence for site characterization is improved. ASCT Borehole Geophysics Checklists (.xlsx version) are provided to support tool selection and use and project management.

4.1.1 Tool Availability

Almost all borehole geophysical investigations involve the application of multiple tools, most of which are readily available. Less commonly used tools (for example, magnetic susceptibility) may require extra coordination with the geophysicist to confirm tool availability and application, for example. It is critical to communicate with the geophysical contractor or operator to ensure project objectives are met, data of known quality is collected, and an accurate schedule and cost is received. Critical site information must be provided to the geophysicist, such as geology, depth to groundwater, borehole conditions, estimated logging footage, field schedule, and site accessibility.

4.1.2 Data Collection Design

Data collection and reporting are important components of geophysical logging programs. Data acquisition and processing are typically provided by a geophysical contractor or qualified practitioners that can purchase or rent the necessary equipment and perform the work themselves. Data processing includes establishing a set datum for depth or elevation matching between geophysical logs, correcting borehole effects, converting log measurements to parameters of interest, and merging logs into a presentable format. A geophysical contractor may not provide data analysis and interpretation unless explicitly requested during the proposal process. Hence, it is important to discuss expectations prior to initiating work so that budgets can be adjusted accordingly.

To effectively communicate with the geophysicist on appropriate tool selection and ensure quality data are collected in a cost-effective manner that meet the project objectives, a good basic understanding of each tool's physical limitations, data processing methods and limitations, and data analytical methods is recommended.

Borehole logging by field personnel is subjective and may vary depending on the skill and experience of personnel. Borehole geophysical logs are typically generated from continuously acquired, objective, and repeatable data from which desired parameters can be qualitatively or quantitatively derived. Geophysical logs provide a significant amount of high-resolution data on lithology, hydrogeologic parameters, and pore fluid characteristics in or near the borehole. While these borehole logs represent detailed vertical interpretations, they must be compared to other borehole logs to provide a planar or horizontal interpretation that can potentially be extrapolated across the site. Multiple parameters can be measured using different tools and the results validated using multiple lines of evidence along with other investigative data for site interpretation.

Borehole geophysical logs can be correlated between multiple borehole locations, providing stratigraphic and structural information. This correlation allows the overall geologic framework to be portrayed in 2-D and 3-D representations (see Figure 4-1 and Figure 4-2). These tools can identify and quantify various bedrock structural features, such as formation contacts and fracture location and orientation. These data can then be correlated between wells. In sediments and sedimentary bedrock, the correlation process uses characteristic curve matching and relies on principles of stratigraphy and sedimentary depositional processes such as Original Horizontality and Walther's Law. These principles state that stratigraphic facies and facies sequences commonly display characteristic compositional and textural changes in the vertical profile that can be observed on geophysical logs and correlated over distances between logs. Once the various facies or facies sequences are identified and correlated, intervals of interest (such as fluid transport pathways) can be assessed.

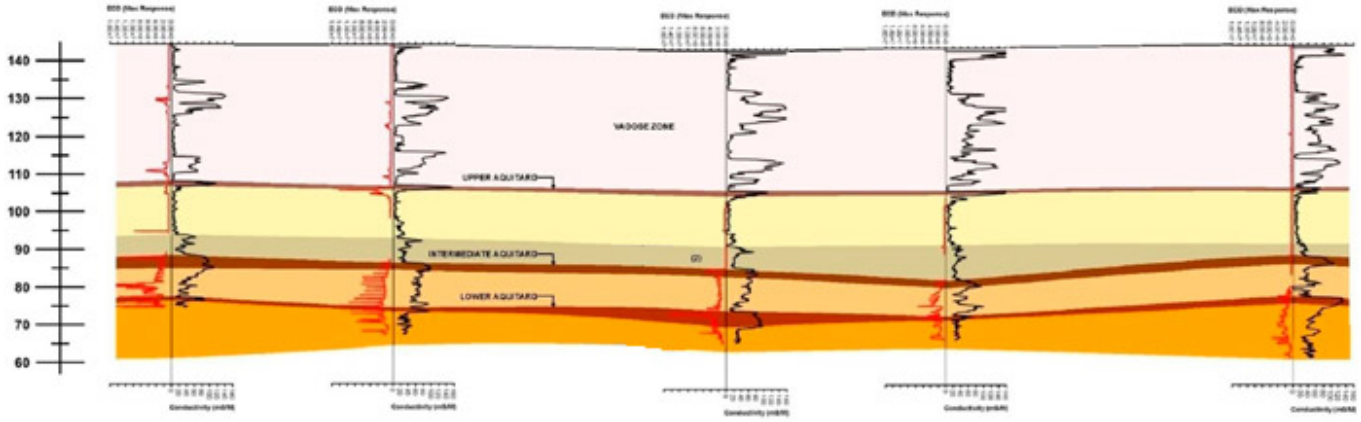

Figure 4-1. View of the overall geologic framework using 2-D representation.
Source: ERM, Used with permission

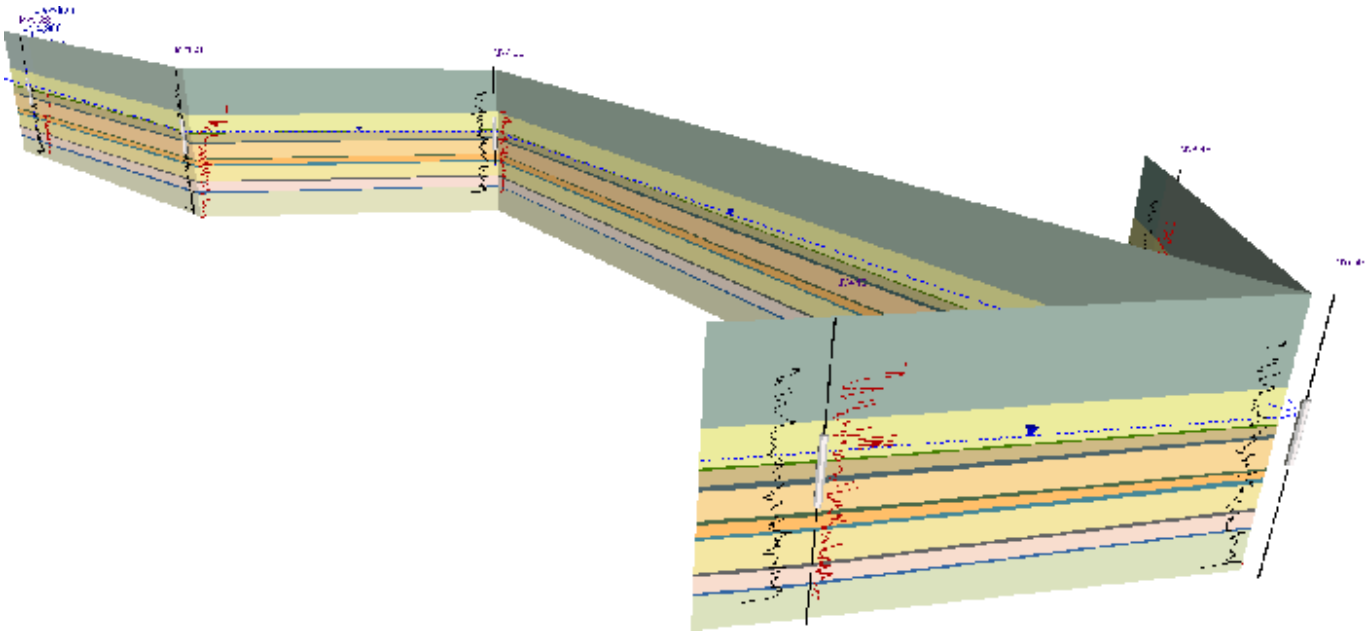

Figure 4-2. View of the overall geologic framework using 3-D representation.
Source: ERM, Used with permission

Whether in sediments or bedrock, the spacing of log data dictates the ability to resolve and correlate features of interest. At the local level and where closely spaced geophysical logs are available, correlating individual stratigraphic or structural features is usually feasible. For projects where geophysical logs represent locations that are several hundred ft or more apart, only larger-scale features that are laterally continuous are generally able to be correlated. A critical part of data acquisition planning is understanding the spacing needed to resolve and characterize geologic features of interest based on the conceptual model for the local geology.

4.1.3 Technical Advantages and General Limitations of Fundamental Logging Tools

The suite of fundamental borehole logging tools highlights a comprehensive set of tools intended to enhance characterization of bedrock and fractured rock systems. All of these tools are widely available for use by qualified geophysicists and logging personnel. Many of these tools are readily deployed during a days' worth of logging and do not involve significant independent costs beyond daily rates offered by many specialty providers. Key technical advantages of these tools include the following:

- Postprocessed data offer a visually familiar record understood by many.
- High-resolution data are easily and rapidly obtained at sub-cm (or lower) accuracy.

- Use of these tools supplements and may even replace the need for rock-core collection and visual logging during bedrock characterizations.
- Downhole tooling and surface cables allow the rapid interchange of probes, sondes, and detectors during logging.
- Select tools can be deployed in both cased and uncased hole settings, which can be advantageous at some sites,
- The combination of tools collectively supports lithologic and structural determinations of bedrock conditions.
- Iterative deployment of tools provides detailed information that assists in the interpretations of other logs, for instance, use of the caliper tool assesses borehole diameter in advance of gamma logging.
- Under certain circumstances, key information may be obtained across air-filled zones.
- Several of the tools provide a useful first step toward determining flow into or out of the borehole independently of more detailed borehole flow-meter assessments.

While there are inherently more technical advantages associated with the fundamental borehole logging tools described herein, a few notable limitations that should be considered when planning a borehole investigation program or interpreting logs. These general limitations include:

- Select tools require the borehole to be at equilibrium with removal of drilling fluids and residual groundwater prior to logging. In addition, image quality may be compromised with turbid fluids.
- Inadvertent damage to sensitive probes or potential drag-down of contaminants can result from the presence of residual NAPL.
- Well pumps, cables, and other potential infrastructure requires removal to allow tools to be lowered and raised in a borehole.
- Certain tools require use of centralizers, which may present a challenge with irregular borehole wall conditions.
- Poor well construction can cause degradation of image and data quality.

4.1.4 Case Studies

An example of how these individual tools were used to develop a CSM is provided in the following case study:

- Conceptual Site Model Development Using Borehole Geophysics at the Savage Municipal Water Supply Superfund Site in New Hampshire.

4.2 Fluid Temperature

Fluid-temperature logging involves using a downhole probe to continuously record the temperature of fluids in a borehole. During logging, a probe is incrementally lowered to directly measure changes in temperature using a thermistor or platinum sensor to estimate geothermal gradients of groundwater or other fluids in direct contact with the probe. Temperature logging is most commonly used in fluid-filled bedrock boreholes to assess flow into or out of the borehole. In some instances, fluid-temperature logging has been used in dry boreholes or discrete borehole zones devoid of fluids to indirectly measure formation temperature. During field application, fluid temperature is routinely logged concurrently with fluid resistivity based on the current configuration of most commercially available tools that combines both tools on the same sonde. Refer to Section 4.3 for a description of the fluid-resistivity tool.

A continuous profile of borehole temperature is also a useful first step prior to deploying a borehole flow meter to identify potential zones of flow into or out of a borehole (see Section 4.8).

4.2.1 Use and Application

Fluid-temperature logging helps quantify geothermal changes and assess the flow of groundwater within a borehole (See Figure 4-3). The tooling is easily deployable using a downhole winch, pulley system, and depth encoder to determine vertical accuracy. To minimize fluid disturbance while the borehole is at equilibrium, the tool should be lowered, rather than raised, while gathering data.

Abrupt changes in fluid temperature may correspond with zones with a discrete inflow or outflow of water from the borehole. Plotting the continuous-temperature profile as one track or strip along with results and data from other conventional logging tools corroborates interpretations using multiple lines of evidence.

Estimating zones of where fluid flow is subsequently used during the characterization process to refine discrete vertical zones where more detailed flow measurements are needed. Additionally, logging can occur while the borehole is under

stress by pumping to potentially enhance water-bearing zone identification.

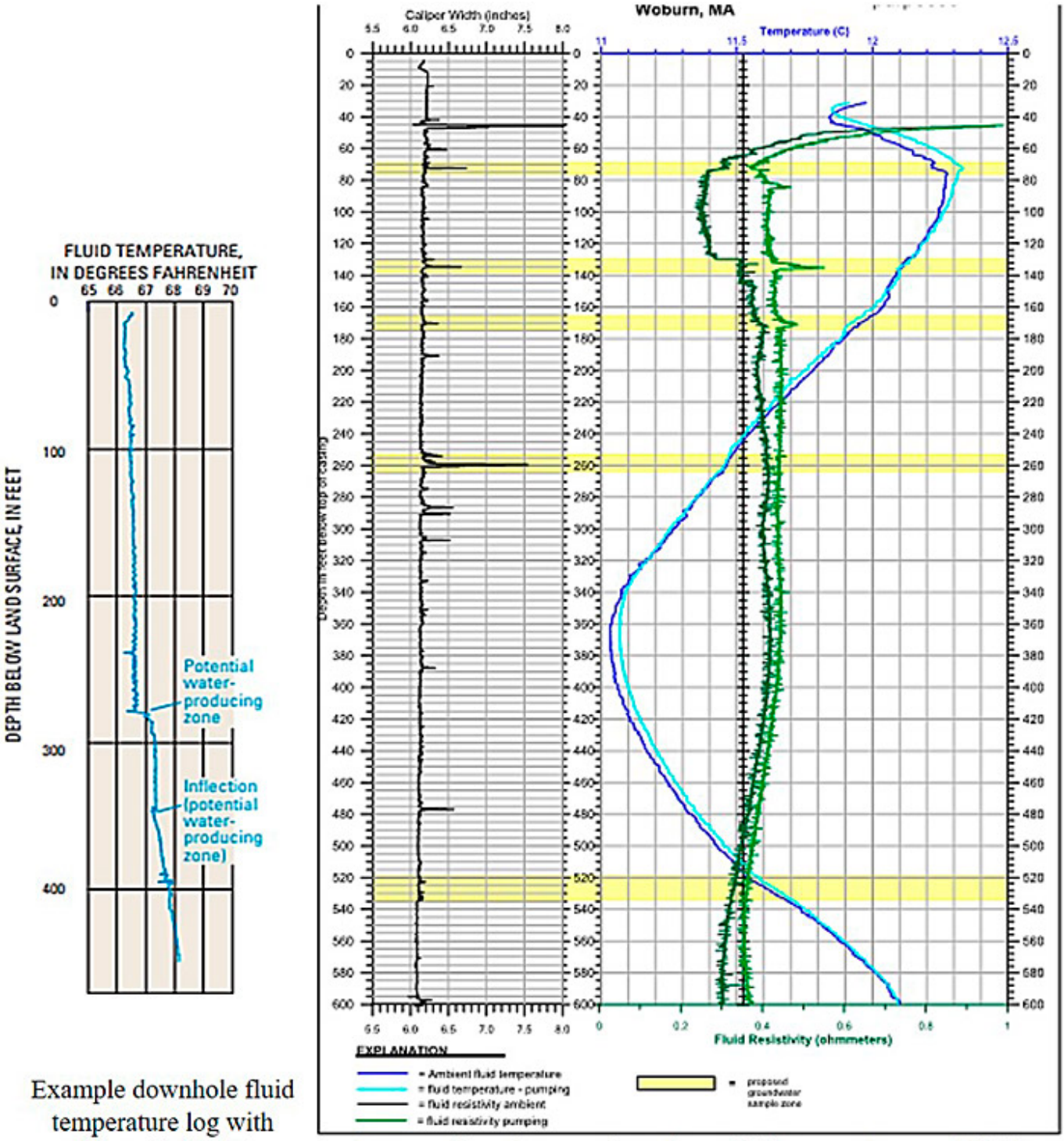

Figure 4-3. Examples of downhole fluid temperature log and composite logs.

Source: Left – Borehole Geophysical Logging of Water-Supply Wells in the Piedmont, Blue Ridge, and Valley and Ridge, Georgia (USGS 2007) and Right – Woodard & Curran, Used with permission

4.2.2 Data Collection Design

Fluid-temperature logging is typically one of the first tools to be used in borehole logging. Because temperature logging

generally occurs downward in a borehole, fluid-temperature logging is performed prior to using tools that are logged upward to minimize water-column disturbance.

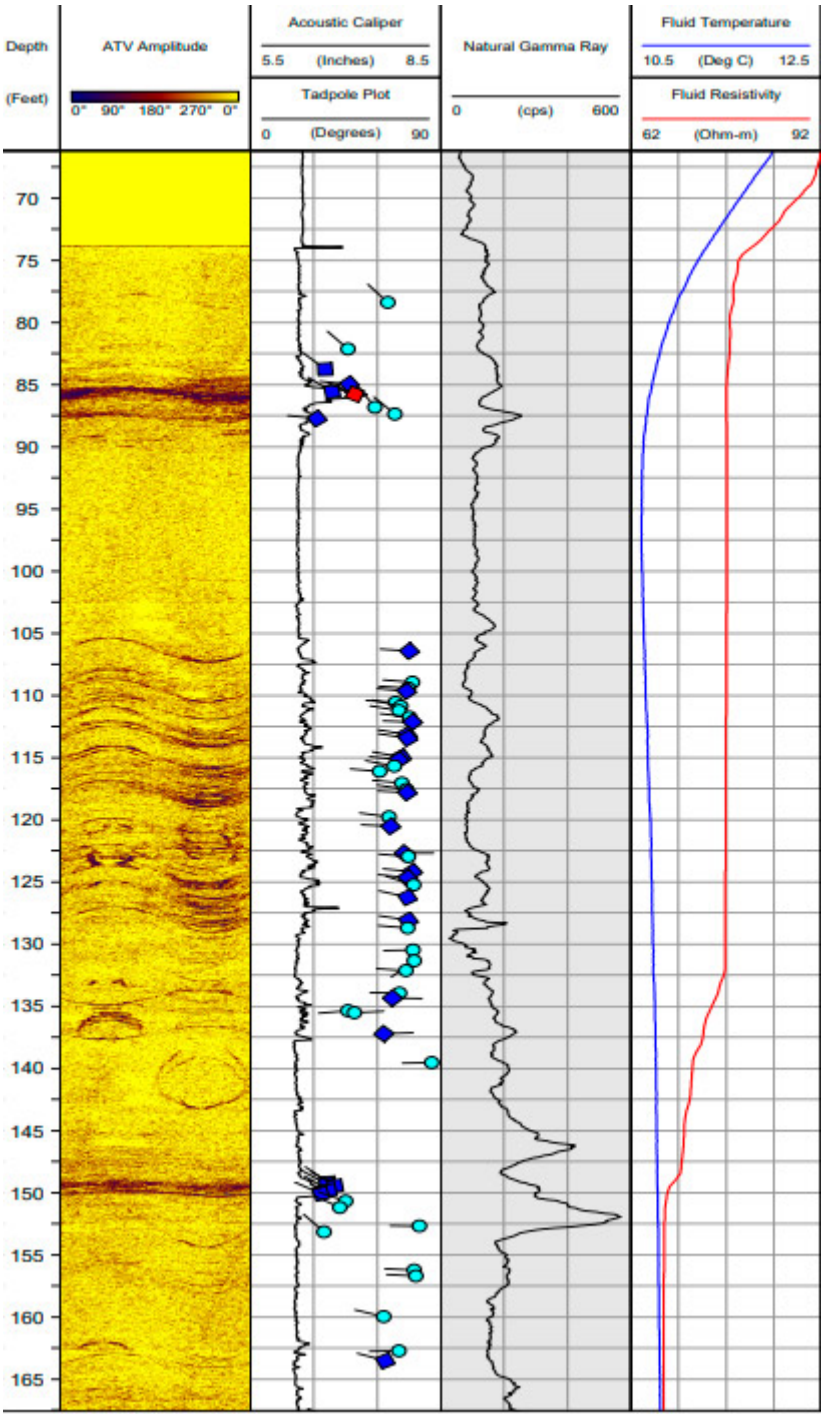

Figure 4-4. Example composite log of fluid temperature (blue line) along with fluid resistivity (red line), natural gamma, acoustic, acoustic caliper, and tadpole plots used to denote structural orientation of planar features.
Source: Image adapted from borehole geophysical logs included in the Remedial Investigation Report for the Savage Municipal Water Supply Superfund Site, Milford, NH, prepared by Weston Solutions Inc., March 2014), Used with permission

4.2.3 Log Intepretation

Fluid-temperature logs provide an index of temperatures in a borehole. Groundwater temperatures often vary based on flow conditions and small-scale changes are a useful indicator to assess inflections on a downhole basis. The sub-mm accuracy of temperature logging may be used to estimate where flow is occurring when corroborated by similar deviations in other logs and borehole wall images identifying planar and subplanar features that suggest fracture locations.

Figure 4-4 provides an example composite log of fluid temperature (blue line) along with fluid resistivity (red line), natural

gamma, ATV (borehole image developed from ultrasonic frequency), acoustic caliper (application of ATV travel times to generate acoustic borehole log based on borehole diameter), and tadpole plots used to denote structural orientation of planar features.

4.3 Fluid Resistivity

Fluid-resistivity logging uses a downhole probe to continuously record the electrical resistance of the fluid in a borehole using a series of electrodes. The downhole resistivity sounding incorporates multiple electrodes for real-time measurement. The electrodes are configured in a stacked array to minimize interferences during logging. Based on interpretations of the generated fluid-resistivity logging profile, areas of inflow or outflow from the borehole are differentiated and then corroborated by changes in fluid temperature, caliper measurements, and other geophysical logs.

Fluid resistivity notably is the inverse of fluid conductance or fluid conductivity[1] and provides a record of changes in the dissolved-solids concentration measured as ohm-meters (Ωm). Many of the tools currently in use have reverted to logging fluid conductivity; it is important to establish the preferred convention prior to logging. Many practitioners prefer to retain the convention of expressing logging results as fluid conductivity for consistency with direct-instrument reading (if such a tool is employed). Expressing logging results as fluid conductivity is also preferred for comparison with other direct-read multiparameter instruments used during groundwater investigations where specific conductivity is measured prior to groundwater sample collection.

4.3.1 Use and Application

Electrical current flow within a formation is governed primarily by fluid-filled pore spaces and the relationship of pore interconnectivity, volume, fluid composition, and temperature. Formation lithology also affects resistivity properties based on mineralogic assemblage and geochemical changes resulting from hydrothermal alteration. The interrelationship of these formation properties and the general ease of fluid-resistivity logging using conventional and commercially available tools has led to resistivity logging in support of various applications, including mineral explorations, oil and gas evaluations, and hydrogeologic assessments. Similarly, due to the strong dependence of fluid resistivity on the presence of dissolved solids, logging is often used to evaluate salt water and fresh water interaction in coastal aquifers.

Fluid-resistivity logging is conducted in fluid-filled open boreholes. Prior to fluid resisitivity logging, the borehole should be flushed of drilling fluids and/or borehole fluid additives and given time to equilibrate. Fluid resistivity logging can also be conducted while the borehole is under stress from pumping to facilitate identification of intervals where water is entering the borehole.

Fluid resistivity is commonly logged concurrently with temperature as an additional line of evidence to delineate water-bearing zones and identify predominant vertical flow conditions within a borehole. This parameter is generally recorded earlier in the logging process to gain a relative understanding of flow in and out of the borehole before the water column has been disturbed by other logging tools. Downhole resistivity probes are typically combined with a temperature thermistor in one probe.

4.3.2 Data Collection Design

Fluid-resistivity logging is conducted using wireline methods in a similar manner as most other borehole geophysical logging tools and must be acquired in open, fluid-filled boreholes. Resistivity logs measure the electrical resistivity that is affected by a number of factors, including include temperature, drilling-fluid resistivity, borehole diameter, mud cake, and drilling-fluid invasion. To use resistivity logs for quantitative analyses, these factors must be documented during logging and recorded in the log headings so they can be factored into the evaluation of the data.

The requirement for open, fluid-filled boreholes means that geophysical logging must be conducted soon after the borehole has reached terminal depth and has been stabilized by the driller. To minimize costs for standby time, communication and coordination with the geophysical service provider is required. Fluid-resistivity logging should be performed early in the logging process along with other primary tools (caliper and fluid temperature) to capture the static and undisturbed state of the borehole.

As with other borehole geophysical tools, logging at a single location provides parameter data only in the immediate vicinity of that location. By logging multiple locations, data can be correlated over greater distances and provide 2-D (cross-sectional) and 3-D conceptual models. The density of well locations to be logged should be based on the stratigraphic

framework and the nature of features that the investigation is attempting to resolve.

4.3.3 Data Interpretation and Presentation

Resistivity log data is usually processed and can be displayed in real-time. An example log is provided in Figure 4-5, along with a subset of key geophysical logging parameters. The dashed oval in the figure highlights the fluid-resistivity deviation that occurs above a notable fracture at approximately 158 ft and concurrent with a change in flow in the heat-pulse flow meter (HPFM) log.

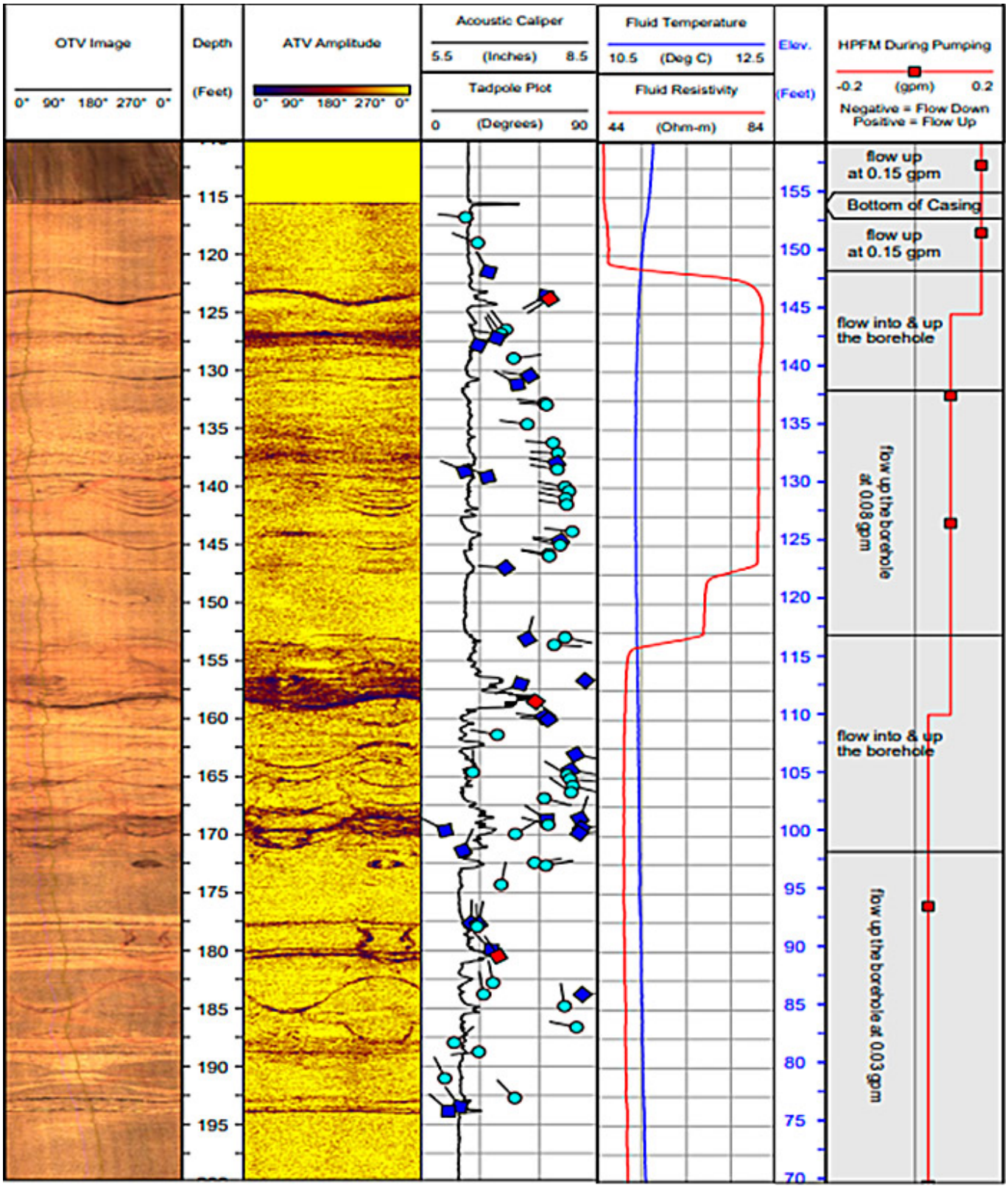

Figure 4-5. Example borehole log including optical/acoustic televiewer, inferred structural characteristics

(tadpole plots), fluid temperature (blue line), fluid resistivity (red line), and stressed HPFM measurements.
Source: Image adapted from borehole geophysical logs included in the Remedial Investigation Report for the Savage Municipal Water Supply Superfund Site, Milford, NH, prepared by Weston Solutions Inc., March 2014), Used with permission

4.4 Mechanical Caliper

A mechanical caliper tool provides a vertical profile of borehole diameter often using either a three-armed or four-armed device. During field application, the caliper is lowered to the bottom of the borehole (or lowest desired depth of measurement) and the arms are opened via direct connection to a laptop computer and pulled upward at a steady rate to record data. The spring-loaded arms reach outward against the edges of the borehole wall and the distance from each arm is recorded on the laptop computer in real-time. The total spacing from each arm is aggregated to determine average borehole diameter on a depth basis.

4.4.1 Use and Application

Mechanical calipers are effective at identifying voids, fractures, and similar openings in borehole walls, but cannot provide information on the orientation or lateral extent of such features. For this reason, the mechanical caliper is commonly used to identify vertical zones where enlargement has occurred. These zones are qualitatively interpreted as intervals where fractures may be present, alterations of the formation along the borehole wall that occurred during drilling, or lithologic and depositional voids.

Calipers are also effective, with or without corollary downhole tools, in locating the bottom of well casings, confirming drill casing diameter, and identifying casing breaks.

4.4.2 Data Collection Design

Caliper logging is often amongst the first of the geophysical tools to be deployed because of its durability and lower cost compared to video, electrical, or acoustic tools. Caliper logging is performed upward from the bottom of the borehole to the ground surface. As noted below, caliper logs are typically presented with other output to readily compare borehole features. The tool can be deployed independently, thus, it can be run at any time during the downhole investigation.

4.4.3 Log Interpretation

A caliper log often includes a corresponding geologic section to demonstrate the possible or likely caliper responses to given strata. Most data interpretation is performed with other standard downhole tool outputs, including natural gamma, fluid temperature, fluid resistivity and electrical logs. Aligning complimentary log outputs supports the multiple lines of evidence approach emphasized by correlating individual strip logs. When interpreting caliper logs, borehole-diameter deviations alone may not be indicative of fluid flow; therefore, correlation with other logs, notably fluid temperature or resistivity, is required to identify flow into or out of a borehole.

4.5 Optical Televiewer

The OTV collects a series of ring-shaped optical images at closely spaced discrete vertical spacings as the tool is moved vertically along the path of the borehole (see Figure 4-6). Coincident with OTV data acquisition, data are collected by orientation sensors (a magnetometer and accelerometers) within the tool. Acquisition and processing software are used with data from these orientation sensors to produce accurate, precisely oriented, cylindrical images of the borehole (see Section 4.6.4). The OTV results in a familiar photographic image, as shown in the figure below, which many practitioners refer to as an image log or virtual core.

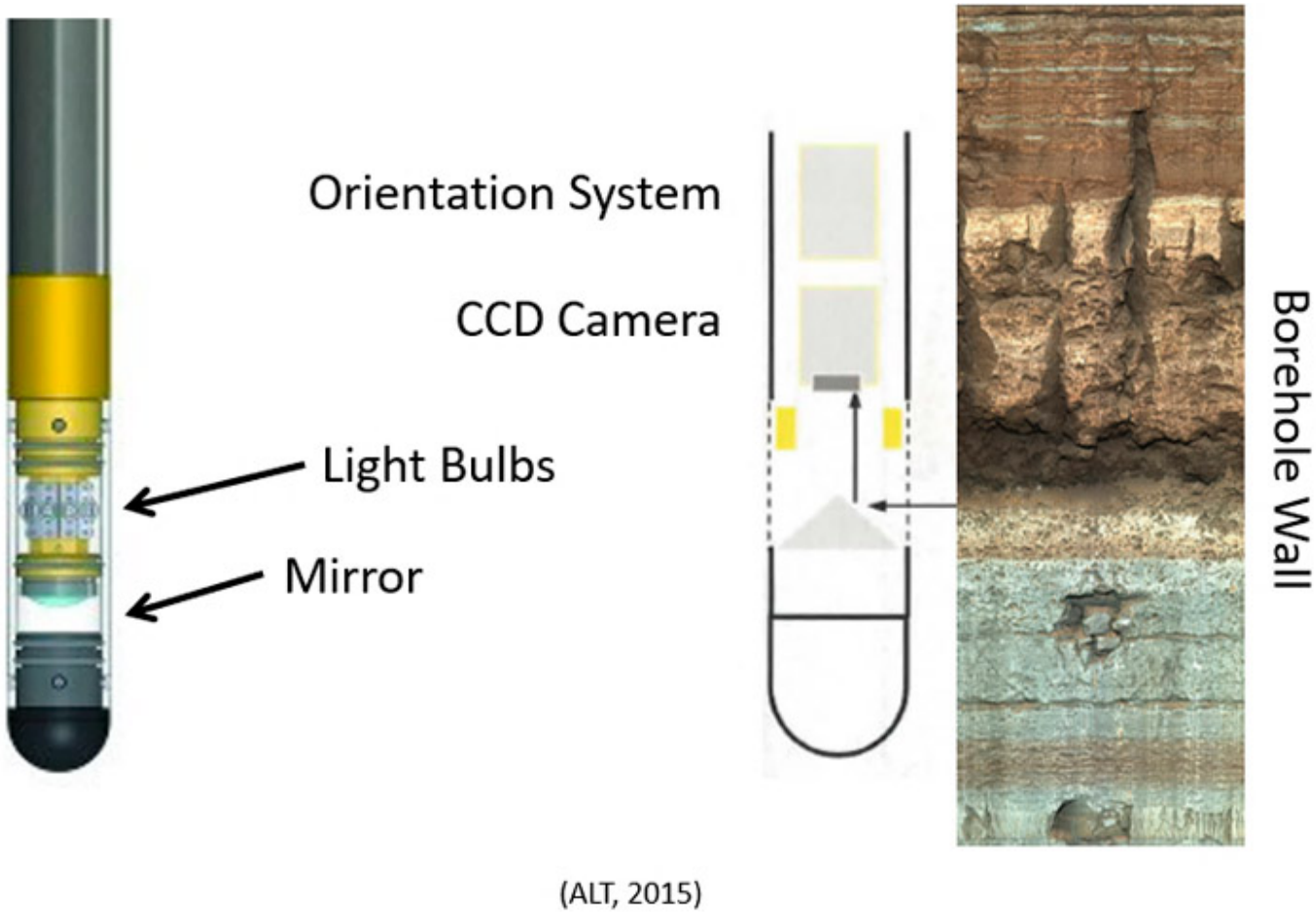

Figure 4-6. Optical televiewer.
Source: Mount Sopris Instruments, Used with permission

The OTV and ATV (discussed in Section 4.6) probes are used during borehole investigations to produce vertically continuous, static images representing conditions at the borehole wall and cased interval in a well.

4.5.1 Use and Application

The OTV tool can be deployed in air- or water-filled open boreholes to assess consolidated formations or in wells completed with screen and casing to evaluate the general condition of the well. The OTV provides a photographic image that is used to assess formation properties such as stratigraphic bedding, contrasting lithologies, and geologic contacts. Fractures are often easily discernable and can reflect regional interpretations involving joints or faults as well as washed out or karstic zones. OTV logs may provide an indicator of groundwater flow within a borehole based on evidence of oxidative staining. If the borehole has been impacted by NAPL, stains or residues from these contaminants may also be observed.

4.5.2 Data Collection Design

The quality of OTV data obtained within the water-filled portion of the hole varies significantly with turbidity. As such, logging should be planned to allow time for suspended materials to settle following disturbances resulting from drilling activities or pump removal.

Chemical precipitation and biological growth may obscure features on the borehole wall; therefore, redevelopment may be appropriate to ensure the best possible image quality in older wells.

In situations where the hole is first cored and subsequently reamed, the smaller-diameter core hole may provide a better OTV (or ATV) image, depending on many factors including lithology and drilling characteristics. In some circumstances (such as soft rocks that may be eroded by drilling-fluid movement during coring), a rapidly drilled air-rotary hole yields a smoother borehole and a superior image. Consulting with the geophysical logging and drilling contractors during project planning can help identify the best approach at a particular site.

OTV logging speed is dependent on the selected vertical and horizontal resolution and the system design and cable type. Typical logging speeds for early-generation OTV systems were on the order of 1 m/min (3.3 ft/min) (Williams and Johnson 2004), while the latest generation of tools can be run at 2 m/min to 5 m/min (6.6 ft/min to 18 ft/min) or higher (ALT 2015).

Color calibration can be achieved using calibration kits supplied by the manufacturer of the OTV probe. The magnetometer and accelerometers are factory calibrated. Field checks on the magnetometer can be made using a compass and oriented cylinder (Williams and Johnson 2004).

4.5.3 Log Interpretation

Structural interpretations generated based upon OTV (and ATV logs) are sensitive to conditions such as borehole deviation and variations in diameter. Borehole deviation, the departure of the borehole from vertical (measured in degrees), and the concepts of apparent dip vs. true dip are illustrated in Figure 4-7. Obviously, a probe run in a deviated borehole does not provide accurate dip (relative to horizontal); therefore, during log processing, deviation measurements collected by orientation sensors within the OTV (and ATV) probe should be used.

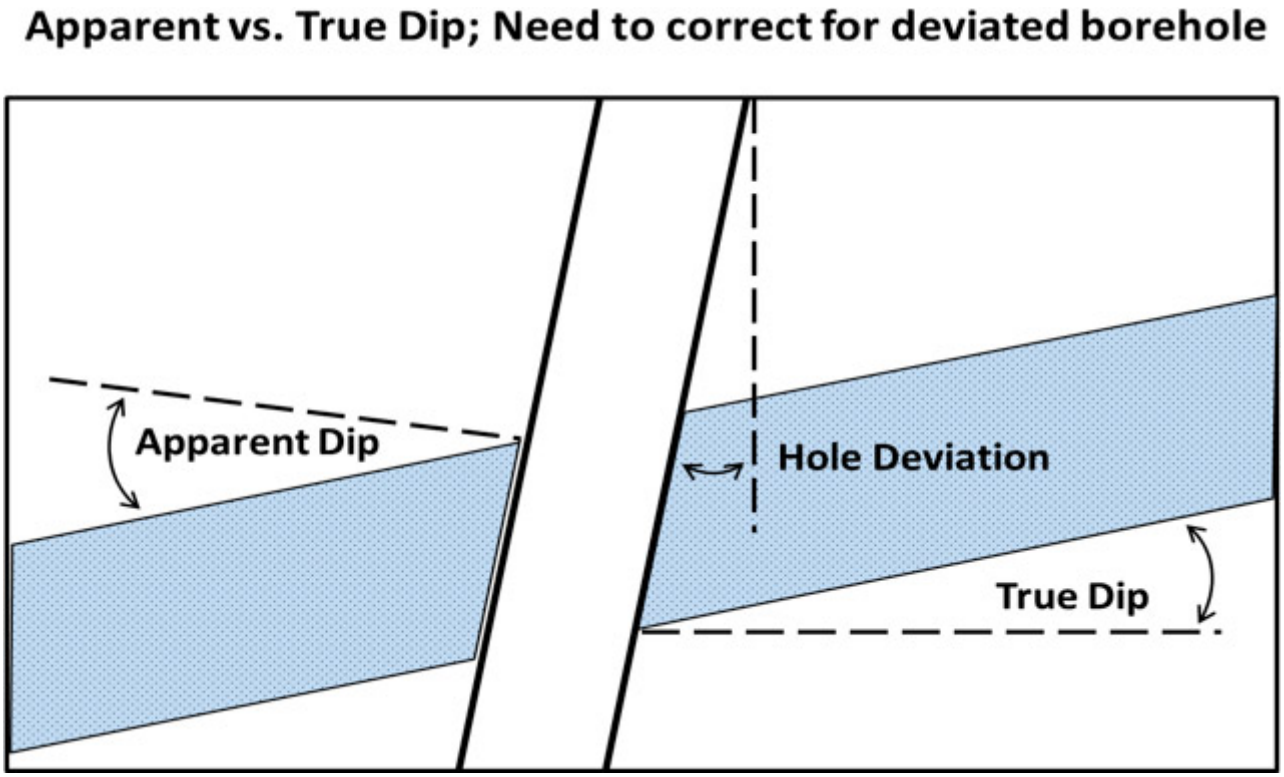

Figure 4-7. Illustration of concepts of apparent dip vs. true dip.
Source: (Peterson 2017), Used with permission

4.6 Acoustic Televiewer

The ATV uses pulses of ultrasonic acoustic energy to generate an image of the borehole wall. A fixed transducer creates high-speed pulses that are directed to a rotating surface or acoustic mirror within the probe. Energy reflected off the mirror travels through the borehole fluid to the borehole wall. Some of the energy reflects back to the mirror and is reflected to a transducer, where it is detected (see Figure 4-8). For each reflected pulse, the amplitude and travel time are recorded. Amplitude is a measure of energy retained in the returning pulse; low amplitudes indicate loss of energy at the borehole wall as a result of soft or fractured rock. Higher amplitudes suggest harder, unfractured rock. Travel time is proportional to distance traveled by the acoustic pulse; where the borehole fluid density is known, borehole diameter can be accurately determined and an acoustic caliper log generated.

The ATV collects up to 360 pairs of amplitude and travel time measurements in each circumferential scan as the tool is moved vertically along the path of the borehole. The vertical spacing between scans is dependent upon tool speed inside the borehole; acquisition software guides selection of logging speed to provide optimal horizontal to vertical resolution. As with the OTV, data are collected by orientation sensors (a magnetometer and accelerometers) within the tool. Acquisition and processing software are used with data from the orientation sensors and the transducer to produce accurate, precisely

oriented cylindrical images of the amplitude and travel time (see Section 4.6.4).

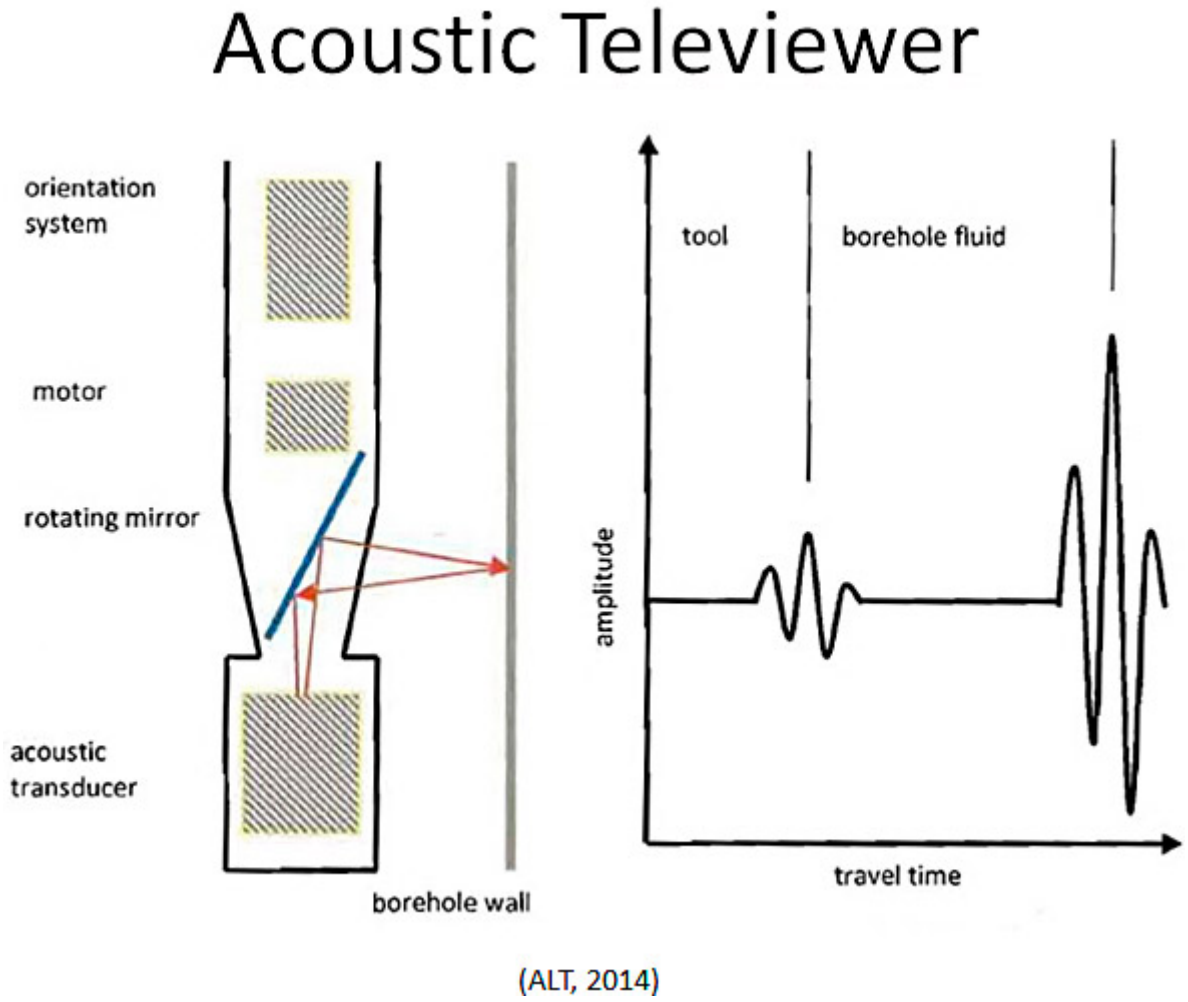

Figure 4-8. Acoustic televiewer.
Source: Mount Sopris Instruments, Used with permission

4.6.1 Use and Application

The ATV is deployed within fluid-filled portions of boreholes, where the fluid (water or drilling mud) transmits the acoustic energy needed to generate the borehole record. The ATV is most commonly used in open boreholes where it is used to assess competent, consolidated formations and provide acoustic caliper and virtual core logs. In addition to the basic elements used for other geophysical logging (winch and wireline, data acquisition unit, field computer with monitor), metal- or plastic-band centralizers are installed on the probe to guide the probe along the central axis of the borehole to maintain consistent proportionality. Use of centralizers also on the tools helps provide accurate estimates regarding the strike and dip of planar and subplanar features. With appropriate processing, the ATV may also be used to evaluate the thickness and corrosion of the steel casing and to assess less competent consolidated formations prone to collapse when a centralized polyvinyl chloride (PVC) liner is emplaced within the borehole. ATV logs are also routinely used to assess casing or well screen conditions.

Consistent with the OTV, the ATV provides an image-based output of the borehole wall that is used to interpret stratigraphy, lithology, and the presence of geologic contacts. Evidence of subsurface fracturing as well as washed out zones in karst environmentas is also possible based on acoustical differences across void spaces.

4.6.2 Data Collection Design

A key comsideration during ATV deployment is the project requriements for vertical and horizontal resolution of the borehole image; this resolution is greatly dependent on logging speed. Typical logging speeds for early-generation ATV systems were on the order of 1 m/min (Williams and Johnson 2004); the latest generation of tools can be run at 2 m/min to 5 m/min or higher (ALT 2015). Acquisition software should be used to evaluate and adjust logging speed as logging proceeds.

Prior to initiating ATV logging, factors such as the borehole fluid type and level as well as the borehole condition should be considered. In general, a better ATV record is obtained in a borehole filled with water instead of drilling mud, so flushing the hole clean before logging may be desirable. Also, adding water to the borehole may allow portions of the borehole above the static water level to be logged, especially for hole completed in low-transmissivity units.

Probe centralization is especially important for good-quality image data and accurate structure orientation during ATV logging. Decentralization on ATV images is indicated by vertically striped transit-time and amplitude images, as shown on Figure 4-9. Adjustable centralizers should be deployed based upon inspection of a mechanical caliper log. Using adjustable centralizers provides a more direct representation of actual borehole diameter compared to the nominal diameter of the tool used during borehole advancement.

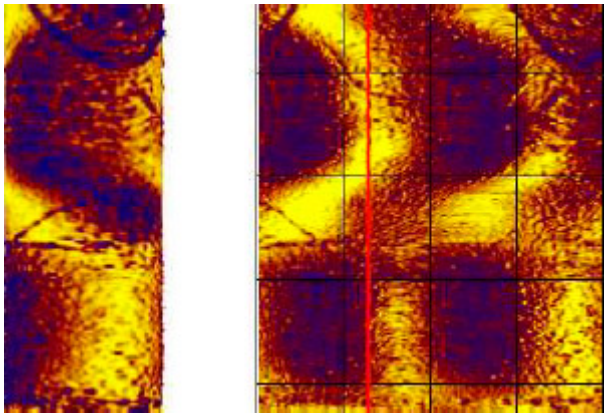

Figure 4-9. Decentralized acoustic image.

Magnetometer and accelerometers are used to provide data on tool orientation during logging. The magnetometer and accelerometers are factory calibrated. Field checks on the magnetometer, however, can be made using a compass and oriented cylinder (Williams and Johnson 2004).

It is important to note that the presence of the steel casing interferes with image orientation. (Williams and Johnson 2004) noted that imaging in a fractured-rock aquifer borehole just below the base of steel surfacing casing is important. Because the magnetometer is affected by steel casing, the interval between the steel casing and borehole plus some overlap should be rerun with the magnetometer turned off. Then the rerun image is matched and spliced into the oriented image for the rest of the borehole.

4.6.3 Log Interpretation

ATV logs are postprocessed using specialty software to quantify the orientation of features identified on the recorded image. The precise orientations of planar features (for example, fractures, sedimentary bedding) identified by the log analyst may be determined and presented in a variety of formats.

To facilitate structural analysis (see Section 4.6.4), the cylindrical image is presented in an unrolled format, cut vertically at North (true or magnetic) and rolled out from left to right, often with vertical lines representing N (at the left), E, S, W, and N (again at the right). In this format, planar features such as fractures intersecting the borehole wall, follow sinusoidal traces, as shown in Figure 4-10.

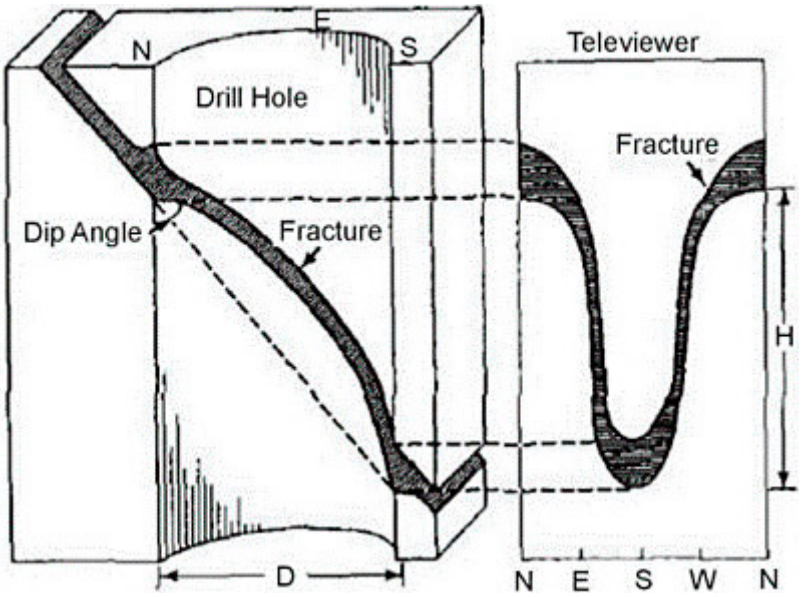

Figure 4-10. Planar features such as fractures intersecting the borehole wall follow sinusoidal traces.
Source: (USACE 1995), Figure 7-30

Structural interpretations generated based upon ATV (and OTV logs) are sensitive to conditions such as borehole deviation and variations in diameter, previously summarized in Figure 4-7. As illustrated in Figure 4-11, where planar features intersect a portion of the borehole with an enlarged diameter, a correspondingly higher-amplitude feature trace results on the sinusoidal structure plot. As a result, if corrections are not made to properly account for the off-gauge condition of the borehole, dips will always be overstated through caving or soft-rock intervals where the hole diameter is enlarged. Experience shows that even a 1-inch enlargement of hole diameter can result in overstatement of dip by several degrees, which is further supported by trigonometric principles. The correction requires reference to a continuous log of borehole diameter (mechanical or acoustic caliper); therefore, either mechanical caliper or ATV logs should also be run when OTV is used to evaluate structure.

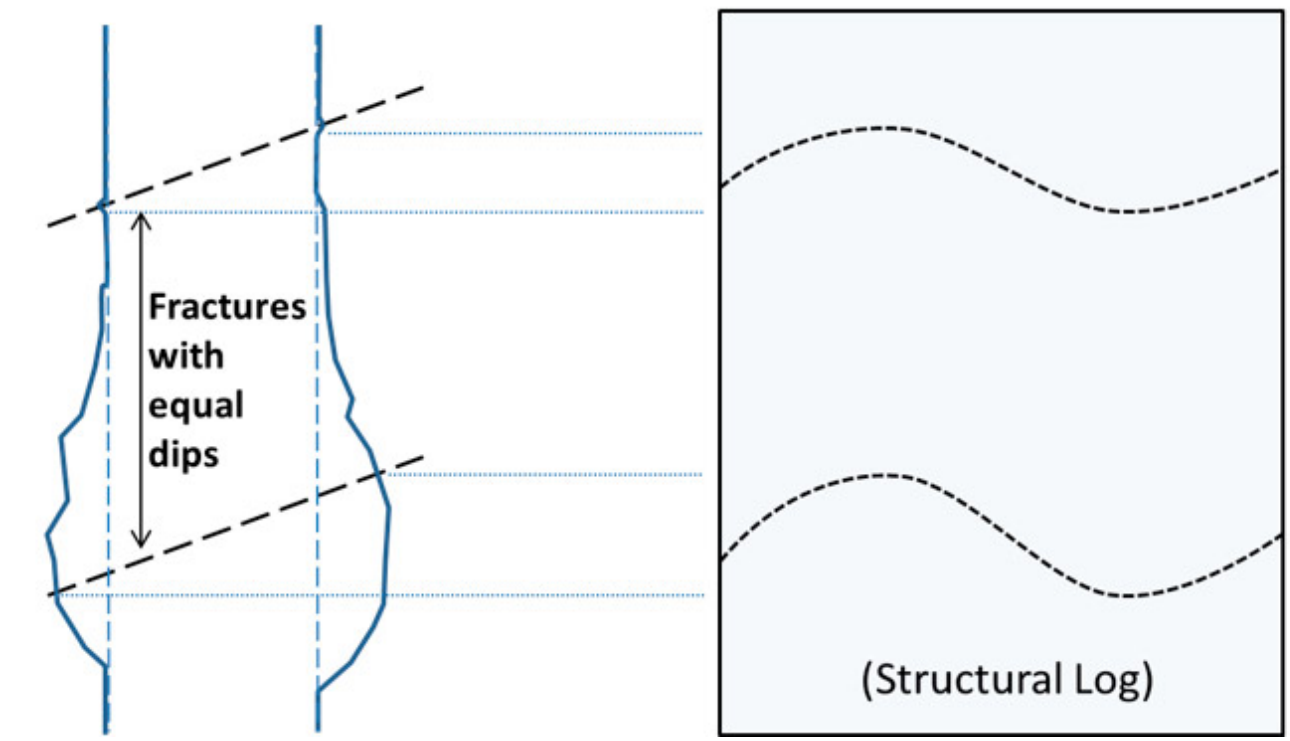

Figure 4-11. Illustration of greater amplitude in washout interval overestimates dip; correction for increased borehole diameter.

Source: (Peterson 2017), Used with permission

While somewhat time consuming, employing these corrections during log processing is necessary to provide results that are accurate and comparable between locations at a site. While the incremental accuracy provided may seem minor, common uses of geophysical logging data imply otherwise. As shown in the down-dip well siting example illustrated in Figure 4-12, dip error as small as 1 degree can result in a typical (10-foot long) monitoring well screen being placed incorrectly, missing the intended monitoring zone. With >5 ft of error in vertical placement, a fracture meant to be located midscreen would be entirely missed at the down-dip location. Therefore, when procuring geophysical logging services, service providers should present the steps that are taken to ensure data quality.

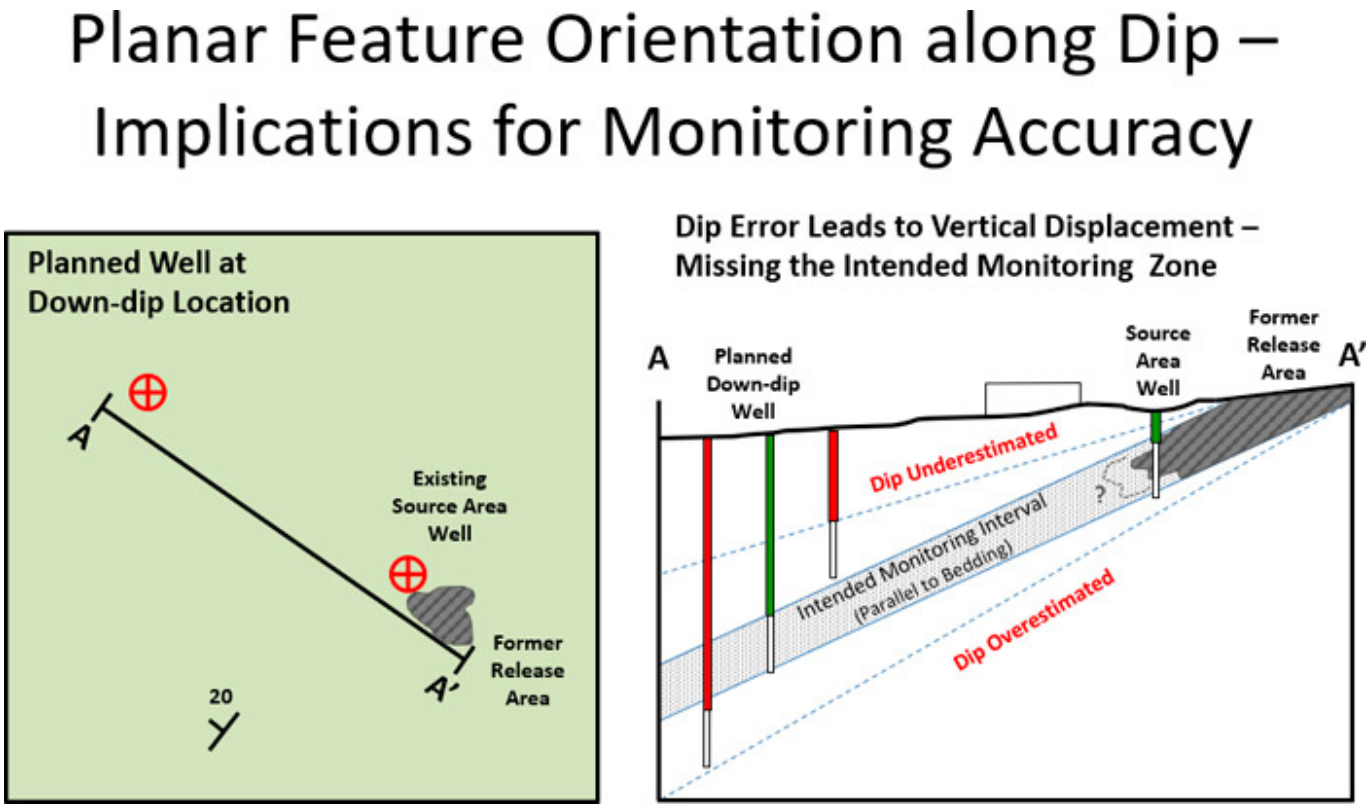

Figure 4-12. Down-dip well siting example (left); planar feature orientation along dip and implications for monitoring accuracy (right).

Source: (Peterson 2017), Used with permission

4.6.4 Virtual-Core Presentation of OTV and ATV Logs

As previously indicated, OTV and ATV probes include orientation sensors (magnetometer and accelerometer) to translate borehole wall images into a 360°, wrapped image referred to as a virtual core. This presentation format provides a consolidated and simplified image of conditions that are useful during log interpretation. Similarly, advances in postprocessing software used to develop virtual cores also allow these logs to be presented adjacent to strip logs from other tools. This section outlines the technical complexity associated with translating borehole images into 2-D projections and key details about presenting structural information.

4.6.4.1 Uninterpreted Data

Using processing software, oriented, uninterpreted image logging data can be presented in several formats, each represented as a single column on the well log. These include the unrolled, virtual-core, and slab-core logs. The unrolled format (see Figure 4-13) shows the borehole image, cut vertically at North (true or magnetic) and rolled out from left to right, often with vertical lines representing N (at the left), E, S, W, and N (again at the right). In this format, planar features such as fractures intersecting the borehole wall follow sinusoidal traces. During interpretation (discussed subsequently), these traces allow the log analyst to determine the attitude (orientation) of the planar features. The low point of the sinusoid corresponds to the compass direction (azimuth) of the dip for the planar feature, while the amplitude (peak to trough distance) is directly proportional to the magnitude of the dip.

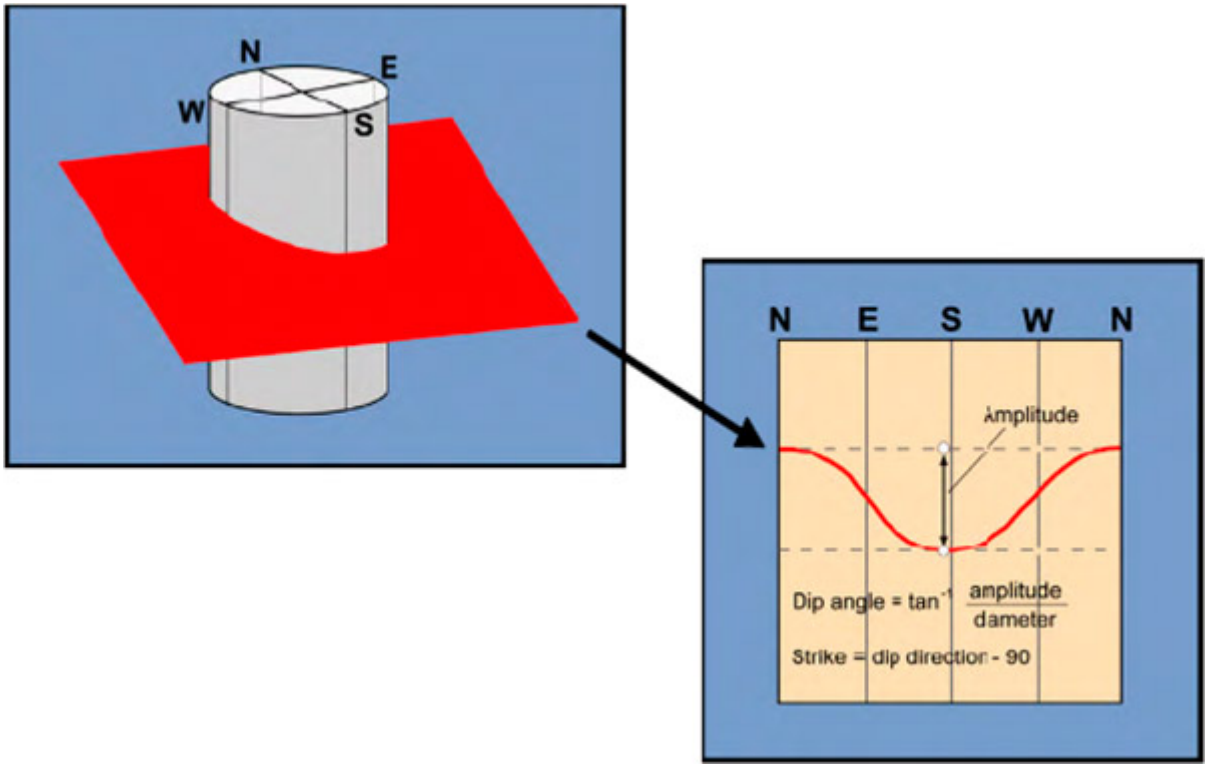

Figure 4-13. Unrolled format shows the borehole image, cut vertically at North and rolled out from left to right, often with vertical lines representing N (at the left), E, S, W, and N (again at the right).
Source: (Weston 2014)

The virtual-core format for OTV or ATV provides a pseudo-3-D view of the borehole as viewed externally. When viewed in the processing software, the core-like image may be rotated to view from all directions. The slab-core format depicts features evident on the viewed side of the borehole as they would appear projected onto a flat surface, mimicking the expected appearance of a slabbed-core or outcrop view. As with the virtual-core format, the slab core is typically shown in reports oriented based either on prevailing structure or arbitrarily aligned (for example, toward North).

4.6.4.2 Interpreted Structure Logs

A log analyst may use the image log output and processing software to prepare interpretive logs, such as a structure log depicting the attitude (strike and dip, or dip/dip azimuth) of each planar feature identified. Commonly, the log analyst uses the output of the image-logging probes (and other probes, discussed below), processing software, and significant professional judgment to prepare an interpretive structure log depicting the attitude of each planar feature. The structure log is usually presented as a plot of colored sinusoidal lines over or next to a copy of either the unrolled OTV or ATV logs, along with accompanying tadpole plots and notes. Tadpole plots represent the azimuth and magnitude of the dip of planar features as follows: dip azimuth is shown by the compass direction in which the tail on the tadpole is pointing, and dip magnitude is shown by the left-to-right position in which the tadpole is placed on a scale from 0° to 90° of dip. Notes are used to describe key features of the well, including the attitude (orientation) of planar features, such as interpreted sedimentary bedding and fractures. An example of a structure log (incorporating both OTV and ATV) is shown in Figure 4-14.

These interpretive logs incorporate significant judgments made by the log analyst, often considering data from more than one logging tool. For example, if both OTV and ATV are used, both are considered when developing the structure log. If the structural-feature classifications employed by the log analyst make reference to apparent capacity of a feature to yield water to the well, the interpretive log depicts the apparent water-yielding fractures or intervals. The analyst's interpretation is based on considering not only the tools used to create the structural log, but also those indicative of potential fluid movement (fluid temperature, fluid resistivity, and heat-pulse flowmeter).

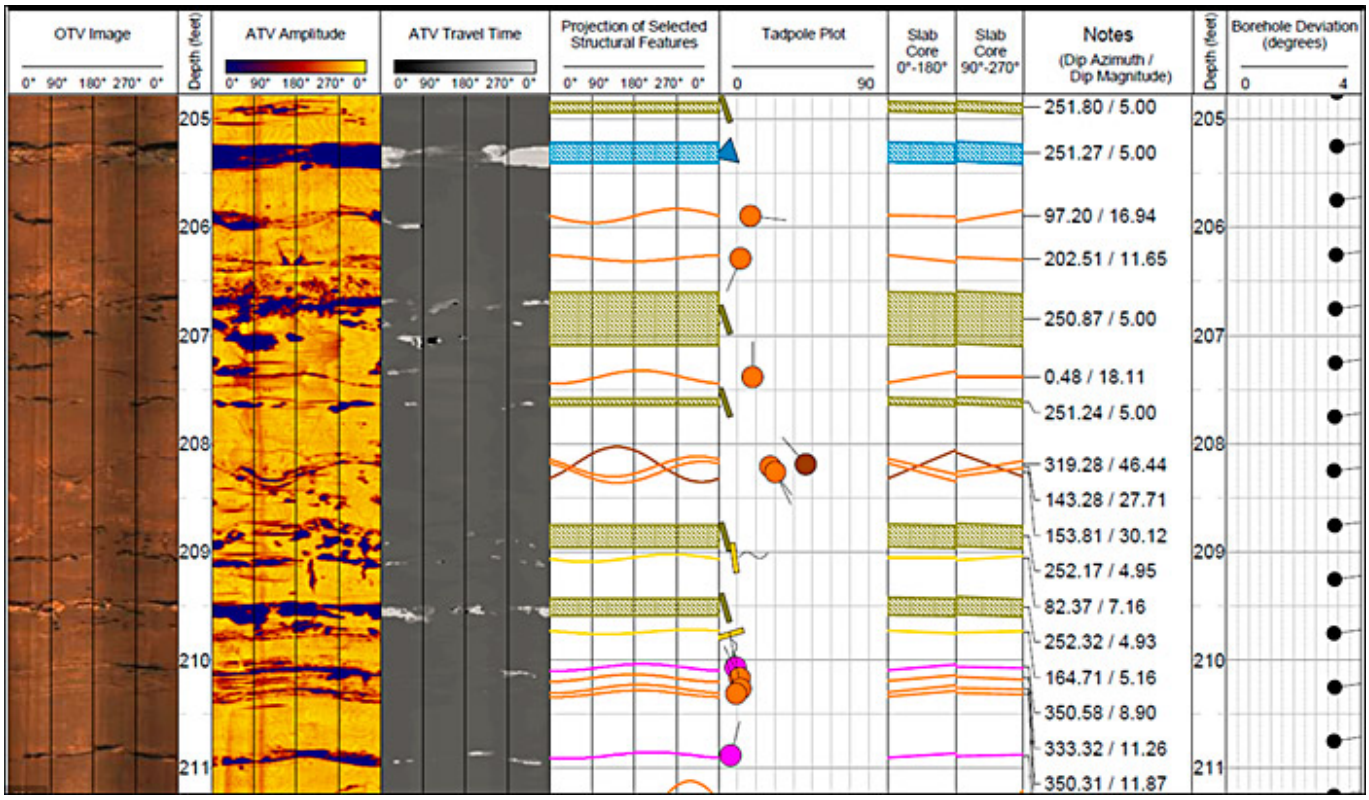

Figure 4-14. Example of a structure log (incorporating both OTV and ATV).
Source: (Peterson 2017), Used with permission

Planar-feature orientation is described using the dip azimuth, dip magnitude convention. The dip azimuth is the compass direction (measured from true north) pointing toward the direction of maximum dip. The dip magnitude is the angle down from horizontal of a line in a planar feature pointing down dip. For example, a designation of 316, 12 refers to a planar feature whose maximum dip is 12° from horizontal, pointing toward azimuth 316° degrees (in the northwest compass quadrant). Colors selected for plotted sinusoids and tadpoles correspond to the specific feature classifications applied by the log analyst.

Structure plots showing lower hemisphere, equal area (or Schmidt) stereonet plots of dip azimuth for interpreted planar features may also be provided, either in a column of the structure log or on separate pages, employing the same feature classification color scheme. When plotted on the structure log, the stereonets can be shown to represent populations of planar features occurring within individual depth intervals (perhaps corresponding to lithologic units). In Figure 4-15, four separate stereonets are provided to show all features interpreted as bedding, banding, or foliation (left column); all identified fractures (center column, top); inferred bedding-parallel fractures (in this case, those fractures with orientations within +/-25° of the bedding dip azimuth and within +/-3.5° of expected bedding dip based on area geological mapping – center column, bottom); and a Rose plot showing dip azimuths of all fractures interpreted from the ATV logs (right column).

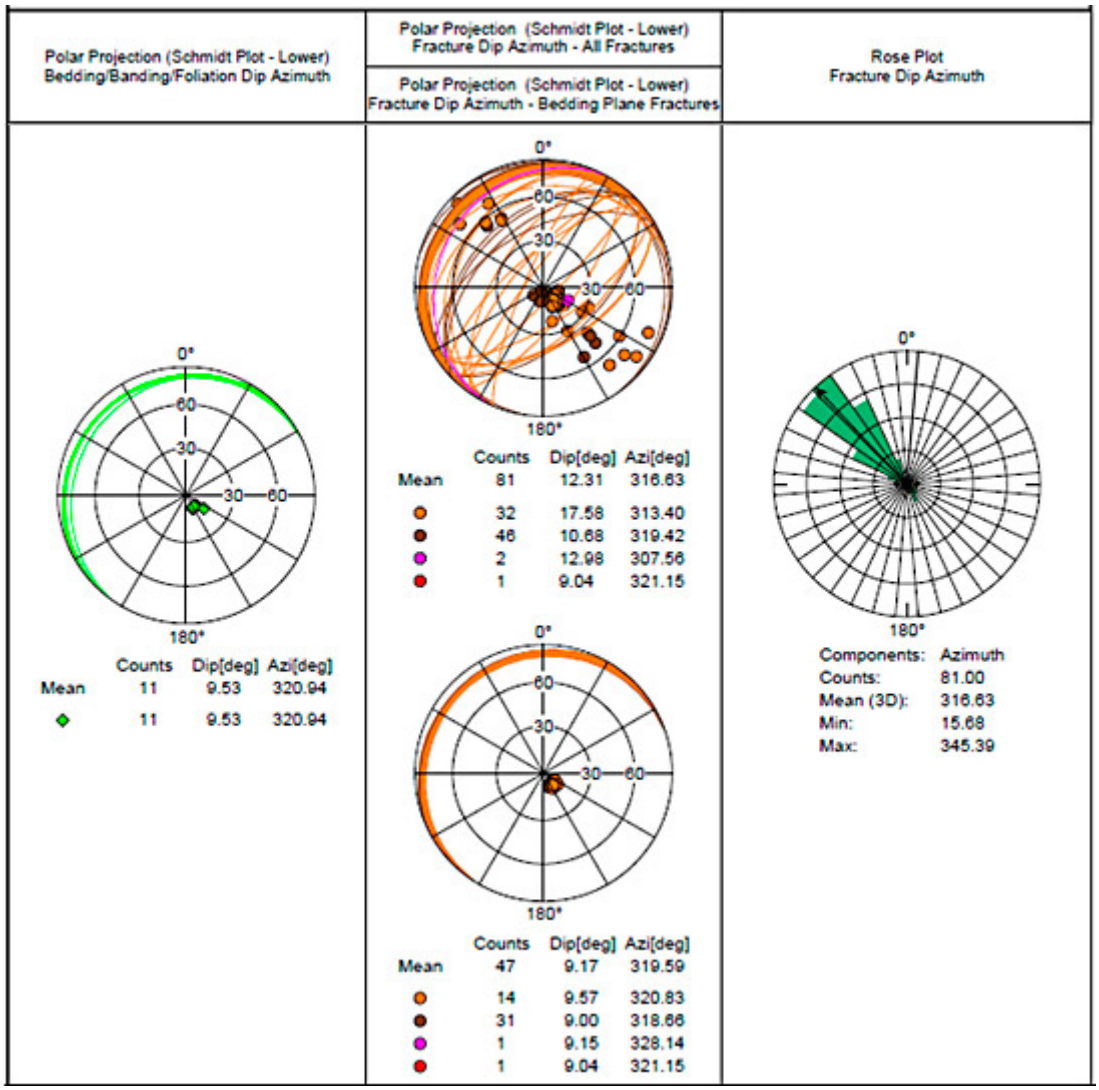

Figure 4-15. Example stereonet plots commonly used to represent conditions throughout the borehole.
Source: (Peterson 2017), Used with permission

Geologists have devised a number of plotting conventions to graphically depict bedrock fabric data and allow for statistical evaluation of these data. The two types used by most geophysical service providers include the compass rose and stereonet plots. The compass rose (shown above at right) shows the strike of a planar feature on a 360° circular compass. The number of measured planes that fall within a specified azimuth arc (typically, every 10°) is indicated by the length of the colored pie-shaped ray comprising the azimuth range. A compass rose plot does not specify planar dip and is therefore a 2-D depiction. The value of this display may be lessened for shallow-dipping or subhorizontal features.

Three-dimensional planar attitudes are represented on a stereonet diagram whereby a line bisecting a plane is shown as a single dot (or pole) projected onto a lower hemisphere. The lower hemisphere is constructed with both compass and angular dip angles represented by lines of latitude and longitude. Equal area stereonets are constructed to contain an equal projection area for each angular field represented by all possible planar orientations. This construction allows the determination of planar orientations by statistically analyzing pole density plotted in a given stereonet cell. Thus, a steeply dipping plane is represented as a single dot near the perimeter of the circular stereonet plot, and the planar strike is normal to the compass heading of the dot. Conversely, a flat-lying plane is plot near the center (or south pole) of the stereonet projection.

It should also be noted that most geophysical service providers report planar orientation from OTV and ATV logging in a dip-azimuth and dip-angle format. Dip azimuth is perpendicular to planar strike and requires data conversion to present the orientation of the plane as a standard strike and dip symbol typically used on geologic maps.

4.6.4.3 Key Considerations for Virtual-Core Interpretation

The familiar (image) format of OTV and ATV logs can lead to errors or misuse when inexperienced users become

overconfident. Common problems include:

- assuming that fracture aperture evident in the borehole image is the same as in undisturbed formation (damage during drilling tends to enlarge fractures at the borehole)
- assuming that all thin, planar features are fractures (while comparison to other logs may reveal them to be filled)
- assuming that all apparently open fractures are hydraulically conductive (while comparison to fluid or HPFM logs may indicate otherwise)
- failing to apply QC measures (for example, not correcting for vertical deviation or borehole diameter), resulting in structure log data of unknown accuracy

When adjusting raw magnetic north data to true north for log presentation, the log analyst must be careful to ensure that the correct direction for the adjustment is applied. It is easy to make the mistake of applying the correct magnitude of declination but wrong direction (introducing dip-azimuth error equal to twice the magnetic declination). Therefore, checking dip-azimuth data against what is known from other on-site or regional studies is always a good idea.

Other considerations relate to how the image log (and other log) data are used in the overall site assessment. The first consideration pertains to the underutilization of geophysical logging data. At times, multiparameter logging projects are conducted at numerous wells on a site, but the resulting data are used only for limited purposes (for example, to support packer testing or well-screen placement). Project objectives in these cases are further advanced by correlating log results between wells to develop a sitewide framework. The second consideration relates the scale of the site and problem at hand. Structural data collected at single location may be suitable to evaluate a small site (for example, a small BTEX plume at an UST site). Investigating more complex conditions over a larger area (for example, chlorinated VOCs plume at a DNAPL site) may warrant a sitewide evaluation that employs multi-well log correlation and three-point structural evaluations. In this case, a structure log from a single borehole probably is not sufficient to characterize the aquifer matrix.

When analyzing data derived from distinct sources or methods, the genesis and population of the data should be considered. A typical outcrop study may result in a dozen or less measurements of planar features over a moderately sized area whereas a single borehole can generate 50 or more such data points from a single point on a site plan. Conversely, it is important to consider that a vertical boring is less liekley to intersect vertical and steeply dipping fractures than horizontal and shallow dipping fractures present within the bedrock formation that may be readily observable in an outcrop. Mixing these data types produces results skewed toward the borehole data, overpowering field measurements and making distinctions difficult to recognize. Other situations may arise where vertical changes in a borehole (such as formation change, fault) may result in distinct data populations from a single borehole. In both cases, the distinct datasets should be analyzed separately to evaluate results and collectively identify similarities and differences in the datasets. These decisions regarding data analysis can be somewhat subjective and require informed expertise regarding the regional and local site geology and data procurement methods.

4.7 Natural Gamma Logging

Gamma logging uses a passive detector lowered in a borehole via wireline to measure natural gamma radiation in the borehole. Gamma radiation is emitted from common radioisotopes, primarily potassium-40 and daughter products of uranium and thorium decay, which are useful indicators of lithology. The strength of the natural gamma radiation decreases with distance from the borehole wall. Thus, the larger the diameter of the borehole, the lower the resolution of the natural gamma log.

Earth materials have varying amounts of naturally occurring gamma emitters. Potassium-40 and, to a lesser extent, uranium and thorium tend to be more concentrated in clays and fine-grained materials. Clean silica sands generally contain few gamma emitters. Many factors affect the radioactivity of soil and rock materials and need to be considered when interpreting gamma logs. Sands that contain high amounts of potassium feldspar emit higher gamma radiation due to the potassium content. The potential for uranium deposition in certain regions and environments must also be considered when interpreting logs.

4.7.1 Use and Application

The most common application of gamma logging is for lithologic characterization and stratigraphic correlation. Gamma-logging results are objective and repeatable, and, when viewed in vertical profile, stratigraphic information can be derived and used to develop CSMs through characteristic curve-matching and cross-borehole correlations. Where clay minerals

contribute to a significant portion of the gamma response, gamma logs can be used to estimate the fraction of clay present, represented by the clay volume divided by the total rock volume.

In igneous and metamorphic rocks, gamma response is generally dependent on minerals in the rock, although water-bearing fractures can exhibit high gamma response due to the precipitation of uranium or other radioactive minerals along fracture walls. Under certain circumstances, gamma logs can be a good indicator of water-bearing fractures.

Key considerations during gamma logging are logging speed and distance from the source to the detector. Based on background conditions, logging speeds can be optimized to observe variations between clay-bearing and clean sandy soils. Slower logging rates may be required to obtain a higher resolution of data across a site and identify smaller variations in lithology; higher logging rates, which increase the footage rate of data collected, may be sufficient to characterize geologic lenses that are of greater thickness. A consistent borehole diameter is optimal in reducing the variability caused by the distance between the detector and the soil matrix. Gamma logging should always be accompanied by a caliper log when logging in open boreholes. The accompanying caliper logging is used to identify potential variabilities of the borehole wall diameter that might impact data quality. A centralizer is also recommended to keep the gamma detector within the center of the borehole. Where borehole washouts are present, the gamma response is reduced regardless of soil or rock type.

4.7.2 Data Collection Design

Gamma logs are acquired in a similar manner as most other borehole geophysical logs but do not require fluid-filled boreholes or casing. When logging in existing monitoring or extraction wells, certain well construction features that could affect data quality, including the original borehole diameter, annular fill outside the casing, and casing material, should be considered. Smaller borehole and casing diameters provide higher-quality results with better vertical resolution.

As with other borehole geophysical tools, logging at a single location provides parameter data only in the immediate vicinity of that location. By logging multiple locations, data can be correlated over greater distances and provide 2-D (cross-sectional) and 3-D conceptual models. The density of well locations to be logged should be based on the stratigraphic framework and the nature of features that the investigation is attempting to resolve.

4.7.3 Log Interpretation

Gamma log data are usually processed and can be displayed in real-time. Geophysical reports may present the gamma logs for different borings on different response scales for counts per second, especially if logging occurs over multiple field events. When interpreting gamma responses and correlating logs between boreholes, verify that the response scaling is the same. Some geophysical contractors color code the response curve with a filled hatch pattern, which can be useful for rapid visual correlations, but misleading if the response scalings differ. Data interpretation is straight forward as shown in the example log displayed below (see Figure 4-16). Other example logs are available on the USGS Geophysical logs – gamma logs webpage (USGS 2000a).

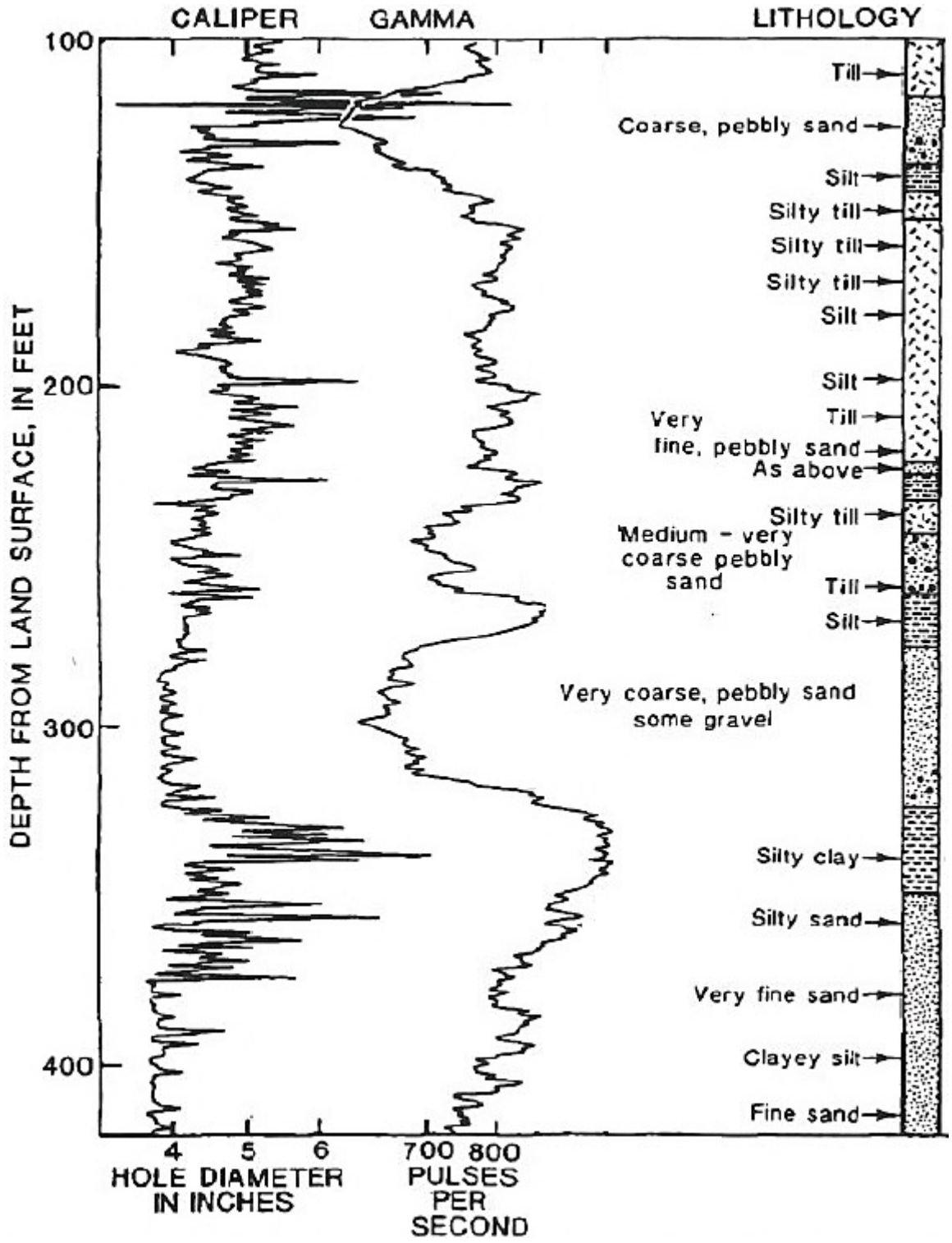

Figure 4-16. Example gamma log output with caliper log and lithology.

Source: Adapted from (USACE 1995), Figure 7-8

4.8 Borehole Flow Meters

Understanding flow within the subsurface is a critical component of any CSM. Historically groundwater potentiometric surface maps have been used to illustrate hydraulic-head differences across a site and aid in the interpretation of lateral flow within the subsurface. In addition, setting a group of wells at a location with the screens of the individual wells set at varying depths (for example, a well cluster) can provide a general understanding of vertical hydraulic gradients within and between different aquifers present at a site. The use of specialty tools that allow for the direct measurement of flow within the borehole can supplement this information and provide a flow-measurement rate as opposed to simply a change in hydraulic head.

4.8.1 Heat-Pulse Flow Meter Logging

The HPFM measures the vertical direction and rate of groundwater flow in an open borehole completed in bedrock. The HPFM uses a pulse of heated water to detect vertical groundwater flow, hence the name of the tool. The HPFM is run after the borehole has been completed to depth and flushed of cuttings and other logs have been run and analyzed to select potentially transmissive features (targets) in the borehole (for example, fractures, bedding planes, joints). The HPFM works as follows (see Figure 4-17):

- The HPFM is run in the water-filled interval of an open borehole.
- The instrument is positioned at a station above or below a target and held stationary in that position until the test is completed. Care must be taken by the operator when selecting a station to position the instrument close to the target and in a section of borehole wall where the diverter can form a good seal with the borehole wall.
- A diverter with a diameter flush with the borehole wall channels vertical groundwater flow through the instrument.
- The instrument is triggered by the operator and an electric element in the center of the instrument rapidly heats up a small volume of water to generate a pulse of heated water.
- Vertical groundwater flow carries the heated water up or down where it is detected by thermistors positioned above and below the heating element.
- After data are collected, the reading can be repeated or the instrument is moved to the next station.

Heat-pulse data are collected in the borehole under ambient, or natural, flow conditions and then under pumped conditions. Under pumped conditions, a submersible pump is installed in the well near the top of the water column and run at a low flow rate, typically about 1 gallon per minute (gpm). This flow rate allows the head in the borehole to change yet remain stable. The HPFM log is then repeated at the same stations as the ambient flow log. The developed from the pumped conditions may identify transmissive features that were not detected by the ambient log because the head in the borehole and the fracture were the same under ambient conditions.

Data are typically only collected in one direction. The HPFM is run alone and not in combination with other probes.

4.8.1.1 Uses

The value of the HPFM is that its resulting data reveal features in the borehole that are transmissive, that is, where water is entering and exiting the borehole. HPFM data also reveal the relative head distribution in the borehole. For example, features where water is entering the borehole have a higher head than features where water is existing the borehole (see Figure 4-17f). This information, coupled with data from other logs, is used to define the site geologic framework, the hydrogeologic framework, and groundwater contaminant migration pathways.

4.8.1.2 Tool Availability

A heat-pulse flow meter is pictured in Figure 4-17. The diameter of this tool is about 50 mm (2 inches); it is about 1.2-m (48 inches) long and weighs about 5 kilograms (12 pounds). The typical flow measurement range of this instrument is 0.03 gpm to 1.0 gpm (0.113 L/m to 3.785 L/m). The HPFM requires centralization and uses a diverter to channel vertical flow in the borehole through the body of the instrument (see Figure 4-17). A geophysical logging contractor performs HPFM logging due to the specialized nature of the HPFM and the expertise and experience required to use the associated software.

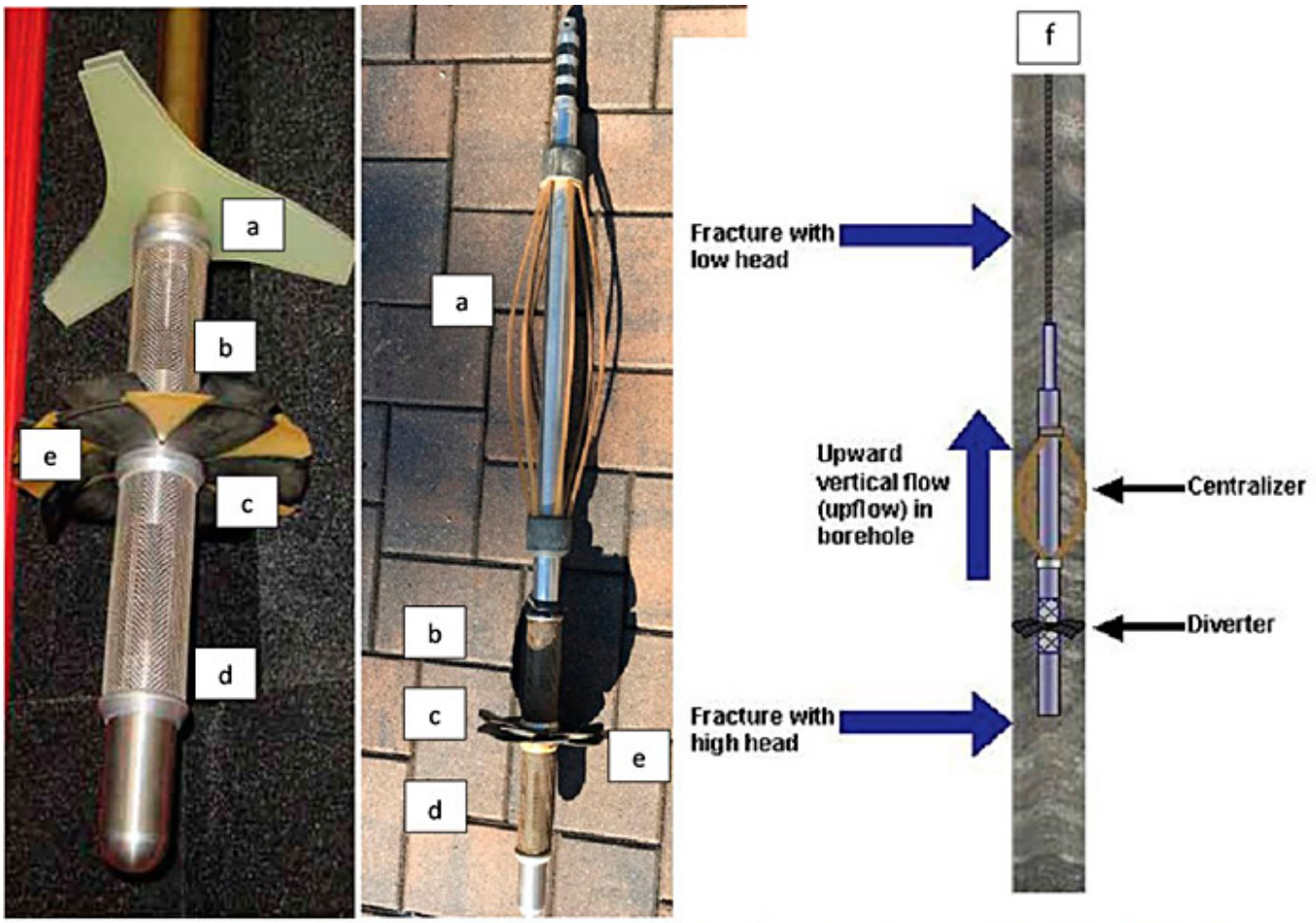

a) Centralizer, b) upper thermistor chamber, screened to allow water to pass through it, c) flexible diverter petals (channel flow through the HPFM), d) lower thermistor chamber screened to allow water to pass through it, (e) heating element located in the center of the HPFM body, and (f) HPFM measuring upward vertical flow in an open bedrock borehole.

Figure 4-17. HPFM.

Source: Left and right images -(USGS 2016b); middle image: Robert Garfield, Hager Richter Geosciences, Used with permission

4.8.1.3 Technical Advantages and Limitations

Compared to other logs that provide an image of the borehole wall or measure the physical properties of the formation, the technical advantage of the HPFM is that it measures the direction and rate of vertical groundwater flow in the borehole. This, coupled with data from other logs, can be used to define the site geologic framework, the hydrogeologic framework, and groundwater contaminant migration pathways.

The limitations of the HPFM are that it detects the most transmissive features in a borehole due to its range of operation. The minimum flow rate it can detect is about 0.03 gpm; therefore, a reading of zero flow should be interpreted as flow <0.03 gpm. It is important to note that transmissive features may be present outside the range of detection of the HPFM. Likewise, the maximum flow rate the HPFM can detect is about 1 gpm, which is sufficient for many site investigations. (A spinner flow can be used to measure higher flow rates; see Section 4.8.2) Another limitation of the HPFM is associated with the diameter of the borehole. Because flow must be diverted through the instrument, it is best to conduct the log in boreholes ranging from 4 inches to 8 inches in diameter.

4.8.1.4 Quality Control

QC when using the HPFM consists of the following elements:

- Before, during, and after use, document that the instrument is working and accurately measuring flow. To test operation, position the HPFM near the top of the water column, ideally in the casing; install the pump above the

HPFM, and run the pump at a specific flow rate (for example, 0.5 gpm). Measure the discharge from the pump to confirm the flow rate, and then check the flow rate reported by the HPFM. The two values should match within the accuracy and resolution of the instrument.

- Allow fluid flow to stabilize after the HPFM is moved to a specified depth in the borehole is reached before proceeding with flow measurements. Moving the HPFM can cause vertical flow.
- Collect multiple measurements to allow for the differentiation between tool-induced flow and borehole flow.
- Monitor the water level in the borehole during logging under ambient and pumped conditions.
- Under pumped conditions, allow the borehole to stabilize (drawdown) before beginning the log and collecting measurements. During logging, maintain a constant flow rate to facilitate adequate data interpretations.
- To determine if the flow rate is beyond the range of detection for the HPFM (<0.03 gpm or >1.0 gpm).
- Move the instrument, stop it, trigger it immediately, to detect if flow is caused by instrument movement.
- If flow is detected, keep the instrument stationary, and trigger the instrument again. Repeat this process. If the flow rate is zero, each subsequent pulse takes longer to reach the thermistor because the movement of water caused by the motion of the instrument is dissipating.
- If flow should be present based on other logs and previous flow measurements and is not, modify the diverter to increase bypass around the instrument and decrease flow through the instrument into the range the HPFM can detect. Document modifications in the geophysical report and consider modifications when interpreting results.

4.8.1.5 Data Collection Design

The HPFM is typically used as part of a suite of borehole logging tools and is used after other logs, such as caliper, ATV, OTV, and fluid temperature and conductivity, have been completed and analyzed to identify potentially transmissive (water bearing) features. These potentially transmissive features are termed targets. Stations for HPFM readings are identified above and below each target where the borehole wall is relatively smooth. Readings are collected at each station and then compared to assess whether water is entering or exiting the borehole at the feature. The HPFM is then run alone (it is not run in combination with other probes).

4.8.1.6 Data Interpretation and Presentation

Figure 4-18 illustrates the interpretation and presentation of HPFM data, outlined in red, in context with other geophysical logs, a FLUTe™ transmissivity profile, sample results, and a FLUTe™ multilevel well design. The OTV, ATV, natural gamma, caliper, and fluid conductivity, and temperature are run first and then interpreted to identify targets and stations for HPFM readings). The HPFM ambient log is then run followed by the HPFM pumping log. To facilitate analysis, the HPFM logs are overlain on one another and the horizontal scale the same for each log: flow in gpm with zero in the middle. In this example, the ambient log (blue circles) shows no vertical flow. The pumped log (red circles) shows water-entry zones at about 120 ft, 110 ft, and 100 ft. (Water is flowing into the borehole from these features to supply the pump.) This information is used to locate downhole samples and design the FLUTe™ well (shown to the left of the HPFM log). The HPFM data can be modeled to estimate the transmissivity of features in the borehole using the flow-log analysis of single holes (FLASH) model developed by the USGS as described in (Day-Lewis 2011) and using the computer code described in (Day-Lewis et al. 2011).

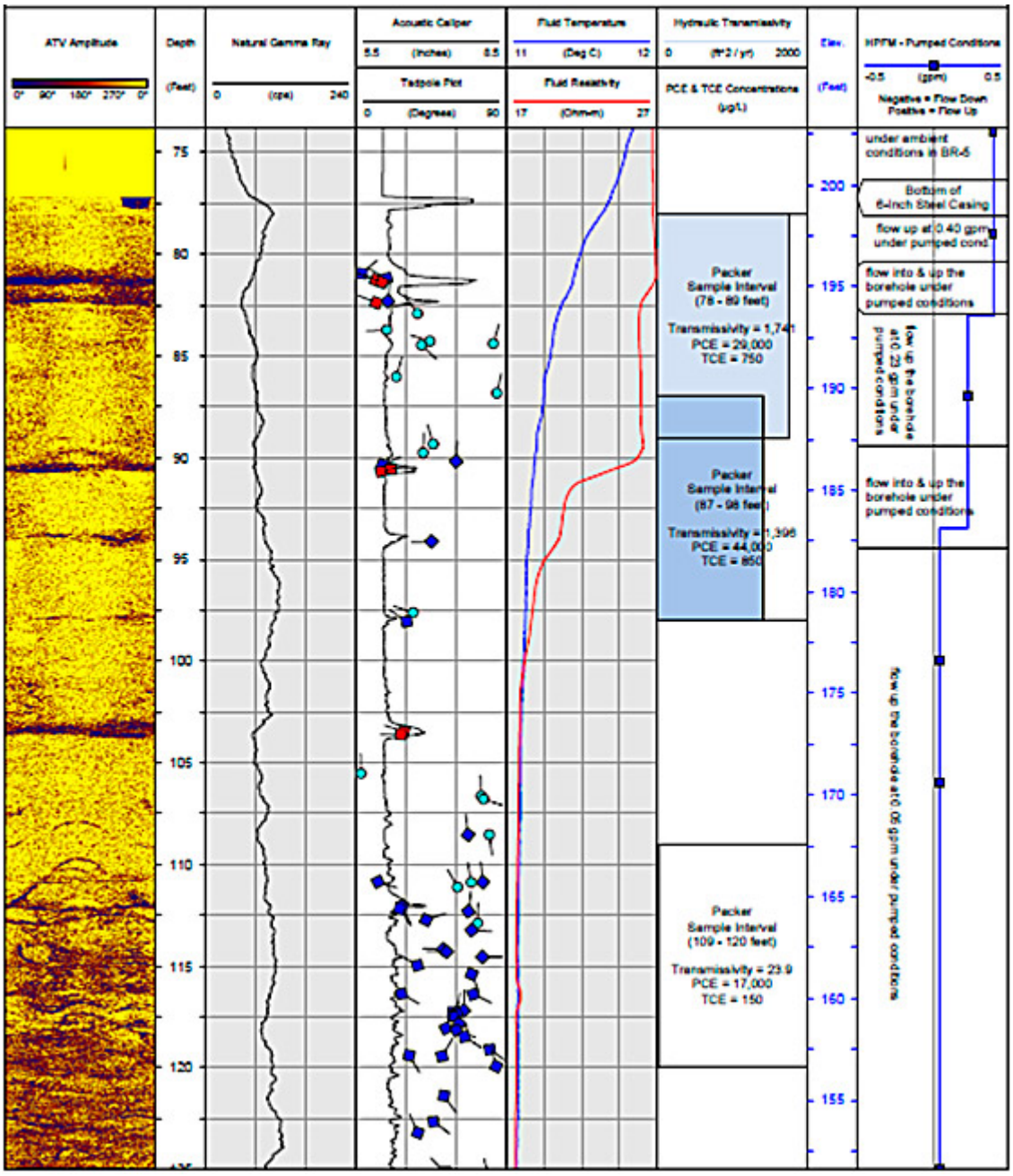

Figure 4-18. Heat pulse flow meter data presentation and analysis.

Source: (Weston 2014)

4.8.2 Impeller Flow Meter Geophysical Logging

The impeller, or spinner, flow meter (see Figure 4-19) is used to measure the rate and direction of vertical fluid movement in a borehole produced by a difference in hydraulic head between two permeable units. This tool was developed over 70 years ago for the petroleum industry and is one of the oldest borehole logging tools for measuring fluid flow in a borehole. Impeller flow meters may be made out of stainless steel, plastic, brass, or titanium. Additional components include centralizers and a protective basket or cage around the impeller. The tool has a sensor, a low-inertia mechanical impeller mounted on precision tungsten carbide or jeweled bearings that revolve in response to fluid flow. As the impeller revolves, it generates electrical pulses that are converted to counts per second or per minute. The count rate is related to the fluid velocity and converted to fluid flow rate by use of a calibration curve. The two most common technologies for rotation sensors are Hall-effect sensors (magnetic) and optical. An overview of this tool and associated literature references is available on the USGS Vertical Flowmeter Logging webpage (USGS 2016a).

Figure 4-19. Spin flow meter probe.
Source: Photo courtesy of Mount Sopris Instruments, Used with permission

4.8.2.1 Uses

The impeller flow meter can be run in a cased well and in an open borehole. It can be used to measure the rate and direction of vertical fluid movement produced by a difference in hydraulic head between two permeable units. It can also be used to measure relative hydraulic gradients, identify permeable units or fractures, identify leaking casing, or characterize the flow within a screened interval.

4.8.2.2 Tool Availability

Impeller flow meters are produced by most borehole logging tool manufacturers and usually come with multiple sizes of impellers, cages, and centralizers to accommodate a range of borehole diameters. When selecting an impeller flowmeter to use, choose the one with the largest impeller blades and lowest friction bearings that produce the highest number of pulses per revolution. Most impeller flow meters can be run on a single or four-conductor logging cable and require a logging winch with tripod and uphole electronic panel or controller to interface to a computer.

4.8.2.3 Technical Limitations

The impeller flow meter is generally considered a low-resolution tool. The low-threshold velocity of a typical impeller flow meter is around 5 ft/min, which limits its use to conditions with higher flow rates. The logging speeds for this tool can be quite high, so attention must be paid to the location in the well or borehole in relation to the bottom and to the placement of the pump. The Hall-effect sensor and optical rotation sensor are both subject to malfunctioning if the borehole fluid has debris, sediment, grease, or sand. Moreover, if the tool is assembled with too much pressure on the impeller bearing, the rotation will be impaired and provide incorrect data. Another interference source can come from variations in the viscosity of the borehole fluid, such as caused by gas bubbles.

4.8.2.4 Quality Control

The impeller should always be run centralized so that the best sample of the laminar flow region of the center of the borehole or well can be collected. The logging speed should be maintained constant and recorded with the flow meter data. A caliper log must be run; logging data should be presented with the flow meter data for borehole and casing diameter corrections. Runs should be made logging down and logging up for a select suite of logging speeds, and repeat runs should

be made. Calibration data should be recorded in the cased portion of the well, when possible, logging up and logging down for at least three different logging speeds to generate a calibration curve.

4.8.2.5 Data Collection Design

The impeller flow meter can operate under ambient conditions and under stressed conditions (pumping or injecting) while moving down or up or while the impeller is held stationary at a specific depth. When planning an open-hole impeller flow meter test, it is important to know the water level in the borehole or well, and the configuration of the borehole or well (for example, bottom of the borehole or well, bottom of surface casing, the position of the well screen or open interval). Supporting borehole geophysical logs, such as caliper, fluid temperature and conductivity, and televiewers provide insight to probable flow zones. When running stress tests, it is critical to maintain a constant pumping or injecting rate and monitor the rate to obtain good quality data.

4.8.2.6 Data Interpretation and Presentation

Impeller flow meter data can be viewed and plotted in standard borehole logging software packages and processed in Microsoft Excel. Additionally, flow meter results can be modeled for transmissivity and head using readily available code such as the USGS's FLASH (USGS 2018a).

4.9 Advanced Borehole Logging Tools

4.9.1 Electrical Resistivity

Resistivity logging is most commonly used in bedrock or deep boreholes where high-resolution data cannot be collected using direct sensing methods. Resistivity logging includes several downhole wireline tools that measure the degree to which subsurface materials resist the flow of electrical current. Tools are available to measure the resistivity of various downhole materials, including borehole fluids, the invaded zone (formation materials in the immediate vicinity of the borehole that have been invaded by borehole fluids), and deeper volumes of the formation beyond the invaded zone. Resistivity is the direct inverse of EC and is measured in Ωm. It is a fundamental property of the material sampled defined as:

$$R = r_{*}S/L$$

where R = resistivity (Ωm), r = resistance (Ω), S = the cross-sectional area being measured (m^2), and L is the length (m)

The resistivity of formation materials is affected by properties of both the matrix material (mineralogy, porosity, permeability) as well as material occupying the pore spaces (gas or pore fluids). Clay minerals and metallic minerals are typically more conductive than other minerals, such as quartz. In water-saturated pores, resistivity is a function of the concentration of dissolved electrolytes in the water (salt water is highly conductive; fresh water is less conductive. Deionized water and air are infinitely resistive, as are many hydrocarbons. Because of these differences, resistivity can often be used as a lithologic indicator as well as an indicator of formation porosity, permeability, and pore fluid chemistry. The relative resistivity of various earth materials is shown in Table 4-2.

Table 4-2. Typical electrical resistivities of earth materials

Source: (Wightman 2004)

Material	Resistivity (Wm)
Clay	1-20
Sand – wet to moist	20-200
Shale	1-500
Porous limestone	100-1,000
Dense limestone	1,000- 1,000,000
Metamorphic rocks	50-1,000,000
Igneous rocks	100-1,000,000

Normal resistivity is the most commonly-used resistivity-logging tool and incorporates four electrodes set at two electrode

spacings (usually 16 inches and 64 inches) that provide variable depths of investigation. The shorter spacing measures resistivity of the invaded zone, and the longer spacing measures resistivity of the invaded zone and deeper native formation. The tool measures apparent resistivity, which must be converted to true resistivity for quantitative interpretations. Another resistivity-logging tool is the lateral log, which incorporates electrodes in a different configuration designed to measure only the resistivity of the native formation beyond the invaded zone. In addition, focused resistivity logging tools, such as the guard log, have an even greater depth of investigation and can provide higher resolution and thin-bed detection.

Resistivity logs must be collected in fluid-filled open boreholes. An alternative to resistivity logging is induction logging which measures formation conductivity (the inverse of resistivity). Induction logging is accomplished by transmitting an alternating current (AC) that generates a magnetic field that induces eddy currents in conductive materials. The eddy currents result in a secondary magnetic field that induces a voltage in a receiving coil. The magnitude of the voltage is a function of the conductivity of the formation material. An advantage of induction logging is that it can measure formation conductivity (and thus resistivity) with or without fluid in the borehole and through plastic casing in existing wells.

4.9.1.1 Uses

The most common application of multielectrode-resistivity logging is lithologic characterization and pore-water quality determination. Due to the many factors that contribute to apparent resistivity measurements, experience interpreting resistivity logs is advantageous when performing quantitative analyses. The methods and algorithms used for quantitative interpretation are beyond the scope of this document but can be obtained from a number of available sources.

Like other lithologic characterization tools, resistivity logs can serve as a correlation tool (where multiple logs are available within reasonable proximity to each other) to resolve desired stratigraphic features. Resistivity logs can also be useful when investigating salt-water and fresh-water issues associated with aquifers.

Downhole-resistivity logging is a useful method to assess lithology and pore-fluid characteristics. It is one of the most common borehole geophysical logging methods used and is widely available from most geophysical services providers. Qualitative interpretation is facilitated by an understanding of the primary factors that influence apparent resistivity responses. Quantitative interpretation can provide insight into parameters of interest such as formation pore-water quality and porosity. The type and configuration of the resistivity-logging tool selected depends on site-specific conditions and the investigation goals. Multielectrode-resistivity logs are often acquired with other logs (spontaneous potential, single-point resistance) as part of a suite of tools providing multiple lines of evidence.

4.9.1.2 Technical Limitations

The primary limitation of resistivity logging is that quantitative interpretation can be complicated by a number of variables. Collectively, these variables result in nonunique solutions to established analytical approaches. Corrections for temperature, drilling-fluid resistivity, borehole diameter, mud cake, and drilling-fluid invasion may be necessary to convert apparent resistivity to true resistivity. Complicating matters, normal logs can be affected by bedding thickness as a function of electrode spacing and provide erroneous results. As such, quantitative interpretation requires experience and a thorough understanding of the regional and local geologic framework so that the proper assumptions for analytical solutions are made. Collecting ancillary data, such as water-quality sampling at sites in proximity to the area of interest can facilitate quantitative interpretations.

4.9.1.3 Quality Control

Resistivity-logging tools are calibrated using fixed resistors between electrodes. A field geologist familiar with the local hydrogeology should be present during data acquisition to assist in evaluating real-time data and identifying potential issues. As with other borehole logging tools, site-specific information (such as location, elevation, well construction details) should be recorded in the log headings for future reference.

4.9.1.4 Data Collection Design

Resistivity logging is conducted using wireline methods in a similar manner as most other borehole geophysical logging tools and must be acquired in open, fluid-filled boreholes. Alternatively, induction logs can be acquired with or without fluid in the borehole and in existing wells with plastic casing. Resistivity logs measure apparent resistivity within the zone of investigation and are influenced by a number of factors, such as temperature, drilling-fluid resistivity, borehole diameter, mud cake, and drilling fluid invasion. To use resistivity logs for quantitative analyses, these factors must be considered during logging and recorded in the log headings.

The requirement for open, fluid-filled boreholes means that geophysical logging should be conducted soon after the borehole is completed and stabilized by the driller. This approach requires communication and coordination with the geophysical service provider to minimize costs for standby time. Logging is usually conducted on a borehole-by-borehole basis rather than logging multiple boreholes in a single mobilization. In cases where the well design requires telescoping casing, mobilization and logging must be conducted prior to setting each casing string.

As with other borehole geophysical tools, logging at a single location provides parameter data only in the immediate vicinity of that location. By logging multiple locations, data can be correlated over greater distances to provide 2-D and 3-D conceptual models. The density of well locations to be logged should be based on the stratigraphic framework and the nature of features that the investigation is attempting to resolve.

4.9.1.5 Data Interpretation and Presentation

Resistivity-logging data are usually processed and displayed in real-time. A typical log suite, referred to as an electric log, is shown in Figure 4-20 with lithologic interpretation.

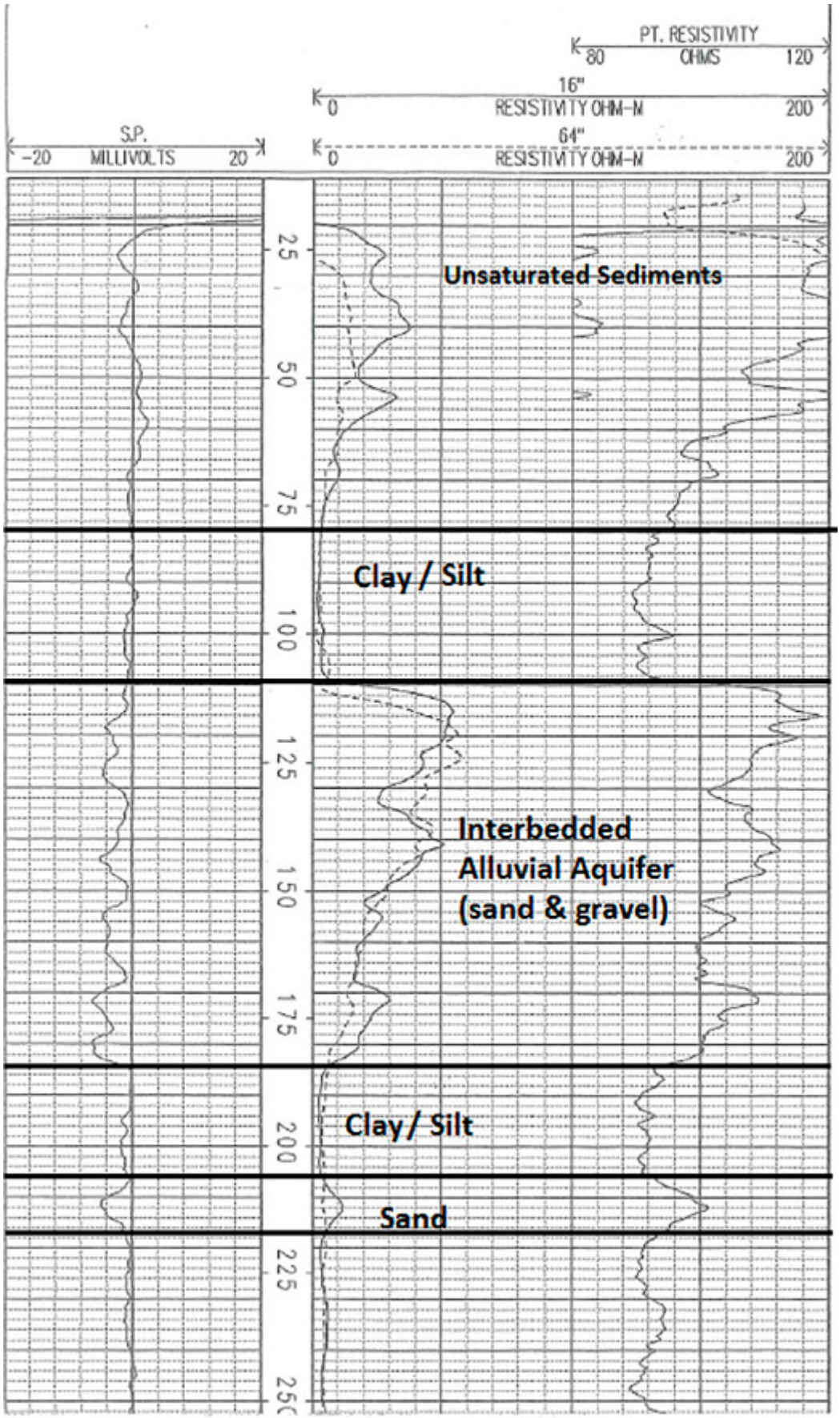

Figure 4-20. Example electric log with spontaneous potential (left column), normal resistivity (16 inch and 64 inch) and single-point resistance outputs.

Source: ERM, Used with permission

In Figure 4-20, lithologic interpretations are based on inflections of the resistivity curves to the right of the baseline,

indicating an increase in resistivity associated with nonclay-bearing sediments. Clay intervals have an apparent resistivity of <5Ωm while the alluvial aquifer interval has an apparent resistivity between 20 Ωm and 50 Ωm. In this example, the pore fluid in the alluvial aquifer is fresh water. If saline or brackish water were present, the apparent resistivity would be significantly lower, which would make determining lithology more difficult. Another example of a resistivity log results are available on the USGS Geophysical logs – Spontaneous-potential log webpage (USGS 2000b).

Quantitative interpretation of resistivity logs involves making corrections to apparent resistivity (logged values) by applying various correction factors for such measurements as borehole diameter, drilling-fluid resistivity, depth of drilling-fluid invasion, and bed thickness. Logging manuals with correction charts are readily available on the internet and elsewhere to assist with log analysis (Schlumberger 2009).

4.9.1.6 Data Misuse

Many factors affect the material resistivity within the zone of investigation and the apparent resistivity log response. While qualitative interpretation can be straightforward for most near-surface investigations in fresh-water saturated sediments, quantitative interpretation requires experience and a thorough understanding of log responses to a number of variables. Reference materials are readily available to facilitate log interpretation, although familiarity with resistivity logging and the local geologic and hydrogeologic framework are critical.

4.9.2 Nuclear Magnetic Resonance

NMR technology uses a quantum physical property of hydrogen atoms and the response of hydrogen atoms to magnetic field perturbations, similar to magnetic resonance imaging used in the medical industry. NMR geophysics has been widely used in the petroleum industry as an exploration and oil-field development tool since the 1960s. Traditionally applied, NMR provides quantitative estimates of total porosity, pore-size distribution, permeability, and relative pore-fluid saturations of oil and water. The oil-field NMR tools were developed for deep subsurface bedrock applications and are typically expensive and cumbersome to deploy, making them impractical for near-surface investigations. In recent years, modified NMR logging tools have been developed that are easily and cost effectively used to acquire high-resolution hydrogeologic parameter data for shallow unsaturated (vadose) zone and aquifer investigations. NMR logging provides continuous, high-resolution data throughout the interval logged using either wireline or push-tool data acquisition methods. Surface NMR geophysical methods are also available but are not discussed in this document. Wireline data acquisition can be applied in stable open boreholes or in existing groundwater monitoring or extraction wells provided the casing materials are nonmetallic. Data are acquired from multiple narrow bands of soil matrix at various radii from the center of the NMR logging tool (called the sensitive diameter, see Figure 4-21). This method allows formation conditions beyond the disturbed area in the vicinity of the borehole or well to be assessed.

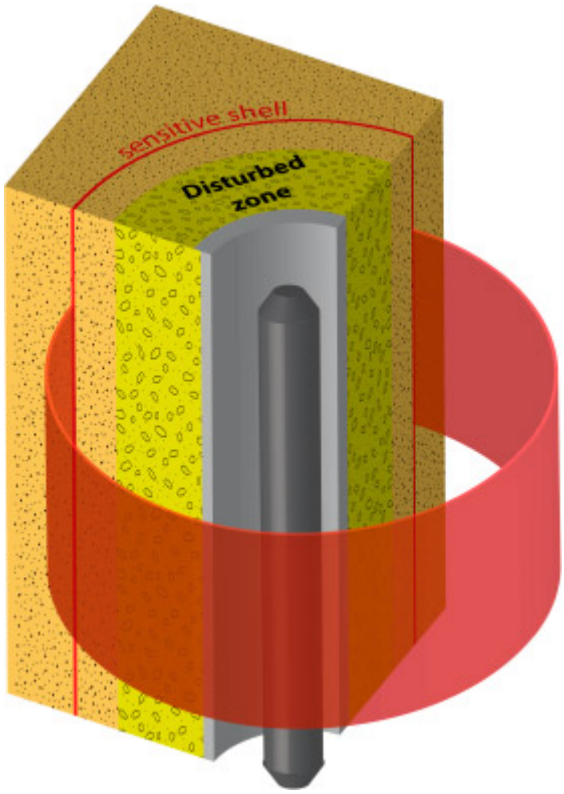

Figure 4-21. Sensitive shell (diameter from center of tool) where NMR data collected.
Source: Vista Clara, Inc., Used with permission

4.9.2.1 Use

Parameters that can be quantified include residual-water saturation (vadose zone), total porosity, mobile porosity, bound porosity (clay or capillary bound), hydraulic conductivity, and multiphased saturations for certain NAPL that are present in the aquifer. Based on pore-size distributions and relative mobile versus bound water content, lithology can be indirectly inferred. As stated previously, NMR can be deployed in stable boreholes, existing groundwater monitoring or extraction wells, or advanced using push-tool methods to collect high-resolution data over the interval logged.

4.9.2.2 Tool Availability

Currently, only a few geophysical service providers offer turnkey near-surface NMR logging; however, NMR logging equipment can be rented and shipped by the manufacturer to most locations in the U.S. as well as globally. This option allows users to perform the logging themselves or have the equipment shipped to their preferred geophysical service provider. The basic equipment required includes the logging tool, a tripod and sheave wheel, a cable spool and winch, an electronics unit and laptop computer, a reference coil to detect background noise, and a generator. The system is designed to be easily set up and operated via user-friendly interfaces on the laptop. Following data acquisition, software installed on the laptop processes the data to provide viewable output of results in real-time.

4.9.2.3 Tool Advantages

NMR is the only available borehole geophysical tool that concurrently measures porosity, pore-size distribution, and hydraulic conductivity. Based on the pore-size distribution, NMR can also differentiate between mobile porosity and bound porosity (silt and clay) fractions. Neutron logging yields quantitative estimates of total porosity but requires using a radioactive source. This requirement can raise concerns when investigating near surface and drinking-water aquifer systems (see ASCT Borehole Geophysics Summary Table). Another advantage of NMR is its ability to detect and differentiate between water and certain petroleum hydrocarbons in pore fluids and provide quantitative estimates of the relative saturations of each.

A key advantage of NMR logging is that it can be conducted in existing PVC-cased monitoring wells, eliminating the need for additional intrusive drilling and derived-waste handling. The depth of investigation is not limited by soil conditions that preclude tool advancement, as can be the case with direct sensing tools. In addition, variations in parameters over time, such as hydrocarbon saturation or reductions in porosity due to biofilm formation, can be monitored by periodically relogging

wells. The NMR tooling can also be deployed using direct-push methods, if desired.

4.9.2.4 Tool Limitations

NMR vertical resolution is somewhat limited compared to other borehole geophysical methods. Data are generally acquired in stages based on tool specifications (coil spacing) and are averaged across each stage. Most NMR tools generally provide approximately 0.5 m (approximately 1.5 ft) of vertical resolution; the direct-push NMR tool provides approximately 9 inches of vertical resolution. Tools typically log between two and four sensitive shells simultaneously with the maximum sensitive diameter varying between 6 inches and 20 inches depending on which tool is used. It is important to know the original borehole diameter to ensure that the sensitive diameter of the tool being used is measuring undisturbed soil matrix beyond the borehole wall. Table 4-3 provides a summary of the various tools and associated features.

Table 4-3. Example NMR tool specifications

Source: (Spurlin et al. 2019), Used with permission

Features	JP525	JP350	JP238	JP175(B)	JP175D	Dart
Probe diameter (inches)	5.25	3.50	2.38	1.75	1.75	1.75
Sensitive diameter (inches)	20	15	12	8 (10)	10	6
Probe length (ft)	5.5	6.3	7.1	7.2	7.2	4.3
Vertical resolution (ft)	1.5	1.5	1.5	3	1.5	9
Echo spacing (milliseconds)	0.7	0.7	0.7	0.9	0.9	0.5
Number of shells	4	4	4	2	2	2
Logging speed (ft/hour)	200	200	200	75 (50)	25	15

4.9.2.5 Quality Control

NMR tools are calibrated by the manufacturer prior to use in the field. The processing software also includes calibration files that are used prior to each logging run to establish data acquisition specifications and procedures relevant to site conditions. The calibration files also specify appropriate logging speeds. Industrial noise such as power lines and electric generators in close proximity to logging can interfere with NMR signals. The equipment should be grounded, and a reference coil box must be used when logging to measure background noise. Background noise can be minimized during data processing to improve the signal-to-noise ratio. For assessing data quality during data acquisition, the signal-to noise-ratio can also be monitored in real-time using the processing software provided by the manufacturer.

4.9.2.6 Data Collection Design

NMR logging is a fairly slow process compared to other borehole geophysical methods. Logging rates of 15 m/h (approximately 50 ft/h) are typical, and for some applications the logging rate is slower. Considering time for mobilization, demobilization, and decontamination between wells, 60 m to 75 m (200 ft to 250 ft) is the maximum log production expected in a typical work day for most near-surface applications. For deeper wells with a single mobilization, greater log production is feasible.

When logging in existing monitoring or extraction wells, certain well construction considerations must be considered, including casing material (nonmetallic only), casing diameter, and the original borehole diameter. The casing diameter determines which tool can be used. In larger-diameter casings, a larger NMR tool can be used to increase the maximum sensitive diameter and improve vertical resolution. The sensitive diameter must be greater than the original borehole diameter to avoid logging the annular material outside the casing. Conversely, if the nature of the annular material of the well is of interest, a tool with a sensitive diameter can be selected to measure parameters within the annular space.

When implementing NMR logging using push-tool advancement techniques, data collection follows similar protocol to other direct sensing methods. In this case, a small-diameter casing is advanced to the maximum depth to be logged and the tool is inserted into the casing. The casing is then retracted in stages to expose the tool to the soil matrix. Following logging at each stage, the tool is raised into the casing and the casing is retracted, ready for the next logging stage. Alternatively, a blank PVC casing (permanent or temporary) can be installed in an open borehole for logging purposes.

As with other borehole geophysical tools, logging at a single location provides parameter data only in the immediate vicinity

of the location. By logging multiple locations, data can be correlated over greater distances to provide 2-D and 3-D conceptual models. Based on mobile- and bound-water porosity information, transport pathways and storage intervals can be identified and mapped. The density of well locations to be logged should be based on the stratigraphic framework and the nature of features that the investigation is attempting to resolve.

4.9.2.7 Data Interpretation and Presentation

The laptop computer provided by the supplier includes software for processing and displaying the data in real-time. Data interpretation is straight forward as shown in the example log displayed below (see Figure 4-22).

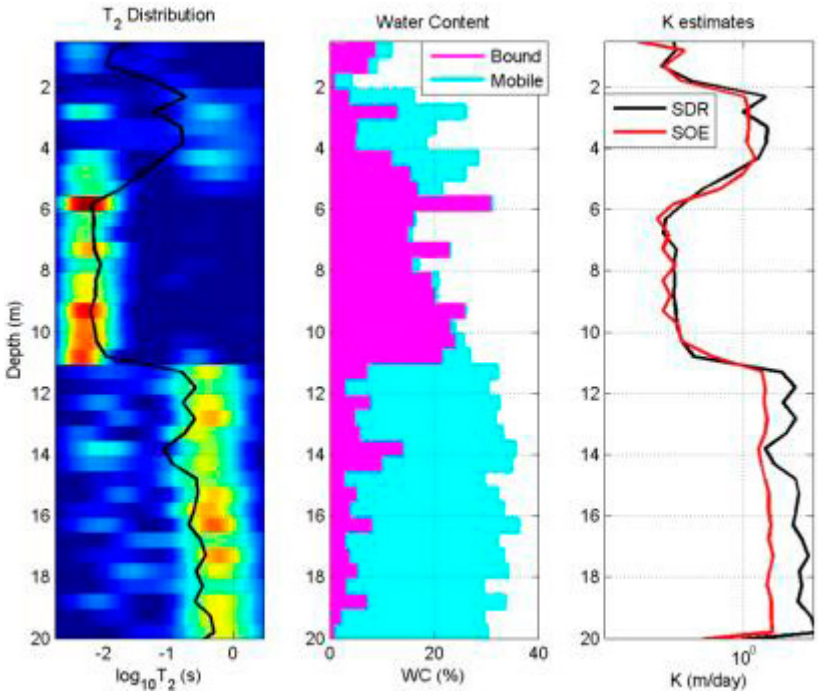

Figure 4-22. Example NMR output.
Source: Vista Clara, Inc., Used with permission

The left column in Figure 4-22 shows the transverse relaxation time (T2) distribution of excited hydrogen molecules derived from composite spin echo trains measured by the NMR tool. The integral of the T2 distribution reflects total water content, and the distribution along the T2 axis is indicative of water mobility. The center column shows the relative amounts of mobile and bound water, and the combination of these represents the total water content. In unsaturated media, total water content reflects the residual-water saturation. In saturated media, the total water content reflects the total porosity of the matrix material. Intervals with a high percentage of mobile water are indicative of highly permeable coarse-grained soils, and intervals with a high percentage of bound water are indicative of low permeable clays and fine-grained soils. The right column shows the estimated hydraulic conductivity distribution for the logged interval. Hydraulic conductivity is estimated from total porosity and pore-size distribution using multiple algorithms developed and empirically tested on various soil and rock types.

Other properties of pore fluids that can be measured by the NMR tool are hydrogen index and fluid diffusivity. Fluid diffusivity is the extent to which molecules move at random in the fluid. There is little difference between the hydrogen index of water and that of petroleum hydrocarbons, although the presence of petroleum hydrocarbons affects fluid diffusivity and has an inverse effect on T2 relaxation times. Using oil-field NMR technology, NMR data can be processed to evaluate those properties and derive estimates of hydrocarbon saturation within the pore space. Testing this analytical method (Spurlin et al. 2019) has shown that hydrocarbon saturations of less than 5% can be detected and semiquantitatively estimated within a reasonable margin of error. This analysis can be performed in stages within intervals of interest identified following initial NMR logging.

4.9.2.8 Data Misuse

The primary considerations when using NMR data are the vertical resolution and the sensitive diameter where data are collected. Vertical resolution is defined by the vertical length of the stage where data are collected and represents average properties of the soil matrix over the interval. If the sensitive diameter is close to or less than the original borehole diameter

(and potentially disturbed zone beyond the borehole), the results obtained may not accurately reflect native soil matrix conditions. It is best to use a tool with a sensitive diameter that extends 2 inches or more beyond the original borehole wall. If the original boring was drilled with mud, the invaded zone may impact formation properties even deeper.

4.9.3 Borehole Video Survey

Borehole video surveys provide a visual record of the actual condition of a well and allows the viewer to see the actual condition of the borehole walls first hand. Under adequate conditions, the viewer can explore a wide range of subsurface environments – from 2-inch diameter monitoring wells to open boreholes and production wells exceeding 12 inches in diameter. Dual-viewing (both downhole and 360° side view), high-resolution cameras allow the viewer to identify and classify geologic features, well construction details, and obstructions, if present. Digital video recordings can be saved to a variety of electronic media or uploaded to a cloud-based platform in the field.

Borehole video camera systems range from portable systems that can reach 1,000 ft in depth to truck-mounted units capable of reaching 5,000 ft or more. Most borehole cameras are fitted inside stainless-steel housings and pressurized with nitrogen. Some models are reportedly waterproof up to 2,500 psi, which is equivalent to a submerged to a depth of 5,880 ft underwater. The housings typically range from 1.6 inches to 3.5 inches in diameter (see Figure 4-23) and up to 22 inches in length. Digital video feeds are transmitted over single-conductor (coaxial) wireline, wrapped with armored cable.

Figure 4-23. Example borehole video camera systems.
Source: Photos courtesy of Mount Sopris Instruments,Used with permission

In addition to the descriptions in the following paragraphs, see the example video of a video survey in bedrock (Allegheny 2013). In addition to the descriptions in the following paragraphs, see the example temperature log on the USGS Geophysical logs – Temperature log webpage (USGS 2000c).

4.9.3.1 Use

Borehole video surveys can be used to perform the following activities:

- Inspect well casing and screen.
- Document well construction.
- Identify and classify fractures.
- Identify seeps from fractures in the vadose zone.
- Identify water-bearing zones.
- Characterize lithologic or geologic features.
- Identify obstructions.
- Confirm changes in conditions before or after work.
- Document regulatory compliance and pre-well abandonment.

An important aspect of conducting a successful borehole video survey is the ability of the camera's light source to reach the borehole walls. With the advancement of LED technology, modern borehole cameras are outfitted with more powerful and efficient LED light rings or forward-facing bulbs (pictured above). Note that halogen lighting techniques also remain in use.

Centralizer bands (thin lengths of bowed metal or plastic affixed to collars that slide over the camera) are used to keep the camera centered in the borehole or well casing throughout the survey. Real-time adjustments to the camera's focus, light intensity, and rotation (during the side-viewing portion of the survey) are controlled remotely at the surface.

A depth encoder, often located at or near the camera system's winch, provides the depth of the camera's lens, from a reference point selected by the user, to the nearest tenth of a foot, on screen. Camera diagnostics, such as internal temperature and humidity, are also available to monitor the condition of the unit or for troubleshooting purposes.

4.9.3.2 Advantages

Borehole video surveys have the following advantages:

- Surveys can be conducted in submerged or open-air environments.
- The viewer is able to observe the condition of the borehole walls first hand, which is useful for classifying the subsurface geology and lithology and planning subsequent tasks (for example, hydraulic packer testing and well construction).
- If present, inflowing and outflowing features are clearly defined to an exact depth.
- The tool can be used to remove well obstructions (for example, small hand tools, piping and tubing, sampling equipment dropped or lost down a well).
- This tool is readily available for rent, purchase, or contract through a vendor.
- Surveys can often be completed in a matter of hours for wells up to 500-ft deep.
- Surveys are electronic and can be uploaded and downloaded, reproduced, or distributed quickly after completion.

4.9.3.3 Limitations

- The clarity of the image is solely reliant on the amount of light reaching the borehole walls. If the water is or becomes turbid, the camera does not receive sufficient light and the image is compromised or lost. If permitted, constantly running clean water into the well or removing water via pumping before or during the survey usually resolves the turbidity issue.
- In wells that are deviated, the camera may favor one side of the borehole wall, compromising the image.
- Many cameras are not equipped with a compass, which limits the viewer's ability to reference or orient the features observed. Using an ATV or OTV, which include internal magnetometers (for orientation) and inclinometers (for tilt), along with a borehole video survey compensates for this limitation.
- Potential interference during the survey may include electrical issues caused by the power source or the physical hazards associated with open rock wells (for example, collapse, loose material, obstruction).

4.9.3.4 Quality Control

The following activities are recommended to control data quality:

- Check camera diagnostics such as internal temperature, pressure, humidity, and voltage/amperage during each survey, in real-time, to ensure safe camera operation, or for troubleshooting purposes.
- Reset the on-screen depth measurement prior to conducting each borehole video survey to maintain project-specific reference points. This depth measurement can be calibrated as frequently as necessary.
- Prior to performing a borehole video survey, the viewer should confirm with the operator the exact location on the camera where the depth is being referenced. It is important to note that during each portion of the video – both downhole and side view – the reference depth does not change, and the side-viewing window is often located slightly above the downhole camera lens.
- Before logging, identifiy the diameter of the well casing and borehole and adjust the camera's centralizer bands should be adjusted to fit loosely against the borehole/casing wall.
- Note the relative size of the borehole or well and account for the camera's proximity to the borehole wall. The viewing window may exaggerate the size of certain features. For example, a void that might appear cavernous may only be a couple of inches in length. It is important to note the relative size of the borehole or well and account for the camera's proximity to the borehole wall. Additionally, other geophysical probes, such as a mechanical caliper or acoustic televiewer can more accurately estimate the size of the features in question.
- Before logging, confirm with the operator the planned logging speed and adjust as necessary, to meet the goals of the survey.
- Check recording devices sat regular intervals to confirm the collection (and storage) of video files.

4.9.3.5 Data Collection Design

Although the standard operating procedure for obtaining borehole videos may change from vendor to vendor or by operator and client preferences, the common practice is to record the first portion of the survey moving downward through the

borehole, viewing through the downhole lens. Newer cameras allow the operator to pan and tilt the lens, but generally speaking the lens continues to point downward during this initial portion of the survey. The operator notes features of interest until the total depth of the well is reached. During this process, care should be taken to avoid borehole disturbance which could reduce camera visibility.

The second portion of the video survey is conducted while pulling the camera upward, recording through a side-viewing window. The camera lens is rotated 360° to view each side of the borehole wall. This rotation can be performed while the camera is in a static (stopped) position or while the camera is moving vertically through the hole. Because of the limited speed of the lens' 360° rotation, a side-viewing survey is typically conducted at a slower speed than the downward-viewing survey.

Video surveys are typically viewed on a monitor or laptop computer screen provided by the operator or camera rental company. The software necessary for video display and processing should also be included. Examples of screenshots from a number of borehole video surveys are included in Figure 4-24.

Downhole view of casing joint

Downhole view of borehole wall. Note groundwater flow on right side of image.

Figure 4-24. Examples of screenshots from several borehole video surveys.

Video surveys can be recorded as MPEG video files, which could become large files. Wi-Fi capabilities in the field may allow the operator to upload video files to a cloud-based platform for easy distribution.

---

[1] Where specific conductance (SC) can be converted from fluid resistivity using the following equation: SC (uS/cm) = 10,000 * 1 / fluid resistivity (Ωm)

5 Surface Geophysics

Surface geophysical tools are a class of nonintrusive geophysical instruments used to evaluate the subsurface. They indirectly measure physical properties of materials from signals produced by natural or generated sources and rely on contrasts in the properties of different materials. Surface geophysical tools are generally portable, can cover a large area and can "see" between wells. The portability of the tools and technological advances in computing power allow surface geophysical methods to be efficiently used in large-scale investigations (for example, area geology) and small-scale site characterizations (for example, identifying an UST at a corner retail store). Surface geophysical tools can also be used as part of remote sensing investigations (see Section 9.16) and can be paired with other tools discussed in this document (see the ASCT Selection Tool), as well as Section 3 and Section 4) as site investigations progress.

Surface geophysical tools are an indirect method. They can be used to image subsurface features that control contaminant transport and, under optimal conditions sense proxies of contamination, but cannot see concentrations of specific contaminants. They require correlation or interpretation and can be subject to misinterpretation. For these reasons, surface geophysical tools are most powerful when used in combination with conventional measurements when they have the potential to reduce characterization and monitoring costs. For example, surface geophysics is often performed to obtain additional data. Additional data collection could involve a drilling program designed to intercept anomalies detected, such as interfaces of interest, voids, faults, fractures. In addition, excavation activities could be designed to verify the depth of buried debris, tanks, or pipes. In many cases, surface geophysical tools can be used to identify the approximate locations of subsurface utilities, so the subsequent invasive phases avoid utility strikes.

5.1 How to Select and Apply Surface Geophysical Tools Using this Document

Projects typically have the following phases: data acquisition, data reduction and processing, modeling, and geological interpretation

- Data acquisition: the tool sends an impulse along a linear transect or across a 3D grid. The signal propagates through the subsurface and is picked up by the tool's receiver. A single transect typically has constant data spacing, with resolution based on the target, and is perpendicular to the target. When multiple transects are combined, a 3D grid of stations and contoured results can be formed. The signal (the data that is desired) to noise (unwanted fluctuations in the measured data that may be spatial or temporal) ratio is improved by repeated measurements.
- Data reduction and processing: The raw data from the data acquisition transect (or survey) must be corrected for geometric effects controlling signal transmission and attenuation. This process is referred to as data reduction. This can include correcting data for unwanted variations unrelated to the variation in subsurface properties (for example, gravity survey is often corrected for surface topography). Digital signal processing, including time series analysis (for example, Fourier analysis) is used to enhance signals relative to noise and geometric effects or signal processing. Be aware that even if a good signal to noise ratio is obtained, target detection is dependent on resolution (see ASCT Surface Geophysics Tool Summary Table) for tool specific resolution) (Mussett and Khan 2000). Targets are recognized as an "anomaly" in the data (for example, values are above or below the surrounding data averages). However, not all geophysical targets produce spatial anomalies.
- Modeling: Data modeling occurs following data reduction. The intent of the model is to describe the variation in subsurface properties that explain the acquired datasets. The model should only be as complex as the data allows. The modeling process falls into two exercises: (1) forward modeling and 2) inverse modeling. Forward modeling takes a model for the distribution in subsurface properties (like a geologic cross section) and uses a mathematical algorithm to approximate the geophysical response that might be seen with a tool (for example, given some set of variables, what is the result). Inverse modeling starts with having observed geophysical data (typically obtained from a tool) that is used to produce a model of the subsurface physical property distribution from the data (for example, when given some measurements, what caused them). A simple example is using the arrival times of seismic p-waves (See Section 5.4) to determine depth to the bedrock interface. A more sophisticated example is demonstrated by the Scenario Evaluator for Electrical Resistivity (SEER) tool discussed

in Section 5.2.2, which generates an estimate of the 2D resistivity distribution from multiple samples of the electrical field induced by injecting electrical current into the Earth.

The model dimensionality depends on the data coverage. It may be a 1-D vertical profile from a sounding around a single point, a 2D model from a single profile of data or a 3-D model from a set of parallel transects. Many geophysical models suffer from being non-unique; the models contain more cells (or parameters) than independent measurements acquired. It is then impossible to find a "unique" model without additional information. For this reason, additional assumptions are made to constrain the model.

Models are inevitably simpler than reality as the heterogeneous nature of the subsurface is never fully captured. Models produced from tomographic imaging methods (for example, electrical resistivity imaging or seismic tomography) usually employ a smoothness constraint to generate a minimal structure image from the range of plausible non-unique models. Images are thus a blurry representation of the subsurface, making it difficult to discern the exact shape and size of anomalies, especially when stations are not close enough to reveal all details of the signal (Mussett and Khan 2000).

- Interpretation: Following modeling, the results are interpreted into a geological or site characterization context. For example, a region of higher EC could indicate the presence of higher salinity groundwater. However, interpretations are typically non-unique as many geophysical properties respond to a wide range of physical and chemical variations. The geophysical model must be combined with all available data (including geologic, geophysical, outcrops, and chemical data) to update the site conceptual model (Mussett and Khan 2000).

Answering of the following targeted questions about site characteristics is the first step in identifying which surface geophysical tool, or series of tools, can be used to meet the project goals:

- What is the objective of the project? For example, is the focus on determining geology? Is the focus on locating the water table? Is the focus on identifying a metallic object such as a utility or buried drum?
- What is the size of the site? For example, is it a large expansive site so that extensive transects can be installed? Is the property a small corner retail store?
- What is the resolution needed? For example, is large-scale resolution sufficient or is a finer-scale needed?
- What is the depth of the feature? For example, is it shallow or is the feature expected to be deep?
- What comprises unconsolidated and consolidated material? For example, is it dry, sandy soil? Does it contain thin layers?
- Are there cultural features (such as roads, heavy equipment, power lines, electrical boxes) that could interfere with the results and result in poor data quality?

Figure 5-1 provides a high-level decision flow chart for selecting and applying the surface geophysical tools discussed in this section. The Geophysical Decision Support System (Harte and Mack 1992) can provide additional decision-making support.

The ASCT Surface Geophysics Tool Summary Table provides a screening process to determine tools to use based on site and project parameters and project objectives. The USGS Fractured Rock Geophysical Toolbox Method Selection Tool (USGS 2018b)can be used to select appropriate tools. More than one tool may provide the data required. By using different tools to collect similar data, supporting evidence is provided and data confidence for site characterization is improved. ASCT Surface Geophysics Checklists (.xlsx version) are also provided to support tool selection and use and project management.

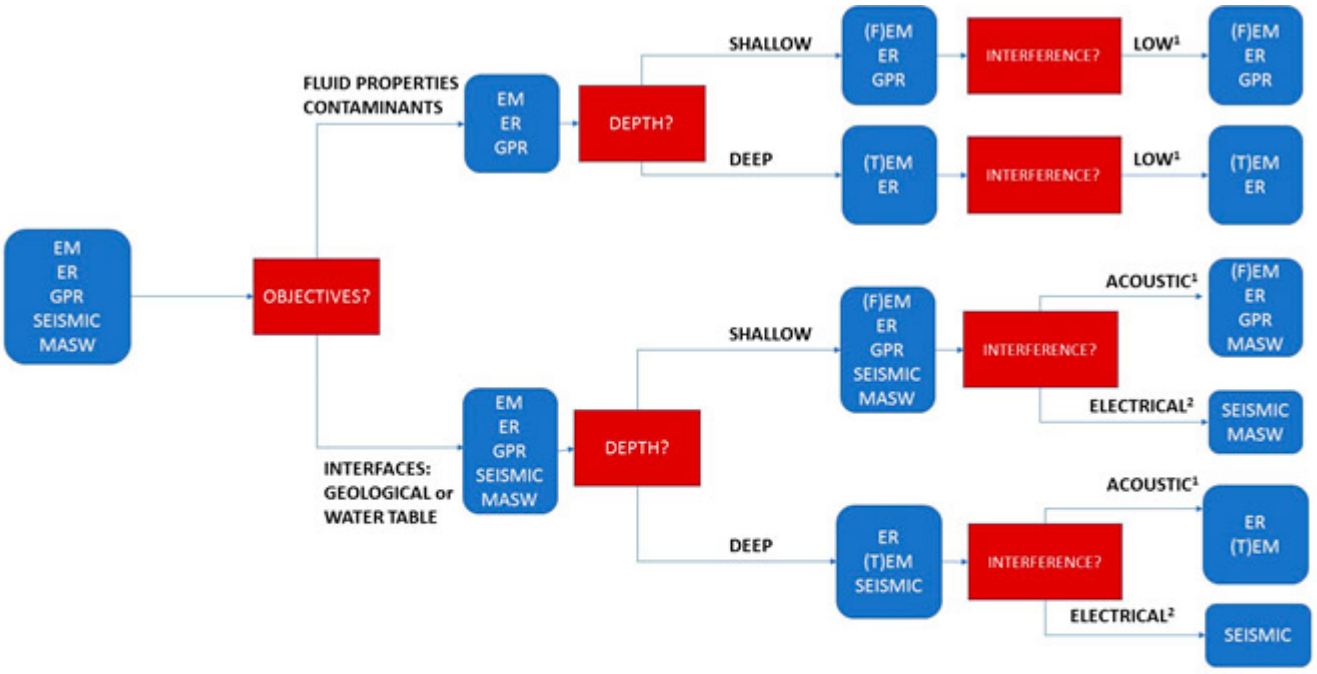

Notes:
-This flowchart provides a high-level overview regarding tool applicability. Specific tool details (e.g. resolution, applicable depth, appropriate geologic setting, study objectives, considerations) is included on Table 5-1.
-For this flowchart, "seismic" refers to both seismic reflection and seismic refraction.
-For this flowchart, "shallow" is generally within 120 feet of the ground surface. "Deep" is generally greater than 120 feet from the ground surface.
[1]Electrical methods can be effective if the degree of electrical interference/noise (e.g., power lines, generators, etc.) is limited. Electrical methods are less affected by acoustic interference/noise. MASW may overcome acoustic interference with vertical stacking of data acquisition to increase signal to noise ratio.
[2]Seismic methods may still be effective in conditions with high degree of electrical interference/noise.

Figure 5-1. Flow chart summarizing major decision factors when selecting surface geophysical tools.

Tools discussed in this section include ERI, ground penetrating radar (GPR), seismic reflection and refraction, multichannel analysis of surface waves (MASW), and both time domain and frequency domain EM surveys.

5.2 Electrical Resistivity Imaging

The ERI method, also known as electric resistivity tomography (ERT), is used to noninvasively determine the spatial variations (both laterally and with depth) of the electrical resistivity of the subsurface [see (Binley 2015) for a recent review]. Electrical resistivity describes the intrinsic resistance of the subsurface to transport an electrical charge via conduction mechanisms. The reciprocal of resistivity gives the EC of the subsurface. Electrical resistivity is a valuable geophysical property to measure as it varies over many orders of magnitude and depends on several physical and chemical properties of interest in high-resolution site characterization.

The electrical resistivity of the subsurface is a function of lithology (porosity, surface area), pore-fluid characteristics (for example, saline water, fresh water, NAPL), water content, and temperature. Ion-rich pore fluids, formations with high interconnected porosity, and formations with a high surface area (for example, fine-grained formations, especially clays), increase the EC of the subsurface, which decreases resistivity. Unsaturated soils increase resistivity (air is a perfect insulator), as does the presence of air-filled voids and or free-phase gasses. The presence of metallic features (for example, ore minerals, infrastructure) also increases EC.

The sensitivity of ERI to multiple subsurface physical and chemical properties makes ERI a highly versatile surface geophysical method. It can be used to image the hydrogeological framework controlling groundwater transport, the distribution of inorganic contaminants in groundwater, and variations of moisture content in the subsurface. This versatility also means that ERI results in nonunique interpretations of subsurface properties, as multiple unknown factors influence subsurface resistivity.

Resistivity imaging has many advantages relative to invasive methods of exploring the subsurface and other geophysical technologies. The primary advantages of the technology result from the (1) wide range of resistivity encountered in geological media, and (2) strong dependence of resistivity on multiple subsurface physical and chemical properties (including moisture content, porosity, fluid salinity, and grain-size distribution). Consequently, ERI has a wide range of

potential applications.

5.2.1 Use

Electrical resistivity relies on galvanic (direct) contact between the transmitting instrument and the Earth which differentiates it from the EM methods described elsewhere in this section. The basic measurement is obtained using four electrodes placed on the surface of the Earth or in boreholes for more specialized cross-hole applications. Two current electrodes are used to drive electrical current ( ) into the subsurface and a second pair of potential electrodes record the resulting electrical potential difference between the electrodes. The source of electrical current is a transmitter (typically a few hundred Watts capacity for site investigation applications) and voltage differences are recorded using a receiver that is synchronized with the transmitter. An overview of the survey is given in Figure 5-2.

The transfer resistance is calculated for each measurement that is often converted to an apparent resistivity. The apparent resistivity represents the equivalent resistivity for a homogenous Earth that results in the measured transfer resistance. These data are representations of the raw measurements. Inverse methods are used to generate images of the variations in the actual resistivity structure (for a heterogeneous Earth) beneath the electrodes.

The electrodes are usually rods or spikes driven into the ground at regular intervals. In some cases, it is necessary to increase the size of the electrodes to reduce the contact resistance (more technically, impedance) between the metal and porous ground. High-contact resistances reduce the current flowing in the subsurface and, consequently, the resulting voltage differences at the receiving potential electrode pairs (leading to lower signal-to-noise ratio). Large electrodes can help improve the signal-to-noise ratio, but their use may violate basic assumptions when interpreting data.

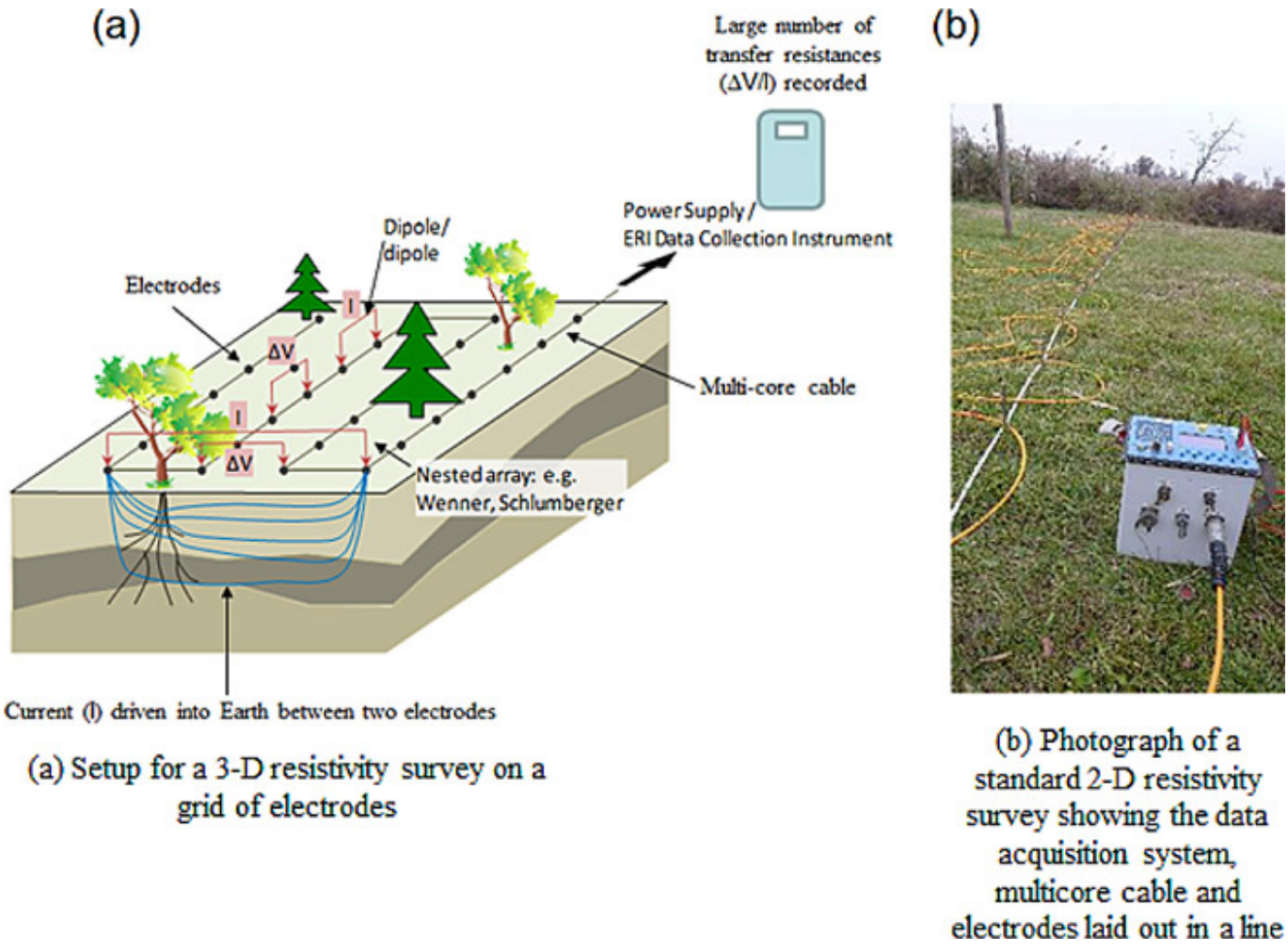

Figure 5-2. Basic components of a resistivity imaging.
Source: Rutgers University Newark, Lee Slater, Used with permission

Electrode configurations can include:

- nested arrays, such as the Wenner array shown in Figure 5-2, which are popular for sensing horizontal interfaces

in the Earth.

- the Dipole-Dipole array, where the current injection and potential recording electrode pairs are separated by some integer multiple of the electrode spacing. These arrays are popular for sensing vertical contacts in the Earth and result from the different sensitivity patterns that arise based on the relative locations of the four electrodes.

The most common application of ERI is in the form of a 2-D transect, where the objective is to obtain a 2-D cross section of the resistivity structure of the Earth. Large transects are typically built up using a set number of electrodes and associated cabling that is progressively rolled along to cover extensive terrain. A major limitation of the 2-D transect is that the imaging (see below) results in a model of the resistivity structure that is constant in the plane perpendicular to the image. Such a 2-D earth assumption may be reasonable in some cases (for example, a resistivity survey perpendicular to a buried pipeline), but in most cases the subsurface is inherently 3-D. A 3-D resistivity survey requires electrodes to be placed on a grid, rather than a survey line. Commercially available software packages for processing resistivity imaging datasets now fully support 3-D surveys.

5.2.2 Data Collection Design

Certain rules of thumb for survey design can guide implementation of the resistivity method. There is an inherent tradeoff between resolution and imaging depth (or imaging distance away from a borehole). Generally, the best possible image resolution is approximately equal to the electrode spacing. This optimal resolution only exists in the shallow subsurface below the electrodes as resolution decreases greatly with distance from the sensing electrodes (with depth below a surface array). The maximum investigation depth depends on the total length of a 2-D ERI survey. If the sequence of four electrode measurements to acquire is well designed and includes four electrode combinations with large electrode spacings, the maximum imaging depth can be roughly estimated as some fraction (for example, 0.75) of the total survey length. This estimation typically assumes a homogenous earth and underscores the need for caution when making assumptions dependent on unknown resistivity distributions.

Developing a resistivity conceptual model provides a better way to assess image resolution and investigation depth. First, a synthetic resistivity distribution is developed based on the CSM (see Figure 5-3). All available information on the subsurface geology and target of interest is used to develop the model. Educated guesses are usually required when assigning probable resistivity values for targets of interest and geological units. These guesses are constrained by data from available borehole logs, groundwater geochemical data, and tabulated values of typical resistivities for different geological materials. A forward model calculation generates a synthetic resistivity dataset contaminated with representative noise for the site so that it simulates the data acquired from a true field survey. Then the model is inverted (see Figure 5-3) to assess which survey design provides the most information to meet the project objectives. A geophysical contracting company experienced in resistivity imaging can perform these simulations and these simulations should be part of a competitive bid for a contract. The scenario evaluator for electrical resistivity (SEER) is a technology-transfer tool developed by the USGS in collaboration with Rutgers University Newark (Terry et al. 2017) that can be helpful when evaluating the likely effectiveness of a resistivity survey for a specific application. SEER is packaged as an Microsoft Excel spreadsheet that can be downloaded from the USGS Scenario Evaluator for Electrical Resistivity (SEER) Survey Pre-Modeling Tool webpage (USGS 2018c).

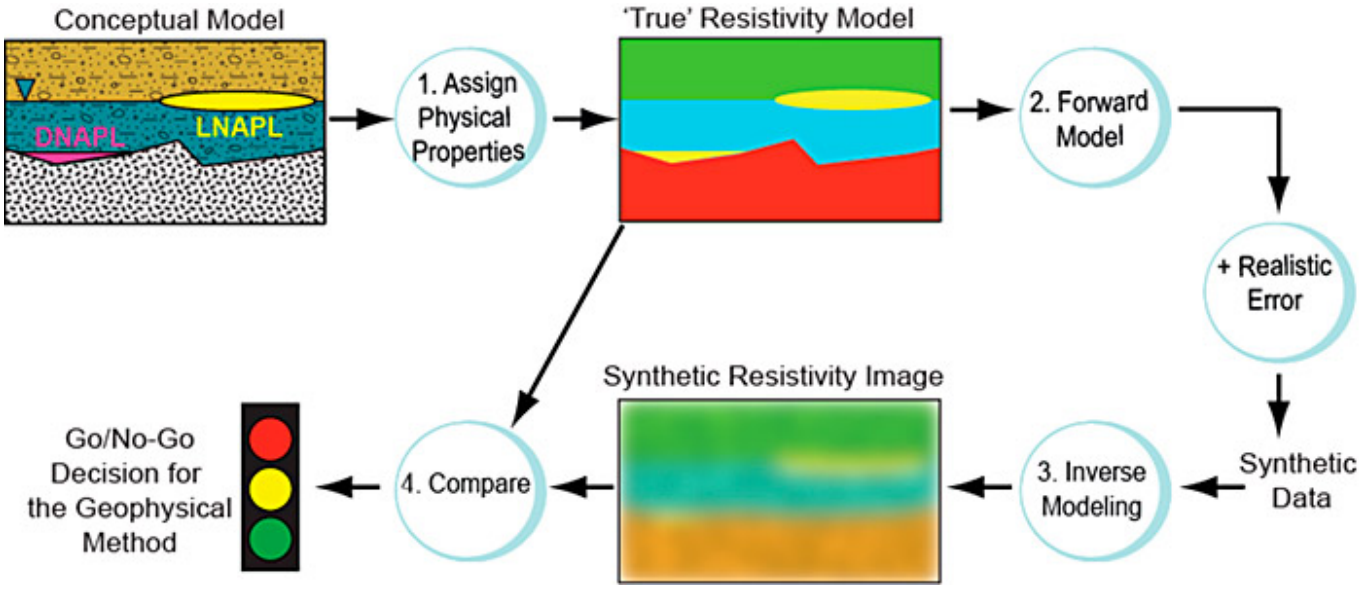

Figure 5-3: Workflow to evaluate the likely effectiveness of a resistivity survey for a specific application.
Source: Rutgers University Newark, Lee Slater, Used with permission

In the example shown in Figure 5-3, the conceptual model is for unconsolidated sediments overlying bedrock, with hypothetical plumes of DNAPL and LNAPL. The workflow tests the likely resolution of the subsurface based on assigned electrical properties for the site geology and contaminants. Based on assumed electrical properties, the water table in the unconsolidated sediments and the bedrock interface is expected to be well resolved. LNAPL may be detected, the deeper DNAPL is not resolvable. The example highlights the inherently low resolution of resistivity imaging (Day-Lewis et al. 2017).

5.2.3 Data Processing and Data Visualization

Inverse methods are used to process field resistivity datasets to compute a subsurface resistivity distribution that is consistent with acquired measurements. Typically many more parameters than measurements are included the subsurface resistivity model. As a result, inverse models generate nonunique solutions to the resistivity structure. Additional constraints on the model structure are included to favor certain models or images over others to narrow the plausible resistivity structure further. By far the most common constraint is called smooth inversion or smoothness-constrained inversion because it produces models with smooth variations in physical properties (deGroot-Hedlin and Constable 1990).

Inverse methods involve an iterative approach in which a mathematical model is used to minimize the difference between the field measurements and the simulated values based on a numerical-forward model for a synthetic structure of the Earth. Finite difference or finite element models are used in the numerical-forward modeling. Iterative parameter updates continue until these differences are less than a specified value defining a convergence criterion. At this point, the estimated model is considered a plausible representation of the resistivity structure of the subsurface. Because an inexperienced user can easily abuse it, the processing should be done by an experienced practioner. To ensure the representation is plausible, experts use a variety of methods to assess the quality of the input data and information content of the inverted image and identify red flags. Unfortunately, geophysical contractors may not always use image appraisal tools to assess the realistic information content in the inverted images. Contractors should provide evidence of image appraisal as part of the delivery of ERI results.

ERI data interpretation is best done as part of a multitechnology approach to refining site conceptual models. Interpretations of ERI survey images should be constrained by other information available at site. Interpretations of resistivity images presented by a contractor should never be simply accepted without careful consideration of whether the interpretation is consistent with existing site information. Used appropriately, the spatially rich information provided from an ERI survey significantly helps CSM refinement.

5.2.4 Quality Control

Numerous QC checks should be performed during the acquisition of field resistivity datasets. The repeatability of the recorded voltages in response to an injected current should be assessed from repeating individual measurements multiple times. A much more robust quantification of the error in the field measurement is achieved from a 'reciprocal' measurement, whereby the electrode pairs being used for current injection and the electrode pairs being used for voltage measurement

are switched over. The principle of reciprocity states that the normal and reciprocal measurement must be identical. Differences in the normal and reciprocal measurement provide a rigorous estimate of the measurement error (Slater et al. 2000). These errors depend on multiple factors, some of which can be addressed during the field survey. One factor is the contact resistance between the electrodes and the Earth. This resistance limits the flow of current into the ground and consequently limits the magnitude of the recorded voltages. Poor contact resistances result from resistive ground, poorly placed and inserted electrodes, and bad contacts between the electrode and the resistivity instrument. Most resistivity instruments allow the user to assess contact resistances and correct issues prior to the start of a survey. Naturally high-contact resistances resulting from the ground conditions can be reduced by watering the electrodes.

Poor data quality also results from buried infrastructure, particularly electrical utilities. The site should be carefully evaluated for the presence of buried utilities, particularly at brownfield sites or within industrial complexes. Identifying the location of utilities helps to isolate anomalous structures in the resistivity images caused by such infrastructure.

Accurate recording of the electrode locations is another important QC consideration. Electrodes are typically put out with the intention of uniform spacing, which is sometimes prohibited by site conditions. When site conditions dictate that the electrodes be offset from the nominal spacing, exact electrode locations should be recorded. Incorrectly documented electrode locations result in model errors during inversion that manifest as artificial image structure at shallow depths close to the electrodes. The topography also should be recorded when the land surface deviates significantly from horizontal. Slopes greater than 10% should be documented and resistivity data modeling should account for the steeper topography. All modern ERI software has the capability to account for topography during inverse modeling.

QC should also be considered during data processing. A correct estimate of the errors in the measurements s necessary to accurately weight the relative importance of the different measurements that the resistivity structure. Unlike errors determined from repeatability tests, reciprocal measurement errors can identify systematic errors that are not apparent from stacking.

As previously noted, image appraisal is important in assessing the significance of the estimate of the resistivity structure; a measure of the depth of investigation to identify well-resolved regions of the subsurface is important. An additional simple but often overlooked QC consideration during the data processing stage is the measure of misfit between the measured field data and the synthetic data determined using the estimated model for the resistivity structure. If this misfit criterion is not adequately minimized, the resulting image should not be considered the best possible estimate of subsurface resistivity.

5.2.5 Limitations

Despite the wide range of ERI applications, some practitioners make overly bold claims that resistivity is a direct NAPL detection tool. Although it is reasonable to assume that a new spill of electrically resistive NAPL forming a continuous, sufficiently thick layer may be detectable, ERI is highly unlikely to directly detect an aged NAPL spill in the subsurface. More accurately, the NAPL biodegrades and results in resistivity signatures (Atekwana and Atekwana 2010). Another example signature is the ionic concentration increase in the porse fluid that results from mineral surface weathering in the presence of organic acids generated by microbial degradation of LNAPL. Finally, resistivity can appear to correlate with LNAPL and DNAPL distribution because of mutual dependence on low-permeability zones. The low permeability materials that tend to lock up NAPL (and act as long-term, sources of contamination driven by back diffusion) are typically fine-grained materials that are electrically conductive and easily resolvable in electrical images.

The relatively low resolution of ERI (see Figure 5-3) is a major limitation that tends to be overlooked; structure smoothing is necessary to obtain a meaningful image. Although ERI can often resolve some degree of subsurface heterogeneity, heterogeneity at a scale below the resolution of the imaging may go undetected or exert strong influence on flow and transport not incorporated into the CSM. It is important to recognize that resolution decreases dramatically with distance below the surface (when electrodes are at the surface) so the best possible resolution only applies to the first layer of the Earth with a thickness equal to approximately half the electrode spacing. Claims of high resolution (a few meters) or better at depth (beyond the top 5 m to 10 m) are suspect because they are inconsistent with the physics of the method. In addition, images that show a lot of structural variability at large distances from the electrodes are suspect because resolution with this method decays substantially with depth. The structural variability results from the inversion of noisy datasets and inappropriate constraints placed on the model structure. Similarly, images containing strong lateral contrasts at depth (vertical contacts in the images at depth) are most likely an artifact resulting from modifying the inversion settings to favor rough-image structure.

Another common error in the interpretation of resistivity images from a standard 2-D survey is that (in this case) the

inversion routine solves for a 2-D subsurface structure; no variation in resistivity is assumed in the direction perpendicular to the image. Although this is a reasonable assumption in some cases (for example, transects perpendicular to a pipeline or across a valley filled with sediments deposited in a low energy environment), 2-D imaging is often done in complex 3-D terrain (for example, over karst) where the 2-D assumption is not valid. In this case, the image produced cannot be expected to represent reality and will contain image artifacts because 3-D structures are being represented by a 2-D model.

5.2.6 Cost

The cost of a ERI survey depends on the complexity of the survey and site conditions. A standard 2-D resistivity imaging survey can be performed by two people in the field. A two-person crew may be able to advance over 300 electrode locations in a day under good site conditions. Productivity declines considerably in the presence of more complex terrain. A resistivity survey is expected to cost $2,000 to $4,000 per day for field data acquisition. Data processing costs depend on the complexity of the survey; a reasonable assumption is half a day of data processing time for every day of field data acquisition.

5.2.7 Case Studies

Examples of how ERI can be applied are provided in the following case studies:

- ERI Provides Data to Improve Groundwater Flow and Contaminant Transport Models at Hanford 300 Facility in Washington
- Surface and Borehole Geophysical Technologies Provide Data to Pinpoint and Characterize Karst Features at a Former Retail Petroleum Facility in Kentucky

5.3 Ground Penetrating Radar

GPR is a high-resolution EM technique that has been developed over the past 40+ years to investigate the subsurface in environmental, engineering, and archaeological investigations (Daniels 2000). GPR is a widely accepted imaging and characterization tool. Its effectiveness depends strongly onsite conditions. Similar to navigational radar, GPR identifies the location, shape, and size of subsurface features based on the reflection of high frequency [10 to 1,500 megahertz (MHz)] EM pulses or waves transmitted from a radar antenna (Daniels 2000); (USEPA 2016d).

Due to the wide range of frequency antennas that can be used, GPR is capable of a high degree of lateral and vertical resolution that often exceeds that of other surface geophysical methods, (ASTM 2011a). Large areas can be covered quickly in the field using GPR. When applied in the right setting, GPR is highly efficient and a reliable source of high-quality 2-D and 3-D data. The real-time capability of GPR allows a geophysicist to interpret the results qualitatively to evaluate site conditions and adjust the field program as needed (NJDEP 2005).

GPR detects changes in EM properties in the subsurface, such as dielectric permittivity, conductivity, and magnetic permeability, that are a function of soil and rock properties, water content, and bulk density (ASTM 2011b). Dielectric permittivity (also known as dielectric constant) is a measure of the ability of a material to store an electric charge by separating opposite polarity charges in space; it effectively measures a material's ability to be polarized by electric displacement due to an electric field and has units of farads per meter (F/m) (ASTM 2011b). It is more convenient in practice to use relative dielectric permittivity, which is the ratio of the dielectric permittivity of a material to the permittivity of a vacuum and is a dimensionless term (Annan 2003). The relative dielectric permittivity of geological materials varies from 1 for air to a maximum of around 80 (depending on the temperature) for water. Solid minerals or rocks have a low relative dielectric permittivity (less than 10). The relative dielectric permittivity of sediments and rocks varies widely depending on the porosity and the water content. Low-porosity rocks and dry unconsolidated sediments (for example, hydraulic conductivity whereas porous rocks and saturated sediments have high relative dielectric permittivity (Everett 2013); (USEPA 2018b). Most geophysics textbooks include tables where representative values of hydraulic conductivity are published for different geological materials; actual values strongly depend on porosity and water content.

GPR senses variations in the hydraulic conductivity, which controls the velocity at which EM waves travel between a transmitter and receiver. The arrival time of the transmitted wave recorded at the receiver is usually stated in Ns (10^{-9} sec) (Daniels 2000); (USEPA 2016d). EM waves travel at 0.3 m/Ns (speed of light) through the air and less than 0.3 m/Ns through geologic media (Daniels 2000); (USEPA 2016d). Variations in the subsurface result in reflected EM waves that are returned to the instrument from interfaces or irregularities with hydraulic conductivity contrasts. Abrupt variations in water content and porosity are usually the primary cause of reflections returned to the instrument. The returning portion of the EM wave is

captured by the receiving antenna where its amplitude, wavelength, and two-way travel time are recorded for processing and interpretation (Dojack 2012). Short EM wavelengths (high frequency) yield a high resolution of interfaces and objects (Daniels 2000).

GPR is most often a shallow subsurface tool (for example, 100 ft or less) due to the many variables that affect EM penetration, reflection, and scattering. GPR service providers should be equipped with multiple antennas of different frequencies to adjust for site-specific conditions, if needed. As an example of the relationships between antenna frequency, resolution, and penetration depth, a 100-MHz antenna can penetrate up to 60 ft in a clean, dry sand setting and have a resolution capable of identifying a 2-ft pipe at 20 ft. In comparison, a 1,000-MHz antenna can penetrate to only 6 ft in a clean, dry sand but resolve shallow wire mesh and a 3/16-inch hose at 6 ft (see US Radar Inc – Ground Penetrating Radar FAQ website (USRadar 2019)). An inherent tradeoff between penetration depth and resolution must be evaluated critically and is discussed in greater detail in Section 5.3.4.

5.3.1 Use

GPR equipment typically consists of a radar-control unit, transmitting and receiving antennas, electronics, and recording devices (see Figure 5-4). The transmitting and receiving electronics are kept separate (Daniels 2000). The radar-control unit sends synchronized trigger pulses to the transmitting and receiving antennas at up to thousands of times per second (USEPA 2018b). The antenna is typically shielded to maximize the energy path to and from the subsurface target to reduce the energy transfer between the transmitter and receiver as well as into the air and to minimize external noise from interferences (Annan 2009). The system is digitally controlled, and data are digitally recorded for processing and display (Daniels 2000). The GPR system contains a microprocessor, internal memory, and data storage.

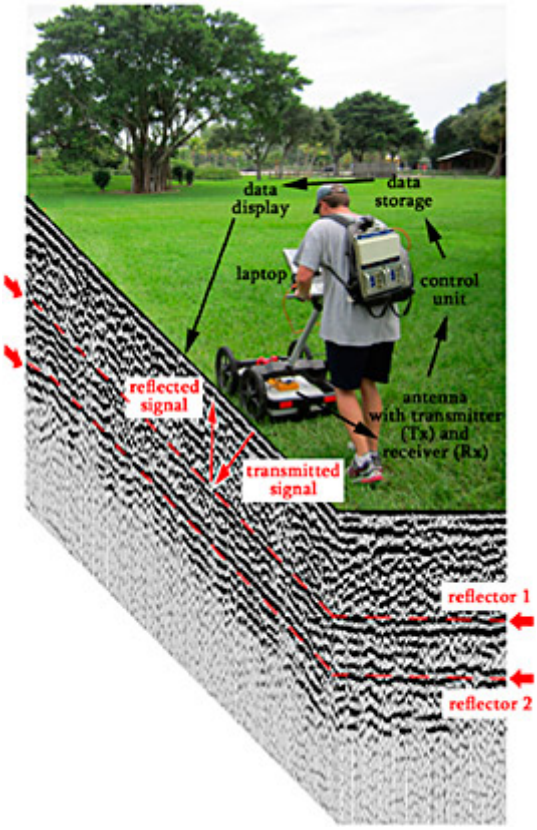

Figure 5-4. GPR implementation involves a pulse of EM energy traveling from a transmitter (Tx) to a receiver (Rx) antenna and contrasts in hydraulic conductivity return a reflection in the GPR record.

Source: Florida Atlantic University, Used with permission

Reflection profiling is the most common type of GPR deployment. Radar waves are transmitted, received, and recorded each time both antennas have been moved a fixed distance across the ground surface (USEPA 2018b). GPR is often deployed along linear transects. The number of transects is a function of the anticipated propagation of the EM wave in the geologic environment. The transects are completed in one direction and then an additional set is completed in a perpendicular direction to improve resolution since the reflected EM pulses are only acquired in the narrow band directly below the transect and could miss objects aligned parallel to the transects. Compiling responses along each transect line enables a

clearer interpretation of the subsurface along a profile.

GPR applications in geologic studies include identifying the depth to bedrock, depth and thickness of soil strata, depth to the water table, and location of cavities or fractures in bedrock (USEPA 2016d); (USEPA 2018b). GPR applications also include locating subsurface structures such as pipes, drums, waste and landfills, tanks, cables, trenches, pits, fill material, unexploded ordnance (UXO), and munitions. GPR may be used for QC testing of soil surveys or on road paving and asphalt projects (Annan 2009). In addition, GPR may be able to detect subsurface contamination provided the contaminant changes the dielectric permittivity to a detectable degree (for example, above background noise in the data). For example, the relative dielectric permittivity of a common organic solvent, trichloroethene, is 3.42 compared to 1.0 for air and 78 for water at 25°C; if such a contaminant displaces water sufficiently in the subsurface, a distinct change in the relative dielectric permittivity occurs for this region of the subsurface (Knight 2001). Similarly, the presence of an immiscible phase of liquid, such as NAPL, may provide an even greater change in the dielectric constant than it would as a dissolved phase in the same media. When a pure NAPL displaces pore water, there is a reduction in conductivity and dielectric permittivity in the media which translates to an increase in the EM wave velocity and decrease in attenuation (Redman 2009). However, in practice, NAPL identification with GPR is typically limited to recent releases that exhibit little weathering of the NAPL via biodegradation or other chemical interactions.

GPR works best in dry, coarse-grained materials such as sand and gravel. High-conductivity soils and saltwater applications are highly detrimental to GPR application because of the high likelihood of EM attenuation (ASTM 2011b). Because clayey fill (high conductivity) is frequently present in the shallow subsurface at most industrial sites, penetration depths may be less than 30 ft (about10 m) for most environmental investigations (USEPA 2016d).

GPR equipment and software are complex and technical training is needed for proper use, data filtering and processing, and interpretation. Training is particularly important for environmental applications of the technology; GPR manufacturers provide integrated tools for utilities detection that are often operated by a less experienced operator. GPR services should be contracted to specialty providers with the proper training and experience; the end user is advised to be wary of contractors who treat GPR as a “black box” (where data goes into a computer and generates results with no processing or data interpretation). Users of GPR data should seek references and project examples from potential GPR providers to vet their experiences and backgrounds. Project objectives and GPR capabilities should be established with the contractor early in the project based on conditions at the site. The GPR contractor should provide input on the advantages and limitations of GPR for the site. GPR services are often contracted using a daily rate, particularly for short, well-defined projects.

For additional information on accepted and recommended procedures for implementing GPR, please refer to (ASTM 2011b).

5.3.2 Data Collection Design

GPR is often one of the first tools employed at a site as the CSM is being developed. Many factors at a site can attenuate the EM wave energy from GPR and, if not well understood and addressed in the investigation design, reduce the effectiveness of GPR. Three factors that should be understood prior to deploying GPR are the following:

- expected site stratigraphy and saturation data (including the types of sediments, stratigraphical order, depths, thicknesses, and water table depth) available from regional to local geologic literature and previous site characterization, if available
- presence of subsurface utilities and other potential interferences such as rebar-reinforced concrete, including their approximate locations based on aboveground indicators (for example, manholes, gas line markers), composition, depths
- aboveground access and interferences that could constrain equipment deployment and locations of potential aboveground interferences such as fences, signs, power lines

Having a solid grasp of these site characteristics is vital for the successful use of GPR.

The knowledge of the expected depth of investigation and relative suitability of soils can aid potential GPR users in refining their methods search. For example, the EC of near-surface sediments is a critical consideration as GPR is often rendered ineffective as a result of excessive signal attenuation by conductive soils (for example, clayey soils, high salinity soils).The USDA Natural Resources Conservation Service has used the soil attribute data from the State Soil Geographic (STATSGO) and the Soil Survey Geographic (SSURGO) databases to develop thematic maps showing relative suitability of soils for many GPR applications (See the USDA NRCS Ground-Penetrating Radar Soil Suitability Maps website (USDA 2009). A generalized map of the U.S. and each state (excluding Alaska) is listed and can be downloaded as a PDF. GPR suitability is rated on a

scale of one to six. Some areas have not been digitized and have no data (USDA 2009). These maps are a guide and local conditions may vary.

Additional considerations include information gained by answering the following questions (Annan 2003):

- Is the target within the detection range of GPR regardless of the subsurface characteristics of the site?
- Will the target elicit a response that is detectable and discernable above background noise?
- Are multiple targets that need to be included in the study design likely to be present?
- Are there other conditions that would preclude using GPR?

A GPR study must be designed knowing the desired resolution and the depth of assessment that can be reliably attained for that level of resolution. The EM pulse frequency is inversely proportional to signal penetration and data resolution (the lower the frequency of the EM pulse, the deeper the signal penetration but the poorer the data resolution, and vice-versa). Two commonly used rules of thumb for evaluating the resolution of GPR are (1) the resolution may be approximated as the maximum depth of the investigation divided by 100 and (2) GPR will be ineffective if the actual target depth is greater than 50% of the maximum depth of the radar (Annan 2003). Additionally, when detecting subsurface utilities, the diameter of a conduit capable of detection is 1 inch per foot of burial (for example, minimum 4-inch-diameter conduit located 4 ft below ground surface).

GPR data may be collected using two modes: moving and fixed. In the moving mode, the transmitter and receiver are maintained at a fixed distance and are moved together along a line to produce a profile (Daniels 2000); (USEPA 2016d). The size of the target and survey objectives must consider the spacing between the traces received by the equipment (Daniels 2000). This mode offers the advantage of rapid data acquisition (See Figure 5-4 and Figure 5-5). In fixed mode, the transmitting and receiving antennas are moved independently to different points to make discrete measurements. The EM wave is transmitted, the receiver is turned on to receive and record the signals, and then the receiver is turned off (Daniels 2000). The measurements recorded create a trace, a time history of the travel of an EM pulse from the transmitter to the receiver. This mode is more labor intensive but provides greater flexibility than moving mode.

5.3.3 Data Processing and Data Visualization

Collected GPR data require considerable iterative postprocessing to improve data quality prior to interpretation. This postprocessing is performed with specialty software and should be conducted by a competent and trained practitioner. Because advanced data processing often includes a higher degree of interpreter bias, it is important to discuss the assumptions made by the practitioner processing the data (Annan 2009).

The GPR trace recorded must be converted from two-way travel time to a depth. The travel time is a record of the changes in amplitude of the EM wave as it travels through the subsurface and encounters reflectors that send the wave back to the ground surface (see Figure 5-4). The propagation velocity of the EM wave is calculated by dividing the propagation velocity of an EM wave in a vacuum (3×10^8 m/s) by the square root of the dielectric permittivity of the subsurface materials (obtained from literature sources). Once the propagation velocity has been estimated based on published values or professional judgment, it is multiplied by the measured two-way travel time to determine the equivalent depth (ASTM 2011b).

The objective of GPR data presentation is to depict a visual image that approximates the subsurface and position of any anomalies. Oftentimes, GPR results include subtleties that do not produce sharp boundaries. These subtleties often represent gradational boundaries that can complicate GPR data interpretation. Examples include heterogeneous fill materials or the water table (Annan 2003). These subtleties in data interpretation should be carefully considered. A significant amount of data filtering is required to produce usable and unbiased GPR images of subsurface data. Corrections to the recorded EM wave are made to account for the effects of attenuation due to geometric spreading, removal of low-frequency energy that subsequently distorts the recorded waveform, and topography. More sophisticated processing includes a step known as migration to correct the location of reflections coming from interfaces that are not vertically below the instrument. Further details can be found in (Annan 2009).

GPR displays are most often presented as 2-D cross sections showing travel times for reflection events. These plots depict distance at ground surface on the x axis versus depth travel time (surrogate for depth below ground surface) on the y axis. An example of a 2-D image illustrating the location of a sewer line is shown in Figure 5-5. This figure also shows how dragging the GPR across a localized target (such as a sewer line) results in a characteristic hyperbola in the reflection record.

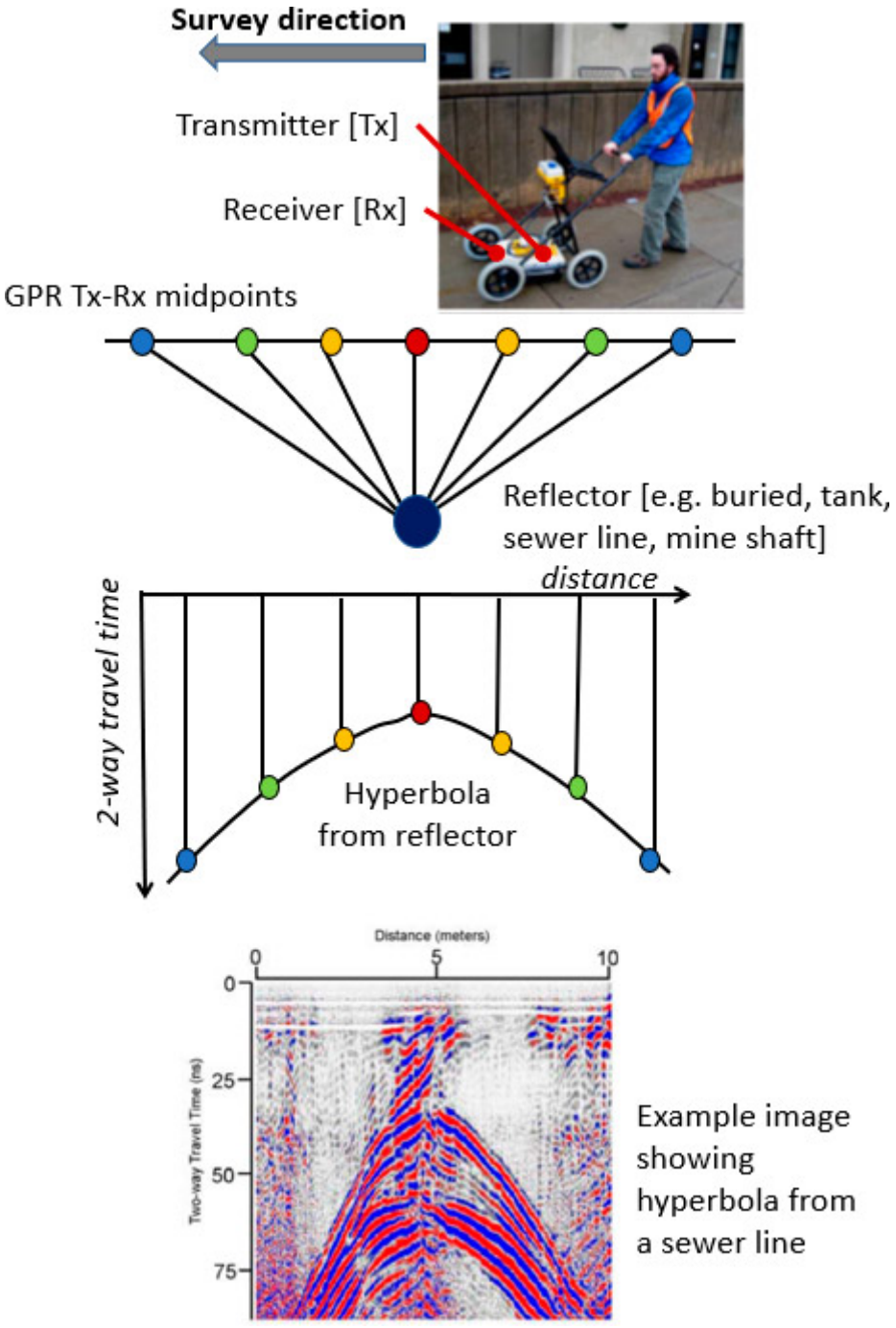

Figure 5-5. Schematic of a GPR survey of buried tank.
Source: Rutgers University Newark, Lee Slater, Used with permission

Another useful representation of GPR datasets is a 3-D block diagram showing relative amplitudes of EM energy at different levels or slices. These block diagrams are useful for identifying and isolating features of interest but can be more challenging for nontechnical reviewers to understand. For a 3-D image to be useful, the amplitude color ranges should be assigned thoughtfully with a minimum number of colors. The viewing angle is another important visualization aspect to consider. A comparison of 2-D and 3-D images for the same target is shown in Figure 5-6.

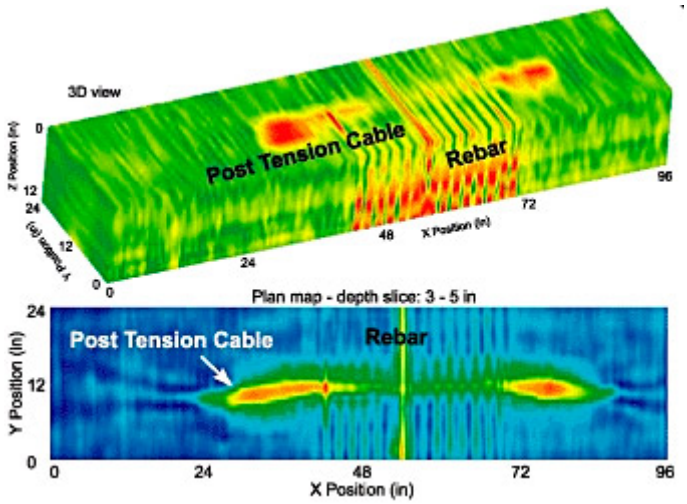

Figure 5-6. 3-D GPR block view of response contrast for metallic objects in relation to 2-D horizontal slices.
Source: (USEPA 2016d)

5.3.4 Quality Control

QC procedures apply to GPR field procedures and data processing and interpretation activities. In the field, test lines are used to obtain the system settings that are optimal for the site. Field logs should be maintained to document system settings and field procedures and changes to either. Site conditions at the time of the survey (weather, ambient conditions) should be recorded because they can influence test data. Equipment calibration is usually performed in accordance with manufacturer's specifications. Operational checks should be performed prior to use and throughout the day as a periodic check. Corrective actions taken to fix equipment or troubleshoot problems should also be recorded. Data should be reviewed as quickly as possible in the field so that scans can be rerun if necessary. It is good practice to rerun the test line to confirm proper system operation (ASTM 2011b).

5.3.5 Limitations

GPR has depth limitations depending on the contrast of electrical properties of the geological formations and the variability in signal attenuation. These factors result in signal losses due to EC, the dielectric constant, and scattering (ASTM 2011b). The effectiveness of a GPR survey is strongly dependent on the rate of attenuation of the EM energy as the signal propagates into the earth. At some distance, the attenuation is so excessive that the returned signal is no longer detectable above the EM noise levels. The attenuation of EM waves is largely from EM energy converting to thermal energy, an effect that increases with the EC of soil, rock, and fluids (USEPA 2018b). The attenuation rate determines the penetration depth of a GPR instrument at a site. In rocks and soil, the degree of saturation, content of pore fluid (for example, free ions in solution), clay mineralogy, and soil types have a strong influence on the bulk material's conductivity and ability to transmit an EM wave (ASTM 2011b).

Unfortunately, site conditions often preclude optimal performance of GPR. The ionic strength of site groundwater and thickness of clay deposits reduce signal-penetration depth. In general, signal penetration is best in dry, sandy, or rocky soils and worse in moist, clayey, and conductive soils (USEPA 1993). Signal attenuation can be 3 ft (1 m) or less in conductive materials such as seawater, mineral-rich clays, or metallic materials. Conversely, penetration depths have been reported up to 100 ft in water saturated sands to nearly 1,000 ft in granite (ASTM 2011b). In a quartz sand-rich environment with the water table at 15 ft, depths of 20 ft are easily obtainable.

Similarly, the presence of surface and buried conductive (metallic) debris on a site can severely hamper subsurface investigations. Radar waves are predominately attenuated by EC (Everett 2013). Reinforcing rods in concrete, buried railway tracks, and even metal underground tanks whisk radar wave energy away leaving little energy for the required detection of reflections.

Finally, accessibility issues on a site can limit effective GPR deployment. GPR equipment must be physically moved across the study area. Although the equipment is portable and often pushed manually by one person via a cart comparable in size to a shopping cart (see Figure 5-5), heavily wooded sites, congested areas, or heavily sloped areas can limit GPR. Air-wave

interferences are also problematic because they reflect the EM signal, which is then captured by the receiver. Air-wave reflections can occur from overhead power lines, telephone poles, walls, fences, vehicles. (Annan 2003).

5.3.6 Cost

Estimates for GPR surveys are typically quoted on a day-rate basis. A typical GPR survey for the purpose of searching for USTs or performing utility surveys, can cost about $3,000 for 1 acre to 1.5 acres. GPR surveys geared to locate subsurface voids may require tighter line spacing so the cost increases to approximately $3,500 for 0.5 acres. These daily rates normally include costs for personnel, equipment, acquisition, interpretation, and reporting.

The number of GPR personnel needed to run a survey depends on the type of survey. A wildcat survey (random lines) can be performed by one person; a grid survey requires at least three people). Sometimes both techniques can be used at a site. Generally, a wildcat survey is used to identify a more specific area of interest where a grid survey is performed. Mobilization and per diem costs are based on the location of the site and the distance from the contractor's office.

5.3.7 Case Studies

Examples of how GPR can be applied are provided in the following case studies:

- Surface and Borehole Geophysical Technologies Provide Data to Pinpoint and Characterize Karst Features at a Former Retail Petroleum Facility in Kentucky
- GPR Data Show Location of Buried Debris and Piping Associated with a Former Gas Holder in Minnesota

5.4 Seismic Methods

Seismic exploration methods are commonly used to determine site geology, stratigraphy, and rock quality. These techniques provide information about subsurface geology, and they make use of the properties of sound waves as they propagate through earth. The methods are based on the fact that geologic materials have different acoustic impedance (the product of density and seismic velocity). This difference results in body waves that reflect or refract at the interface of two strata, and surface waves that disperse (spread out) as they travel across the surface of the Earth.

Seismic reflection and refraction techniques measure the travel time of two types of body waves from surficial shots (an energy source, usually in the form of a sledgehammer striking a metal plate flat on the ground). The primary wave (P wave) and the secondary wave (S wave). The P wave, also called compression wave, is the fastest traveling wave and, consequently, the first to arrive to a strata boundary. The S wave, also called the shear or transverse wave, travels slightly slower than the P wave and is produced by the conversion of a P wave at a boundary. Seismic-wave velocities depend on the elastic moduli and the densities of the geologic material in which the wave travels through. Elastic moduli are a set of constants that define how a material responding to stress deforms, then recovers to its original shape after the stress stops. For example, a sound wave travels at a speed of 300 m/sec to 800 m/sec through unconsolidated sand while traveling at a speed between 4,600 m/sec to 7,000 m/sec through granite.

MASW is a seismic technique that uses surface waves (specifically Rayleigh waves) from a similar energy source (for example, sledgehammer striking a metal plate) to determine shear-wave velocity (Vs) profiles in the subsurface. The basis of this technique is the dispersive characteristics of surface waves when traveling through a layered medium; different wavelengths propagate with different velocities depending on their penetration depth. There are two types of MASW techniques (passive and active); active MASW is the most common and is discussed in this section.

Applications for seismic methods include mapping depth to bedrock and bedrock topography, mapping depth to groundwater, identifying and mapping faults, identifying geologic settings for NAPL transport, mapping stratigraphy, and mapping subsurface geologic structures. In addition, MASW is commonly used for mapping variation in soil stiffness (Vs is a direct indicator of ground stiffness) and identifying low-velocity anomalies (for example, karst terrain, voids and sinkholes, severely weathered bedrock, waste pits, and surface bedrock features).

Although seismic methods (especially reflection) can be more expensive than other geophysical methods, they are cost effective for the information they provide compared to nongeophysical intrusive methods. Equipment is readily available, portable, and nonintrusive, and seismic measurements have good resolution and provide relatively rapid coverage of a large area.

5.4.1 Use

A linear array of geophones (a recording device used to convert velocity into voltage) is typically established along the ground surface. Surficial shots (a seismic energy source, usually obtained by hitting a metal plate placed flat on the ground with a sledgehammer) are generated to provide a seismic wave in the form of a strong vibration that is recorded by the geophones. Shots are fired, in turn, at each geophone, and active geophones are progressively added ahead of the shots in a roll-along fashion. The geophones receive and transmit data to a data processing unit where software algorithms process the signal. The data processed are used to produce an image of the subsurface stratigraphy (Sheriff and Geldart 1995).

5.4.1.1 Multichannel Analysis of Surface Waves

In this method, the ground is struck multiple times with a sledgehammer to enhance the amplitude of the surface wave and minimize background noise. This process is called vertical stacking. Data are recorded and analyzed via dispersion and inversion analysis.

Because higher frequency signals are mostly refracted energy and refracted energy noise, low-frequency geophones are needed; low-frequency, vertically-polarized geophones are commonly used to record surface wave data because they can record extremely low-frequency data and attenuate higher frequency signals. The desired surface-wave energy to analyze in MASW usually ranges between 5 Hz and 40 Hz. Figure 5-7 illustrates an overview of the method, including:

- data acquisition and the multichannel record obtained (note that it contains multiple frequencies despite looking like only one)
- dispersion image generated from each record along with its extracted dispersion curve
- one-dimensional shear-wave velocity profile that is back calculated from the curve
- final 2-D shear-wave velocity profile map produced using an appropriate interpolation method

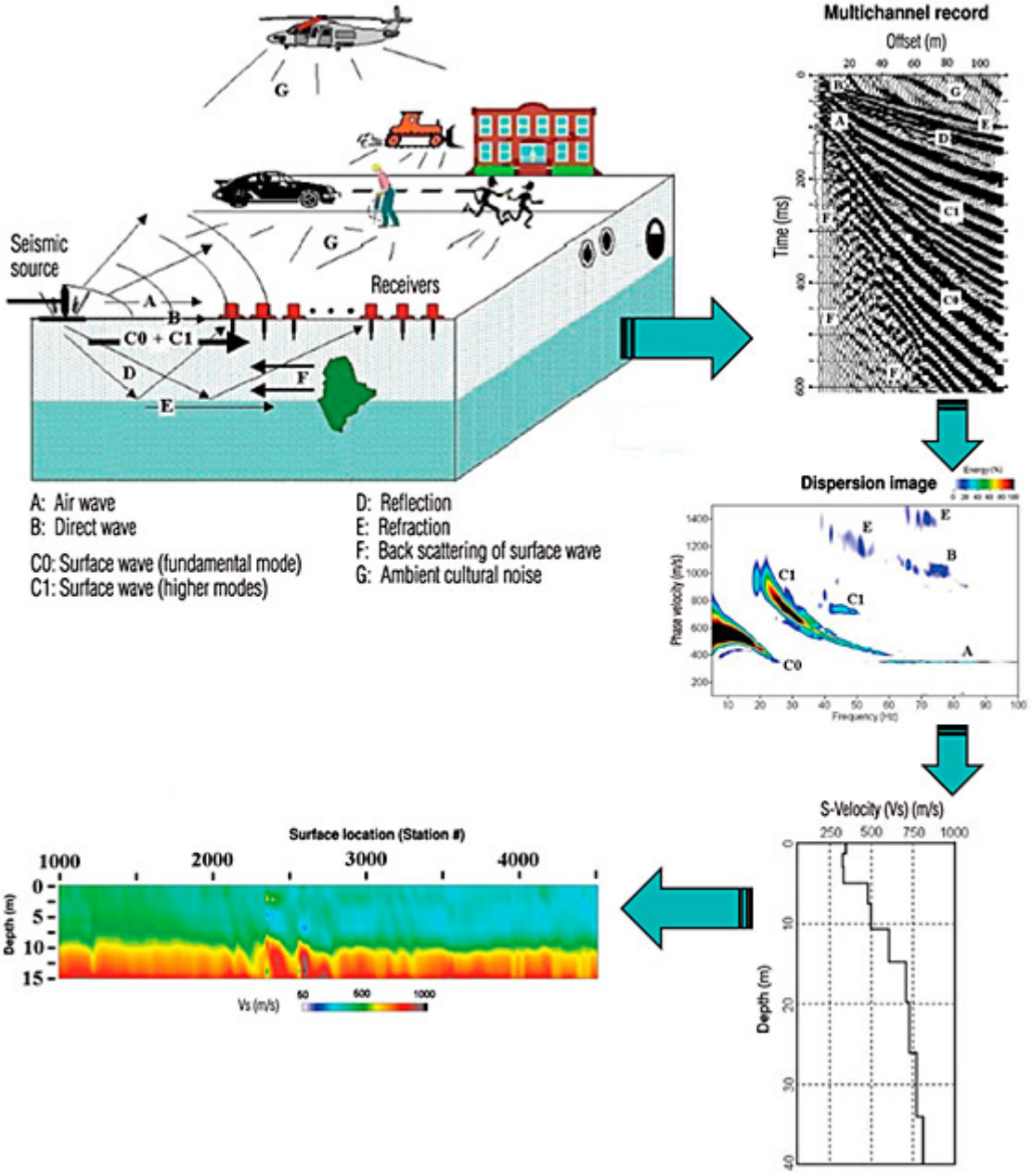

Figure 5-7. Overall procedure and application of MASW.
Source: Modified after (Park et al. 2007), Used with Permission

5.4.1.2 Reflection

Reflection surveys use geophones to record the arrival of the P waves after they have reflected from a subsurface horizon. As the first seismic wave (the P wave) generated by the shot source (for example, sledgehammer) travels through the geologic media, it propagates in three different ray paths. One path is along the ground surface (direct ray). The second path is represented by the reflected wave. The reflected wave consists of the wave that travels down to the interface layer, hits the interface, and travels upwardly from the refracting layer (reflected ray). The third path (critically refracted ray) is represented by the refracted wave, which has three legs. The first leg travels downwardly across the first layer and with an off-set x from the downward reflected ray, hits the interface, and produces the second leg of the refracted wave that travels along the second layer (at the speed of the lower layer). The third leg travels upwardly through the refracting layer or refractor by critical refraction). A simplified diagram of the method is shown in Figure 5-8.

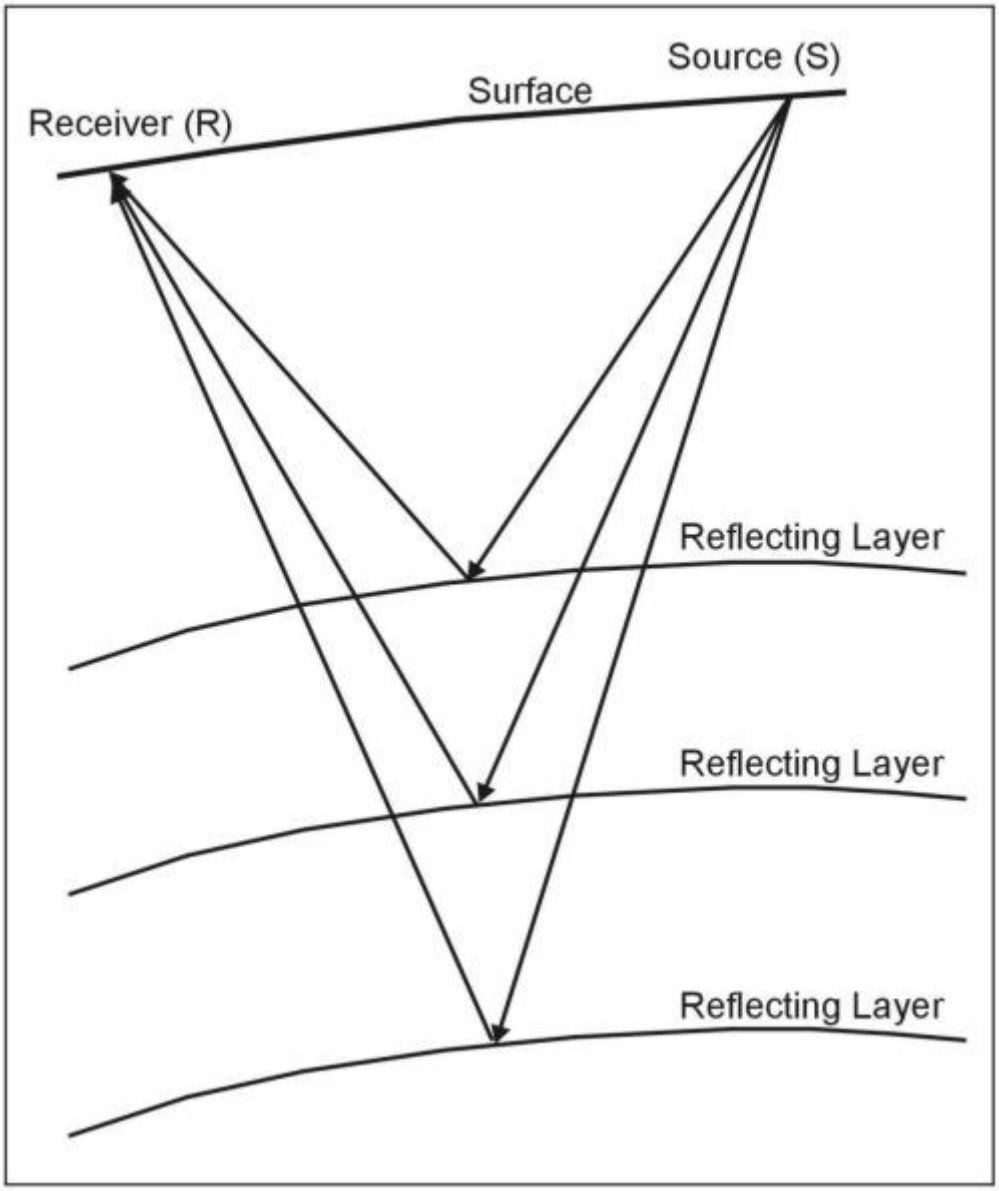

Figure 5-8. Schematic of the seismic reflection method.
Source: (USEPA 2016a)

5.4.1.3 Refraction

The seismic refraction technique analyzes the refracted wave along the different stratigraphic interfaces by recording the signatures on each geophone in the spread implanted in the ground. Ray paths go downward to the boundary, are refracted along the boundary, and return to the surface. The recorded signal response is plotted and processed as a function of the distance (off set) from the source. The processed signal produces a cross section of the seismic wave velocity, which, in turn, conveys information about the geological stratigraphy (Sheriff and Geldart 1995); (Council 2000). The seismic reflection technique generates an image of the subsurface impedance contrast for the area investigated. The image provides data related to the distance and travel time of the reflected wave (Council 2000). Figure 5-9 provides a schematic of a seismic refraction survey. First arrivals near the shot have paths directly from the shot to the detector. Rays traveling along the boundary are the first to arrive at receivers (geophones) away from the shot because the lower material has a higher velocity (V2 > V1).

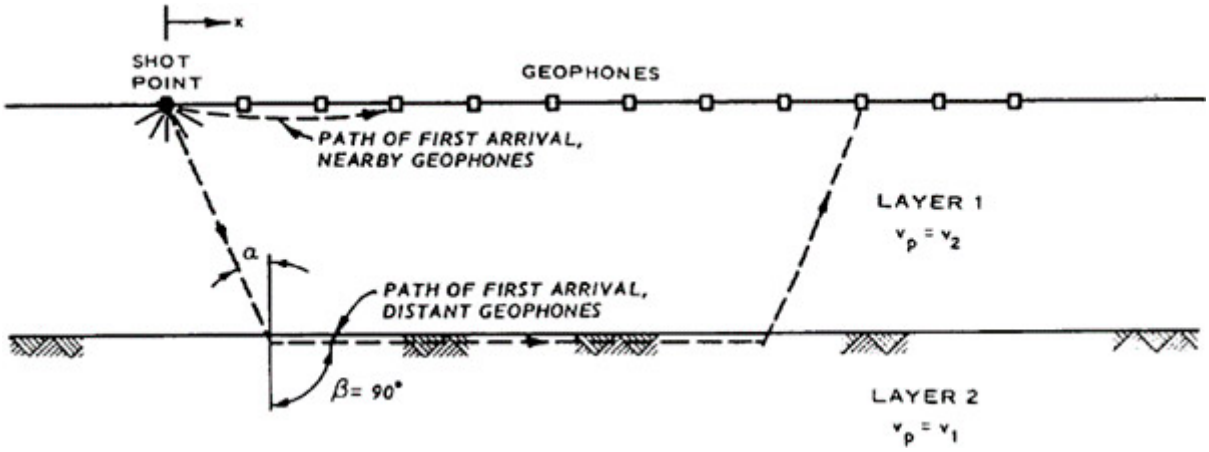

Figure 5-9. Seismic refraction schematic.
Source: (USACE 1995)

5.4.2 Data Collection Design

The maximum depth and resolution of the data depend on the energy and frequency of the initial pulse and arrangement (geometry) of the geophones. Factors to consider which energy source to use include:

- its energy output (the stronger it is, the better the signal to noise ratio), for most environmental work, the best possible source is a 14 or 16 lb sledgehammer
- frequency content (higher frequencies offer high resolution but decay more quickly than lower frequencies; this lowers the depth of investigation)
- a source should allow for stacking measurements to improve the signal to noise ratio (it should be repeatable)
- the source signature should be well-defined (the wave energy should be known exactly) to significantly enhance the imaging quality (GPG 2017).

Common geometries of survey designs include multichannel and common midpoint (CMP) (GPG 2017). A multichannel design can be a split spread, which has a central shot with receivers on both sides, or a single-ended spread where the receivers are always on one side of the source. Seismic traces belong to a single source, a common source gather. A CMP design uses multiple shots and receivers in specifically so that some subsurface points are sampled more than once. The goal is to identify all reflections to a point on various profiles and stack them to get an enhanced signal-to-noise ratio. The degree of multiplicity from a particular location is known as fold. For example, a 24-channel seismograph is commonly used to gather 12-fold data.

Additional general considerations for survey design are as follows (GPG 2017):

- Seismic reflection surveys are typically designed to detect a reflection from a particular subsurface point multiple times. This approach improves the ability to detect and image a given event because the method makes it more difficult to discern direct arrivals and sound waves traveling through the air.
- Seismic refraction surveys are most useful at sites where velocities increase with depth (for example, a sand or gravel layer overlies a clay layer instead of a clay layer overlying a sand or gravel layer).
- The depth of penetration is approximately one-fifth of the length of the geophone spread, including off-set shots. For example, if the depth of investigation must be 10 m, at least 50 m (measured from off-set shot to off-set shot must be available for the survey (GPG 2017).
- Vertical resolution for seismic data is how thin a layer can be before the reflections from its top and bottom become indistinguishable. Vertical resolution is dependent on the signal wavelength, which is dependent on the frequency and velocity of the material). The theoretical minimum thickness is ¼ wavelength (for example, careful processing could extract the pulses if they overlap by half a wavelength) (GPG 2017).
- For MASW investigations, the resolvable depth of investigation that can be obtained with the highest accuracy is related to the receiver spacing. The receiver spacing should be greater than 30% of the investigation depth but not exceed the investigation depth (MASW 2018). In practice, the length of spread is usually limited in the range of 10 ft to300 ft and the maximum depth of investigation is less than 150 ft. Note that surface waves generated by most seismic sources are attenuated and are not useable at the end of a long receiver spread because they become noisy (Park, Miller, and Xia 1999).

- For MASW investigations, topography influences the quality of the field measurements; surveying should be conducted on relatively flat ground for best results. The overall topographic variation might not affect the data, but the ground should be nearly flat, at least within the receiver span (Park 2006).

5.4.3 Data Processing and Visualization

Qualified specialists typically perform data processing. These individuals should have all available information (for example, well logs, known depths, results from ancillary methods, and the expected results).

The data from seismic surveys are usually plotted on time distance graphs and as a profile of stacked data of distance versus time. Most seismic instrumentation is capable of drawing a vertical cross section through the ground, or profiles, that are a layer-cake representation of depth to acoustic boundaries (stratigraphic horizons) and types of acoustic anomalies. Figure 5-10 provides a seismic reflection record. The receivers are arranged to one side of a shot, which is 15 m from the first geophone.

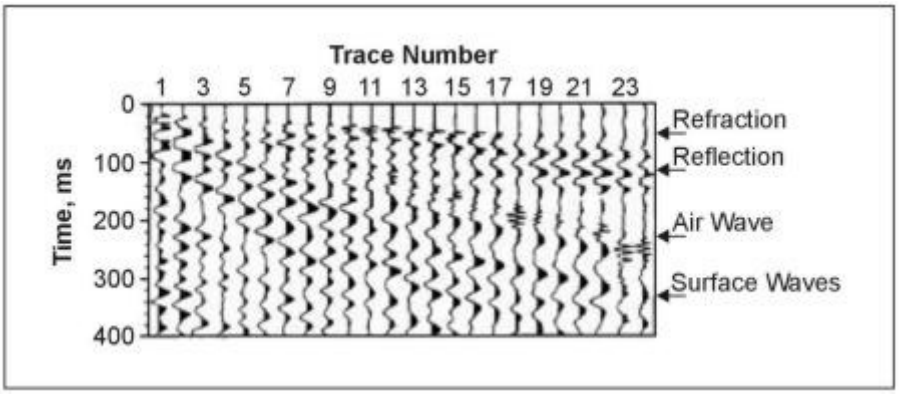

Figure 5-10. Simple seismic reflection record.
Source: (USEPA 2016a)

Data processing consists of three primary activities: deconvolution, CMP stacking, and migration. Deconvolution restores a waveshape to its form before filtering. CMP stacking uses a stack of common midpoint to gather traces. Migration performs an inversion so that reflections and diffractions are plotted at their true locations (Yilmaz 2001).

5.4.3.1 Seismic Reflection

The essential steps to process seismic reflection data (Baker 2019) are as follows:

- Obtain common source-point gathers.
- Sort into CMP gathers. (Reflection events appear as hyperbolic trajectories, and the goal is to stack them to a single trace.)
- Perform a velocity analysis for each event to find the stacking velocity.
- Perform a normal moveout correction and stack to yield a single trace corresponding to a coincident source and receiver.
- Composite the traces into a CMP-processed section.

These techniques can be expensive due to software cost and the need for a qualified specialist to interpret the results, but technically robust and excellent results can be achieved. An important outcome of the processing is obtaining a true depth section. This requires conversion of the times of the reflections to depths by derivation of a velocity profile. Well logs and check shots are often necessary to confirm the accuracy of this conversion.

5.4.3.2 Seismic Refraction

The generalized reciprocal method (GRM) is typically used to acquire, process, and interpret seismic refraction data. GRM is an interpretation method designed to accurately map undulating refractor surfaces from in-line refraction data using both forward and reverse shots. The method is related to the Hales and the reciprocal seismic refraction interpretation methods. In this method, it is crucial to acquire at least seven shots per spread. Assuming a 24-channel acquisition system, one center shot is required between geophones 12 and 13, one shot between each of geophone pairs 6 and 7 and 18 and 19, a near-off-set shot from each end geophone (geophones 1 and 24), and one far-off-set shot from each end of the spread. In practice,

often 13 shots are used per spread for high-resolution investigations. To map the refractor surface, an off-end shot must be located at each end of the spread so that each first arrival on the geophone spread is a bedrock arrival.

Blind zones and hidden layers may be encountered. A hidden layer is an intermediate velocity, intermediate depth layer whose thickness or velocity is such that rays from a deeper, higher velocity layer arrive at the ground surface sooner than rays from the hidden layer. Standard seismic refraction interpretation schemes yield significant errors in calculated refractor depths in the presence of blind zones or hidden layers. The GRM is the only method capable of overcoming this problem.

Data processing includes the selection of first-break arrival times, the generation of time-distance plots for each line, the assignment of selected portions of the travel-time data to individual refractors, and the phantoming of travel-time data for the target (lower) refractor. Once this preprocessing work is complete, GRM processing begins. Layer thicknesses and velocities are calculated, and a geophysical interpretation of the geological parameters is made. The end product is a seismic refraction profile that indicates the seismic layers detected, the depths to the interfaces between layers as they vary along the line, and the seismic velocities encountered.

5.4.3.3 MASW

After seismic data are uploaded into the MASW software (SurfSeis), the velocity at which each different frequency propagates is automatically analyzed. Each multichannel record is transformed from the space-time domain to the frequency domain, and a dispersion image (also called overtone image) is produced. The dispersion image shows fundamental and higher modes of the Rayleigh waves. A fundamental mode dispersion curve is then extracted from each dispersion image (Park 2006). Accurate extraction of the dispersion is the most critical step because its primarily determines the accuracy of the final shear-wave velocity profile. In a trial-and-error approach, the user can run the dispersion program several times for different phase velocity ranges and select the optimum dispersion curve. To improve the estimation of the optimum dispersion curve, multiple curves are extracted from several multichannel records and are combined into a single experimental curve.

The final step is developing the shear-wave velocity profile from the dispersion curve using an inversion process. Rayleigh waves are the product of interfering compressional and shear waves; therefore, inversion of the dispersion curve results in compressional and shear-wave velocities as a function of depth. In the inversion process, several possible soil models are estimated, and a dispersion curve model that best fits the experimental dispersion curve is selected. The theoretical dispersion curve of the models is first computed and compared to the experimental dispersion curve based on the root mean square error (RMSE) between the two curves. If the calculated RMSE is greater than the specified minimum error, the soil model is modified, and a new dispersion curve is calculated. The procedure is repeated until either the specified minimum error or the maximum number of iterations is reached. The shear-wave velocity profile of the model resulting in the best fit is the final output of dispersion-inversion analysis (Olafsdottir, Bessason, and Erlingsson 2018).

Spatial interpolation methods can be used to create a 2-D shear-wave velocity map by assigning each 1-D shear-wave velocity profile at the surface coordinate in the middle of the receiver spread used to acquire the corresponding record (Park 2005).

5.4.4 Quality Control

To ensure seismic data are properly recorded, the geophones should have the following:

- a digital converter to convert electrical signals into a time series of numbers
- the ability to start digitizing at the same time the shot is initiated
- a computer to manage input and to plot signals so that data quality can be checked visually
- in-built software to carry out initial data interpretations (GPG 2017)

To acquire data of sufficient quality, the surveyor should ensure no noise is generated at the geophones by confirming that the geophone has a good contact with the ground surface. Adding salty water to moisten the soil at the geophone location can enhance wave acquisition. In addition, ambient noise should be kept to a minimum during the survey. Avoid noise from people walking, cars, or heavy equipment movement in the proximity of the geophones.

Source offset (the distance between the source and first receiver) is an important consideration for MASW investigations because surface waves are formed at a certain distance from the source. If the first receiver is placed closer than this distance to the source, ambient noise is recorded rather than the surface waves. Source offset has been suggested to lie within the range of 25% to 50% of the receiver array length (MASW 2018); (Park and Carnevale 2010); (Park, Miller, and Xia

1999).

In addition to data-acquisition quality discussed above, the field data for MASW investigations require a number of preprocessing and processing considerations:

- Raw seismic data are converted into Kansas Geological Survey data processing format (KGS or SEG-Y), named for the Kansas Geological Survey who first developed the method. Field geometry should be correctly assigned during the data format conversion.
- Field data should be inspected, and bad records removed.
- Field data are inspected for the consistency in the alignment of surface waves in neighboring records.
- Filtering and muting are used to identify and eliminate noise.
- Sometimes preliminary data processing is performed to investigate the optimum ranges of phase velocity and frequency.
- To improve the estimation of the optimum dispersion curve, multiple curves are extracted from several multichannel records and are combined into a single experimental curve.
- Inversion of the data further reduces the uncertainty associated with the experimental dispersion curve estimates.

5.4.5 Advantages

5.4.5.1 Seismic Reflection

Seismic reflection can define sequential stratigraphy to great depths (>1,000 m or 3,281 ft), although a thick sequence of dry gravel greatly affects the depth of penetration. Depending on the application, seismic reflection can resolve layers down to 1 m (3 ft) thickness and is not affected by highly conductive electrical surface layers. Other advantages include:

- Data permits mapping of many horizons with each shot.
- The method can work regardless of velocity at depth (for example, reflection surveys are not hampered by clay layer overlying a sand/gravel layer).
- Observations can be more readily interpreted in terms of complex geology.
- Observations use the entire reflected wavefield (the time history of ground motion at different distances between the source and the receiver).
- The subsurface is directly imaged from the acquired observations.

5.4.5.2 Seismic Refraction

Seismic refraction is often used in shallow areas (less than 30 m or 100 ft) where the principal goal is to map bedrock topography beneath a single overburden unit. It also is employed to map weathered bedrock and fracture zones during water prospecting. If the velocity of the transmitting unit used with seismic refraction increases with depth, results may have to be modified or discarded. For example, a low-velocity thin-sand unit that is overlain by a high-velocity clay unit may not be resolvable with the refraction technique. Recent advances in inversion of seismic refraction data make it possible to image relatively small, nonstratigraphic targets such as foundation elements and perform refraction profiling in the presence of localized low-velocity zones such as incipient sinkholes. Other advantages include:

- Refraction observations generally employ fewer source and receiver locations and are thus relatively cheap to acquire.
- Little data processing is performed on refraction observations with the exception of trace scaling or filtering, which helps pick the arrival times of the initial ground motion.
- Because such a small portion of the recorded ground motion is used, developing models and interpretations is no more difficult than with other geophysical surveys.

5.4.5.3 MASW

MASW is a low-cost, noninvasive method that does not require heavy machinery for data measurement. Measuring geophones are placed in the ground and do not require coupling to the ground. Therefore, data are acquired relatively quickly without leaving lasting marks on the surface. Compared to seismic reflection and refraction methods, MASW is applicable in a wider range of field conditions.

The main advantage of MASW method compared to seismic reflection and refraction is that it determines stiffness profiles with far greater precision. Surface waves have stronger energy than body waves; hence, higher signal-to-noise ratios are

usually obtained in surface methods (Park, D.Miller, and Miura 2002); (Gouveia, Lopes, and Gomes 2016).

5.4.6 Limitations

The disadvantages of seismic methods are in the interpretation of data, which requires ground-truthing, information from other tools, and substantial expertise to interpret. The performance of seismic methods can be significantly affected by cultural noises, such as highways and airports, as well as buried building foundations. Seismic methods do not perform well in heterogeneous settings where thin discontinuous layers may be missed. Additionally, depth penetration may be sacrificed due to lack of low-frequency seismic energy (Anderson 2014). Other tool-specific limitations are discussed below.

5.4.6.1 Seismic Reflection

Seismic reflection costs more than refraction and is limited to penetration depths generally greater than approximately 50 ft. At depths less than approximately 50 ft, reflections from subsurface density contrasts arrive at geophones at nearly the same time as the much higher amplitude ground roll (surface waves) and air blast (the sound of the shot). Reflections from greater depths arrive at geophones after the ground roll and air blast have passed, making these deeper targets easier to detect and delineate. It is possible to obtain seismic reflections from shallow depths, perhaps as shallow as 3 m to 5 m if the following activities are performed.

- Vary field techniques depending on depth.
- Contain the air blast.
- Place shots and geophones near shallow or surface groundwater.
- Use severe low-cut filters and arrays of a small number (one to five) of geophones.
- Ensure reflections are visible on the field records after all recording parameters are optimized.
- Guide data processing by the appearance of field records; use extreme care to avoid stacking refractions or other unwanted artifacts as reflections.

Additional disadvantages are as follows:

- Because many source and receiver locations must be used to produce meaningful images, reflection seismic observations can be expensive to acquire.
- Reflection seismic processing requires appropriate software and requires a relatively high level of expertise. Thus, processing observation data is relatively expensive.
- At later times in the seismic record, more noise is present, making the reflections difficult to extract from the unprocessed data.

5.4.6.2 Seismic Refraction

Seismic refraction is generally applicable only where the seismic velocities of layers increase with depth. Therefore, where higher velocity (for example, clay) layers may overlie lower velocity (for example, sand or gravel) layers, seismic refraction may yield incorrect results. Additionally, seismic refraction requires geophone arrays with lengths of approximately four to five times the depth to target of interest. This limits its application to mapping features at depths less than 100 ft. Greater depths are possible, but the required array lengths may exceed site dimensions, and the shot energy required to transmit seismic arrivals for the required distances may necessitate using large explosive charges. Furthermore, the lateral resolution of seismic refraction data degrades with increasing array length due to migration of seismic waves. Other disadvantages include:

- Observations require relatively large source-receiver off sets
- Observations are generally interpreted in terms of layers that can have dip and topography.
- Observations only use the arrival time of the initial ground motion at different distances from the source (off sets).
- A model for the subsurface is constructed by attempting to reproduce the observed arrival times.

5.4.6.3 MASW

Rayleigh wave amplitudes decrease exponentially with depth; therefore, resolution diminishes markedly with increasing depth. As a result, investigations using MASW are limited to much shallower depths than either reflection or refraction (Park et al. 2007). Consequently, the application of MASW is limited when identifying thin deep layers and depth of deeper interfaces. Because MASW data are recorded using receiver arrays and averaging (lateral and vertical) occurs during data acquisition, the use of MASW at complex sites where the bedrock depth and soil properties vary significantly is limited

(Anderson 2014).

5.4.7 Cost

5.4.7.1 Seismic Reflection

The cost of a seismic reflection survey depends on the complexity of the survey and the site conditions (for example, terrain, topography, accessibility, surface hardness dictating ease of planting electrodes). A standard reflection imaging survey can be performed by three to five people in the field. A three-person crew may be able to perform 400 shots in a day under good site conditions. This equates to approximately 900 ft (300 m) of line for a shallow survey. Productivity declines considerably in the presence of more complex terrain. A seismic reflection survey is expected to cost $2,000 to $4,000 per day to acquire field data. The costs involved to process resistivity data also depends on the complexity of the survey. At least a day of data processing time for every day of field acquisition is a reasonable estimate.

5.4.7.2 Seismic Refraction

Similar to a seismic reflection survey, the cost of a seismic refraction survey depends on the complexity of the survey and site conditions. A standard refraction imaging survey can be performed by two to three people in the field. A three-person crew may be able to place 600 ft (200 m) of lines per day. Productivity declines considerably in the presence of more complex terrain. A seismic refraction survey is expected to cost $1,000 to $2,000 per day to collect field data. Data processing costs also depend on the complexity of the survey. A day of data processing time for every day of field acquisition is a reasonable estimate.

5.4.7.3 MASW

MASW is relatively rapid and cost-effective method of estimating shear-wave velocity. The utility of this method is generally more economical in terms of data acquisition, data processing, and overall cost than obtaining these measurements using refraction, downhole, and cross-hole techniques (Park et al. 2007).

5.4.8 Case Studies

Examples of how seismic methods can be applied are provided in the following case studies:

- Resistivity, Seismic Exploration, and GPR Provide Data to Evaluate Clay Reserves at a Commercially Mined Pit
- Seismic Refraction, Electric Resistivity, and Multichannel Analysis of Seismic Waves Provide Data to Locate Monitoring Well Locations in a Mixed-Use Area in Northern Virginia
- Surface Geophysical Methods Provide Data to Identify Prospective Utility Waste Landfill Sites in Karst Terrain in Missouri

5.5 Electromagnetic Surveys

EM methods are methods that use an energy source (either an electric field or a changing magnetic field) to excite ground current. The ground current follows two fundamental principles of EM induction. Faraday's law of electromagnetic induction estimates how a magnetic field interacts with an electric current to produce an electromotive force; Ampere's law states that electric currents generate magnetic fields. Together, these two tenets embody the most fundamental EM phenomena: that a varying magnetic field will result in a varying electric field that will create another varying secondary magnetic field. When an electrical current is inducted into the ground (a conductor), a varying magnetic field is generated. The induction of the electrical current varies depending on the composition of the subsurface, and the secondary magnetic field provides information about the EC of the subsurface. The main objective of EM methods is to extract this information from measured data and translate it to electrical resistivity or EC images of the subsurface.

This section describes two sets of tools: frequency domain electromagnetic (FDEM) surveys and time domain electromagnetic (TDEM) surveys. FDEM surveys measure the electrical response of the subsurface at several frequencies to obtain information about conductivity variations with depth. TDEM surveys achieve the same results by measuring the electrical response of the subsurface to a pulsed wave at several time intervals after transmission.

5.5.1 Use

5.5.1.1 FDEM

FDEM instruments consist of a transmitter and receiver that use inductive coupling between electrical coils and subsurface

conductors to identify subsurface targets (see Figure 5-11). A primary alternating current magnetic field generates electrical currents (known as eddy currents) to flow in subsurface conductors. These eddy currents generate a secondary magnetic field. The receiver coil of the FDEM instrument measures the resultant field (vector sum of the primary and secondary fields). FDEM instruments generally have two configurations. One configuration involves two loops or coils that consist of a transmitter coil and a receiver coil where one person carries each. The receiver coil receives the primary and secondary magnetic fields. A second FDEM configuration includes a single instrument that houses the transmitter and receiver and is typically used with a field computer and a GPS.

Most EM equipment allows measurement of both the in-phase component and the 90° out-of-phase, or quadrature, components of the resultant field. Common FDEM systems use a low-induction approximation where the out-of-phase component is proportional to the EC. In this case the instruments are often described as terrain conductivity meters. The instrument records apparent EC, which is typically reported in mS/m. The in-phase component is a ratio of the secondary magnetic field and primary field and is measured in parts per thousand. It is a strong indicator of metal content.

FDEM is often used as a reconnaissance tool to guide more detailed surface geophysical surveys. The inductive coupling of the instrument to the subsurface means that measurements can be acquired rapidly without the need for direct ground contact, which allows for quick and efficient data collection relative to galvanic electrical resistivity imaging surveys. FDEM surveys are typically used for lateral geologic and hydrogeologic profiling in the subsurface, contaminant plume mapping, fill and waste delineation, and locating tanks and buried drums, buried structures, and underground utilities.

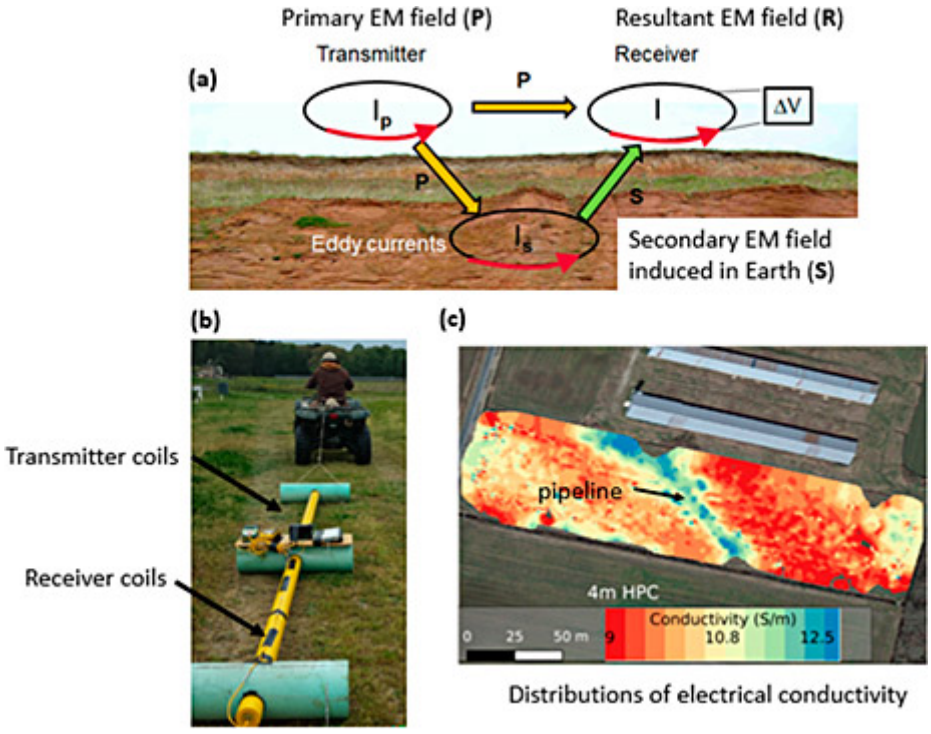

Figure 5-11. FDEM instrument components.
Source: Rutgers University Newark, Lee Slater, Used with permission

5.5.2 TDEM

TDEM surveys measure variations of EC (inverse of resistivity) in the subsurface. EC correlates well with several physical and chemical properties of subsurface materials, including particle size, texture, porosity, and ionic content (salinity), so it provides a detailed picture of subsurface material. TDEM surveys measure the amplitude of a signal as a function of time; the signal is transmitted as an electric current pulse (for example, by turning off the current quickly), and measurements are obtained after the primary field disappears (only in the presence of the secondary field).

TDEM instruments consist of a transmitter and receiver that send and receive an electrical signal. An electrical current is passed through an ungrounded loop (which requires no direct contact with the ground) that generates a magnetic field that, in turn, generates electrical eddy currents in the subsurface. Eddy currents are dependent on the subsurface electrical conductivity and geometry of the layers and are measured using an induction coil [see Figure 5-12 (a)]. The current diffuses more slowly in conductive materials compared to resistive materials. Soundings, information about the subsurface

conductivity as a function of depth, are measured in the receiving coil.

Transient soundings can be conducted by placing a wire in a square loop on the ground. The wires are then connected to the transmitter, and the receiving coil is placed in the middle of the transmitter loop. The receiving coil is connected to the receiver and the receiver is connected to the transmitter. These connections allow synchronization between the transmitter and receiver [see Figure 5-12 (b)]. TDEM data recording is completed in time windows called gates. The gates are set from a few microseconds up to tens or even hundreds of milliseconds after the transmitter current has been turned off. The gates are arranged logarithmically, increasing time lengths to improve the signal-to-noise ratio at later times; these later signals provide information on deeper layers.

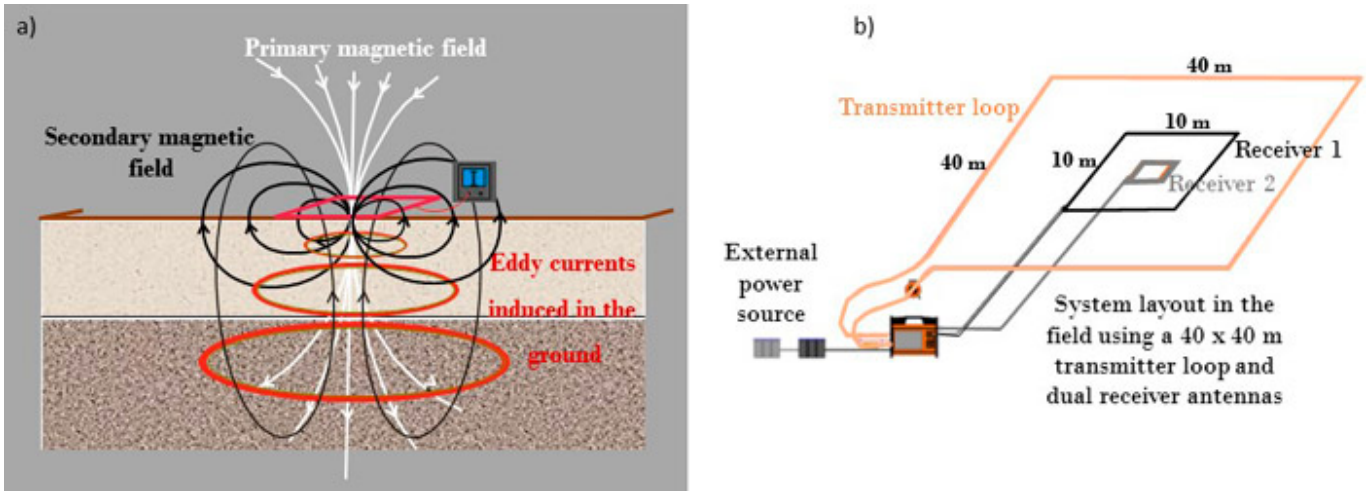

Figure 5-12. Example of duo central receiver coils with the WalkTEM system.
Source: Courtesy of MALÅ Geoscience/Guideline Geo, Used with permission

TDEM equipment can be suspended from an aircraft (fixed wing or helicopter) for airborne EM methods, placed or pulled on the ground for ground-based surveys, or towed by a boat for waterborne surveys. TDEM ground arrays allow for larger transmitter loops that increase depths of measurement. Because towed arrays can cover considerably larger areas, they are often used in mineral prospecting for identifying conductive ore bodies or other large-scale projects. TDEM systems for environmental studies can sound the depth, thickness, and conductivity of layers down to about 300 m (about 1,000 ft) below surface (Sørensen and Auken 2004); (Christiansen and Auken 2012); (Auken, Boesen, and Christiansen 2017).

5.5.3 Data Collection Design

5.5.3.1 FDEM

FDEM surveys are generally performed by walking or towing an instrument behind a vehicle in even-spaced transects in a grid pattern (see Figure 5-13). The lateral resolution of the data is determined by the spacing of data collection points; therefore, transect spacing should be selected based on the size of the desired target. For example, transect spacing can be greater for landfill or plume delineation and smaller for buried metallic debris identification.

The distance between the transmitter and receiver coils influences detection depth and data resolution. A greater coil separation allows for a greater depth of detection and, conversely, lower data resolution. Greater depths of detection are useful for profiling geologic and hydrogeologic features or identifying large-scale features that do not need high-resolution results. Features that warrant high-resolution profiling (such as buried utilities or minor changes in soil types) should generally be collected with smaller coil spacing; however, this limits the investigation depth. Generally, a coil spacing of 12 ft has an effective exploration depth of approximately 15 ft to 20 ft.

The instrument orientation (vertical dipole or horizontal dipole modes) can have an influence on detection depths. In-phase and out-of-phase measurements are collected at greater depths and lower resolution when in vertical dipole mode. Measurements collected in horizontal dipole mode are shallower and higher resolution.

FDEM instrumentation commonly consists of a single transmitter and a single receiver that collects in-phase and out-of-phase measurements simultaneously. Newer FDEM instruments have multiple receiver coils (at different separations and orientations) that can provide measurements of both the in-phase and quadrature-phase components at multiple depth

ranges simultaneously.

5.5.3.2 TDEM

TDEM data can be collected in a rectangular grid pattern (for example, readings taken at the nodes of the grid) or along a traverse or profile. The survey configuration is site-specific and dependent upon site conditions and the size and orientation of the target. For example, mapping or searching buried metallic objects at a large site should be conducted by a grid configuration; mapping a fault line or a geologic contact requires completion of a profile. Generally, it is most beneficial to place the profiles perpendicular to known or expected geological structures. The length of the profile and grid sizes are crucial parameters to conducting an effective investigation. Note that it is always recommended to extend data collection far enough beyond the conductive target to obtain background levels (NJDEP 2005). For airborne TDEM, flight speed is a trade off between lateral resolution, mapping depth, and costs. A low flight speed provides a high data density, improved lateral resolution, and a higher mapping depth and vice versa.

To achieve the required depth of investigation and resolution, both the size of the side lengths of the transmitter and the amount of current carried by the loop should be established. Usually, most TDEM systems are equipped with software that is used in the field during data acquisition. Within the software, inputs like antenna loop size, gate time, current, power-line frequency (for example, 50 Hz for Europe and 60 Hz for USA), and source of noise in EM data can be changed in the field. Generally, longer gate times are needed to investigate greater depths.

Obtaining proper sounding intervals during data acquisition is important to ensure high-lateral resolution. For example, if an electrically conductive contaminant plume is to be investigated, several stations should be within the plume. The sounding interval near the suspected edge of the plume should also be adjusted for an accurate resolution of the conductivity gradient. As a rule, the higher the spatial sampling density, the higher the lateral resolution. As with other geophysical surveys, elements such as monitoring wells, property lines, and potential sources of cultural interference should be noted. The surface topography should also be collected to aid in data interpretation.

5.5.4 Data Processing and Data Visualization

5.5.4.1 FDEM

FDEM resulting data should only be used for qualitative purposes. Data files are downloaded from the field computer following data collection. Depending on the instrument type and model, GPS measurements may be incorporated into the data file during the survey. Data are processed using various software programs and assessed for data quality. Data processing software interpolates data between actual measurement points. Data are then typically presented in a color-contoured, plan-view map showing the amplitude of the bulk conductivity and the in-phase modes for a specific approximate investigation depth. Data from multifrequency FDEM instruments can be inverted to produce 2-D or 3-D variations in EC across a site.

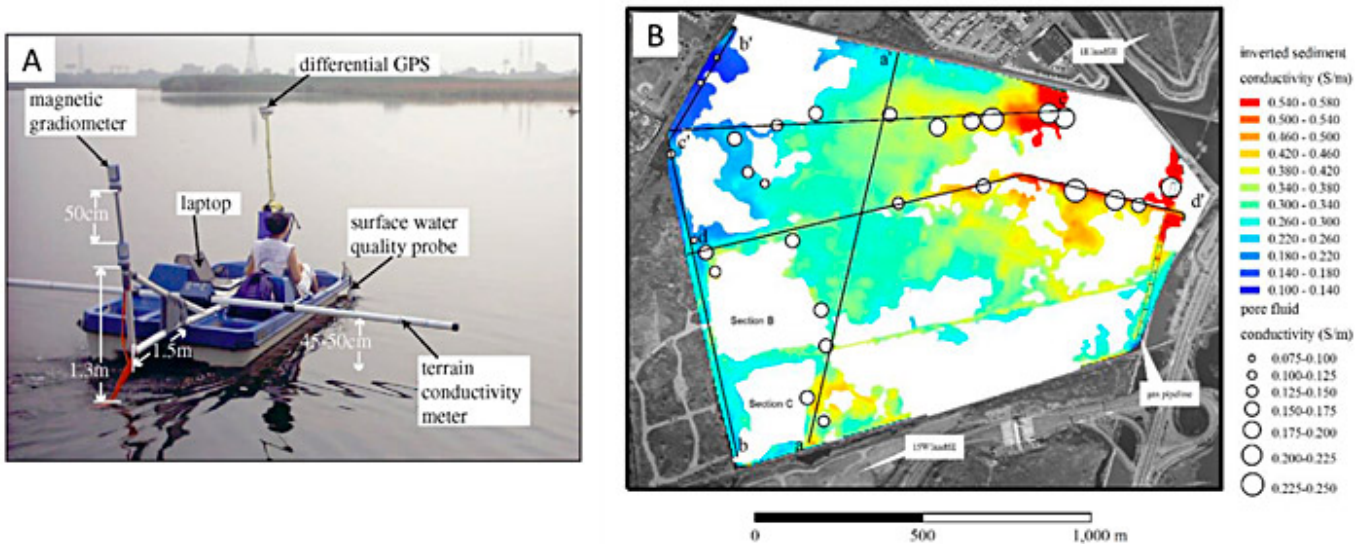

Figure 5-13. Example of a FDEM survey mapping variations in conductivity across a wetland impacted by leachate plumes from landfills.

Source: Modified from (Mansoor 2006), Used with permission

Figure 5-13 shows (a) a paddleboat equipped with terrain-conductivity meter, differential GPS, surface-water quality probe, and a magnetic gradiometer (for mapping metals) and (b) the resulting interpolated image of EC of the sediments from over 12,000 data points, with direct measurements of pore fluid conductivity extracted from sediment samples. The plume from the landfill in northeast of the wetland is immediately obvious from the high EC of the sediments.

5.5.4.2 TDEM

TDEM systems allow the user to visualize the acquired data in the field with minimal preprocessing. For accurate presentation and interpretation of the subsurface model, noise removal and inversion of the raw data must be performed. To prepare the acquired data for geophysical inversion and interpretation, distorted or noisy data must be removed and data should be averaged to improve the signal-to-noise ratio. Variations in topography (or elevation) should be used when interpreting the sounding data. Accounting for topography/elevation will provide more accurate depths to subsurface features such as water-table interface throughout the sounding.

Noisy or distorted data are removed manually by visually assessing the data. Once the raw data are relatively free of noise, data are averaged to form soundings for inversion. Averaging is essential to improve the signal-to-noise ratio. Various averaging methods are available in different processing software. Averaging filter widths can range from small to large. A small averaging filter width is preferable where the signal-to-noise ratio is good and in situations where lateral resolution is a priority; a large averaging filter width improves the signal-to-noise ratio, especially when handling noisy data or mapping deeper geologic structures is a priority.

Inversion of the processed TDEM data is usually performed using computer algorithms. Currently, advanced computer software allows processed TDEM data to be automatically inverted to a layered earth model. The inversion results are usually presented as 2-D cross sections, contour maps, and mean resistivity maps. For example, inversion results for TDEM data acquired in grid format should be presented in detailed, scaled 2-D profile and contour maps, indicating the contour interval with scaled profile plots (traverses shown on map). Anomalous resistivity areas showing targeted features (for example, probable drum burial or contaminant plumes), should also be indicated on the contour map. Pertinent information related to the instrumentation (system technical specification), field operations, and site conditions and issues that may affect data quality, processing workflow and interpretation techniques should be recorded.

A geophysical datum always consists of two numbers – the measurement itself and the uncertainty of the measurement, because the measured data consist of both the earth response and the background noise. When performing a single transient in a TDEM sounding, the signal can be significantly affected by noise sources. Some noise sources such as lightning and communications equipment can be effectively decreased through repeated measurement (for example, stacking) where noise is decreased, and the signal is enhanced. Other noise sources such as man-made structures (high voltage power lines, fences, pipelines, cables) can overwhelm the receiver and cause the data to be unusable. In those cases, the survey should take place further away from the noise source.

5.5.5 Quality Control

5.5.5.1 FDEM

Most FDEM instruments need to be calibrated prior to data collection, typically more than once per day, to avoid significant data drift that occurs during an extended data collection period. Instrument calibration should be documented using standardized forms and procedures.

Survey pattern and orientation can have an impact on interpolated data results. For example, collecting data perpendicular to a linear anomaly (like a utility) is preferred, and collecting data in a transect pattern versus a meandering, nonlinear pattern is preferred. It is good practice to periodically download data and check for quality issues. Field conditions and notable features should be recorded during the survey.

Several different data interpolation methods can be used to process FDEM data. There is not a single appropriate interpolation method; multiple methods may need to be considered to determine which one is most appropriate. QC may include reviewing daily static test data to verify calibration results, data repeatability, and reliability. Spatial variation between GPS and coils should be considered. Electronic lag time is also corrected during data processing, as well as, drift.

QC for processing inverted data from multifrequency FDEM instruments may include reviewing inversion mis-fits and the robustness of the inversion parameters and comparing inverted results with validation data.

5.5.5.2 TDEM

QA/QC checks are essential and should be performed before, during, and after data collection. Prior to the survey, the TDEM system should be calibrated to establish the absolute time shift and data level to facilitate precise modeling. Prior site information (for example, existing boreholes or other reference models) can be used to correct leveling and drift during calibration modeling. Making these corrections prior to the survey ensures accurate data when estimating depth and mapping near-surface features.

An inventory of infrastructure close, around, and buried at the site should also be conducted prior to surveying. Infrastructure is the major source of noise in TDEM data and can adversely affect data quality. Planning TDEM profiles parallel and within 100 m (328 ft) of potential noise sources should be avoided.

Field-data processing and visualization are essential to identifying buried sources of noise for removal during final data processing. After data collection, readings must be evaluated as part of the QC process. Readings should be considered inaccurate (unless determined otherwise) when the midpoint between the transmitter and receiver coils is within four coil separations from a metal fence, pipeline, power line, or other source of cultural noise (NJDEP 2005).

5.5.6 Advantages and Limitations

5.5.6.1 FDEM

Advantages of a using FDEM technology (versus galvanic resistivity surveys) include relatively fast and easy collection of EM field measurements, nonintrusive data collection that can be done on foot or from a vehicle at low speeds (see Figure 5-13), and minimal data processing. In general, FDEM can provide high-quality lateral resolution when collecting continuous measurements; the resolution is determined by the spacing between the transmitter and receiver coils, as well as the spacing between the measurements (ASTM 2018).

Misuse of this tool usually occurs when FDEM is used beyond its limitations or because the physical limitations and disadvantages of the method are not understood. FDEM surveys can be highly susceptible to interference (noise) when conducted near metallic objects, fences, and power lines.

Limitations to consider include:

- geologic and cultural interference (utilities, metal fences, power lines)
- depth of detection limits
- data resolution expectations (generally, greater depths will have lower resolution and shallower depths will have higher resolution)
- inadequate survey set up or poor-quality data collection
- data processing and interpolation requires specialized knowledge
- significant labor for some methods
- variations in data resolution between survey methods

5.5.6.2 TDEM

The main advantages of TDEM surveys when compared to alternative direct current methods are that it provides high lateral resolution, deeper depth of penetration, and denser data coverage. In addition, TDEM is noninvasive and capable of resolving three or more layers in the subsurface. Finally, airborne TDEM surveys can be performed quickly and can produce large amounts of data over a relatively short period of time.

5.5.7 Cost

5.5.7.1 FDEM

The cost of a FDEM survey depends on the type of instrument and site conditions. A standard FDEM survey includes one (single instrument) or two (separate coils) field personnel. A single person using a single instrument that houses both coils can survey approximately 2 acres to 3 acres (with 5-foot or greater line spacing) in a day under good site conditions. A two-person crew using separate coils can survey approximately 3 acres to 4 acres per day under good site conditions. Productivity declines in the presence of more complex terrain. A FDEM survey is expected to cost $2,000 to $3,000 per day for field data acquisition. The cost involved in data processing varies, but approximately one-half day of data processing time per day of field acquisition is a reasonable estimate.

5.5.7.2 TDEM

The cost of a TDEM survey depends on the survey type (airborne or ground-based survey). For airborne surveys, the daily cost depends primarily on the survey size (line-km covered), location of the survey area, and the time of year. This information is used to estimate the cost of mobilizing and demobilizing the system and crew, daily fixed cost of the crew on site, helicopter availability and rate, equipment requirements, fuel requirement, system endurance, survey duration, and the applicable standby rate. For example, a survey that is in close proximity [<25 km (<16 mi)] from a base of operations (for example, ease of access to roads, fuel, hotel, landing site) is far less expensive than one performed in a remote area. A survey involving >1,000 line-km (>621 line-mi) is much less expensive on a line-km rate basis than a small survey [<100 line-km (>62 line-mi)]. Late fall and winter survey periods are more unpredictable and therefore more expensive than spring-summer surveys, specifically regarding weather-related standby. The cost to conduct an airborne survey is expected to range from $16,000/day to $25,000/day. Beyond survey charges, data QC, processing, reporting, and sometimes interpretation are included in the survey price. Please note, most companies conducting airborne TDEM surveys provide a quote on a per job basis rather than daily basis.

Ground-based TDEM surveys are quoted on a daily basis. A daily cost includes personnel, geophysical equipment, GPS, vehicle, and data processing and typically ranges from $1,800/day to $5,000/day. Ground-based TDEM surveys range from small (for example, shallow targets such as pipes, UXOs) up to large, deep targets such as ore bodies for the minerals industry. As a result, typical daily costs have a large range, primarily depending on loop size, number of operators, and terrain. For example, at the smallest scale, one person operates the TDEM system mounted on a wheeled cart; at a larger scale, several people are needed to move the large transmitting loop. Overall, the size of the survey, site conditions, site location, and time of year, are the deciding factors affecting the total cost for ground-based and airborne TDEM.

5.5.8 Case Studies

The following case studies demonstrate the use of these surveys:

- Surface Geophysical Methods Provide Data to Identify Prospective Utility Waste Landfill Sites in Karst Terrain in Missouri
- Airborne Time-Domain Electromagnetic Method Maps Sand Distribution along the Illinois Lake Michigan Shore

6 Remote Sensing

Remote sensing technology acquires information from a distance and has traditionally depended on aircraft or satellites for gathering data. This document focuses on remotely piloted aircraft system (RPAS). This terminology is used by the U.S. Federal Aviation Administration (FAA) for aircraft operated without the possibility of direct human intervention from within or on the aircraft (see 14 CFR 107.3). Other terms like remotely piloted vehicle (RPV), unmanned aircraft systems (UAS), unmanned aerial vehicle (UAV), or small unmanned aircraft system (SUAS) are commonly used. In this section, the colloquial term drone is used to refer to a vehicle with or without attached remote sensing equipment that legally operates under Part 107 of the FAA regulations (for example, weighs ≤55 pounds, including cargo or payload, and operates under 400 ft). This document does not address operations not covered under Part 107 (medium-altitude, long-endurance). see Section 6.2.5 for a summary of Part 107.

Using drones with remote sensors for site characterization is relatively new but rapidly becoming commonly used because of several important technological developments, including improved battery efficiency; compact and lightweight onboard computers; increased data-storage capacity; and inexpensive, widely available, and generally reliable high-resolution lightweight cameras. These hardware changes are coupled with new practical features (for example, autonomous flight, which can precisely fly the drone along predetermined flight paths with limited human control). As a result, data collection that previously required workers to traverse difficult terrain on foot can now be performed with a drone. Drones also have the ability to fly into potentially hazardous areas keeping people out of harm's way. Under Part 107, drones must fly at altitudes less than 400 ft above the ground, which is advantageous to spatial and spectral resolution for both passive and active sensors. Ease of drone deployment supports frequent, routine flight operations, allowing better recording of and ultimately understanding of temporal changes. Similarly, the evolution of drones is intricately connected to supporting advances in computer processing which enables tremendous amounts of data to be acquired and processed in a relatively quick timeframe.

6.1 How to Select and Apply Remote Sensing Tools Using this Document

Using remote sensing requires a basic understanding of the tools that are deployed and how the sensors collect data. The following remote sensing tools and spectral data collected by drones are discussed in this section:

- visible spectrum camera
- multispectral and hyperspectral camera
- Long-Wave Infra-Red (LWIR) camera
- LiDAR
- photogrammetry software

Visible spectrum aerial photographs and video are the most common products produced using a drone, but there are a variety of other sensors that can be carried by a drone. In general, remote sensors are categorized as passive sensors or active sensors. Passive sensors record reflected, ambient light across a defined EM spectrum. The most commonly used bands include the red band, green band, blue band, near-infrared, red edge, and long-wave infrared (LWIR) bands. Examples of passive sensors include visible spectrum cameras (see Section 6.3), multiple spectrum cameras, and hyperspectral cameras (see Section 6.4.1.11), and LWIR band cameras (see Section 6.4.1.12). Active sensors transmit a signal that is detected when it returns to the source. Common examples of active sensors include light detection and ranging (LiDAR; see Section 6.4.1.13) or radio detection and ranging (RADAR).

Drones can also be used to collect water, air, and soil samples, and collection techniques are rapidly developing. Section 6.6 focuses on water sample collection as the architype physical sampling and, to a lesser degree, air sampling. Soil sampling techniques are being developed but are not ready for commercial application at this time.

Drone applicable technologies are developing rapidly with new tools and with improvements to older tools appearing regularly. These developments are occurring in a highly competitive market such that pricing and performance are improving concurrently. The emerging nature of this technology and its application to site characterization will continue to rapidly evolve over the coming months and years.

Beyond sensors and aerial platforms, significant advances in computing capabilities have allowed for the generation of many

useful data products. Desktop and cloud-based software is available for photo stitching and georeferencing of orthomosaics, digital elevation models (DEM), digital surface models (DSM), point cloud, classifying and mapping surface features, performing analyses of plant health, survey maps, and cut/fill volumes of mining and landfills.

This section provides discussion of remote sensing technologies, how they work, appropriate use, advantages and limitations, data collection design, quality controls, data interpretation and presentation. The ASCT Remote Sensing RPAS Summary Table provides information for common sensors used with RPAS. The ASCT Remote Sensing Checklist (.xlsx version) provides information to be considered while preparing for a flight and prior to, during and after a flight.

6.2 Drones

6.2.1 Platform Selection

Key drone components include the airframe, propulsion system, navigation equipment and flight controller (often composed of GPS, on-board stabilization, and autonomous flight computer), and its payload (for example, camera.). When selecting a drone for remote sensing, it is important to consider the basis of the intended payload and type of data collection needed to achieve project objectives. Drones are available in different types and configurations, each providing its own set of unique advantages and disadvantages. It is important to understand the capabilities and limitations of each type when selecting a drone for a specific application. The primary types of drone are as follows:

- fixed wing
- rotary wing (helicopter)
- multirotor
- hybrid

Table 6-1 summarizes features of the various platform types and may not properly represent certain makes and models of drones. Users should evaluate the performance, cost, and capabilities between several manufacturers before selecting a drone for a specific project.

Table 6-1. Drone platform summary

Platform Type	Payload Capacity	Capable of Vertical Take Off and Landing	Complexity
Fixed Wing	High	No	Low
Rotary Wing (Helicopter)	High	Yes	High
Multirotor	Moderate	Yes	Low
Hybrid	Low	Yes	Moderate

6.2.1.1 Fixed-Wing

Fixed-wing drones are the most power-efficient platform type and can generally fly longer and carry more payload than other drones. The primary disadvantage of fixed-wing aircraft is the need for a suitable take off and landing site. Most small fixed-wing drones are hand-launched because smooth runway areas are often not available. Landing the drone generally takes more space. Landing gear is seldom used, and most aircraft are skid landed. Small fixed-wing drones are commonly constructed of durable expanded polypropylene or expanded polyolefin foams.

6.2.1.2 Rotary Wing

Rotary-wing or helicopter configurations allow hovering and vertical take offs and landings. Rotary-wing drones are more efficient than multirotor drones due to their long and narrow rotor blades. Rotary-wing drones are often used to carry payloads that are too heavy for a multirotor. These drones are more mechanically complex because the rotor blades constantly change pitch through each rotation. Although electronic stabilization systems have reduced the complexity of some of these mechanisms, rotary-wing drones require more maintenance than other drones. One significant advantage of rotary-wing drones is that they can be powered by a single motor, making them well suited to internal combustion or turbine power, which allows the drones to fly much longer than battery-powered aircraft.

6.2.1.3 Multirotor

Multirotor drones, which dominate the current drone market, usually have an even number of electric motors that turn fixed

pitch propellers. The four- and six-propeller configurations are most common. The torque of the propeller pairs turning one direction is countered by an opposing torque of propeller pairs turning the other direction. Pitch and roll are accomplished by varying the motor speed. Yaw (rotation around the vertical axis of the drone) is accomplished by varying the speed of propeller pairs to unbalance the torque in the desired direction. Multirotor drones are mechanically simple with as few as four moving parts. Their mechanical complexity is replaced by electronics and software, making them reliable and easy to operate. Multirotor drones are generally battery powered and not as well suited to fuel power; they typically have a flying time duration of less than 30 minutes.

6.2.1.4 Hybrid

Hybrid drones combine vertical take-off and landing capabilities with the ability to transition to a more efficient fixed-wing forward-flight mode. Some hybrid drones use multirotors for lift and a separate motor and propeller for forward thrust. These drone types are called separate lift and thrust. After transitioning to forward flight, the lifting motors are turned off. Some hybrid drones articulate the lifting motors to a forward orientation to transition to fixed-wing mode. Another configuration uses a fixed-wing drone with sufficient thrust from multiple forward-facing motors to achieve vertical take off. This is referred to as a tailsitter and is less mechanically complex because it does not have to use separate lift motors or articulate the motors. The transition from hover to forward flight and then back to hover is challenging to automate, and the performance of each manufacturer's product depends on both proper aerodynamic and software design. The advantage of the design is increased flight time but is someone hampered by decreased payload capacity. Decreased payload capacity results because it is necessary to vertically lift a wing. Upon take off, this action does not contribute lift to the drone's flight.

6.2.2 Global Navigation Satellite System (GNSS)

To produce an accurately scaled and geographically positioned dataset, drone position information is required. Two instruments play crucial roles in ensuring the quality of the collected data are the GPS and the inertial measurement unit (IMU). The GPS tracks of the drone location, and the IMU accounts for the effects of roll, pitch, and yaw. Together these instruments track the geographical coordinates during flight and are vital during data postprocessing. Multiple GPS systems are available:

- navigational GPS, sometimes called GNSS as GPS is a subset of GNSS
- real-time kinematic (RTK) GPS
- ground control points (GCPs)

6.2.2.1 Navigational GPS

Most drones have a navigational GPS that enables position holding and autonomous flight functions. The GPS coordinates are inserted into the image exchangeable file (EXIF) data which helps simplify integration into GIS applications. The EXIF often contains information such as aperture, shutter speed, ISO, focal length, camera model, and flight date. Given the value of such data, agencies should consider standards such as the USGS Unmanned Aircraft Systems Data Delivery Specification (USGS 2018d) or others as they develop their specifications. Although the navigational GPS may only be accurate to about 30 ft horizontally, photogrammetry software can produce scaled products suitable for many applications. The relative horizontal accuracy of a photogrammetry product, supported only by navigational GPS, can be accurate to within several ft and precise to within several inches.

6.2.2.2 Real-Time Kinematic GPS

RTK GPS units use at least one additional GPS receiver at a nearby known static position to continuously correct the airborne GPS position. This method provides GPS horizontal accuracies of a few tenths of an inch. Drones using RTK GPS units can produce data with horizontal and vertical accuracies less than 0.5 inches without ground control. RTK has an additional benefit in that it enables the drone to fly and land precisely. When a short loss of communications between the fixed base and the aircraft occurs, the airborne GPS can revert to a less accurate floating mode, resulting in unusable image coordinates.

Postprocessed kinematic (PPK) GPS units have an advantage over RTK GPS units in that a continuous communication link between base and aircraft is not necessary. A base station must be set prior to flight operations. PPK uses logs from the base station or a network of continuously operating reference system (CORS) receivers to correct image coordinates after the flight. Raw logs from the onboard GPS as well as PPK methods can provide equivalent accuracies to RTK methods but require postprocessing that may be complex.

These methods are costly compared to using a navigational GPS or a navigational GPS paired with GCPs (see Section 6.2.2.3). When high-accuracy data are required but deployment of GPCs is dangerous or inconvenient relative to the data needs, RTK may be worth the cost.

6.2.2.3 Ground Control Points

GCPs are an effective way to georeference drone data and greatly improve accuracy for navigational GPS. This method can also be used with images that contain no geographic coordinates. This method involves manually identifying surveyed ground targets within the postprocessing software. Temporary targets are often used but features clearly visible in several photos can be used as GCPs. Products produced using ground control can achieve accuracies of less than 0.1 ft horizontally and vertically. Some software products allow extra targets to be designated as check points. Check points are not used by the software to georeference the point cloud but rather to measure error between calculated and surveyed coordinates.

6.2.3 Data Collection Design

6.2.3.1 Employing Available Imagery to Support Drone Operations

A wide variety of satellite imagery data are available online, much of free. For example, NASA, NOAA, and USGS provide satellite data. It is common practice to use aerial photography available through Google Earth or other platforms when investigating a site. Similarly, airborne LiDAR data are available from the United States Interagency Elevation Inventory (NOAA 2019b). Some other common locations for this type of data include:

- NASA Earthdata Imagery (NASA 2019)
- NOAA Satellite Imagery and Data (NOAA 2019a)
- USGS EarthExplorer (USGS 2019)

An online search of satellite imagery data yields many sources of data. States and local municipalities may also provide imagery data. Available data must be examined prior to collecting data to potentially narrow and focus additional data collection. When using satellite imagery data, note the timeframe of the imagery and how it corresponds to the timeframe of the proposed project. Although imagery data may be available, image processing may be required. Prior to purchasing imagery data, available data should be researched; many states have no-cost LiDAR data available. When weighing the option of employing available remote sensing data versus collecting drone data, it is crucial to know the needed temporal resolution, spatial resolution, and spectral resolutions required for the specific project.

6.2.3.2 Site Specific Considerations

Prior to implementing drone operations at a site, it is critical to evaluate the site-specific physical characteristics that may either impede or improve data collection. Some common considerations include the following:

- Topography changes may impede safe operations and must be considered in flight planning. For example, the amount of overlap needed to produce quality data for both active and passive sensor changes with topography, flight pattern, objects being imaged, and available light. In rugged mountains, the light available to illuminate the pixels on the sensor from a shady slope is relatively weak; the light illuminating the pixels on the sensor from a sunny slope is stronger. Additionally, different objects (for example, rocks verse vegetation) reflect more or less light. These ambiguities can significantly affect remote sensing data accuracy.
- Sun position, cloud cover, and time of day may contribute to lighting effects that negatively impact data collection. Harsh midday light, for example, can cause excessive contrast, blown highlights, hard shadows, and washed images. Changing light conditions, such as dynamic cloud cover, may also cause issues with a passive sensor. Full cloud cover, on the other hand, may reduce shadowing and variations in light intensity. Too much cloud cover or fog may not only block reflected light, but also pose operational safety hazards.
- Ground-cover variations may lead to errors in photo stitching and processing. Ground cover such as snow, water, or tall grass moving in the wind may cause difficulty in finding tie points between images (see Section 6.2.2.1 for more details). Heavy vegetation may also reduce the effectiveness of active sensors in penetrating canopies and may obscure the ground surface from passive sensors.
- Temperature variations in the air or between the ground and the air may influence gradients observed during thermal data collection efforts. Additionally, some sensors have a recommended operating temperature range. Operating outside that range may reduce sensor performance or cause the sensor to fail.
- Water, including ponded water, may obscure active or passive sensors from an aerial platform. Many sensors have a limited ability to penetrate beyond a few centimeters of water.

- Many drones are not designed for use in high winds or rain, and such conditions may influence operational safety and data collection.

6.2.4 Best Operational Practices

The following operational practices were adapted from drone sampling as described in (Castendyk et al. 2017). Drone operations are best performed by a two-person sampling team of a pilot and a spotter. The pilot is responsible flying, defining a safe flight area and ensuring equipment is operating properly. The spotter is responsible for ensuring no one enters the safe flight area, watching for changes in environmental conditions (for example, weather, birds, vehicle traffic); assisting the pilot in positioning the drone over the sample point; and, when using the drone for sampling, collecting the sample(s) when the drone returns.

- Upon arrival at the site, review weather conditions. Moderate to strong wind can make the drone difficult to control. Note that wind speeds are typically lower in the early morning. Precipitation and condensation from fog or clouds can damage exposed circuitry.
- Establish the safe flight area, a 20-ft by 20-ft area delineated with cones or other brightly coloured markers, where the drone takes off and lands. The safe flight area must have an unobstructed, line-of-sight view of media to be sampled or area from which data are being collected. Avoid hazards such as the top of a cliffs, the bottom of highwalls, trees, powerlines, and active vehicle traffic. During drone operations, only the pilot and the spotter are allowed to enter the safe flight area. Typically, the pilot and spotter stand just outside of the area when the drone is turned on and off.
- Prior to flight, install fully charged batteries. Used batteries must be placed in a charging station.
- As appropriate for planned operations, attach sampling equipment and check sensors, controls, and the condition of the drone.
- Thereafter, raise the drone and payload, position the system relative to the sampling point or point at which sensor data collection is initiated. Initiate planned flight pattern or route to sampling point. As noted above, the selected flight pattern should be advantageous for data collection and safe navigation.
- Once the allotted flight time has passed or data collection goals are met, land the drone within the safe flight area. For active sampling, such as water sampling, an experienced team can generally complete Step 5 in approximately 15 minutes to 20 minutes.
- Replace the batteries with a fresh set and repeat Step 5 until all samples or sensor data are collected.
- Prepare the sampling report, which should include at a minimum: (1) notes regarding weather conditions, (2) the sampling and data collection coordinates, (3) the sampling point (in 3-D for water sampling), and (4) justification for the selected sampling point(s) or data collection area.

6.2.5 Regulations and Policies

The FAA recognized the importance of integrating drone operations into the NAS and adopted updated regulations (14 CFR Part 107) in 2016. The FAA presently supports two options for certifying public agency drone operations. The original mechanism was through a blanket Certification of Waiver or Authorization (COA) referred to as a Section 333 exemption. This exemption permitted flight below 400 ft in Class G (uncontrolled) airspace and self-administered pilot certification, with a need to apply for an emergency COA (e-CAO) for special circumstances. These mechanisms also required specific commercial pilot training rather than the current lower level of certification. The initial application process for a COA is extensive and operations remain subject to the application andreview process for e-COA for many flights. The FAA is phasing this out in favor of operations under the Part 107 rule.

Part 107 applies to government entities and commercial operators alike (FAA 2019c). Requirements include remote pilot certification by the FAA (written test), drone registration, and limitations on airspace and operational conditions. The FAA has continued to expedite this program, simplifying the online application process for flights that deviate from the Part 107 requirements (for example, a Certificate of Waiver or Airspace Authorization is required for flights in Air Traffic Controlled airspace, beyond Line-of-Sight, and flights outside of daylight hours) (See FAA Part 107 Waivers (FAA 2019b)).

On August 29, 2016, 14 CFR, Part 107 went into effect for both civil and public use of drones. A new pilot certificate termed the “remote pilot” along with associated testing requirement were part of the rule. The rule also established a registration process for small drones flown commercially. The remote pilot must pass the written FAA exam and register their aircraft. Commercial operation includes work performed for compensation as well as work performed without compensation in the furtherance of a business or for research. Flying drones for educational or instructional purposes (for example, teaching a

STEM class or a drone training program) may operate either under Part 107 or as a recreational flier (See FAA Educational Users (FAA 2019a)). Part 107 rules allow small unmanned aircraft to operate with the following summarized restrictions (See FAA Press Release – New FAA Rules for Small Unmanned Aircraft Systems Go into Effect (FAA 2016b):

- Less than 55 lbs
- Visual line-of-sight (VLOS) only
- No operations over unprotected nonparticipants or moving traffic
- Daylight only, civil twilight with lighting visible for three miles
- Drone must yield right of way to other aircraft
- First-person view (video from a drone) requires a visual observer with VLOS
- Maximum ground speed of 100 mph
- Maximum altitude of 400 ft above the ground or a structure
- Weather visibility of at least three miles
- Class G airspace only without air traffic control permission
- One aircraft per pilot
- No operations from a moving aircraft
- No operations from a moving vehicle unless over a sparsely populated area
- No careless or reckless operations
- No carriage of hazardous materials

Unmanned aircraft regulations constitute a large portion of the 2018 FAA Reauthorization Act. The act distinguished between the operational risks associated with manned versus unmanned aircraft. Section 336 was repealed, thereby allowing the FAA more authority to regulate and register hobbyist aircraft. Unmanned traffic management systems, counter drone techniques, fee mechanisms, and the flexibility to regulate a rapidly changing industry are key parts of this act.

The FAA has recently instituted the Low Altitude Authorization and Notification Capability (LAANC), allowing near real-time processing of airspace authorizations for drone operations. Further regulatory changes regarding flying over people, beyond VLOS, and other operational parameters are being released by the FFA on a regular basis.

The FAA's website is the official source of drone information and registration. Drone regulations are continually evolving, and it is important for pilots to stay up to date on current regulations. Useful resources for drone regulations and information include:

- FAA Unmanned Aircraft Systems web page (FAA 2019c)
- FAA DroneZone web page (FAA 2019d)
- Know Before You Fly web page (KBYF 2015)

The document links below cover the material on the FAA Remote Pilot Airman Knowledge Test:

- Remote Pilot – Small Unmanned Aircraft Systems Study Guide (FAA 2016a)
- US DOT Advisory Circular: Small Unmanned Aircraft Systems (FAA 2016b)
- Part 107 Drone Exam Practice Tests: Questions 1-10 (3DR 2019)

6.2.5.1 Environmental Considerations

Incidents have been reported where birds, particularly large birds of prey, have directly attacked drones. Such attacks could result in damage to the drone and possibly fatal injuries to bird. To protect the drone and wildlife, a spotter equipped with binoculars can constantly scan the flight area to alert the pilot of bird activity. If birds are spotted, drone flight should cease until the birds have exited the area.

6.2.5.2 Legal Considerations

Drone work may require new service agreements or riders to existing agreements and changes in insurance policies, delaying work. It can take time to establish a new contract for drone water sampling owing to legal requirements. Client agreements or aircraft use policies within a company may not have anticipated drone use. Liabilities for aircraft may be based on the crash of a manned-helicopter or fixed-wing aircraft, which grossly overstates the liability related to a drone.

6.2.5.3 Regulatory Considerations

Some drone uses may be new to regulators. It may be helpful to invite regulators to observe a drone water-sampling event. This approach was used in Nevada for the Department of Environmental Protection (Newman et al. 2018) and in Montana for

the Montana Department of Environmental Quality (MDEQ) and the U.S. Bureau of Land Management (BLM) (Williams et al. 2018). In these instances, regulators accepted drone water samples for regulatory compliance purposes. After observing the methodology, one regulator wrote, “The methodology is acceptable for regulatory purposes and allows for multiple samples to be collected while maintaining human and environmental safety” (Newman et al. 2018).

6.2.6 Public Acceptance

The potential to invade privacy is a significant concern associated with drone flight. Drone flights, particularly by government and law enforcement entities, are problematic in this regard. While local laws and ordinances can address safety and nuisance concerns, privacy and potential government surveillance are problematic issues. In response to the privacy concerns associated with using drone-mounted cameras, a presidential memorandum dated February 15, 2015 initiated a series of multistakeholder efforts resulting in guidelines for private and commercial use. These voluntary best practices address privacy, accountability, and transparency issues (See Voluntary Best Practices for UAS Privacy, Transparency, and Accountability (NITIA 2016)).

It should be noted that certain drone applications (for example, where a physical sample is collected) (see Section 6.6) may not drive privacy concerns to the same degree as image collection. Thus, when dealing with stakeholders, communicating the goal and product associated with a particular flight may help to alleviate potential concerns.

Regardless of intentions and goals associated with drone use, state and private organizations should establish and enforce drone operating procedures that explicitly protect public privacy.

6.3 Visible Spectrum Camera

Drones have brought aerial mapping within reach due to the ability to scale costs and requirements to a site-specific nature.

With advancements in video technology, aerial video is becoming more popular. Oblique video is commonly shot from drones to assist in site characterization. The unique perspective of aerial videography and photography allows for an unprecedented level of understanding at a variety of sites (large and small). In addition, using geospatial data imbedded in information collected by the drone, video may be embedded with meta data and later synced with a video mapping program. Similarly, photos and video may be georeferenced or attached to geotagged photo locations to provide assistance in site characterization. These basic methods are relatively inexpensive and require a limited infrastructure of software to implement.

Beyond photo and video, the next most common application of drones is the collection of visible spectrum data as a collection of overlapping datasets. Software that can extract three-dimensional information from two-dimensional image data has transformed drones into powerful mapping and surveying tools.

The drone camera is the tool most often used in site characterization due to its low cost, high availability, and simplicity of the self-explanatory nature of a picture. Additionally, the operational requirements and technical knowledge required to use a camera are low relative to other sensors. Off-the-shelf camera drones cost approximately $1,000 or more. Detailed technical information about these cameras is provided in the following sections. Similar but abbreviated technical information is available in the ASCT Remote Sensing RPAS Summary Table for other common sensors.

Photos and video can be used for inspection, documentation, change detection, and many other purposes. Low-altitude photos and video can yield valuable information about a site that is not apparent from ground observations.

Drones flying less than 400 ft above the ground allow ground sampling distances of inches or less versus feet for conventional visible spectrum aircraft photography. Drones often use wide-angle lenses which are less prone to distortion due to vibration than longer lenses. Using a gimbal to stabilize a wide-angle lens can yield focused images in a variety of lighting conditions. In many areas of the country, atmospheric haze is a common problem when obtaining aerial photographs. Drone sensors benefit from less atmosphere between the subject and sensor and, thus, less distortion from atmospheric interference or weakening of specific EM bands.

Furthermore, in most cases, uncorrected photographs are of less use than the postprocessed outputs. The most recognized postprocess image is the orthomosaic. Orthomosaics are *geometrically corrected to remove distortion caused by topographic relief, lens distortions, and camera position. The orthomosaic can be used to measure true distances because it is an accurate representation of the Earth’s surface*. Organizations should consider the need for and methods to archive not only the uncorrected photos but the processed products.

6.4 Camera Features

This section provides basic information for properly selecting and using a camera in drone operations. The visible spectrum camera is a model for other sensors and their characteristics; therefore, most lessons that apply to it also apply to sensors that collect spectral data outside the visual range (for example, hyperspectral and infrared cameras).

6.4.1 Camera Spatial Resolution

Spatial resolution is a measure of the finest detail distinguishable in an image and is determined by the sensor dimension and pixel pitch (aperture), focal length, and distance from the object being imaged (see Figure 6-2). For drones, the distance from the object is typically the height above the ground.

6.4.1.1 Sensor Dimensions

Sensor dimension is equivalent to the film base in a film camera. A large sensor collects more light, which corresponds to a better image. The dimensions of a sensor are described by two parameters: size and aspect ratio.

Generally, a larger sensor is preferred because a larger sensor receives more light and allows for a wider ISO while reducing noise. Sensor size is reported in inches based on optical format, which is larger than the true diagonal size of the sensor. The diagonal length of the sensor multiplied by 3/2 is approximately the sensor width reported in inches. For example, a 6.4-mm by 4.8-mm sensor has a diagonal of length of 8.0 mm and an optical format of 8.0 x 3/2 ≈ 12 mm. This value converts to about 0.5 inches and therefore designated a 0.5-inch sensor.

Aspect ratio describes the screen shape in a height-to-width ratio of the displayed image. Two choices exist: 4:3 and 16:9. An aspect ratio of 4:3 is squarer; an aspect ratio of 16:9 corresponds to modern computer monitors. CCD sensors have an aspect ratio of 4:3. Complementary metal–oxide–semiconductor (CMOS) sensors have an aspect ratio of 16:9, although some CMOS cameras allow selection of either ratio. The squarer 4:3 aspect ratio is created by cropping the sides of the 16:9 aspect ratio image, decreasing the field and spatial resolution. An aspect ratio of 16:9 is preferred for images displayed and processing on a modern computer monitor, but CDDs have other advantages and are discussed with sensor types.

6.4.1.2 Pixel Pitch

While sensor size and aspect ratio describe the physical size of the sensor, a sensor may also vary in pixel count. Pixel pitch relates the width of an individual pixel on a sensor to sensor width. To compare sensors, the sensor's size and absolute number of pixels must be compared by using pixel pitch (see Figure 6-1). Pitch is calculated by dividing the sensors width by the number of pixels in a row on the sensor. As an example, the sensor size of a Phase One iXU 1000 drone camera is 53.4 mm by 40 mm and the pixel count is 11,608 by 8,708. Using one side of the rectangular sensor, the pixel pitch is 40 mm/8,708 pixels = 0.004593 mm/pixel, reported as 4.6 microns. When two sensors have the same number of pixels, the larger sensor has the better image. It is possible for the smaller sensor to have many more pixels and, therefore, it will have a better image. Pixel pitch balances these two sensor aspects; generally, a smaller pixel pitch provides greater resolution.

6.4.1.3 Aperture

Aperture is usually denoted by the f-number, which is the ratio of the focal length to the diameter of the opening (length over diameter; see Figure 6-1). Thus, f/2 is an aperture with a diameter 1/2 the size of the focal length of the lens, f/4 is 1/4 the size of the focal length, and f/1.0 is an opening equal to the focal length. The larger the value in the denominator, the smaller the aperture opening. For digital cameras, pixel size is equivalent to the aperture opening that allows light through the lens in a film camera. The smaller the opening through which light must enter, the greater the spreading of light (diffraction). A larger pixel pitch is equivalent to a larger opening for light and, therefore, less diffraction.

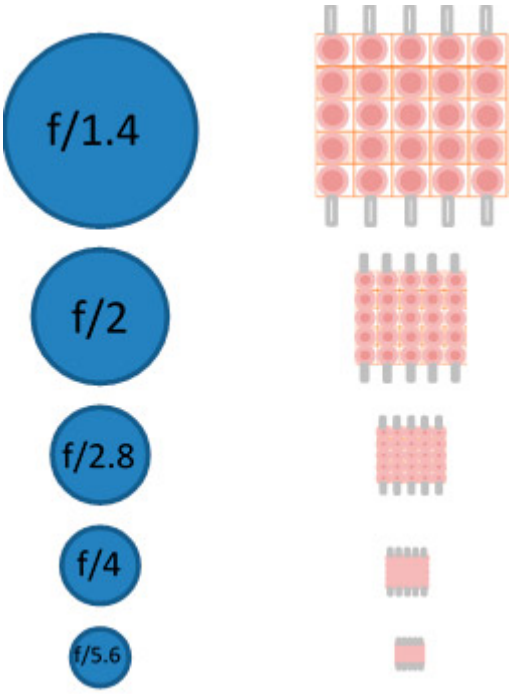

Figure 6-1. Comparison of aperture to pixel pitch.

Figure 6-1 allows a comparison between aperture and sensor pixel size. As seen in the Figure 6-1, two sensors may have different physical sizes but the same pixel counts. Alternatively, pixel count can vary for sensors of the same size. Thus, pixel size and pixel count both influence image quality. The aperture, denoted by f-number, is the ratio of focal length to pixel size (the opening allowing light to enter the camera).

Presently, small drones may use small CMOS sensors like a mobile phone camera sensor. For environmental work, where we assume larger drones and emphasize picture quality, it is expected that the sensor is, generally, 1/2.3 inch or larger CDD. In the drone market CDD sensors presently dominate. This statement is constantly being tested as new CMOS sensors are developed, so check contemporary research.

6.4.1.4 Focal Length

The second key element that influences spatial resolution is focal length, which is the distance between the lens and sensor when the camera is correctly focused on an object. (In textbooks, focal length is described as that same distance when the object is at infinity.) Focal length is a characteristic of the lens. Typically, drone cameras have focal lengths from 10 mm to 1,200 mm. Shorter focal lengths (effective focal lengths of 24 mm to 35 mm) are best for producing quality pictures when the drone is flying at typical operational height (above 50 ft) because distortion is reduced in images taken for larger geospatial applications. If a drone is used as an inspection camera to inspect a stack, a longer focal length would perform better.

The relationship between actual focal length and the focal length of a full 35-mm camera is expressed as a focal length multiplier called a crop factor. The crop factor of a camera can be calculated by dividing the diagonal length of a 35-mm frame by the diagonal length of the camera sensor. Crop factors are available on the internet and usually provided by the camera or drone manufacturer. The crop factor is a valuable method to compare focal lengths. If a camera has a crop factor of two, a 35-mm film frame is twice as large as the camera sensor.

6.4.1.5 Flight Height

Drone flight height is the distance from the object on the ground to the camera lens and a determinant of spatial image resolution. The further the object is from the camera, the more difficult it is the see clearly. Likewise, if an object is too close, it is also hard to see. Camera settings and flight height may be adjusted to optimize image quality. Camera parameters must be selected to match the intended use of the camera.

6.4.1.6 Ground Sampling Distance

Ground sampling distance (GSD) is a composite concept used to describe spatial resolution in terms of the dimension of a

square pixel per area on the ground. Thus, GSD is the distance in the x and y directions that a sensor sees or images. For drones, GSD may be thought of as the area on the ground covered by each pixel when the camera is stationary. For example, a GSD of 2 inches means that one pixel in the image represents two linear inches on the ground or 2 x 2 = 4 square inches. The smaller the distance between pixels (a small GSD) the greater the accuracy of the corresponding ground image. The larger the GSD, the lower the spatial resolution of the image. An aerial survey cannot be more accurate than the GSD.

GSD, as a formula, is the ratio of the sensor width (Sw) times flight height (H) divided by focal length (f) times the object width in number of pixels. Therefore, the GSD is reported in distance per pixel.

(Sensor Size (Width) x Flight Height) / (Focal Length x Object Width in Pixels)

Note the same formula applies to sensor height and object height.

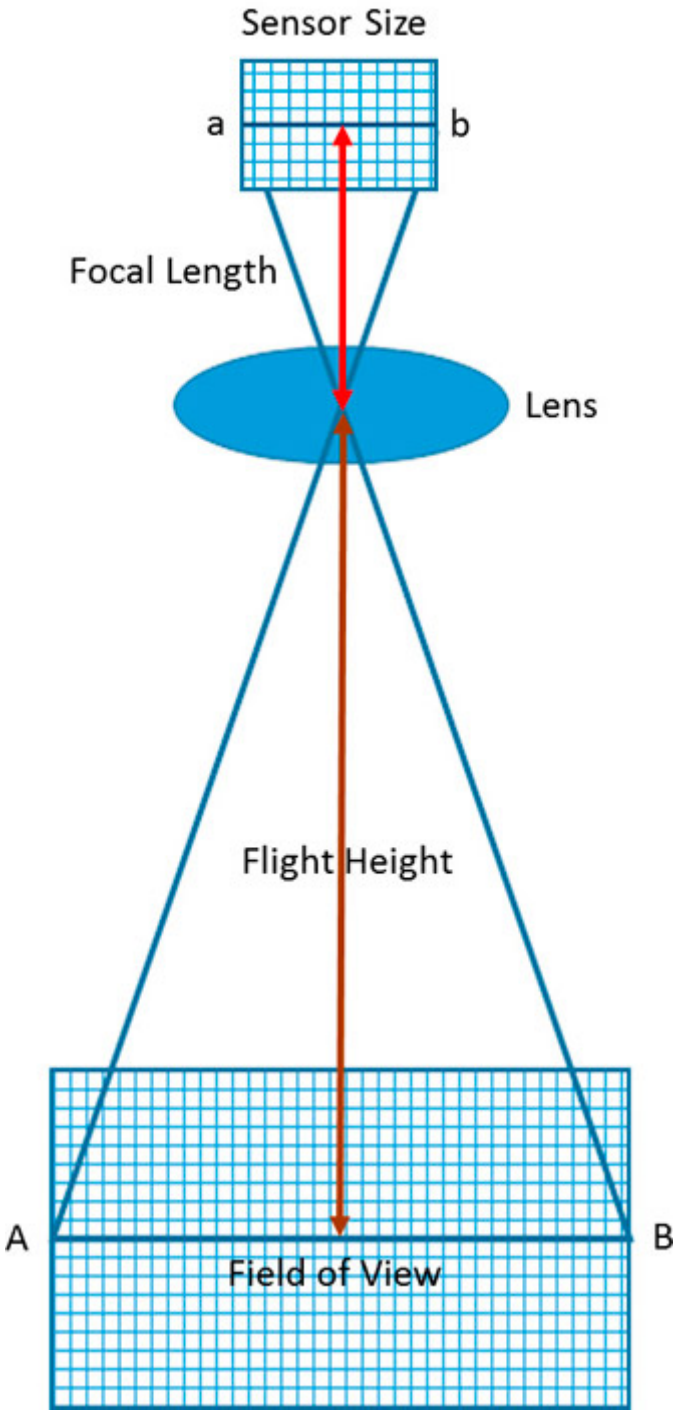

Figure 6-2. Relationship between sensor dimension, focal length, flight height and field of vision.

Figure 6-2 illustrates the relationship between sensor dimension (sensor size in x, y, and diagonal), focal length (distance from lens to sensor), flight height, and field of vision. The distance from the object being viewed is the flight height relative to that object. The GSD can be used to determine the proper flight height needed to acquire the desired image. A rule of thumb is to double the GSD; another rule of thumb is that any image you want to see clearly should be covered by 10 pixels to 20 pixels. Using the 20-pixel value, the smallest object imaged should be at least 10 inches in size at 100 ft above the ground. Note: If you reduce the flight height by half, the size of the object clearly imaged doubles.

6.4.1.7 Light Exposure

Three factors control the light exposure of the sensor: ISO, shutter speed, and aperture. Aperture was discussed previously. ISO is the light sensitivity of the digital sensor. Quality drone cameras allow ISO to be adjusted along with shutter speed; adjustability typically ranges between 100 (low sensitivity) to 12,800 (high sensitivity). As a point of perspective, ISO 200 is double the sensitivity of ISO 100. Low ISOs, like 100 or 200, are most often used in low light or when the camera or subject is stationary and the shutter opening is set for a longer time. A lower ISO is less grainy, has better color, and captures details better. In bright light or when either the camera or subject is moving, higher ISO and faster shutter speed are preferred. A higher ISO may result in grainy images because the light had less time to interact with the sensor. Keeping the ISO as low as possible is recommended to achieve the highest quality image (balanced against movement of either the camera or subject).

6.4.1.8 Field of View

Field of view (FOV) measures the area on the surface of the ground that is observed by a single sensor. FOV is similar to GSD, which is the area on the ground observed by a single pixel. The FOV is, however, used to describe the angular extent of the scene that the camera can image. The larger the FOV, the larger the area covered (assuming all other aspects are equal).

6.4.1.9 Gimbal

A gimbal is a camera mount that allows the camera to move up and down and left to right. Using a gimbal allows the camera to stay focused on an object or area of interest regardless of the motion of the drone. For example, the gimbal keeps the camera steady when the drone is buffeted by wind. For stable video footage and quality photos, a gimbal is needed.

6.4.1.10 Camera Settings

Most dronesproduce quality images when the camera settings are the default out-of-the-box camera settings. When collecting images for geoprocessing, the camera should be optimized to do as much of the work as possible without manual adjustments. The shutter speed, aperture, and ISO should be set to automatic. If a test flight results in blurry or noisy images, these parameters should be manually adjusted. There is a tradeoff between the shutter speed, aperture, and ISO sensitivity. Quality images with the least amount of noise are obtained when lighting is bright and consistent, the ISO is relatively low, and the shutter is as open as possible. Poor lighting results in noisy images. A shutter speed that is too fast produces grainy images similar to when there is insufficient light. Poor images interfere with image processing and the accuracy of the results. Initial settings are noted below.

- Shutter speed should be fixed and set to a medium speed (for example, between 1/300 second and 1/800 second) that does not produce blurry images. If more than 5% of the images are subject to a directional blur, the shutter speed should be slightly increased. When adjusting shutter speed, a rule of thumb is to set the speed to double the frame rate. If the picture appears too white or too black, increase shutter speed to reduce white but reduce shutter speed to reduce black.
- ISO should be set as low a value that supports crisp images and does not produce shaky images. In low light, the ISO should be decreased. To reduce noise in the picture, decrease the ISO. For faster flight speeds, increase the ISO. Keep in mind that high ISO in the daylight can produce overexposed and noisy images.
- Aperture should be set to automatic to allow the camera to compensate for changing light levels. When setting the aperture manually, set the aperture as low as possible. Adjust the aperture before shutter speed.
- Set the focus on infinity or automatic when flying above 50 ft when the images are for geoprocessing. Images obtained for inspection work may require manual focus.
- Once the shutter speed is adjusted, the exposure may be adjusted. The goal is to center the exposure value scale.
- Saving images for editing. RAW format saves more information than JPEG.

6.4.1.11 Multispectral and Hyperspectral Cameras

Multispectral and hyperspectral cameras are differentiated by the width and number of wavelength bands detected. Both cameras typically record reflected light in the red, green, and blue (RGB) as well as near-infrared. Some cameras have broader spectral ranges. From a practical perspective, the cameras are differentiated by spectral resolution, which is a combination of band width specificity and band number. Multispectral cameras typically collect data on three to nine relatively wide bands, while hyperspectral cameras suitable for small drones collect data on tens to hundreds of narrow bands.

Generally, multispectral cameras collect data in the near-infrared and red spectra. Some cameras also collect data in the blue and red-edge or other selected bands within wavelengths from 400 nm to 950 nm. While multispectral data can be collected by adding a filter to an RGB sensor, a camera specifically built to collect multispectral data has a dedicated sensor for each wavelength band collected. This design vastly increases the amount of data collected and increases the data-mining opportunities compared to cameras using filters. The multispectral camera is the dominant camera used in agriculture where resulting data are used to differentiate between healthy and diseased plants.

Hyperspectral cameras collect data on more bands than the multispectral camera, allowing for greater characterization of the area or items imaged. Some hyperspectral cameras can discern between certain minerals in the short wavelength infrared (SWIR) range from 1,000 to 2,500 nm. The camera can differentiate between healthy and diseased plants, as well as stages of plant growth, hydration status, the presence of herbaceous pests, plant varieties, and some nutritional deficiencies. Furthermore, these cameras can identify objects, materials, or physical processes not discerned by multispectral analysis (for example, mineral and surface chemical composition (see (GISGeography 2018)). The drawback of hyperspectral cameras versus multispectral cameras is cost. The hyperspectral camera is more expensive and the data-rich output makes analysis more complex and increases needed storage.

When using these cameras, vegetation appears green because chlorophyll absorbs red (630 nm to 680 nm) and blue wavelengths (450 nm to520 nm), leaving the green (520 nm to 600 nm) to be reflected. Reflectance at these three wavelengths is employed as a measure of active plant chlorophyll. A sick plant reflects more red and blue relative to green due to reduced photosynthesis. Accordingly, multispectral cameras capture relatively broad band of wavelengths in the RGB light. When vegetation is dense, the blue and red may be scattered and absorbed; an additional spectral range of the hyperspectral camera may help with characterization. The ratios of the NIR and red indicate plant biomass, general health, and hydration status. The cellular structure of vegetation causes infrared light (680 nm to 700 nm) to be reflected; this reflectance varies with plant cycle, season, climate, habitat, and other parameters (Adão et al. 2017). Stress and dead leaves significantly reduce near-infrared reflectance. The narrow near-infrared band (700 nm to 730 nm) marks a sudden change in reflectance from absorption of red to reflection of near infrared.

A multispectral camera can be used to obtain data that can serve as a baseline for monitoring plant health or implementing conservation or restoration efforts. Multispectral imaging supports parsing the ratio of reflected near-infrared radiation to red radiation. This allows the discernment of a unique spectral for different plants, which is rooted in the number of chloroplasts present in a plant leaf, the amount of active photosynthesis occurring, health status, nutritional status, or stage of growth. Specific known spectral reflectance curves can be used to identify various plant species.

The wavelengths that are typically used for hyperspectral imaging of plants range from UV (starting at about 250 nm) to SWIR (about 2500 nm). Cameras usually capture a certain subrange, such as the visible and near-infrared range (VIS–NIR, 400–1300 nm), SWIR (1300–2500 nm), or UV (250–400 nm). These ranges are combined in some sensors to increase the coverage of the spectrum. It is common to have more bands in a true multispectral image, perhaps including light in the infrared region (wavelength over 700 nm.) Additionally, a hyperspectral image typically contains hundreds of contiguous narrow wavelength bands over a spectral range. The approach produces a dense, information-rich color dataset with enough spatial resolution to have many hundreds of data points (pixels) per leaf.

If a release of a particular hazardous, toxic, or characteristic waste is known to impact plant health or stress vegetation, biasing sampling using either multispectral or hyperspectral data may be useful. Either is a significant improvement over the typical ground field survey that often result in the reported finding of “no stressed vegetation.” If plant health, vegetation cover, and plant species diversity are valid indicators of the presence of a release or the health of land, then a finding of “no stressed vegetation” would be improved by quantitatively measuring and objectively characterizing plant health using these cameras.

Finally, hyperspectral camera imagery is being used to monitor cyanobacteria blooms in fresh water. The camera can

differentiate the reflected wavelength differences between chlorophyll *a*, contained by particular cyanobacteria, and chlorophyll *b* typical of plants and green algae.

6.4.1.12 Long-Wave Infrared (LWIR) Camera

LWIR cameras use a sensor to detect wavelengths above 10,000 nm, a range that is referred to as thermal infrared. These cameras are more expensive and have lower resolution than visible light cameras butcan be paired with them. Radiometric LWIR cameras provide a measured temperature value for each pixel; standard LWIR cameras provide approximate temperatures. LWIR cameras can be used to assess heat loss from sources such as buildings, infrastructure, people and animals, or seepage of landfill gases. Similarly, these cameras can be used to assess thermal properties of different substances like snow versus rock or timber (see the High-Resolution and Thermal Aerial Images Identify Mine Openings at an Abandoned Colorado Mine case study).

6.4.1.13 LiDAR

LiDAR tools can be used to measure the heights of objects and features on the ground with a high degree of accuracy. Practical applications are the ability to build a topological map through vegetation, generate highly accurate terrain mapping, and perform basic infrastructure inspections. For these applications, LiDAR uses near-infrared light (about 1,000 nm) to image objects. Pulses of laser light are used to measure distances; 4000 pulses per second is typical for a lower cost LiDAR but these values can be in the hundreds of thousands or even millions of pulses per second. When the laser light strikes an object, the light is reflected. A sensor detects the reflected laser light and records the time from the laser pulse to the received reflection. This value is converted into a distance, and these measured distances are combined point by point to produce a 3-D image called a point cloud. Each point is assigned a classification such as ground, water, vegetation, man-made object, and others. Classified point clouds are more easily manipulated because undesired features, such as vegetation, can be filtered out. The point clouds generated with LiDAR inherently do not include color information; however, some manufacturers merge color image data from a camera to colorize the point cloud. Additionally, laser data points are compared with the GPS locations of the drone and balanced against the systems on the drone that record pitch, roll, and heading. By integrating this information, site-specific features such as elevation models and ground contours can be constructed.

LiDAR tools offer a number of advantages over visual cameras:

- high accuracy
    - small FOV (0.1 to 1 milliradian) for detailed mapping on a local scale
    - large FOV for more complete relational maps
- all data is geo-referenced cover larger area per time
- less impacted by shadows and steep terrain
- large dataset to manipulate
- no external light source requried

Considerations for flight planning for LiDAR include:

- fying at night is possible (requires FAA waiver)
- increase overlap by 30 to 50% in steeper terrains
- run multiple passes in urban areas to transcend building shadows
- optimize flight elevation to specific LiDAR employed

6.4.2 Additional Information

- Cameras and settings for aerial surveys in the geosciences: optimizing image data (O'Connor, Smith, and James).
- Multi-Camera Imaging System for UAV Photogrammetry (Wierzbicki 2018).
- Geology 883, Remote Sensing Image Analysis and Application, Pennsylvania State University (PennState 2018).
- ESRI's The ArcGIS Imagery Books (ESRI 2019).
- Digital terrain modeling: principles and methodology (Li, Zhu, and Gold 2005).

6.5 Photogrammetry

Software employing techniques such as georeferenced orthomosaics, point clouds, triangulated irregular network (TIN)

meshes, digital elevation models (DEM), and digital terrain models (DTM) can extract 3-D information from 2-D images. Images with a high level of overlap taken from various positions, even without spatial orientation, can thus be used to generate 3-D models.

A typical work flow involves programming the drone to fly a series of flight lines back and forth over the subject, capturing images with overlap front to back and side to side. Overlap requirements vary depending on the site and mapping objectives, but, as a rule of thumb, at least 60% overlap is needed to reconstruct terrain maps with a high degree of accuracy. Subjects with vertical facades or geologic features not visible in straight down (Nadir) images can be reconstructed from photos taken at an angle that captures the facade. If a single structure is being captured, a series of circular orbits around the structure at two or more different altitudes are often combined with Nadir images. Most drone flight-planning software automatically calculates the flight lines, image intervals, and camera gimbal positions from a polygon or point of interest to support such image development.

These techniques work best for subjects with adequate contrast and stationary features. Water or featureless surfaces such as sand cannot be modeled because they lack sufficient contrast to match pictures. Movement creates distortion because the sensor reads out the image one line at a time rather than all at once. These rolling shutter or electronic shutter sensors can introduce distortion as the camera-subject relationship changes during a single photo. Using fast mechanical shutters and gimbals help to compensate for the lack of adequate contrast and movement.

6.5.1 Data Collection Design

Data management and sharing should be considered early in the development of a drone program. Proper data management leverages data collected from multiple sources and allows data to be easily located and shared. Data sharing can enhance safety and lower costs by reducing the need for redundant flights. A drone can collect gigabytes of data in a single flight. Information technology resources and GIS may not be prepared for the vast amount of resulting data; cloud-based computing and data storage should be considered in these instances.

6.5.2 Data Certification Requirements

Depending on the purpose of the georeferenced data, data generated from a drone flight should be verified by licensed professional surveyors or other professionals with mapping experience.

6.5.3 Data Visualization and Analysis

Software packages for data collected via drone include ENVI, ERDAS IMAGINE, ArcGIS, TNTMips, GRASS GIS, QGIS, and TerrSet. The programming languages R and Python have several libraries for processing remote sensing data. These programs can be used to build automated data processing chains and are required to use leading-edge machine learning tools (use of artificial intelligence (AI) to automatically learn and improve from experience) with remote sensing data. Selecting appropriate software packages should be based on project goals and future anticipated projects.

6.6 Sample Collection and Monitoring using Drones

Drones may be used to collect water, air, and soil samples, particularly samples that may be difficult or dangerous for a human to collect. The area of physical sample collection via drones is developing rapidly. The following sections focus on water sample collection as the architype physical sampling. Air sampling and, to a lesser degree, soil sampling applications are developing and are not extensively addressed.

Figure 6-3. Example drones.

Source: Photos courtesy of Kentucky Department of Transportation and the Division of Waste Management

The Kentucky Department of Transportation and the Division of Waste Management with the help of Ardupilot open source project built a hexacopter and quadrotor. The hexacopter, pictured in Figure 6-3 (left), carries an air pump and sorbent tube to determine the potential presence of hazardous air pollution produced by fires. The quadrotor, pictured in Figure 6-3 (right), collects a water sample using a double-valve bailer on a tether. The expanded polypropylene foam pool noodle frame material is light weight, which increases payload capacity, enables water landings, and minimizes propwash over the sample area.

6.6.1 Water Sampling Devices

Multiple water-sampling devices have been developed and demonstrated for drones (see Table 6-2). In general, drone water-sampling devices fall into two categories: surface-water sampling devices, and deep-water sampling devices. Table 6-2 provides a description of drone water sampling equipment cited in literature at the time of this writing. Many of these tools were developed by universities and may not be available for commercial deployment.

Ultimately, the best equipment for a given job satisfies the following criteria:

- Has it been tested and demonstrated to work?
- Is it commercially available for rent or purchase?
- Can it collect water samples from the required depths?
- Does it collect the required sample volume in one flight?
- Will regulators accept water samples collected with this method (see below)?

Table 6-2. Description of sampling devices

Reference	Sample volume	Sample depth	Description of sampling device
(Ore et al. 2015)	20 mL	<1 m	1-m-long tube with onboard pump
(Cornell, Herman, and Ontiveros 2016)	50 mL	0 m	Falcon tube dipped below surface
(Koparan et al. 2018)	130 mL	0.6-0.8 m	Thief-style, messenger-triggered bottle
(Terada et al. 2018)	250 mL	<0.8 m	Sample tube with check-valve
(Washburn et al. 2018)	500 mL	5 m	Bottle closes autonomously at a specified pressure
(IRYS 2016)	1000 mL	0 m	Thin tray submerged in water

Reference	Sample volume	Sample depth	Description of sampling device
(Castendyk, Straight, and Filiatreault 2017)	1250 mL	80 m	Niskin sample bottle
(Williams et al. 2018)	2000 mL	83 m	Proprietary sampling device

6.6.1.1 High-Lift-Capacity Drones

The drone used to collect water samples should be able to lift (1) the weight of the drone, (2) the weight of the water sampling device when filled with water, and (3), if applicable, the weight of specialized equipment added to the payload, such as a messenger and a messenger-release device. Small drones useful for photography may not have the lift needed.

6.6.1.2 Flight Distance and Power Supply

A drone loaded with a water sample may have a flight time of approximately 15 minutes. A margin of error should be added to this time to ensure the safe return of equipment. Given the time available and weight carried, drone flight range may be limited to 1,000 to 1,500 ft from take off to the sample point.

6.6.2 Quality Control

The ability to verify sampling depth is important. In the field, the water-sampling device is suspended at a known distance below the drone; thus, the elevation of the drone can be used to estimate the sample collection depth. Similarly, the tether holding the sampler can mark depth using brightly coloured tags placed at known intervals. Furthermore, if the water parameters are known, density, salinity, conductivity, and temperature may be used as indicators of depth. This approach requires consistency in these water parameters for the body of water at a specific depth and as measured by the device. Pressure may also be used to indicate depth; a small pressure transducer, such as a Van Essen, Micro-Diver, DI610 (approximately $1200) has a depth error of +/- 25 inches at 328 ft depth and provides a good measure of sample depth.

6.6.3 Advantages and Disadvantages

The advantages of water sampling using drones include the following:

- Improve safety by eliminating the need for humans to work on or near water. Standard practices for water sampling involve a person filling water bottles from a shoreline or from a boat. Working on or near water presents several risks to human health. In October 2017, a contractor drowned after falling into a coal-ash pond in Kentucky (See WDRB News article (WDRB 2017)). In addition to the obvious concern of drowning, some stratified basins can accumulate large quantities of dissolved gases (CO_2, H_2S, CH_4), and rapid degassing events can displace atmospheric oxygen leading to asphyxiation or, in the case of hydrogen sulfide, cause acute toxicity.
- Reduce costs associated with water sampling (no need for a boat or an access road; fewer staff).
- Allow increased sampling frequency due to ease of sampling and reduced cost.
- Enable better water quality management because of better understanding of water quality and shorter response time to changes in water quality.

Drone water sampling has several disadvantages compared to boat-based practices. As the practice gains wider acceptance and regulatory approval, some of these disadvantages may be eliminated.

- Sample volume is limited due to the weight of a loaded water sampler.
- Sample depth is restrained by regulatory restrictions on drone height. Methods that involve suspending the sampler on a tether below the drone (Castendyk, Straight, and Filiatreault 2017); (Castendyk et al. 2018) are restricted to maximally 400 ft below the drone and sampling can only occur to a depth of the tether.
- Off-the-shelf equipment for drone water sampling is not widely available. One engineering firm sells water-sampling equipment (Hatch Associates Consultants, Mississauga, Canada). Interested companies either need to: (1) purchase their own specialized equipment, develop custom attachments, and train crew or (2) contract for this service.
- Drone water sampling is new and unfamiliar to regulators and the industry, leading to caution when adopting nonstandard techniques.
- Establishing legal approval to conduct drone water sampling may hinder its use.

6.6.3.1 Sample Locations

To collect representative water samples, the depth and surface area of the water body must be taken into account. Typically, water samples are collected from the point directly above the maximum depth of the water body. Assuming there are no lateral changes in water chemistry, sampling from this point should allow an assessment of the entire water body. Water bodies, such as, ponds and lakes having large surface areas or multiple floor depressions, or sub-basins, may require multiple sampling points. A bathymetry map, if available, shows the locations of depressions which may have a unique water chemistry characteristic as compared to the larger water body.

6.6.3.2 Number of Samples

Stratification may occur in the water column, resulting in discrete layers with different water chemistry. Stratification is caused by vertical density difference between shallow and deep water which result from surface water warming faster than deep water, high salinity water being added to the water body from surface or groundwater, or both. Sampling only the surface of a stratified water body can give a false indication of the overall water quality, especially if fresh rainwater has diluted the surface water layer relative to the deep layer. For this reason, the State of Nevada requires that mine pit lakes deeper than 25 ft be sampled at a minimum of three intervals: near the surface, in the middle, and near the bottom.

To appropriately characterize a water body, at least one water sample should be collected from each homogeneous layer. For shallow ponds less than ten ft deep, a single surface sample may be sufficient assuming that the water column is well mixed by wind energy. For water bodies deeper than 25 ft, this requires: (1) a water sampling device capable of collecting water samples from depth (see below), and (2) knowledge of the depth intervals of stratified layers within the body. To complicate matters, the depth of stratified layers changes seasonally, such that the appropriate sampling depths used during one site visit may be inappropriate on another site visit. Guessing the appropriate sample depths, without knowledge of water column~~,~~ structure can result in missing an important layer. Over-sampling may result in chemically redundant samples.

To avoid these outcomes, it is best to profile the in situ physiochemical properties of the lake before sampling (Castendyk, Straight, and Filiatreault 2017); (Castendyk et al. 2018

). One useful device for this purpose is YSI *CastAway*® CTD (approximate cost $6,500; (SonTek 2019)). The *CastAway* is a hand deployable conductivity, temperature, and depth instrument for hydrologic profiling. It measures *in situ* temperature, electrical conductivity and water density as a function of depth at five times per second during its decent and accent. The data set is sent to a laptop, and the associate software illustrates profiles of each variable. Such data can be used to identify homogeneous layers and to select sampling depths.

6.6.3.3 Sample Volume

To determine the volume of sample needed consider the following:

- What contaminants of concern need to be measured? For example, the suite of parameters listed on an applicable effluent discharge permit;
- Are both total and dissolved concentrations are required.
- Ask the receiving analytical laboratory for the number of water bottles needed to measure the suite of parameters and the volumes of each water bottle.

6.7 Cost Considerations

Companies throughout the U.S. offer product and support ranging from turn-key equipment packages to individual items or services such as hardware, software, postflight, image processing and analysis, data visualization, and pilot training. Most providers offer finished mapping and surveys, aerial imagery, and videography while slightly fewer companies provide multispectral, hyperspectral, infrared, LiDAR, or comparable services. Limited numbers of companies offer water and stack testing. Aerial imagery and videography are inexpensive and broadly useful such that companies are developing in-house expertise. The drone services market is continuously evolving and competitive such that new equipment and services arise almost continually.

Complete drone packages are readily available that include the unmanned aircraft vehicle (fixed wing or multirotor), camera (still and video), mission planning software for creating autonomous missions, and postprocessing and analytical software for generating orthoimagery, analyzing vegetative health, creating 3-D digital elevation and surface models, and calculating cut

volumes or change-in elevations. Such systems are generally adapted for mapping surveys using photogrammetric methods. Prices for a simple camera drone and supporting software can be as low as about $1,000. More complex systems are usually in the range of $10,000 to more than $30,000.

6.8 Case Studies

- Drone Technology Expedites and Streamlines Site Characterization at a Former Golf Course in Missouri
- High-Resolution and Thermal Aerial Images Identify Mine Openings at an Abandoned Colorado Mine
- RPAS Collects Water Samples to Avoid Safety Concerns at Montana Tunnels Mine

7 Stakeholder and Tribal Perspectives

This section provides guidance to regulators, technology vendors, and responsible parties on identifying and engaging with public and tribal stakeholders. This section also provides guidance to public and tribal stakeholders on the use of ASCT in the evaluation, monitoring, and remediation of contaminated sites; outlines some potential issues, needs, and concerns that stakeholders may have; and supplies examples of how stakeholders can engage in and improve upon site characterization.

Public and tribal stakeholders include affected tribes, community members, representatives of environmental and community advocacy groups, and local governments. Stakeholders are generally open to using innovative technologies and approaches, particularly if the technologies help improve CSMs, accelerate the remediation process, test the effectiveness of a remediation process, and lead to faster solutions. Affected stakeholders are not limited only to residents adjacent to a site. Residents located downgradient of a site, for example, may be affected. Tribes also may have treaties or other pacts with the federal government that grant them fishing, hunting, or access rights in areas that are not necessarily near present-day reservations; this issue is an especially important consideration in the identification of affected tribes. Additionally, at some sites, tribes have regulatory oversight and, thus, play a major regulatory role that is different from that of other stakeholders.

Individual states and Native American communities recognize certain tribes that are not recognized by the federal government. A list of federally recognized tribes, by state, may be obtained from the National Conference of State Legislatures (NCSL) (NCSL 2019). For state-recognized tribes, refer to the individual states. Current lists of state-recognized tribes may be incomplete. One such list is available from NCSL (NCSL 2019). Another is a list of nonfederally recognized tribes (Giese 1997).

Peoples who lifestyles are not anticipated in the thinking of the majority culture nor accounted for in standardized risk assessments may be disproportionately affected by environmental contamination. In Native American communities, those who practice subsistence fishing may be more affected than the general population by contaminants in water. Those who practice the sweat lodge ritual may perhaps be disproportionally affected by inhalation of contaminants in water. It is important to make remedial decisions informed by the actual practices of the people who are potentially impacted as opposed to attributing majority culture practices upon such communities.

Tribes are sovereign nations and should be approached as such, with the proper protocol. Each tribe has its own customs and protocols, and it is important to learn about them in advance. General protocol requires that tribal leaders be addressed with their appropriate title (such as Chairman, Chairwoman, Chief, Councilman, Councilwoman) and treated with the same respect afforded for equivalent heads of state or members of the federal legislature.

Public and tribal stakeholders should be approached early and often in the site characterization process. They often have valuable information about site characteristics and history that can enhance the evaluation process and improve the CSM, leading to better-quality remediation decisions. Public and tribal stakeholders should be asked about their aspirations for future use of land and resources and whether they have specific desires about reclamation and property redevelopment. If mutual trust and respect have been established through open and honest communication from the beginning of the project, consensus can be reached in favor of a scientifically meritorious solution. Problems can be addressed faster, and remediation efforts can proceed more smoothly and efficiently when decisions have earned the support of the stakeholders.

While stakeholders are generally open to innovative technologies, the lack of existing agency guidelines for ASCTs in some states may be a source of apprehension or suspicion. It is important to present the facts about the efficacy of ASCT methods as clearly and honestly as possible. Explanations for how ASCT methods work should be offered.

At sites where remediation objectives have not been achieved, stakeholders may have lost trust in technical professionals and therefore be skeptical of new technologies proposed. Particularly at these sites it is important to show evidence of the effectiveness – and limitations – of ASCT methods. Honest communication, with evidence presented in understandable forms, is essential to achieve stakeholder agreement.

An example of how stakeholders contribute to the site characterization process is summarized below.

Example – How the Great Falls Citizens Association Helped Characterize a MTBE Site

Great Falls is an unincorporated city in Northern Virginia. The website of the Great Falls Citizens Association (GFCA) (GFCA 2019) states: “Since Great Falls is not legally a city, we lack a town government to represent our local interests. GFCA acts in an unofficial capacity to represent the voices of the citizens of Great Falls.” The population of Great Falls is generally well educated and includes former USEPA employees. Most homes in Great Falls have private wells.

About five years ago, concern arose about MTBE contamination in the aquifer from a closed gas station. The plan for the site was to install monitoring wells to the southeast. GFCA members believed that a fracture zone was present to the south near a subdivision and posed a risk to private wells. GFCA members recruited three outside experts to evaluate the site free of charge and eventually convinced the state agency to address their concerns.

ASCTs, specifically surficial geophysical methods including seismic refraction, ER, and MASW, were used to guide placement of the monitoring wells. Results confirmed the suspicions of the GFCA members– a fracture zone was present to the south. Monitoring wells were installed in the areas of the vadose zone and fractured rock. As suspected, high levels of MTBE were found. Remediation in the form of pump and treat has been ongoing for about four years.

The engineers of the responsible party held several meetings with GFCA members, sometimes with about 100 citizens in attendance. Citizens were accepting of the ASCTs and use of the ASCTs enabled their assertions to be confirmed and their concerns to be addressed.

After four years of pumping and treating the groundwater, MTBE concentrations have gradually reduced to below the end points set by the state agency. GFCA members continue to monitor results of postcleanup monitoring.

8 Regulatory Perspective

In 2018, the ITRC completed a state survey to gauge the extent of familiarity and use of ASCTs by regulators and identify the limitations and barriers to achieving wider acceptance and use of these tools. This section provides a brief summary of the 55 contacts who responded to the survey, representing 37 states plus Puerto Rico. Some states provided multiple responses. Results are presented indicating the percentage of respondents. Respondents were not required to answer every question.

Of the 55 people responding to our inquiry about their level of experience with ASCTs, most (85%) were very familiar with ASCTs. Forty respondents reported that they had limited or moderate experience and two reported that they were very experienced. Slightly over 50% of the respondents had used ASCTs on only a few (<10) sites; the rest reported more extensive experience using ASCT.

The ITRC specifically queried states on the following technology groups:

- direct sensing (downhole) tools (for example MIP, HPT)
- borehole geophysical tools (for example televiewer, flow meters)
- surface geophysical tools (for example GPR, EM, seismic surveys)
- crosshole geophysical tools (for example seismic, ER)
- remote sensing (for example aerial surveys)

Respondents were most familiar with downhole direct sensing tools, borehole geophysical tools, and surface geophysical tools. With downhole direct sensing tools, it appears that respondents generally have the most experience with MIP and LIF (UVOST®). Respondents use HPT less frequently, and OIP is used even less. Use may be a function of when the tool was introduced to the market. MIP and LIF have been on the market since about 2007, HPT became available about 2015, and OIP became available about 2016. Respondents seem to have the most experience with EM and GPR surveys (surface geophysical tools), with reported usage that greatly exceeds the usage of seismic tools. This increase experience may be due to the extensive use of EM surveys to locate buried steel tanks and the use of GPR to identify tanks and utility lines. Seismic surveys generally do not have sufficient resolution to identify small- or near-surface objects and calibration, processing, and interpreting seismic data is more difficult and therefore subject to additional error. Cross-hole geophysical tools and remote sensing surveys were used the least frequently. Possible reasons include cost, limited availability, lack of stakeholder familiarity, and applicability (that is, the techniques were judged to be unnecessary for the project due to small size, contaminant type, or geology.).

Many respondents reported that ASCTs were advantageous when used after a new or catastrophic release event, and 87% reported that ASCTs were most advantageous when used for sites that had not achieved remedial objectives. Most also agreed that ASCTs were very useful for remedial purposes. In these situations, ASCTs were used to obtain specific technical information often after traditional site characterization methods had produced unsatisfactory results. Although survey results show that the regulatory community recognizes that using ASCTs can be beneficial, the respondents were generally neutral on whether their state would recommend or require use of ASCTs. The general consensus from comments was that the responsible party and its consultant should evaluate and recommend how to investigate a release site. It was acknowledged that, in some circumstances, responsible parties and consultants wished the regulatory agency would initiate a discussion of ASCTs.

8.1 Challenges and Solutions

Distinct challenges must be overcome to increase the use of ASCTs. Resolving these challenges should be a consideration for all stakeholders. In spite of the perception that using ASCTs is beneficial, respondents noted the following barriers to their effective use: cost, lack of understanding of tool capabilities, lack of training for interpreting the data collected, and lack of ASCT availability. Regulatory issues and other considerations were reported as less significant barriers.

8.1.1 Cost

Cost was the most frequent barrier reported in the survey. Eighty-seven percent of those who responded indicated that costs were the primary barrier to ASCT use; 71% responded that costs would be a consideration in selecting an approach, potentially because the site investigation is being paid with government funding. Approximately half of the respondents

reported that their state would reimburse or otherwise pay for using ASCTs, and cost versus perceived benefit (reduced remedial time and cost) would be one of the most important considerations for selecting ASCTs over more traditional methods. Some states have overcome cost uncertainity andby soliciting bids for contracts that include ASCTs to establish per-foot or per-sample rates. Other possible solutions include drafting work plans to solicit prices on a case-by-case basis from companies using ASCTs, requesting consultants to provide itemized cost comparisons for using ASCTs as an alternative to more traditional methods, and controlling costs by limiting ASCTs to specific scopes of work or certain types of sites.

8.1.2 Lack of Understanding

The lack of understanding and knowledge of the tools appears to be equally shared among the regulatory community, the consultant, and the responsible party. This lack of understanding appears in two parts: the need to understand the operation, capabilities, and limitations of ASCTs and the need to independently interpret the data so the consultant and regulator can confirm data, make site decisions, and take actions based on the data. Too often consultants and regulators rely solely on the ASCT vendor for data interpretation or vendor assistance with data interpretation is incomplete or not included in the scope of work. These interpretations may not take into account relevant site information that the vendor may not know.

8.1.3 Lack of Training

The lack of training, familiarity, and experience with ASCTs by regulators are reflected in the paucity of state guidance. Only five states in our survey have guidance for the appropriate use of ASCTs and only one (Wyoming) offered detailed information. Guidance documents signal regulatory acceptance of ASCTs, even if only under certain circumstances or parameters, and encourage the knowledge and use of ASCTs.

One solution may be for industry to inform and train regulators and encourage regulators to suggest that consultants consider using ASCTs when regulators believe these tools may be appropriate. Consultants often hesitate to propose actions they fear regulators will not approve, worrying it will cause clients to doubt their expertise. Coincidentally, some responsible parties fear that using ASCTs will reveal previously unknown contamination, increasing project lifetime and liability. I In fact, ASCTs are likely to reveal conditions that allow reductions in such concerns.

8.1.4 Availability

A general lack of ASCT availability is identified as a third major hurdle. As might be expected, all ASCTs are not useful in all geographic areas. A partnership between the ASCT industry to train regulators and consultants how to use ASCTs and interpret the resulting data seems to be a path forward to regulators becoming more accepting of the tools. Increased usage should result in increased availability and decreased costs. This transition is likely to take at least a decade because each step is interrelated and interdependent. Perhaps if vendors offered incentives for ASCT use (for example, reduced mobilization fees, multiday discounts), there would be more motivation to propose ASCT use and prove their benefit.

8.1.5 Regulatory Issues

Survey respondents generally reported that their agency either suggests or recommends using ASCTs, yet regulatory issues were reported to be a primary barrier by 7% of respondents. Regulatory issues may include the inability to approve or pay for innovative technologies or the requirement that physical sampling and laboratory analysis is necessary to support decisions. In the latter case, using ASCTs is deemed extraneous or not cost beneficial). ASCTs do not replace but *complement and enhance* the interpretation of data gathered by traditional methods. Compliance with regulatory requirements and meeting the technical needs of a project may require variations in how ASCTs are applied (for example, using ASCTs in a limited capacity while using traditional methods for confirmation or limiting ASCT use to source-zone determination or treatment).

9 Case Studies

Case Study #	Case Study	ASCT Type	Technology
9.1	MIP Boring Data Allow On-Site Decisions to Fill Data Gaps and Reduce Uncertainty during Triad Approach Evaluation at Five South Dakota Sites	Direct Sensing	MIP
9.2	MIP Allows Real-Time Identification and Delineation of DNAPL Plume at a Former Naval Air Station in California	Direct Sensing	MIP
9.3	OIP-Green Probe Delineates Extent of Coal Tar NAPL at a Former Gas Manufacturing Plant in Kansas	Direct Sensing	OIP-G
9.4	LIF Survey with UVOST® Provides More Accurate Representation of LNAPL Plume at a Former Bulk Petroleum Storage Facility in New Hampshire	Direct Sensing	LIF-UVOST®
9.5	UVOST® Differentiates LNAPL Types to Allocate Financial Liabilities at a Retail Petroleum Facility in Tennessee	Direct Sensing	LIF-UVOST®
9.6	TarGOST Determines DNAPL Extent and HPT Confirms Site Lithology at a Former Creosote Facility in Louisiana	Direct Sensing	LIF-TarGOST and HPT
9.7	9.7 CPT Borings and Hydropunch Sampler Optimize Site Characterization at an Aviation Industrial Complex in California	Direct Sensing	CPT and Hydropunch
9.8	Waterloo APS, CPT, and LIF Data Update CSM and Help Optimize Selected Remedy at a Former Refinery in Oklahoma	Direct Sensing	Waterloo APS, CPT, and LIF
9.9	Conceptual Site Model Development Using Borehole Geophysics at the Savage Municipal Water Supply Superfund Site in New Hampshire	Borehole Geophysics	Borehole caliper, fluid temperature/ resistivity, natural gamma, OTV, ATV, and HPFM
9.10	ERI Provides Data to Improve Groundwater Flow and Contaminant Transport Models at Hanford 300 Facility in Washington	Surface Geophysics	ERI
9.11	Surface and Borehole Geophysical Technologies Provide Data to Pinpoint and Characterize Karst Features at a Former Retail Petroleum Facility in Kentucky	Borehole and Surface Geophysics	ER, FDEM, GPR
9.12	GPR Data Show Location of Buried Debris and Piping Associated with a Former Gas Holder in Minnesota	Surface Geophysics	GPR
9.13	Resistivity, Seismic Exploration, and GPR Provide Data to Evaluate Clay Reserves at a Commercially Mined Pit	Surface Geophysics	ERI, GPR
9.14	Seismic Refraction, Electric Resistivity, and Multichannel Analysis of Seismic Waves Provide Data to Locate Potential Monitoring Well Locations in a Mixed-Use Area in Northern Virginia	Surface Geophysics	Seismic Refraction, ER, MASW
9.15	Surface Geophysical Methods Provide Data to Identify Prospective Utility Waste Landfill Sites in Karst Terrain in Missouri	Surface Geophysics	ERI, MASW
9.16	Airborne Time-Domain Electromagnetic Method Mappings Sand Distribution along the Illinois Lake Michigan Shore	Surface Geophysics	TDEM

Case Study #	Case Study	ASCT Type	Technology
9.17	Drone Technology Expedites and Streamlines Site Characterization at a Former Golf Course in Missouri	Remote Sensing	Orthoimagery
9.18	High-Resolution and Thermal Aerial Images Identify Mine Openings at an Abandoned Colorado Mine	Remote Sensing	High resolution imagery, Thermal aerial imagery
9.19	RPAS Collects Water Samples to Avoid Safety Concerns at Montana Tunnels Mine	Remote Sensing	Water quality monitoring samples

9.1 MIP Boring Data Allow On-Site Decisions to Fill Data Gaps and Reduce Uncertainty during Triad Approach Evaluation at Five South Dakota Sites

John McVey
South Dakota Department of Environmental and Natural Resources – Petroleum Release Compensation Fund
john.mcvey@state.sd.us

In 2004, the South Dakota Petroleum Release Compensation Fund conducted a study to evaluate and report on the effectiveness of using the triad approach to manage decision uncertainties associated with five petroleum release sites across South Dakota (SDPRCF 2015). The goal of the study was to apply the principals of the triad approach to rapidly characterize the sites, develop accurate CSMs, establish clear clean-up goals and move the languishing sites toward regulatory closure as quickly as possible. A MIP coupled with an electron capture device, photoionization detector, flame ionization detector and Columbia Technologies SmartData Solutions® (Columbia 2019) data processing and visualization platform were selected to allow for real-time assessment and decision making. Standard confirmation sampling was used to verify the rapid site assessment.

Similar to other sites included in the study, the former T&T Standard site was stalled in the assessment process and not moving toward regulatory closure. A release (see Figure 9-1) was discovered in December 1991, and assessments were performed in 1992, 1993, 1994, and 1999. Three underground storage tanks (USTs) (one 10,000-gallon gasoline, one 8,000-gallon gasoline, and one 3,000-gallon diesel) and about 900 cubic yards of contaminated soil were removed in 1992. Two USTs (one 270 gallon and one 100 gallon) and about 10 cubic yards of soil were removed in 1994. Groundwater monitoring was performed from 1992 to 2003. An additional assessment was required to define the extent and evaluate potential for risk to underground structures (utilities) and city water supply wells. For this study, objectives included the following:

- Confirm background data using perimeter test holes.
- Identify all potential sources and determine if source areas are separate or co-mingled.
- Resolve potential sources between on- and off-site properties.
- Determine extent of dissolved plume relative to Source Water Protection Area.
- Determine if deeper lithology is consistent with aquifer material.
- Evaluate potential of excluding site from Source Water Protection Area.
- Identify all downgradient pathways and receptors.
- Identify location, depth, and construction of utilities and determine impacts.
- Take confirmation soil & groundwater samples.
- Analyze soil and groundwater samples for TPH-G, BTEX, MTBE, EDB, TPA.
- Determine need for additional compliance monitoring wells.
- Develop corrective action plan.

A total of 23 MIP borings were advanced over three days, resulting in approximately 13,000 data points collected over 640 ft of drilling. In addition, three conventional direct-push confirmation borings were installed, resulting in approximately 65 data points over 55 ft of drilling. An abandoned storm sewer filled with waste oil and two previously unidentified USTs were discovered, partially due to the density of data provided by the MIP borings. Additional assessment was required to define extent and evaluate the potential for risk to underground structures (utilities) and city water supply wells.

The major objectives were completed, and a Corrective Action Plan was developed. It was determined that groundwater beneath the site is not hydraulically connected to the drinking water source and not necessary to meet drinking water MCLs. No Further Action status was received in January 2007, slightly over two years after the MIP assessment.

At the former T&T Standard site, as well as the other sites included in the study, the availability of real-time data provided the flexibility to augment the project work plan during the same mobilization, minimizing the need for future site visits to collect additional data. Consequently, the time and costs associated with redundant mobilization and demobilizations, generation of interim reports, revision of work plans, and additional contracting to complete the necessary work were avoided. Of the three sites that had prior assessment data, MIP assessment costs ranged from 15% to 70% less expensive than conventional assessments.

Lessons learned from the triad approach study were as follows:

- Pre-planning and establishing objectives up front proved invaluable in identifying and resolving differences in assessment objectives, establishing site-specific remedial goals, and developing decision metrics for real-time decision making as assessment data became available.
- Prior to beginning work, consideration should be given to other technologies that can provide specialized characterization (for example, LIF to assess a NAPL plume).
- More up-front training on direct sensing technologies such as MIP and LIF would have been helpful before beginning field work.
- On-site real-time data collection proceeded smoothly and results were invaluable. On-site decisions were made with regard to collecting additional data to fill data gaps and reduce uncertainty.
- Heavier petroleum did not clear the MIP trunk line well and carry over was evident on logs from one boring location to the next. Note: The exact nature of the heavier petroleum is not known, but it likely contained a mixture of diesel, grease, and asphaltic tar.

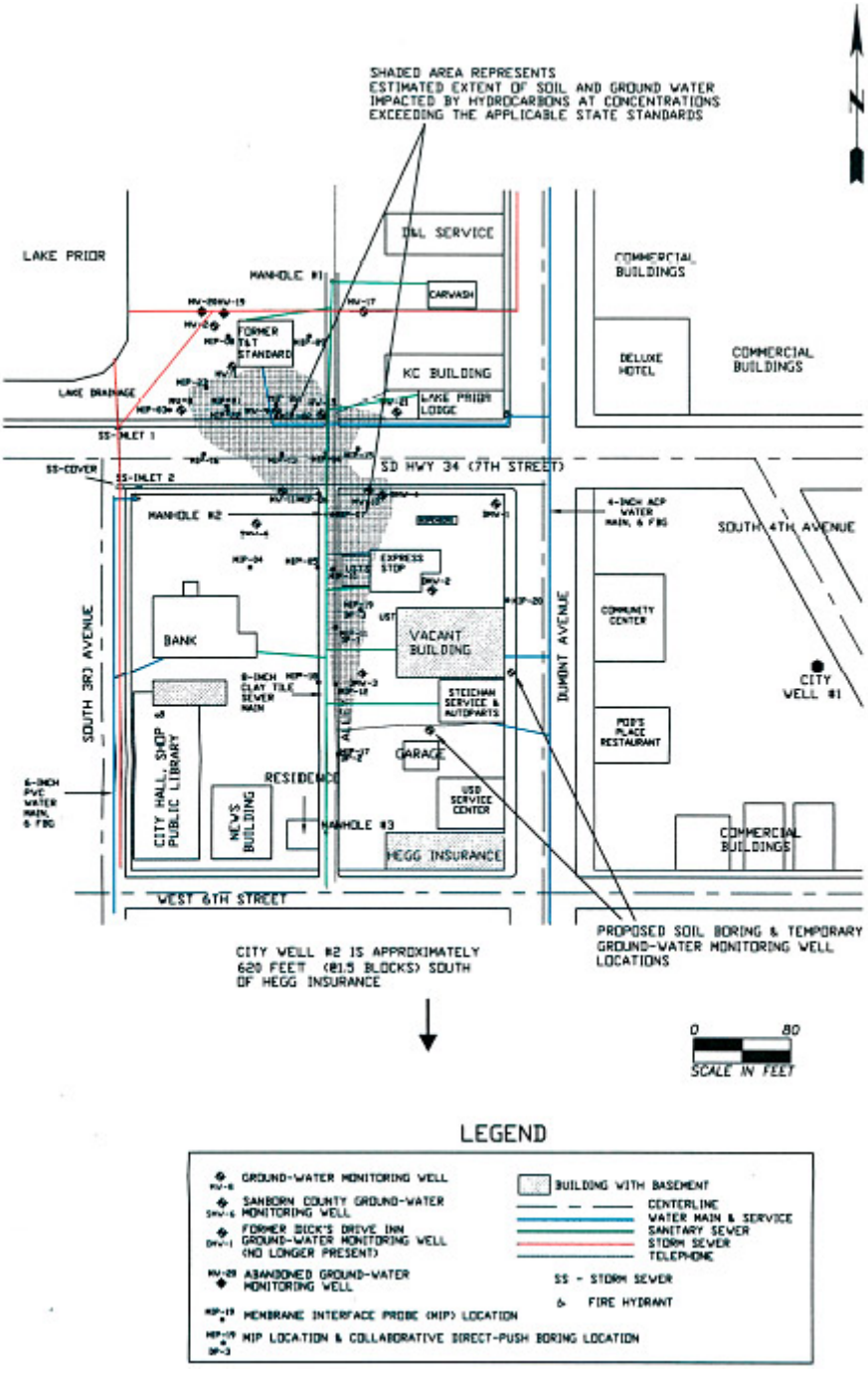

Figure 9-1. Former T&T Standard site.

9.2 MIP Allows Real-Time Identification and Delineation of DNAPL Plume at a Former Naval Air Station in California

Eliot Cooper
Director of Technology Innovation
Gregg Drilling, Remediation Division
ecooper@greggdrilling.com

Information presented in this case study is based on investigations conducted by Shaw Environmental and Vironex Field Services

In 2010 the U.S. Navy engaged in remediation for Operable Unit (OU) 2B Installation Restoration Sites 3, 4, 11, and 21 at the Former Naval Air Station (NAS) Alameda in Alameda, California. Site 4 (Aircraft Engine Facility) covers approximately 22.7 acres and includes Building 360, which was used for aircraft engine and airframe overhaul. Building 360 operations contributed to the existence of a large VOC plume located within OU-2B. A portion of the plume located within Site 4, referred to as Plume 4, consists of two lobes that trend east-west through Site 4. The northernmost lobe of the plume is associated with source area 4-1.

Despite years of groundwater sampling indicating the presence of DNAPL, DNAPL could not be located or identified, impeding overall remediation of a Plume 4. Because the probability of sufficiently defining both the vertical and horizontal extent of a DNAPL zone with traditional sampling is low, site characterization was perfomed using a MIP advanced by direct-push drilling. This was followed by continuous soil core sampling and use of Sudan dye to help identify the presence of a high TCE mass (see Figure 9-2) and, if identified, determine if this mass was DNAPL.

The MIP uses up to four detectors (PID, FID, ECD and XSD) to respond to volatile chlorinated solvent contaminants. These detectors provide responses as eV that can be used to assess the amount of contaminant mass in the subsurface. Based on years of experience in logging chlorinated solvent sites and corresponding traditional soil and groundwater sampling, levels greater than 1 x 10^6 to 1 x 10^7 uV from the PID detector may indicate contaminant mass at DNAPL levels.

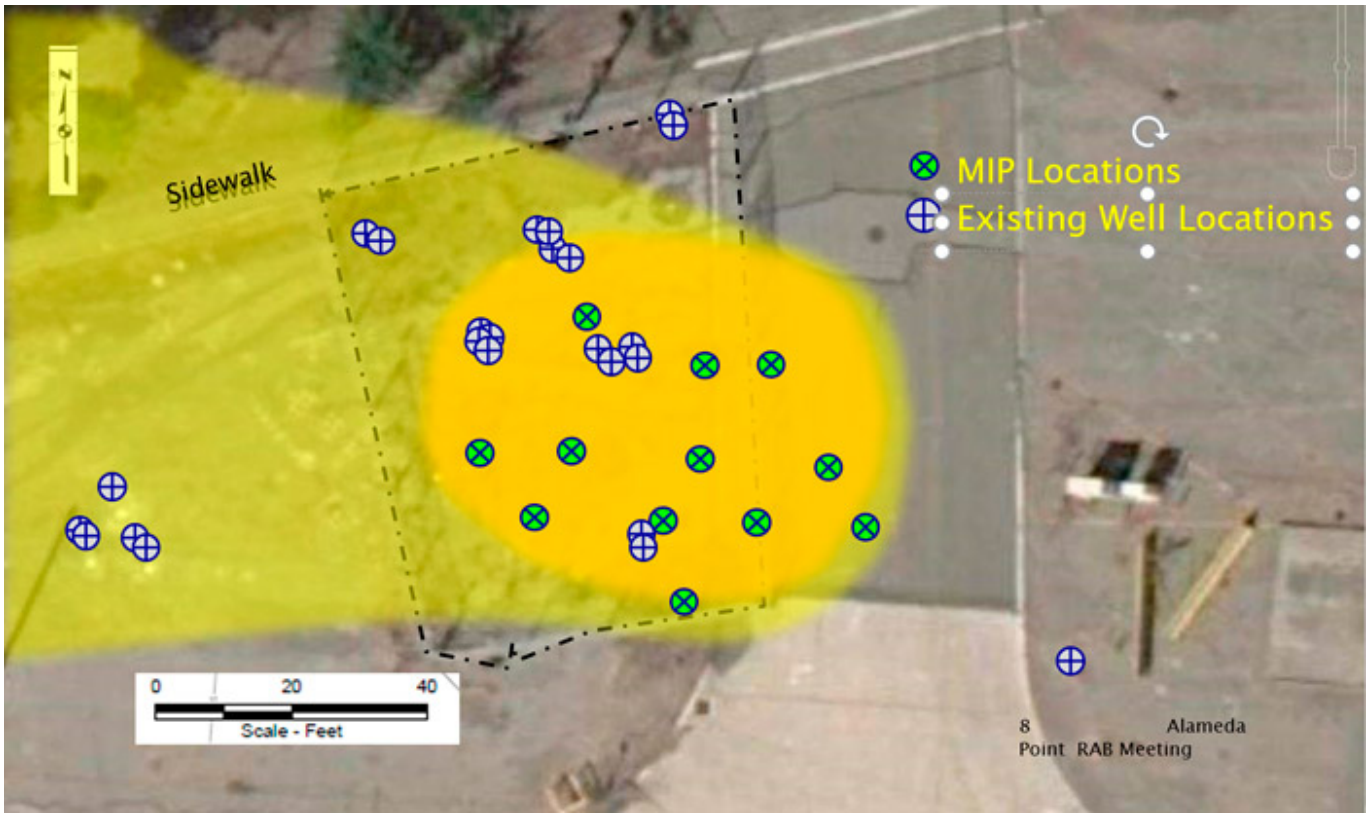

Figure 9-2. Locations of existing wells and MIP borings in assumed source (dark yellow) and plume (light

yellow).

Based on the level of responses of both the ECD (>1.4 x 10^7 *u*V) and PID (>1 x 10^6 to 1 x 10^7 *u*V), a potential DNAPL zone was identified from approximately 15- to 22-ft below ground surface (see Figure 9-3 and Figure 9-4).

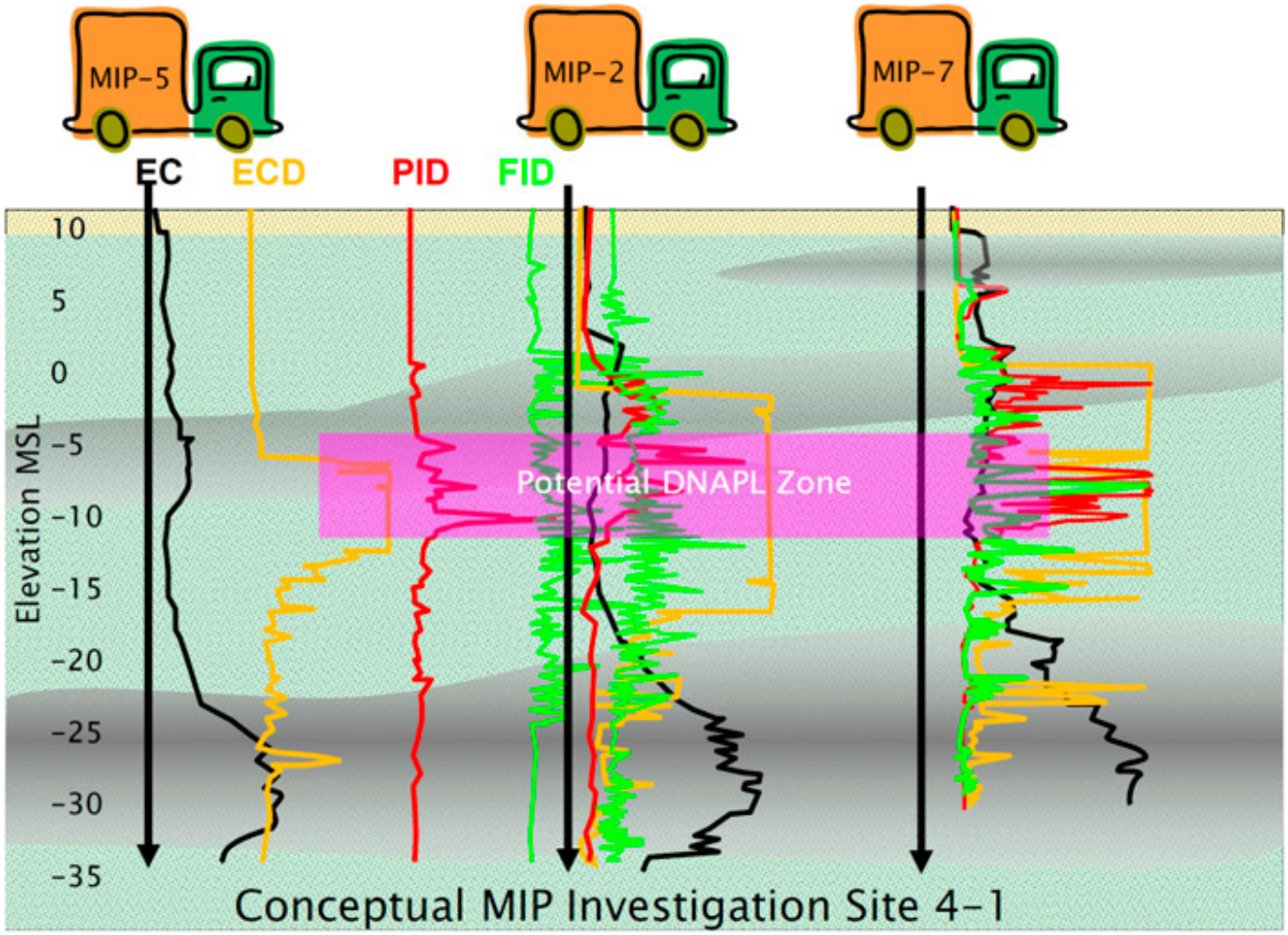

Figure 9-3. Potential DNAPL interval identified by ECD and PID tools.

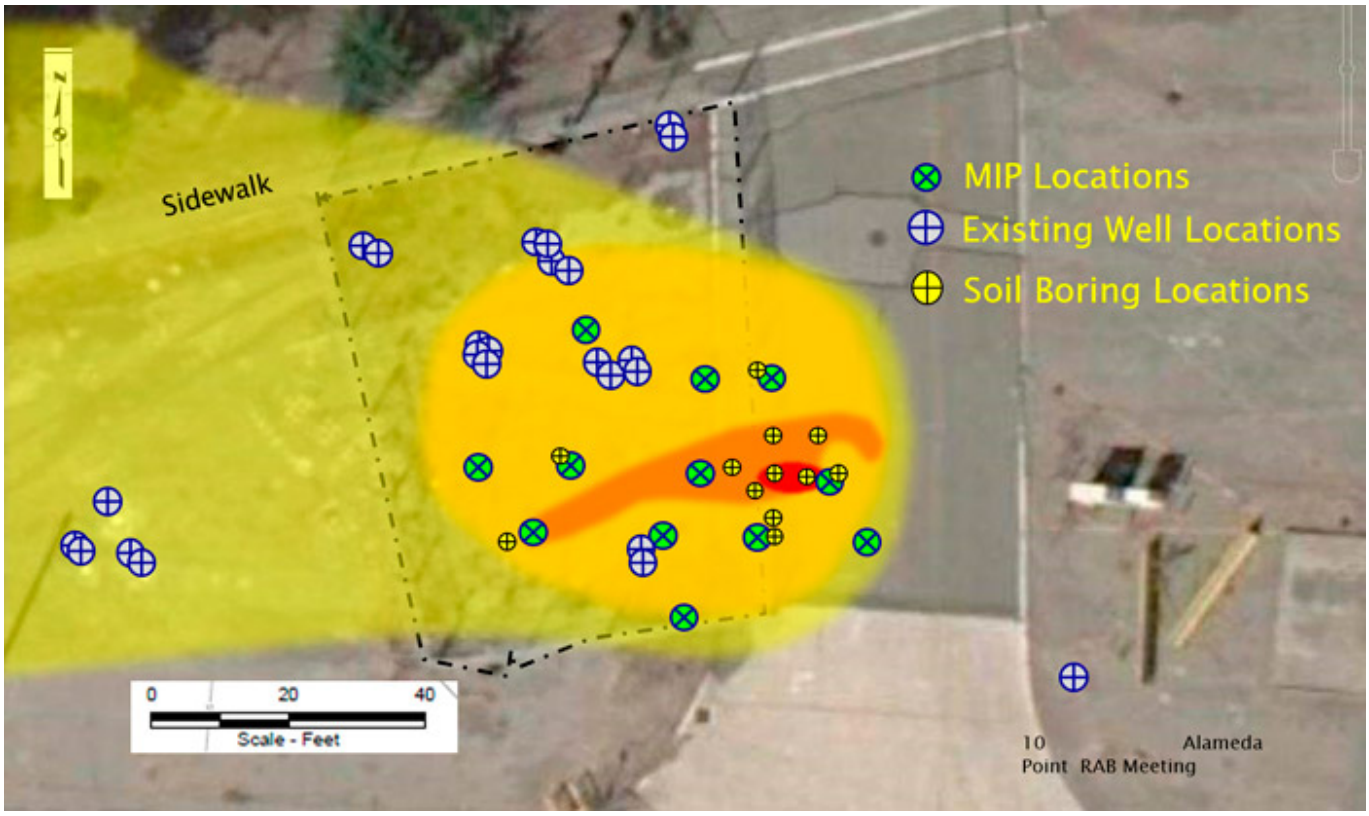

Figure 9-4. Identified source core (light red) and DNAPL area (dark red).

Following the MIP screening, discreet groundwater samples were collected from the high-PID-response depth intervals (see Figure 9-5). Based on these results, corresponding soil samples were collected (see Figure 9-6) and DNAPL was confirmed through staining with Sudan red dye (see Figure 9-7).

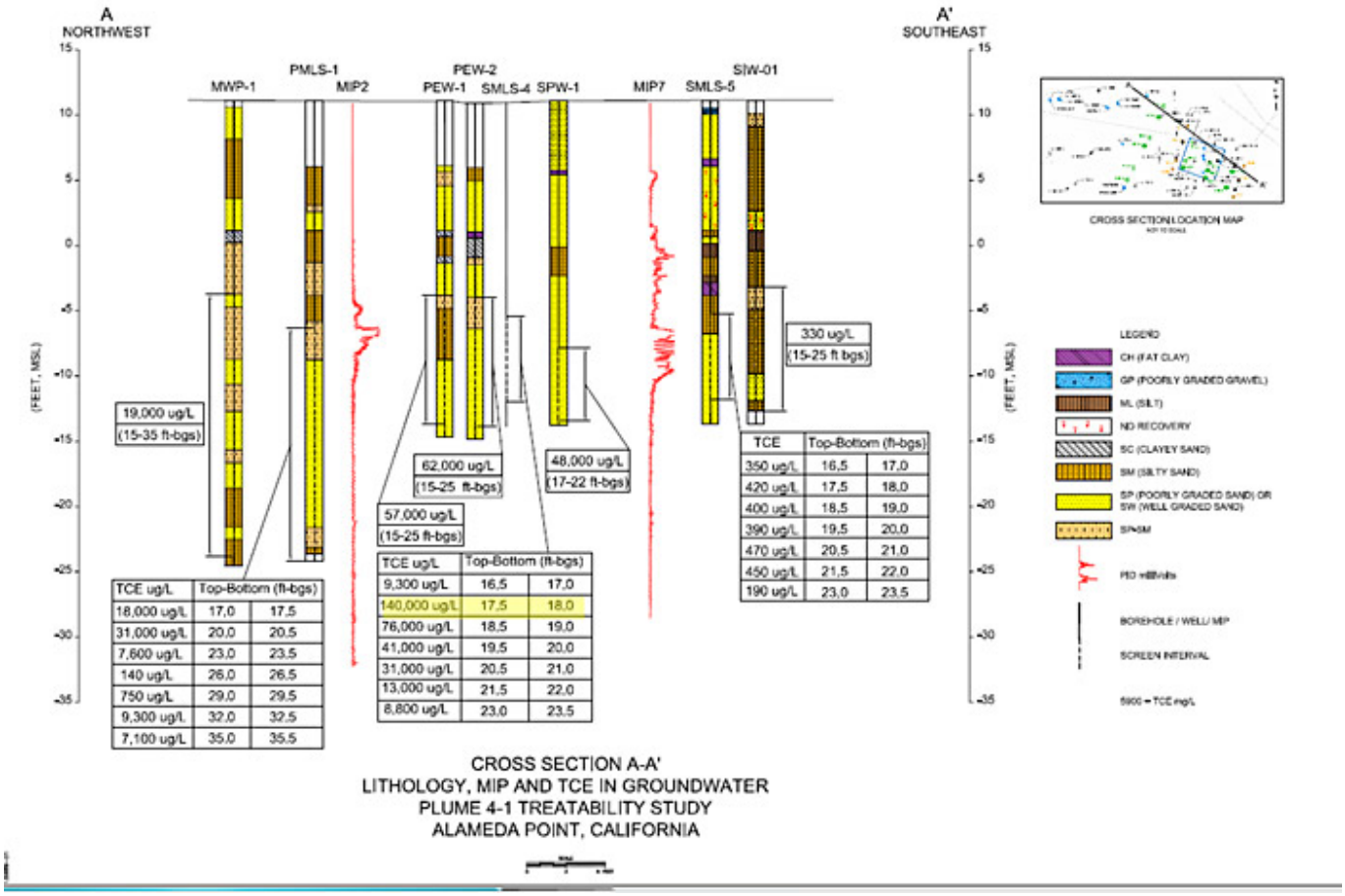

Figure 9-5. TCE Groundwater concentrations in µg/l.

Figure 9-6. Soil core collection with Geoprobe DT8040.

Figure 9-7. Sudan Dye staining indicating TCE DNAPL.

Previous attempts to locate the suspected TCE DNAPL source area were costly and unsuccessful. The cost associated with this integrated approach provided an excellent return on characterization investment. After identifying the TCE DNAPL source zone, a targeted DNAPL treatment strategy was applied, leading to expedited cleanup of the source area and plume.

9.3 OIP-Green Probe Delineates Extent of Coal Tar NAPL at a Former Gas Manufacturing Plant in Kansas

Wesley McCall, P.G.
Geoprobe Systems®, Salina, KS
mccallw@geoprobe.com

Jonathan L. Stephenson, I.G. Environ. Spec.
KDHE BER Orphan Sites Unit, Topeka, KS
jonathan.stephenson@ks.gov

The former Wellington manufactured gas plant was constructed around 1896 and operated until 1906. In the 1910s the community converted the closed plant into its first community park. Due to a tight community budget, municipal waste was used to backfill the gasholder (shown in Figure 9-8) prior to construction of the park. The backfill created a significantly heterogeneous subsurface (VanDeventer n.d.). Currently, the plant building operates as a local railroad museum, with school children from across the area visiting the museum several times each year.

Figure 9-8. Wellington former manufactured gas plant under construction circa 1896. Gas holder in right foreground and plant building at left

Environmental investigations at the facility began as early as 1993 and have continued intermittently until the present. Dozens of soil samples from multiple borings have been analyzed for PAHs and other contaminants. Contaminants detected in soils include naphthalene and benzo-a-pyrene. Shallow and deep nested monitoring wells were installed at 12 locations across the site and coal tar DNAPL has been observed in at least three of the wells located between the former gas holder and the plant building (KDHE 2014a); (KDHE 2014b). Thickness of DNAPL observed in the wells has ranged from a trace to one foot. nd areas where coal tar contamination was present.

In March of 2011, nine trenches were excavated with a backhoe to assess contaminant distribution (KDHE 2014b). Several of the trenches encountered a “black, wet oily waste” and analysis of one such sample contained 22,800µg/kg benzo-a-pyrene and a total PAH load of 617,790 µg/kg. KDHE decided that additional information on coal tar NAPL distribution was needed to better assess remediation/removal options for this facility. KDHE then coordinated with Geoprobe to run logs with the recently developed OIP-G probe to assess the distribution of coal tar NAPL to better characterize the site and guide remedial actions.

The OIP-G probe was used to assess the distribution of coal tar NAPL. This direct-push probe is designed with a green (525 nm) laser diode to induce fluorescence of coal tars and creosote. The green light illuminates the soil through a sapphire window on the side of the probe. A small CMOS camera mounted behind the window captures images of the fluorescent light. The images are analyzed by the OIP software to provide a digital log of percent area of fluorescent versus depth as the

probe is advanced at 2 cm/sec. An EC dipole also provides a log of bulk formation EC to evaluate lithology.

Log locations were selected based on previous site data and to fill data gaps (see Figure 9-9). Thirty-four OIP-G logs were obtained with depths between about 25 ft to 30 ft.

Historical reports indicate the gas holder was 15-25 ft deep. Drilling determined the actual depth to be 16.5 ft (Burns & McDonnell 2004). The OIP log completed within the gas holder showed the gasholder's base had been structurally compromised, with contamination (fluorescence) being logged to a depth of 25ft.

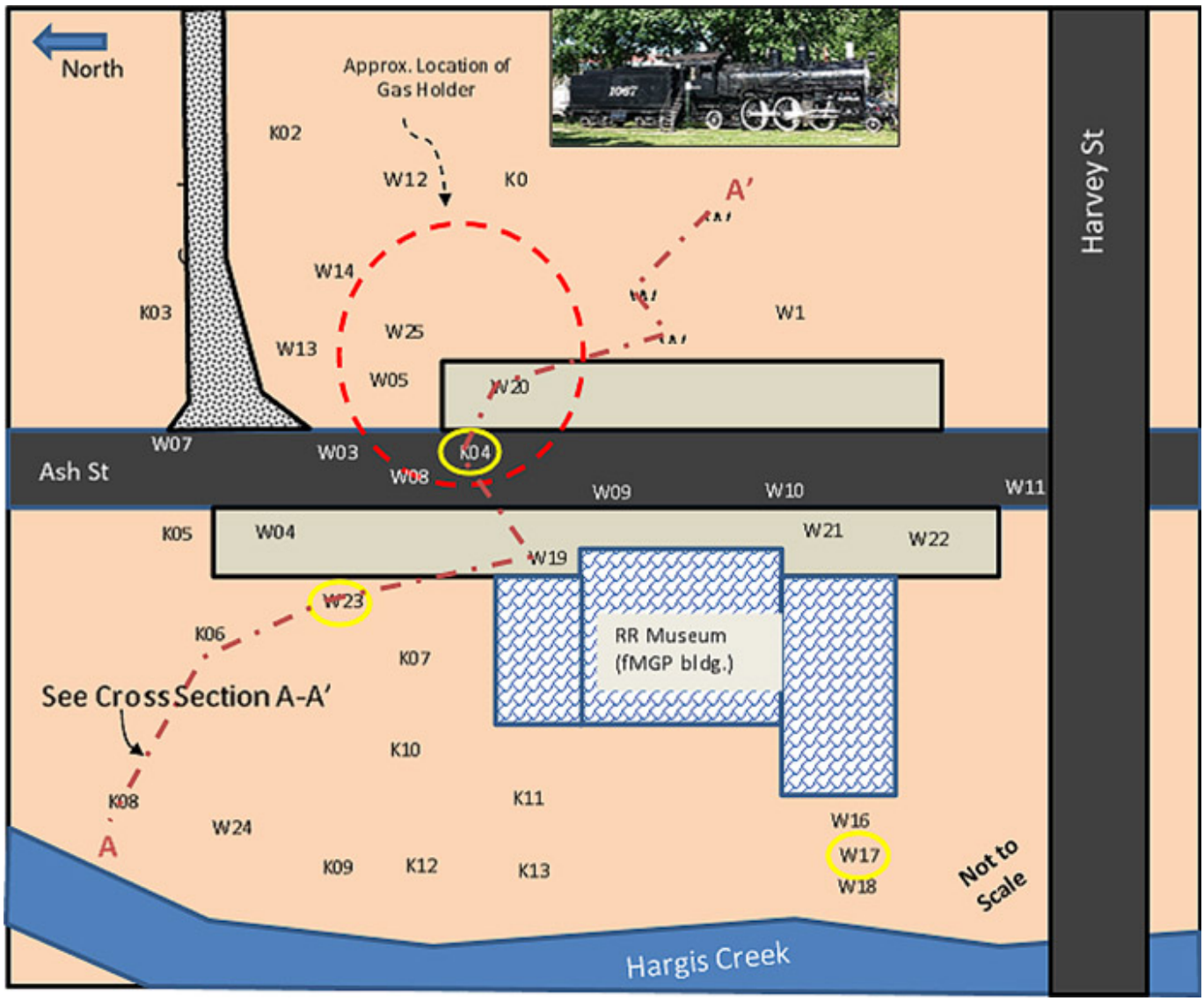

Figure 9-9. Site sketch map with log and cross section locations.

Log K04 showed high fluorescence levels between about 13 ft to 20 ft below ground surface (see Figure 9-10). A soil core sample was collected from 13.5 ft to 17.5 ft at this location. Coal tar DNAPL was poured out of the soil liner into a 4-oz. jar before subsampling the soil for analysis. The soil sample analysis revealed a total PAH load of 6,016,000 µg/kg. Log W23 (see Figure 9-10) showed high EC spikes in the upper 10 ft indicating the presence of buried metal. Log W23 also showed several zones of elevated fluorescence. A soil core was collected from 9 ft- to 11ft interval and submitted for analysis. The results revealed a total PAH load of 2,724,000 µg/kg.

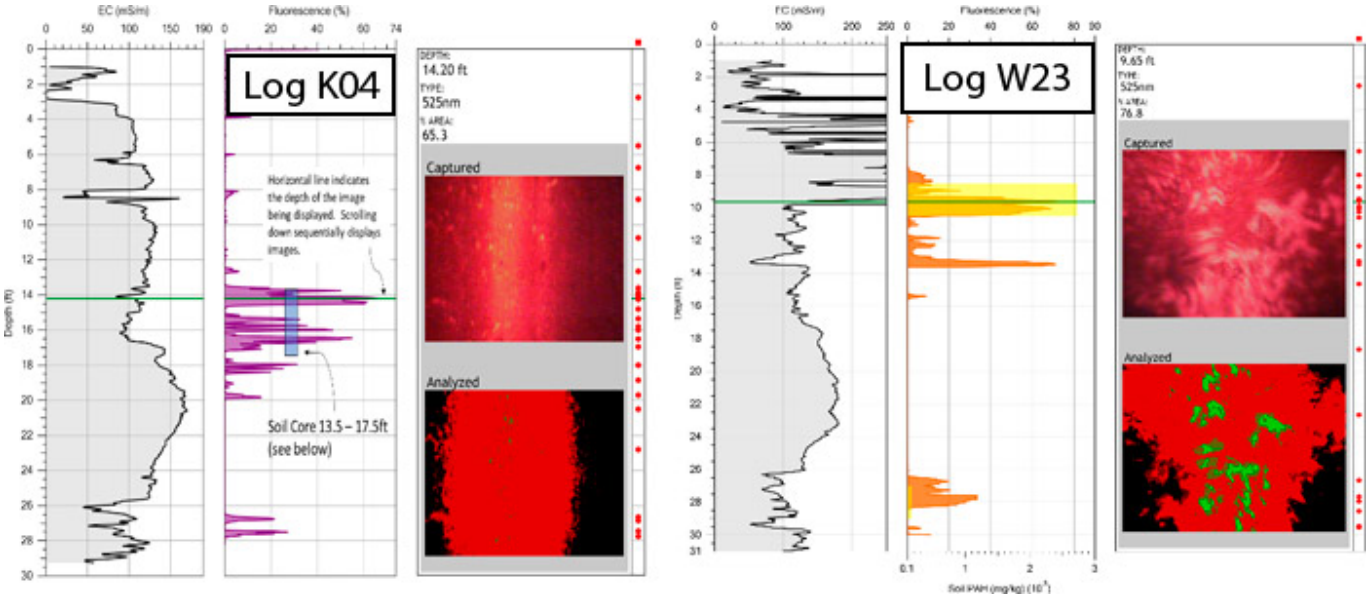

Figure 9-10. K04 and W23 logs.

Many of the EC logs displayed lower EC near the middle of the formation (for example, about 14 ft to 17 ft in log K04) and then again just above the shale bedrock (for example, about 26 ft to 28 ft in log K04). Samples collected across these low EC intervals typically had a higher sand and gravel content and were therefore more permeable. High fluorescence readings were often observed in the lower EC zones, especially just above the shale bedrock. A cross section of logs (see Figure 9-11) reveals a high EC zone near the middle of the formation. Samples from these zones revealed the soils to be a low permeability, silty clays. Gray shading in Figure 9-11 also shows total PAH results from soil samples collected at those approximate depths. Orange shading in Figure 9-10 represents percent fluorescence from 0% to 90%. The cross section also shows that the coal tar NAPL typically lies above and below the low permeability zone, as indicated by elevated fluorescence levels. (McCall, Christy, Pipp, Jaster, Bean, et al. 2018). Confirmation sampling verified that fluorescence observed by the OIP-G successfully identified coal tar contamination at multiple locations across the area investigated. Cross sections with the logs were able to provide a clear guide to the distribution of coal tar NAPLs.

This project cost KDHE approximately $30,000 in mobilization, and Geoprobe operating costs during two assessment events. Approximately 1,733 ft of OIP-G logging was completed and 40 soil samples were collected for PAH analysis at depths of up to 30 ft. Geoprobe provided expertise, training, and the OIP-G tool, which assisted in reducing costs.

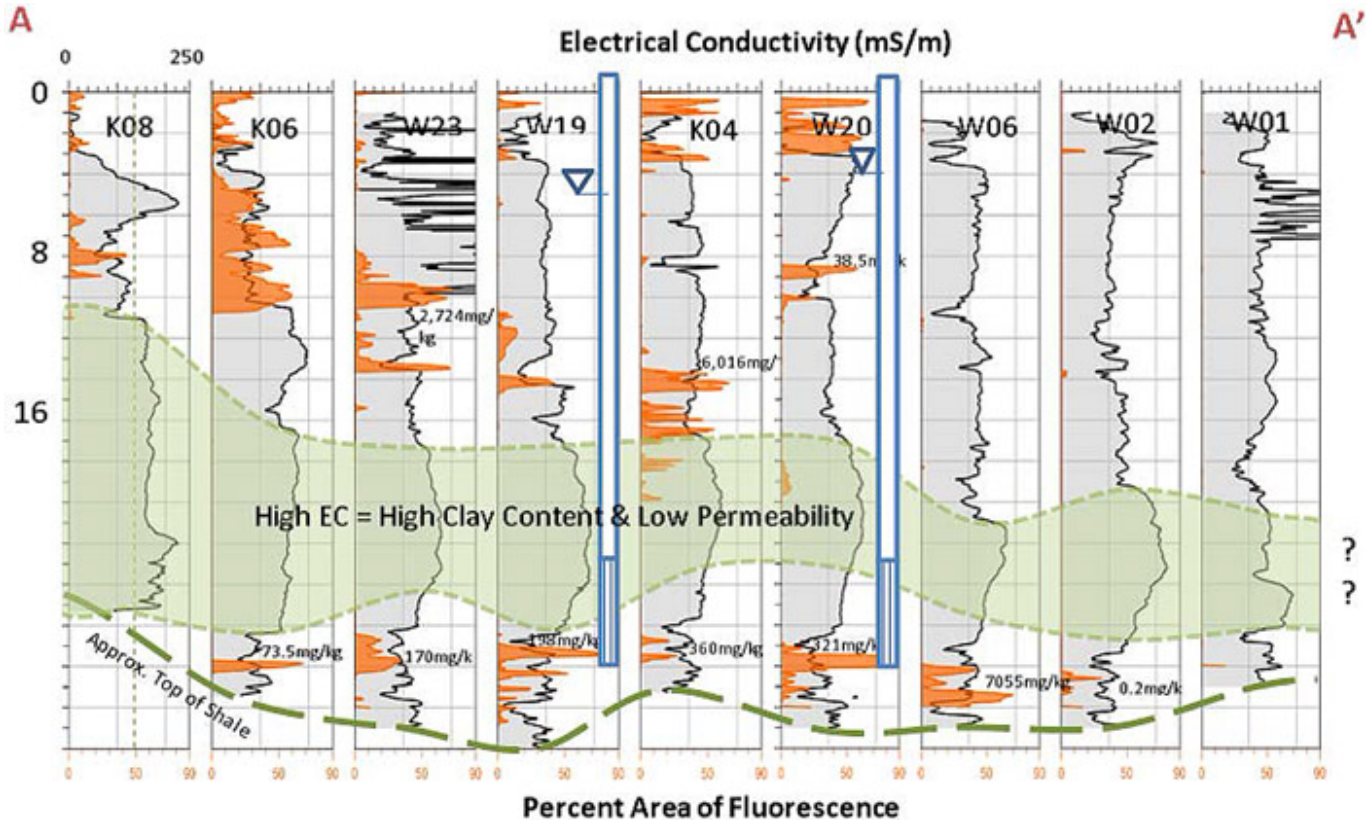

Figure 9-11. Cross section A – A' (see Figure 9-9 for location; not to scale).

The advantages of using OIP-G at this location were as follows:

- The ability to simultaneously run an EC log to assist with lithology interpretation while obtaining the fluorescence logs
- Facilitation of real-time decision-making regarding sampling locations based on fluorescence log
- Ability to identify sampling intervals while in the field, reducing the number of samples requiring lab analysis
- compared to conventional core sampling and trenching methods, reduced investigation-derived waste on the order of 95%, which also reduced worker exposure.

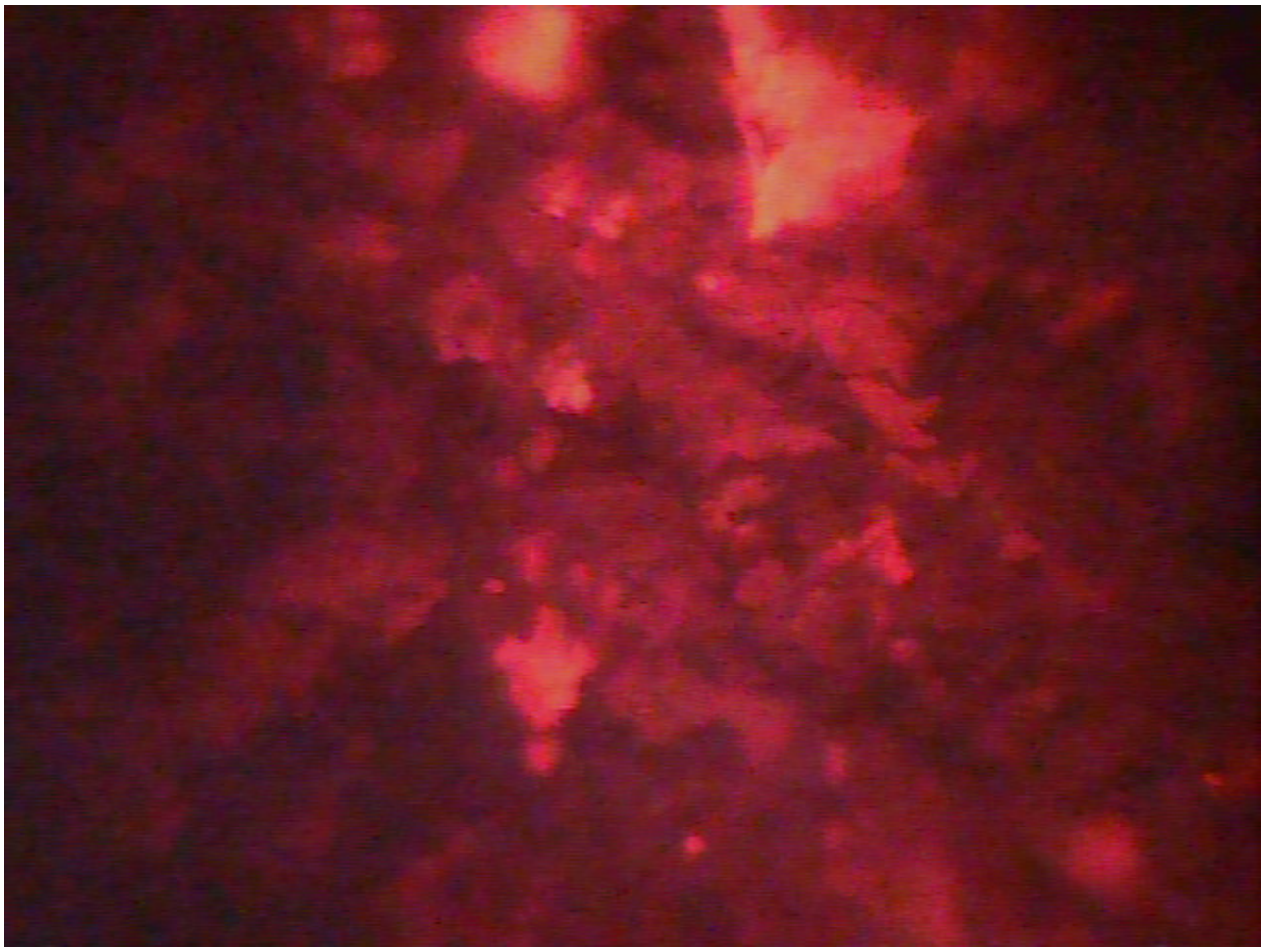

Figure 9-12. Red-orange fluorescence of calcareous minerals observed under green (525 nm) source light.

The biggest disadvantage of this tool is that it can produce false positives in fluorescence if there are calcareous materials present in the path of the probe. At this site, elevated fluorescence (about 40%) in the red-orange wavelength typical of coal tar was observed at locations W17 and W18 (see Figure 9-12). Soil coring results showed no coal tar contamination at these locations but light-colored particles were observed in the soil. A test with dilute hydrochloric acid produced effervescence, indicating calcite/limestone. Calcite is known to fluoresce. It is thought that limestone-based sand and gravel may have been used as fill material along the stream bank at this location. Similar fluorescence was observed from small caliche nodules present in the soil. Geoprobe is attempting to reduce the false positive problem by using an infrared LED to differentiate between dark-colored contaminants and light-colored minerals. In the meantime, targeted soil sampling may be required to verify the cause of fluorescence.

9.4 LIF Survey with UOVOST® Provides More Accurate Representation of LNAPL Plume at a Former Bulk Petroleum Storage Facility in New Hampshire

Joshua Whipple
NH Department of Environmental Services
MtBE Remediation Bureau
Concord, NH
joshua.whipple@des.nh.gov

Information presented in this case study is based on investigations conducted by GeoInsights, Inc. and Columbia Technologies

In 2006, an investigation was performed at a former petroleum bulk storage facility in Conway, New Hampshire. The site occupies an area of approximately 0.9 acre and abuts the Conway Scenic Railroad to the north. During the investigation, soil and groundwater contaminated with petroleum were discovered in the area of a former fueling rack. Subsequent soil and groundwater investigations revealed the presence of LNAPL in the central area of the site where the fueling rack, pump house, and product piping were formerly located. A dissolved-phase petroleum contaminant plume was also discovered extending off site to the north (see Figure 9-13).

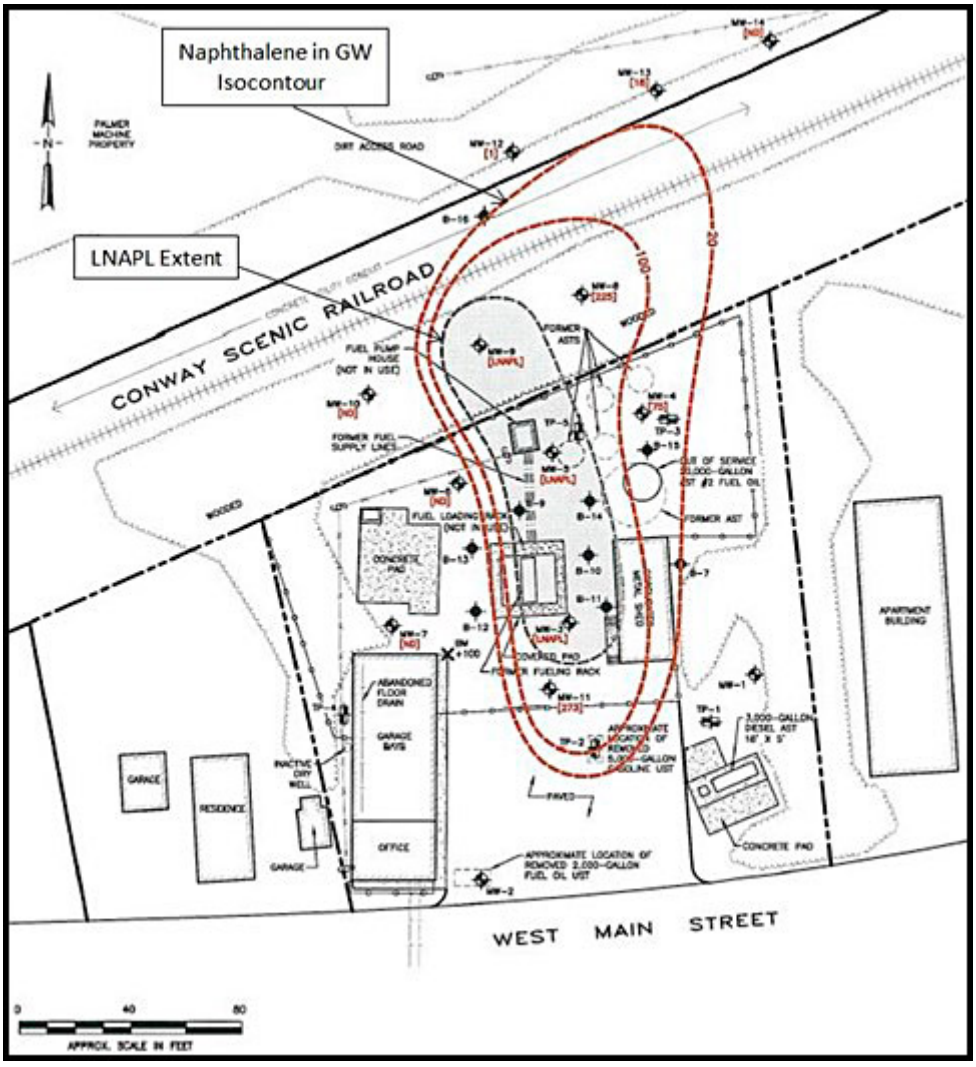

Figure 9-13. Site Plan showing extent of LNAPL observed in monitoring wells (GeoInsight 2009).

The investigation included the installation of 30 soil borings using a direct push method and 18 monitoring wells using hollow-stem augers. Soil beneath the site consisted primarily of loose to medium-dense, stratified, tan fine sand with lesser amounts of medium sand and interbedded silt (GeoInsight 2007) to depth of 20 ft below ground surface. The water table was observed at depths ranging from 10 ft to 15 ft below ground surface and fluctuated an average of 2.5 ft over six years of groundwater monitoring. LNAPL was observed in three of the monitoring wells at thicknesses ranging from 0.04 to 0.93 foot.

Based on soil sampling and field screening results, most of the soils impacted above NHDES Soil Remediation Standards (SRS) were observed at depths between 10 ft and 16 ft (see Figure 9-14), with shallower impacts observed in the area where LNAPL was present. Elevated field-screening results above 100 mg/l were observed at a maximum investigation depth of 20 ft below ground surface. The dissolved plume, defined mainly by naphthalene concentrations above New Hampshire's Ambient Groundwater Quality Standard, extended off site beneath the railroad tracks and the adjacent property to the north.

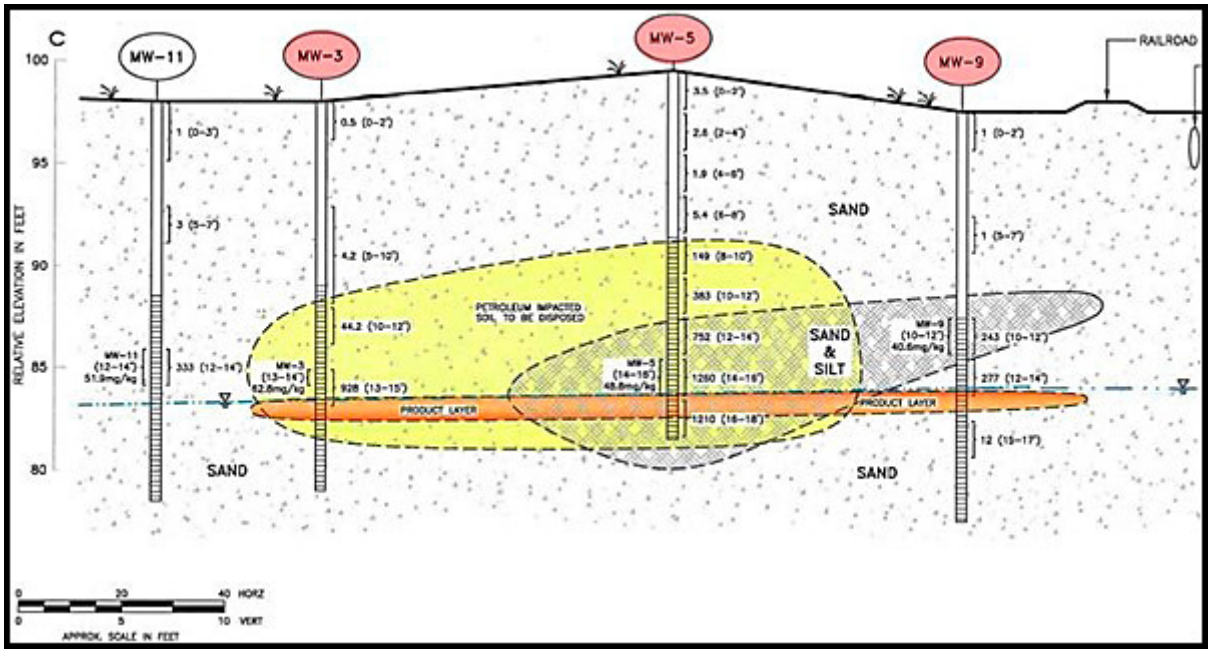

Figure 9-14. Initial cross section showing the vertical extent of petroleum impacted soil and LNAPL observed in monitoring wells (GeoInsight 2010).

Although the site investigation facilitated a good understanding of site geology and the horizontal extent of soil and groundwater impact, the following constraints were observed:

- A lack of sufficient soil data due to many of the soil samples being collected through hollow stem augers with a 2-foot split spoon sampler every five ft.
- Insufficient soil sample recovery with an average of approximately 50%, in the sandy subsurface material.
- The investigation was conducted over several phases resulting in inconsistent soil descriptions.
- Several of the soil borings were only advanced to the initial depth of the water table resulting in elevated field screening results and SRS exceedances at the deepest extent of the investigation

With questions regarding the vertical extent of soil and LNAPL impact, the project team considered other investigation techniques. Initial cross sections (see Figure 9-14) present the LNAPL thickness observed in the monitoring wells. This creates a misperception that LNAPL is only present in a distinct layer rather than varying degrees of LNAPL saturation that may actually be present. Because of the favorable drilling conditions and a release that consisted mainly of heavier heating oil petroleum product, a soil boring program using LIF/UVOST® was conducted in 2011. A total of 26 UVOST® borings were advanced using a Geoprobe direct-push drilling rig with a LIF probe (Columbia 2011).

Eight of the UVOST® borings exhibited fluorescence greater than 50% RE, and six borings had a response greater than 25% (see Figure 9-15, Figure 9-16 and Figure 9-17). When compared to waveforms of common petroleum products, the resulting wavelengths were closest to the diesel standard, which was consistent with the historical site use. The UVOST® investigation results revealed LNAPL at depths of up to 7 ft below the water table, much deeper than originally anticipated. The thickness

of the zone impacted by LNAPL was measured up to 7 ft rather than the approximately 1-foot thickness observed in the monitoring wells.

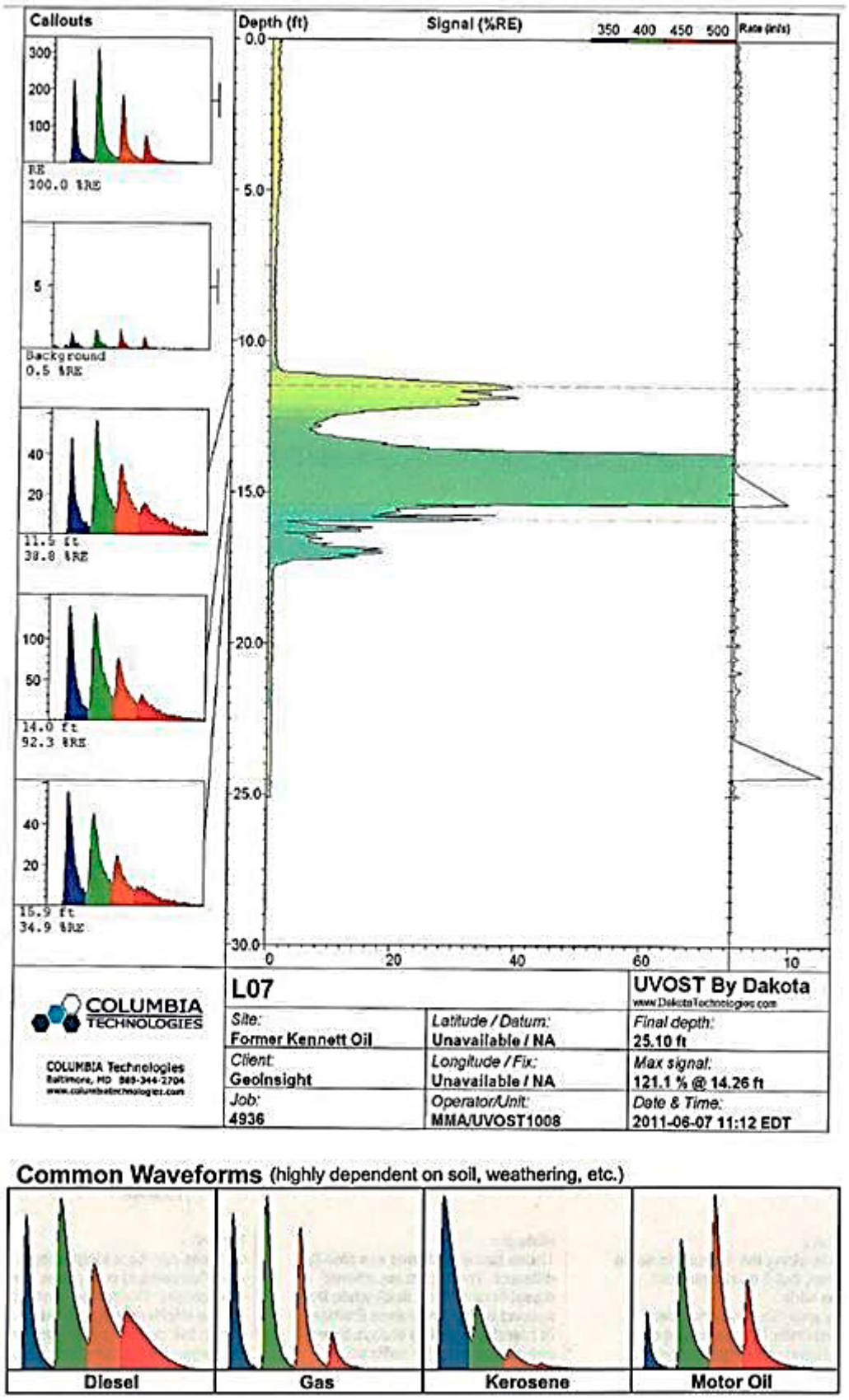

Figure 9-15. Log from one of the soil borings within the former fueling rack area (Columbia 2011).

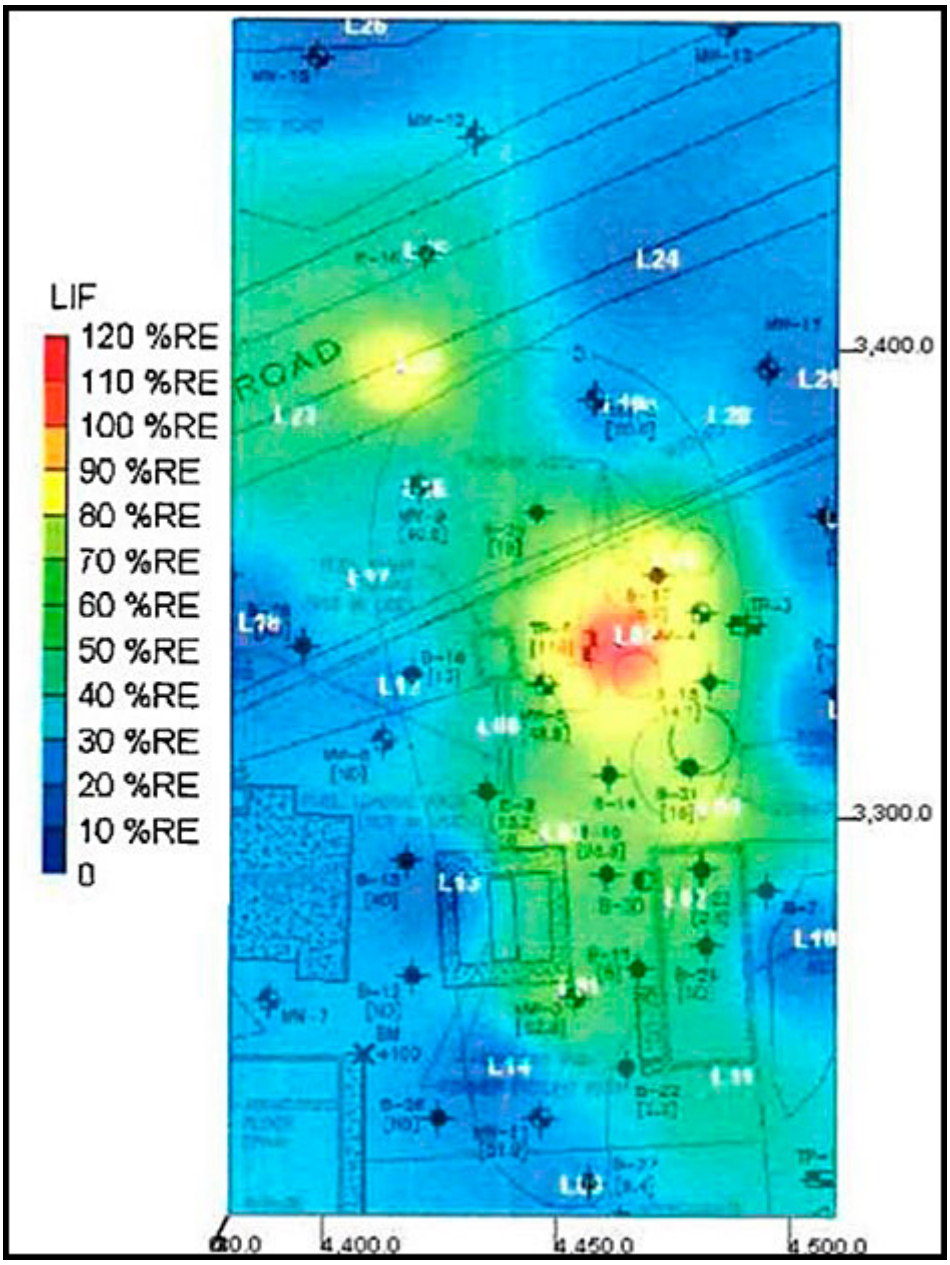

Figure 9-16. Areal extent of LNAPL detection (Columbia 2011).

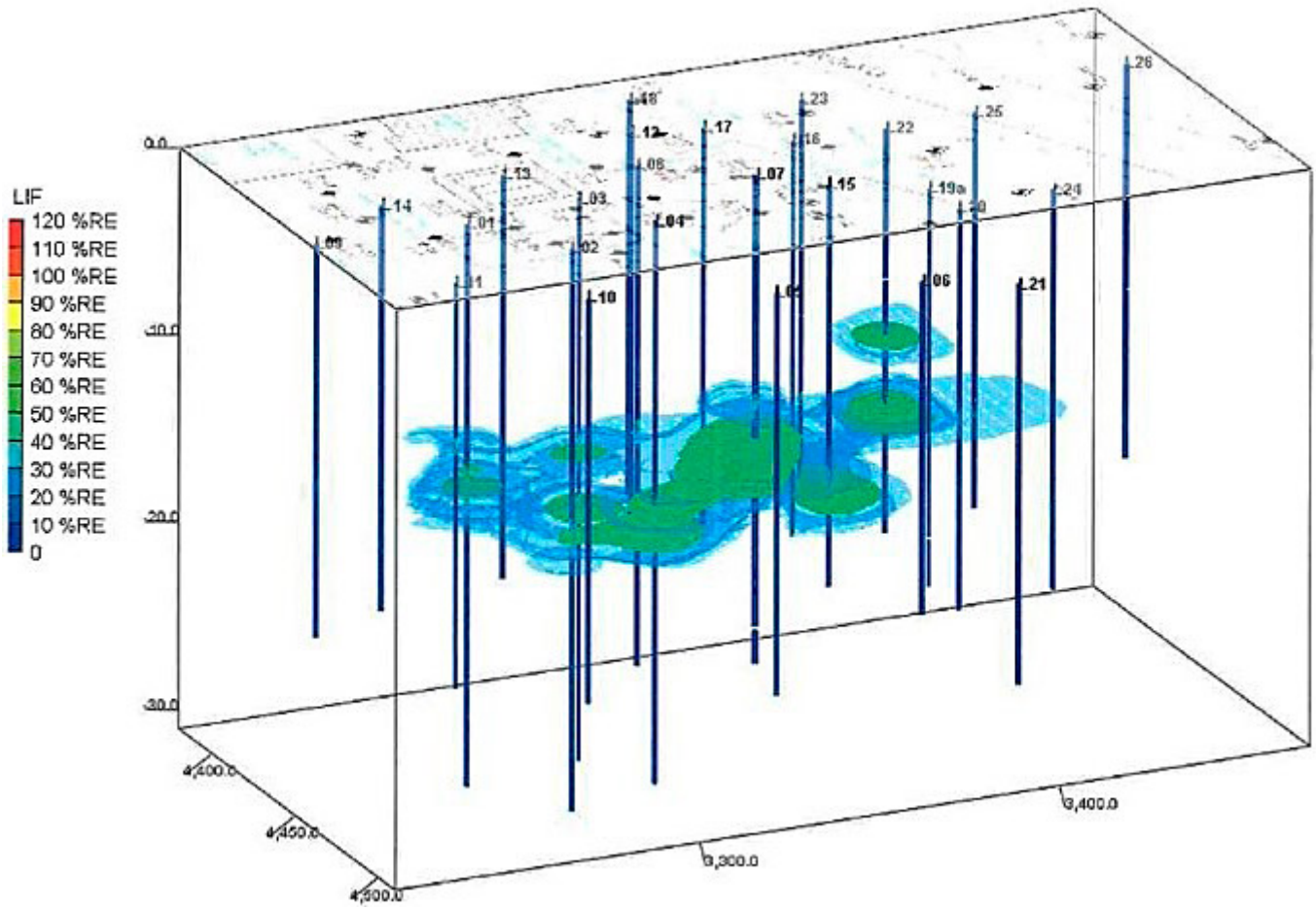

Figure 9-17. 3D representation of LNAPL detection (Columbia 2011).

The UVOST® data were incorporated into the existing CSM to show that the LNAPL impact appears more like the vertical equilibrium LNAPL plume model with LNAPL at residual saturation on the fringes of the plume and depths below the water table (see Figure 9-18 and see ITRC's Technical Guidance Document "LNAPL Site Management: LCSM Evolution, Decision Process, and Remedial Technologies" [LNAPL-3] (ITRC 2018) for more detail on LNAPL plume characteristics).

The total cost for the UVOST® was approximately $30,000 investigation with roughly half of the cost attributed to engineering and consulting oversight and half for the UVOST® contractor. The project field work spanned one week and resulted in a relatively detailed summary report updating the CSM and evaluating potential remedial alternatives to address the more accurate representation of the site conditions.

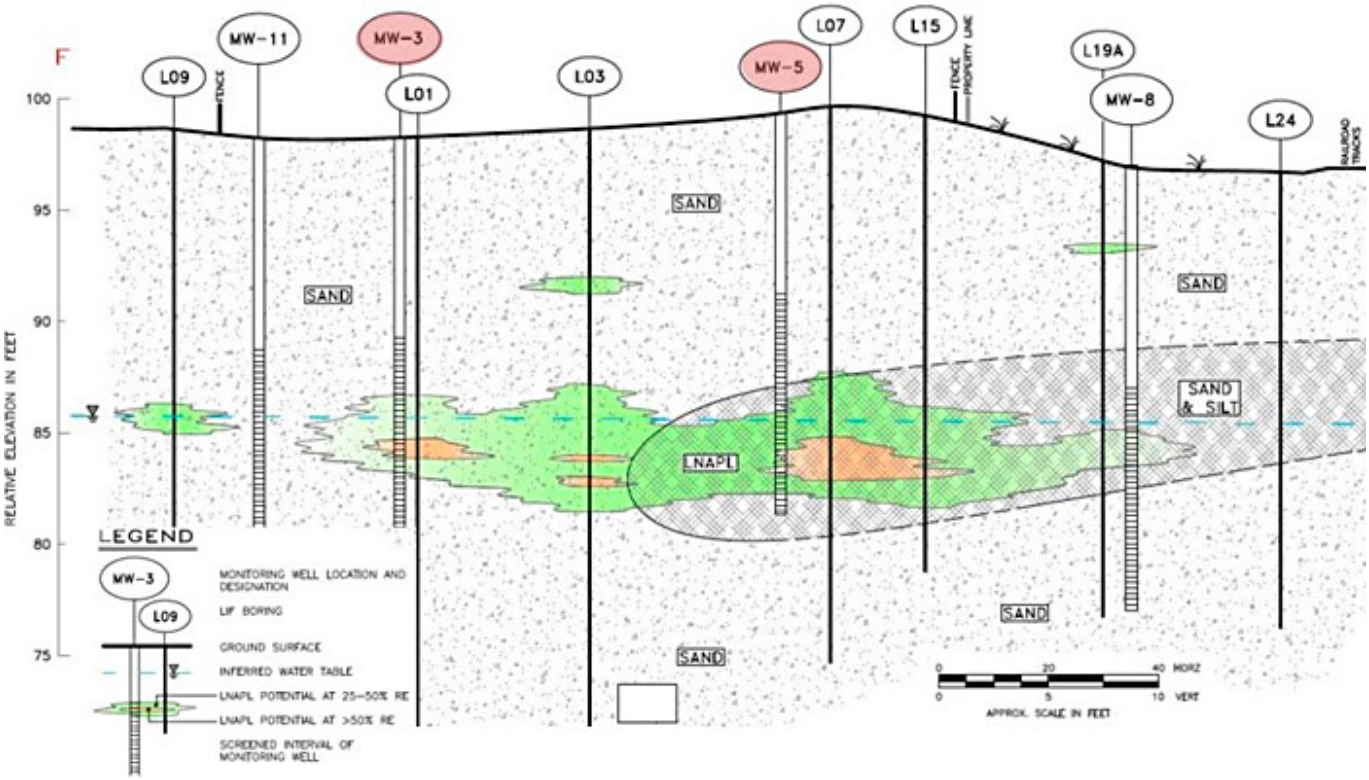

Figure 9-18. Areal extent of LNAPL detection (GeoInsight 2011).

Although suggesting additional soil characterization at a site where several soil borings and wells have already been installed can be difficult, this investigation demonstrates the value of doing so. Ultimately, soil excavation was determined to be the most appropriate remedial approach, and, in 2012, approximately 6,300 tons of petroleum-contaminated soil were removed. Because of LIF survey results, the soil volume to be excavated was defined, a more accurate request for proposal was prepared for bidding contractors, and a chance for complete removal of the source material was improved.

9.5 UVOST Differentiates LNAPL Types to Allocate Financial Liabilities at a Retail Petroleum Facility in Tennessee

Randy St. Germain
Dakota Technologies, Inc.
Fargo, North Dakota
stgermain@dakotatechnologies.com

Ed Creaden
Dakota Technologies Company, LLC
Overland Park, Kansas
ecreaden@dakotatechnologies.com

Information presented in this case study is based on investigations conducted by Southern Environmental Management & Specialties, Inc and Dakota Technologies Company – See source information below

The Tennessee Department of Environment and Conservation (TDEC), Division of Underground Storage Tanks (UST Division) oversees the management of UST petroleum release sites. The UST Division operates a fund to reimburse registered UST site owner and operators for certain costs associated with petroleum release assessment and cleanup. Allocation of financial liabilities can be difficult to assess where multiple sources of contamination are present, such as when an off-site petroleum release from an ineligible facility migrates onto an otherwise fund-eligible petroleum release site. Differentiation of various types of LNAPL based on high-resolution insitu data can provide key information for these determinations.

A TDEC UST Fund-eligible site located in Jackson, Tennessee, is an active retail petroleum station in operation since the 1950s, storing and dispensing gasoline from five USTs. An adjoining facility operates aboveground storage tanks (ASTs) used for storage of diesel that is not eligible for UST Fund reimbursement. Evidence of a gasoline release was suspected when an elevated benzene concentration was measured in samples from an offsite groundwater monitoring well installed during an investigation of a nearby UST site in 2012. LNAPL was subsequently identified in onsite groundwater monitoring and recovery wells in 2014.

The site is located within a wellhead protection area, with the nearest municipal well about 0.75 mile of the site. No documented drinking water wells are within 0.5 mile of the site, and the nearest surface water is approximately 0.3 mile to the northwest. The presumed direction of groundwater flow is to the southwest, and depth to groundwater typically varies from approximately 27 ft to 34 ft below ground surface. Figure 9-19 depicts the general layout of the site, showing monitoring well, recovery well, and soil boring locations installed during previous investigation activities. Based on soil boring and monitoring well installation logs, soil generally consists of orange, gray, and brown silty clay to 10 ft to 15 ft below ground surface. From approximately 15 ft to 40 ft, unconsolidated sediment consists primarily of orange, pink, brown, and white sand with some clay, silt, and gravel.

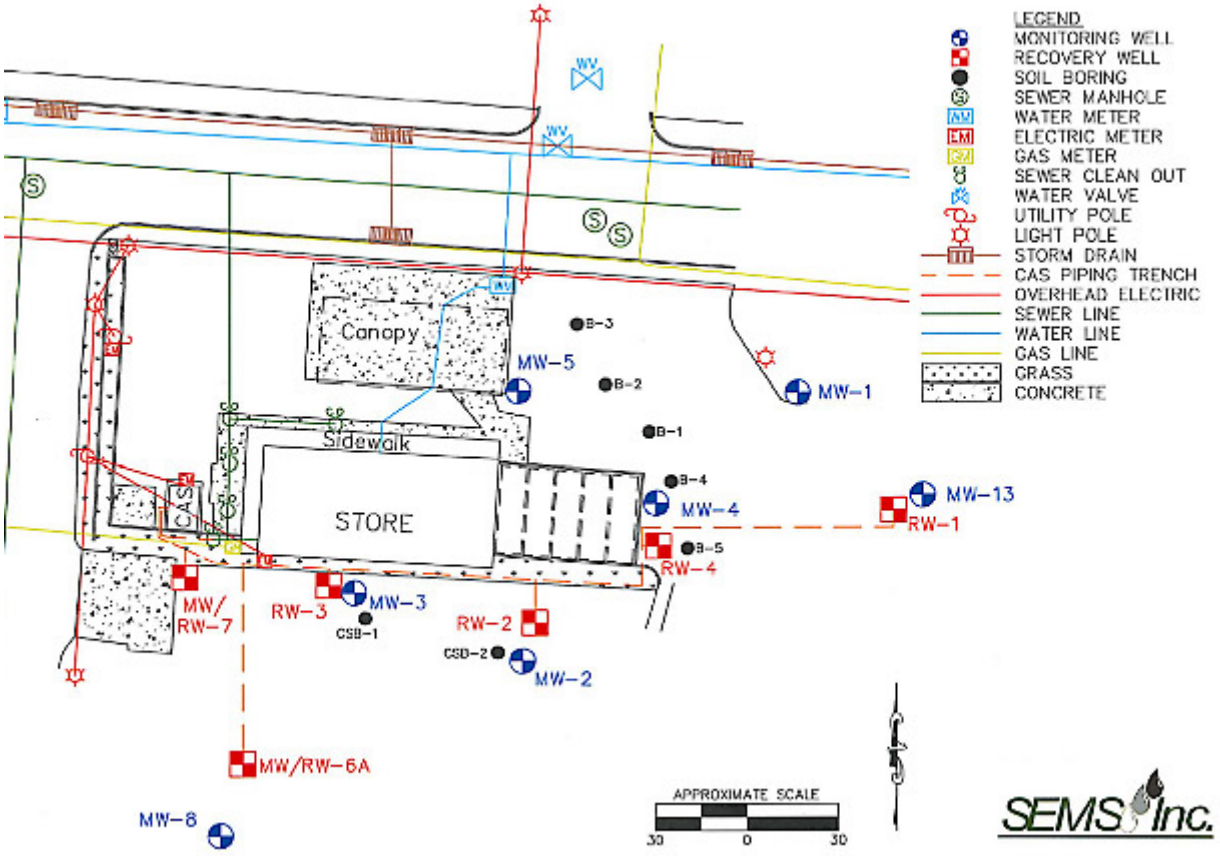

Figure 9-19. Site map.

In April 2012, a new petroleum release case was opened for the site by TDEC based on an elevated benzene concentration in a groundwater sample from an offsite well associated with an offsite UST. The offsite well was located within approximately 10 ft of the site property line, raising concerns of a possible gasoline release at the site. Analytical results reported for a site check in July 2012 confirmed the presence of petroleum hydrocarbons in onsite soil above TDEC Initial Screening Levels.

A corrective action plan was developed in June 2013, and remedial action was taken using mobile-enhanced multi-phase extraction corrective action technology (MEME-CAT) two months later. In August 2014, LNAPL was discovered in six on-site monitoring and recovery wells, with thicknesses ranging from 0.03 ft in well MW-4 to 4.50 ft in well MW-7. Additional recovery wells were installed. Due to the persistent presence of LNAPL in MW-7, the well was converted into a recovery well in June 2016. No measurable LNAPL has been documented in the well since that time. In June 2017, an additional monitoring well (MW-6A) was converted into a recovery well (RW-6A). Elevated concentrations of benzene (greater than 3 mg/L) persisted at five monitoring wells (MW-2, MW-3, MW-4, MW-6A, and MW-8) based on February 14, 2018 monitoring data. On February 26, 2018 0.03 ft of LNAPL was measured in one monitoring well (MW-8).

Based on the presence of LNAPL and elevated dissolved petroleum hydrocarbons in onsite monitoring wells, TDEC requested a UVOST® site characterization of the site in 2018. UVOST® and its predecessor, the Rapid Optical Screening Tool (ROST™), are the only commercially available laser-induced fluorescence (LIF) technologies used for high-resolution three-dimensional mapping of light nonaqueous phase liquids (LNAPLs) in the subsurface. Combining advanced analysis techniques of UVOST data with other lines of evidence such as formation hydrostratigraphy, soil and groundwater contaminant data, and historical site operational information supports the development of more robust LNAPL conceptual site models (LCSMs).

Thirty-one UVOST® borings were advanced on the site in April 2018. The average depth of the borings was 42.70 ft below ground surface. A total of 1,323.95 ft of UVOST® logging was completed over a four-day period with an average daily production of approximately 331 ft. LNAPL was detected in 28 of the 31 borings, ranging in depth from approximately 10 ft to 40 ft below ground surface. Figure 9-20 depicts the UVOST® boring, monitoring, and recovery well locations overlain on an aerial photograph of the site.

Figure 9-20. UVOST® boring and monitoring well locations.

UVOST logs of total fluorescence versus depth were produced for all borings. Figure 9-21 is the UVOST log from boring 20-LIF, which was installed near the gasoline USTs and dispensing pumps.

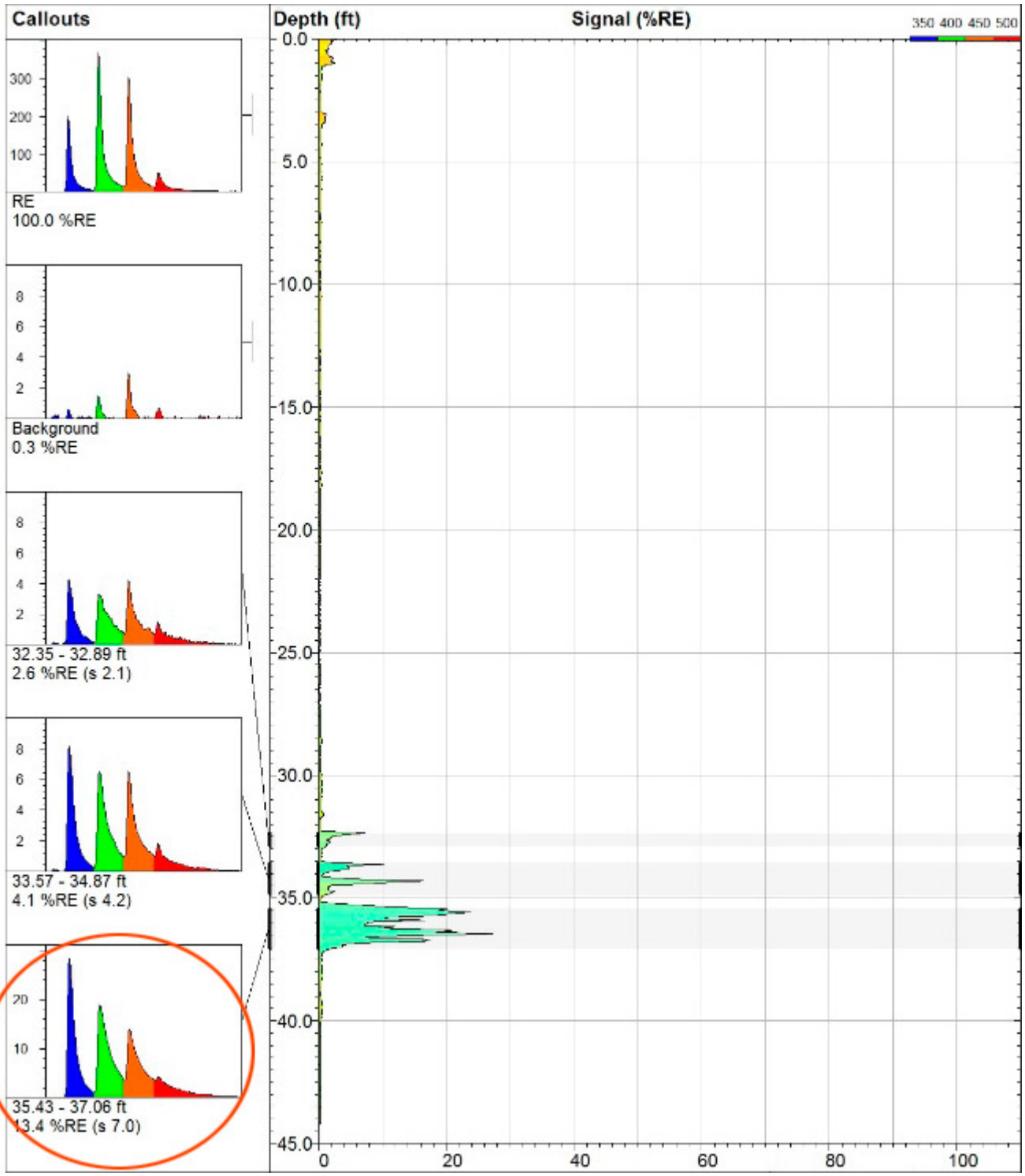

Figure 9-21. UVOST® log for boring 20-LIF.

The waveforms from the LNAPL-bearing zone identified at approximately 35 ft to 37 ft below ground surface in this log are indicative of the presence of intact (unweathered) gasoline (see circled waveform callout in left column of log). The 350-nm channel shown as blue on the waveform callout has a fluorescence lifetime only modestly shorter than the other three channels and a relatively high intensity. The calculated color for this waveform is shown in the log as light blue (blue-shifted), which is characteristic of an intact gasoline's fluorescence response.

In contrast to this log, the UVOST® log from boring 05-LIF (refusal encountered at 32.60 ft) shown in Figure 9-22 exhibits a strikingly different signature. This boring was installed near the diesel aboveground storage tanks and, of the 31 borings installed, this boring was the only one to encounter refusal before achieving the targeted depth of approximately 40 to 45 ft. The waveforms from the LNAPL-bearing zone encountered at approximately 29 ft to refusal are indicative of the presence of diesel. The 350-nm channel (blue peak) has a dramatically shorter lifetime and less intensity than the three long lifetimes in

the subsequent channels, which is the hallmark of a diesel fuel.

The 350 nm channel (blue peak) has a dramatically shorter lifetime and less intensity than the three long lifetimes in the subsequent channels, which is the hallmark of a diesel fuel. The calculated fill color has also dramatically red-shifted to yellow in comparison to the teal green gasoline responses in log 20-LIF.

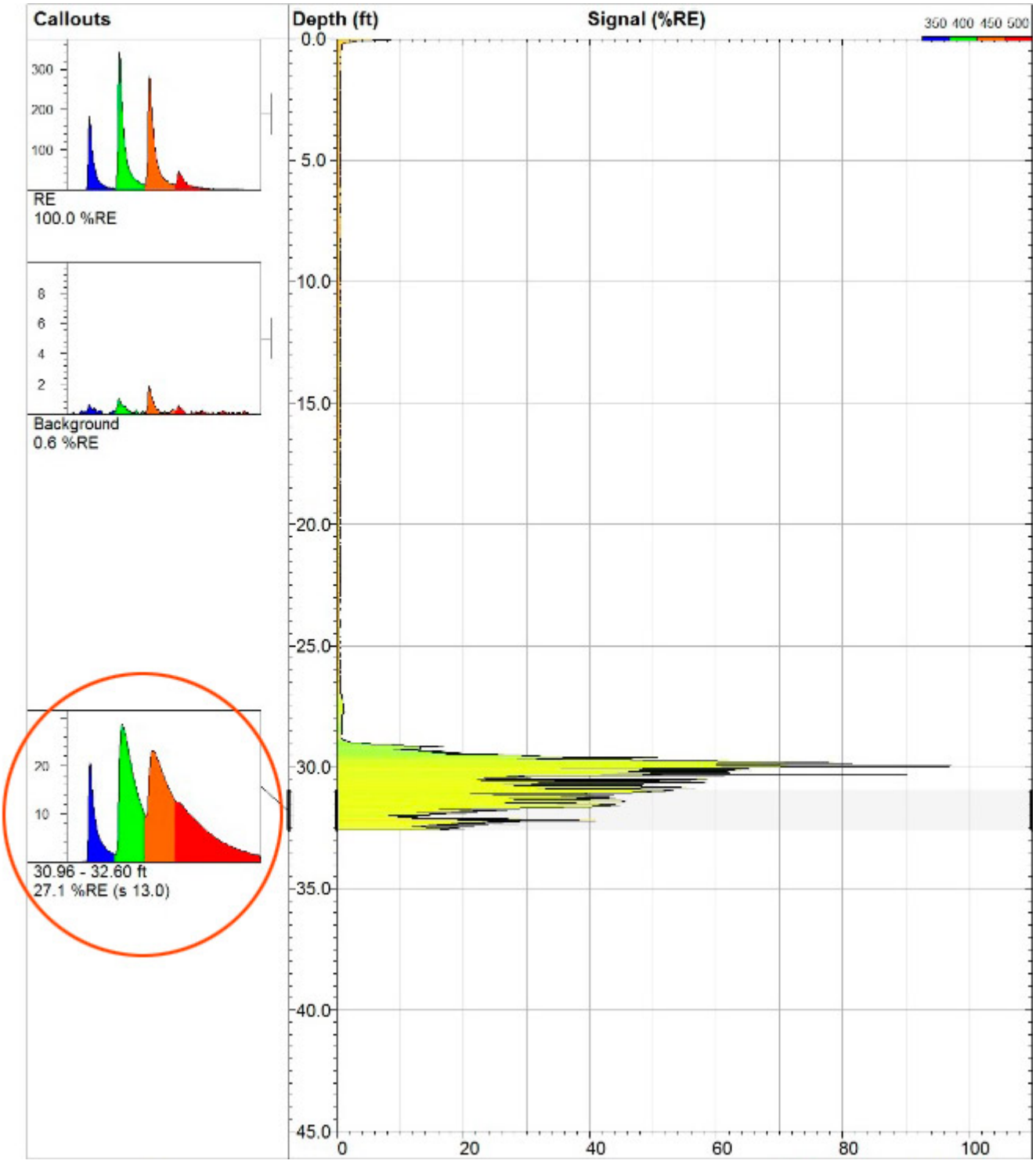

Figure 9-22. UVOST® log for boring 05-LIF.

These waveforms and their resulting color shift in the logs alerted the investigative team in real-time that the fluorescence response at location 05-LIF was indicative of diesel fuel as opposed to the expected gasoline response.

Figure 9-23 is the UVOST® log from boring 12-LIF, which was installed near the gasoline dispensing pumps. This boring intersected a relatively shallow, perched zone of gasoline at approximately 15 ft to 17 ft below ground surface that exhibited

waveform characteristics consistent with that of weathered gasoline. The 350-nm channel has a similar fluorescence lifetime to the other three channels; however, the intensity of the 350-nm channel is relatively low (likely due to washing out of naphthalenes). The result is a red-shifted waveform and a calculated fill color that appears greener than the bluer intact gasoline response. Although less pronounced, this red-shifting and apparent weathering can also be observed in the waveform callouts in Figure 9-21 at the 32- to 35-foot depth.

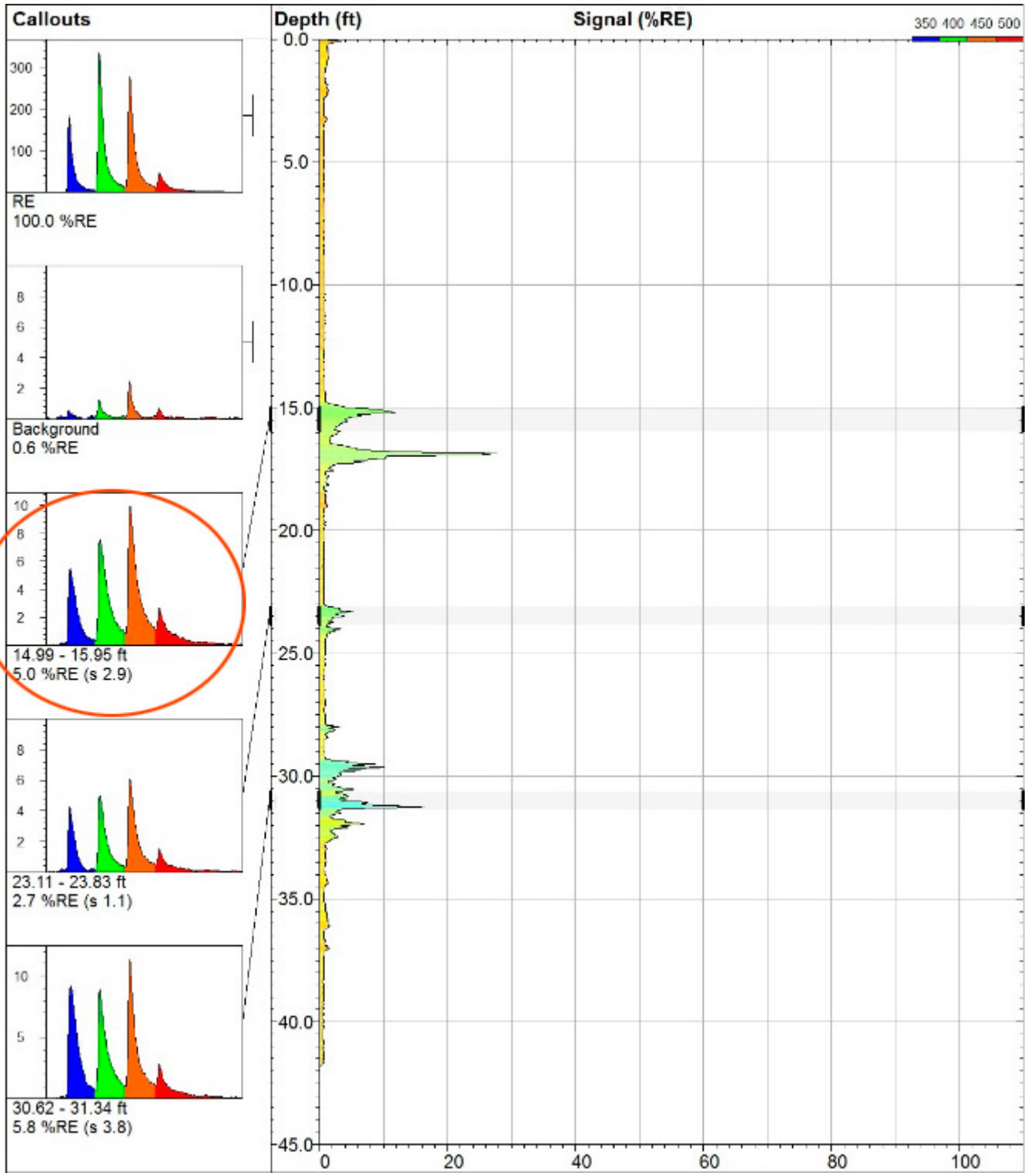

Figure 9-23. UVOST® log for boring 12-LIF.

Investigation results indicated the likely presence of three unique types of LNAPL on site (shown in Figure 9-21, Figure 9-22, and Figure 9-23) because UVOST® data exhibit characteristics of intact (unweathered) gasoline, weathered gasoline, and diesel fuel. TDEC requested advanced analysis of UVOST® data to support the differentiation of LNAPL sources and

subsequent visualization in a four-dimensional CSM. The allocation of remediation and financial responsibilities will be considered based on these findings. Future investigative activities designed to confirm these findings are ongoing.

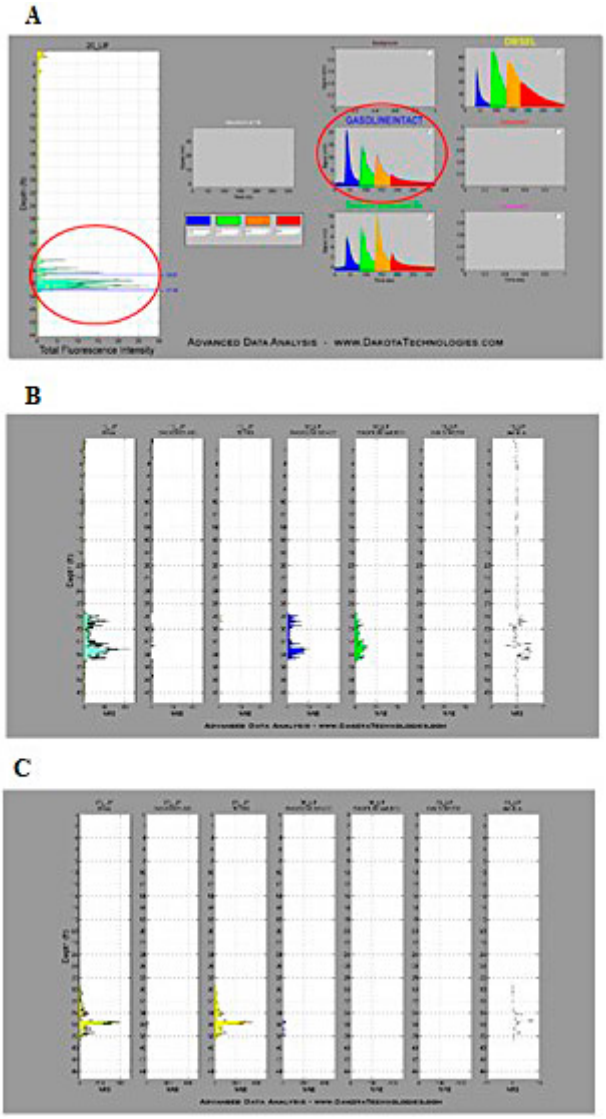

Figure 9-24. Examples of Waveform Harvesting and NNLS Results.

In the advanced analysis, a Basis Set was created by harvesting waveforms from field logs or bench-top tests to define the various types of fluorescence encountered such as various fuel types or false positive fluorescence encountered at the site. Once the various fluorescence waveforms were accounted for in the Basis Set, software automatically fits the Basis Set waveforms to the log's insitu waveforms, which can be in the thousands of waveforms. The analysis software passes each raw waveform, along with the Basis Set waveforms, to a non-negative least squares (NNLS) routine that determines the proportion of each of the Basis Set waveforms that is required to optimally fit the insitu waveforms and returns a %RE contribution for each Basis Set waveform. RE stands for Reference Emitter, which normalizes the LIF response similar to how using isobutylene to normalizes the response on a handheld PID. Once all the waveforms in a log have been analyzed, the software plots the original raw LIF log next to the logs that represent the fluorescence intensity that was mathematically attributable to each of the Basis Set waveforms.

Figure 9-24 (A) depicts the harvested waveform from UVOST® boring 20-LIF, which was selected based on its close match to known intact gasoline waveform responses. In addition to intact gasoline, the fluorescence signatures of diesel, weathered gasoline, and calcite were also encountered, so they were included in the Basis Set. Panels B and C in Figure 9-24 show the resulting LIF buckets for the Basis Set that can be independently plotted in transects or 3D visualizations.

Consideration of other lines of evidence such as general site knowledge, proximity to suspected release source(s), clustering diagrams, analytical data from prior sampling events, or any other available data that reduce uncertainty can be useful in the harvesting process.

The NNLS outputs were used to develop 3D data visualizations that depict interpolated LNAPL plume bodies, distinguished by different colors representing each unique class of fluorescence waveform (and thus fuel type).

Figure 9-25 presents a 3D view of all the LNAPL fluorescence without regard to the type, showing UVOST® signal strength ranging from 2 %RE in blue to greater than 50 %RE in red.

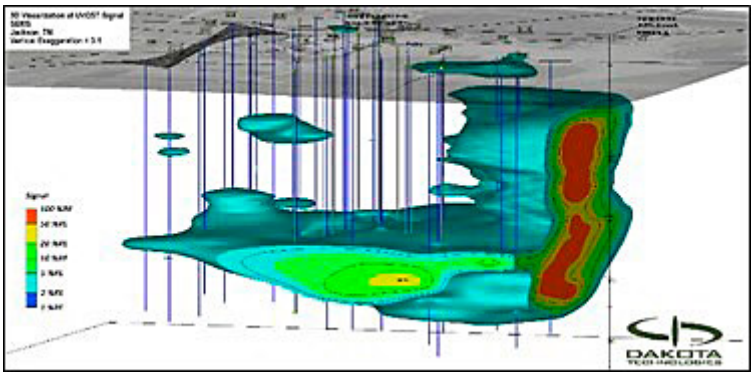

Figure 9-25. 3D Visualization of UVOST Response >2 %RE

3D LNAPL bodies of each Basis Set fluorescence type were also generated. Visualizations of the various fuels were developed with various perspectives of the site, including horizontal slicing, vertical slicing and low to high range %RE UVOST response levels. Figure 9-26 (A) intact Gasoline, (B) weathered Gasoline, and (C) diesel depict a 3D view with the isolation of the primary waveform classifications, based on NNLS analysis. Based on the analysis the southern area of the site contains the highest saturations of diesel LNAPL, extending as deep as 10 ft into the saturated zone. The vertical distribution of the apparent diesel LNAPL is greatest near the southern property boundary in near proximity to the diesel ASTs and an associated loading dock.

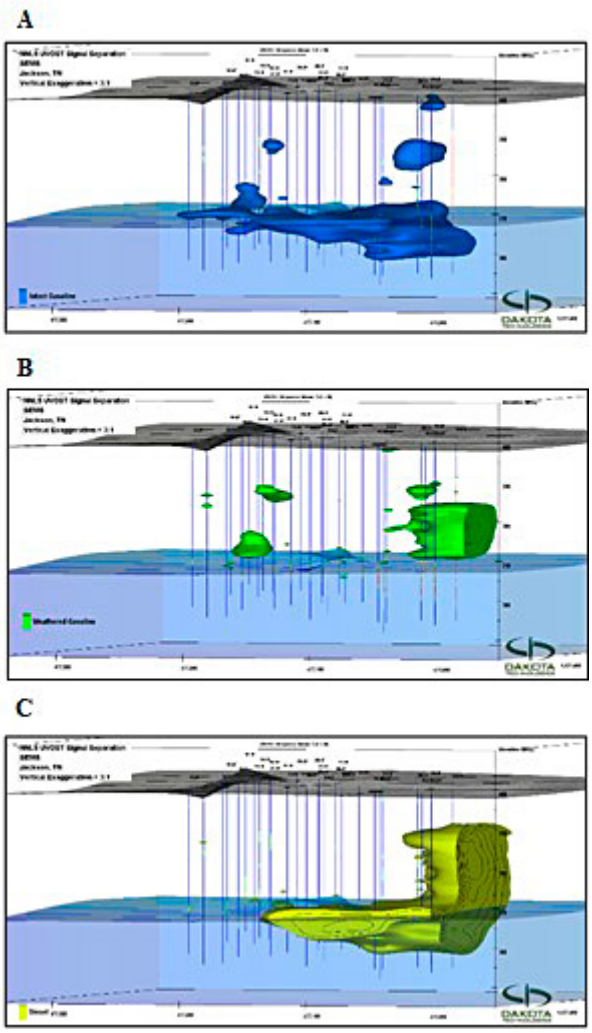

Figure 9-26. 3D Visualizations of NNLS UVOST® Basis Set. (A) Intact Gasoline. (B) Weathered Gasoline. (C) Diesel.

In the areas closer to the gasoline USTs and dispensing pumps, discontinuous masses of *weathered* and *intact* gasoline LNAPL appear to be perched in the vadose zone, as much as 15ft above the water table. Apparent diesel LNAPL in these areas of the site appears to be at greater depth than observed in the southern portion of the site, tapering off to absent in the northern portion of the site.

A definitive determination of specific LNAPL products cannot be made from LIF data alone. Typically, the LIF data provide a basis from which targeted sampling plans can be developed for confirmation, along with examination of other available lines of evidence. In this case, Dakota worked with the client and regulators to determine optimal locations for targeted sampling that would provide samples necessary to determine with confidence whether the initial LIF waveform interpretation, the NNLS analysis, and the resulting 3D visualizations were correct.

Select LIF locations and depths were sampled and cores were examined whole at Dakota's lab. Sub-samples were selected and sent to a forensic lab for analysis by USEPA Methods 8015M and 8270M. There was generally agreement between the a priori LIF NNLS CSM model and analytical lab results, with highlights being:

- Soil from 05-LIF (29.5-30.0'), shown on Figure 4, contained LNAPL as indicated by LIF, 66.5% diesel and 33.5% gasoline, supporting the "DIESEL" ID made in the field and assumed in the NNLS CSM
- Soil from 12-LIF (16.0-16.5'), shown on Figure 5, was found to contain LNAPL, 99% weathered gasoline, supporting the "GASOLINEWEATH" ID made in the field with LIF and assumed in the NNLS CSM; 12-LIF's location just under the dispensers probably precluded it from receiving diesel from the assumed nearby AST release
- Soil from 20-LIF (36.7-37.0'), shown on Figure 3, contained LNAPL, 65% weathered gasoline and 35% diesel, semi-supportive of the "GASOLINEINTACT" interpretation in the field (NAPL was gasoline-dominated). The field interpretation and the NNLS CSM are in disagreement with the lab's 35% diesel finding (the waveform and N2

purging studies showed little indication of diesel).

The total cost for the UVOST® site characterization was approximately $22,000, which includes the costs for mobilization, per diem payments, four days of UVOST operation, and direct-push technology rig operators and equipment. The cost for preparing the data visualization package and advanced data analysis (not described here) was approximately $8,500. The validation sampling and forensic analysis that resulted in confirmation of the CSM cost approximately $9,200. Costs can vary depending on the size of the site, the complexity of the data, and the desired visualization outputs.

While the cost of the UVOST® site characterization and data analysis process is significant, the real-time screening for the presence, distribution and classification of LNAPL at a scale-appropriate resolution provides key information in a multiple-lines-of-evidence approach to a comprehensive and adaptive assessment process. It should be noted that advanced analysis is not always necessary or even advised. Experienced UVOST practitioners often process the waveform types, false positives, and relative impacts intuitively in three dimensions without the need to perform advanced data analysis and computerized visualization.

9.5.1 Source Information

High Resolution Site Characterization Report – UVOST-EC Investigation, Dakota Technologies Company, LLC, April 18, 2018

Initial Response and Hazard Management Report, Southern Environmental Management & Specialties, Inc., November 20, 2012

Initial Site Characterization Report (ISCR), Southern Environmental Management & Specialties, Inc., March 28, 2013

Corrective Action Monitoring Report (CAMR), Southern Environmental Management & Specialties, Inc., October 4, 2018

9.6 TarGOST Determines DNAPL Extent and HPT Confirms Site Lithology at a Former Creosote Facility in Louisiana

Jennifer Lindquist, P.G
Leaaf Environmental LLC
Gretna, Louisiana
jlindquist@leaaf.com

Keith Horn
Louisiana Department of Environmental Quality
Baton Rouge, Louisiana
Keith.Horn@la.gov

Information presented in this case study is based on investigations conducted by Leaaf Environmental, Inc. and USEPA.

Releases of creosote are suspected to have occurred at a creosote wood preserving facility (Bayou Bonfouca Superfund site) in Slidell, Louisiana, during its operational life from the late 1800s through the early 1970s. A fire occurred at the facility in the early 1970s and caused several large tanks to rupture. Creosote flowed across the site and into Bayou Bonfouca, contaminating soil, the bayou (creek and channel bottom sediments), surface water, and groundwater. The facility was abandoned after the fire.

Several investigations were completed from 1976 to 1987, and the site was added to the National Priorities List in 1982. In 1991, groundwater treatment was initiated as a remedy to clean up the creosote groundwater plume.

The groundwater treatment system continues to operate at the facility. The system recovers groundwater from two on-site recovery well arrays (arrays 1a and 2) and one off-site array (array 3) located on the opposite bank of the bayou. Approximately 100 gallons of DNAPL are recovered every month from the treatment system, and DNAPL has been observed in recovery wells in all three arrays (see Figure 9-27).

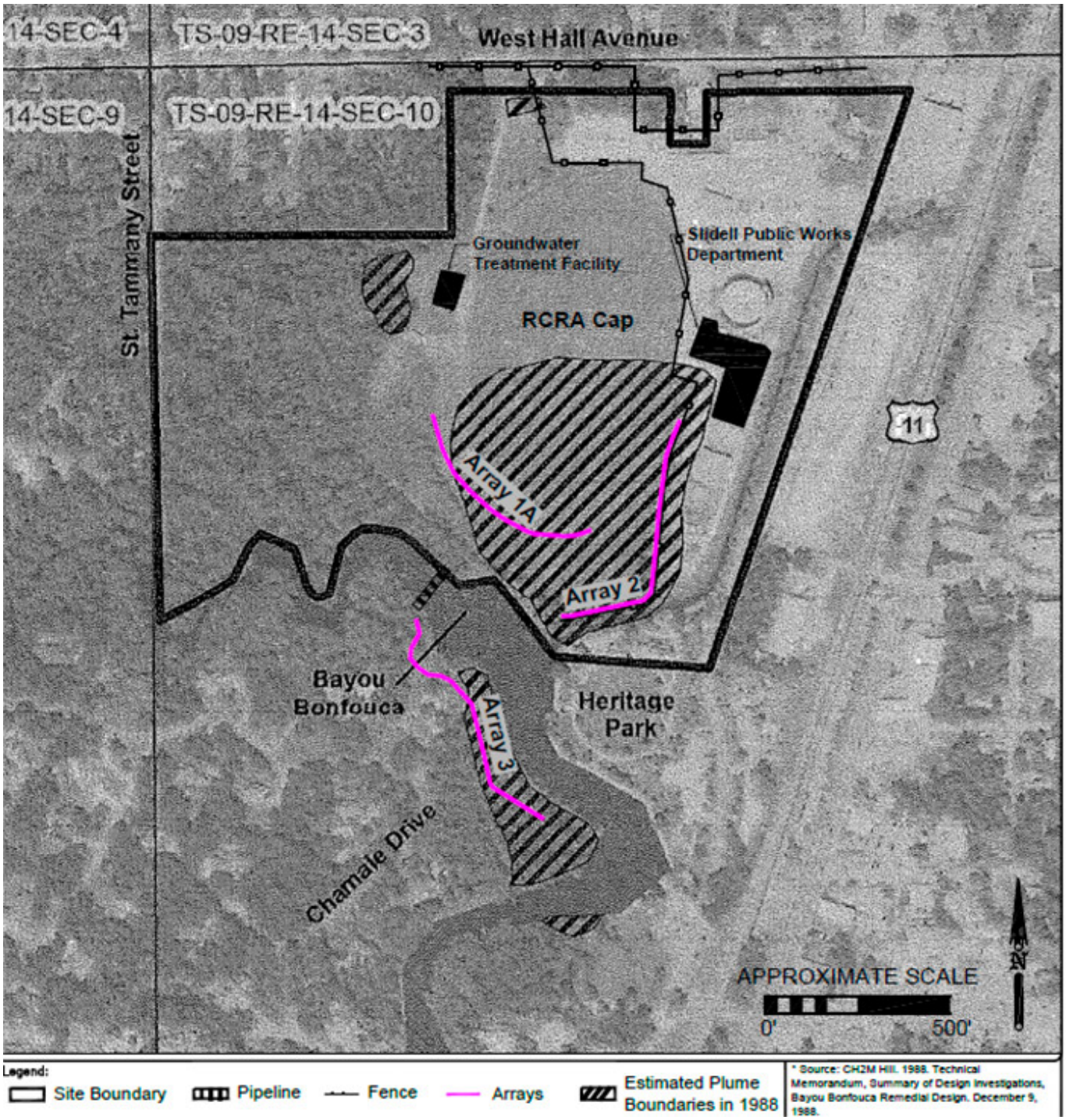

Figure 9-27. 1988 DNAPL plume and site features.

Recent evaluations provided information showing that groundwater cleanup goals have not been met. An assessment of remedy effectiveness showed that the pump-and-treat system is restricting DNAPL plume movement rather than remediating the plume as intended.

An investigation using TarGOST in conjunction with the HPT was performed in 2018 to approximate the extent of subsurface DNAPL and assist in assessing the effectiveness of the current remedy. The tar-specific Green Optical Screening Tool (TarGOST) tool was selected to conduct subsurface screening in an effort to delineate the current extent of the DNAPL plume associated with the site. The initial objectives of the investigation included:

- field screening using existing wells and TarGOST to approximate the extent of subsurface DNAPL and
- collection of soil, groundwater, sediment, and landfill ash samples at selected locations to confirm TarGOST findings and determine current concentrations of historical wood preserving The assessment was designed to determine the presence/absence of DNAPL and was not intended to produce quantitative results.

The HPT was added to the screening effort to estimate hydraulic conductivities and the complex fluvial subsurface lithology, which consists of inconsistent interbedded sand, silt, and clay that can trap DNAPL in unexpected locations.

The TarGOST tool was selected to characterize *in situ* DNAPL due to proven performance at another creosote site in Louisiana, its selective detection of creosote, its ability to provide immediate data, and its ease of use via direct push methods. In addition, minimal investigation-derived wastes are generated. The TarGOST system makes direct fluorescence measurements by directing fast pulses of 532 nanometer (green) laser light onto the soil through a sapphire windowed probe. If creosote is present, the polycyclic aromatic hydrocarbons in it will absorb some of the light and emit pulses of fluorescence that are detected back through the window and are recorded by the TarGOST's time-resolved detector. The HPT was added to the screening effort to approximate hydraulic conductivities and to estimate the complex fluvial subsurface lithology, which consists of inconsistent interbedded sand, silt, and clay that can trap DNAPL in unexpected locations.

Prior to field work, the fluorescence response of a sample of recovered creosote was measured via TarGOST. The resulting response was high, indicating that TarGOST would readily detect the NAPL in situ. The field survey was initiated in March 2018. Screening was conducted using the TarGOST within the footprint of the DNAPL plume as estimated in 1988. Thirty-three locations were screened during five days in March and April 2018. An additional 14 locations were screened during four days in November 2018 (see Figure 9-28). The maximum screening depth was 55 ft below ground surface, coinciding with a clayey cohesive unit into which the creosote has not historically penetrated. Confirmation soil and groundwater sampling, as well as soil logging, were conducted at approximately 25% of the screening locations to confirm the TarGOST observations and identify contaminants within the creosote plume.

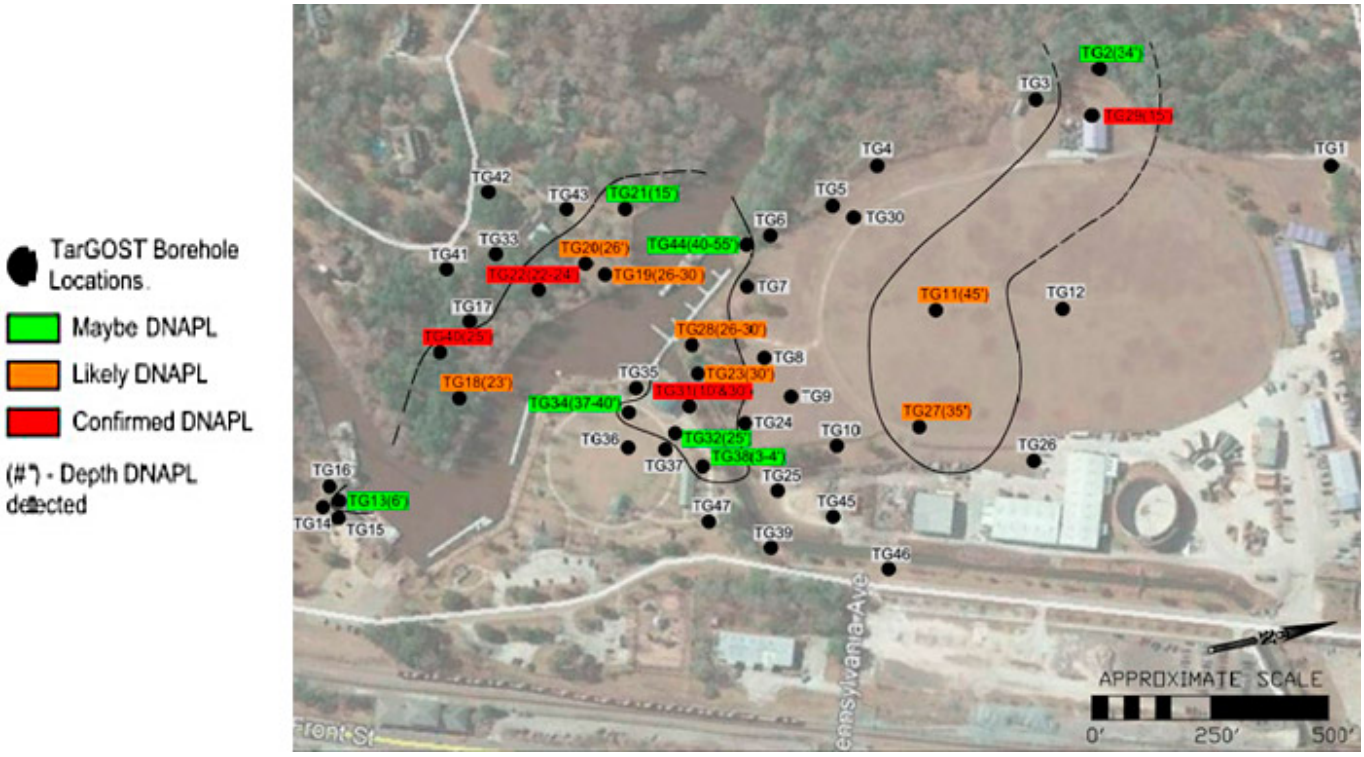

Figure 9-28. 2018 TarGOST sample locations and current plume interpretation.

While the DNAPL plume has not been fully delineated, the TarGOST defined the extent and relative amount of DNAPL present at sampled locations both on and off site (see Figure 9-29). This information will be used when evaluating the effectiveness of the current remedy. The HPT confirmed the site lithology that was described in the 1980s and 1990s.

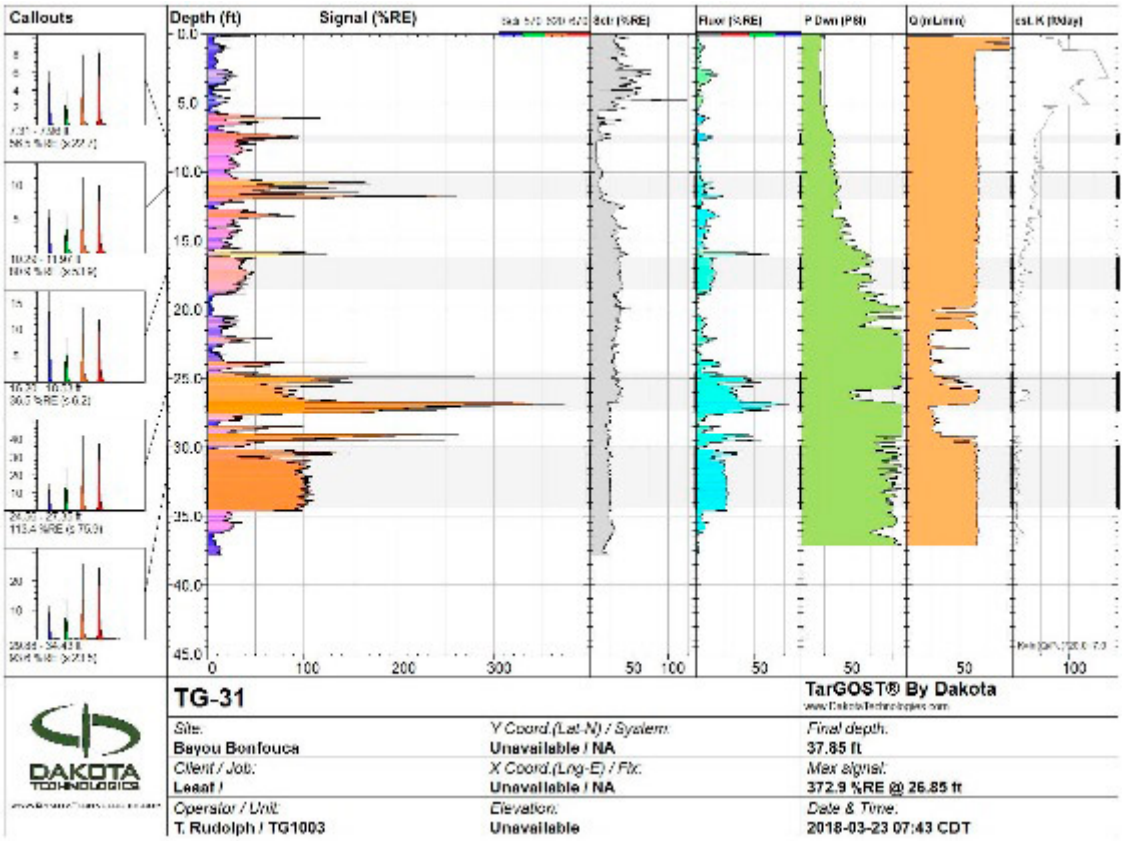

Figure 9-29. TarGOST and HPT log showing creosote fluorescence and water pressure responses.

Natural organic material can and does fluoresce similarly, but not identically, to creosote, and this occurred to some extent at this site. Organic clay, which exhibited high fluorescence, was observed in confirmation samples at one location. Roots and organic debris, which exhibited variable fluorescence, were observed in confirmation samples at several locations (see Figure 9-30 and Figure 9-31). The time-resolved fluorescence waveforms generated by the TarGOST, along with advanced analysis of these waveforms such as cluster diagrams, played a key role in discerning between the target DNAPL and organic matter. Confirmation sampling was essential to eliminate false interpretation of organic matter fluorescence. For each log with a response that was not confirmed with a soil boring, a determination as to whether DNAPL was “maybe present” or “likely present” was made based on the degree to which the unconfirmed logs were similar to the logs for confirmed DNAPL.

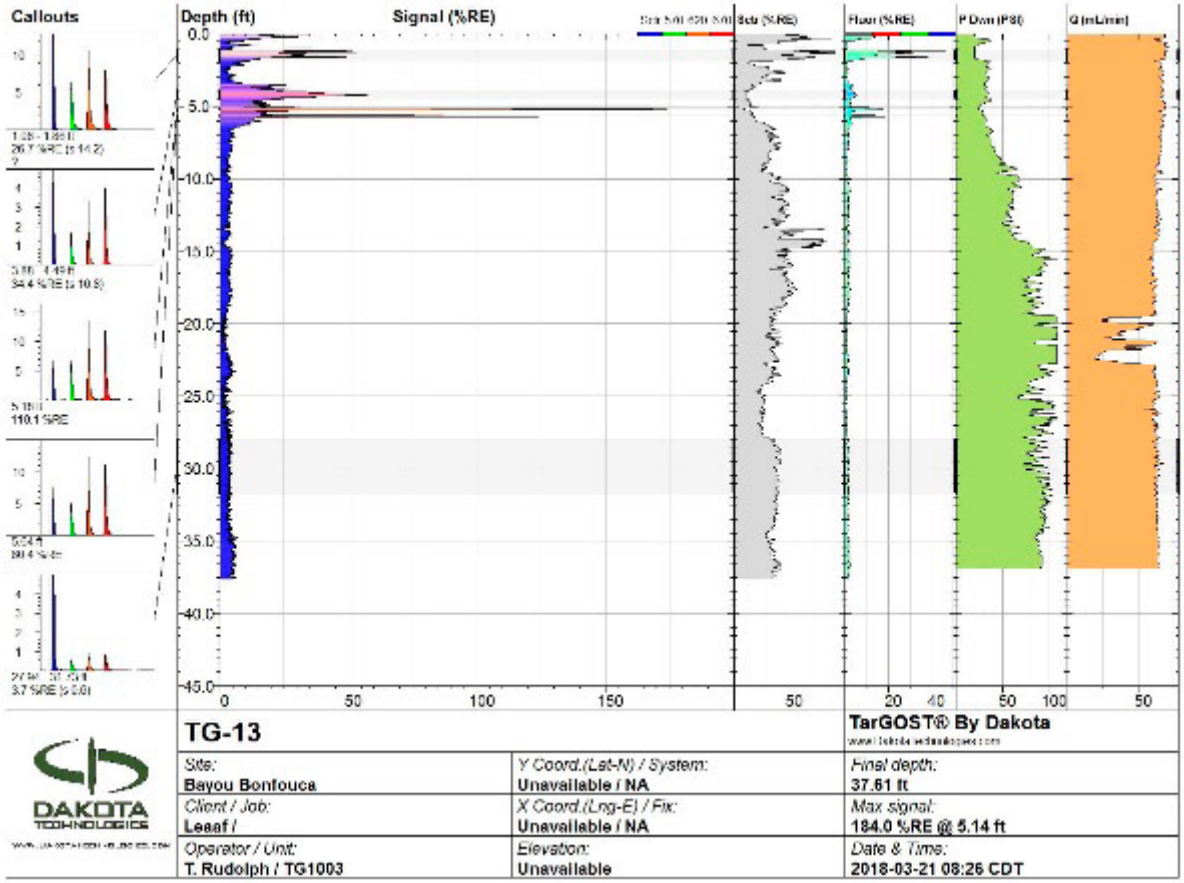

Figure 9-30. TarGOST and HPT log showing organic clay fluorescence near the surface.

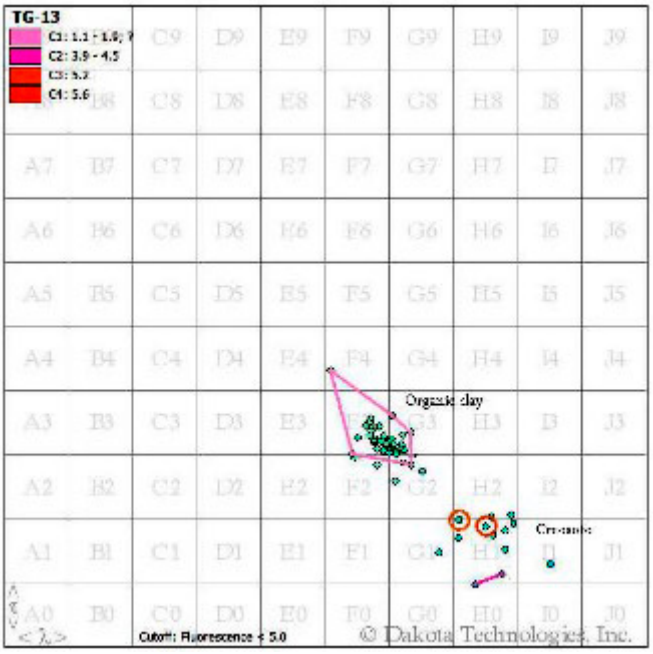

Figure 9-31. Wavelength scatter for organic clay and creosote.

The total costs for the two TarGOST screening investigations, including soil and groundwater confirmation sampling, at the site was approximately $233,000. Specifically, the cost of the TarGOST equipment, operator, direct-push rig, and crew totals approximately $7,000 per day. The remaining costs included personnel; analytical for ash characterization, soil, groundwater, and sediment sampling; on-site utility location; and characterization and removal of investigation-derived wastes. Cost savings could be affected by reducing the number of confirmation samples to the minimum recommended

(10%).

The advantages of using TarGOST at this site were as follows:

- allowed for a relatively rapid assessment of the extent of the DNAPL plume
- easily deployed via a standard direct-push drilling rig
- ability to provide immediate data
- minimal investigation-derived wastes
- reduced cost by approximately 60% compared to traditional sampling and analysis methods
- reduced field time required to gather the information by approximately 75% compared to traditional methods
- minimized public exposure at sampling locations adjacent to public park
- allowed the objectives of the investigation to be met in a timely and cost-effective manner

9.6.1 Source Information

Tar-specific Green Optical Screening Tool (TarGost), Dakota Technologies (DTI 2017).

Fifth Five-Year Review Report for Bayou Bonfouca Superfund Site, Slidell, St. Tammany Parish, Louisiana. USEPA, July 2016.

Site Investigation Submittal, Bayou Bonfouca Superfund Site, Slidell, Louisiana. Leaaf Environmental, Inc., May 14, 2018.

Additional Site Investigation Work Plan, Quality Assurance/Quality Control Plan and Technical Sampling & Analysis Plan, Bayou Bonfouca Superfund Site, Slidell, Louisiana. Leaaf Environmental, Inc., August 2018.

9.7 CPT Borings and Hydropunch Sampler Optimize Site Characterization at an Aviation Industrial Complex in California

Kenda Neil
NAVFAC Engineering and Expeditionary Warfare Center
Port Hueneme, CA
kenda.neil@navy.mil

Information presented in this case study is based on investigations conducted by ESTCP – See source information below

The largest aviation industrial complex on the west coast is located in San Diego, California, and surrounded on three sides by San Diego Bay and the Pacific Ocean. The site is located on relatively flat land with an average elevation of approximately 20 ft above sea level. The site has been graded for development using hydraulic fill consisting of medium- to coarse-grained, poorly graded sands and silty sands. In some areas, the fill is underlain by organic silts and clays.

An operable unit, located in the northeastern portion of the site, is in a heavy industrialized area with several processes including aircraft testing, maintenance shops, and associated chemical storage tanks and pipelines. The groundwater level in this area is approximately 5 ft above mean sea level. The groundwater gradient is relatively flat, from 0.001 to 0.002 foot per foot. Groundwater flow direction is to the north/northeast and discharges into the San Diego Bay. The primary groundwater contaminants are chlorinated VOCs and hexavalent chromium. A chlorinated VOC plume in the area is over 0.5-mile long and is believed to migrate into distinctive zones. For example, immediately downgradient of the source area, the plume migrates into a narrow band 200-ft wide but reduces in width more than 50% further downgradient where it also appears to migrate deeper.

To address data gaps pertaining to both the stratigraphy and contaminant distribution in the area, CPT borings were advanced and hydropunch samples were collected (see Figure 9-32.). Because the utility corridors on site make well installation difficult and, in some cases, prohibit use of a traditional drill rig, the smaller footprint of a CPT rig allowed access in these tight areas. The stratigraphic data obtained were used to prepare cross sections and helped to determine that downward migration was due to structural or depositional features. CPT boring and Hydropunch data were used to assess areas of interest without having to collect soil samples and determine well-screen intervals. As a result, specific zones of interest were identified and sampled quickly and fewer permanent wells were needed.

An additional 10 CPT borings were advanced in a row downgradient of the plume to evaluate soil and analytical results. The screen intervals for these wells were based on CPT boring data and hydropunch sample concentrations. The advantages of using CPT borings at this location are as follows:

- allowed for the collection of continuous and much more complete data sets with limited possibility of bias from field personnel regarding soil type interpretations
- allowed the selection of intervals of different (and distinct) hydraulic characteristics from which to collect groundwater samples
- improved the understanding of the site and permitted better mapping of the local structure (faults), which, in turn, allowed remediation strategies to be designed
- Obtained more data (and more quickly) at approximately 50% less cost than when using traditional characterization approaches.

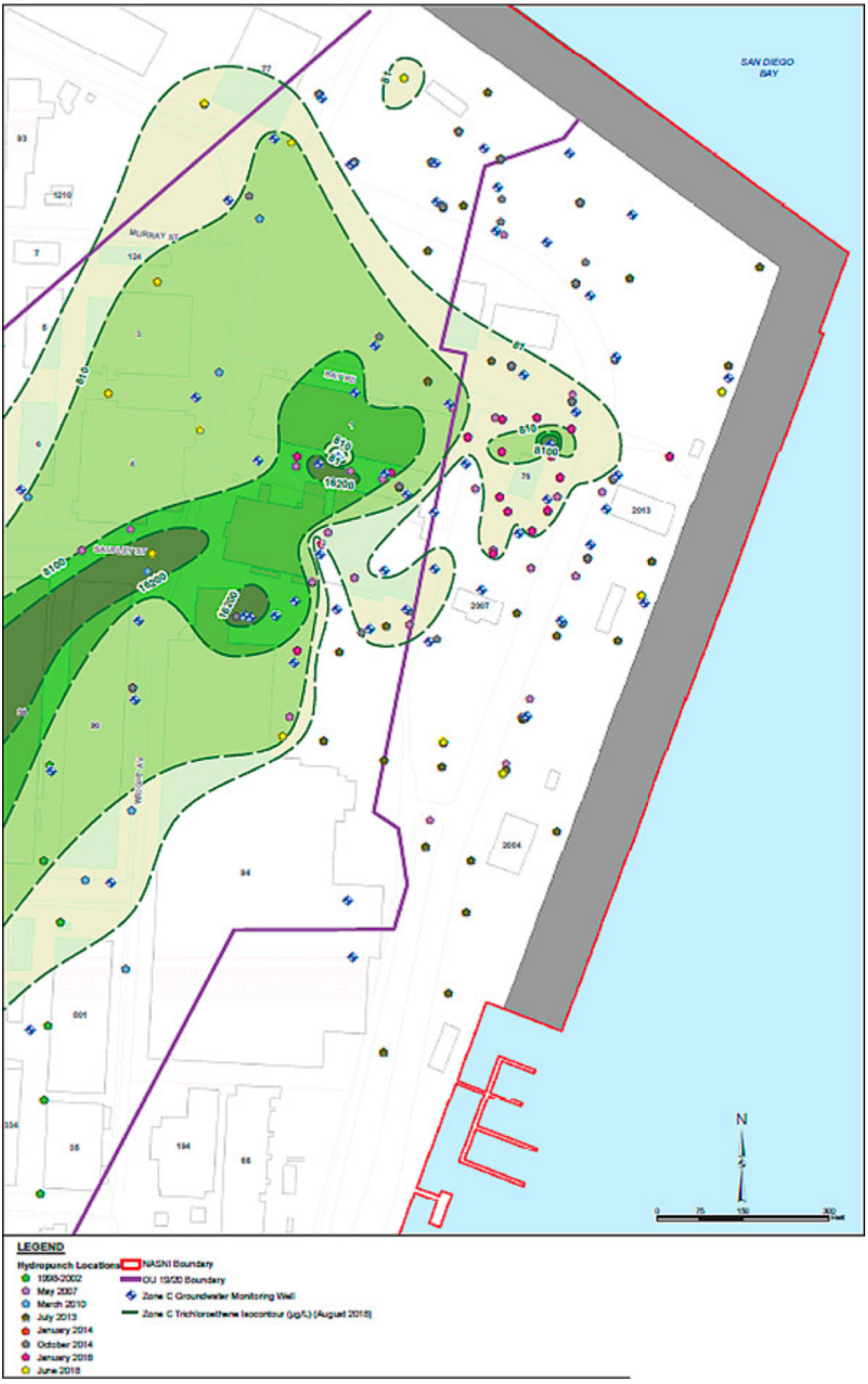

Figure 9-32. CPT boring and hydropunch sample locations.

9.7.1 Source Information

Parallel InSitu Screening of Remediation Strategies for Improved Decision Making, Remedial Design, and Cost Savings (ESTCB 2012).

9.8 Waterloo APS, CPT, and LIF Data Update CSM and Help Optimize Selected Remedy at a Former Refinery in Oklahoma

Hank Unterschuetz
Oklahoma Department of Environmental Quality
Oklahoma City, OK
Hank.Unterschuetz@deq.ok.gov

Amy Brittain
Oklahoma Department of Environmental Quality
Oklahoma City, OK
amy.brittain@deq.ok.gov

Information presented in this case study is based on investigations conducted by ERM.

A former refinery in southern Oklahoma stretches over 400 acres with a long operational history. It was first constructed in the 1920s and operated until 1983 through multiple expansions and changes in ownership (ERM 2015). Soil and groundwater at the site are contaminated with VOCs, PAHs, and metals. In addition to the presence of LNAPL, a previous soil-vapor investigation identified new areas potentially contaminated with LNAPL. Previous investigations were not focused on the horizontal and vertical extent of dissolved-phase groundwater contamination, contaminant mobility, and associated risk(s) to receptors. The risk pathway of highest concern is a nearby stream, located on the eastern boundary of the site.

Although much of the site is underlain by shallow sedimentary bedrock (sandstone with siltstone and mudstone inclusions), the portion of the site closest to the stream is underlain by quaternary-age alluvium, which overlies the sedimentary bedrock (see Figure 9-34). The alluvium consists of silt to fine-grained sand with silty or sandy clay and is thickest along a valley located immediately west of the stream. Groundwater within the alluvium discharges to the stream, presenting the most significant risk pathway for site contaminants (ERM 2013b).

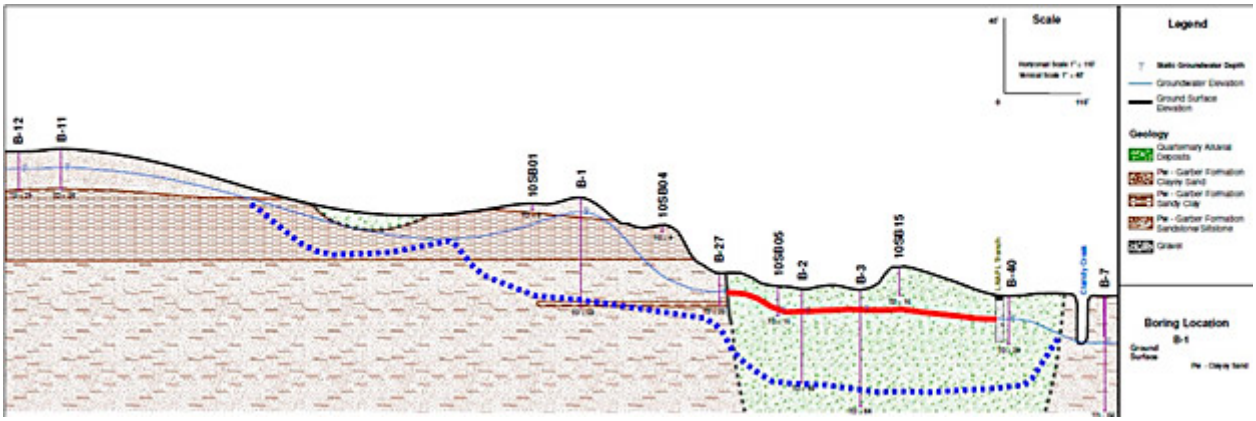

Figure 9-33. West-east site geology cross section.

9.8.1 Waterloo Advanced Profiling System (APS)

The Waterloo APS was used to collect groundwater samples for analyses of VOCs, SVOCs, and metals at multiple vertical intervals from multiple boring locations in the portion of the site underlain by alluvium. Using a direct push method for sample collection in conjunction with a mobile laboratory for real time sample analysis allowed for extremely quick sampling and decision making.

The Waterloo APS is a direct-push, real-time measurement tool that provides hydro-stratigraphic data and allows for discrete-interval water sampling. The instrument reports a continuous log of the Index of Hydraulic Conductivity (Ik) by injecting a small amount of clean water into the geologic formation as it is being pushed. The tool monitors the depth, pressure, and flow rate of the injected water, and generates a continuous log of relative permeability of the formation. With this knowledge, the user can select intervals for sample collection. Multiple discrete-interval groundwater samples can be collected from a single boring without having the remove the tooling for sample collection or decontamination (ERM 2013b).

The Waterloo APS collects groundwater samples from a 2- to 5-inch vertical interval, which is a much narrower sample interval than a traditional monitoring well screen. Because the sample is collected from a narrow interval, samples from the Waterloo APS often have higher concentrations than a traditional monitoring well samples, which represent the average

groundwater concentration across the well screen interval (often several ft). For these reasons, Waterloo APS is deemed a conservative environmental sample and is useful for efficiently and accurately delineating dissolved phase contamination, and for identifying locations where wells should be installed for future monitoring or recovery.

Groundwater from the entire eastern site perimeter and part of the southern site perimeter was evaluated. Thirty-eight borings were advanced and 52 groundwater samples were collected from the most permeable zones within the alluvium using the Waterloo APS (see Figure 9-34). Results indicated no groundwater contamination on the southern boundary of the site and revealed previously unknown contamination on the northeast site boundary. The dissolved-phase data gathered was used to accurately determine locations and appropriate screening intervals for the installations of a limited number of additional monitoring wells (ERM 2013a).

The Waterloo APS was only one tool used in this site-wide application of direct-push tools. Combined with the information gleaned from CPT and LIF, the complex subsurface was better characterized efficiently. After monitoring wells were installed, the CSM was updated and used to guide various remedial actions. Current remedial actions to remove petroleum related wastes in the subsurface adjacent to the creek have been efficient and effective because of the high-resolution site characterization data generated by the Waterloo APS and other direct-push methods.

The conventional approach to monitoring this risk pathway would have been to install dozens of wells at various screening intervals around the creek and on the boundaries of the site. However, use of the Waterloo APS saved time and better guided well installation (ERM 2015). A total of 16 wells were installed between 20 and 40 ft. Using interval data from the Waterloo APS, new well screens were targeted to characterize dissolved-phase plumes or perform LNAPL bail-down tests which minimized well construction costs while ensuring quality data from the installed wells.

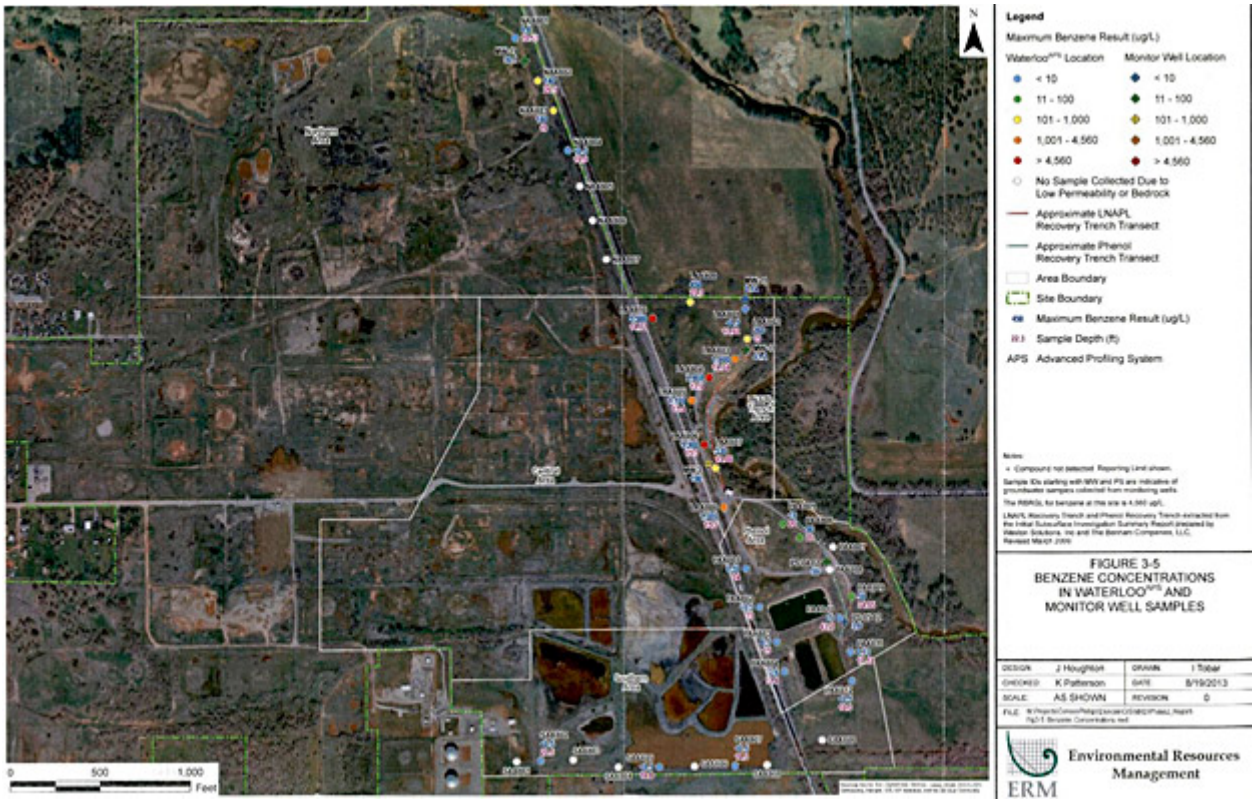

Figure 9-34. Maximum benzene results at monitoring wells and Waterloo APS locations.

9.9 Conceptual Site Model Development Using Borehole Geophysics at the Savage Municipal Water Supply Superfund Site in New Hampshire

Andrew M. Fuller, PG
Weston Solutions, Inc.

James Soukup, PG, RG, LSP
Weston Solutions, Inc.

Kenneth A. Richards, PG, PE
Hazardous Waste Remediation Bureau
NH Department of Environmental Services

Historical use of tetrachloroethene (PCE) at the Savage Municipal Water Supply Superfund Site in Milford, NH has impacted the overburden and bedrock aquifers underlying the site and a nearby municipal water supply well and resulted in a groundwater contamination plume approximately 6,000-ft long. Figure 9-35 shows the site location. Geology at the site consists of highly transmissive glacial outwash and a relatively thin discontinuous till unit overlying fractured crystalline bedrock.

First developed in 1950, the Savage Municipal Water Supply well provided potable drinking water to approximately 10,000 residents in the Town of Milford, NH. Sampling of the well conducted in the early 1980s discovered volatile organic compounds (VOCs) including 1,1,1-trichloroethane (1,1,1-TCA), trichloroethene (TCE), trans-1,2-dichloroethene (trans-1,2-DCE), PCE, and 1,1-dichloroethane above drinking water standards. A Remedial Investigation (RI) completed in June 1991 identified multiple sources of the VOCs found in groundwater, including the former OK Tool Company; which manufactured metal cutting tools and hardware from approximately 1940 to 1987.

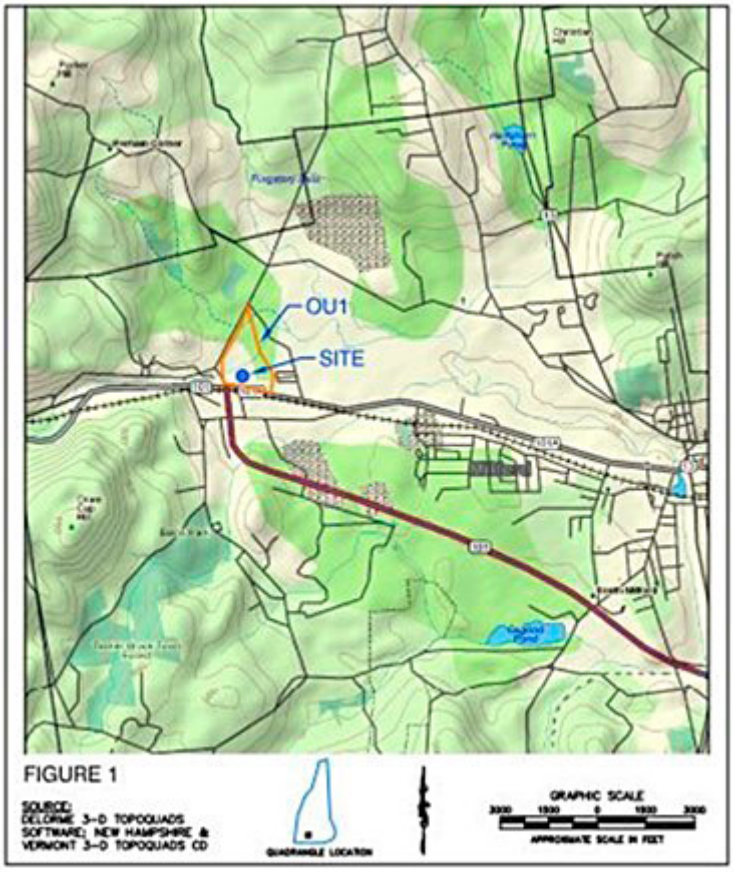

Figure 9-35. Site location.

Based on previous investigations, the final remedy selected for the site included institutional controls, a subsurface barrier (slurry) wall to isolate the source area, groundwater extraction wells (inside and outside the barrier), soil vapor extraction, air sparging, and groundwater monitoring. The treatment system, which has operated since 1999, successfully reduced VOC concentrations in groundwater outside the barrier wall to below drinking water standards at nearly all monitoring wells screened within the unconsolidated deposits.

Site geology consists of a 50 to 110 ft thick highly transmissive sand and gravel glacial outwash and a relatively thin discontinuous till unit (<10 ft) overlying fractured crystalline bedrock. Historically the aquifer present within the unconsolidated deposits has generally been divided into three units, including the shallow overburden (0-30 ft below ground surface), intermediate overburden (30-70 ft below ground surface), and deep overburden 70-110 ft below ground surface). The initial CSM for the site assumed that the deep bedrock was highly competent with few fractures and that the remaining source of chlorinated solvents, possibly DNAPL, was located in the unconsolidated deposits. It was believed that VOCs would not migrate into the bedrock aquifer unless hydraulic containment was not maintained, and downward hydraulic gradients were allowed to develop inside the slurry wall. Therefore, the vertical extent of characterization activities was limited to the deep unconsolidated deposits directly above the bedrock surface and the shallow bedrock aquifer (<50 ft below the bedrock surface). Initial results from these wells identified VOC concentrations that were several orders of magnitude less than those observed in the sand and gravel overburden aquifer. Although VOC concentrations in shallow bedrock wells historically had been significantly lower than those in overburden wells, increasing VOCs concentrations continued to be observed over time in the shallow bedrock monitoring wells after remedy implementation. In addition, expanded residential development has occurred to the north and northwest of the site and these homes rely on individual deep bedrock wells for potable water.

This investigation expanded upon both the lateral and vertical extent of the previous characterization of the bedrock aquifer performed during the RI. Bedrock monitoring well installation, borehole geophysical logging, packer sampling, and a pumping test were all performed to help refine the bedrock CSM. These tools were used to evaluate the bedrock fabric, fracture geometry, and groundwater quality, as well as identify hydraulically active fractures within each monitoring well, and assess the anisotropy of the bedrock aquifer.

Several bedrock monitoring wells were installed, and one existing monitoring well was deepened as part of the investigation. Depths of the investigations were based on the documented construction of the residential water supply wells to the northwest of the Site. Immediately following installation, a standard suite of geophysical logs was completed at each location including borehole caliper, fluid temperature/resistivity, natural gamma, OTV, ATV, and HPFM. HPFM readings were collected under both ambient and pumping conditions. The borehole caliper, OTV, and ATV logs were used to identify bedrock fractures, foliation and bedding within each borehole and their orientation. Natural gamma and OTV logs provided information regarding the lithology of the bedrock formation beyond the classification of drill cuttings during well installation. The fluid temperature/resistivity and HPFM logs were used to identify hydraulically active fractures within each borehole by detecting flow into or out of the boreholes.

A constant rate pumping test was conducted to further evaluate properties of the bedrock aquifer. The objectives of the pumping test included: understanding the hydrogeology of the deep bedrock aquifer including the anisotropy and potentially identifying specific inter-fracture flow; understanding the interaction of the deep bedrock aquifer with the shallow bedrock and deep overburden aquifers; and monitoring contaminant trends in groundwater for the purpose of evaluating future remedial options for the bedrock aquifer.

During the pumping test, water level monitoring was expanded to evaluate piezometric head variations within the deep unconsolidated deposits directly above the bedrock surface, shallow bedrock within the upper 50 ft of the bedrock formation, and deep bedrock zones in response to the applied stress on the deep bedrock source well. The HPFM was used within multiple deep bedrock boreholes prior to the culmination of the pumping test to evaluate inter-fracture flow under pumping conditions.

Borehole geophysical logging identified an overall fracture strike direction of northeast-southwest and a primary dip direction to the northwest with a lesser number of fractures dipping to the southeast. Fractures identified during the analysis are moderate to steeply dipping (55º to 70º). HPFM testing did not identify ambient vertical flow at the Site suggesting near-horizontal flow in the bedrock but did identify multiple inferred transmissive zones within each well under pumping conditions. Figure 9-36 is a rose diagram presenting the geophysical fracture analysis for the entire Site. A short sample of a well log is also included.

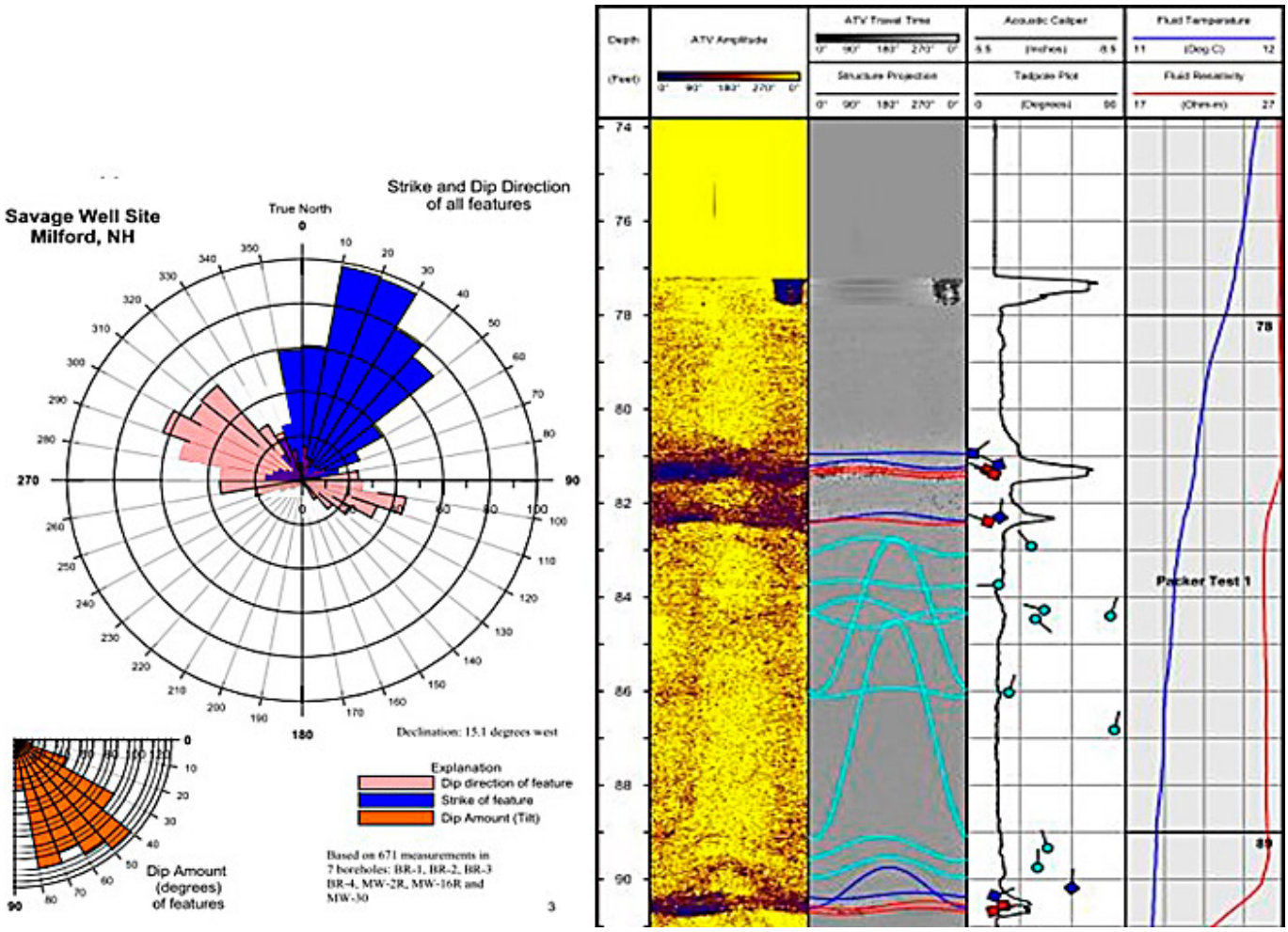

Figure 9-36. BR-5 geophysical log (inferred transmissive fractures identified in red).

Reported concentrations of PCE in bedrock groundwater ranged from below laboratory detection limits to approximately 100,000 ppb. Concentrations of this magnitude suggest DNAPL may be present in the deep bedrock beneath the source areas. Samples collected during the packer testing identified PCE concentrations generally increasing with depth in source area wells and decreasing with depth in peripheral wells. This observation within source area wells would be expected given the higher specific gravity of chlorinated hydrocarbons and the moderate to steeply dipping fracture network. The rapid decrease in contaminant concentrations in peripheral wells suggests a significant vertical component to the contaminant migration. No Site COCs were identified in the proximity of the residential area to the north and northwest of the Site.

Groundwater elevation measurements at the culmination of the aquifer test indicated an elongated pattern to the groundwater surface with the axis in the south-southwest to north-northeast orientation. This pattern is illustrated on Figure 9-37 and differs from the inferred easterly direction of groundwater flow under static conditions; however, the asymmetrical cone of depression correlates with the fracture strike orientations measured during the borehole geophysical logging. This identifies the anisotropy of the bedrock aquifer, a preferential pathway for contaminant migration at the Site.

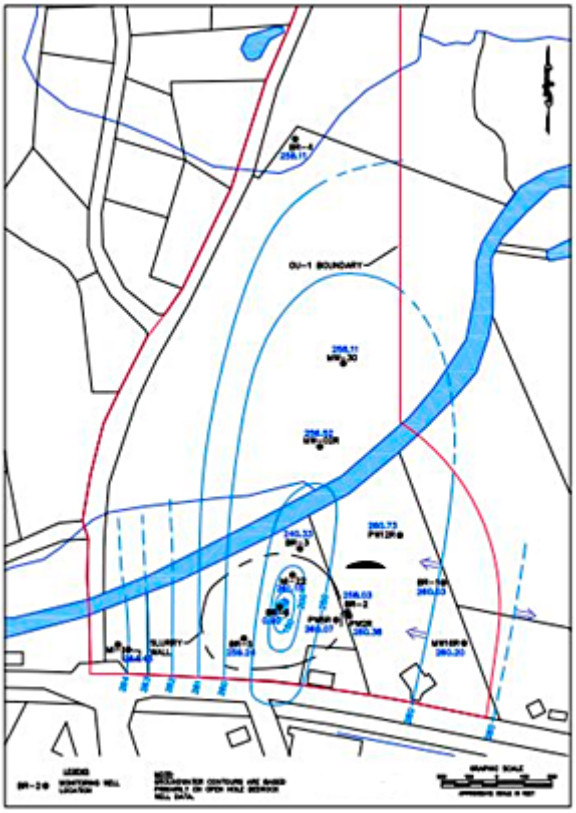

Figure 9-37. Groundwater elevation pattern

The characteristic purple color of sodium permanganate ($NaMnO_4$) was observed in purge water approximately 2 hours after the start of the pumping test. Sodium permanganate was applied to the deep overburden aquifer within the barrier wall during an ISCO program implemented between 2008 and 2010. The observation of $NaMnO_4$ in the deep bedrock during the pumping test illustrates the significance of the hydraulic connection between the pumping well and the deep overburden within the barrier wall.

Although groundwater elevation data did not identify any observable impact to the overburden aquifer during the pumping test, the rapid presence of $NaMnO_4$ in purge water indicates that when a stress is applied to the bedrock aquifer, the overburden is a significant source of recharge. In addition, the lack of $NaMnO_4$ presence at the start of the test indicates that the natural head distribution may not allow the oxidant to flow there. The lack of influence to groundwater elevations for wells screened within the unconsolidated deposits is not surprising due to the saturated thickness (~85 ft), high hydraulic conductivity (>1,000 ft/day) of the overlying sand and gravel aquifer, and the magnitude of difference of storage coefficients between the overburden and bedrock aquifers. These characteristics would mask the minimal influence resulting from a 10 gpm withdrawal.

Concentrations of PCE and TCE each decreased over the duration of the pumping test. The reduction in concentrations over the course of the pumping test suggests that extended pumping from the source area induces flow from other portions of the Site, which exhibit lower concentrations of contaminants.

During the HPFM logging conducted on the final day of the pumping test, flow was detected in the open bedrock portions of boreholes located near the pumping well. The HPFM testing identified a lateral connection by way of deeper fractures, located at depths greater than 112 ft below the bedrock surface, or approximately 212 ft below ground surface. This lateral connection was accentuated when the stress of the pumping test was applied to the bedrock aquifer. In addition, the primary source of recharge to the bedrock aquifer is likely from the overburden via a network of shallow steeply-dipping fractures, generally positioned less than 50 ft below the bedrock surface, or approximately 150 ft below ground surface. This is supported by the shallow recharge observed in each of the wells that exhibited drawdown during the pumping test.

Analytical results from samples collected during packer-interval sampling suggest that very high concentrations of chlorinated hydrocarbons are present in the bedrock beneath the source area within the barrier wall, possibly in the form of DNAPL. Downhole geophysics data from deep bedrock boreholes indicate that most shallow fractures are steeply dipping;

which is consistent with the presence of high contaminant concentrations in the deep bedrock fractures in the proximity of the overburden source area, because these fracture characteristics would facilitate the vertical migration of contamination into the deep bedrock within a short distance of the source area. The significant reduction in contaminant concentrations with respect to distance from the source area suggests that there is a stronger vertical component to contaminant migration than lateral.

The results from the pumping test and water table elevation monitoring identified clear north-northeast anisotropy to the bedrock aquifer, which correlates with rose diagrams generated with fracture strike/dip information compiled during the borehole geophysics program. This anisotropy represents the most significant contaminant migration pathway at the Site. Results from the HPFM testing conducted during the pumping test identified a lateral connection by way of deeper fractures. In addition, the primary source of recharge to the bedrock aquifer is from the overburden via a network of shallow fractures. Shallow recharge was observed in each of the wells that exhibited drawdown during the pumping test. Although the deep overburden is a primary source of recharge to the bedrock aquifer as evidenced by the presence of $NaMnO_4$, the pumping test did not result in influence on the water table elevation in the unconsolidated deposits. This lack of impact to overburden groundwater elevations is not surprising due to the large saturated thickness, high hydraulic conductivity of the overlying sand and gravel aquifer, and the magnitude of difference of storage coefficients between the overburden and bedrock aquifers.

The data obtained from this investigation provided critical information to refine the CSM for the Site. The updated CSM indicates that significant contaminant concentrations exist in deep bedrock, including the possibility of DNAPL, representing a secondary, ongoing source of groundwater contamination. Mapping of the bedrock fracture system has identified a higher frequency of shallow but steeply dipping fractures that tend to promote vertical migration of the impacted groundwater and a deeper system of fewer fractures that are less steeply dipping and tend to allow more lateral migration. A strong north-northeast trending anisotropy was identified in the bedrock that represents the most likely direction of lateral contaminant migration in deep bedrock.

The findings of this study resulted in the completion of a RI/FS for the bedrock aquifer at the Site. Several remedial alternatives were evaluated as part of the RI/FS process, and the updated remedy for the Site includes bolstering of the slurry wall containment system, additional oxidant injections, and continued operation of the groundwater extraction system at the Site in conjunction with a Technical Impracticability (TI) waiver.

9.9.1 Source Information

Geohydrology of, and Simulation of Ground-Water Flow in, the Milford-Souhegan Glacial-Drift Aquifer, Milford, New Hampshire, Harte, P.T. and Mack, T.J., 1991, USGS Water-Resources Investigations Report 91-4177.

The Use of Specific Capacity to Assess Transmissivity in Fractured-Rock Aquifers, Huntley, David, Roger Nommensen, and Duane Steffey, 1992, Ground Water. Vol. 30, No. 3, pp. 396-402.

9.10 ERI Provides Data to Improve Groundwater Flow and Contaminant Transport Models at Hanford 300 Facility in Washington

Lee Slater
Rutgers University Newark
Newark, NJ
lslater@newark.rutgers.edu

The ERI method, also known as electric resistivity tomography (ERT), is used to noninvasively determine the spatial variations (both laterally and with depth) of the electrical resistivity of the subsurface (see Section 5.2 for details). At the U.S. Department of Energy's Hanford 300 Facility in Richland, WA, ERI was used to improve the understanding of the hydrogeological framework regulating the exchange of groundwater with surface water. The basic geology of the site is described as a coarse-grained aquifer (the Hanford Formation) underlain by a lower permeability, fine-grained confining unit (the Ringold Formation). The thickness of the Hanford Formation varies between 14 m (45.9 ft) and 17.5 m (57.4 ft) in boreholes close to the Columbia River, with thickness increasing inland. Due to historical nuclear waste processing and disposal at the site, radionuclide-contaminated groundwater may have been discharged into the Columbia River. Of concern is the possible presence of relict paleochannels incised into the Ringold Formation that could act as permeable pathways for contaminants to rapidly migrate from the aquifer into the river. The risks of radionuclide contamination result in a high cost of drilling at this site; ERI is a more cost-effective investigation technique.

Two-dimensional resistivity surveying was performed to investigate variations in the depth to the Hanford-Ringold contact across the site and identify evidence for incisions in the Ringold Formation that might represent paleochannels (see Figure 9-38). The rationale for applying ERI was the expected strong contrast in electrical resistivity between the coarse-grained Hanford sediment (more resistive) and the fine-grained Ringold sediment (less resistive). A series of parallel, 2-D ERI lines was acquired on 400- to 500-m-long lines using a 5- and 10-m electrode spacing (see Figure 9-38a). Challenges faced in deploying these lines included steep terrain and high contact resistances due to dry soil. The latter was overcome by watering electrodes with a high-salinity solution.

The resulting images of an approximately 40-m investigation depth clearly defined the Hanford-Ringold contact and identified locations close to the river where the resistivity structure suggests the presence of paleochannels (see Figure 9-38c). An interpolated plan view showing the elevation of the sharp contrast in electrical resistivity representing the Hanford-Ringold contact (constructed using the 10 2-D transects shown in Figure 9-38) is presented in Figure 9-38. This figure also highlights (1) the path of a key paleochannel that coincides with the location of temperature anomalies from distributed temperature sensing (DTS) indicative of pronounced groundwater-surface water exchange, and (2) high uranium concentrations sampled in the river sediment. The DTS was performed using a fiber-optic DTS line placed along the river bed; temperature is inferred by scattering light transmitted along the cable. Uranium contours are based on concentrations measured in the boreholes (see Figure 9-39) across the site.

The 2-D assumption used in the inversion of the ERI dataset is reasonable for the lines parallel to the river, as evident by the strong similarity in structure between these lines. Simplified logs from two boreholes that were drilled at the site confirm that the imaged depth to the Hanford-Ringold contact is reasonable, given the inherent smoothing and limited resolution of the technology at depth. The results of this survey have been used to improve groundwater flow and contaminant transport models at the site.

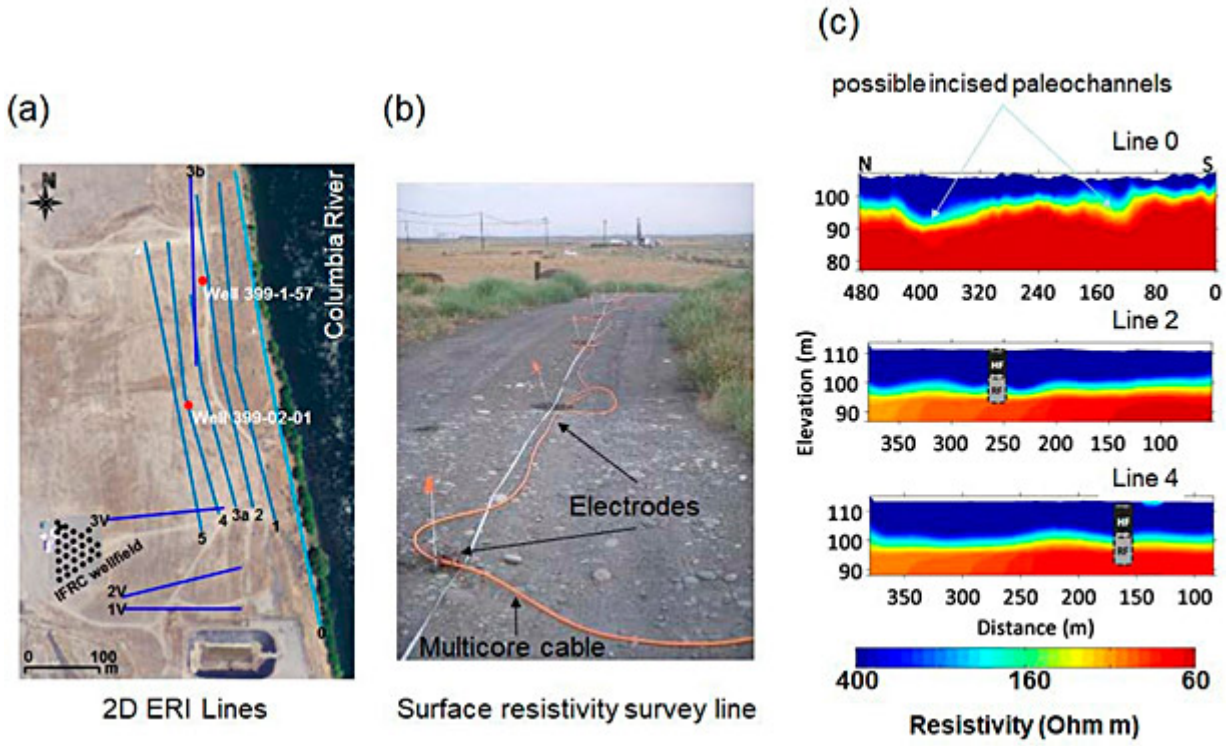

Figure 9-38. ERI survey at the DOE Hanford 300 Area, Richland, WA: (a) 2-D ERI survey line locations, (b) example of line showing site conditions and multicore cable/electrodes, (c) example 2-D images for three of the 10 lines showing strong electrical contrast between Hanford Formation (HF) and Ringold Formation (RF), with location of two boreholes with simplified log shown.

Source: Modified from (Mwakanyamale et al. 2012)

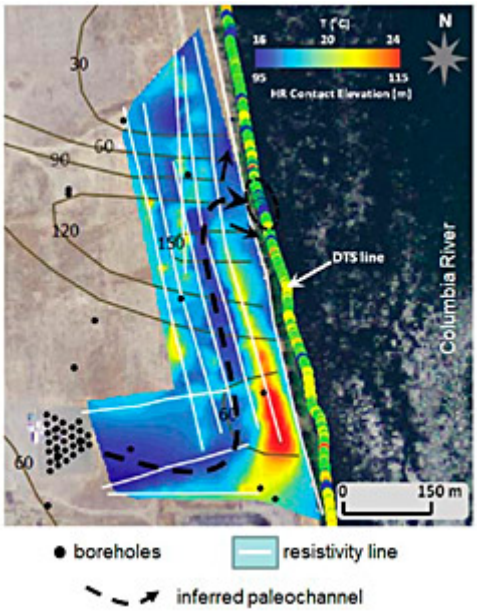

Figure 9-39. Elevation of Hanford-Ringold contact compared to temperature anomalies (from distributed temperature sensing [DTS]) showing [1] groundwater-surface water exchange locations, and [2] contours of uranium concentrations (mg/L) in aquifer from boreholes.

Source: Modified from (Mwakanyamale et al. 2012)

9.11 Surface and Borehole Geophysical Technologies Provide Data to Pinpoint and Characterize Karst Features at a Former Retail Petroleum Facility in Kentucky

Michael Albright
KY Underground Storage Tank Branch
Frankfort, KY
michael.albright@ky.gov

Brad Highley
KY Underground Storage Tank Branch
Frankfort, KY
alan.highley@ky.gov

Information presented in this case study is based on investigations conducted by Mundell and Associates, Hinkle Meyer Environmental Services, and Shield Environmental Associates – See source information below.

Many UST sites in Kentucky are located within the four distinct karst areas underlying the Commonwealth. Karst geomorphology and hydrogeology create unique challenges to effectively characterizing contaminant location and extent as well as characterizing flow dynamics at these sites. Traditional characterization of UST releases in karst terrain involves the initial collection of soil samples (saturated and unsaturated) and groundwater samples from the water table aquifer. Monitoring wells are often installed in rock without adequate knowledge of the karst geomorphology and hydrogeology specific to the point of installation. Monitoring wells thus installed typically provide insufficient information regarding contaminant mass in the epikarst, in solution-enhanced fractures, and in well-developed karst conduits. To address this insufficiency, surface geophysical methods such as two-dimensional ERI, refraction micro tremor, frequency domain electromagnetic conductivity, and low-frequency electromagnetics were used to identify potential bedrock monitoring well locations. Once the borehole was established, geophysical methods, including caliper, gamma log, borehole resistivity, optical televiewer, acoustic televiewer, and heat-pulse flowmeter are employed. Combining these methods increases well-placement efficiency, which supports effective site characterization.

A recent investigation conducted at a former retail petroleum facility in the Eastern Pennyroyal Karst Area near Mt. Vernon, Kentucky demonstrates the critical importance of implementing borehole geophysical technologies to characterize contaminant mass storage and transport in karst terrain. The B&F Gulf Service Station has an extensive history of environmental and public health issues such as vapor in adjacent off-site structures, LNAPL in public utility lines, and LNAPL in off-site monitoring wells. While site investigations spanning the last 20 years had determined that minor amounts of LNAPL and gasoline contaminants are present in overburden soil, shallow epikarst features, and deeper karst features, traditional investigation methods failed to produce sufficient data for construction of a comprehensive conceptual site model. Surface geophysical investigations were performed to identify additional monitoring well locations. Once the new boreholes were established, borehole geophysical logging was performed to 1) locate, differentiate, and map the differing lithologic units underlying the sites; 2) locate and identify karst features, fractures, and bedding planes that may be acting as pathways for the transport and distribution of contaminants; 3) determine the construction of monitoring wells; and 4) refine the CSM.

To characterize the perceived karst terrain underlying the site, a surface geophysical survey was performed in August 2015. Given the required imaging depth of 20 ft to 50 ft below ground surface and the desire to image the vertical and horizontal extent of subsurface features, the survey included seven ER profiles along with FDEM and GPR (see Figure 9-40). This approach was selected because unfractured carbonate rocks in karst terrains are highly resistive and fractured and solution-enhanced rocks have lower resistivity values. When combined with known lithological and structural information, these anomalies can help identify and characterize karst features often at great depths. ER data was collected using an Advanced Geosciences SuperSting™ R8 earth-resistivity meter; FDEM data was collected using a GEM-2 broadband electromagnetic sensor manufactured by Geophex LTD. The surface geophysical survey identified:

- Numerous karst features (sinkholes, springs) during field reconnaissance.
- Several clay and residuum-filled sinkholes
- Several local vertically-aligned low-resistivity zones within the limestone bedrock possibly acting as preferential flow paths, both vertically and horizontally.
- Solution- enhanced fractures and bedding planes are possibly acting as reservoirs and conduits for contaminant transport.

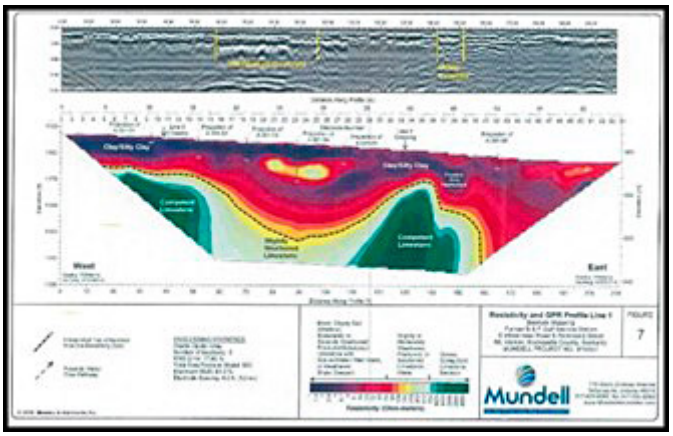

Figure 9-40. Electrical Resistivity and GPR Profile Line 3

To verify these findings, five boreholes were advanced and logged near the B&F Gulf site in October 2016. In May 2018, two additional boreholes were advanced and logged geophysically. Drilling locations were determined using prior surface geophysical survey data. Borehole logging was performed using an optical televiewer probe, acoustic televiewer probe, natural gamma probe, three-arm caliper probe, and EM resistivity probe. The selected tools will allow for well installation in relation to karst features which may be acting as reservoirs and conduits for LNAPL and dissolved phase petroleum hydrocarbons.

Borehole geophysical logging results indicated the following:

- Solution-enhanced fractures and bedding planes are acting as reservoirs and conduits for contaminant transport.
- Borehole logging with the optical televiewer tool identified the presence of LNAPL at the soil\bedrock interface and in the epikarst. The LNAPL is most likely the source of vapor intrusion (see Figure 9-41). Historical vapor intrusion investigations failed to identify the source of petroleum vapor intrusion in adjacent structures.

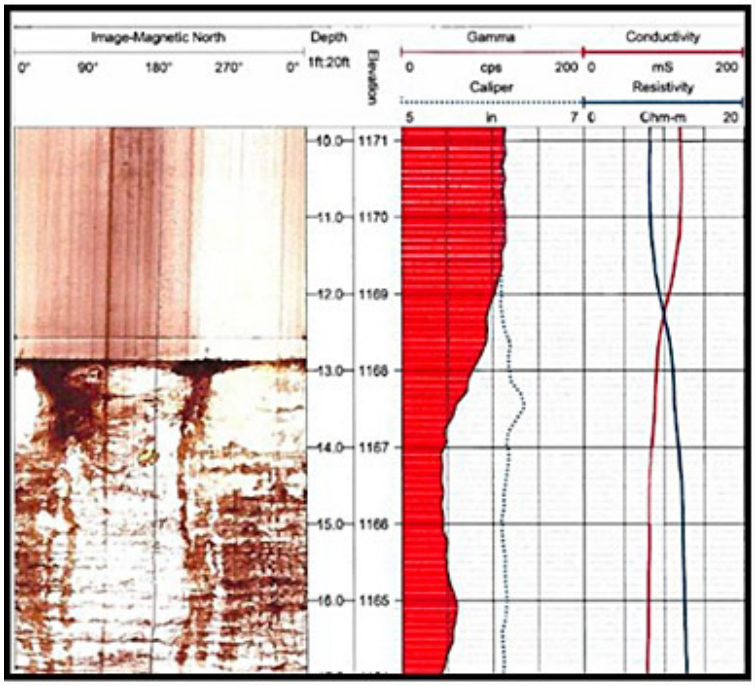

LNAPL Seeping into Borehole from Epikarst Observed by Optical Televiewer in MW-17D

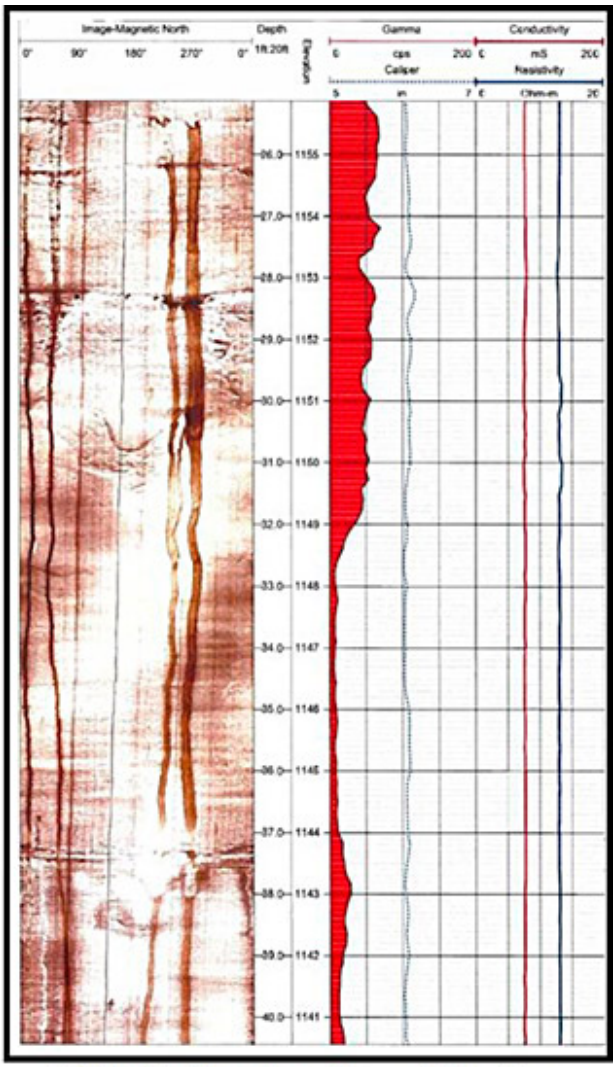

LNAPL Seeping from Solution-Enhanced Fractures Observed with Optical Televiewer in MW-17D

Figure 9-41. LNAPL observed by optical televiewer

The total cost for the surface and borehole geophysical investigations at the site was approximately $83,600. Specifically, the cost of the surface geophysical field investigation and analysis was $16, 800 with an additional $7,000 for project management. The cost of the borehole geophysical investigations was approximately $59,800, which included $37,700 for borehole geophysical logging and $22,100 for borehole advancement and monitoring well installation.

While these costs, and the cost of geophysical investigations in general are significant, the resulting high-resolution datasets allowed the appropriate placement of horizontal and vertical monitoring wells as well as the determination of the appropriate screened interval. This reduced the overall cost and duration of the site characterization and facilitated CSM refinement, which ultimately will lead to timely and cost-effective site remediation.

9.11.1 Source Information

Report of Geophysical Survey: Subsurface and Bedrock Mapping, Former B&F Gulf Service Station, Mt. Vernon, KY, Mundell and Associates, Former B&F Gulf Service Station, Mt. Vernon, KY, Shield Environmental Associates, Hinkle Meyer Environmental Services, November 4, 2015

Intermediate Site Investigation Report, Former B&F Gulf Service Station, Mt. Vernon, KY, Shield Environmental Associates, Hinkle Meyer Environmental Services, January 25, 2017

Report of Geophysical Survey: Geophysical Borehole Logging, Former B&F Gulf Service Station, Mt. Vernon, KY, Mundell and Associates, Shield Environmental Associates, Hinkle Meyer Environmental Services, January 24, 2017

Preliminary Report of Geophysical Survey: Geophysical Borehole Logging, Former B&F Gulf Service Station, Mt. Vernon, KY, Mundell and Associates, Shield Environmental Associates, Hinkle Meyer Environmental Services, May 2018

9.12 GPR Data Show Location of Buried Debris and Piping Associated with a Former Gas Holder in Minnesota

Jennifer Jevnisek
Minnesota Pollution Control Agency
St. Paul, MN
Jennifer.jevnisek@state.mn.us

In 2014, the City of Duluth formally enrolled a vacant city lot in the state's Voluntary Remediation Program. The site, which was planned for redevelopment, is located on a 3.10-acre vacant lot northwest of the intersection of Jay Street and 41st Ave in Duluth, Minnesota (see Figure 9-42).

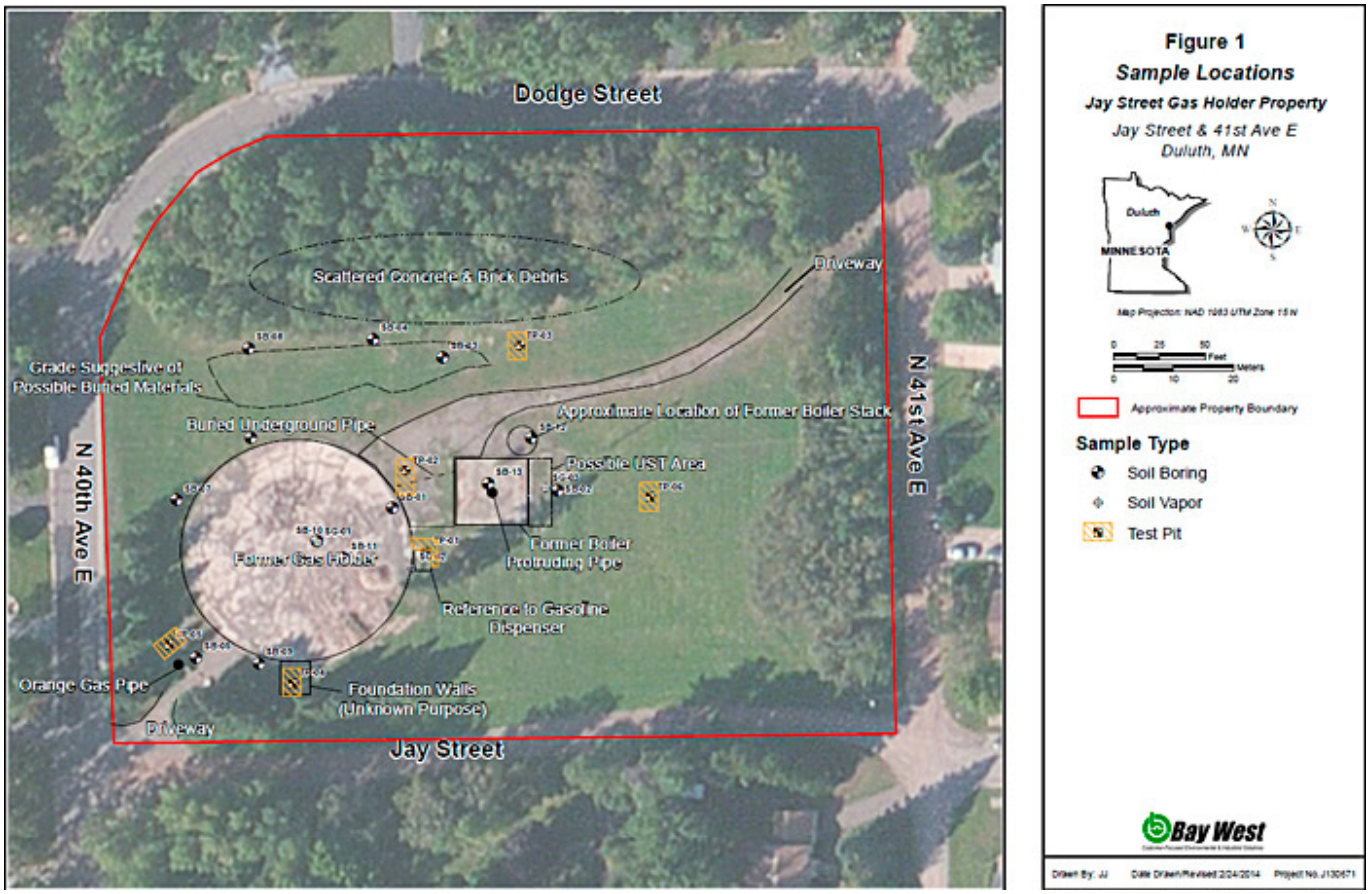

Figure 9-42. Site location of former gas holder in Duluth, MN.

A Phase I Environmental Site Assessment (ESA) (BayWest 2013) noted that the site was previously occupied with a gas holder (a facility used to provide storage in connection with manufactured gas plants). The gas holder was on-site from approximately 1923 until 1960 when the facility was demolished and the associated equipment may have been partially buried on site. Historical documents indicate that the location of the actual manufacturing gas plant site was located miles away. Exact building specifications and demolition information of the gas holder are unknown.

A Phase II ESA, conducted to prepare a Response Action Plan (RAP) for the project, noted that site geology consists primarily of sand and gravel with layers of silty sand, sandy silt, silty clay, and silt. The report also noted that bedrock was not encountered in borings placed as deep as 20 ft below ground surface. Investigation work encountered groundwater at depths ranging from 3 ft to 17 ft below ground surface.

In October 2013, a site reconnaissance was conducted as part of due diligence efforts. (BayWest 2013) noted building debris in the wooded area directly north of a former boiler and an area of elevated ground surface consistent with the description of

where chimney debris associated with the former gas holder would have been buried. Because the extent of buried debris and demolition material was unknown, a limited GPR investigation (see Figure 9-43) was conducted in November 2013 to assess the location of this material. GPR was selected based on its ability to noninvasively provide images of man-made objects in the near subsurface.

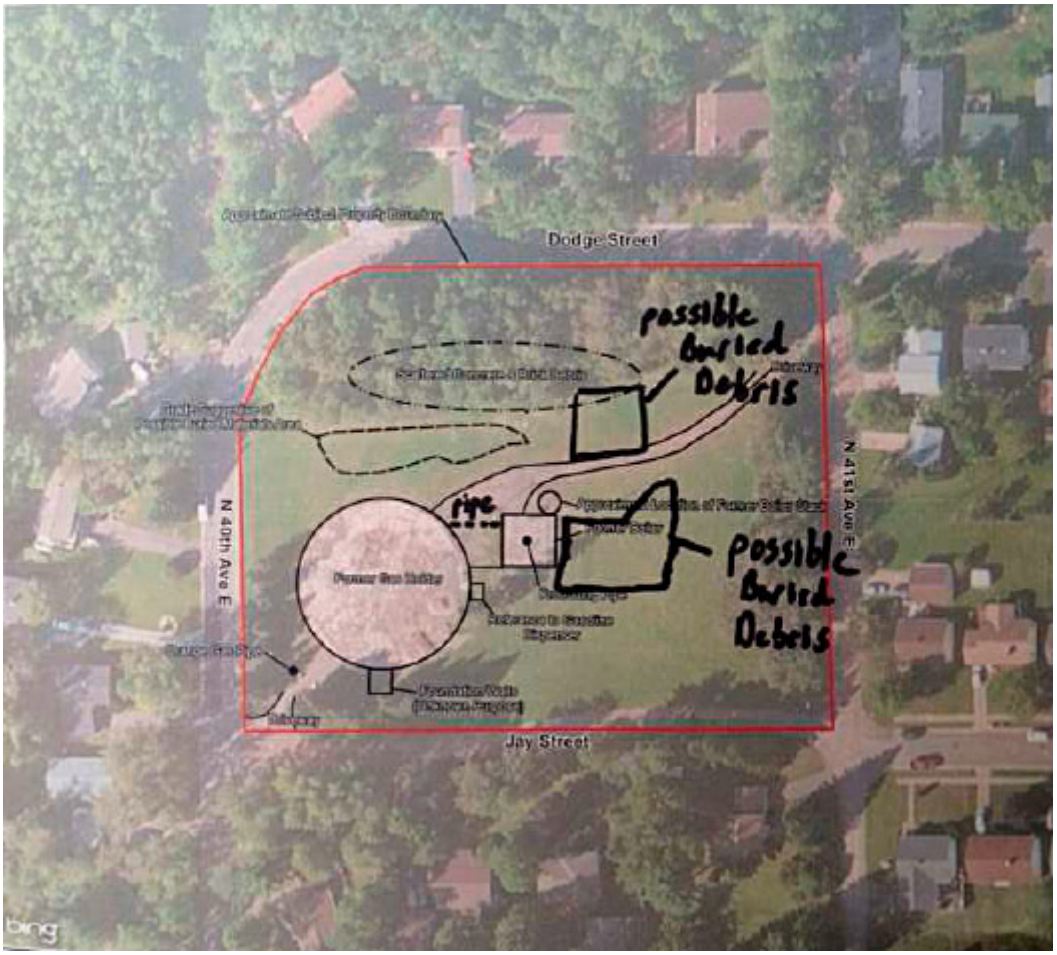

Figure 9-43. GPR investigation area, as presented in report from contractor.

Scans were collected with the GPR unit in parallel lines approximately 3 ft on center. The GPR unit was able to detect to approximately 4 ft below ground surface. The assessment revealed two locations with possible buried debris at depths of 2 ft to 4 ft below ground surface (see Figure 9-44 and Figure 9-45) near test pits TP-03 and TP-06 (see Figure 9-42 for test pit locations). The data images in Figure 9-45 for TP-06 were from scans performed just east of the former boiler room. The GPR equipment consistently picked up images of either fill material or disturbed soil in this area. The cost of this assessment was $3,200.

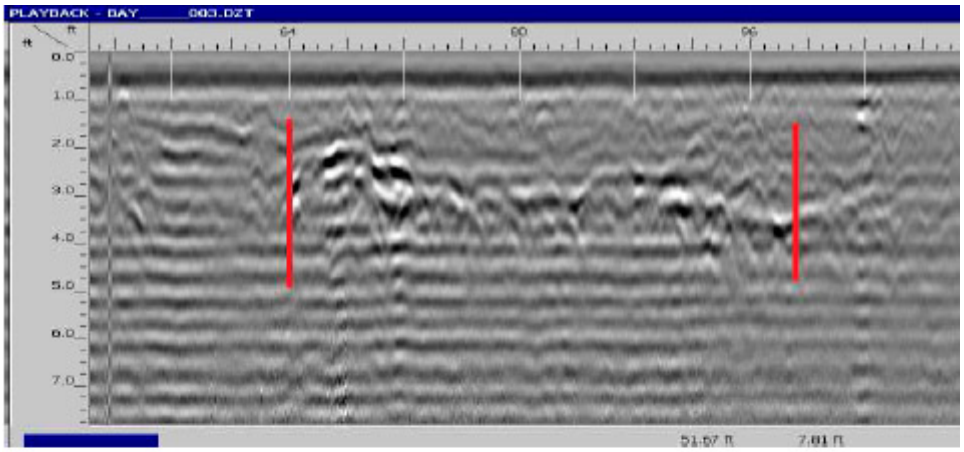

This data image shows some possible buried debris at 2-4 feet deep. The next picture corresponds with this data image.

Figure 9-44. GPR scan and input from GPR contractor. Location pertains to TP-03.

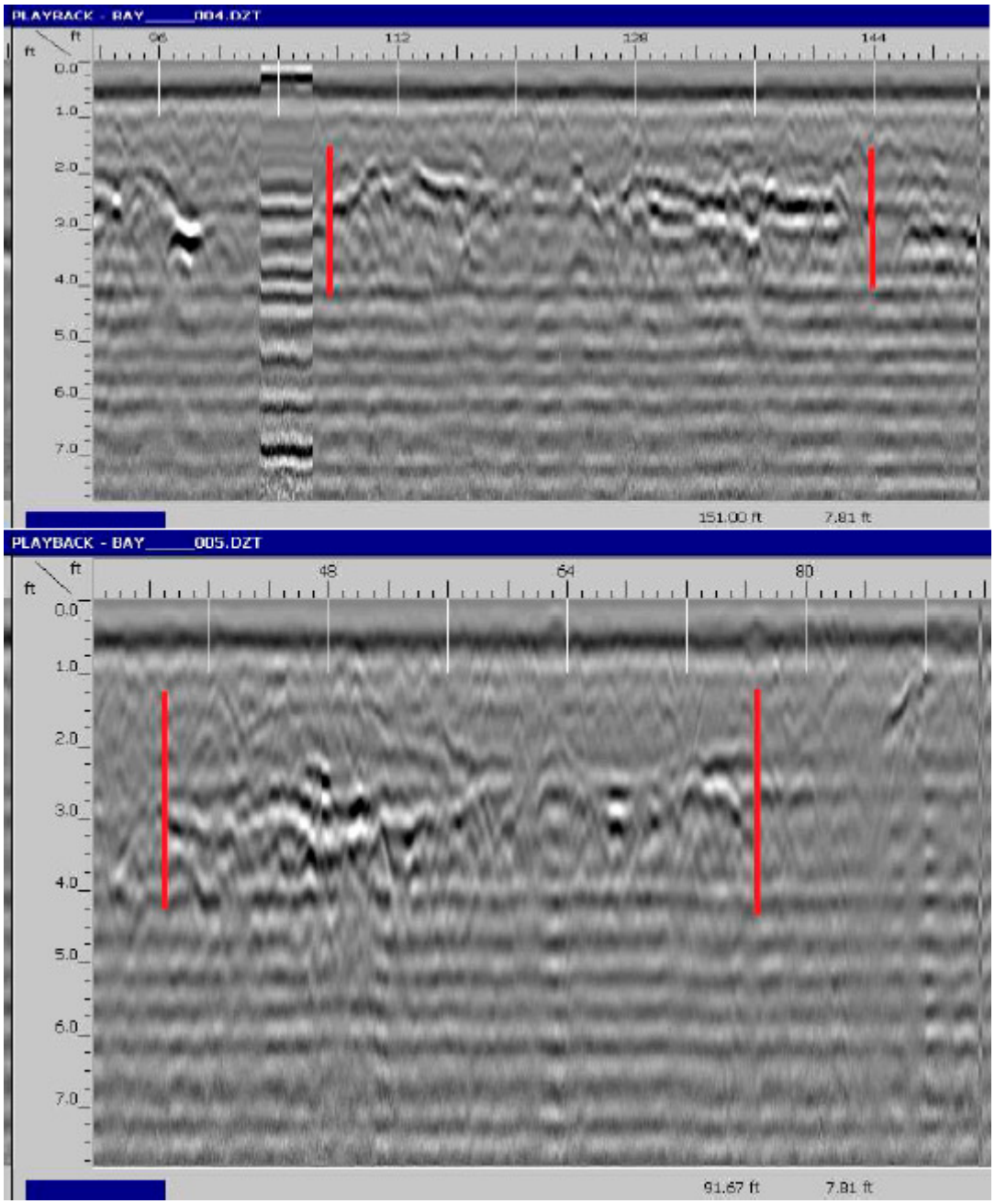

Figure 9-45. GPR scan near TP-06 (see Figure 9-42 for location of TP-06).

A subsequent test pit investigation was performed in January 2014 to confirm the findings of the GPR assessment (BayWest 2014). The investigation confirmed the presence of debris at TP-03 at a depth of 2 ft to 6 ft below ground surface. The GPR assessment also identified a pipe connecting the former gas holder to the former boiler at approximately 2 ft to 2.5 ft below ground surface (see Figure 9-46); its presence was confirmed at test pit TP-02 where it was encountered at approximately 2 ft below ground surface.

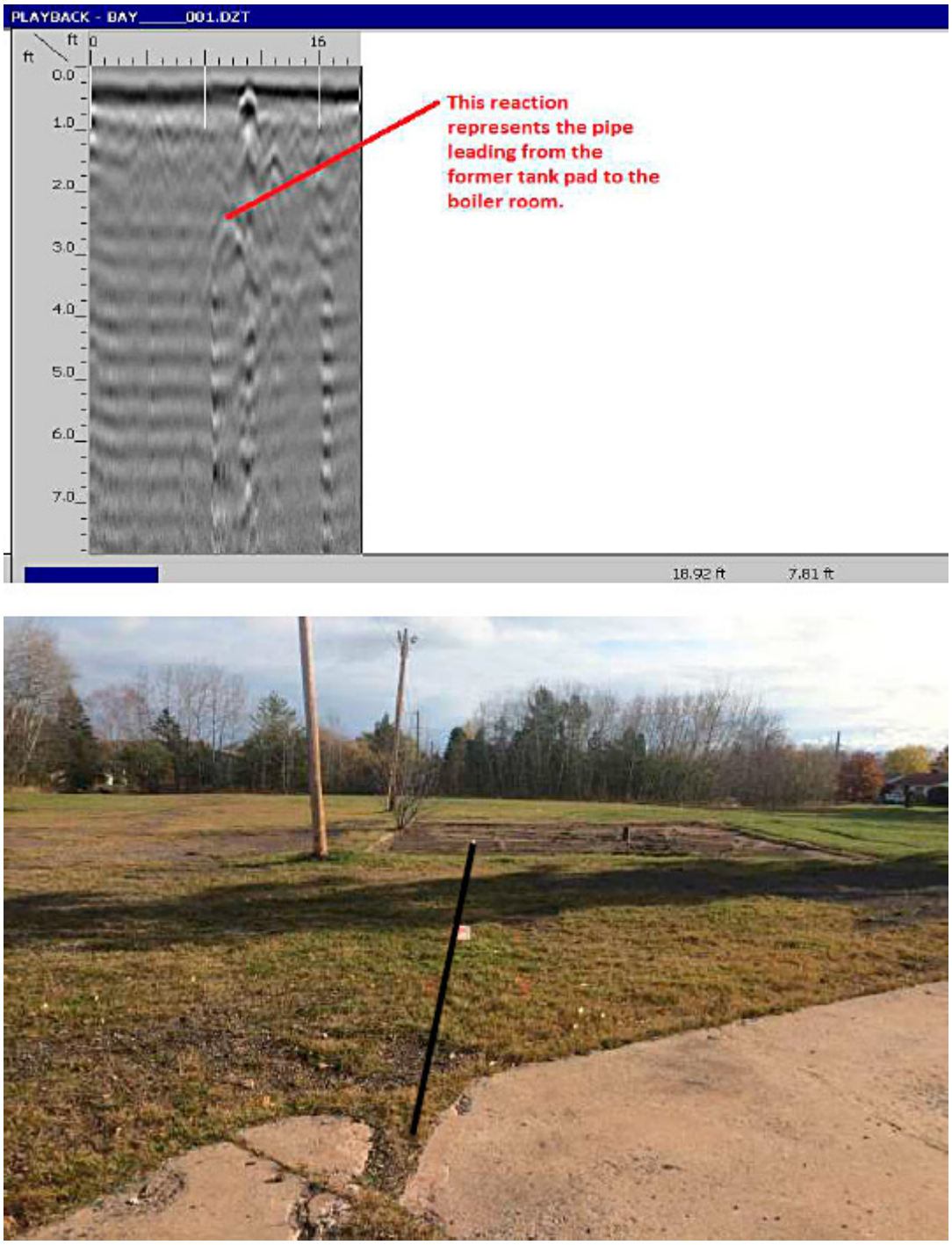

Figure 9-46. GPR scan and photo near TP-02 (see Figure 9-42 for location of TP-02).

Data obtained from the GPR assessment and test pit excavation were used in conjunction with supplemental soil and groundwater data to develop a RAP, (BayWest 2016). Response actions included soil stabilization, excavation, and disposal, removal of concrete and asbestos containing material, and the removal of debris comingled with soil (BayWest 2016).

The city representative noted that while the tool was effective at identifying features in the survey area, a significant amount of material had been overlooked and was discovered during redevelopment (BayWest 2016). The suspicion was that overlooked material was not due to technology failure, but because a portion of the site had not been investigated with the tool. The discovery of overlooked material and associated costs resulted in project overruns and a fair amount of bad will among project stakeholders.

9.13 Resistivity, Seismic Exploration, and GPR Provide Data to Evaluate Clay Reserves at a Commercially Mined Pit

Lisandro Suarez
CT Department of Energy and Environmental Protection (DEEP)
Hartford, CT
lee.suarez@ct.gov

The purpose of this case study was to evaluate the clay reserves at a commercially mined clay pit. Geophysical techniques including GPR, ERT, and seismic exploration were used to help characterize a shallow stratigraphy. For clay mining purposes, the main objectives of performing these tests were to proof a clay deposit (with the intention of planning extraction operations). GPR techniques were not good to use on materials that exhibit low ER, such as clays. Nevertheless, GPR provided an estimate of the thickness of the top sand layer and an approximate depth to perched groundwater or depth to water table. In contrast to GPR, ERT was used particularly on materials that exhibit low resistivity. Resistivity-supplied information related to the clay-layer thickness and its heterogeneity. Seismic exploration was used to provide a better estimate of the thickness of the clay layer and the depth to bedrock.

Prior to the geophysical survey, a review of the U.S. Geological Survey bedrock geological map for the project quadrant was performed to help in understanding the local stratigraphy and soil characteristics.

Figure 9-47 is an aerial photo that shows where the geophysical surveys were performed. Line 1 (150 m) was the west-east line profile where DC-resistivity and seismic exploration were performed. Line 2 (150 m) was the south-north line profile for DC-resistivity and seismic exploration surveys. The GPR profile was performed along the arrow marked as GPR.

Figure 9-48 contains the Dipole-Dipole method (top image) and Schlumberger method (bottom image) resistivity test result for line 2. The north-south profile (line 2) in Figure 9-48 was adjusted for topography by using Global Positioning System (GPS) technology. In general, all three profiles showed a clay layer with resistivity values between 10 and 150 Wm. The clay was fairly homogeneous throughout the first 20 m to 30 m below the sand layer. Perched groundwater or saturated sand and clay were found at the contact between the two distinct permeability layers (sand overlying clay) as indicated by the high resistivity values found toward the south end of the profile. In the instance when the underlying soil became saturated, the perched groundwater elevation became, by definition, the water table elevation. The survey profile for line 1 was similar to line 2 and indicated that the clay layer was relatively homogeneous.

Figure 9-47. Aerial photo showing the approximate location where the geophysical surveys were performed.

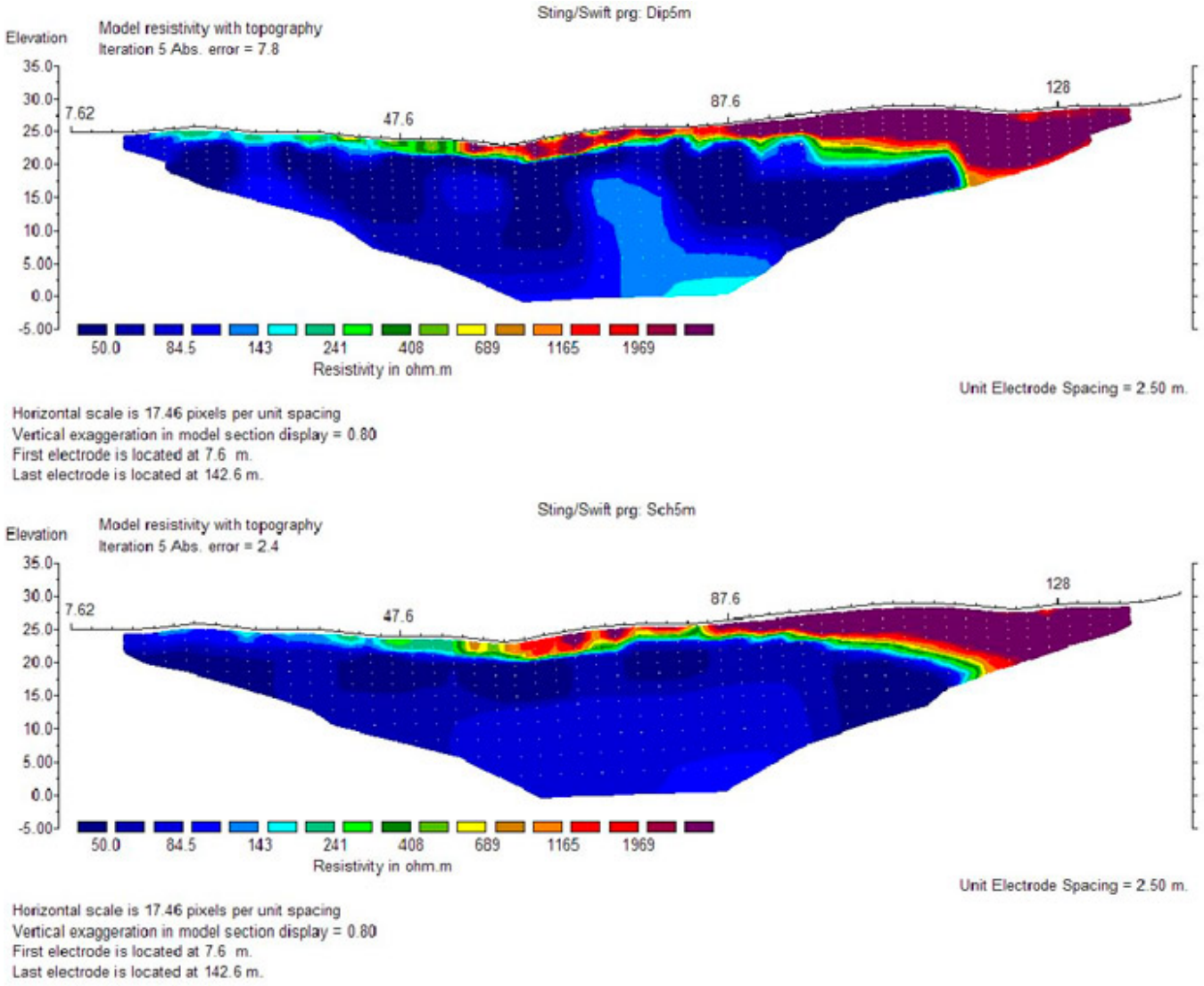

Figure 9-48. The the inverse model for line 2 (north to south, from left to right of the profiles above) in which the true resistivity values of the subsurface tested were represented. (All distances in meters).

The goal of the seismic survey was to determine the approximate depth-to-bedrock. The data obtained to construct the site's depth-to-bedrock profiles were mined by using refraction and reflection. Basically, three soil layers were found: A thin sand layer, a thick clay layer, and bedrock. Figure 9-49 shows the north-south lithostratigraphy and depth-to-bedrock graph based on refraction and reflection techniques (north to south). The sand layer was delineated in pink. The west-wast lithostratigraphy was similar and showed bedrock at approximately 30 m of depth.

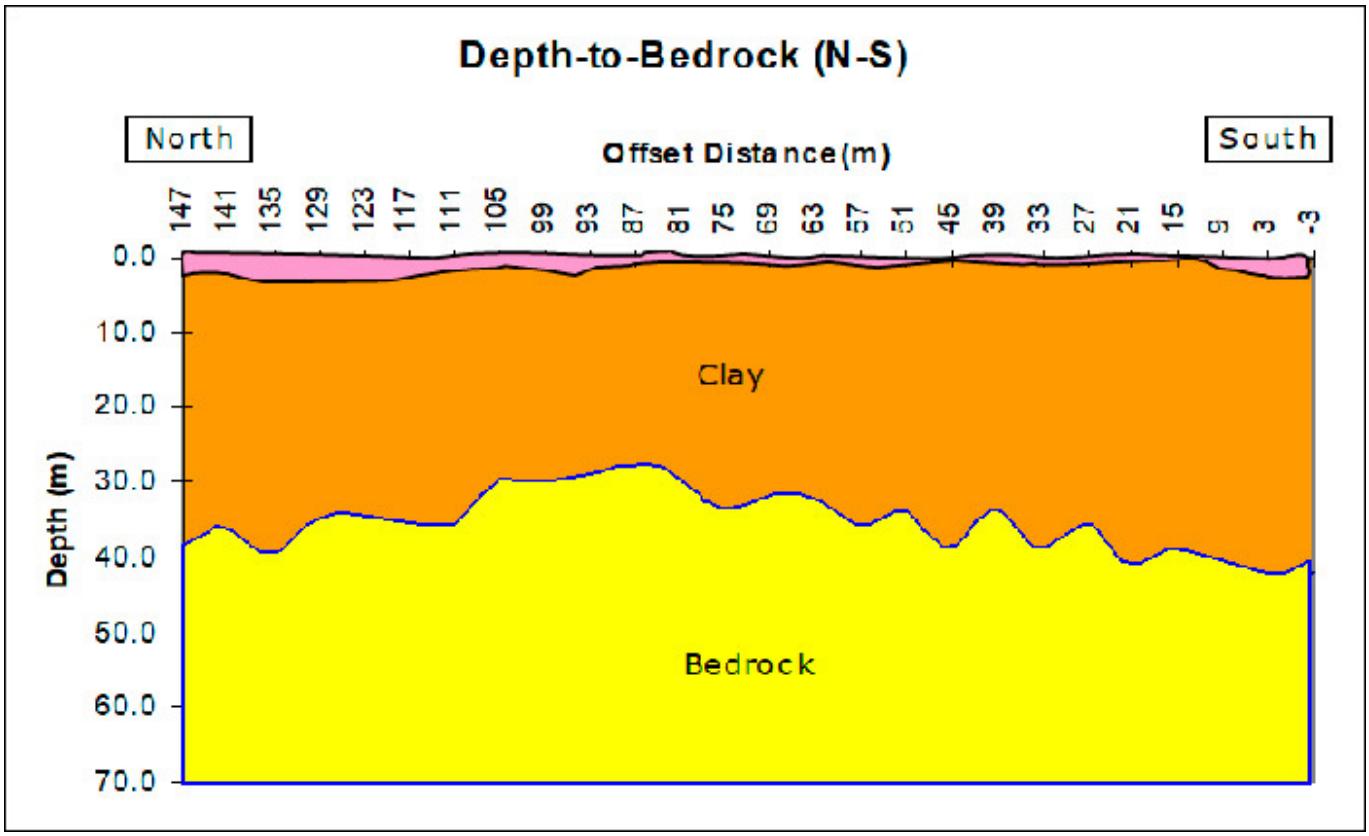

Figure 9-49. North-South lithostratigraphy and depth-to-bedrock graph based on refraction and reflection techniques (north to south).

The purpose of the GPR survey was to delineate the sand layer from the clay layer with the intention of evaluating the volumetric tonnage of sand necessary to be stripped off before the clay layer could be properly mined. The resultant information was also used to plan and calculate the equipment necessary in the process as well as labor hours and other logistical issues.

The GPR survey (see Figure 9-50) showed a layer of sand of about 2 m thick present on the north side of the site; it gradually decreased its thickness at a rate of about 2 cm/m toward the south. At about 100 m from the benchmark, the thickness of the sand layer was just a few inches. A clay layer was under the sand and the GPR could not penetrate it. It was expected that groundwater flowed at the interface between the sand and the saturated clay layers. No surface topography adjustment was made as the surface had relatively minor changes in elevation (zero-slope, man-made dirt road).

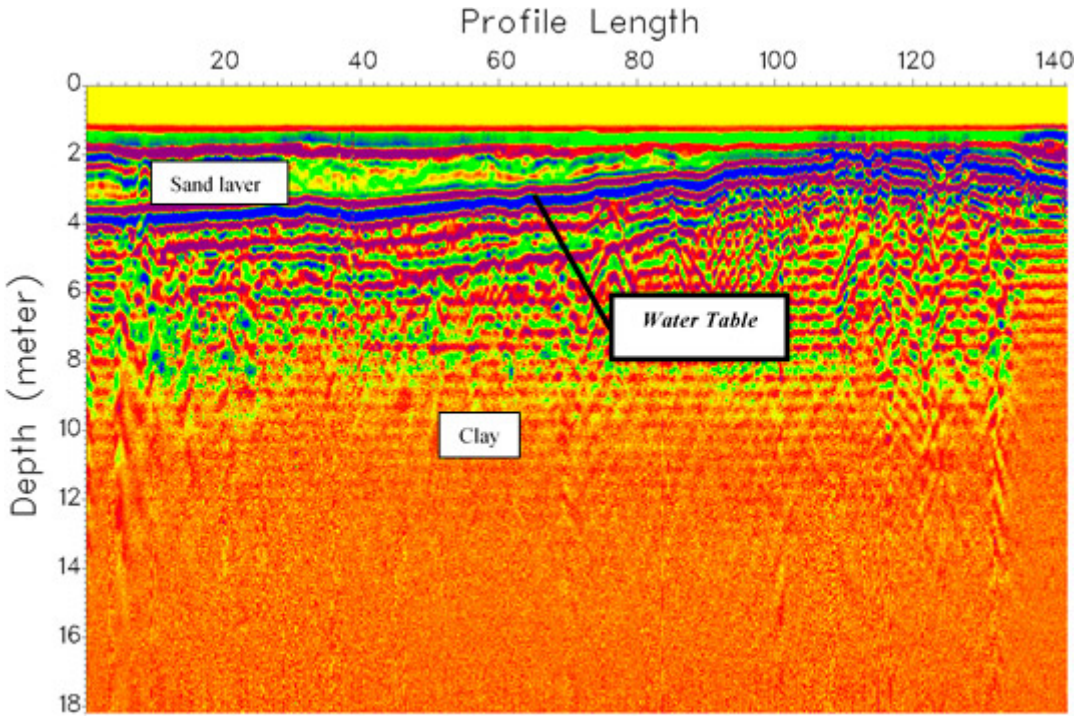

Figure 9-50. GPR test result. The profile run from the north end of the proposed area (left corner, at 0 m) to the south end (right corner, at 140 m).

This combination of geophysical methods was performed to support decisions made by the management of a brick manufacturing company. Because bricks are made primarily out of clay, brick manufacturing companies are continuously monitoring their clay reserves and the clay properties that affect quality. Test results obtained on this project provided sufficient evidence that the clay was of great quality and there was plenty of volume to continue manufacturing bricks for many years to come.

The cost associated with this project was less than $100; in-kind services were provided by the University of Conneticut and the USGS.

9.14 Seismic Refraction, Electric Resistivity, and Multichannel Analysis of Seismic Waves Provide Data to Locate Monitoring Well Locations in a Mixed-Use Area in Northern Virginia

Nathan Stevens, PG
Kleinfelder, Inc. (Maine)
Westborough, MA
nstevens@kleinfelder.com

At a site in a mixed commercial and residential area in northern Virginia, a recent assessment identified MTBE in bedrock groundwater at locations cross gradient to groundwater flow. Based on these results, additional bedrock monitoring wells were needed. Area mapping and local reconnaissance, in combination with borehole geophysical and aquifer testing, indicated that relatively discrete, steeply dipping fractures were potentially responsible for both movement of contaminated groundwater from the overburden to bedrock and transport of MTBE away from the site. Surficial geophysical technologies were selected to allow the determination of appropriate and feasible monitoring well locations and because the methods overcame the following site-specific challenges: density of development in the area; the proximity of potential receptors (private potable wells)' and properly identifying top of bedrock, potential fractures, and feasible drilling locations. In addition, the methods needed to be acceptable to the regulatory authority, understandable to the public, readily available, and cost effective.

Seismic refraction (SR), ER, and MASW were used to identify potential monitoring well locations. A total of 550 linear ft of ER survey, 1,500 linear ft of MASW, and 2,100 linear ft of SR were performed over three days along roadways or through commercial parking lots.

Based on the initial data described above, two ER lines were conducted south of the site using an Advanced Geosciences SuperSting™ R8 earth-resistivity meter and Swift automatic electrode system in dipole-dipole arrangement (see Figure 9-51). Approximately 3,000 soundings were collected. The electrode spacing (dipole size) was 6.6 ft to 10 ft and used 32 and 35 electrodes. ER data, when analyzed, identifies contrasts in the conductivity (inverse of resistivity) of the subsurface. Patterns in the contrast of conductivities are a line of evidence to the location of clays, bedrock, and potentially saturated fractures. The end result is an illustration of basic stratigraphy of the study area.

Figure 9-51. ER lines conducted on the site

Seven SR lines were conducted using a 24-channel Geode Seismograph with 10-Hz geophones and a 10-pound manual hammer. Two of the SR lines were conducted in a roll-along setup to maintain vehicle traffic in the public roads. Each line used 10-foot geophone spacing and five source locations. SR ER data, when analyzed (see Figure 9-52 for an example), identifies differences in seismic velocity due to the bending of seismic waves as identified by the time required for the signal to travel from the source (hammer) though the subsurface and to the receiver (geophones). Patterns in the contrasts of seismic velocities can indicate the depths and locations of weathered and competent rock as opposed to overburden unconsolidated materials. The end result is an illustration of the stratigraphy of the study area.

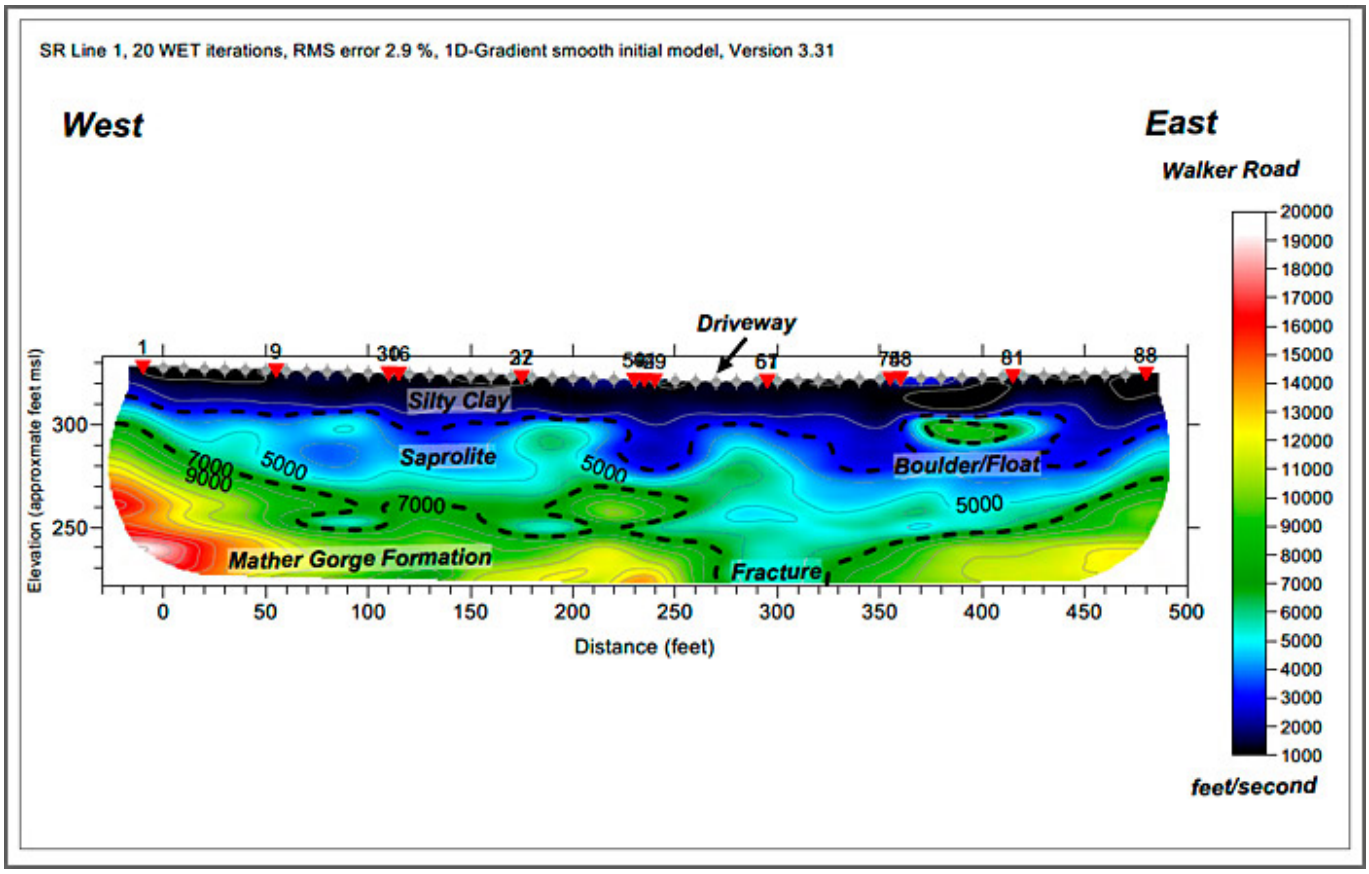

Figure 9-52. Seismic refraction profile along line 1

Five MASW lines were conducted. Data collection was performed using a 24-channel Geode Seismograph with 10-Hz geophones and a 12-pound hammer. Sources were placed at each end and on 10-foot centers. MASW uses the surface wave component of the seismic signal, in conjunction with the body-wave component used by SR, within a frequency/velocity model to identify anomalies in the stratigraphic model developed using SR. These anomalies can represent fractures or fracture zones, especially those that intersect the top of the competent bedrock as determined by SR and ER (see Figure 9-53 for an example).

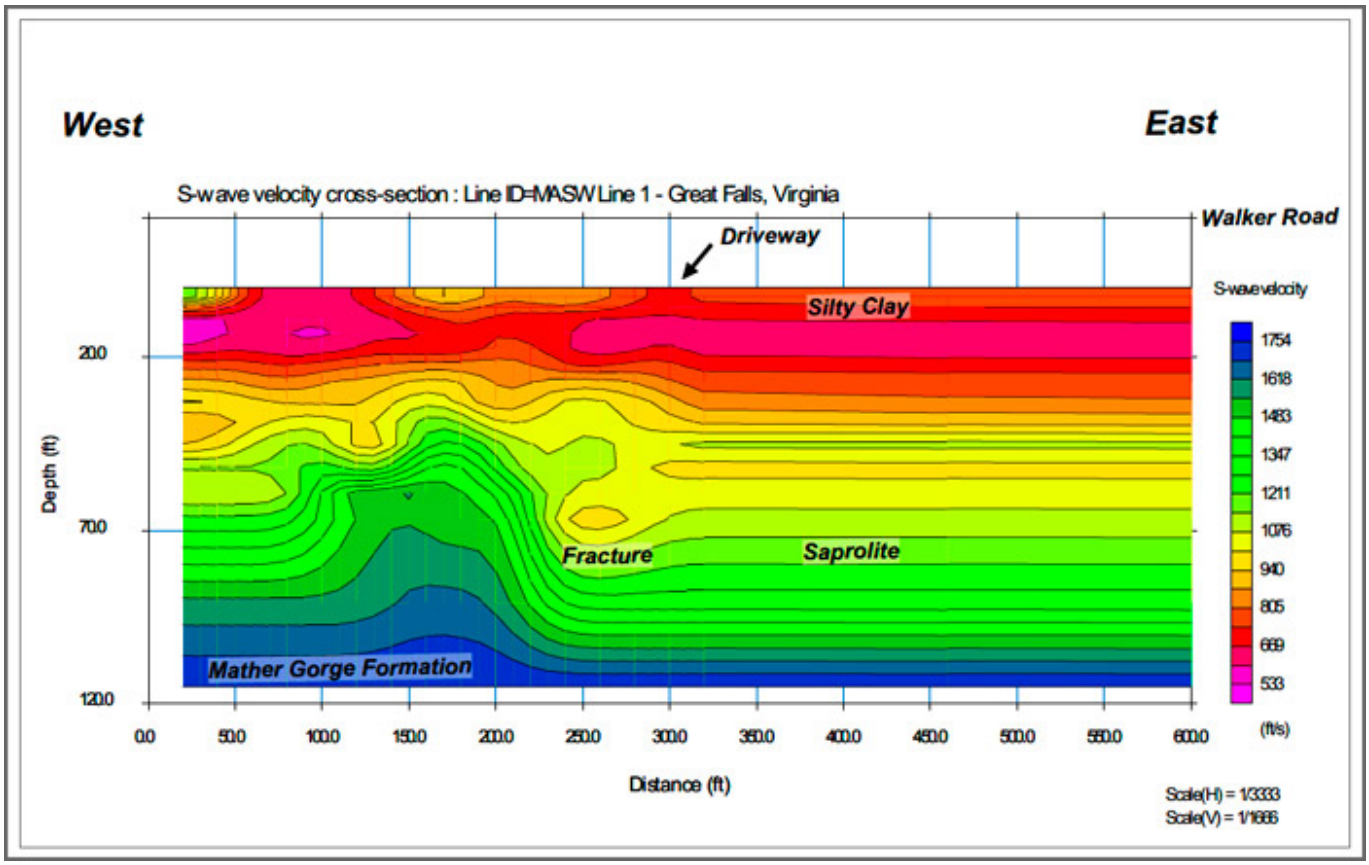

Figure 9-53. MASW profile along line 1

Surficial geophysical results allowed the identification of a trend of anomalies categorized as a fracture zone and the subsequent determination of monitoring well locations. The justification for these locations was easily understood by the regulator and public because of the developed figures. The figures provided documentation of the various lines of evidence offered by each technique, profiles of the interpreted subsurface, and plan shown on an aerial photo base. This approach became the basis for installing sentinel monitoring wells between the site and potential receptors and served as an important component when presenting the CSM subsequent meetings.

The cost of the geophysical survey was approximately $15,000, which was less than one-half the cost of a single well and provided important assurances to all stakeholders that the selected monitoring well locations were appropriate.

9.15 Surface Geophysical Methods Provide Data to Identify Prospective Utility Waste Landfill Sites in Karst Terrain in Missouri

Elanz Siami-Irdemoosa
Missouri Department of Natural Resources
Jefferson City, MO
elnaz.siami-irdemoosa@dnr.mo.gov

A 42-acre utility waste landfill (UWL) is permitted through the Missouri Department of Natural Resources (MDNR) to receive coal combustion residuals from the combustion of coal at the John Twitty Energy Center (JTEC). The JTEC is a coal-fired power station located at the southwest boundary of the City of Springfield in Greene County, Missouri (Springfield 2016). As the existing UWL was filling to capacity, a new UWL was required to be located and developed at the 800-acre JTEC site.

The bedrock surface at the site consists of Burlington-Keokuk Limestone. Its thickness may vary from 150 ft to 250 ft due to high degree of weathering. The weathered and irregular bedrock is hidden below a mantling of chert clay residuum with thicknesses varying from a few feet to over 40 ft. Most karst features in southwest Missouri are developed within this formation, which includes solution-widened joints, pinnacles, solutional sinkholes, and collapse sinkholes (MDNR-SWMP 2015). The MDNR had two main concerns in siting a UWL in karst terrain: 1) ensure sinkhole collapses do not result in failures of the landfill liner system or instability of the landfill foundation and 2) monitor the uppermost continuous aquifer beneath the landfill. ERT and MASW methods were selected to characterize the nature and extent of the karst system at the site and identify a suitable UWL site (MDNR-SWMP 2015). ERT and MASW techniques have proven to be the best geophysical methods for investigations in karst terrain, particularly when the overburden soil is clay dominated (Van Nostrand and Cook 1966); (Frankline et al. 2019); (Zhou, F. Beck, and B. Stephenson 2000). The high contrast in resistivity values between carbonate rock and clayey soil allows the determination of the soil-bedrock contact (Siami-Irdemoosa 2017).

A total of 374,922 linear ft of ERT data was acquired along 183 traverses. The length of the traverses varied from 625 ft to 8,680 ft. ERT data were collected mostly along parallel west-east oriented and north-south oriented traverses. MASW data were acquired at 240 specific locations along west-east oriented ERT traverses and (mostly) at 400 ft intervals (see Figure 9-54) (MDNR-SWMP 2015).

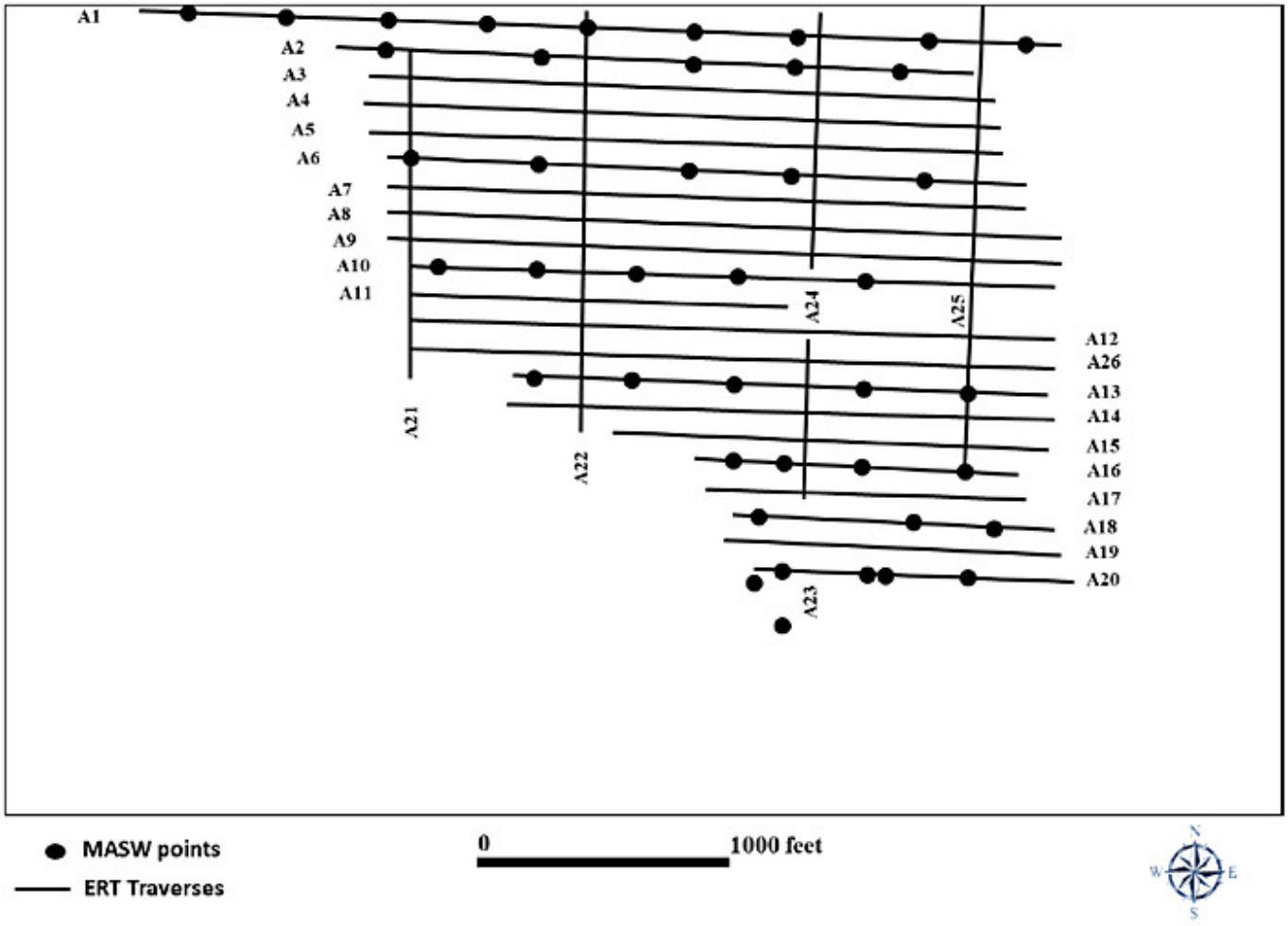

Figure 9-54. Layout of ERT traverses and MASW locations at the investigation site (Area A).
Source: (Siami-Irdemoosa 2017)

ERT data were interpreted to map the soil-bedrock interface, soil thickness, variation in rock quality, and joint sets and to characterize the existing sinkholes (see Figure 9-55b). The MASW data were also interpreted to map the soil-bedrock interface, map variation in soil thickness, determine the engineering properties of soil and rock, and validate the ERT interpretation (especially with respect to mapped top of rock) (see Figure 9-55a and Figure 9-55c) (MDNR-SWMP 2015).

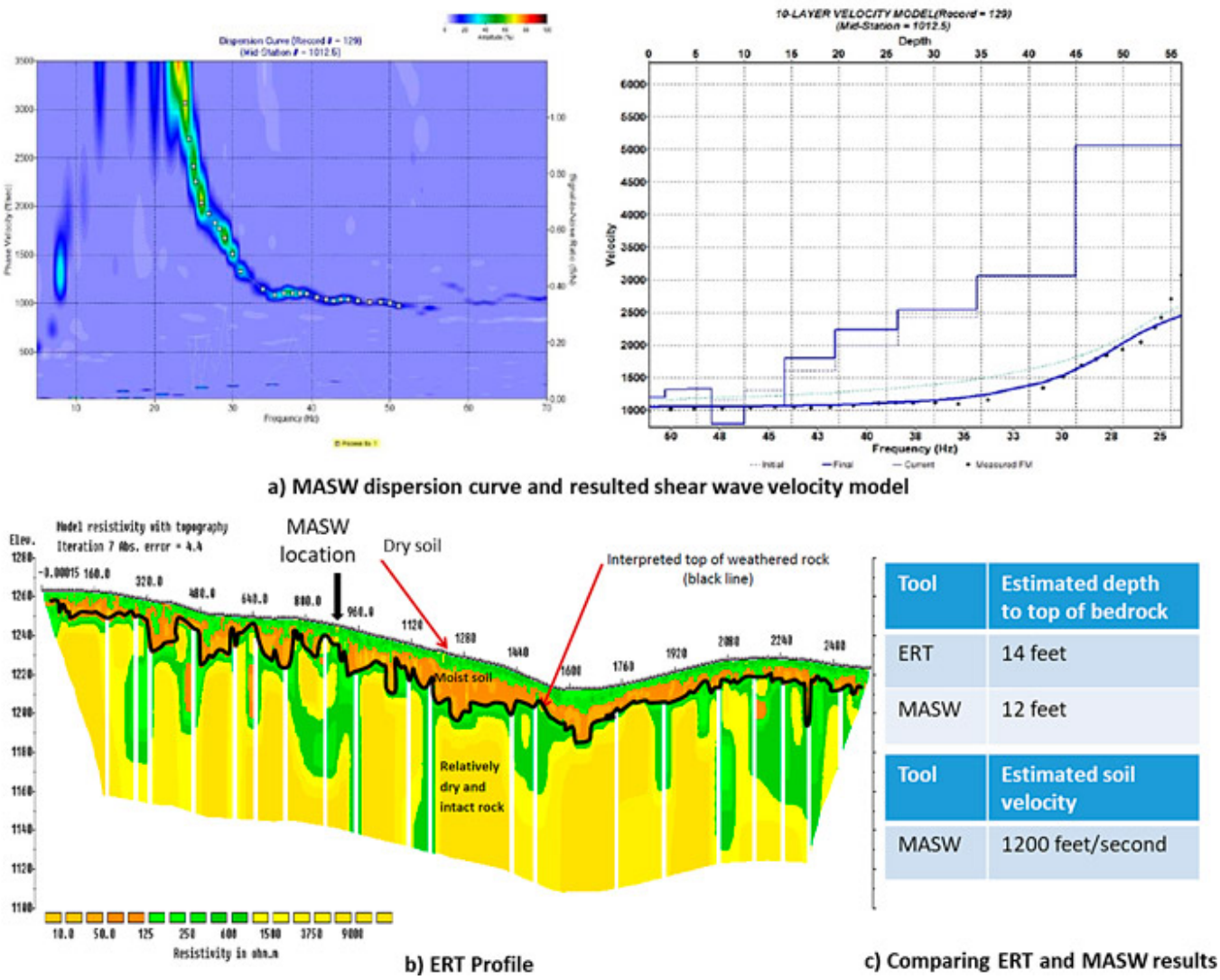

Figure 9-55. ERT and MASW data interpretation; a) MASW array dispersion curve and shear-wave velocity model.

Source: (MDNR-SWMP 2015)

The geophysical surveys were complemented by site reconnaissance, confirmatory drilling, downhole video, and downhole LiDAR. Data from fifteen (15) boreholes were correlated with the interpreted ERT profiles and MASW data to validate the interpretation. A hollow-stem auger was used to drill the boreholes on the bedrock surface, and the bedrock was core drilled using HQ™ core barrels and NQ™ core barrels. A corehole encountered a subsurface void immediately east-southeast of a large solutional sinkhole along an ERT profile. A high-resolution downhole camera was used to inspect the subsurface void. An LED-based detection and ranging (LEDDAR) technology was employed to further map the encountered void (MDNR-SWMP 2015).

The primary findings of the site investigation include the following:

- The interpreted soil-bedrock interfaces from ERT profiles and MASW correlate well with borehole control.
- Soil thickness is variable at the site and varies between about 5 ft and 30 ft.
- Two sets of visually prominent orthogonal joints were identified on site: the north-south trending joint sets and the west-east trending joint sets. The north-south trending joint sets are more prevalent on site, with a density of approximately 1/100 ft. The density of the west-east trending joints sets is approximately 1/200 ft.
- Aerial photographs of the site revealed that most visually prominent joint sets are associated with either cultural features that concentrate runoff, natural surface drainage features, or confirmed sinkholes. Over half of the identified visually prominent joint sets are culturally influenced and more than 80% are cultural or drainage influenced.
- A few numbers of solutional sinkhole, collapse sinkhole, and closed depressions were identified during the site

reconnaissance. The potential for a sinkhole collapse is low based on the investigation findings.

Based on the results of ERT survey, MASW control and supplemental investigation, two prospective sites were identified as the best alternatives for UWL development.

9.16 Airborne Time-Domain Electromagnetic Method Maps Sand Distribution along the Illinois Lake Michigan Shore

Kisa E. Mwakanyamale
IL State Geological Survey
Prairie Research Institute
Univ. of IL at Urbana-Champaign
Champaign, IL
kemwaks@illinois.edu

Steven E. Brown
IL State Geological Survey
Prairie Research Institute
Univ. of IL at Urbana-Champaign
Champaign, IL

Andrew C. Anderson
IL State Geological Survey
Prairie Research Institute
Univ. of IL at Urbana-Champaign
Champaign, IL

Ethan J. Theuerkauf
IL State Geological Survey
Prairie Research Institute
Univ. of IL at Urbana-Champaign
Champaign, IL

From Kenosha, Wisconsin to Chicago, Illinois the Lake Michigan coastline is a dynamic system of land uses and habitats where lasting benefits start with scientific understanding of how it all works together. Sediment distribution along this shoreline is constantly changing in response to increased human activities and complex natural coastal processes associated with wave action, short- and long-term fluctuations in lake level, and the influence of coastal ice. Beach sand is a critical coastal resource that helps alleviate beach and bluff erosion, often endangering sensitive ecosystems and habitats. Most sand along the Illinois Lake Michigan coast is transported from north to south as a result of the dominant waves approaching the shoreline from the north and northwest. Sand is also diverted and trapped by harbors and lake-fills along the Illinois shore, depleting the supply of littoral sand for longshore drift, also resulting in significant dredging costs, and impacts on recreational and commercial boating. The Illinois Coastal Management Program (ICMP) at the Illinois Department of Natural Resources is prioritizing sand management to protect the natural and cultural resources along this important shoreline.

This project complements efforts of the ICMP and the Illinois State Geological Survey (ISGS) to improve regional sand management along the Illinois Lake Michigan shoreline by mapping the thickness of nearshore sand. Developing a regional coastal information system is one of the main components of the long-term sand management plan. This project is focused on filling the information gap on sediment distribution in coastal waters off the Illinois coast. Understanding the characteristics and dynamics of nearshore sediment distribution is critical in unraveling patterns and processes of coastal erosion and accretion. To inform a regional sand management strategy, high-resolution, helicopter-transient electromagnetic (HTEM) data were collected along the southwestern Lake Michigan coast, surveyed about 73 miles from Kenosha, Wisconsin to Chicago, Illinois and about 0.6382 miles lakeward (see Figure 9-56). New developments in airborne time-domain electromagnetic method in terms of instrumentation, data processing, modeling, interpretation algorithms, and measurement techniques coupled with the ability to measure large areas during short time periods make HTEM a cost-effective method for providing regional coverage. The HTEM method was used in this study to improve the quality of data and ground coverage of the entire shoreline.

The main project objectives are to 1) map the distribution of unconsolidated sand along the entire 73-mile stretch of the southwestern Lake Michigan coast and 2) demonstrate the value of collecting high-density HTEM data to improve the resolution and reliability of lithological mapping, and 3) show its applicability to long-term monitoring. The intended results from this project are maps and cross sections showing the extent and thickness of sand deposits, both around structures as well as further lakeward, and the extent of erosion and lake-bottom down-cutting. Understanding sand, the degree of erosion, and extent of down-cutting will facilitate decision making regarding the protection and improvement of critical coastal infrastructure. Identifying sand sources will aid in developing a regional sand redistribution model, possibly allowing the comparison of economies and efficiencies of various beach nourishment methods.

9.16.1 Survey and the Study Site

The Lake Michigan bottom is underlain primarily by sandy glacial deposits, and the bedrock under the glacial deposits is dolomite. Lake-bottom sand is distributed over the clayey glacial deposits, but areas along the south of the Illinois shoreline have dolomite near or at the land or lake-bottom. Using a dual-moment HTEM system allows both deep and shallow deposits of sand and clayey till to be targeted, with the possibility of mapping the bedrock topography. A line spacing of 100 m (328 ft) was used to provide high-lateral resolution of the thin sand layer overlying the clayey glacial sediment.

The HTEM survey covered nine approximately 117-km (about 73-mile)-long traverse lines running north-south along the

coastline approximately 100 m (328 ft) apart (see Figure 9-56), with several perpendicular lines of variable lengths where possible (areas with little to no cultural features). The total line km flown was 1,049 km (652 miles). The survey outline is presented in Figure 9-38 with lines stretching from Kenosha in the north of the study area to south of Chicago.

The Illinois Lake Michigan coast is highly urbanized, resulting in challenges during data collection and causing noise in the acquired data. The presence of cultural features close to the lake (for example, buildings, boats, roads, and power lines) pose safety risks and are a source of noise to the HTEM data, causing survey (flight) lines to be diverted lakeward to the safe distance (see Figure 9-56). The safe distance is counted as the distance between any point on the transmitter-receiver setup and the man-made conductor. The safe distance to any man-made conductor is at least 100 m over an earth with an overall resistivity of 40 Ωm-m to 60 Ωm-m (Ωm).

Weather conditions were another challenge. The Lake Michigan coast is consistently windy throughout the year. Strong winds and heavy clouds delayed data acquisition efforts over several time intervals during the study.

Figure 9-56. Map showing the helicopter survey lines (green) at 100 m spacing, on the southwestern Lake Michigan shore. The top inset show example of perpendicular flight lines east of Illinois Beach State Park (IBSP). The bottom inset show the flight lines ~100 m away from infrastructures and buildings in Chicago.
Source: (Mwakanyamale et al. 2018)

9.16.2 Outcome

All HTEM data was processed (noise removal) and inverted using Aarhus Workbench software. Then, all filtered data were modeled using spatially constrained inversion (SCI). In this SCI algorithm, a group of time-domain EM soundings are inverted simultaneously using one-dimensional models. Each sounding yields a separate layered model, and then the models are constrained laterally. The result of the SCI inversion is a model section that varies smoothly along and across the profiles and yields a resistivity model that combines high-resolution shallow and deep subsurface information.

Layered models (resistivity) resulting from the inversion of collected HTEM data are presented as maps of mean resistivity in depth intervals and as layered 2-D resistivity profiles. Resistivity is shown on a logarithmic scale, the conductive (blue color)

and resistive (purple color) features appear with the same weight. The white shading at the bottom of the 2-D profiles indicates the estimated lower depth of investigation. The maps in Figure 9-57 show the distribution of resistivity for each layer in a model. The elevation slices were extracted from the interpolated 1-D resistivity models from collected HTEM data. The depth interval at 2 m (6.6 ft) for each layer is stated on the maps as elevation above sea level (see Figure 9-57).

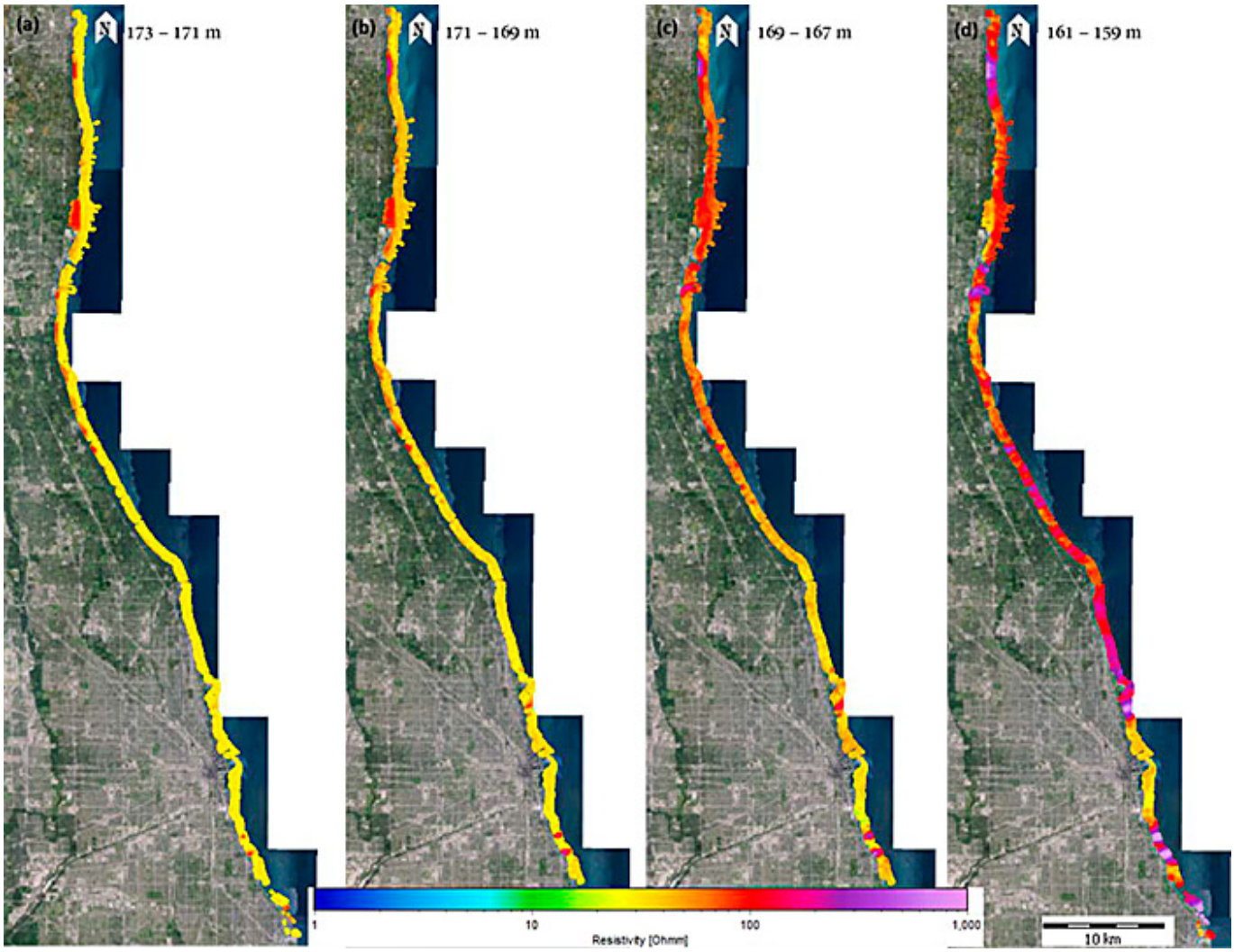

Figure 9-57. Map showing distribution of resistivity in Ωm. The maps represent change in resistivity with depth, from the elevation of 173 m – 159 m (568 ft – 522 ft) at 2 m (6.6 ft) intervals. The variation in resistivity is due to difference in electrical conductivity properties within various geological units (lake water – bedrock).
Source: (Mwakanyamale et al. 2018)

Resistivities were modeled between 173 m (568 ft) to 159 m (533 ft) elevation (see Figure 9-57 (a-d), respectively), As expected, resistivity significantly changes with depth. Low resistivities (less than 50 Ω m) predominate the water column and some shallow sediment (not visible in the map), but layers of much higher resistivity material (greater than 500 Ω m) are observed in the deeper layers (bedrock). At shallow depths, 171 m – 167 m (561 ft to 545 ft) (see Figure 9-57 (b) and (c)) the north side of the map is dominated by resistivities of about 100 Ω m. Zones of high resistivity material are present at the south end of the site at both 171 m to 169 m (561 ft to 554 ft) and 169 m to 161 m (554 ft to 528 ft) elevation.

Figure 9-58 shows a map of filtered HTEM soundings (white dots) used in modeling of resistivity data, overlaid by selected 2-D resistivity profiles (resistivity distribution with depth) (see Figure 9-59 and Figure 9-60).

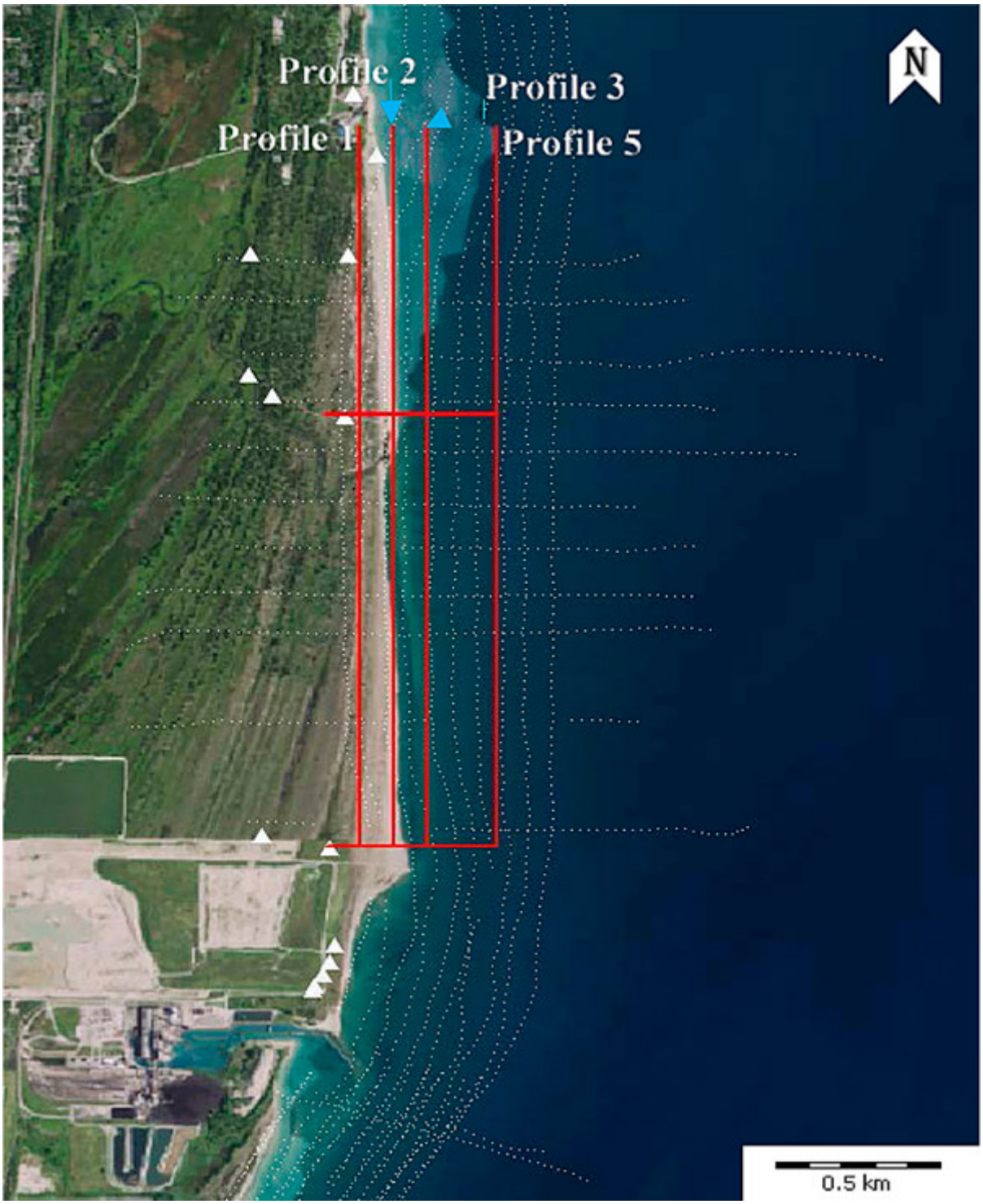

Figure 9-58. Map showing filtered HTEM soundings (white dots) and selected profiles (red lines) to present 2-D resistivity distribution below. White triangles are borehole locations close to HTEM lines.
Source: Modified from (Mwakanyamale et al. 2018)

The 2-D inversions of the HTEM data resulted in a six-layer framework (including the water column) across the profiles. The observed sharp contrast in resistivity from the lake water to the bedrock material is due to changes in electrical conductivity properties within the different units of the framework. This observed variability in resistivity values across the layers (see Figure 9-59 and Figure 9-60) is consistent, for example, with changes in grain size and rock material between shallow <150 m (492 ft) elevation (unconsolidated glacial sediment (for example, sand, silt and clay) and deeper >140 m (459 ft) elevation (bedrock material, for example, dolomite, shale and limestone) layers. These observations are confirmed by shallow borehole information along the shoreline. Boreholes that penetrate fully through the sand and clay glacial deposits are absent, but the low resistivity layer was interpreted as clay-till. Boreholes 2951 and 2952 encountered a sand layer of about 8.8 m (29 ft) thick with clay at the bottom of borehole 2952 (see Figure 9-60). As shown above, the hot colors (purple)

indicate resistive features (for example, dolomite, Figure 9-59 and Figure 9-60), while the cooler colors (blue) indicate conductive features (for example, shale, Figure 9-59 and clay Figure 9-60, respectively).

Thin layers beneath the water column are shown on the expanded depth axis in Figure 9-60 (y-axis). The yellow to brown color (between 80 Ω m to 120 Ω m) is interpreted as sand (see Figure 9-59). Depending on the grain size and level of water saturation (for example, sand at the beach) a different resistivity value will show compared to the sand on the lake bottom. This is also confirmed by the borehole 2951 and 2952 in Profile 1.

The water column is clearly seen in Profiles 2, 3 and 5 (see Figure 9-59 and Figure 9-60) as an approximate30 Ω m layer (resistivity value was recorded using a conductivity meter).

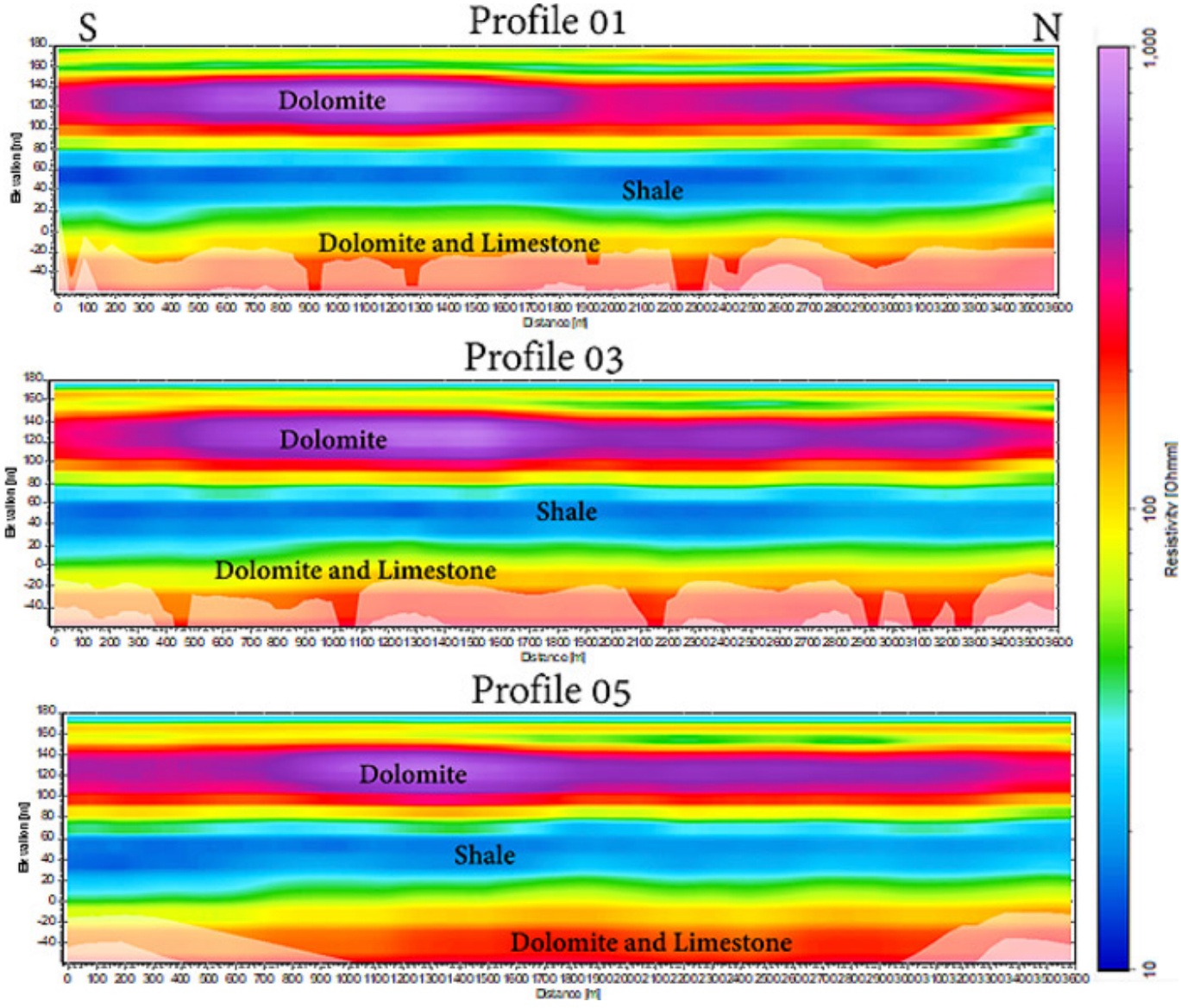

Figure 9-59. Electrical resistivity results from 2-D modeling of the airborne electromagnetic. There is a sharp contrast in resistivity values with depth indicative of difference in electrical conductivity within geological units.

Source: Modified from (Mwakanyamale et al. 2018)

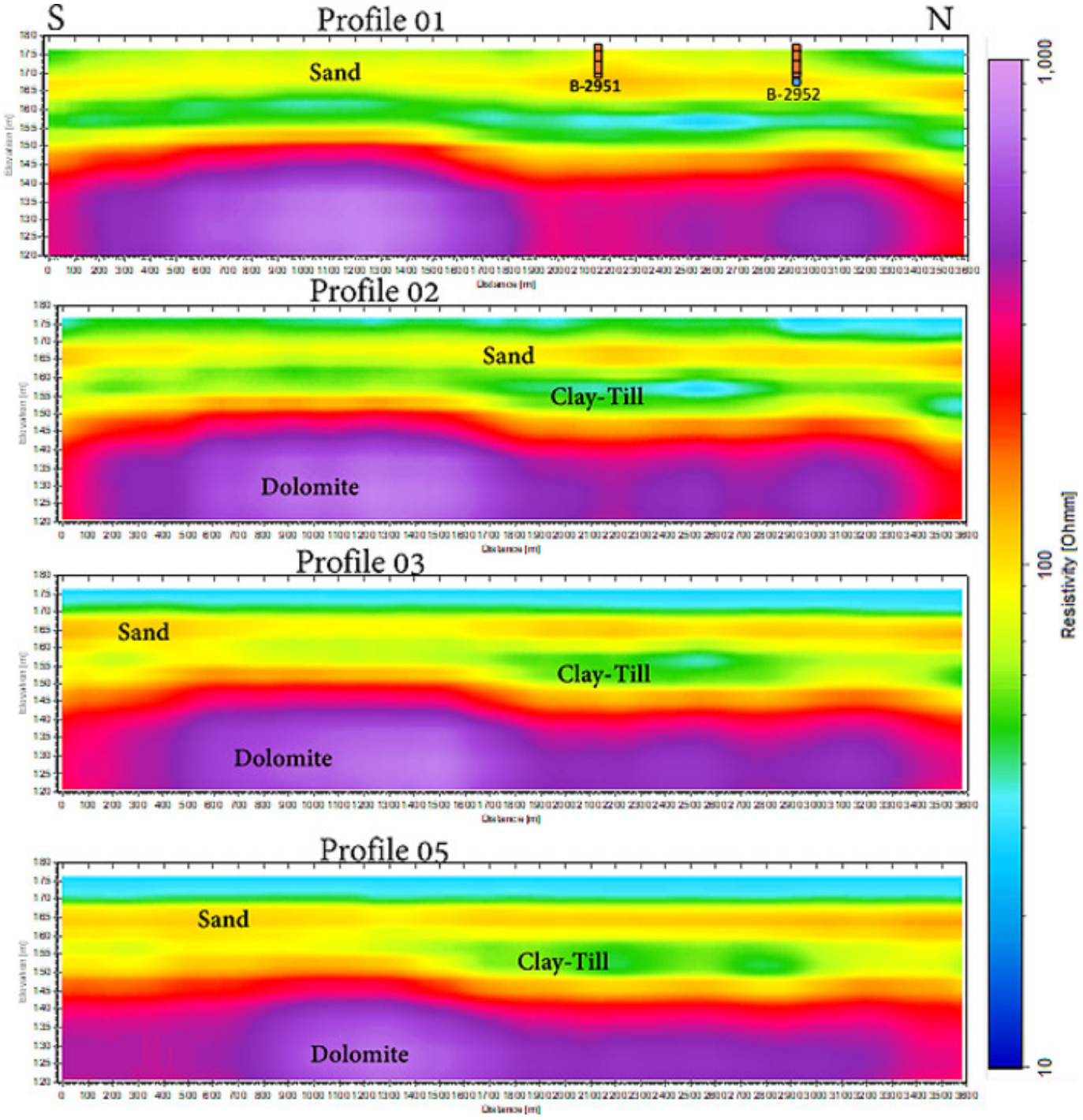

Figure 9-60. Electrical resistivity results from 2-D modeling of the airborne electromagnetic data at the IBSP in Zion, IL. The thin clay and sand layer is clearly seen in these cross sections. The cylinders in Profile 1 are borehole number 2951 and 2952 showing presence of sand layer (brown) of about 8.8 m (29 ft) for both boreholes, with clay (blue) at the bottom of borehole 2952.

Source: Modified from (Mwakanyamale et al. 2018)

The overall distribution of the sand body along the shoreline from Kenosha to south Chicago is shown in Figure 9-61. This 3-D view of the resistivity data shows a trend in sand thickness that has been reported consistently (for example, (Fraser and Hester 1974); (Shabica and Pranschke 1994). As expected, the models indicate a thick layer of sand (yellow layer) on the northern section of the shoreline (north of Great Lakes Naval Station), albeit with some patches of thin sand, silt/clay (green layer), or exposed bedrock (red/ purple) in some locations. This portion of the shoreline, which is adjacent to the lake, allows the largest (≥10 m (+33 ft)) littoral sand deposit observed in the entire shoreline. South of the Great Lakes Naval Station and north of Winthrop Harbor to Kenosha, sand deposits are relatively thin, and the bedrock is exposed in most areas. A thin coating of silt/clay is present on north and south of W. Foster Ave and Winnetka and absent south of the city of Chicago and around Kenosha, exposing the dolomite bedrock (red or purple color).

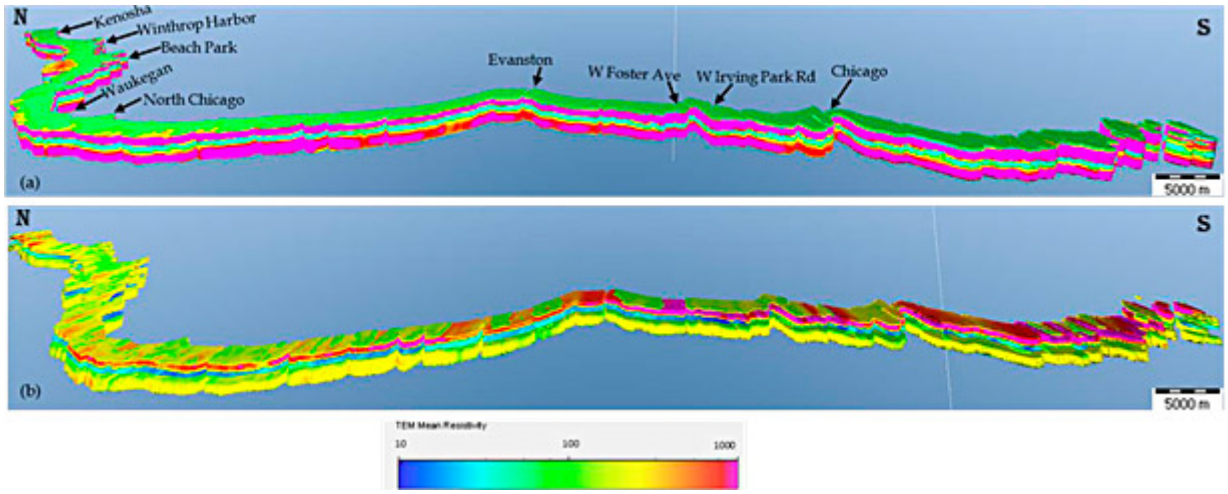

Figure 9-61. D view of the resistivity results along the SW Lake Michigan shoreline. (a) 3D view of all the interpreted geological layers, with the water column shown as pale green; (b) the water column is removed to expose the units on the lake bottom.

Source: Modified from (Mwakanyamale et al. 2018)

9.16.3 Summary

HTEM results from the airborne survey provide insights into the variability in distribution and thickness of unconsolidated sand along the southwest Lake Michigan shoreline. This study aimed to provide both qualitative and quantitative information on sand thickness, sand distribution, and bathymetry along the 73-mile (117 km)-long shoreline from Kenosha, Wisconsin to the Illinois state line south of Chicago. The resistivity images provide unique continuous information on the spatial variation in distribution and thickness of the unconsolidated sediment on the nearshore. Here, the resistivity of unconsolidated sand and gravel is assumed to be in the range of 90 Ω m to 200 Ω m (Culley, Jagodits, and Middleton 1976); (Telford et al. 1976). The resistivity of lake water was measured during the waterborne ERT survey with a conductivity meter reading of 30 Ω m. The 2-D modeling of the resistivity data confirms that a major portion of the Illinois nearshore is comprised of a thin layer of unconsolidated sand with numerous bedrock outcrops.

The resistivity results are consistent with available borehole information on the thickness of the sand layer, especially in the IBSP area. The borehole records date from 20 years to 40 years ago. Littoral sand thicknesses may have changed significantly since that time, so the correlations are considered tentative. Most boreholes close to the shore were only drilled to penetrate the sand layer; few have information on the bedrock material. As a result, much of the available borehole data is too shallow to be used in interpretation of the resistivity data. Layers of clay, silt, dolomite, and shale were encountered in a few boreholes which penetrated bedrock. Due to the dynamic nature of the nearshore sand, only boreholes close (about 50 m (164 ft)) to HTEM lines were used to interpret resistivity data. Due to littoral transport, abrupt changes in thickness of unconsolidated sediment are possible within a short distance; hence, comparison between borehole information and resistivity data that are not in close proximity to one another can be misleading. Further efforts to obtain cores to verify thicknesses of surficial sand and geologic units in the subsurface are planned, including hydraulic probing surveys to directly compare the mapping (Fraser and Hester 1974); (Shabica and Pranschke 1994).

9.17 Drone Technology Expedites and Streamlines Site Characterization at a Former Golf Course in Missouri

Mike Rawitch
Ramboll US Corporation
Overland Park, KS
mrawitch@ramboll.com

A former golf course in Missouri ceased operation in the middle to late 2000s and remained vacant for more than a decade. At the time of the investigation typical golf course features such as greens, tee boxes, and stockpiles were not readily observable. The purpose of the investigation was to determine the nature and extent of arsenic, lead and mercury contamination previously detected in samples from the greens, putting green, tees, fairway, driving range, and pitch-and-putt course to complete the site characterization. In July 2018, a site characterization was conducted to determine the nature and extent of arsenic, lead, and mercury contamination previously detected in samples from the greens, putting green, tees, fairway, driving range, and pitch-and-putt course. A drone with a visual camera was used to help identify key on-site features through spatial referencing and document visuals prior to and after soil removal. A web-based GIS system allowed field teams and office staff to access collected data quickly.

High-resolution aerial photographs of the site were collected with a DJI Phantom 4 Pro, a multirotor quadcopter. Prior to flight operations, Skyward (Drone Fleet Management software) was used to ensure compliance with FAA guidelines in 14 CFR part 107 (FAA 2018). Data collection planning and processing were accomplished using the cloud-based processing software DroneDeploy. The flight plan was developed and included considerations such as avoiding nearby residences and trees that obscured visual line-of-sight.

The survey was limited to the approximate property boundaries (228 acres). Data collection resulted in 563 individual perpendicular aerial images and several dozen oblique aerial photographs. The perpendicular images were processed to create a single high-resolution orthomosaic of the site. Additionally, these images were processed using photogrammetric methods to create a digital surface model. Accuracy was reported as root mean square error of approximately 53 inches for the optimized camera location in XYZ coordinates. The absolute accuracy was calculated as the root mean square error of the difference between the image location recorded by the navigational GPS and the corrected image location calculated during map processing in the X, Y, and Z plane. The ground sampling distance of the imagery captured was approximately 1.3 inches per pixel.

The processed orthomosaic imagery was brought into a web-based/mobile GIS platform (ArcGIS Online) using a Web Tile Layer created by DroneDeploy to allow the imagery to be viewed on an iPad Pro with a Bluetooth connection to a Trimble R1 global navigation satellite system (GNSS) receiver. This setup supports submeter location accuracy for the sample points directed by the imagery data. Field teams collected soil samples informed by the drone data, which were provided as a mobile GIS map. The collected samples were used to inform and direct excavation. Postexcavation, a second imagery dataset was captured. The combined dataset supported a GIS presentation of the site postexcavation. A replicate drone survey was performed following the excavation activities. The soil from the excavations was consolidated into four stockpiles for ease of loading for disposal. DroneDeploy was used to estimate the volume of the soil stockpiles and to denote the locations of excavation areas apparent on orthoimagery. The volume of the four stockpiles was estimated at approximately 301 cubic yards.

Anecdotal information suggested that, as part of previous remediation efforts, the golf greens were scraped and the excavated soil was stockpiled on the northern portion of the site. To locate these potential stockpiles, a drone was used to collect visual images. The images were examined, and photogrammetric analysis revealed no elevated areas indicative of soil stockpiles or areas of obvious tone or texture differences indicative of soil disturbance. Additionally, high-resolution orthoimagery was integrated into mobile GIS to assist in confirming sample locations and their relative location to historic course features (see Figure 9-62, Figure 9-63 and Figure 9-64 for example images).

Figure 9-62. Pre-excavation site characterization of one area where soil removal was documented

Figure 9-63. Postexcavation of one area with soil stockpile next to equipment

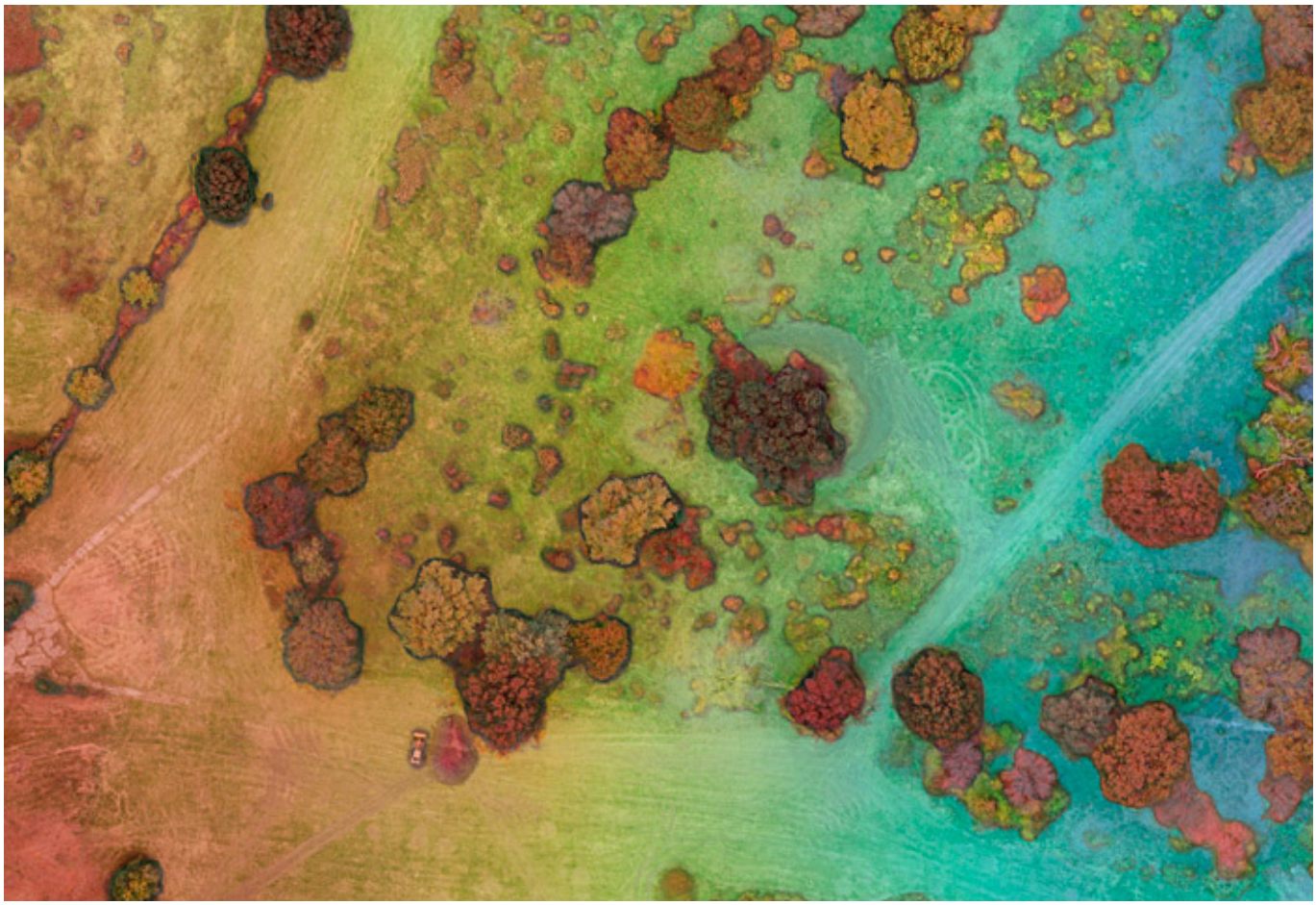

Figure 9-64. Postexcavation digital surface model with soil stockpile next to equipment

Site closure was achieved in early 2019. While the site could have been inspected on foot and supported by older aircraft or satellite images, using a drone with a visual camera provided distinct advantages, including, but not limited to, the following:

- Speed: The 228-acre site was surveyed in a matter of a few hours.
- Detail: Certain areas of the site were difficult or impossible to access on foot and, even if the site were canvased on foot, findings would have been difficult to document.
- Collaboration: The data were made available for all interested parties to review. Data were easily shared between the teams conducting activities in the field and the office, which allowed for efficient remedial and characterization efforts the field team to remain oriented to site features during the characterization.

When compared to reviewing aerial imagery alone, the method used provided distinct advantages, including, but not limited to, the following:

- Spatial resolution: The ground sampling distance of 1.3 inches is a much finer spatial resolution than available with traditional aerial imagery.
- Temporal resolution: The ability to fly the drone immediately before characterization and after soil remediation activities provided visual documentation of the completed work.

In total, the effort cost approximately $2,500, including developing a flight plan, collecting samples (bulk of the effort), uploading data for cloud-based processing, paying fees associated with remotely piloted aircraft system (RPAS) equipment and data processing, performing a quality review of processed data, and conducting analysis and interpretation. Analysis and interpretation included the identification of historical features, integration into mobile/web-based GIS, and measuring of stockpiles postremediation. The total cost does not include mobilization to the site or additional reporting efforts beyond the initial characterization.

An estimate of costs to survey the entire 228 acres on foot would be on the order of $5,000 to $10,000. In addition to these avoided costs, the costs avoided by applying this technology and improving efficiencies are intangible but most definitely beneficial.

9.18 High-Resolution and Thermal Aerial Images Identify Mine Openings at an Abandoned Colorado Mine

Mike Rawitch
Ramboll US Corporation
Overland Park, KS
mrawitch@ramboll.com

An abandoned mine in Colorado ceased operation in the 1980s and has remained vacant for the past several decades with a recent addition of a water treatment facility to decrease acid mine drainage. In Spring 2018, an investigation was conducted to identify all mine openings and subsidence features to restrict both access to the mines and the production of acid mine drainage water.

To improve the spatial accuracy of the data collected and allow the imagery to be used with existing maps and drawings, 18 ground control points were captured using a high-precision GPS unit (TrimbleGeoXH). High-resolution visual, aerial imagery of the site was collected using a multirotor DJI Phantom 4 Pro. DJI Goggles (see Figure 9-65) were used for oblique photography and video inspections on the side of vertical cliff faces. The DJI goggles consist of two high-quality screens that sit in front of the pilot's eyes and allow control of both photo and video capture. To capture temperature differences between mine openings and the surrounding topography, thermal imagery was collected using a Matrice 210 quadcopter fitted with a Zenmuse XT infrared camera.

The Zenmuse XT camera was selected to identify areas with thermal contrast between the mine openings and the surrounding ground. The thermal characteristics of open mines increase between 0.5°C to 1°C in contrast to surrounding ground surface temperatures. The agility of the quadcopter and use of DJI goggles allowed the many mountainous features across the site to be visually inspected (see Figure 9-65). The combination of geolocated, oblique thermal images, visible spectrum images, and nadir thermal and visible spectrum imagery provided detail that is generally not available from areal maps or aerial photographs from airplanes or satellites.

The survey was initiated at a known mine opening to calibrate the equipment to the temperature of the air leaving the mine. To ensure compliance with FAA guidelines in 14 CFR part 107 (FAA 2018), a preflight airspace check was completed using Skyward (Drone Fleet Management software solution). Data collection planning and processing were facilitated by the cloud-based processing software DroneDeploy and Drone2Map.

Figure 9-65. Remotely piloted aircraft system (RPAS) being piloted with DJI Goggles.

Multiple flights occurred over more than 450 acres during a five-day period between April 23 and April 27, 2018. Historic maps and reports were digitized and used for flight data collection planning. During flight, a series of geolocated infrared and visible spectrum images were captured for each mine feature documented in the inventory as well as for previously unidentified potential mine features based on thermal and visible anomalies. In total, more than 1,500 individual thermal images and 2,000 individual visible spectrum images were captured. These images were processed using DroneDeploy and Drone2Map to create two high-resolution composite images: one for the thermal spectrum and one for the visible spectrum. Additionally, these images were used to create a 3-D model and a digital surface model (DSM). To produce a DSM, vegetation and buildings were removed and replaced with an interpolated surface (see Figure 9-66).

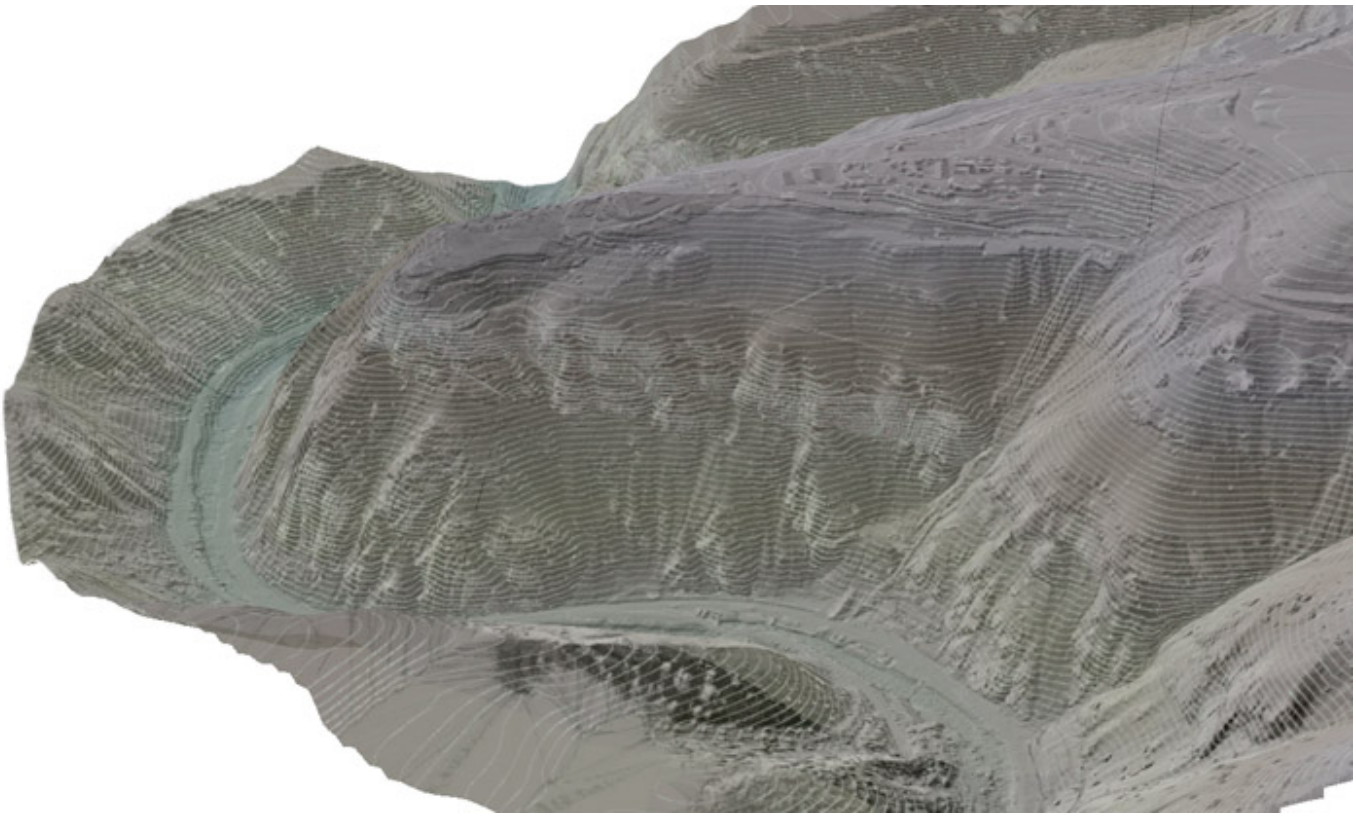

Figure 9-66. Digital surface model projected in three-dimensional visualization with 10-foot contour lines.

Accuracy was reported as the optimized camera location in horizontal (X, Y) as a root mean square error at approximately 5.5 inches, and 15.8 inches in vertical (Z). The absolute accuracy was calculated as the root mean square error difference between the image location recorded by the navigational GPS and the corrected image location calculated during map processing. The ground sampling distance of the imagery captured was approximately 2 inches per pixel (see Section 6.4.1.6).

In total, 84 potential adits or shafts were identified at the site. Forty-one features were considered to have a high probability of being a mine feature, and an additional 43 features were suspected of being a mine feature. Data from the drone survey, combined with percent slope and the known hydrology (local surficial drainage patterns), were used to develop and prioritize a list of features for investigation and closure. Note that the percent slope calculated from the data can be used to support plans for hiking or driving into the area by identifying potential access routes.

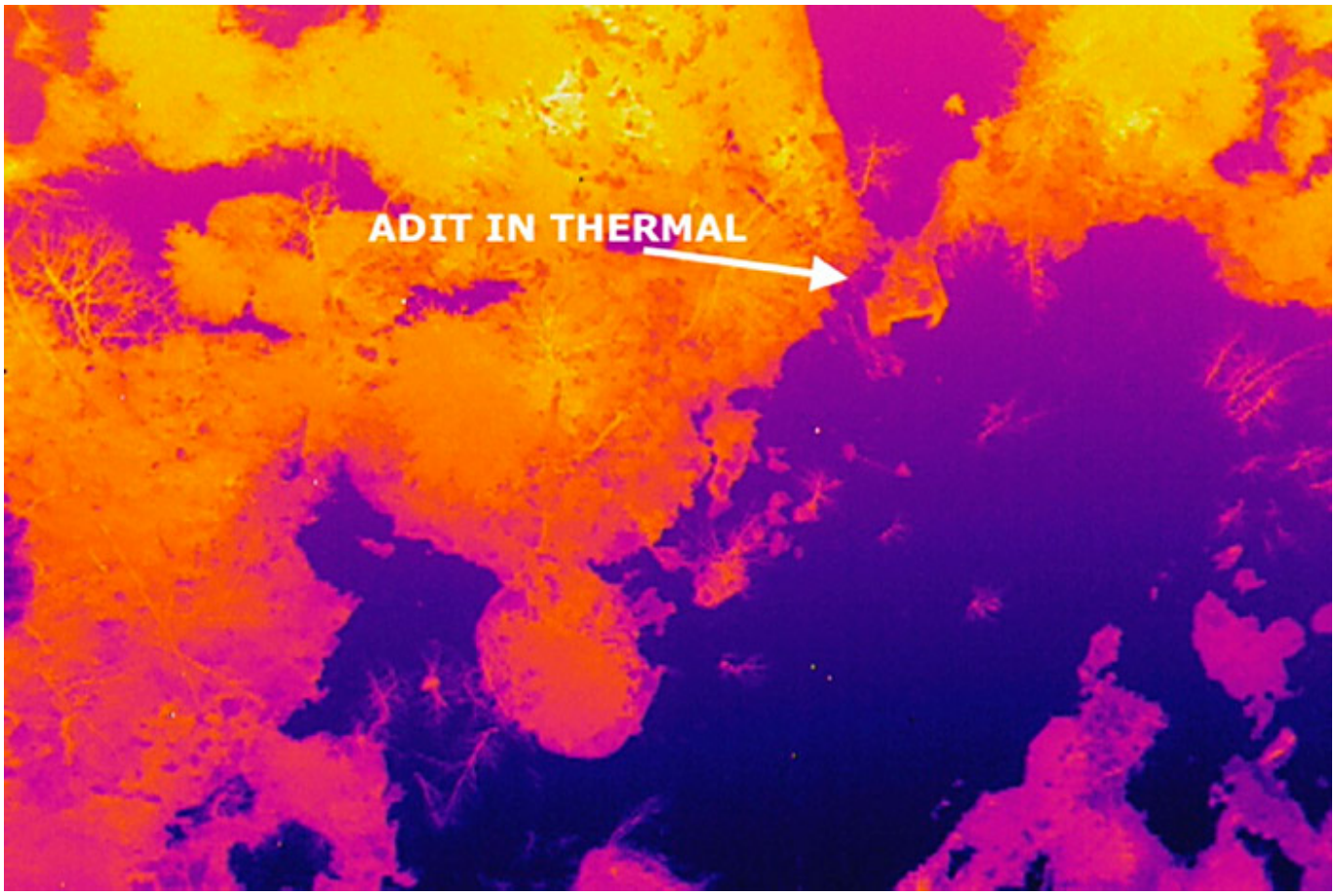

Figure 9-67. Adit identified in thermal imagery.

The processed orthomosaic imagery was brought into a web-based/mobile GIS platform (ArcGIS Online) using a Web Tile Layer created by DroneDeploy (see Figure 9-67). The unprocessed geolocated images were also brought into GIS and provided as a final data product. Therefore, field teams working at the site could view all imagery to be viewed on mobile GIS equipment (an iPad Pro with a Bluetooth connection to a Trimble R1 GNSS receiver). The integration of this digital data continues as part of site management and is available to support remedial efforts and facilitate optimization of actions in support of remediation.

Plants obscured potential adits. Compared to a manual survey, drone flights were advantageous in the following aspects:

- Safety: Using the drone avoided performing a survey and searching for unidentified mine openings on foot, which requires trained climbers and some rappelling. Drone use avoided the risks associated with this activity, such as injuries and becoming disorientated or lost.
- Detail: A traditional, manual survey only documents part of a large site and records limited photographs and written descriptions. Using this technology allowed the entire site to be surveyed in greater detail than would have been possible on foot.
- Accuracy: GNSS systems provided limited accuracy at certain times of the day due to the steep topography and associated interference. Compared to the 1986 survey (completed with an altimeter and compass), features were identified with a higher degree of accuracy. In some cases, features were located several hundred yards from where they were originally mapped.
- Collaboration: Data were easily shared between the office and field team, which supported dynamic characterization and remedial efforts.

Figure 9-68. Mine opening only visible from oblique imagery.

When compared to reviewing historical aerial imagery or maps alone, the method used provided distinct advantages, including, but not limited to, the following:

- Spatial resolution: The ground sampling distance of 1.3 inches is a much finer spatial resolution than available with traditional aerial imagery (typically on the order of 6 inches to 12 inches for this area)
- Temporal resolution: The ability to fly the RPAS immediately before characterization and after soil remediation activities provided a tremendous benefit to the project.
- Agility: The ability to fly parallel to cliff faces allowed the identification of many features that are impossible to see from a nadir perspective. For example, adits were not visible in the nadir; the oblique imagery was invaluable.
- Accuracy: The site closed prior to the availability of GPS technology, so many of the site feature locations were mapped inaccurately. Many older maps are lost, damaged, or not in a digital format.

In total, the effort cost approximately $60,000, including developing a flight plan, collecting samples, uploading data for cloud-based processing, paying fees associated with equipment and data processing, performing a quality review of processed data, conducting analysis and interpretation, integrating data into mobile/web-based GIS, and developing online reporting tools. The total cost does not include mobilization to the site or additional reporting efforts beyond the initial characterization.

An estimate of costs to survey the 450 acres on foot is $40,000 and includes significant safety hazards with potentially inadequate data results. Flying the site with new aerial imagery is not a practical option given the scale of the site and the extreme topography. In addition to replacing a manual survey, the savings associated with the application of this technology and improved efficiency are difficult to calculate but presumed beneficial. Also, a reduction in costs associated with the reduction and treatment of acid mine drainage water over time should be considered.

9.19 RPAS Collects Water Samples to Avoid Safety Concerns at Montana Tunnels Mine

Devin Castendyk, PhD, MSc
Senior Geochemist
Golder Associates Inc.
Denver, Colorado
Devin_Castendyk@golder.com

On October 23, 2018, a three-person team from Golder Associates Inc. (Golder) in Denver, Colorado, collected three water samples in the Montana Tunnels Pit Lake near Jefferson City, Montana. Water quality monitoring was conducted for the first time at a flooded former open pit gold mine (now known as the Montana Tunnels Pit Lake) near Jefferson City, Montana. The use of a remotely piloted aircraft system (RPAS) avoided the significant safety risk of posed by unstable pit walls. Three water samples were collected from 0- , 92-, and 184-ft deep.

The work was contracted by the MDEQ and observed by representatives from the MDEQ, U.S. Bureau of Land Management (BLM), and Montana Tunnels Mining Company. (Williams et al. 2018) described this sampling event in an inspection report, copies of which can be requested from the Butte, Montana office of the BLM.

The RPAS was flown above a point on the water surface that was believed to overlie the deepest location within the pit lake. Flight 1 lowered a CastAway CTD through the water column that recorded the maximum depth (230 ft) and measured in situ profiles of temperature and electrical conductivity. Temperature and electrical conductivity were uniform throughout the water column, indicating that the lake had recently undergone complete mixing through a process known as fall turnover (see Figure 9-69).

Based on evidence of homogeneous conditions in the water column, three water samples were collected with uniform sample spacing across the water column. After discussions with MDEQ, sample depths of 0 ft, 98 ft, and 197 ft were targeted for sampling. Flight 2 collected a two litre (2L) water sample from the deepest depth. Flight 3 attempted to collect a sample from the immediate surface of the water, but upon return, the sample chamber contained only 0.6 L. Flight 4 lowered the sampling device a few feet deeper and returned with a 2L sample. Flight 5 collected a 2L sample from the mid-depth of the lake. Postprocessing of pressure transducer data showed the actual sample depths to be 0-, 92-, and 184-ft deep.

The sampling event provided data to meet MDEQ requirements and demonstrated the ability of aerial drones to perform water sampling. Given that the original request for proposals required only two water samples from 10- and 50-ft deep, the sampling team was able to provide an additional sample and significantly greater vertical distribution than requested at no additional charge. Most importantly, use of RPAS water sampling equipment significantly improved safety compared to boat-based methods. The MDEQ accepted the samples for routine monitoring purposes.

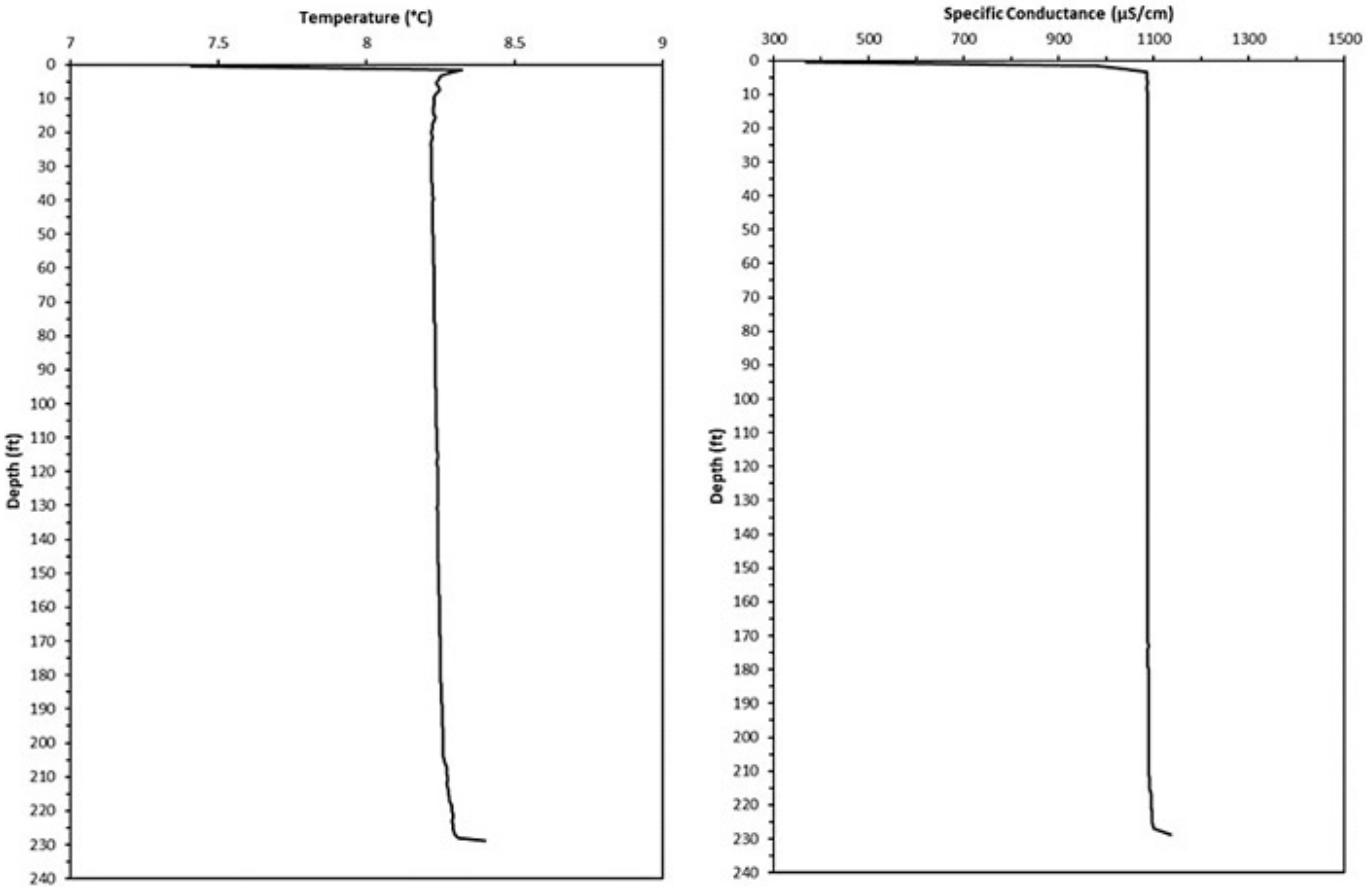

Figure 9-69. In situ temperature (left) and specific conductivity (right) measured in the Montana Tunnels pit lake on October 23, 2018.

Appendix A. Tool Tables and Checklists

Title	Document File Name
ASCT Selection Tool	ASCT Selection Tool
Section 3 – ASCT Direct Sensing	
Tool Summary Table	ASCT Direct Sensing Tool Summary Table
Checklists	ASCT Direct Sensing Checklists (.xlsx version)
Section 4 – ASCT Borehole Geophysics	
Tool Summary Table	ASCT Borehole Geophysics Tool Summary Table
Checklists	ASCT Borehole Geophysics Checklists (.xlsx version)
Section 5 – ASCT Surface Geophysics	
Tool Summary Table	ASCT Surface Geophysics Tool Summary Table
Checklists	ASCT Surface Geophysics Checklists (.xlsx version)
Section 6 – ASCT Remote Sensing	
RPAS Summary Table	ASCT Remote Sensing RPAS Summary Table
Checklists	ASCT Remote Sensing Checklists (.xlsx version)

Tool	Primary Parameter	Parameter Resolution	Drilling Methods	Typical Productivity per Day	Vertical Parameter Resolution	Limitations	Potential Tool Combinations
Downhole Analytical							
LIF – UVOST® / ROST™	Light PAH NAPL	LNAPL only, can resolve product type	Percussion or static driven DPT	150 – 250’	cm/in	Limited to lithologies that can be pushed, aviation gasoline, chlorinated DNAPL, Heavy PAH NAPL	EC, Injection Flow Logging, CPT
LIF – DyeLIF™	Chlorinated DNAPL	Chlorinated DNAPL	Percussion or static driven DPT	150 – 250’	cm/in	Limited to lithologies that can be pushed, can’t specify product type	EC, Injection Flow Logging, CPT
LIF – TarGOST®	Heavy PAH NAPL	Heavy PAH NAPL (Coal Tar, Creosote, crude oil)	Percussion or static driven DPT	150 – 250’	cm/in	Limited to lithologies that can be pushed, not effective on light PAH NAPL, chlorinated DNAPL	EC, Injection Flow Logging, CPT
OIP – UV	Light PAH NAPL	LNAPL only, photos of fluorescence, formation	Percussion or static driven DPT	150 – 250’	cm/in	Limited to lithologies that can be pushed, can’t specify product type, Chlorinated DNAPL	EC, Injection Flow Logging, CPT
OIP – Green Laser	Heavy PAH NAPL	Heavy PAH NAPL (Coal Tar, Creosote, crude oil)	Percussion or static driven DPT	150 – 250’	cm/in	Limited to lithologies that can be pushed, not effective on light PAH NAPL, chlorinated DNAPL	EC, Injection Flow Logging, CPT
MIP	VOC distribution	Low ppb to low ppm	Percussion or static driven DPT	100 – 200’	cm/in	Limited to lithologies that can be pushed, NAPL problematic	EC, Injection Flow Logging, CPT
Downhole Physical							
Hydraulic Profiling (Injection Flow Logging)	Flow and pressure, used to estimate hydraulic conductivity	Hydraulic conductivity 0.1 to 75 ft/day	Percussion or static driven DPT	150 – 250’	cm/in	Not effective in high permeability formations	EC, MIP, LIF, OIP, GWS
CPT	Lithologic / hydrogeologic parameters	Soil type, relative density, porewater pressure	Static driven DPT	150 – 300’	cm/in	Limited to lithologies that can be pushed, refusal in bedrock and rocky formations	MIP, LIF, OIP XRF, injection flow logging, electrical conductivity
EC Logging	Formation soil conductivity	Electrical conductivity of formation and/or TDS of groundwater	Percussion or static driven DPT	150 – 250’	cm/in	Log provides non-unique solution that can respond to different subsurface factors	Commonly used as an accessory tool for many direct sensing applications
FLUTe (T-Profiler)	Estimated Transmissivity	Transmissivity range from 0 to 1 cm^2/sec	Needs open borehole for deployment. Unconsolidated and bedrock applications	Varies	0.5 to 1 ft	Limited to consolidated lithologies, requires pre-planning for borehole diameters and depth	FACT system, blank liner, NAPL FLUTe

Tool	Primary Parameter	Parameter Resolution	Drilling Methods	Typical Productivity per Day	Vertical Parameter Resolution	Limitations	Potential Tool Combinations
High Resolution Sampling and Profiling							
Screen Point GW Sampler	Aqueous samples	Aqueous samples, parameter based on analytical method used	Percussion or static driven DPT	Varies based on objectives	inches - 1 ft	Low permeability formations	Pneumatic slug testing, mobile lab
Direct-Push Temporary Well Point Systems	Aqueous samples	Aqueous samples, parameter based on analytical method used	Percussion or static driven DPT	Varies based on objectives	1 ft	Limited to lithologies that can be pushed, refusal in bedrock and rocky formations	MIP, LIF, OIP XRF, injection flow logging, electrical conductivity, mobile lab
Soil/ Bedrock Cores	Soil and/or rock samples	Lithologic descriptions, Solid media samples with parameters based on analytical method used	Percussion or static driven DPT, hollow stem auger with sampler, sonic, bedrock coring methods	Varies based on objectives and drilling method	As needed	Limited recovery in some lithologies	Mobile lab, DFN, PID, FID, XRF
HPT - GWS	Estimated hydraulic conductivity, aqueous samples	Aqueous samples, parameter based on analytical method used	Percussion or static driven DPT	Varies based on frequency of sample collection	cm on hydraulic profiling, depth-discrete over 3- to 4-inch interval for groundwater samples	Not effective in lower permeability formations, potential fouling in finer grained formations	Electrical conductivity
Waterloo APS	Estimated hydraulic conductivity, aqueous samples	Aqueous samples, parameter based on analytical method used	Percussion or static driven DPT	Varies based on frequency of sample collection	cm on hydraulic profiling, depth-discrete over 3- to 4-inch interval for groundwater samples	Not effective in lower permeability formations, potential fouling in finer grained formations	Electrical conductivity
FLUTe (FACT)	Vertical profile of VOCs	Limited to analytes that adsorb to carbon. Results reported in mass of VOC per mass of carbon.	Needs open borehole for deployment. Unconsolidated and bedrock applications	deployed in hours, wait time 1-2 weeks	Continuous carbon profile, resolution based on sampling	Not applicable for constituents that do not adsorb to carbon	FLUTe T-Profiler, blank liner, NAPL FLUTe
FLUTe (NAPL)	Presence and depth of NAPL	LNAPL and DNAPL	Needs open borehole for deployment. Unconsolidated and bedrock applications	deployed in hours, wait time 1+ hours	Continuous profile, NAPL detection based on visual inspection of liner	Can't specify NAPL type	FLUTe T-Profiler, blank liner, FACT System
DFN	Distribution of VOCs in bedrock (fractures and matrix)	VOCs, physical rock properties	Bedrock Coring	Varies based on rock type and frequency of sampling	inches to feet, depth-discrete sampling, interval based on objectives and geology	Data representative of mass diffused in the matrix, not a direct measure of dissolved concentrations	Mobile lab
Multi-Level Well Systems	Vertical profile of contaminants	Aqueous samples, parameter based on analytical method used	Any, depends on lithology	Varies	Depth interval determined based on objectives	Depends on system, e.g., FLUTe only in consolidated and direct-push only in unconsolidated or soft consolidated	FLUTe T-Profiler, downhole physical and analytical tools

Direct Sensing Proposal Considerations		
1	Do the data quality objectives and scope of work meet the project objectives?	
2	Does the proposal specify the equipment and order of tools to be used (for example, equipment model, software version)?	
3	Is the tool appropriate for the site?	
	Has the tool matrix (resolution, scale, targets, weaknesses/limitations of tool) been reviewed to determine tool applicability?	
	Has the considerations for the tool checklist been evaluated to determine tool applicability?	
	Can the tool measure for the target analyte type, phase, concentrations?	
	Have target analyte sample(s) been bench tested on the instrument?	
	What site conditions may prove challenging for implementation?	
	What potential is there for false positive signals? What are they and have they been tested for response?	
	What is the methodology for QA/QC in field and during post-processing?	
	Are there any deviations or recommendations from a requested suite of tools with supporting justification?	
4	Has a rationale for survey design been provided?	
	Has (or will) the proposer reviewed background information for the site (for example, geologic and hydrogeologic maps, previous studies, geography, aerial photographs, site history, historic fire insurance maps)?	
5	Does the proposal provide a description of the workflow process?	
	How the tool will be implemented?	
	What method will be used to ensure data location accuracy?	
	Does the proposal address several “what if” scenarios to deal with special issues?	
	Is there flexibility in the proposed work to expand the footprint and depth of the investigation?	
	Is there a plan and budget for targeted confirmatory sampling when unexpected, interesting, or questionable responses are observed?	
6	Does the proposal comply with safety requirements for the site?	
	What safety concerns may make the site unusual?	
	Are field personnel properly trained?	

Direct Sensing Proposal Considerations		
7	Does the proposal specify the data deliverables?	
	Will raw data digital files be provided?	
	Will locational data be provided (for example, will I be able to relocate the area at a later time?)	
	Will copies of field notebooks be provided?	
	Will a report or memo summarizing the investigation and data interpretation be provided?	
8	Does the proposal provide detailed costs?	
	Are subcontractors identified?	
	Are proposed hours appropriate?	
	Are equipment costs appropriate?	
	Are commodities/supplies appropriate?	
	Has a comparison of costs per day versus production (feet/day) per day been conducted to see which is likely to be more cost effective?	
9	Does the proposal provide a clear project timeline?	
10	What is the contractor's level of experience?	
	Are resumes provided?	
	Are references and other projects of similar scope provided?	
10	Are any permits required?	
12	What are the insurance requirements?	

Direct Sensing Report Checklist		
1	Is there a summary of the tools and methods utilized?	
2	Does the report include limitations that constrained the study physically (for example, interferences, safety considerations, access) or due to other reasons beyond control of the contractor?	
3	Was the solicited scope of work followed as requested or were there deviations from the scope that were performed? If so, is there adequate justification for the deviations and was the user aware of them/approving of them in advance?	
4	What type of post processing was performed on the data? Does the report summarize the methods and assumptions used?	
5	What type of QA/QC was performed? Were there QA/QC steps in the field that were adequately followed? Was there data processing/interpretation QA/QC performed and is it described? Were there any deviations from the QA/QC plan?	
6	Is there a narrative summary of the findings and results?	
	Is there a description of the types of responses observed, their potential origins, and whether they were confirmed with sampling?	
	Is there a description of lines of evidence observed to support/refute on-site interpretations?	
	Were there any limitations of the technology (were there any suspected false negatives)?	
	Are there recommendations for follow-up sampling locations if definitive confirmation was not accomplished during the `investigation?	
7	Are raw data files provided?	
	Are summary tables of logs provided?	
	Are logs presented in at least two appropriate scale factors (typically very low for absence/presence determinations and high for semi-quantitative site-wide comparisons of impact)?	
8	Is there at least one plan view figure of the study area and the transects?	
9	What types of graphics are provided to illustrate the findings? Are there 2D or 3D profiles of responses with adequate scale, color ramp definitions?	

MIP-Quality Control Checks to Expect to See During Site Work		
1	Proper calibration with relevant standards during response testing, before and after each boring.	
2	Rods are in very good condition with threads properly maintained (reduces costs due to breakage).	
3	Ensure there is a consistent hold period at predetermined intervals (this depends on the response test).	
4	Check condition of probe and associated ports/detectors for plugging or damage upon probe retrieval from ground.	
5	Conduct occasional duplicate borings or compare other nearby logs to ascertain localized heterogeneity.	
6	Spares - additional trunk-lines and probes are on hand and at the ready in case they are needed.	
7	Comprehensive field notes are being taken.	

OIP-Quality Control Checks to Expect to See During Site Work		
1	Proper response testing before and after each boring.	
2	Rods are in very good condition with threads properly maintained (reduces costs due to breakage).	
3	Check sapphire window for fogging or damage and check associated ports/detectors for plugging or damage upon probe retrieval from ground.	
4	Conduct occasional duplicate borings or compare other nearby logs to ascertain localized heterogeneity.	
5	Spares - additional trunk-lines and probes are on hand and at the ready in case they are needed.	
6	Comprehensive field notes are being taken	

LIF-Quality Control Checks to Expect to See During Site Work		
1	Proper reference emitter and background waveforms are achieved/recorded (background should not exceed 1% RE, if possible).	
2	If used, electric conductivity probe is tested and found to be functioning properly.	
3	Rods are in very good condition with threads properly maintained (reduces costs due to breakage).	
4	Push rate - assure that depth recording is accurate, and rate is not too fast (~1 inch/sec).	
5	Condition of sapphire window checked for fogging or damage and fluid port is checked for plugging or damage upon probe retrieval from ground.	
6	Pre-mob or on-site screening of site-specific NAPLs and false positives to generate a site- specific library of in-situ signals for proper interpretation.	
7	Conduct occasional duplicate borings or compare other nearby logs to ascertain localized heterogeneity.	
8	Confirmatory soil borings are both budgeted for and performed when unexpected, interesting, or questionable responses are observed (almost universally the case).	
9	Spares - additional fiber/probe setups are on hand and at the ready in case they are needed.	
10	Comprehensive field notes are being taken.	

CPT-Quality Control Checks to Expect to See During Site Work		
1	Functional checks before and after each boring using zero load as a baseline.	
2	Inspection of the cone by operator after each advancement checking for possible damage.	
3	Decontamination of equipment between boreholes where contamination is (or is suspected to be) present to prevent cross contamination.	
4	Careful observation of screens during CPT advancement to determine any potential problems.	
5	Monitoring advancement rate.	
6	Collection of confirmatory samples to compare to CPT results.	
7	Comprehensive field notes are being taken.	

HPT-Quality Control Checks to Expect to See During Site Work		
1	Proper calibration, before and after each boring.	
2	Rods are in very good condition with threads properly maintained (reduces costs due to breakage).	
3	For applicable dissipation tests, ensure there is a consistent hold period to reach equilibrium in a semi-permeable zone.	
4	Check condition of probe and associated screens for plugging or damage upon probe retrieval from ground.	
5	Conduct occasional duplicate borings or compare other nearby logs to ascertain localized heterogeneity.	
6	Spares - additional trunk-lines and probes are on hand and at the ready in case they are needed.	
7	Comprehensive field notes are being taken.	

EC-Quality Control Checks to Expect to See During Site Work		
1	Proper calibration during response testing, before and after each boring.	
2	Rods are in very good condition with threads properly maintained (reduces costs due to breakage).	
3	Check condition of probe for damage upon probe retrieval from ground.	
4	Conduct occasional duplicate borings or compare other nearby logs to ascertain localized heterogeneity.	
5	Spares - additional trunk-lines and probes are on hand and at the ready in case they are needed.	
6	Comprehensive field notes are being taken.	

Tool	Property																								
	Lithology Thickness	Thin bed resolution	Depositional Environment	Shale/Clay Content	Lithologic Contacts	Mineral identification	Potassium, Uranium, Thorium Content	Bulk Density	Formation Resistivity	Strike & Dip of Bedding/Foliation/Fracture	Permeability	Fracture Detection	Fracture Aperture	Fracture Density	Porosity Type(s)/Distribution	Porosity Value	Fluid Flow	Fluid temperature	Borehole Fluid Conductivity	Formation water conductivity	Water Level in Formation/saturation	Casing Integrity	Screen/Intake Location	Borehole diameter	Borehole deviation	Examination Behind Casing	Well completion evaluation (e.g., cement bond, seal/grout location)	Location of debris in well
Nuclear magnetic resonance (NMR)	6	6	6	6	6						6																	
Mechanical caliper	9	9										9	9		9							10	10	10				10
Impeller flow meter																	1											
Optical televiewer	4	4	4		4					4		4	4	4	4							5	4, 5		4, 5			4, 5
Acoustic televiewer	1	1	1		1					1		1	1	1	1							3	2, 3	1	1, 2, 3			1, 2, 3
Borehole video	4	4	4		4							4	4	4	4		4					4	4				4	4
Fluid temperature/differential temperature													1				1	2, 3			2	2, 3	2					
Natural gamma	10	10	10	10	10																				10			
Resistivity	1	1	1	1	1				1			1			1					1	1							
Heat pulse flowmeter																	1											
Fluid resistivity (or conductivity)																	1		1, 2, 3	2	2	2, 3	2					
Other Tools																												
Induction conductivity	6	6	6	6	6				6											6	6					6	6	
Single-point resistance	1	1	1									1									1							
Spontaneous potential	8		8	8	8												8			8	8							
Spectral gamma	10	10	10	10	10	10	10																					
Neutron porosity (neutron-neutron)	7, 10		7, 10	7, 10	7, 10											7, 10										7, 10	7, 10	
Density log (gamma-gamma)	7, 10		7,10	7, 10	7, 10	7, 10		7, 10													7, 10					7, 10	7, 10	
Acoustic caliper	1	1										1	1		1							1, 3	1, 3	1, 3				1, 3
Radar (borehole GPR)					6							6									6							
Magnetometric resistivity																												
Magnetic susceptibility	6			6	6	6						6											6					
Full wave form seismic				1												1							1				3	
Cement bond log																						3				3	3	

Legend:

Applicable tool to assess property

Potentially applicable tool to assess property

Required hole conditions:

1. Open fluid filled hole
2. Screened or open fluid filled hole
3. Cased fluid filled hole
4. Clear fluid of dry open hole
5. Clear fluid or dry cased hole
6. Open or non-conductive cased hole, dry or fluid filled
7. Active nuclear log to be run in stable holes only
8. Conductivity difference between borehole fluid and formation fluid
9. Open hole
10. No restrictions

Sources:

ASTM Standard D5753-05, June 2005, "Standard Guide for Planning and Conducting Borehole Geophysical Logging" ASTM International, West Conshohocken, PA

Day-Lewis, F.D., Johnson, C.D., Slater, L.D., Robinson, J.L., Williams, J.H., Boyden, C.L., Werkema, D., and Lane, J.W., 2016, A Fractured Rock Geophysical Toolbox Method Selection Tool: Groundwater. doi:10.1111/gwat.12397 (https://water.usgs.gov/ogw/bgas/frgt/).

Department of the Army, 1995. Engineering and Design: Geophysical Exploration for Engineering and Environmental Applications, Engineer Manual EM 1110-1-1802 (31 August 1995). U.S. Army Corps of Engineers, Washington D.C.

Keys, W.S., Crowder, R.E., and Henrich, W.J., 1993, Selecting geophysical logs for environmental applications, *in* Seventh

Borehole Geophysics Proposal Considerations		
1	Do the data quality objectives and scope of work meet the project objectives?	
2	Does the proposal specify the equipment and order of tools to be used (for example, equipment model, software version)?	
3	Is the tool appropriate for the site?	
	Has the tool matrix (resolution, scale, targets, weaknesses/limitations of tool) been reviewed to determine tool applicability?	
	Has the considerations for the tool checklist been evaluated to determine tool applicability?	
	What site conditions may prove challenging for implementation?	
	What potential is there for false positive signals? What are they and have they been tested for response?	
	What is the methodology for QA/QC in field and during post-processing?	
	Are there any deviations or recommendations from a requested suite of tools with supporting justification?	
4	Has a rationale for survey design been provided?	
	Has (or will) the proposer reviewed background information for the site (for example, geologic and hydrogeologic maps, previous studies, geography, aerial photographs, site history, historic fire insurance maps)?	
5	Does the proposal provide a description of the workflow process?	
	How the tool will be implemented?	
	What method will be used to ensure data location accuracy?	
	Does the proposal address several “what if” scenarios to deal with special issues?	
	Is there flexibility in the proposed work to expand the footprint and depth of the investigation?	
	Is there a plan and budget for targeted confirmatory sampling when unexpected, interesting, or questionable responses are observed?	
6	Does the proposal comply with safety requirements for the site?	
	What safety concerns may make the site unusual?	
	Are field personnel properly trained?	
7	Does the proposal specify the data deliverables?	
	Will raw data digital files be provided?	
	Will locational data be provided (for example, will I be able to relocate the area at a later time?)	
	Will copies of field notebooks be provided?	
	Will a report or memo summarizing the investigation and data interpretation be provided?	

Borehole Geophysics Proposal Considerations		
8	Does the proposal provide detailed costs?	
	Are subcontractors identified?	
	Are proposed hours appropriate?	
	Are equipment costs appropriate?	
	Are commodities/supplies appropriate?	
	Has a comparison of costs per day versus production (feet/day) per day been conducted to see which is likely to be more cost effective?	
9	Does the proposal provide a clear project timeline?	
10	What is the contractor's level of experience?	
	Are resumes provided?	
	Are references and other projects of similar scope provided?	
11	Are any permits are required?	
12	What are the insurance requirements?	

Borehole Geophysics Report Considerations		
1	Is there a summary of the tools and methods utilized?	
2	Does the report include limitations that constrained the study physically (for example, interferences, safety considerations, access) or due to other reasons beyond control of the contractor?	
3	Was the solicited scope of work followed as requested or were there deviations from the scope that were performed? If so, is there adequate justification for the deviations and was the user aware of them/approving of them in advance?	
4	What type of post processing was performed on the data? Does the report summarize the methods and assumptions used?	
5	What type of QA/QC was performed? Were there QA/QC steps in the field that were adequately followed? Was there data processing/interpretation QA/QC performed and is it described? Were there any deviations from the QA/QC plan?	
6	How are borehole logs provided?	
	How soon are draft borehole logs provided? Typically can be provided within 1-2 days. If targeting areas for sampling or determining the need to seal off a borehole, you may need to know potential flow zones ASAP depending on your site	
	When are legible finalized borehole logs be provided? Each borehole will have all of the data compiled into a format that should be easily interpreted. Depending on the suite of tooling used this could be one final log or multiple. Typically ATV and OTV are compiled onto one for comparison. Scale should be of such that features can be easily identified.	
7	Is there a narrative summary of the findings and results?	
	Is there a description of the types of responses observed, their potential origins, and whether they were confirmed with sampling?	
	Is there a description of lines of evidence observed to support/refute on-site interpretations?	
	Were there any limitations of the technology (were there any suspected false negatives)?	
	Were fracture traces and interpretation (for example, orientation/open/closed, fluid filled, dip/aperture) provided?.	
	Was fracture analysis performed, and are rose diagrams and stereonet plots provided?	
	Are there recommendations for follow-up sampling locations if definitive confirmation was not accomplished during the `investigation?	
8	Are raw data files provided?	
	Are summary tables of logs and identified features provided?	

Borehole Geophysics Report Considerations		
	Are logs presented in at least two appropriate scale factors (typically very low for absence/presence determinations and high for semi-quantitative site-wide comparisons of impact)?	
	Are raw WellCad files provided?	
9	Is there at least one plan view figure of the study area and the transects?	
10	What types of graphics are provided to illustrate the findings? Are there 2D or 3D profiles of responses with adequate scale, color ramp definitions?	

Borehole Geophysics Quality Control		
1	Log repeat/duplicate runs. What logs are repeated, footage rate are they completed at, and how often?	
2	HPFM requires multiple measurements (3+) at each elevation to confirm readings collected	
3	3-arm caliper results can be compared to results from the acoustic televiewer (ATV) or video survey. ATV results can be utilized to generate a caliper log for a borehole.	
4	Repeat data collection at casing/bedrock interface. Steel casing will influence orientation of some logs/distort results due to internal magnetometer.	
5	Necessary calibration procedures for tools and calibration checks	
6	Start and end elevation footage for measurements. These should be the same to make sure the winch did not slide and/or cable did not stretch	
7	Decontamination procedures (if applicable to your site). Clean tooling	
8	Compare with lithologic logs, do the contact or lithologic changes match depth wise	
9	Inspect equipment – does it appear clean and in good working order	
10	Site cleanup and proper equipment security	

Borehole Geophysics Fluid Temp/Res, Formation Resistivity, ATV/OTV, and Gamma Considerations		
1	Do open boreholes exist that can be logged? While the cost to implement the standard suite of geophysical tools is relatively reasonable, installation of boreholes/wells may be a significant cost to consider depending on subsurface conditions.	
2	Do you have access to the borehole? The equipment is heavy and requires a power source; therefore, you need to be able to get the equipment to the borehole location. Some contractors can only log from a vehicle, while others have remote logging capabilities.	
3	Is the borehole open or is it cased? Some tools require an open borehole to collect measurements. OTV illuminates and collects a direct image of the borehole wall; therefore, logging of a cased borehole would only provide an image of the casing. While the ATV sends out an acoustic signal to generate an image of the borehole, the signal will not effectively travel through casing materials. In addition, steel casing within boreholes can have an adverse effect on image quality for both the OTV and ATV. The borehole image generated by both tools is orientated to north by use of an internal magnetometer, which is influenced when in proximity of the steel casing and requires correction during post-processing of the data.	
4	Is there information available regarding regional/local lithology? Soil types and mineralogy can affect the response for some tools, such as gamma, and proper analysis requires an understanding of the possible soil types that may be present.	
5	Is the borehole fluid filled? Some probes must be submerged in water or light mud-filled intervals of boreholes to transmit and measure signals. Information regarding native formation fluids should be considered as pore fluid salinity/TDS can result in differing response for some tools. Fluid clarity is of concern for OTV as this tool collects a direct image of the borehole wall. Dark or cloudy fluid may not facilitate image collection with the OTV. ATV requires a fluid filled borehole to transmit acoustic signal.	
	Boreholes can be dry for temperature logging and will provide a direct measurement of fluid temperature within the formation.	
	Borehole can be logged while in equilibrium under ambient conditions or when a stress is applied. If conditions in the borehole haven't equilibrated, some of the smaller temperature/resistivity fluctuations may not be evident in the logging results. Logging under pumping conditions may enhance identification of water-bearing zones.	
6	What is the diameter of the borehole? Minimum/maximum diameter for operations of tools. Need >2-inch diameter borehole for most of the tooling and in general the ideal diameter is between 4 and 8 inches.	

Borehole Geophysics Fluid Temp/Res, Formation Resistivity, ATV/OTV, and Gamma Considerations		
7	Is the borehole straight and stable? Unstable and/or uneven borehole walls can result in collapse or the tool getting stuck. These specialized tools are expensive to replace if damaged or lost down a well. The original borehole diameter and any deviations in the borehole diameter are important considerations for proper log analysis as well. Uneven borehole diameter can also result in an adverse effect on image quality. Some of the tools rely on centralizers to keep the tool evenly spaced between the borehole walls. Deviation from the center of the borehole will result in distortion of the image or misinterpretation of the results.	
8	Do you have Safe working area/conditions? Understanding of work zone, contaminants (if applicable), long hours [work at night?]?	

Borehole Geophysics Heat Pulse Flowmeter or Impellert Considerations		
1	Do open boreholes exist that can be logged? While the cost to implement geophysical tools is relatively reasonable, installation of boreholes/wells may be a significant cost to consider depending on subsurface conditions. Open boreholes should be drilled and logged before the tool is utilized.	
2	Do you have access to the borehole? The equipment is heavy and requires a power source; therefore, you need to be able to get the equipment to the borehole location. Some contractors can only log from a truck, while others have remote logging capabilities.	
3	Borehole should be flushed of drill cuttings/sediment and needs to be fluid filled to measure groundwater flow	
4	Have potentially transmissive zones been identified? Borehole needs to have been logged using other geophysical tools, such as caliper, ATV, fluid temp/resistivity, or video, so that potentially transmissive zones can be targeted for flow measurements.	
5	Is there a general understanding of fluid flow within the formation? The limits of detection for the heat pulse flowmeter ranges from 0.03 gpm to 1.0 gpm. Use of the impeller flowmeter is typically required for rates greater than 1.0 gpm. This needs to be considered and evaluated during the logging process to ensure all zones of flow are identified and the objectives of the investigation are met.	
6	Are the flow measurements are going to be collected under stressed/pumped conditions? Are proper management of investigation derived waste needs to be considered?	
7	What is the diameter of the borehole? Need >2-inch diameter borehole for most of the tooling and in general and there are limitations on how large the borehole can be. The ideal diameter for boreholes ranges from 4-8 inches.	
8	Is the borehole straight and stable? Unstable and/or uneven borehole walls can result in collapse or the tool getting stuck. These tools are expensive, and no one wants to lose one down a borehole ($$$$). Uneven borehole diameter can also result in an adverse effect on image quality. The tools both rely on centralizers to keep the tool evenly spaced between the borehole walls. Deviation from the center of the borehole will result in distortion of the image, especially with the ATV tool.	
9	Is the working area/conditions safe? Understanding of work zone, contaminants (if applicable), long hours [work at night?]?	

Borehole Geophysics Nuclear Magnetic Resonance Considerations		
1	How are NMR data acquired? NMR logs can be acquired in open boreholes, using Geoprobe direct-push methods, or in wells constructed with nonconductive casings or screens (for example, PVC). When logging in open boreholes, a temporary casing is recommended if the borehole could potentially be unstable (unconsolidated material). There is no requirement for the borehole to be fluid-filled.	
2	Are you in a highly industrialized area? Industrial “noise” such as power lines and electric generators in the proximity of the logging location can interfere with NMR signals.	
3	What is the diameter of the original borehole and well casing? Various NMR tools are designed to accommodate different well casing diameters, and each will have a corresponding maximum sensitive shell diameter that must be greater than the original borehole diameter to collect data within the geologic unit of interest. Conversely, if conditions in the well’s annular space is of interest, select a tool with the appropriate sensitive shell diameter.	
4	What vertical resolution is necessary to identify features of interest? Different NMR tools provide different levels of vertical resolution ranging from 1 meter (approximately 3 feet) to less than ½ meter (1.5 feet or less).	
5	How many locations and vertical feet of logging are desired? NMR logging is a fairly slow process compared to other borehole geophysical methods. Logging rates of 15 meters per hour (approximately 50 feet per hour) are typical, and for some applications the logging rate is slower. Considering time for mobilization/demobilization and decontamination between wells, 60 to 75 meters (200-250 feet) is the maximum log production that should be expected in a typical work day for most near-surface applications. For deeper wells with a single mobilization greater log production is feasible.	
6	If self-performing the data acquisition, do you have staff trained on the use of the equipment? While designed to be user friendly, some level of training (typically 1-2 days) is needed to be proficient in data acquisition and processing. Alternatively, a geophysical service provider can rent the equipment and perform logging on your behalf.	
7	Do you have a secure location to store NMR tools when not in use? NMR tools are expensive (typically in the range of $250,000) so security and insurance requirements need to be considered while the equipment is in your possession.	

Borehole Geophysics Nuclear Magnetic Resonance Considerations		
8	Is the working area/conditions safe? Understanding of work zone, contaminants (if applicable), long hours [work at night?]. Be mindful of weather conditions, particularly electrical storms, that can affect data acquisition and cause damage to equipment. Be aware that the NMR tool contains powerful magnets that can disrupt pacemakers in the proximity of the tool.	

Method	Measured Properties	Study Objectives	Lateral Scale (feet)	Depth (feet)	Resolution (feet)	Geology/lithology	Large area needed	Acoustic/ Vibration Interference	Cultural Interference (metalic objects, power lines, utilities, pipes, fences, rebar, etc.)	Electromagnetic Interference (power lines, vehicles, atmospheric storms)	Limitations	Other supporting geophysical tools	Self Perform or Contractor
	Objectives					Considerations							
ERT	Electrical potential from applied current	Fracture zones, voids/solution features, lithology, buried debris, monitoring applied amendments, landfill leachate, saltwater intrusion, LNAPL	10 to 300	1 to 300	3 to 30	Low resistivity (high conductivity) soils	X		X			MASW, GPR	contractor due to high equipment costs
GPR	Amplitude and arrival time of reflected EM wave	Water table, lithology, buried debris, subsurface utilities, UST, voids, top of bedrock, unexploded ordinance (UXO), LNAPL	10 to 3,000	1 to 150	1 to 30	Dry, sandy soils provide best conditions for performance; high clay content greatly reduces penetration depth			X		Site access contstraints, interferences at ground surface, relatively flat terrain reduces topographic correction uncertainty, shallow water table reduces resolution and penetration depth	Magnetometer ERT	contractor due to high equipment costs
Seismic Reflection	Amplitude and arrival time of reflected acoustic waves	Top of bedrock, geologic contacts, faults, fractures, lithology, water table	1 to 3,000	1 to 1500	1 to 30	Saturated, fine-grained soils	X	X			Source to geophone distance 1-2X target depth	Seismic refraction ?	rental equipment available for self-performing with qualified personnel
Seismic Refraction	Amplitude and arrival time of refracted acoustic waves	Top of bedrock, geologic contacts, faults, fractures, lithology, water table, soil and rock properties	1 to 3,000	1 to 1500	1 to 30	will not detect thin layers	X	X			source to geophone distance 3-5X target depth	Seismic reflection?	rental equipment available for self-performing with qualified personnel
Frequency Domain Electromagnetics	Electrical conductivity of the subsurface using the magnitude and phase of the secondary field resulting from induced EM current	Mapping of contaminant plumes, hydrogeologic mapping, locating and mapping buried wastes, metal drums and tanks, and metal utilities	Unlimited (lateral extent is limited by battery life, or site features (such as trees, buildings, etc.))	1 to 200	Measurement Resolution +/- 0.1% of full scale	Low resistivity (high conductivity) soils	X		X	X		TDEM?	rental equipment available for self-performing with qualified personnel

Surface Geophysics Summary Table

Method	Measured Properties	Study Objectives	Lateral Scale (feet)	Depth (feet)	Resolution (feet)	Geology/lithology	Large area needed	Acoustic/ Vibration Interference	Cultural Interference (metalic objects, power lines, utilities, pipes, fences, rebar, etc.)	Electromagnetic Interference (power lines, vehicles, atmospheric storms)	Limitations	Other supporting geophysical tools	Self Perform or Contractor
Time Domain Electromagnetics	Electrical resistivity of subsurface by inducing pulsed currents with a transmitter loop	Primarily used for soundings to determine depth and thickness of geologic and hydrologic layers and for detection and mapping of inorganic plumes, seepage from brine pits, and salt-water intrusion	1 to 3,000	20 to 3,000	N/A	Low resistivity (high conductivity) soils	X			X	Areas of measurable resistivity contrast between subsurface layers	FDEM?	rental equipment available for self-performing with qualified personnel
MASW	Amplitude and arrival time of surface waves	Top of bedrock, karst features, soil layers, lithology, soil and rock properties (variation in soil or rock strength), rippability of material	10 to 300	0.1 to 120	0.1 to 20	Unconsolidated materials provide best performance. Will not detect deep thin layers and deep interfaces, will not work well with varaible lithologic interfaces and soil or rock properties					Shallow penetration depth, Relatively flat terrain	ERT Seismic Refraction GPR	rental equipment available for self-performing with qualified personnel
sources:													
Lee Slater - Envirowiki													
ASTM D6429-99 (reapproved 2006)													

Surface Geophysics Proposal Considerations		
1	Do the data quality objectives and scope of work meet the project objectives?	
2	Does the proposal specify the equipment and order of tools to be used (for example, equipment model, software version)?	
3	Is the tool appropriate for the site?	
	Has the tool matrix (resolution, scale, targets, weaknesses/limitations of tool) been reviewed to determine tool applicability?	
	Has the considerations for the tool checklist been evaluated to determine tool applicability?	
	What site conditions may prove challenging for implementation?	
	What potential is there for false positive signals? What are they and have they been tested for response?	
	What is the methodology for QA/QC in field and during post-processing?	
	Are there any deviations or recommendations from a requested suite of tools with supporting justification?	
4	Has a rationale for survey design been provided?	
	Has (or will) the proposer reviewed background information for the site (for example, geologic and hydrogeologic maps, previous studies, geography, aerial photographs, site history, historic fire insurance maps)?	
5	Does the proposal provide a description of the workflow process?	
	How the tool will be implemented?	
	What method will be used to ensure data location accuracy?	
	Does the proposal address several “what if” scenarios to deal with special issues?	
	Is there flexibility in the proposed work to expand the footprint and depth of the investigation?	
	Is there a plan and budget for targeted confirmatory sampling when unexpected, interesting, or questionable responses are observed?	
6	Does the proposal comply with safety requirements for the site?	
	What safety concerns may make the site unusual?	
	Are field personnel properly trained?	
7	Does the proposal specify the data deliverables?	
	Will raw data digital files be provided?	
	Will locational data be provided (for example, will I be able to relocate the area at a later time?)	
	Will copies of field notebooks be provided?	
	Will a report or memo summarizing the investigation and data interpretation be provided?	

Surface Geophysics Proposal Considerations		
8	Does the proposal provide detailed costs?	
	Are subcontractors identified?	
	Are proposed hours appropriate?	
	Are equipment costs appropriate?	
	Are commodities/supplies appropriate?	
	Has a comparison of costs per day versus production (feet/day) per day been conducted to see which is likely to be more cost effective?	
9	Does the proposal provide a clear project timeline?	
10	What is the contractor's level of experience?	
	Are resumes provided?	
	Are references and other projects of similar scope provided?	
11	Are any permits are required?	
12	What are the insurance requirements?	

Surface Geophysics Report Considerations		
1	Is there a summary of the tools and methods utilized?	
2	Does the report include limitations that constrained the study physically (for example, interferences, safety considerations, access) or due to other reasons beyond control of the contractor?	
3	Was the solicited scope of work followed as requested or were there deviations from the scope that were performed? If so, is there adequate justification for the deviations and was the user aware of them/approving of them in advance?	
4	What type of post processing was performed on the data? Does the report summarize the methods and assumptions used?	
5	What type of QA/QC was performed? Were there QA/QC steps in the field that were adequately followed? Was there data processing/interpretation QA/QC performed and is it described? Were there any deviations from the QA/QC plan?	
6	Is there a narrative summary of the findings and results?	
	Is there a description of the types of responses observed, their potential origins, and whether they were confirmed with sampling?	
	Is there a description of lines of evidence observed to support/refute on-site interpretations?	
	Were there any limitations of the technology (were there any suspected false negatives)?	
	Are there recommendations for follow-up sampling locations if definitive confirmation was not accomplished during the `investigation?	
7	Are raw data files provided?	
	Are summary tables of logs provided?	
	Are logs presented in at least two appropriate scale factors (typically very low for absence/presence determinations and high for semi-quantitative site-wide comparisons of impact)?	
8	Is there at least one plan view figure of the study area and the transects?	
9	What types of graphics are provided to illustrate the findings? Are there 2D or 3D profiles of responses with adequate scale, color ramp definitions?	

Surface Geophysics ERT Considerations		
1	Is site in an urban area?	
	Urbanized areas may prohibit the ability to achieve the required transect lengths for the desired depth.	
2	Is study area paved with impervious surfaces?	
	Electrodes require direct contact with subsurface soil which will be impaired by the presence of asphalt and concrete.	
	Capacitively coupled systems exist for settings with impervious surfaces, however, the resolution and depth of study is reduced.	

Surface Geophysics GPR Considerations		
1	Is the water table depth less than 5 feet from ground surface?	
	Shallow water table attenuates the GPR signal and thus reduces resolution and penetration depth.	
2	Are there aboveground interferences?	
	Standing water can cause loss of resolution.	
	Aboveground tanks, fences, power lines causing air wave interference.	
3	Is the site terrain relatively flat?	
	Flat terrain is ideal -topographic correction and ease of operator use.	
	Significantly undulating terrain will require topographic correction and can be more challenging to implement by the operator.	

Surface Geophysics Seismic Reflection/Seismic Refraction Considerations		
1	Is site in an urban area?	
	Urbanized areas provide high potential for excessive interferences and noise that can compromise data quality.	
	Extensive pre-planning is required (for example, background data collection, identification of interferences). Seismic tools may still be effective in locations with a high degree of electrical interference.	

Surface Geophysics MASW Considerations		
1	Are there aboveground interferences?	
	Ambient noise can be minimized by vertical stacking (combining multiple records).	
2	What is the site terrain relatively level?	
	Surface reliefs with dimension greater than about 10% of receiver-spread length or surface slope greater than 10° are not recommended.	
	Ground should be nearly flat at least within the receiver span.	

Surface Geophysics EM TDEM Considerations		
1	What is the water table depth?	
	Some FDEM instruments used to obtain vertical soundings are sensitive to vertical geologic features including groundwater in fractured bedrock.	
2	Are subsurface features present?	
	Rebar in reinforced concrete can cause interference.	
	Buried utilities will have an impact on vertical soundings.	
3	Are aboveground interferences present?	
	Buildings, fences, reinforced concrete, and high-power utilities can cause interference and must be accounted for in the study design and planning.	

Surface Geophysics EM TDEM Considerations		
1	Where is the study area? Urban or Rural area?	
	Time domain electromagnetic (TEM) method is more susceptible to interference from cultural features in urban areas, for example, Power lines, electric fences, roads, cars, any metals close to or by the study site. This will cause noise in the data.	
	Buried utilities (for example, pipe lines, cased wells) will significantly interfere with the EM signal, causing noise in the data.	
2	What is the scale of the project?	
	Airborne TEM is more suitable for larger area, it provides large ground coverage at relatively short time.	
	Groundbased TEM is more suitable for small projects. Depending on the available manpower, average of 16 soundings can be collected per day.	
	Choice of the size of the transmitting antenna will also depend on the size of the area, for example, a site big enough for the Walktem's 40 m x 40 m square loop.	
3	What are the site conditions?	
	Sites covered with tall grass, shrubs or bushes are not suitable for groundbased TEM. This will cause difficulties in placement of antenna. Complete removal of shrubs and bushes can resolve this.	
4	What is the geology of the site?	
	TEM is sensitive to conductive features (clay and shale), current system moves slowly in the subsurface which in turn results in a shallower depth of investigation.	
	Current system moves fast in the subsurface for intermediate to resistive features (for example, sand and gravel), typical for environments encountered in groundwater mapping, allows for higher depth of investigation.	
5	What is the intended depth of investigation?	
	For deeper targets >426 feet (>130 m), for example, in mining projects, airborne EM is more suitable.	

Sensor Type	Typical Data Products	Use Case Examples	Relative Cost Range	Limitations and Considerations
Visible Spectrum Camera	High-resolution nadir and oblique aerial photography High-resolution video High-resolution orthomosaic imagery Photogrammetrically derived Digital Surface Models (DSM) and Digital Terrain Models (DTM) Three-dimensional models Three-dimensional point cloud data (typically a .LAS or .LAZ file format)	Photogrammetry (measuring of lengths, heights and observation of features) from orthomosaic imagery Mensuration (geometric measurements) Generating surfaces and volumes Slope calculations for access or stability Surficial flow modelling Hydrologic analysis Video and photographic inspections Hazardous and confined space inspections Horizontal feature inspections Vertical infrastructure inspections Habitat mapping Stereographic viewing	$-$$$	Typically restricted in areas where dense vegetation canopies exist. Additional characteristics around time of day should be considered.
Multispectral Camera	High-resolution orthomosaic imagery Multi-spectral composite imagery	Vegetation mapping Habitat mapping Identification of certain gases Water quality assessment	$$-$$$	Cost, payload weight, and wavelength required for required task are all significant considerations. Multispectral instruments are typically restricted in areas where dense vegetation canopies exist. Additional characteristics around time of day, seasonality should also be considered.
Hyperspectral Camera	Hyperspectral data cube	Mineral or metals identification Vegetation mapping Habitat mapping Identification of certain gases	$$$$-$$$$$	Requires large processing capabilities and specific technical knowledge. Hyperspectral instruments are typically restricted in areas where dense vegetation canopies exist.

Sensor Type	Typical Data Products	Use Case Examples	Relative Cost Range	Limitations and Considerations
Thermal/Long-Wave Infra-Red (LWIR) Camera	High-resolution thermal video High-resolution thermal images (oblique and nadir) Orthomosaic thermal imagery map	Equipment inspections Wildlife surveys Identification of groundwater seeps Mapping of surface water mixing zones Identification of abandoned mine entrances Vegetation mapping Soil moisture mapping Snow/ice cover mapping	$-$$$	Thermal/LWIR sensors are typically restricted in areas where dense vegetation canopies exist. Additional characteristics around time of day, seasonality and field temperatures should also be considered.
Light Detection and Ranging (LiDAR)	Three-dimensional point cloud data (typically a .LAS or .LAZ file format) Digital Surface Models (DSM), Digital Terrain Models (DTM), Digital Elevation Models (DEM)	Hydrologic modelling Bare-earth measurements of volumes and surfaces (effective in vegetated areas) Identification of surficial features under canopy cover Vegetative canopy measurements Wetland mapping Mensuration (geometric measurements) Generating surfaces and volumes Slope calculations for access or stability Surficial flow modelling Hydrologic analysis	$$-$$$$$	Cost, payload weight, and point density are considerations for LiDAR. Point density per area is a consideration depending on the required task, and is often correlated with costs. LiDAR does not penetrate water.

*Table does not include less-common remote sensing devices such as magnetometers, gravimeters, and others.

Remote Sensing Safe Flight Initial Remote Assessment		
1	Verify FAA Airspace Regulations are being followed including verification of airspace restrictions. In particular, make sure the following areas are considered:	
	Controlled airspace.	
	Airports within 5 miles.	
	Heliports within 1 mile.	
	Restricted or prohibited areas.	
	Densely populated areas.	
	National Parks.	
2	Ensure pilot certified under FAA's Small UAS Rule (14 CFR Part 107).	
3	Review any state or municipal rules involving drones.	
4	Obtain written permission from the person with legal authority under your flight path.	
5	Verify appropriate insurance requirements are met.	
6	Ensure site-specific personal protective equipment, hazards, hazardous materials, or other special considerations are taken into account.	
7	Note safety equipment available (ABC fire extinguishers, first-aid kit) as appropriate.	
8	Design primary objectives of data collection and associated flight plans.	
9	Anticipate obstructions to Line-of-Sight, and plan accordingly (smaller flight segments or a visual observer).	
10	Review weather forecast at site prior to mobilization and planning.	
11	Note sunrise and sunset times to avoid unauthorized nighttime operations.	
12	Check the drone firmware and other relevant manufacture provided software for updates.	
13	Familiarize with the individual drone involved in operation and expected data products.	

Remote Sensing Safe Flight Final Remote Assessment		
1	Review weather forecast at site prior to mobilization and planning	
	Include appropriate health and safety equipment for weather conditions	
2	Final review of flight legality under 14 CFR Part 107 including reviewing temporary flight restrictions	
3	Check drone firmware and other relevant manufacture provided software for updates	
4	Complete a final inventory and physical inspection of:	
	Drone	
	Remote controller	
	Payloads	
	Batteries	
	Connecting cables	
	Storage media	
	Ground control devices	
	Other required equipment	
5	Verify batteries are charged and/or power source is available	

Remote Sensing Safe Flight Onsite and Launch		
1	Follow FAA regulations including, but not limited to:	
	Maintaining visual line-of-sight at all times.	
	Avoiding flying over people.	
	Avoiding flying at night.	
	Avoiding flying more than 400 feet above ground level.	
2	Final review of flight legality under 14 CFR Part 107 including reviewing temporary flight restrictions.	
3	Verify weather and wind conditions are appropriate for the duration of the flight.	
4	Identify an appropriate takeoff and landing area.	
5	Note the location of the nearest ABC fire extinguisher if you have one on-site.	
6	Inspect the drone, associated parts and batteries for damage or other defects.	
7	Note any potential obstructions and make ensure your flight path is above these areas.	
8	Verify that the aircraft is ready for power-up. This includes, but is not limited to:	
	Ensuring that any propellers are secure and clear.	
	Ensuring that the landing and takeoff are is clear of obstructions and traffic.	
	Battery in the controller is adequately charged.	
	Battery in the drone is adequately charged.	
	Data or sample storage is adequate.	
	Removing gimbal clamps.	
9	Ensure any appropriate safety gear is donned.	
10	Power up the drone, and verify the following:	
	Flight control app launches.	
	System statuses are signifying no errors.	
	If appropriate, a return-to-home location is set with settings for return-to-home height.	
	If appropriate, a maximum flight altitude is set.	
	If required, perform a compass and/or gimbal calibration.	
	Confirm a GPS signal lock.	
	Confirm remote controller connection with the drone.	
	Final flight plan verification.	
	Camera lens cap is removed.	
	Storage media or data collection devices are installed.	
	If applicable, ground control is deployed.	

11	Verbally announce that the drone is taking off and the launch area should be clear. The launch area should be marked off to prevent entrance.	
12	Confirm the launch area is clear.	
13	Takeoff with the drone.	

Remote Sensing Safe Flight In-Flight		
1	Capture required data. Maintain situational awareness (cars driving near control area, tripping hazards).	
2	Routinely check battery levels.	
3	Listen and look for aircraft, people, and vehicles entering your airspace.	
	Yield to all aircraft.	
4	Routinely monitor the drone location and maintain line-of-sight at all times.	
5	If applicable, maintain regular communication with any visual observers.	

Remote Sensing Safe Flight Landing		
1	Check the landing area for obstructions or people.	
2	Verbally announce that the drone is landing, and the landing area should be clear.	
3	Confirm the landing area is clear.	
4	Land the drone.	
5	Power off the drone.	

Remote Sensing Safe Flight Post-Landing		
1	After the drone is powered off, download any relevant data or take appropriate measures with any samples.	
	Perform relevant check for data collection.	
2	Inspect the drone, associated parts and batteries for damage or other defects.	
3	As appropriate, log the flight and any post-flight maintenance.	

Glossary

A

Active sensors – A solid-state chip that collects the return of a transmitted signal from an emitting source, for example, the return signal from a radar or light detection and ranging (LiDAR) camera.

Advection – Transport of solutes by flowing groundwater.

Alluvial – Unconsolidated rock or sediment that has been shaped by water and redeposited in a non-marine setting

Alluvial channel – A feature formed by the scouring effect of a river, typically under high energy conditions. It is therefore often coarser grained and more permeable than adjacent geological units.

Aperture – The ratio of the focal length to the diameter of the opening that allows light into the camera or onto the sensor.

B

Bedrock fabric – When applied to rocks, includes the complete spatial and geometrical configuration of all those components that make up the rock. It covers terms such as texture, structure and preferred orientation and so is an all-encompassing term that describes the shapes and characters of individual parts of a rock mass and the manner in which the parts are distributed and oriented in space. The individual parts are only considered as contributing to a fabric if they occur repeatedly in a reproducible manner form one sample of rock to another. (Hobbs B. E. 1976)

C

Capillary boundary – The pore spaces in soil just above the water table that may contain water above the static level from interactive forces between the water and soil.

Charged coupled device (CCD) sensors – A type integrated circuit made-up of a capacitor array that accumulates electric charge relative to light intensity and converts the charge to voltage.

Complementary metal–oxide–semiconductor (CMOS) sensors or active-pixel sensor – A type integrated circuit with amplifiers in each pixel capacitor that accumulates electric charge relative to light intensity and converts the charge to voltage.

Conceptual site model (CSM) – Representation of the site that summarizes and helps project planners visualize and understand available information. The CSM is the primary planning and decision-making tool used to identify the key issues and the data necessary to transition a project from characterization through post-remedy. It documents current site conditions and serves to conceptualize the relationship between chemicals in environmental media, sources, and receptors through consideration of potential or actual migration and exposure pathways.

Constituents/contaminants of concern (COCs) – Chemicals, compounds, elements detected in environmental media (soil, ground water, surface water, sediment, air) above regulatory criteria or that pose an unacceptable risks to human health and the environment, as identified in the risk assessments.

Continuously operating reference system (CORS) – A network of continuously operating ground stations, maintained by the United States National Geodetic Survey, that provide global satellite data consisting of carrier phase and code range measurements to support of three-dimensional positioning throughout the United States, its territories, and a few foreign countries.

D

Dense non-aqueous phase liquid (DNAPL) – A liquid (for example, tetrachloroethene) that has a density greater than water and is immiscible with water.

Dielectrical permittivity – A measure of the ability of a material to store an electric charge by separating opposite

polarity charges in space; it effectively measures a material's ability to be polarized by electric displacement due to an electric field and has units of farads per meter. Also known as dielectric constant.

Diffusion – The process of ionic or molecular constituents moving in the direction of a concentration gradient.

Digital elevation models (DEM) – A digital image, where each pixel has an elevation value, that representation of the ground surface terrain or relief not the contour of trees, building, or other objects that may obscure the ground surface or protrude above the ground surface.

Digital surface model (DSM) – A digital image, where each pixel has an elevation value, that representation of the surface relief such as the tree canopy, buildings, or bare ground when it is exposed.

Direct-push technology – Casing is pushed into the subsurface without drilling or auguring. Little or no annular space is created using this method.

Dispersion – The spreading of dissolved substances due to the combined effects of physical forces such as mechanical mixing, diffusion, and browning movement.

Dissolution – The process of dissolving.

Drive rod – The sections of direct push drilling rod added to the direct sensing probe to extend the depth.

Drone – The airframe, propulsion system, navigation equipment, and flight controller (often composed of GPS, on-board stabilization, and autonomous flight computer), and its payload (for example, camera).

E

Electrical resistivity – The intrinsic resistance of the subsurface to transport an electrical charge via conduction mechanisms.

F

Field of view (FOV) – A measure of the area on the surface of the ground that is observed by a single sensor.

Focal length – The distance between the lens and sensor when the camera is correctly focused on an object.

G

Gimbal – A camera mount that allows the camera to move up and down and left to right.

Ground control points (GCPs) – Manually surveyed ground targets that are clearly visible in in the collected data which can be used to measure vertical and horizontal error between the calculated point coordinates and the surveyed coordinates.

Ground sampling distance (GSD) – A description of spatial resolution in terms of the dimension of a square pixel per area on the ground.

H

Halogenated – Natural and synthetic chemicals that contain one or more halogens (fluorine, chlorine, bromine, or iodine) combined with carbon and other elements.

Heavy NAPL – Commonly DNAPL due to their higher density including coal tars, creosote, tank bottoms, bunker (marine) fuel, and chlorinated solvents that were used for degreasing.

Hydraulic conductivity – The rate that water can move through a saturated porous medium; defined as a proportionality constant (which includes the intrinsic permeability, the fluid density, a gravitational constant and the dynamic viscosity).

Hyperspectral camera – A camera that collects spectral data on tens to hundreds of narrow spectral bands over its coverage range.

I

Inertial measurement unit (IMU) – Electronic measurement of roll, pitch, and yaw, which is combined with GPS data to determine the drone's geolocation.

ISO – Is a scale of light sensitivity for a digital sensor which is comparable to ISO of film.

J

[bedrock] Joint – A fracture or break in rock that lacks any visible or measurable movement parallel to fracture surface.

K

Karst – Rock formations, typically limestone or dolomite, formed by dissolution of rock and often characterized, topographically, by sinkholes, sinking streams, closed depressions and characterized in the subsurface and by porosity features such as bedding planes, pinnacles, conduits, and caves.

L

LiDAR – A camera that uses pulses of laser light, near-infrared (about 1,000 nm), to image objects and measure distances.

Light non-aqueous phase liquid (LNAPL) – A liquid (e.g., petroleum oil, gasoline, diesel fuel) that has a density less than water and is immiscible with water.

Lines of evidence – Pieces of evidence organized to show relationships among multiple hypotheses or complex interactions among agent, events, or processes. A weight of evidence approach includes the assignment of a numeric weight to each line of evidence.

Lithology – Soil or rock type and origin.

Long-wave infrared camera (LWIR) – A camera having a sensor to detect wavelengths above 10,000 nm, a range that is referred to as thermal infrared.

M

Membrane – A semi-permeable, thin film polymer that is permeable to gas but impermeable to liquids.

Multispectral camera – A camera that collects data on three to nine relatively wide bands in near-infrared and red spectra.

N

Navigational GPS – Satellite-based system that provides geolocation and time information to a global positioning system (GPS) receiver using four or more GPS satellites.

Non-aqueous phase liquid (NAPL) – A liquid that is immiscible with water.

O

[fracture] Orientation – The strike and dip of an inclined plane.

Orthomosaic – A consolidated image, built from a collection of aerial images, corrected to remove distortions caused by camera perspective.

P

Passive sensors – A solid-state chip that collects reflected, ambient light across a defined region of the electromagnetic spectrum, for example, the light collected by a camera.

Permeability – Intrinsic measure of the ability of a porous material to allow fluids to past through it.

Photo stitching – The combining multiple photographic images, having overlapping fields of view, to produce high-resolution image or panoramic image.

Pixel pitch – The width of an individual pixel on a sensor relative to the width of the whole sensor.

Plume – An elongated body of groundwater containing contaminants, emanating from a point source and migrating within a hydrogeologic unit(s). The shape and movement of the mass of the contaminated water is affected by the geology, bio/geo chemistry, contaminant(s), and the flow characteristics of the groundwater. Because they often travel through discrete fractures and fracture sets, bedrock plumes are commonly asymmetrical in shape. Therefore, in bedrock, it may be more appropriate to use the terms “contaminant distribution” or “area of impact”.

Point cloud – A collection of data points (latitude, longitude, and altitude) within a defined coordinate system that are assembled in digital space to represent a surface.

Porosity (primary, secondary) – The ratio of the void volume to the total volume in geologic material. For primary porosity the void volume is the intergranular or inter-crystalline space. For fracture porosity the void volume is the space within fractures.

Postprocessed kinematic (PPK) GPS – The use location data from a base station or a network of operating reference system receivers to correct image coordinates after the flight data collection.

Precipitation – The process of chemical deposit formation from a solution.

Preferential pathway – A high-permeability conduit for contaminant migration such as a utility penetrations, lines, or drains; building sumps or drainage pits; elevator shafts; fractures in bedrock; or gravel channels.

Probe – Direct sensing instrument attached to the lead end of a drilling rod.

Q

Qualitative data – Qualitative – An indirect measurement (for example, LIF and PID measurements provide a relative measure of absence or presence but are not suitable as stand-alone tools for making remedy decisions.

Quantitative Data – Compound-specific values in units of concentration based on traceable standards (for example, µg/l, ppm, ppbv).

R

Real-time kinematic (RTK) GPS – The use of at least one additional GPS receiver at a nearby known static position to continuously supplement the GPS data from a satellite-based system.

Receptor – An individual, plant or animal that has the potential to be exposed to a contaminant in the environment media.

Remote-sensing – Gathering of data from distance by use of an airborne detector.

S

Saturated zone – Area below the unsaturated zone in which all the soil pores and rock fractures are filled with water.

Semi-quantitative data – Compound-specific quantitative measurements based on traceable standards but in units other than concentrations (for example, ng or ug) or provides measurements within a range.

Semi-volatile organic compounds (SVOCs) – A subgroup of volatile organic compounds that tend to have a higher molecular weight and higher boiling point temperature.

Sensor – A solid-state chip that converts an optical image to an electronic signal.

Site characterization – Site characterization is the process of developing an understanding of the geologic, hydrologic and engineering properties at the site including the soil, rock, along with groundwater and in many cases, human-modified conditions in the subsurface (e.g. utilities, structures, mines and tunnels) that can impact site conditions (Benson and Yuhr 2016).

Stakeholder – A stakeholder can be a person, a group, or an organization that is either affected, potentially affected, or has any interest in the project or in the project’s outcome, either directly or indirectly (Commission 1997).

Stratigraphy – The sequence of soil and rock layers in the subsurface, typically informed by an understanding of the natural processes that led to that sequence (e.g. deposited in a marine environment vs laid down by a river).

String Potentiometer (aka 'String Pot') – A transducer used to detect and measure linear position and velocity using a flexible cable and spring-loaded spool. Used to measure the depth of a probe in a borehole during advancement.

Surface geophysical tool – A class of nonintrusive geophysical instruments used to evaluate the subsurface. They indirectly measure physical properties of materials from signals produced by natural or generated sources and rely on contrasts in the properties of different materials.

T

Time-resolved – Activities measured with respect to time.

Transmissivity – The product of hydraulic conductivity and aquifer saturated thickness. For a discrete fracture the aquifer saturated thickness is the effective aperture.

Trunk line – Cable connecting a probe instrument to the above ground data acquisition instruments.

U

Unconsolidated formation – A soil or rock that has not been hardened by burial or geologic processes. Typically easy to excavate and penetrate with direct push tools but may collapse easily.

V

Volatile organic compounds (VOCs) – Organic chemicals that have a high vapor pressure at ordinary room temperature.

References

3DR. 2019. “Part 107 Drone Exam Practice Tests: Questions 1-10.” 3d Robotics, Inc. https://3dr.com/faa/drone-practice-tests/.

Adamson, D. T., S. Chapman, N. Mahler, C. Newall, B. Parker, S. Pitkin, and M. Rossi. 2014. “Membrane Interface Probe Protocol for Contaminants in Low-Permeability Zones.” *Groundwater.* 52 (4):550-565. doi: https://doi.org/10.1111/gwat.12085.

Adão, T., J. Hruška, L. Pádua, J. Bessa, E. Peres, R. Morais, and J.J. Sousa. 2017. “Hyperspectral Imaging: A Review on UAV-Based Sensors, Data Processing and Applications for Agriculture and Forestry.” *Remote Sensing* 9 (11). doi: https://doi.org/10.3390/rs9111110.

ADEC. 2017. Field Sampling guide. Division Of Spill Prevention and Response Contaminated Sites Program Alaska Department of Environmental Conservation. Juneau, Alaska. https://dec.alaska.gov/media/11956/field-sampling-guidance-august-2017-final.pdf.

Aldstadt, J., R., Germain, T., Grundl & R., Schweitzer. 2002. An In-Situ Laser-Induced Fluorescence System for Polycylic Aromatic Hydrocarbon-Contaminated Sediments (Final Report – Project Number GL975149-01-0, Submitted to United States Environmental Protection Agency Great Lakes National Program Office, Chicago, Illinois).

Allegheny. 2013. “Downhole Video Inspection Of 8-Inch Diameter Bedrock Well.” Allegheny Instruments. https://www.youtube.com/watch?v=Wa2isgVjgiY.

ALT. 2015. “OBI-402G Tool Specifications, product image copied from website in 2015.”. https://www.alt.lu/optical_televiewer.htm.

Anderson, N.L. 2014. Surface Waves (MASW) and Ground Penetrating Radar (GPR) Lecture Notes. Missouri S&T.

Annan, A.P. 2003. *Ground Penetrating Radar: Principles, Procedures & Applications*: Sensors & Software Incorporated, https://books.google.com/books?id=1nm4tgAACAAJ.

Annan, Peter. 2009. “Chapter 1. Electromagnetic Principles of Ground Penetrating Radar.” In *Ground Penetrating Radar: Theory and Applications*, 1-40. doi: 10.1016/B978-0-444-53348-7.00001-6.

Apitz, Sabine, Lisa M. Borbridge, Kim Bracchi, and Stephen H. Lieberman. 1993. “Fluorescent response of fuels in soils: insights into fuel-soil interactions.” *Environmental Process and Treatment Technologies, SPIE* 1716.

ASTM. 2010. D6187-10. In *Standard Practice for Cone Penetrometer Technology Characterization of Petroleum Contaminated Sites with Nitrogen Laser-Induced Fluorescence.* ASTM International, 100 Barr Harbor Dr., West Conshohocken, PA. www.astm.org.

ASTM. 2011a. D6429-99. In *Standard Guide for Selecting Surface Geophysical Methods. (reapproved 2011).* ASTM International, 100 Barr Harbor Dr., West Conshohocken, PA. www.astm.org.

ASTM. 2011b. D6432-11. In *Standard Guide for Using Surface Ground Penetrating Radar Method for Subsurface Investigation.* ASTM International, 100 Barr Harbor Dr., West Conshohocken, PA. www.astm.org.

ASTM. 2012a. D5778-12. In *Standard Test Method for Electronic Friction Cone and Piezocone Penetration Testing of Soils.* ASTM International, 100 Barr Harbor Dr., West Conshohocken, PA. www.astm.org.

ASTM. 2012b. D6001-05. In *Standard Guide for Direct-Push Groundwater Sampling for Environmental Site Characterization.* ASTM International, 100 Barr Harbor Dr., West Conshohocken, PA. www.astm.org.

ASTM. 2013. D7242/D7242M – 06(2013)e1. In *2013 Standard Practice for Field Pneumatic Slug (Instantaneous Change in Head) Tests to Determine Hydraulic Properties of Aquifers with Direct Push Groundwater Samplers.* ASTM International, 100 Barr Harbor Dr., West Conshohocken, PA. www.astm.org.

ASTM. 2017. D7352-17. In *Standard Practice for Direct Push Technology for Volatile Contaminant Logging with the Membrane Interface Probe (MIP).* ASTM International, 100 Barr Harbor Dr., West Conshohocken, PA. www.astm.org.

ASTM. 2018. D6639-18. In *Standard Guide for Using the Frequency Domain Electromagnetic Method for Subsurface Site Characterizations,*. ASTM International, 100 Barr Harbor Dr., West Conshohocken, PA. www.astm.org.

Atekwana, Estella A., and Eliot A. Atekwana. 2010. "Geophysical Signatures of Microbial Activity at Hydrocarbon Contaminated Sites: A Review." *Surveys in Geophysics* 31 (2):247-283. doi: 10.1007/s10712-009-9089-8.

Auken, Esben, Tue Boesen, and Anders V. Christiansen. 2017. "Chapter Two – A Review of Airborne Electromagnetic Methods With Focus on Geotechnical and Hydrological Applications From 2007 to 2017." In *Advances in Geophysics*, edited by Lars Nielsen, 47-93. Elsevier. doi: https://doi.org/10.1016/bs.agph.2017.10.002.

Baker, Gregory. 2019. "Processing near-surface seismic-reflection data : a primer." *Society of Exploration Geophysicists*.

Baker, Michael. 2004. Final Supplemental Groundwater Characterization Report Bishop Tube Site Baker Corporation. Harrisburg, Pennsylvania. files.dep.state.pa.us/RegionalResources/SERO/SEROPortalFiles/Community%20Info/Bishop%20Tube/Reports/July%202004%20Final%20Supplemental%20Groundwater%20Characterization%20Report%20-%20TEXT.pdf.

BayWest. 2013. Phase I Environmental Site Assessment of Jay Street Gas Holder Site, MPCA file SR1338.

BayWest. 2014. "Phase II Environmental Site Assessment of Jay Street Gas Holder Site. MPCA file SR1338."

BayWest. 2016. "Response Action Plan Implementation Report of Jay Street Gas Holder Site. MPCA file SR1338."

Beck, Frank P., Patrick J. Clark, and Robert Puls. 2000. "Location and Characterization of Subsurface Anomalies Using a Soil Conductivity Probe." *Ground Water Monitoring and Remediation – GROUND WATER MONIT REMEDIAT* 20:55-59. doi: 10.1111/j.1745-6592.2000.tb00265.x.

Benson, Richard, and Lynn Yuhr. 2016. "What Is Site Characterization." In, 99-106. doi: 10.1007/978-94-017-9924-9_11.

Berlman, I.B. 1971. *Handbook of fluorescence spectra of aromatic molecules.*, *Academic Press, New York*: Academic Press. doi: https://doi.org/10.1016/B978-0-12-092656-5.X5001-1.

Binley, A. 2015. "11.08 – Tools and Techniques: Electrical Methods." In *Treatise on Geophysics (Second Edition)*, edited by Gerald Schubert, 233-259. Oxford: Elsevier. doi: https://doi.org/10.1016/B978-0-444-53802-4.00192-5.

Bumberger, Jan, Dirk Radny, Andreas Berndsen, Tobias Goblirsch, Johannes Flachowsky, and Peter Dietrich. 2011. "Carry-Over Effects of the Membrane Interface Probe." *Ground water* 50:578-84. doi: 10.1111/j.1745-6584.2011.00879.x.

Burns & McDonnell. 2004. Wellington Former Manufactured Gas Plant Soil Boring (Gas Holder) Summary and Air Monitoring (Tech.). Wellington, KS.

Cascade. 2019. "Membrane Interface Hydraulic Profiling (MiHPT)." Cascade. https://cascade-env.com/technologies/site-characterization/membrane-interface-hydraulic-profiling-mihpt/.

Castendyk, D., B. Hill, P. Filiatreault, B. Straight, A. Alangari, P. Cote, and W. Leishman. 2018. "Experiences with Autonomous Sampling of Pit Lakes in North America using Drone Aircraft and Drone Boats." Proc. 11th Inter. Conf. on Acid Rock Drainage (ICARD) & Inter. Mine Water Assoc. (IMWA) 2018 Ann. Conf., Pretoria, South Africa, Sep. 10-14.

Castendyk, D., B. Straight, and P. Filiatreault. 2017. Apparatus connecting a water sample bottle to an unmanned aerial vehicle (UAV) in order to collect water samples from below the surface of a water body. edited by US Patent Office Application. patents.google.com/patent/US20170328814A1/en.

Castendyk, D., B. Straight, P. Filiatreault, S. Thibeault, and L. Cameron. 2017. "Aerial Drones Used to Sample Pit Lake Water Reduce Monitoring Costs and Improve Safety." Society of Mining Engineering, Feb 19-22, 2017.

Christiansen, Anders Vest, and Esben Auken. 2012. “A global measure for depth of investigation.” *GEOPHYSICS* 77 (4):WB171-WB177. doi: 10.1190/geo2011-0393.1.

Christy, T.M. 1996. “A driveable permeable membrane sensor of volatile compounds in soil.” Tenth National Outdoor Action Conference, Dublin, Ohio.

Cohen, Robert M., Anthony P. Bryda, Scott T. Shaw, and Charles P. Spalding. 1992. “Evaluation of Visual Methods to Detect NAPL in Soil and Water.” *Groundwater Monitoring & Remediation* 12 (4):132-141. doi: 10.1111/j.1745-6592.1992.tb00072.x.

Coleman, A., D. Nakles, M. McCabe, F. DiGnazio, T. Illangasekare, and R. St. Germain. 2006. Development of a Characterization and Assessment Framework for Coal Tar at MGP Sites. Electric Power Research Institute (EPRI). Palo Alto, CA.

Columbia. 2011. Subsurface Characterization Using Laser Induced Fluorescence (LIF) Technology – Former Petroleum Bulk Storage Facility in Conway, New Hampshire. LLC Columbia Technologies. Rockville, Maryland.

Columbia. 2019. “Columbia Technologies SmartData Solutions®.” Columbia Technologies, LLC. https://www.columbiatechnologies.com/technologies/smartdata-solutions/.

Commission, Presidential/Congressional. 1997. *Framework for Environmental Health Risk Management : Final Report*. Translated by The Presidential/Congressional Commission on Risk Assessment and Risk Management. Vol. Volume 1. Washington, DC, https://www.google.com/url?sa=t&rct=j&q=&esrc=s&source=web&cd=1&ved=2ahUKEwivv73DyZnlAhUCa60KHVh4BZcQFjAAegQIABAC&url=https%3A%2F%2Foaspub.epa.gov%2Feims%2Feimscomm.getfile%3Fp_download_id%3D36372&usg=AOvVaw1nlpBlDO-3OtjaNja-yuvF.

Considine, Thomas, and Jr Albert Robbat. 2008. “On-Site Profiling and Speciation of Polycyclic Aromatic Hydrocarbons at Manufactured Gas Plant Sites by a High Temperature Transfer Line, Membrane Inlet Probe Coupled to a Photoionization Detector and Gas Chromatograph/Mass Spectrometer.” *Environmental Science & Technology* 42 (4):1213-1220. doi: 10.1021/es702252q.

Cornell, D., M. Herman, and F. Ontiveros. 2016. Use of a UAV for Water Sampling to Assist Remote Sensing of Bacterial Flora in Freshwater Environments. In *Undergraduate External Publications. Paper 17.* St. John Fisher College. http://fisherpub.sjfc.edu/undergraduate_ext_pub/17.

Costanza, J., and W. M. Davis. 2000. “Rapid detection of volatile organic compounds in the subsurface by membrane introduction into a direct sampling ion-trap mass spectrometer.” *Field Analytical Chemistry & Technology* 4 (5):246-254. doi: 10.1002/1520-6521(2000)4:5<246::aid-fact4>3.0.co;2-w.

Council, National Research. 2000. *Seeing into the Earth: Noninvasive Characterization of the Shallow Subsurface for Environmental and Engineering Applications*. Washington, DC: The National Academies Press. doi: 10.17226/5786.

Culley, RW, FL Jagodits, and RS Middleton. 1976. “E-PHASE SYSTEM FOR DETECTING BURIED GRANULAR DEPOSITS.” Publication, November 3, 1976.https://trid.trb.org/view/47246.

Daniels, Jeffrey J. 2000. Ground Penetrating Radar Fundamentals. Appendix to USEPA Region V Report. https://clu-in.org/download/char/GPR_ohio_stateBASICS.pdf.

Day-Lewis, F.D., Johnson, C. D., Paillet, F.L., and Halford, K.J,. 2011. “FLASH: A Computer Program for Flow-Log Analysis of Single Holes v1.0.” *Geological Survey Software Release*, https://dx.doi.org/10.5066/F7319SZC.

Day-Lewis, Frederick D., Carole D. Johnson, Frederick L. Paillet, and Keith J. Halford. 2011. “A Computer Program for Flow-Log Analysis of Single Holes (FLASH).” *Groundwater* 49 (6):926-931. doi: 10.1111/j.1745-6584.2011.00798.x.

Day-Lewis, Frederick D., Lee D. Slater, Judy Robinson, Carole D. Johnson, Neil Terry, and Dale Werkema. 2017. “An overview of geophysical technologies appropriate for characterization and monitoring at fractured-rock sites.” *Journal of Environmental Management* 204:709-720. doi: https://doi.org/10.1016/j.jenvman.2017.04.033.

deGroot-Hedlin, C., and S. Constable. 1990. “Occam’s inversion to generate smooth, two-dimensional models from magnetotelluric data.” *Geophysics,* 55 (12):1613-1624.

Dixon, J.M., M. Taniguchi, and J.S. Lindsey,. 2005. “PhotochemCAD 2. A refined program with accompanying spectral databases for photochemical calculations.” *Photochem Photobiol* 81:212-213.

Dojack, Lisa. 2012. Ground Penetrating Radar Theory, Data Collection, Processing, and Interpretation: A Guide for Archaeologists. Vancouver, British Columbia: University of British Columbia.

DTI. 2017. “Tar-specific Green Optical Screening Tool (TarGost).” Dakota Technologies, Inc. (DTI). http://www.dakotatechnologies.com/services/targost.

Einarson, Murray, Adrian Fure, Randy St. Germain, Steven Chapman, and Beth Parker. 2018. “DyeLIF™: A New Direct-Push Laser-Induced Fluorescence Sensor System for Chlorinated Solvent DNAPL and Other Non-Naturally Fluorescing NAPLs.” *Groundwater Monitoring & Remediation* 38 (3):28-42. doi: 10.1111/gwmr.12296.

ERM. 2013a. Phase 2 Direct Push Evaluation Report, Former Refinery in Southern Oklahoma. ERM.

ERM. 2013b. Site-Wide Characterization Work Plan Addendum No. 2, Former Refinery in Southern Oklahoma. ERM.

ERM. 2015. Site-Wide Characterization Summary Report, Former Refinery in Southern Oklahoma. ERM.

ESRI. 2019. “The ArcGIS Imagery Book.” Environmental Systems Research Institute, Inc. https://www.e-education.psu.edu/geog883/node/421.

ESTCB. 2012. Parallel InSitu Screening of Remediation Strategies for Improved Decision Making, Remedial Design, and Cost Savings. U.S. Department of Defense Environmental Security Certification Program (ESTCP). Alexandria, Virginia. https://pdfs.semanticscholar.org/d66f/250f074149c031b4baccbd60bb4e0702be4a.pdf.

Everett, Mark E. 2013. *Near-Surface Applied Geophysics*. Cambridge: Cambridge University Press. doi: 10.1017/CBO9781139088435.

FAA. 2016a. “Remote Pilot – Small Unmanned Aircraft Systems Study Guide “. U.S. Department of Transportation, Federal Aviation Administration https://www.faa.gov/regulations_policies/handbooks_manuals/aviation/media/remote_pilot_study_guide.pdf.

FAA. 2016b. “Small Unmanned Aircraft Systems (sUAS) Advisory Circular.” U.S. Department of Transportation, Federal Aviation Administration https://www.faa.gov/documentLibrary/media/Advisory_Circular/AC_107-2.pdf.

FAA. 2018. “Part 107 UAS Operations.” U.S. Department of Transportation, Federal Aviation Administration Last Modified September 27, 2018. https://www.faa.gov/about/office_org/headquarters_offices/avs/offices/afx/afs/afs800/afs820/part107_oper/.

FAA. 2019a. “Educational Users.” U.S. Department of Transportation, Federal Aviation Administration. https://www.faa.gov/uas/educational_users/.

FAA. 2019b. “Part 107 Waivers.” U.S. Department of Transportation, Federal Aviation Administration. https://www.faa.gov/uas/commercial_operators/part_107_waivers/.

FAA. 2019c. “Unmanned Aircraft Systems (UAS).” U.S. Department of Transportation, Federal Aviation Administration https://www.faa.gov/uas/.

FAA. 2019d. “Welcome to the FAADroneZone.” U.S. Department of Transportation, Federal Aviation Administration. https://faadronezone.faa.gov/#/.

Fiacco, Joe. 2010. “High Resolution Site Characterization: A Sustainable Risk Management Approach.” *EHS Journal*, http://ehsjournal.org/http:/ehsjournal.org/joe-fiacco/high-resolution-site-characterization-a-sustainable-risk-management-approach/2010/.

Frankline, A. G., Dwain K. Butler, D. M. Patrick, W. E. Strohm Jr, and Mary Hynes. 2019. “Foundation considerations in siting of nuclear facilities in karst terrains and other areas susceptible to ground collapse.”

https://apps.dtic.mil/dtic/tr/fulltext/u2/a099565.pdf.

Fraser, G. S., and C. Hester. 1974. Sediment distribution in a beach ridge complex and its application to artificial beach replenishment, Environmental Geology Notes. Illinois State Geological Survey. Champaign, Illinois. https://www.ideals.illinois.edu/bitstream/handle/2142/78912/sedimentdistribu67fras.pdf?sequence=1.

GeoInsight. 2007. Level II Site Investigation – Former Petroleum Bulk Storage Facility in Conway, New Hampshire. GeoInsight.

GeoInsight. 2009. Dissolved Contaminant Plume/GMZ Delineation Report – Former Petroleum Bulk Storage Facility in Conway, New Hampshire.

GeoInsight. 2010. Soil Delineation and Monitoring Well Installation Report – Former Petroleum Bulk Storage Facility in Conway, New Hampshire.

GeoInsight. 2011. Laser Induced Fluorescence Plume Delineation Report – Former Petroleum Bulk Storage Facility in Conway, New Hampshire.

Geoprobe. 1994. A Percussion Probing Tool for The Direct Sensing of Soil Conductivity. In *Technical Paper No. 94-100*. Kejr Engineering Inc, Salina, Kansas.

Geoprobe. 2006. Geoprobe® Screen Point 16 Groundwater Sampler, Standard Operating Procedure. In *Technical Bulletin No. MK3142.* Kejr Inc., Salina, Kansas. https://geoprobe.com/literature/sp16-groundwater-sampler-sop.

Geoprobe. 2010. Geoprobe® Screen Point 22 Groundwater Sampler, Standard Operating Procedure. In *Technical Bulletin No. MK3173.* Kejr Inc., Salina, Kansas. https://geoprobe.com/literature/sp22-groundwater-sampler-sop.

Geoprobe. 2014. Geoprobe® Pneumatic Slug Test Kit (GW1600) Installation and Operation Instructions for USB System. In *Instructional Bulletin No. MK3181.* Kejr Inc., Salina, Kansas. https://geoprobe.com/sites/default/files/storage/pdfs/MK3195%20Slug%20Test%20Kit%20Instructions%20USB.pdf.

Geoprobe. 2015a. Geoprobe Systems® Electrical Conductivity (EC) System Standard Operating Procedure. In *Technical Bulletin No. MK3201.* Kejr Inc., Salina, Kansas. https://geoprobe.com/sites/default/files/storage/pdfs/EC_SOP_0115_0.pdf.

Geoprobe. 2015b. Geoprobe® Membrane Interface Probe (MIP) Standard Operating Procedure. In *Technical Bulletin No. MK3010.* Kejr Inc., Salina, Kansas. https://geoprobe.com/sites/default/files/storage/pdfs/MIP_SOP_mk3010_0115_0.pdf.

Geoprobe. 2019. Optical Imaging Profiler (OIP) Standard Operating Procedure. Geoprobe. Salina, Kansas. https://geoprobe.com/sites/default/files/storage/pdfs/OIP%20SOP%20rev.2.1.pdf.

GFCA. 2019. “Great Falls Citizens Association.” Great Falls Citizens Association. https://gfca.org/.

Giese, Paula. 1997. “U.S. Federally Non-Recognized Indian Tribes — Index by State.” Paula Giese. http://www.kstrom.net/isk/maps/tribesnonrec.html.

GISGeography. 2018. “Spectral Signature Cheatsheet – Spectral Bands in Remote Sensing.” Last Modified February 20, 2018, accessed August 8, 2019. https://gisgeography.com/spectral-signature/.

Gouveia, Fátima, Isabel Lopes, and Rui Carrilho Gomes. 2016. “Deeper VS profile from joint analysis of Rayleigh wave data.” *Engineering Geology* 202:85-98. doi: https://doi.org/10.1016/j.enggeo.2016.01.006.

GPG. 2017. “Geophysics for Practicing Geoscientists (GPG).”. GeoSci Developers. https://gpg.geosci.xyz/.

Hale, J. 2011. “Direct-Push, Laser Induced Fluorescence Application to Fractured Rock.” Fractured Rock and Eastern Ground Water Regional Issues Conference., Burlington, Vermont.

Harte, P. T., and Thomas J. Mack. 1992. Geohydrology of, and simulation of ground-water flow in, the Milford-Souhegan glacial-drift aquifer, Milford, New Hampshire. Open-File Reports U. S. Geological Survey Books, Section. http://pubs.er.usgs.gov/publication/wri914177.

IRYS. 2016. “Tallering Peak.” IRYS Drones PTY LTD, Last Modified July 12, 2016. https://www.youtube.com/watch?v=rx4nmuieLDM.

ITRC. 2015. Integrated DNAPL Site Characterization and Tools Selection. ISC-1. Interstate Technology & Regulatory Council, DNAPL Site Characterization Team., Washington, D.C. https://www.itrcweb.org/DNAPL-ISC_tools-selection/.

ITRC. 2017. Characterization and Remediation in Fractured Rock. FracRx-1. Interstate Technology & Regulatory Council, Characterization and Remediation in Fractured Rock Team, Washington, D.C. https://fracturedrx-1.itrcweb.org/.

ITRC. 2018. LNAPL Site Management: LCSM Evolution, Decision Process, and Remedial Technologies” [LNAPL-3]. Interstate Technology & Regulatory Council, Washington, D.C. https://lnapl-3.itrcweb.org/.

KBYF. 2015. “Know Before You Fly.” Association for Unmanned Vehicle Systems International (AUVSI) and the Academy of Model Aeronautics (AMA). http://knowbeforeyoufly.org/.

KDHE. 2014a. Phase I Source Investigation Report: Former Manufactured Gas Plant (FMGP) – Wellington; Site ID: C2-096-70046-8.1. Kansas Department of Health and Environmental. Wellington, Kansas.

KDHE. 2014b. Phase II Source Investigation Report: Former Manufactured Gas Plant (FMGP) – Wellington; Site ID: C2-096-70046-8.1. Kansas Department of Health and Environmental. Wellington, Kansas.

Knight, Rosemary. 2001. “Ground Penetrating Radar for Environmental Applications.” *Annual Review of Earth and Planetary Sciences* 29 (1):229-255. doi: 10.1146/annurev.earth.29.1.229.

Koparan, C., A.B. Koc, C.V. Privette, C.B. Sawyer, and J.L. Sharp. 2018. “Evaluation of a UAV-assisted autonomous water sampling.” Water 10 (655):16. doi: 10.3390/w10050655.

Kram, Mark L., Arturo A. Keller, Steve M. Massick, and Leroy E. Laverman. 2004. “Complex NAPL Site Characterization Using Fluorescence Part 1: Selection of Excitation Wavelength Based on NAPL Composition.” *Soil and Sediment Contamination: An International Journal* 13 (2):103-118. doi: 10.1080/10588330408984082.

Lakowicz, J.R. 1999. “Principles of Fluorescence Spectroscopy, 2nd Ed.” *Kluwer Academic/Plenum Publishers, New York.*

Li, Zhilin, Qing Zhu, and Christopher Gold. 2005. *Digital Terrain Modeling: Principles and Methodology*. doi: 10.1201/9780203357132.

Lunne, Tom, P. Robertson, and John Powell. 1997. “Cone Penetration Testing in Geotechnical Practice.” *Soil Mechanics and Foundation Engineering* 46. doi: 10.1007/s11204-010-9072-x.

Mansoor, Nasser, Slater, Lee, Artigas, Francisco, and Auken, Esben. 2006. “High-resolution geophysical characterization of shallow-water wetlands.” *Geophysics* 71 (4):B101-B109. doi: https://doi.org/10.1190/1.2210307.

MASW. 2018. “Multichannel Analyses of Surface Waves (MASW) – Data Acquisition.”, accessed 11/20/2018. http://www.masw.com/DataAcquisition.html.

McCall, Wesley. 2010. Tech Guide for Calculation of Estimated Hydraulic Conductivity Log from HPT Data. Geoprobe. https://geoprobe.com/sites/default/files/storage/pdfs/tech_guide_estk_v5_0_0.pdf.

McCall, Wesley, T.M. Christy, D. A. Pipp, Ben Jaster, Rick Bean, Ian Smith, Gary Richards, and Jonathan Stephenson. 2018. “Field Tests with the OIP-Green DP Photo-Logging System for Detection of Coal Tars.” Battelle 11th International Conference on the Remediation of Chlorinated and Recalcitrant Compounds, April 2018.https://geoprobe.com/literature/field-tests-oip-green-dp-photo-logging-system-detection-coal-tars.

McCall, Wesley, Thomas M Christy, Daniel A Pipp, Ben Jaster, Jeff White, James Goodrich, John Fontana, and Sheryl Doxtader. 2018. “Evaluation and application of the optical image profiler (OIP) a direct push probe for photo-logging UV-induced fluorescence of petroleum hydrocarbons.” *Environmental Earth Sciences* 77:374. doi: 10.1007/s12665-018-7442-2.

McCall, Wesley, Thomas M. Christy, and Mateus K. Evald. 2017. “Applying the HPT-GWS for Hydrostratigraphy, Water Quality and Aquifer Recharge Investigations.” *Groundwater Monitoring & Remediation* 37 (1):78-91. doi: 10.1111/gwmr.12193.

McCall, Wesley, Thomas M. Christy, Daniel Pipp, Mads Terkelsen, Anders Christensen, Klaus Weber, and Peter Engelsen. 2014. “Field Application of the Combined Membrane-Interface Probe and Hydraulic Profiling Tool (MiHpt).” *Groundwater Monitoring & Remediation* 34 (2):85-95. doi: 10.1111/gwmr.12051.

MDEQ. 2013. Montana Light Non-Aqueous Phase Liquid (LNAPL) Recovery and Monitoring Guidance Remediation Division Montana Department of Environmental Quality. Helena, Montana. http://deq.mt.gov/Portals/112/Land/StateSuperfund/Documents/montana%20LNAPL%20Recovery%20and%20Monitoring%20Guidance%20FINAL%2007_15_13.pdf.

MDEQ. 2017. Senate Bill 96 (2015) Status of $7,000,000 Appropriation from the Orphan Share Account Environmental Quality Council – Final Report July 1, 2015 to June 30, 2017. Montana Department of Environmental Quality. Helena, Montana. https://deq.mt.gov/Portals/112/Land/LUST/Documents/downloadables/Final%20Report%20(July%202017).pdf?ver=2017-08-07-092411-013.

MDNR-SWMP. 2015. Preliminary geophysical investigation: City Utilities John Twitty Energy Center. Missouri Department of Natural Resources. Springfield, Missouri

Milsom, J., and A. Eriksen. 2011. *Field Geophysics, 4th Edition.* UK: John Wiley & Sons Ltd.,. doi: https://doi.org/10.2113/gseegeosci.19.2.205.

Mussett, Alan E., and M. Aftab. Khan. 2000. “Looking into the Earth: An introduction to Geological Geophysics.” *Cambridge University Press.* doi: https://doi.org/10.1017/CBO9780511810305.

Mwakanyamale, K. E. , S. E. Brown, E. J Anderson, and A. C. Phillips. 2018. Mapping Sand Distribution along the Illinois Lake Michigan Shore using Airborne Electromagnetic Method, Contract Report for FY2016, Award NA16NOS4190151. Illinois Department of Natural Resources Coastal Management Program.

Mwakanyamale, Kisa, Lee Slater, Andrew Binley, and Dimitrios Ntarlagiannis. 2012. “Lithologic imaging using complex conductivity: Lessons learned from the Hanford 300 Area.” *GEOPHYSICS* 77 (6):E397-E409. doi: 10.1190/geo2011-0407.1.

NASA. 2019. “EarthData Visualize Data.” National Aeronautics and Space Administration. https://earthdata.nasa.gov/earth-observation-data/visualize-data.

NCSL. 2019. “Federal and State Recognized Tribes.” National Conference of State Legislatures. http://www.ncsl.org/research/state-tribal-institute/list-of-federal-and-state-recognized-tribes.aspx#federal.

Newman, C.P., D. Castendyk , B. Straight, P. Filiatreault, and A. Pino. 2018. “Remote water-quality sampling of Nevada pit lakes using unmanned aircraft systems.” *Geological Society of America, Abstracts with Programs* 50 (5). doi: 10.1130/abs/2018RM-313820.

NITIA. 2016. Voluntary Best Practices for UAS Privacy, Transparency, and Accountability. National Telecommunications and Information Administration U.S. Department of Commerce. Washington D.C. https://www.ntia.doc.gov/files/ntia/publications/voluntary_best_practices_for_uas_privacy_transparency_and_accountability_0.pdf.

NJDEP. 2005. Field Sampling Procedures Manual. Chapter 8. New Jersey Department of Environmental Protection Site Remediation Program. https://www.nj.gov/dep/srp/guidance/fspm/.

NOAA. 2019a. “Satellite and Information Services, Imagery and Data.” U.S. Department of Commerce, National Oceanic and Atmospheric Administration. https://www.nesdis.noaa.gov/content/imagery-and-data.

NOAA. 2019b. “United States Interagency Elevation Inventory.” States Department of Commerce, National Oceanic and Atmospheric Administration. https://coast.noaa.gov/inventory/.

O’Connor, James, Mike Smith, and Mike James. 2017. “Cameras and settings for aerial surveys in the geosciences: Optimizing image data.” Progress in Physical Geography 41:030913331770309. doi: 10.1177/0309133317703092. https://pdfs.semanticscholar.org/a2d4/a2a54c71d3d4e7c0d68ab5ae60b0f37d3b71.pdf?_ga=2.238797632.1981474323.1572121044-763476554.1572121044.

Olafsdottir, Elin Asta, Bjarni Bessason, and Sigurdur Erlingsson. 2018. “Combination of dispersion curves from MASW measurements.” *Soil Dynamics and Earthquake Engineering* 113:473-487. doi: https://doi.org/10.1016/j.soildyn.2018.05.025.

Ore, John-Paul, Sebastian Elbaum, Amy Burgin, and Carrick Detweiler. 2015. “Autonomous Aerial Water Sampling.” *Journal of Field Robotics* 32 (8):1095-1113. doi: 10.1002/rob.21591.

Park, Choon B. 2005. “MASW horizontal resolution in 2D shear-velocity (Vs) mapping.”

Park, Choon B. 2006. SurfSeis User’s Manual V2.0. In *Kansas Geological Survey.* http://www.kgs.ku.edu/software/surfseis/Manuals/Manual20.pdf.

Park, Choon B., and Mario Carnevale. 2010. *Optimum MASW survey – Revisit after a Decade of Use*. doi: 10.1061/41095(365)130.

Park, Choon B., Richard D.Miller, and Hidetoshi Miura. 2002. “Optimum Field Parameters of an MASW Survey.” *SEG-J, Tokyo*.

Park, Choon B., Richard D. Miller, and Jianghai Xia. 1999. “Multichannel analysis of surface waves.” *GEOPHYSICS* 64 (3):800-808. doi: 10.1190/1.1444590.

Park, Choon B., Richard D. Miller, Jianghai Xia, and Julian Ivanov. 2007. “Multichannel analysis of surface waves (MASW)—active and passive methods.” *The Leading Edge* 26 (1):60-64. doi: 10.1190/1.2431832.

Parker, Beth. 2007. “Investigating contaminated sites on fractured rock using the DFN approach. 2007 NGWA/U.S.” *EPA Fractured Rock Conference: State of the Science and Measuring Success in Remediation, Portland, ME*:150-168.

PennState. 2018. “FEOG 883:Remote Sensing Image Analysis and Applications.” Penn State College of Earth and Mineral Sciences. https://www.e-education.psu.edu/geog883/node/421.

Peterson, J. L. 2017. “Borehole Geophysical Logging – Applications for Environmental Site Remediation (New Jersey Site Remediation Professional Licensing Board Course No. 2015-2017).” Princeton Geoscience, Inc. to the New Jersey Licensed Site Remediation Professionals Association and the New York – Philadelphia Chapter of the Association of Environmental and Engineering Geologists.

Quinnan, J.A., Killenbeck, E. and Welty, N.R.H. 2010. “Re-evaluating MIPs – Observations on limitations based on comparison with whole-core and vertical profile sampling.” Battelle 7th International Conference: Remediation of Chlorinated and Recalcitrant Compounds. Oral Presentation.

Redman, J. D. 2009. “Chapter 8 – Contaminant Mapping.” In *Ground Penetrating Radar Theory and Applications*, edited by Harry M. Jol, 247-269. Amsterdam: Elsevier. doi: https://doi.org/10.1016/B978-0-444-53348-7.00008-9.

Robertson, P. 1990. “Soil classification using the cone penetration test.” *Canadian Geotechnical Journal – CAN GEOTECH J* 27:151-158. doi: 10.1139/t90-014.

Robertson, P., John Sully, D. J. Woeller, Tom Lunne, John Powell, and D. G. Gillespie. 2011. “Estimating coefficient of consolidation from piezocone tests.” *Canadian Geotechnical Journal* 29:539-550. doi: 10.1139/t92-061.

Robertson, P.K., and K.L. Cabal. 2008. Guide to Cone Penetration Testing for Geo-Environmental Engineering, 2nd Edition. Inc. Gregg Drilling and Testing. Signal Hill, California.

Robertson, P.K., R.G. Campanella, D.G. Gillespie and J. Greig. 1986. “Use of Piezometer Cone Data.” ASCE Specialty Conference: In Situ ’86: Use of In Situ Tests in Geotechnical Engineering, Blacksburg, GSP 6, ASCE. Specialty Publication, SM 92., Reston, VA.

Schlumberger. 2009. Log Interpretation charts, 2009 Edition. Schlumberger. Sugar Land, Texas. http://pages.geo.wvu.edu/~tcarr/pttc/schlumberger_chartbook.pdf.

Schulmeister, Marcia, James Butler Jr, J. M. Healey, L. Zheng, D. A. Wysocki, and Wes McCall. 2003. “Direct-Push Electrical Conductivity Logging for High-Resolution Hydrostratigraphic Characterization.” *Ground Water Monitoring and Remediation – GROUND WATER MONIT REMEDIAT* 23:52-62. doi: 10.1111/j.1745-6592.2003.tb00683.x.

ScienceDirect. 2016. “Cone Penetration Test.” Elsevier B.V., Last Modified 2019, accessed August 6, 2019. https://www.sciencedirect.com/topics/engineering/cone-penetration-test.

SDPRCF. 2015. A Study of Managing Uncertainties using the Triad Approach. South Dakota Petroleum Release Compensation Fund. Pierre, SD. http://denr.sd.gov/dfta/prcf/triad_pathology.aspx.

Shabica, Charles, and Frank Pranschke. 1994. “Survey of Littoral Drift Sand Deposits Along the Illinois and Indiana Shores of Lake Michigan.” *Journal of Great Lakes Research* 20 (1):61-72. doi: https://doi.org/10.1016/S0380-1330(94)71132-1.

Sheriff, R.E., and L.P. Geldart. 1995. *Exploration Seismology.*, *Cambridge University Press.* doi: https://doi.org/10.1017/CBO9781139168359.

Siami-Irdemoosa, Elnaz. 2017. “Dissolution-enlarged fractures imaging using electrical resistivity tomography (ERT).” Ph. D. in Geological Engineering, Geosciences and Geological and Petroleum Engineering, Missouri University of Science and Technology (2572).

Slater, L., A. M. Binley, W. Daily, and R. Johnson. 2000. “Cross-hole electrical imaging of a controlled saline tracer injection.” *Journal of Applied Geophysics* 44 (2):85-102. doi: https://doi.org/10.1016/S0926-9851(00)00002-1.

SonTek. 2019. “YSI CastAway® CTD.” SonTek. https://www.sontek.com/castaway-ctd.

Sørensen, Kurt, and Esben Auken. 2004. “SkyTEM – A new high-resolution helicopter transient electromagnetic system.” *Exploration Geophysics* 35:194-202. doi: 10.1071/EG04194.

Springfield, City Utilities of 2016. Closure and Post-Closure Care Plan. City Utilities of Springfield. Springfield, Missouri.

Spurlin, Matthew S., Brent W. Barker, Bradley D. Cross, and Craig Divine. 2019. “Nuclear magnetic resonance logging: Example applications of an emerging tool for environmental investigations.” *Remediation Journal* 29:63-73. doi: 10.1002/rem.21590.

St. Germain, R. 2008. Remediation Technology Symposium. Sacramento, California.

St. Germain, R. 2011. “Laser-Induced Fluorescence (LIF) Primer.” *Applied NAPL Science Review, Demystifying NAPL Science for the Remediation Manager.* 1 (9), http://www.h2altd.com/wp-content/uploads/2011/10/ANSR-v1i9.pdf.

St. Germain, R., M. Einarson, A. Fure, S. Chapman, and B. Parker. 2014. “Dye based laser-induced fluorescence sensing of chlorinated solvent DNAPLs.” 3rd International Symposium on Cone Penetration Testing., Las Vegas, Nevada, USA.http://www.dakotatechnologies.com/info/newsletters/article/2014/08/06/dye-based-laser-induced-fluorescence-sensing-of-chlorinated-solvent-dnapls.

St. Germain, R., and T Martin. 2008. North American Environmental Field Conference & Exposition – LIF Workshop Slides. https://clu-in.org/download/char/lif/Dakota-Technologies-LIF-Workshop.pdf.

Telford, W. M., L. P. Geldart, R. E. Sheriff, and D. A. Keys. 1976. “Applied Geophysics.” *Geological Magazine* 113 (5):492-493. doi: 10.1017/S0016756800050858.

Terada, Akihiko, Yuichi Morita, Takeshi Hashimoto, Toshiya Mori, Takeshi Ohba, Muga Yaguchi, and Wataru Kanda. 2018. “Water sampling using a drone at Yugama crater lake, Kusatsu-Shirane volcano, Japan.” *Earth, Planets and Space* 70. doi: 10.1186/s40623-018-0835-3.

Terry, Neil, Frederick Day-Lewis, Judith Robinson, Lee Slater, Keith Halford, Andrew Binley, John Lane, and Dale Werkema. 2017. “Scenario Evaluator for Electrical Resistivity Survey Pre-modeling Tool.” *Ground water* 55. doi: 10.1111/gwat.12522.

USACE. 1995. Geophysical Exploration for Engineering and Environmental Investigations. U. S. Army Corps of Engineers. Washington, DC: U. S. Army Corps of Engineers. https://www.publications.usace.army.mil/Portals/76/Publications/EngineerManuals/EM_1110-1-1802.pdf.

USACE. 2008. Former Kirksville Air force Station, Missouri U.S. Army Corps of Engineers. Kansas City, Missouri: U.S. Army Corps of Engineers. https://dnr.mo.gov/env/hwp/docs/kafspp1108.pdf.

USDA. 2009. “Ground-Penetrating Radar Soil Suitability Maps.” U.S. Department of Agriculture, Natural Resources Conservation Service. https://www.nrcs.usda.gov/wps/portal/nrcs/detail/soils/survey/geo/?cid=nrcs142p2_053622.

USEPA. 1993. Subsurface Characterization and Monitoring Techniques: A Desk Reference Guide. Volume 1: Solids and Ground Water Appendices A and B. U. S. Environmental Protection Agency Land and Emergency Management. Washington, DC. EPA/625/R-93/003a. https://nepis.epa.gov/Exe/ZyNET.exe/30004L8E.txt?ZyActionD=ZyDocument&Client=EPA amp;Index=1995%20Thru%201999%7C1991%20Thru%201994%7C1986%20Thru%201990%7CHardcopy%20Publications &Docs=&Query=EPA%2F625%2FR-93%2F003a&Time=&EndTime=&SearchMethod=2&TocRestrict=n&Toc=&TocEntry =&QField=&QFieldYear=&QFieldMonth=&QFieldDay=&UseQField=&IntQFieldOp=0&ExtQFieldOp=0&XmlQuery= &File=D%3A%5CZYFILES%5CINDEX%20DATA%5C91THRU94%5CTXT%5C00000009%5C30004L8E.txt&User= ANONYMOUS&Password=anonymous&SortMethod=h%7C-&MaximumDocuments=10&FuzzyDegree =0&ImageQuality=r75g8/r75g8/x150y150g16/i425&Display=p%7Cf&DefSeekPage=x&SearchBack=ZyActionE&Back= ZyActionS&BackDesc=Results%20page&MaximumPages=1&ZyEntry=1&SeekPage=x.

USEPA. 2004. The Triad Approach to Managing Decision Uncertainty for Better Cleanup Projects. Washington, D.C.: U.S. Environmental Protection Agency. https://archive.epa.gov/epawaste/hazard/web/pdf/triad.pdf.

USEPA. 2006. Guidance on Systematic Planning Using the Data Quality Objectives Process U.S. Environmental Protection Agency. Washington, D.C. EPA/240/B-06/001 https://www.epa.gov/sites/production/files/documents/guidance_systematic_planning_dqo_process.pdf.

USEPA. 2016a. “Environmental Geophysics Seismic Reflection Methods.” U. S. Environmental Protection Agency, Last Modified May 18, 2016, accessed August 6, 2019. https://clu-in.org/characterization/technologies/geophysics/pages/reference/methods/Surface_Geophysical_Methods/Seismic_Methods/Seismic_Reflection_Methods.htm.

USEPA. 2016b. Expected Site Assessment Tools For Underground Storage Tank Sites: A Guide For Regulators. Chapter 5 Direct Push Technologies. U. S. Environmental Protection Agency Land and Emergency Management. Washington, DC. EPA 510-B-16-004. https://www.epa.gov/sites/production/files/2014-03/documents/esa-ch1.pdf.

USEPA. 2016c. Expedited Site Assessment Tools for Underground Storage Tank Sites: A Guide for Regulators. United States Environmental Protection Agency Office of Underground Storage Tanks. Washington D.C. EPA 510-B-97-001/EPA 510-B-16-004. https://www.epa.gov/ust/expedited-site-assessment-tools-underground-storage-tank-sites-guide-regulators.

USEPA. 2016d. “Ground-Penetrating Radar.” U. S. Environmental Protection Agency, Last Modified May 24, 2016. https://archive.epa.gov/esd/archive-geophysics/web/html/ground-penetrating_radar.html.

USEPA. 2018a. Best Practices for Data Management Technical Guide. United States Environmental Protection Agency. Washington D.C. . EPA 542-F-18-003. https://semspub.epa.gov/work/HQ/100001798.pdf.

USEPA. 2018b. “Ground Penetrating Radar. U.S. EPA Contaminated Site Cleanup Information (CLU-IN). 7 September 2018 (last update).”. U. S. Environmental Protection Agency, Last Modified September 7, 2017. http://clu-in.org/characterization/technologies/gpr.cfm.

USEPA. 2018c. “Membrane Interface Probe (MIP).” U.S. Environmental Protection Agency. https://clu-in.org/characterization/technologies/mip.cfm.

USGS. 2000a. “Geophysical logs – Gamma logs.” Department of the Interior, U.S. Geological Survey. https://www.usgs.gov/media/images/geophysical-logs-gamma-logs.

USGS. 2000b. “Geophysical logs – Spontaneous-potential log.” Department of the Interior, U.S. Geological Survey. https://www.usgs.gov/media/images/geophysical-logs-spontaneous-potential-log.

USGS. 2000c. “Geophysical logs – Temperature logs.” Department of the Interior, U.S. Geological Survey.

https://www.usgs.gov/media/images/geophysical-logs-temperature-logs.

USGS. 2007. Borehole Geophysical Logging of Water-Supply Wells in the Piedmont, Blue Ridge, and Valley and Ridge, Georgia. Washington, D.C.: Department of the Interior, U.S. Geological Survey. Fact Sheet 2007–3048 https://pubs.usgs.gov/fs/2007/3048/pdf/fs2007-3048.pdf.

USGS. 2016a. "Vertical Flowmeter Logging." Department of the Interior, U.S. Geological Survey. https://water.usgs.gov/ogw/bgas/flowmeter/.

USGS. 2016b. "Vertical Flowmeter Logging." U.S. Department of Interior, Last Modified December 26, 2016, accessed August 6, 2019. https://water.usgs.gov/ogw/bgas/flowmeter/.

USGS. 2018a. "FLASH: A Computer Program for Flow-Log Analysis of Single Holes." Department of the Interior, U.S. Geological Survey. https://water.usgs.gov/ogw/bgas/flash/.

USGS. 2018b. "Fractured Rock Geophysical Toolbox Method Selection Tool (FRGT-MST)." U.S. Department of Interior, Last Modified 1/25/2018, accessed 10/15/2019. https://water.usgs.gov/ogw/bgas/frgt/.

USGS. 2018c. "Scenario Evaluator for Electrical Resistivity (SEER) Survey Pre-Modeling Tool." Department of the Interior, U.S. Geological Survey. https://water.usgs.gov/ogw/bgas/seer/.

USGS. 2018d. USGS Unmanned Aircraft Systems, Data Delivery Specification U.S. Geological Survey Department of the Interior. Washington, D.C. DCN 074-2 MOD1.A5915 Version 1.2 https://lta.cr.usgs.gov/sites/default/files/USGS%20UAS%20Data%20Delivery%20Spec1.2_0.pdf.

USGS. 2019. "Earth Explorer." U.S. Geological Survey. https://earthexplorer.usgs.gov/.

USRadar. 2019. "Ground Penetrating Radar FAQ ". US Radar, Inc. http://www.usradar.com/about-ground-penetrating-radar-gpr/faq/.

Van de Putte, W., S. Van Herreweghe, W. Vansina, M. Van Stratten, B. Van Goidsenhoven, I. De Vrieze, and V. Labeeuw. 2012. "On-Site Component-Specifc Detection of Volatile Organic Components with the EnISSA MIP." Battelle 8th International Conference: Remediation of Chlorinated & Recalcitrant Compounds, May 2012.

Van Nostrand, Robert Gaige, and Kenneth L. Cook. 1966. Interpretation of resistivity data. U. S. Department of Interior. Washington, D.C. http://pubs.er.usgs.gov/publication/pp499.

VanDeventer, M. S. n.d. Community Park 1913-1921 Wellington, Kansas.

VDEQ. 2017. DEQ's Northern Region Petroleum Program current understanding of the Robinson Terminal North – the former Washington Post paper depot. Virginia Department of Environmental Quality. Woodbridge, Virginia. https://www.deq.virginia.gov/Portals/0/DEQ/Land/Tanks/rtn_cssummary.pdf.

Washburn, Libe, Eduardo Romero, David Salazar, Andrea Valdez-Shulz, Zoe Welch, and Debora Debora Iglesias-Rodriguez. 2018. "Water sampling from aerial drones for water quality research in coastal and inland waters." *Earth and Space Science Open Archive*. doi: 10.1002/essoar.91b890c2338f2530.0218ab17a1fc4712.1.

WDRB. 2017. Coroner releases name of KU contractor who died in workplace accident in Ghent, Kentucky. *WDRB.com*. https://www.wdrb.com/news/article_b5235045-7d59-50be-aba4-93c890f1cc95.html.

Weston. 2014. Remedial Investigation Report, Savage Municipal Water Supply, Superfund Site OU3, 621 Elm Street, Milford, New Hampshire. Inc. Weston Solutions. Concord, New Hampshire. SDMS Doc IS 556274. https://semspub.epa.gov/work/01/556274.pdf.

Wierzbicki, Damian. 2018. "Multi-Camera Imaging System for UAV Photogrammetry." *Sensors (Basel, Switzerland)* 18 (8):2433. doi: 10.3390/s18082433.

Wightman, W., F. Jalinoos, P. Sirles and K. Hanna. 2004. Application of Geophysical Methods to Highway Related Problems. Central Federal Lands Highway Division Federal Highway Administration. Lakewood, CO. Publication No, FHWA-IF-04-021. https://ntrl.ntis.gov/NTRL/dashboard/searchResults/titleDetail/PB2005102288.xhtml.

Williams, D., S. Haight, W. Jepson, G. Smith, D.. Walsh, J. Mohrmann, D. Danesi, and C. Bell. 2018. MT Tunnels Inspection Report, Montana Tunnels Pit Lake, Jefferson City, Montana. U.S. Bureau of Land Management. Butte, Montana.

Williams, John H., and Carole D. Johnson. 2004. “Acoustic and optical borehole-wall imaging for fractured-rock aquifer studies.” *Journal of Applied Geophysics* 55 (1):151-159. doi: https://doi.org/10.1016/j.jappgeo.2003.06.009.

Yilmaz, Ozdogan. 2001. *Seismic Data Analysis.* Tulsa, Oklahoma: Society of Exploration Geophysicists, https://library.seg.org/doi/book/10.1190/1.9781560801580.

Zhou, W., B. F. Beck, and J. B. Stephenson. 2000. “Reliability of dipole-dipole electrical resistivity tomography for defining depth to bedrock in covered karst terranes.” *Environmental Geology* 39:760-766. doi: 10.1007/s002540050491.

Acronyms

ASCT	Advanced Site Characterization Tools
ATV	Acoustic Televiewer
BTEX	Benzene, Toluene, Ethylbenzene, And Xylenes
CPT	Cone Penetrometer Testing
CSM	Conceptual Site Model
DFN	Discrete Fracture Network
DNAPL	Dense Non-Aqueous Phase Liquid
DyeLIF©	Dye-Enhanced Laser Induced Fluorescence
EC	Electrical Conductivity
ECD	Electron Capture Detector
EM	Electromagnetic
ERI	Electrical Resistivity Imaging
ERT	Electric Resistivity Tomography
EXIF	Exchange Image File
FAA	Federal Aviation Administration
FACT	Flute Activated Carbon Technique
FDEM	Frequency Domain Electromagnetic
FID	Flame Ionization Detector
FLUTe T	FLUTe Transmissivity Profiler
FLUTe™	Flexible Liner Underground Technology
FOV	Field of View
GC	Gas Chromatograph
GCP	Ground control Point
GNSS	Global Navigation Satellite System
GPR	Ground Penetrating Radar
GPS	Global Positioning System
GRM	Generalized Reciprocal Method
GSD	Ground Sampling Distance
HPFM	Heat Pulse Flowmeter
HPT	Hydraulic Profiling Tool
HPT-GWP	HPT Groundwater Profiler
HPT-GWS	HPT Groundwater Sampler
IMU	Inertial measurement unit
IR	Infrared
ISO	Sensitivity of Camera Sensor to Light
LED	Light Emitting Diode
LiDAR	Light Detection and Ranging
LIF	Laser-Induced Fluorescence
LNAPL	Light Non-Aqueous Phase Liquid
LWIR	Long-Wave Infrared
MASW	Multichannel Analysis of Surface Waves
MiHPT	Membrane Interface Hydraulic Profiling Tool
MIP	Membrane Interface Probe
MTBE	Methyl Tertiary-Butyl Ether

NAPL	Non-Aqueous Phase Liquid
NMR	Nuclear Magnetic Resonance
NNLS	Non-negative least squares
OIP	Optical Image Profiler
OIP-G	Optical Image Profiler-Green
OTV	Optical Televiewer
PAH	Polycyclic Aromatic Hydrocarbons
PCE	Tetrachloroethene
PID	Photo Ionization Detector
QA	Quality Assurance
QC	Quality Control
RADAR	Radio Detection and Ranging
RE	Reference Emitter
%RE	Response Relative to A Reference Emitter Calibration Standard
ROST	Rapid Optical Screening Tool
RPAS	Remotely piloted aircraft system
RTK	Real-Time Kinematic
SEER	Scenario Evaluator for Electrical Resistivity
SVOC	Semi-Volatile Organic Compound
TarGOST	Tar-Specific Green Optical Screening Tool
TCE	Trichloroethene
TDEM	Time Domain Electromagnetic
UAS	Unmanned Aircraft Systems
UAV	Unmanned Aerial Vehicle
USEPA	Unite States Environmental Protection Agency
USGS	U.S. Geological Survey
UV	Ultraviolet
UVOST®	Ultraviolet Optical Screening Tool
VIS	Visible Spectrum
VOC	Volatile Organic Compound
VRS	Vertical Resistivity Sounding
Waterloo ASP	Waterloo Advanced Profiling System
XRF	X-Ray Fluorescence
XSD	Halogen Specific Detectors

Acknowledgments

The members of the Interstate Technology & Regulatory Council (ITRC) Implementing Advanced Site Characterization Tools Team wish to acknowledge the individuals, organizations, and agencies that contributed to this technical/regulatory guidance.

As part of the broader ITRC effort, the Implementing Advanced Site Characterization Tools Team effort is funded primarily by the U.S. Department of Energy. Additional funding and support have been provided by the U.S. Department of Defense and the U.S. Environmental Protection Agency.

The members of the Interstate Technology & Regulatory Council (ITRC) Advance Site Characterization Tools Team wish to acknowledge the individuals, organizations, and agencies that contributed to this Technical and Regulatory Web-based Guidance Document.

The ASCT team was led by: Alex Wardle of the Virginia Department of Environmental Quality and Ed Winner of Kentucky Division of Waste Management.

Team leaders were assisted by Program Advisors: Jim Rocco and Lesley Hay Wilson of Sage Risk Solutions LLC.

Specifically, the team recognizes the efforts and important contributions of the following:

State and Local Government

Glenn Anderson
Kentucky Transportation Cabinet

Justin Buckler
Missouri Department of Natural Resources

Tom Fox
Colorado Division of Oil and Public Safety

Andrew Fuller
New Hampshire Department of Environmental Services

Andri Dahlmeier
Minnesota Pollution Control Agency

Maile Gee
Santa Ana, California Regional Water Quality Control Board

Margaret Greene
Tennessee Department of Environmental Control

Minda Hornosky
South Carolina Department of Health and Environmental Control

Ricardo Jaimes
District of Columbia Department of Energy and the Environment

Jennifer Jevnisek
Minnesota Pollution Control Agency

Kelvin Lew
Los Angeles Department of Water and Power

John Mefford

Washington Department of Ecology, Toxics Cleanup Program

Todd Mullins
Kentucky Division of Waste Management

Kisa Mwakanyamale
Illinois Geological Survey

Natalie Pheasant
Tennessee Department of Environmental Control, Division of Remediation

Elnaz Siami-Irdemoosa
Missouri Department of Natural Resources

Harold Templin
Indiana Department of Environmental Management

Tiffany Yee
Arizona Department of Environmental Quality

Federal Government

Edward Gilbert
USEPA Office of Land and Emergency Management, Office of Superfund Remediation and Technology Innovation, Technology Innovation and Field Services Division

Allan Harris
US DOE Environmental Management Consolidated Business Center

Kenda Neil
US Navy NAVFAC Engineering and Expeditionary Warfare Center

Tom Walker
USEPA Office of Underground Storage Tanks

Tribal Stakeholder

Mary Jo Ondrechen
Northeastern University

Academia

Lee Slater
Rutgers University, Newark

Industry Affiliates

Carey Austrins
Golder Associates, Ltd.

Bob Bond
Langan

Mark Bruce
Eurofins

Devin Castendyk
Golder Associates, Ltd.

Janet Castle

Eagle Synergistic

Eliot Cooper
Gregg Drilling LLC

Frederic Cosme
Geosyntec Consultants

Bradley Cross
ERM

Thomas Darby
Arcadis

Safaa Dergham
Ramboll

John Dougherty
CDM Smith

Joann Dyson
GHD

Jaime Feliciano
Geosyntec

Jim Finegan
Kleinfelder

Jason Flagg
Langan

William Flinchum
Duncklee & Dunham, P.C.

John Fontana
Vista Geoscience

David Heidlauf
Ramboll

Todd Kafka
Geosyntec Consultants

Wes McCall
Geoprobe Systems

Robert Meyer
Gregg Drilling LLC

Christopher Mulry
GES, Inc.

Robert O'Neill
Brown and Caldwell

James Peterson
Princeton Geoscience, Inc.

Mike Rawitch
Ramboll

Brian Sandberg
GHD

Alice Sandzen
ERM

Lizanne Simmons
Kleinfelder

John Sohl
Columbia Technologies

Randy St Germain
Dakota Technologies, Inc.

Many others offered advice, suggestions, reviews and edits.

Team Contacts

Team Leaders

Alex Wardle
Virginia Department of Environmental Quality
alexander.wardle@deq.virginia.gov

Ed Winner
Kentucky Division of Waste Management
edward.winner@ky.gov

Program Advisors

Jim Rocco
Sage Risk Solutions LLC
jrocco@sagerisk.com

Lesley Hay Wilson
Sage Risk Solutions LLC
lhay_wilson@sagerisk.com

Direct Sensing

Todd Mullins
Kentucky Division of Waste Management
todd.mullins@ky.gov

Jim Finegan
Kleinfelder
jfinegan@kleinfelder.com

Borehole Geophysics

Andrew Fuller
NHDES
andrew.fuller@des.nh.gov

Brian Sandberg
GHD
Brian.Sandberg@ghd.com

Surface Geophysics

Jennifer Jevnisek
Minnesota Pollution Control Agency
jennifer.jevnisek@state.mn.us

Todd Kafka
Geosyntec Consultants
tkafka@geosyntec.com

Remote Sensing

Glenn Anderson
Kentucky Transportation Cabinet
glenn.anderson@ky.gov

Devin Castendyk
Golder Associates, Ltd.
devin_castendyk@golder.com

Contact

Your opinion is important to us. If you have questions or comments about an ITRC document, training course or ITRC in general, please contact us at itrcweb.org.